# From Protoplanetary Dust to Asteroidal Heating: A mineralogical study of the CO3 chondrites

Enrica Bonato

BSc, MSc

(Università degli Studi di Padova, University College London)

Submitted in fulfilment of the requirements for the

Degree of Doctor of Philosophy

School of Geographical & Earth Sciences

College of Science and Engineering

University of Glasgow


January 2021

# Abstract

Carbonaceous chondrites are among the most primitive extra-terrestrial materials available for study. These meteorites provide a detailed record of the geological processes and events that have shaped our solar system over the last 4.5 billion years. "Ornans-like" carbonaceous chondrite meteorites, also referred to as CO3 chondrites, comprise pristine, primitive mineralogy that has undergone no or minimal aqueous alteration. CO3 chondrites are also known to contain up to $\sim 3.5\%$ carbon in the form of insoluble and soluble organic matter, graphite and carbonates. The CO3 chondrites form a suite of samples that have experienced increasing degrees of thermal metamorphism, from weakly heated CO3.0s such as Colony and DOM 08006, to strongly meta-morphosed CO3.8s such as Isna. Detailed studies of this suite of CO3 chondrites enables firstly a determination of the most primitive and earliest formed aggregates of crystalline, amorphous and organic solids, and their textural relationships from which inferences can be made regarding the nature and composition of the protoplanetary disk; and secondly quantification of the effects of parent body metamorphism on these early solar system solids.

In this thesis I have studied 12 CO3 chondrites that cover the whole metamorphic sequence, namely Colony and DOM 08006 (CO3.0), NWA 7892 (CO3.05), MIL 090010 (CO3.1), Kainsaz (CO3.2), Felix (CO3.3), Ornans (CO3.4), Lancé (CO3.5), Moss and ALHA77003 (CO3.6), War-renton (CO3.7) and Isna (CO3.8). Bulk mineralogy and chemical compositions were quantified using X-ray powder diffraction (XRD) and electron probe microanalysis, and were contextual-ised with in-situ, spatially resolved scanning and transmission electron microscopy (TEM), and synchrotron-based scanning transmission X-ray microscopy (STXM) combined with X-ray ab-sorption near edge structure (XANES) spectroscopy.

XRD was used to quantify the bulk modal mineralogy of the CO3 chondrites. I found that the most primitive samples mostly comprise Mg-rich olivine and pyroxene, and Fe-bearing amor-phous silicates. Samples between CO3.0 and CO3.1 contained $\sim$ 35 % forsterite, $\sim$ 13 % $Fo_{60}$ olivine, $\sim$ 26 % pyroxene, $\sim$ 2.5 % sulphide, $\sim$ 0.7 % metal, $\sim$ 5 % magnetite and $\sim$ 14 % amorphous mate-rial. On heating, forsterite within the primitive samples was systematically replaced by Fe-rich olivine such that all the olivine in the CO3.8 was $Fo_{60}$. This transformation was linear and could be used for rapidly and accurately defining the petrologic grade of a CO chondrite. The amorphous Fe-bearing silicates were fully crystallised by CO3.2, magnetite had disappeared by CO3.3 and nepheline appeared at CO3.3 and gradually increases in abundance up to CO3.8. Changes in the modal mineralogy are reflected in the bulk chemistry with the matrix becoming depleted in Fe and enriched in Mg, due to equilibration with chondrules, and there is a small linear increase in Cr with increasing metamorphism.

Bright-field TEM images show the fine grain size and heterogeneous texture of the matrix in the most primitive CO3 chondrites, which consists of an amorphous groundmass within which is embedded $\sim$ 0.1 $\mu$m silicate, sulphide, metal and phyllosilicate grains. TEM imaging also revealed a systematic change in the porosity of the matrix as a function of metamorphic grade. Recrystallization and equilibration of the low porosity, low permeability matrix in the CO3.0-3.1 chondrites caused by metamorphic heating, progressively increased the porosity and average grainsize of the minerals up to CO3.8. Fe L-edge XANES analysis of the STXM data revealed that the amorphous Fe-bearing silicates and the matrix of the most primitive CO3.0 chondrites are almost fully oxidized with the $Fe^{3+}/\Sigma Fe$ ratio close to 1.0. On heating the Fe becomes rapidly reduced with Kainsaz containing only about 10 % $Fe^{3+}$ and Moss being dominated by $Fe^{2+}$. Lim-ited spatial variation in the Fe L-edge X-ray absorption spectra was observed in DOM 08006, most likely related to the proximity of metal and sulphides to the amorphous silicates. No significant variation in the Fe L-edge X-ray absorption spectra was observed in the silicate fraction of Moss even down to the 40 nm scale.

STXM and XANES at the C, N, and O K-edges reveal spatial variations in the functional chemistry of the organic matter in the most primitive CO3 chondrites. This variation was most evident in the intensity of the aromatic, ketone and carboxyl spectral

features. The presence of carbonate was also occasionally observed most particularly in and close to a $\sim$ 1.3 $\sim$m wide carbonate vein in a sample of NWA 7892. As a function of increased metamorphic heating I found that the aromatic group persists while the ketone and carboxyl groups disappear such that in Moss CO3.6 only aromatic carbon was observed (with a potential trace of carbonate). Graphite was not definitively identified in any of the samples. Spectral features on the O K-edge show the progressive crystallisation of the amorphous silicate into olivine with metamorphic heating.

The effects of metamorphic heating on the primitive CO3 chondrites is to crystallise the amorphous Fe-bearing silicates, systematically modify the modal mineralogy, increase the po-rosity of the matrix and homogenise the molecular speciation in the organic matter. Furthermore, the hydrated amorphous silicates dehydrate within a narrow temperature interval of about 100°C and there is a concomitant reduction of the $Fe^{3+}$ to $Fe^{2+}$ as the amorphous Fe-silicates transform into crystalline minerals. This reduction of the Fe is facilitated by the changing redox conditions likely due to the removal of oxidizing $H_2O$ and the initial presence of reducing agents such as H and C.

I conclude that CO meteorites formed from anhydrous parent bodies in which minimal aqueous alteration took place and the main source of water was hydrated amorphous silicates. I propose that these amorphous silicates were hydrated in the nebula prior to accretion onto the CO parent bodies. Water within the amorphous silicates contributed to the oxidation of the Fe to $Fe^{3+}$. Low porosity and limited permeability in the primitive materials restricted any fluids from circulating within the parent body. Changes from metamorphic heating released water and increased perme-ability such that organic matter became homogenized and subsequently partially dissociated gen-erating a reducing environment. It is possible that the CO parent bodies had an onion shell like structure with high petrologic type COs concentrated in the inner part of the asteroid and low petrologic types closer to the surface.

# Contents

# List of Tables

# List of Figures

# Acknowledgements

Firstly, I would like to thank my supervisors for the opportunity they gave me, for believing in me and for everything they thought me. This PhD was a life changing experienced that shaped me both as a person and as a scientist. Thank you for listening to me, you for being so calm and supportive even in very difficult situations and for making me believing in myself until the end. Sara, Ashley, Paul and Martin, it was a great pleasure working with you, I will never forget these years spent working together and I very much hope they are just the beginning of a long lasting collaboration.

Many thanks my Viva examiners, Rihan Jones and Lydia Hallis, for th very constructive discussion we had during the viva and for the comments that halp me improving the quality of this work.

Many thanks to the Science and Technology Facilities Council for funding this "out of this world" PhD project.

I would like to thank ANSMET for supplying some of their Antarctic meteorites and the Meteorite Collection at the Natural History Museum, in particular Natasha Almeida and Caroline Smith for the collection access, support and advice throughout my PhD.

I would also like to thank the I08 Beamline Team at Diamond Light Source, Burkhard Kaulich, Tohru Araki and Majid Kazemian for their support and time helping on the Beamline. A special thank you must be given to Ridgeway house for their exotic and memorable cuisine.

Thank you to the Imaging and Analysis Centre at the NHM and in particular to Jens Najorka, John Spratt, Tomasz Goral, Tobias Salge, Tony Wighton, Alex Ball and Callum Hatch for all their help in the lab throughout my project.

Thank you to Billy Smith and Colin How of the Kelvin Nanocharacterisation Cen-

tre, at the University of Glasgow, for preparing the FIB sections analysed in the present work and for the technical support at the TEM.

Christian Schröder from the University of Stirling for Mössbauer spectrocopy analyses.

Thank you to Adrian Brearley and Brad De Gregorio for their interest to my project and for the long meetings and helpful conversations we had at several conferences over the years.

Thank you to Eileen Cox and Anna Hutson, for their support at the NHM.

Thank you to my colleagues and friends in the Mineral and Planetary Science Division and my PhD fellows, for being supportive, encouraging and always available for a chat and for partying. I would also like to mention Jack Anderson, Geralllt Hughes, Finley Gilchrist, Mingming Zhang, Sara Motaghian, Sarah (Boozy) Boazman, Zach Dickeson, Carmen Pinto Ward, Bex Summerfield, Mihaiela Swift, Martin Mangler, Emily Brugge and Helena Bates (my fave).

Thank you to *The Keepers Arms* for its top selection of hyper-cold beers that resfreshed my writing over the summer.

Thank you to my Glasgow fellows Luke Daly, Áine O'Brien and Annemarie Pickersgill for their help and friendship up in Glasgow.

Thank you to my friends Silvia, Giovanni, Valentina, Chiara, Betty, Emanuela, Natasha, Simon, Epi, Chris, Elisa and little Thomas, Agata and Agnieszka.

Thank you to Mario, for supporting me during these years and for his help; thank you to Massimo for his long distance support and conversations; thank you to Corrado for being able to daydream all the time not matter what.

Thank you to Evelin and little Maja for their help, support and understanding until the end.

Thank you very much to everyone, this work and these years would have been very different without your presence and intake. You all deserve a special recognition as you all contributed to the creation of this work.

Last, but not least mum, dad and grandparents. Grazie per avermi supportata fin dall' inizio, da quando sono partita nel 2012. In quel momento pensavo di rimanere lontana solo per poco tempo, ma il tempo é volato e sono ancora qui. Sono successe

tante cose in questi anni ma non vi ho mai dimenticati e siete sempre nel mio cuore.

# Declaration

I declare that, except where explicit reference is made to the contribution of others, that this dissertation is the result of my own work and has not been submitted for any other degree at the University of Glasgow or any other institution.

Enrica Bonato

*Al nonno Tito*

# Chapter 1

# Introduction

## 1.1 The formation of the Solar System

The Solar System formed over 4.5 billion years ago as result of the gravitational collapse of a dense part of an interstellar molecular cloud (for a review see Russell (2007); Figures 1.1 and 1.2). The precollapse cloud was mainly composed of light elements such as H and He. About 1% of the cloud was comprised of dust grains which were produced during the previous phases of stellar evolution (Apai & Lauretta, 2010) and another 1% of molecules (e.g. CO) and elements heavier than He (Boss & Goswami, 2006). The collapse of the molecular cloud might have been triggered by the gravitational collapse of a region that was unusually dense or in response to the explosion of a nearby supernova (Figure 1.1). In this second scenario, the explosion produced a shock wave that triggered the collapse and began the formation of the Sun (Boss & Keiser, 2015). Due to the conservation of angular momentum, the molecular cloud began to spin faster during its gravitational collapse which caused the atoms to collide with one another more frequently and the kinetic energy produced in this process was transformed into heat. Consequently, the central material became denser and the increasing temperature and pressure led to the fusion of H into He and the birth of the Sun. This phase is thought to have lasted for about 100,000 years (Russell, 2007). At this stage the proto-Sun was surrounded by a disk of gas and dust; the continued spinning of the disk led to its collapse to the rotational plane of the system to create the protoplanetary disk from which the planets formed. The evolution of the protoplanetary disk is a consequence

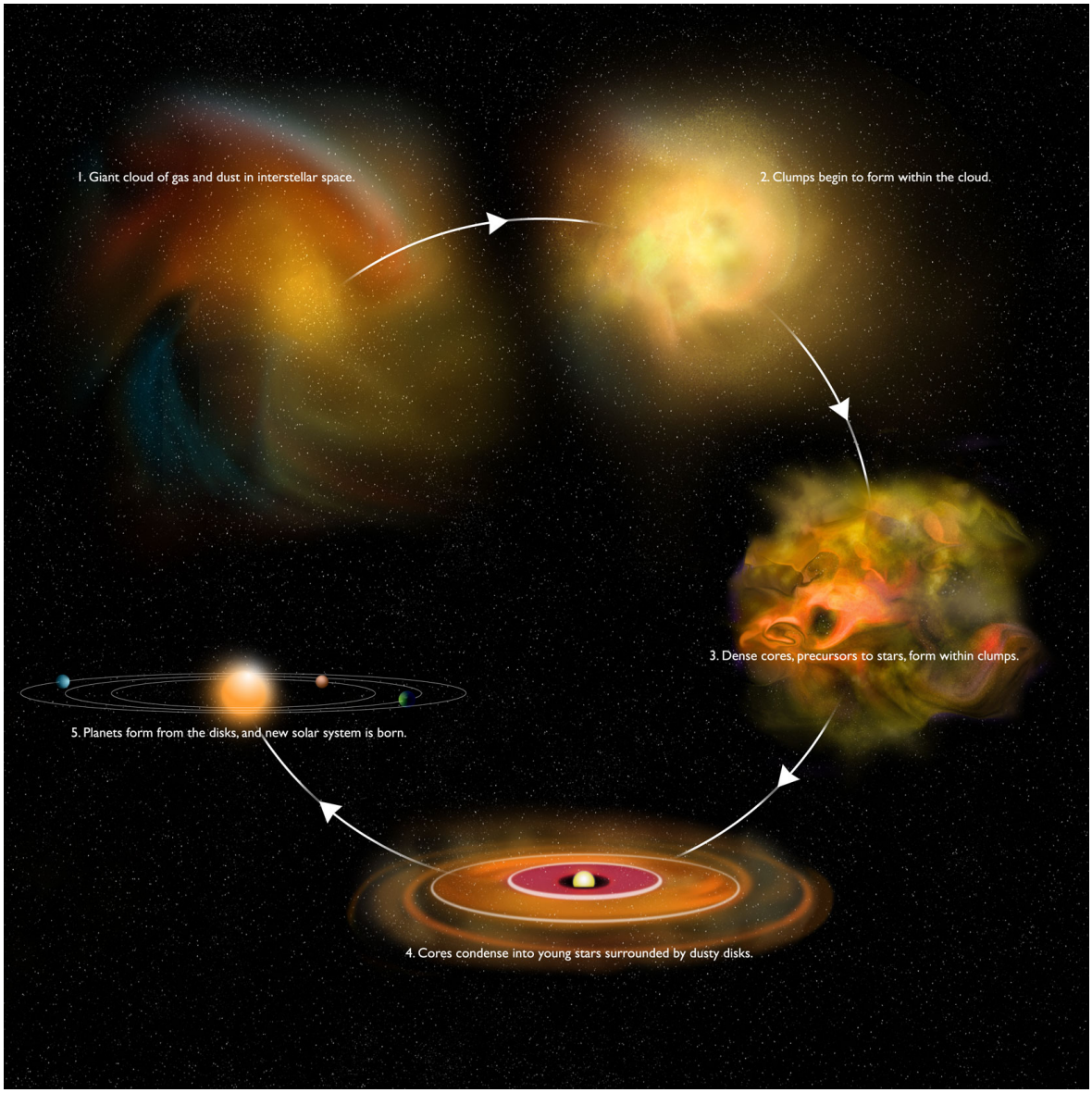


Figure 1.1: *Diagram illustrating the formation of the Solar System; credit to Bill Saxton, NRAO/AUI/NSF*

of different fundamental parameters such as mass and size, but also factors including viscous evolution, grain coagulation, photoevaporation and accretion to the star (Apai & Lauretta, 2010).

The inner part of the disk was hotter than the outermost part, and it is within the inner disk that the terrestrial planets formed. At 4567 Ma the first new solids began to form within the disk (Amelin et al., 2002) (Figure 1.2). These solids are the highly refractory minerals found within Ca, Al-rich inclusions (CAIs), which probably formed close to the Sun (Grossman, 1972; Russell, 2007). Thereafter, chondrules (rounded silicate-rich objects composed primarily of olivine and pyroxene) and metal formed

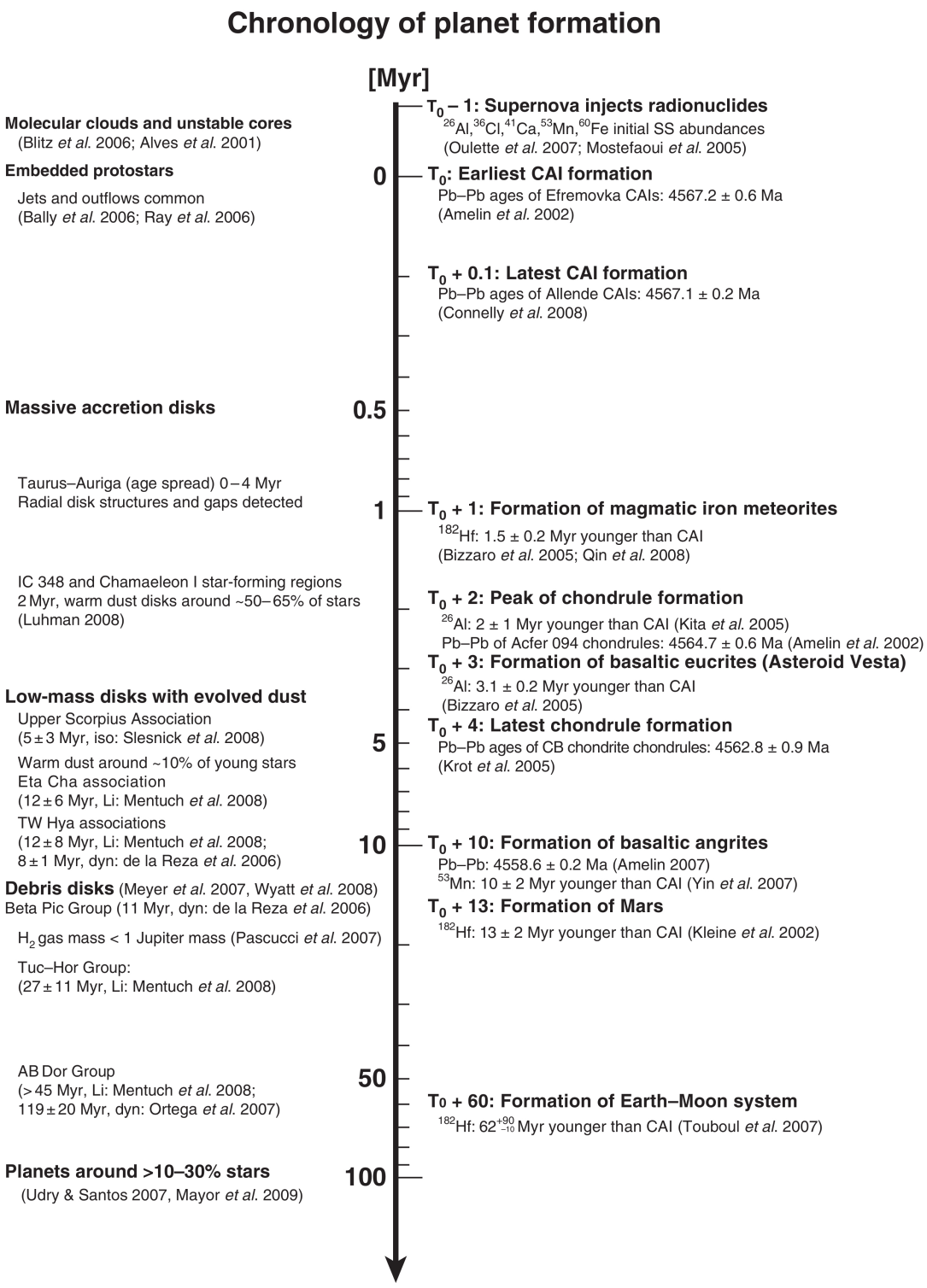


Figure 1.2: *Chronology of planet formation in the Solar System. After Apai & Lauretta (2010)*

from the melting of dust clusters or the dispersion of molten material. Once these building blocks had formed, a fine-grained matrix cemented them all together through a gravitational sedimentation process during which the dust settled in the midplane of the accretion disk (Russell, 2007). Planets formed by accretion, during which dust grains of $\mu$m size clumped together to form cm sized bodies. These bodies kept growing until reaching metre-size and km-size bodies called *planetesimals*. Planetesimals may have grown faster due to the accretion of pebbles affected by aerodynamic drag, a process named *pebble accretion* (Lambrechts & Johansen, 2012). Gravitational interactions among planetesimals led to growth in size through multiple low-velocity collisions; although some of them were subject to larger impacts that caused erosion, melting or fragmentation. It is believed that this phase of planet formation progressed for about 10 to 100 million years (Asphaug et al., 2006).

The way the Solar System is structured can be explained through the *Grand Tack model* by Walsh et al. (2011), where the asteroid belt (located between Mars and Jupiter) is the boundary between the rocky planets, located in the inner Solar System, and the gas giant and ice planets that are found in the outer Solar System. The outer planets are mainly composed of volatiles, mostly H, He, N, $H_2O$ and $CO_2$, as temperatures at those heliocentric distances were below the condensation temperature of water and other volatiles (Russell, 2007). The *Grand Tack model* suggests that Jupiter was the first gas giant planet to form, followed by Saturn which was located further out from the Sun. When Jupiter began to migrate inwards, due to gas drag, along with Saturn, they pushed materials inside their orbit inwards, compressing the disk embryos and scattering outwards some inner-disk planetesimals (Figure 1.3).

At this point Saturn entered a motion resonance with Jupiter which affected their orbits and caused them to invert their migration direction. At about 1.5 AU (known as *the tack point*) they began to migrate outwards from the Sun. During their outward migration they interacted planetesimals that were formed between $\sim$ 2 and 4 AU (S-type) and about 8 to 13 AU (C-type), beyond the gas giants. Most of these planetesimals (asteroids) were ejected from their orbit by the influence of Jupiter and Saturn, but the ones that survived stabilised their orbit within the asteroid belt. These asteroids are rocky bodies orbiting the Sun that can be classified on the basis of their composi-

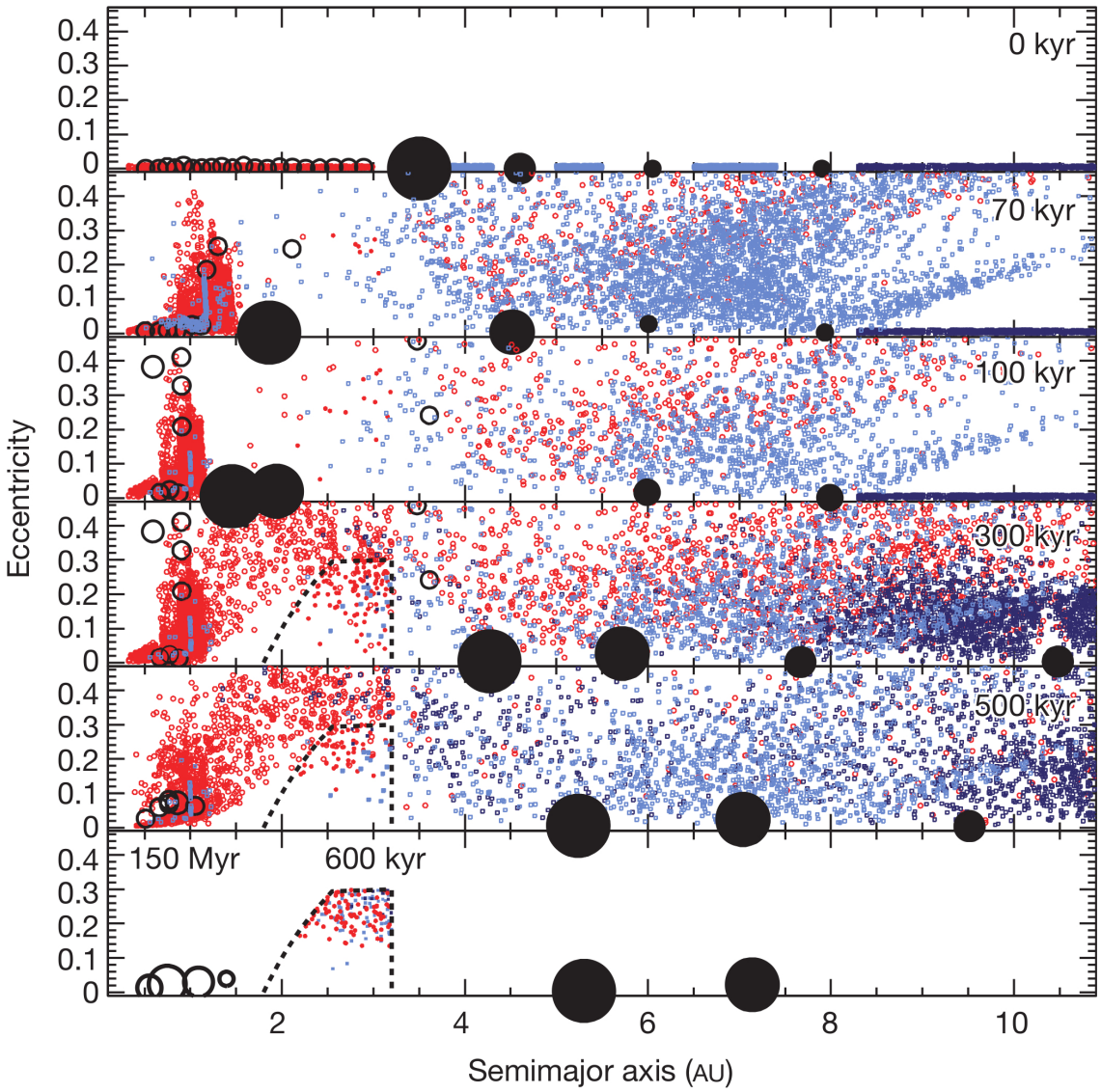


Figure 1.3: *Diagram showing the evolution of the small body population in relation to the migration and growth of gas giant planets after Walsh et al. (2011). Jupiter, Saturn, Uranus and Neptune are represented by large black filled circles, and they migrate inward and outward. The red dots represents S-type planetesimals which were initially located between 0.3 and 3 AU. The light blue dots represent C-type planetesimals, which are located between the giant planets, while the dark blue dots represents the outer-disk planetesimals (initially between 8 to 13 AU). Planetary embryos are represented with open circles.*

tion. The asteroid belt can be divided into the inner asteroid belt, which is dominated by S-type asteroids related to ordinary chondrite meteorites that were located within the inner orbit of Jupiter, and the main and outer belt which is dominated by C-type asteroids (Walsh et al., 2012; DeMeo et al., 2015). C-type asteroids are linked to carbonaceous chondrites that were originally located between and beyond the gas giants (Walsh et al., 2012; DeMeo et al., 2015). The asteroid belt contains numerous irregular bodies (total mass of about $3x10^{21}$kg), collisions between which result in fragmentation and the production of smaller meteoroids which can then enter the Earth's atmosphere, becoming meteorites when they hit the ground (Hutchison, 2004).

Meteorites provide a detailed record of the geological processes that took place in the Solar System over the last 4.5 billion years. Meteorites are very important materials to study as they can provide information about the evolution, age and composition of the Solar System, geological history ofplanetary bodies, stellar evolution through the analysis of presolar grains, and how water and life might have been brought to Earth and the other terrestrial planets (Hutchison, 2004). By looking at meteorites we can see that following initial accretion, asteroids underwent various stages in their evolution such as aqueous alteration, thermal metamorphism, melting and differentiation (Grady & Wright, 2006; Weisberg et al., 2006). Larger asteroids experienced high enough temperatures to melt and differentiate, and these are the parent bodies of the iron and achondrite meteorites. Chondrites are unmelted meteorites from undifferentiated asteroids that nevertheless experienced some thermal metamorphism and aqueous alteration.

## 1.2 Protoplanetary disk and its mineralogy

The formation of the protoplanetary disk is the result of the collapse of the proto-stellar cloud and the conservation of its angular momentum. The Solar System formed from a cloud of gas and dust, and the majority of the dust mass is in the form of amorphous silicates (Kemper et al., 2004). The formation of crystalline silicates is the result of primary processes such as thermal annealing of the amorphous silicates, or vaporisation and gas-phase condensation of the inner region of the disk (van Boekel et al., 2004)

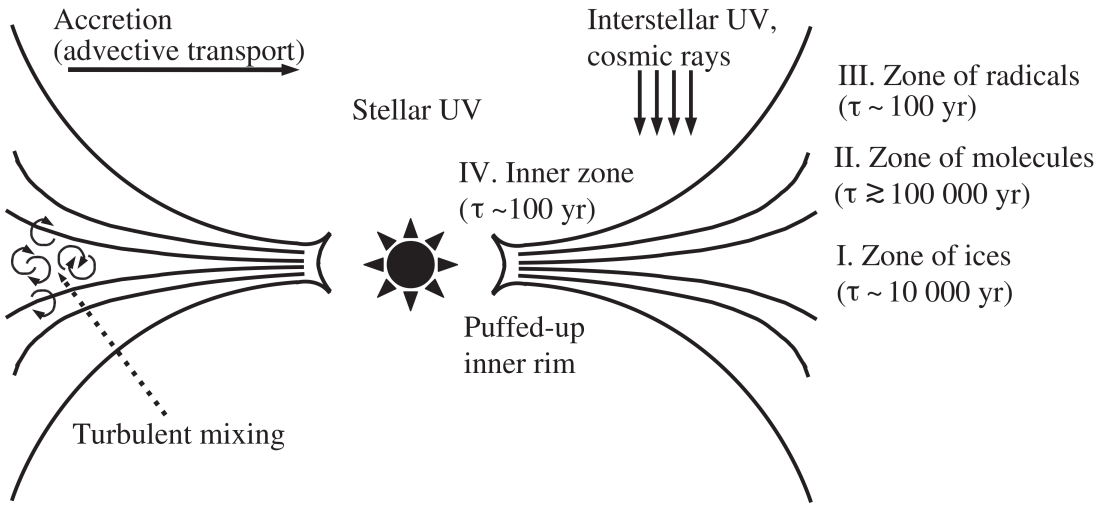


Figure 1.4: *Chemical zones of the protoplanetary disk, with timescales esimated for a radius of 100 AU; after Semenov et al. (2010).*

A protoplanetary disk can be divided into four chemically different zones (Apai & Lauretta, 2010) (Figure 1.4):

- Zone I: Zone of ices, which is mainly cold gas phases and grain-surface reactions and is opaque to the incoming radiation. This region is located in the cold-mid plane.

- Zone II: Zone of molecules, comprises a warmer molecular layer close to the mid plane and processing is dominated by ultraviolet and X-ray induced photochemistry.

- Zone III: Zone rich in radicals, very hot and with low abundance of molecules near the Sun.

- Zone IV: Inner zone, inside the ice line and where planets forms.

Dust grains are an important component of protoplanetary disks and the dominant matter influencing their opacity. The chemistry of the grain surface of the dust particles leads to the formation of molecular ice and of complex organic molecules (Henning & Meeus, 2009) to form a silicate core and icy/organic mantle. The composition of the protoplanetary disk is assumed to partially reflect the composition of the molecular cloud, so of the interstellar medium (ISM), although it can slightly differ because of

the evaporation of volatile molecular ice, oxygen incorporation into water and the subsequent formation of Si atoms from quartz (Henning & Meeus, 2009). The dust in the molecular cloud, or the ISM, is formed mainly from silicates and carbonaceous material. Silicate and carbonaceous dust were therefore the most common cosmic dust species present in a protoplanetary disk, although there are mineralogical variations depending on the regions of the disk. The inner disk was very abundant in crystalline phases, which are subjected to a faster grain growth because of the higher collision rates of the grains. Less crystalline phases were instead more concentrated in the outer disk. The dust model introduced for the first time by Pollack et al. (1994) suggests that the inner disk is mainly populated by Mg-bearing silicates (van Boekel et al., 2004), such as forsterite ($Mg_2SiO_4$), and enstatite ($MgSiO_3$) which is more stable and therefore more abundant (Henning & Meeus, 2009; Apai et al., 2010). The outer disk regions contain iron-magnesium silicates such as olivines and pyroxenes, (van Boekel et al., 2004) with amorphous silicates, quartz, metallic iron, troilite, volatile and refractory organics and water ice in varying amounts.

The dust model of Pollack et al. (1994) divides the products of dust forming elements (O, C, Si, Mg, Fe, S and N) into categories: gases, molecular ices and refractory grains. The molecular ices only exist in the outer disk, as it is cooler, while FeS forms from the condensation of Fe and $H_2S$ at 680 K. Formation of FeS was also described by Lauretta et al. (1996), hypothesising that FeS formed very rapidly and that changes in sulfur content of chondritic material are due to the the removal of metal grains from contact with the gas ($H_2S$) for examples by accretion in larger bodies. Dust material in a disk has restricted stabilities, and their survival depends on their location within the disk and the prevailing physical conditions (e.g. pressure and temperature). Gail (1998, 2003) suggest the following temperature limits for different dust materials:

- $T < 700$ K: FeS formation, Fe-metal, Si present in Mg-rich amorphous silicates, $SiO_2$ is unstable;
- $T \sim 800$ K: FeS disappears, amorphous silicates anneal to crystalline silicates;
- $1300 < T < 1400$ K: crystalline silicates and solid Fe destroyed, only dust particles remaining are refractory-rich (such as $Al_2O_3$);

- $T > 1850$ K: no dust survives.

However, there are also other Al- and Ca- minerals that can exist under the temperature-density constrains of the protoplanetary disk such as hibonite ($CaAl_{12}O_{19}$) and spinel ($MgAl_2O_4$) (Ebel, 2006). Dust material started to form with the cooling of the nebula, allowing solids and liquids to condense, but partially condensed materials also became isolated from the remaining gas, which is reflected by the partial depletion in volatile in planetary bodies located in the inner solar system (Davis & Richter, 2014). As a consequence of this, it is possible to state that evaporation and condensation processes took place in the early solar system.

## 1.3 Chondrite meteorites

Chondrites (Figure 1.5) are a group of unmelted meteorites, which derive from undifferentiated asteroids. Chondrites contain small spheres (average size <1 mm) called *chondrules*, along with refractory inclusions such as CAIs (Calcium and Aluminium rich Inclusions) and AOAs (Amoeboid Olivine Aggregates), sulphides, Fe, Ni-metal, and fine-grained matrix (Hutchison, 2004; Krot et al., 2014b). It is generally accepted that refractory inclusions, Fe, Ni-metal and chondrules formed in the solar nebula as result of high temperature processes such as condensation and evaporation (Krot et al., 2014b). The majority of chondrules and Fe, Ni-metal as well as many CAIs underwent subsequent melting processes as a result of heating events. Matrix material, some CAIs and metal grains, although they managed escaping melting processes, they experienced thermal processing on asteroid parent bodies like thermal and shock metamorphism, hydrothermal alteration (Krot et al., 2014b). Matrix is typically very fine grained (from 10 nm to 5 $\mu$m) and very susceptible to alteration by water or temperature (Scott & Krot, 2005). Moreover, matrix is very important as it contains most of the information about the formation of the Solar System that can be obtained from presolar material and organic matter (Zinner, 2003; Scott & Krot, 2005). Presolar silicates in particular can provide important insights about compaction and accretion processes that took place in primitive meteorites (Haenecour et al., 2018), however they are very susceptible to alteration processes.

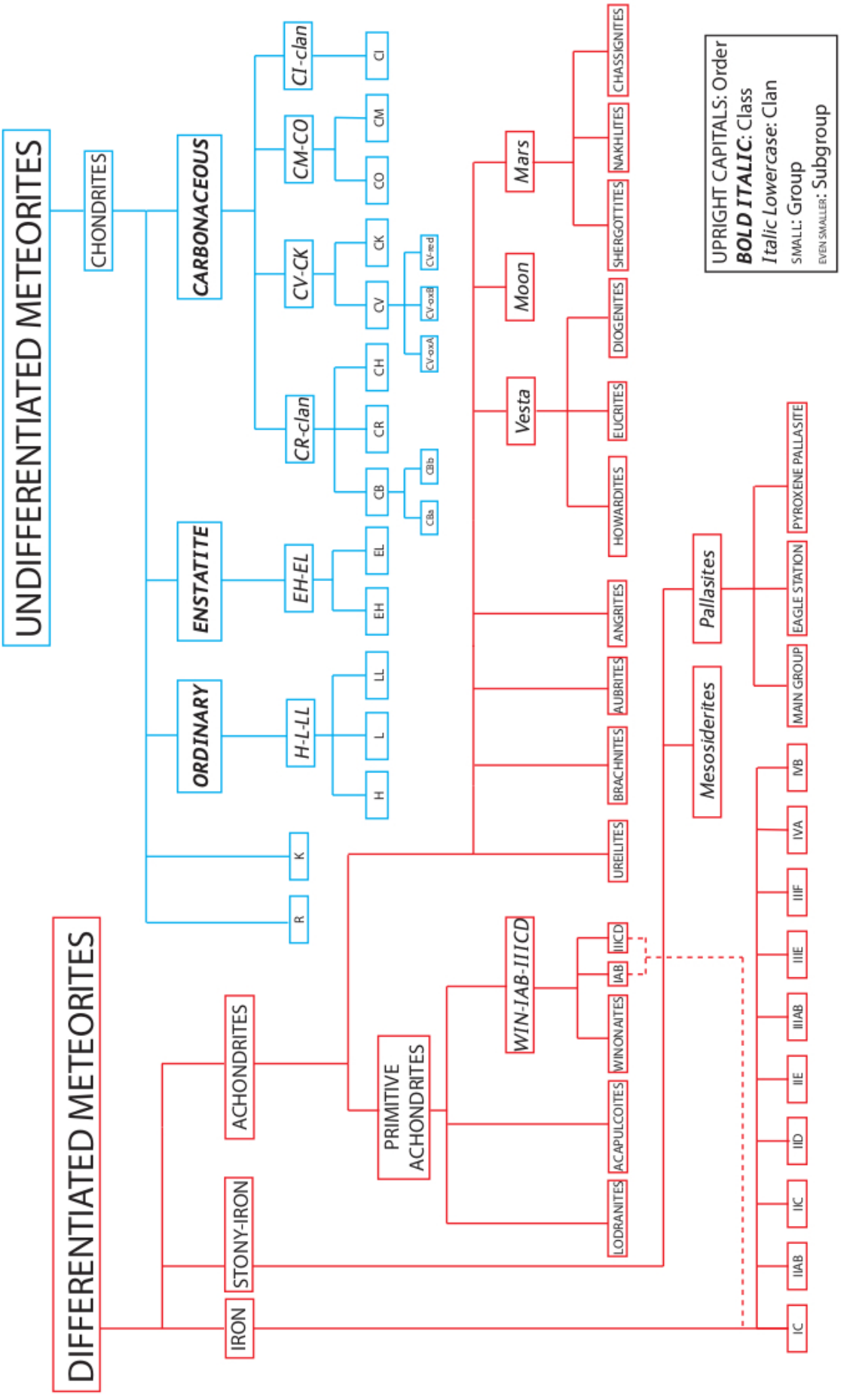


Figure 1.5: *Diagram illustrating the systematics of meteorite classification; after Weisberg et al. (2006).*

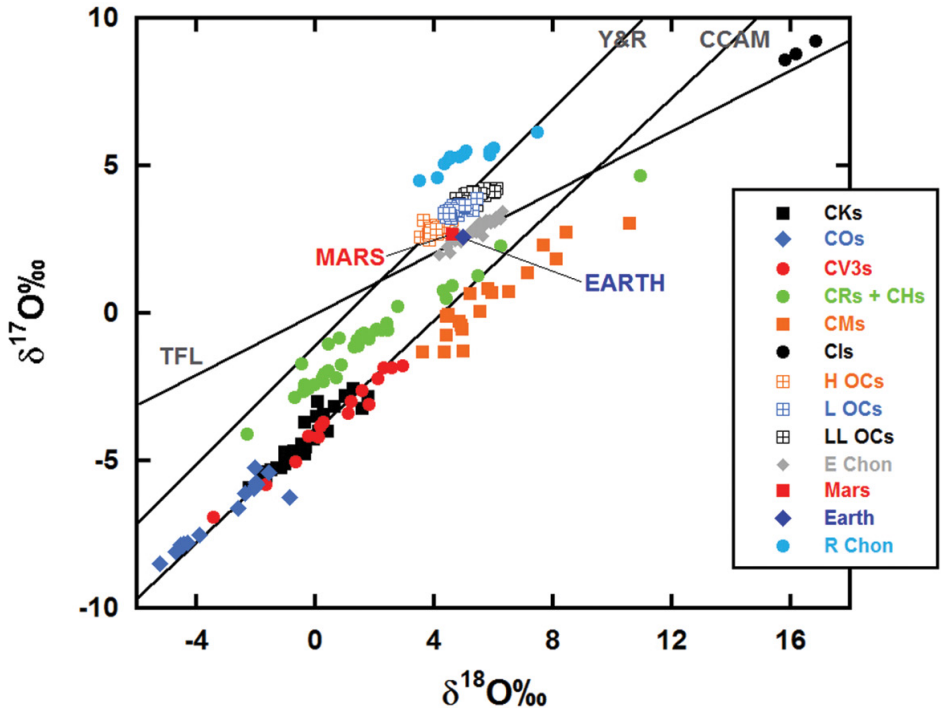


Figure 1.6: *Oxygen isotopic composition of OC, CC, EC, RC, Mars and Earth by Burbine (2016). The carbonaceous chondrites plots below the terrestrial fractionation line (TFL) and the Young and Russell line (Y&R).*

*Organic matter* is "stored" in the matrix, and it provides very useful insights in understanding the formation of the matrix itself. Of particular importance is understanding if the organic matter is associated with specific minerals and assessing its role within alteration processes. This necessity to maintain spatial integrity of the sample has lead to the wide use and development of *in situ* analyses e.g. Cody et al. (2008); De Gregorio et al. (2013); Le Guillou & Brearley (2014a); Le Guillou et al. (2015); De Gregorio et al. (2015b). Chondrites accreted up to 3.5 % of carbon in their matrices (Alexander et al., 2017), which can be present under many forms. Carbon can be present as crystalline graphite, with a size range from 1 to 7 $\mu$m, as amorphous carbon and carbide grains. However, most carbon is in the form of organic matter (Alexander et al., 2017). Organic matter is divided into soluble organic matter (SOM) and insoluble organic matter (IOM), based upon its solubility in solvents (Gilmour, 2003; Alexander et al., 2017). IOM has highly variable isotopic signatures such as D, H/C, N/C and S/C ratios which vary within chondrite groups. This isotopic variability likely reflects the accretion and alteration processes that affected the chondrite parent bodies.

Chondrites can be divided into: ordinary, enstatite, rumurutite (R), kakangarite (K) and carbonaceous (Figure 1.5). Ordinary chondrites (OC) are the most abundant meteorites available for study and make up more than 85 % of the meteorites that have been observed to fall on Earth (Weisberg et al., 2006). They are materials coming from the inner Main Belt region of the asteroid belt (Zolensky et al., 2018). They are characterised by millimetre-sized chondrules, rare CAIs and AOAs and ∼10 - 15 vol% of matrix (Hutchison, 2004; Weisberg et al., 2006). The Hayabusa mission provided a direct link between OCs and S type asteroids (Nakamura et al., 2011). Enstatite chondrites (EC) are highly reduced, which suggests that they formed within the inner Solar System (Hutchison, 2004). They contain Fe-poor silicates and high Si (2-3 %) in the Fe, Ni-metal; enstatite ($MgSiO_3$) is the main mineral present in their chondrules. They also contain a wide variety of sulphide, nitride and metal phases that are absent in other chondrite groups, including oldhamite (CaS), niningerite [(Mg,Fe,Mn)S] and osbornite (TiN) (Hutchison, 2004; Weisberg et al., 2006). R (Rumuruti-like) chondrites have a matrix abundance over ∼70 vol% mainly composed of enstatite $Fs_3$, metal is about 6 - 9 vol%, their average olivine composition is $Fa_2$ and enstatite $Fs_4$, and refractory-lithophile and volatile-element abundances ar similar to OC (Weisberg et al., 2006; Krot et al., 2014a). K (Kakangari-like) chondrites are characterised by a high abundance of matrix material (∼ 50 vol%), high oxidation states, very little abundance of CAIs, refractory lithophile and moderate abundance of volatile elements, mostly metamorphosed and brecciated (Weisberg et al., 2006; Krot et al., 2014a). Carbonaceous chondrites (CC) are characterised by close to solar elemental abundances, low-Fe metal content, high carbon content (up to 5 wt%) and enrichments in volatile elements (Krot et al., 2014a; Zolensky et al., 2018). The CCs have Mg/Si ratio $> 1$ and high concentrations of refractory lithophile elements (Grossman & Score, 1996; Hutchison, 2004). Petrology and geochemical characteristics including texture, mineralogy, whole-rock chemical composition, O-isotopic signature (Figure 1.6), and the ratio of chondrules to matrix are used to classify them into chemical groups (Figure 1.5). Chondrite chemical compositions are commonly expressed as Mg- or Si- normalised abundances relative to CI chondrites (Ivuna-like), as CIs bulk composition is close to that of the solar photosphere (Weisberg et al., 2006). The most pristine meteorites

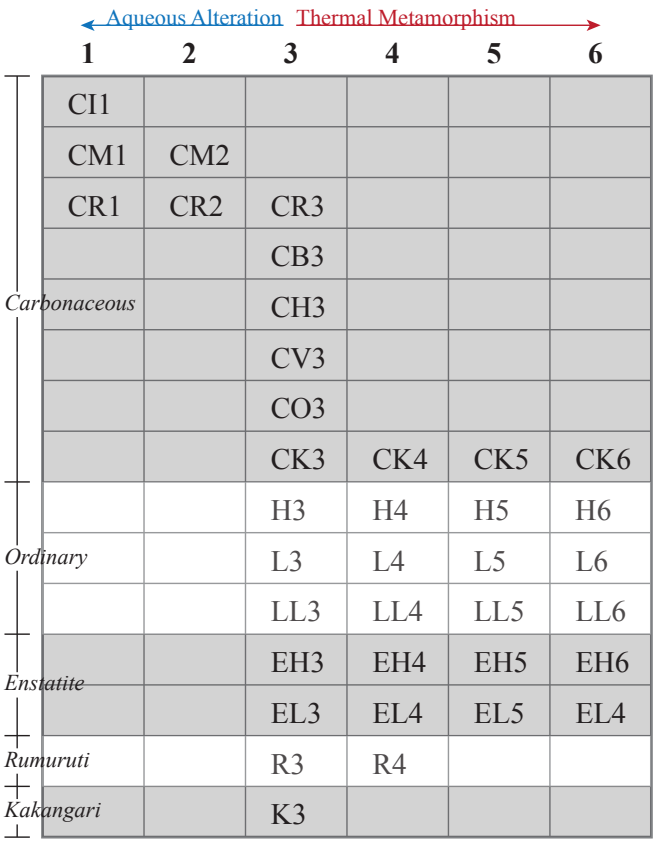


Figure 1.7: *Table illustrating the petrologic types for each chondrite group; after Weisberg et al. (2006).*

are classified as petrologic type 3.0; chondrites of petrologic types 1 and 2 are those affected by aqueous alteration at low temperature, while those classified as petrologic types from 4 to 7 underwent changes at high temperatures, such as recrystallisation (Brearley & Jones, 1998; Weisberg et al., 2006) (Table 1.7).

## 1.4 Chondrite Processing: metamorphism & aqueous alteration

Chondritic materials were subject subject to three main parent body processes: thermal metamorphism, aqueous alteration and impacts. It is thought that most of the components which chondrites are made from were accreted in a "cold" environment, but experienced parent thermal metamorphism (Dodd, 1969; Huss et al., 2006). The *autometamorphism* or *hot accretion* model suggests that a mass of hot material accreted

to form a parent body, which at a certain point began to cool (Hutchison, 1996). This theory suggests that the portion of material that cooled down more rapidly developed into type 3 chondrites, while the material that cooled more slowly became type 6 chondrites (Rubin & Brearley, 1996; Huss et al., 2006). However, the most widely accepted theory is *prograde-metamorphism* in which a cold and unequilibrated material was progressively heated on a parent body. There are several potential heat sources that could have caused metamorphism of chondrite parent bodies (Brearley & Jones, 1998; Huss et al., 2006), including: i) accretional or collisional heating: during parent body accretion the kinetic energy produced by high velocity impacts of smaller planetesimals was transformed into heat; ii) radioactive decay of $^{26}$Al and $^{60}$Fe; iii) electromagnetic induction by the solar wind; iv) FU-Orionis-type events, which are an increase in the brightness of a star (e.g. the Sun) over a time-scale of 1 and 100 years. Consequent increases in temperature can lead to the heating of planetesimals to temperatures over 1200°C (Huss et al., 2006). Thermal metamorphism results in incremental changes in the chemical and textural equilibrium of the primary components of the asteroid. There is strong evidence that the most important source of heat responsible for the majority of the thermal metamorphic features is the decay of $^{26}$Al (Scott & Krot, 2014; Zolensky et al., 2018), which was adequately mixed within the solar nebula, while the abundance of $^{60}$Fe was not high enough in the early solar system (Scott & Krot, 2014). The peak temperature that can be reached in the metamorphic process for chondrites is estimated to be below 950°C which corresponds with the appearance of partial melts in the Fe-Ni-S system (Brearley & Jones, 1998).

Among carbonaceous chondrites CO (Ornans-like) and CV (Vigarano-like) and CK (Kakangari-like), are the most affected by thermal metamorphism. and they can be subdivided in subtypes ranging from 3.0 to 3.8 for COs, from 3.1 to 3.6 for CVs and in types from 3 to 6 for CKs. The peak of the metamorphic temperature in COs was modelled by Scott & Jones (1990) through the changes in composition of the olivines and estimated to be of about 200 °C for CO3.0, 300 °C for CO3.2 and up to $600 - 700$ °C for COs 3.6-3.8. The metamorphic temperatures for CV3s were estimated by Huss et al. (2006) on the basis of observations carried out by Huss & Lewis (1994a), Huss & Lewis (1994b) and Bonal et al. (2006) with the following temperatures: Leoville $\sim$250

°C; Vigarano, Mokoia, Kaba, Efremovka ∼300 - 400 °C, Grosnaja ∼ 500 °C, Axtell and Allende 550-600 °C. CH (ALH 85085-like), CB (Bencubbin-like) and CR (Renazzo-like) chondrites show very little evidence of thermal metamorphism. The CK group has both metamorphosed and un-metamorphosed members (Kallemeyn et al., 1991), but it has just a few petrologic type 3 samples which are not enough for a systematic study of the metamorphic properties (McSween, 1977). Most of the CI (Ivuna-like) and CM (Mighei-like) chondrites the effects of thermal processing (< 200 °C) are not very easily recognisable as it has been overprinted by severe aqueous alteration.

In oxidised CV and CO carbonaceous chondrites metasomatic processes also took place. In oxidised CVs metasomatism led to enrichments in alkalis (Na, K and Rb), halogens (Cl, I, Br) and in volatile elements (Mn, Fe, Cu, Zn,Cr, Au, Ga and Si) with alteration of the CAIs bulk composition showing evidence of phase replacement (with formation of phases such as nepheline, sodalite grossular, wollastonite hendebergite and ferroan spinel) happening at low temperatures (< 1000 K) (Brearley, 2003). Similar effects were also recorded in chondrules, with replacement of chondrule mesostasis and plagioclase mainly with nepheline and sodalite, and in the matrix (Brearley, 2003). Effects of metasomatism in COs are similar to those experienced by oxydised CVs. The most visible effects of metasomatism in COs are recorded in plagioclase rich chondrules and in primary anorthite in type I chondrules, which show replacement of the anorthyte with nepheline (Brearley, 2003; Tomeoka & Itoh, 2004).

Most CCs experienced some degree of aqueous alteration leading to the formation of secondary phyllosilicates, carbonates, sulphates, oxides and sulphides, although the process is more extensively recorded in the CI, CM and CR chondrites (Figure 1.5) (Brearley, 2003). Aqueous alteration could have happened in the nebula with high temperature condensates reacting with water vapor, or with anhydrous dust becoming hydrated in icy regions (Ciesla et al., 2003) or within the asteroidal parent bodies (Brearley, 2003; Zolensky et al., 2018), with the latter the favored model.

## 1.5 Ornans type Chondrites: A Petrological Overview

CO ("Ornans-like") chondrites are classified as CO3s, as they are relatively pristine CCs having undergone minimal aqueous alteration. The CO chondrites petrologic subtypes range from 3.0 to 3.8. and they can be defined as a metamorphic sequence since samples belonging to this meteorite group are chemically similar to each other (Ebel et al., 2016). COs experienced thermal metamorphism which led to the progressive equilibration of their mineral composition (McSween, 1977; Scott & Jones, 1990). Moreover, unlike other groups, the effects of thermal metamorphism on CO chondrites were not overprinted by aqueous alteration. Therefore they are an ideal group of samples for undertaking extensive studies about the effects of thermal metamorphism and asteroid parent body.

CO chondrites are mainly composed of olivine, low Ca-pyroxene, calcic plagioclase, melilite, spinel, kamacite, troilite, magnetite and sulphide and some other minor minerals (McSween, 1977; Krot et al., 2014b; Zolensky et al., 2018). The concentration of volatile elements and rare gases in CO3 chondrites can be correlated with the degree of metamorphism. Sodium is the only major element showing a substantial variation with different degrees of metamorphism; Na/K and Na/Si ratios increase with metamorphic grade. The carbon content in contrast is lower at higher petrologic subtype (McSween, 1977; Alexander et al., 2017). Ornans is more depleted in rare gases than the other CO chondrites (McSween, 1977) and this can be explained by the *Ornans paradox* as on the basis of its chemical properties it belongs at a higher petrologic subtype than on its petrographic properties. However, more recent studies demonstrated that bulk content in nobel gas cannot be used as a reliable indicator of metamorphic processes Bonal et al. (2007), and therefore the Ornans paradox does not exist.

COs are characterised by small chondrules, with average sizes of $\sim 150$ $\mu$m (Rubin, 1998) and abundance of about 51.3 vol % (Ebel et al., 2016). Type-I chondrules are the most abundant, mainly characterised by fosteritic olivine (Fo), contain kamacite and taenite metal nodules, have a spongy appearance (Hutchison, 2004). In Kainsaz, chondrule olivine phenocrysts reach up to Fa$>$ 5 mol% and into the type-II chondrule composition (Berlin et al., 2011). Type-II chondrules are also present in COs, they are

porphyritic FeO-rich olivine ($Fo_{52-88}$) and contain chromian hercynite in dark brown glass, but less abundant compared to type-I (Krot et al., 2014b; Zolensky et al., 2018). Most of the chondrules in COs are porphyritic ( $\sim 95\%$) (Scott & Krot, 2014), and they include porphyritic olivine-pyroxene (POP), porphyritic pyroxene (PP) and porphyritic olivine (PO); while the remaining 5% is constituted by nonporphyritic type chondrules such as barred olivine (BO), radial pyroxene (RP) and cryptocrystalline (C) (Scott & Krot, 2014). Tomeoka & Itoh (2004) described that, due to metasomatism, mesostasis in type-I chondrules of COs that underwent a weak heating process are characterised by glass and plagioclase, while in more heated samples they contained nepheline. Berlin et al. (2011) noticed that mesostasis in type-II chondrules is more $Al_2O_3$-rich, and had low $SiO_2$, $TiO_2$, $P_2O_5$ and S in comparison to mesostasis in CR and ungrouped ordinary chondrites (UOC) chondrules. Due to their grain size, chondrules are less affected by thermal metamorphism than the matrix, but their olivine and pyroxene still show enrichment in FeO with increasing temperatures (McSween, 1977). Overall, type-I and type-II chondrules give the biggest contribution in terms of coarse silicates in CO chondrites as they are the most abundant (Scott & Jones, 1990).

CAIs constitute about 2.3 vol% of the CO meteorites (Ebel et al., 2016), they have different compositions and they can be defined as melilite-rich, spinel-pyroxene and hibonite-rich CAIs (Zolensky et al., 2018). Melilite content in CAIs decreases with increasing petrologic subtype and is absent from CO3.6 onwards which is suspected to be related to secondary processes, such as metamorphism on the parent body (Russell et al., 1998; Huss et al., 2006). Unaltered melilite inclusions in CO3.0 do not show evidence of secondary alteration and they are Al-rich and contain Fe. With increasing metamorphic grade the outer part of melilite-rich inclusions frequently contain secondary nepheline, pyroxene and FeS. The amount of FeO in CAIs increases with the metamorphic grade (Russell et al., 1998). It is very common in COs to find CAIs rimmed with spinel surrounded by diopside. The amount of Fe in spinel increases until reaching the petrologic subtype 3.4 where the spinel contains about 50-60 mol% hercynite (Russell et al., 1998; Hutchison, 2004).

AOAs compose $\sim$3.5 vol% of CO chondrites, with an average size of ranging between 20 $\mu$m and $\sim$ 1 mm (Chizmadia et al., 2002), and their mineralogy is characterised

by olivine, anorthitic plagioclase, diopside, and opaques. All these phases increase with metamorphism with the exception of the opaques which show a reduction in their abundance. AOAs are among the first phases in COs to be affected by metamorphism because of their fine-grained nature. FeO content in AOAs is very low in CO3.2, while it shows a great variability in 3.3, 3.4 and 3.5 reflecting the Fe/Mg exchange with the matrix (Rubin, 1998). In petrologic subtypes 3.7 and 3.8 the constant FeO/MgO ratios show that there is an equilibration with the matrix (Chizmadia et al., 2002).

Another feature of CO chondrites are the so-called dark inclusions (DIs), which are present at 1 vol% and consist of fine-grained (up to 40 $\mu$m) aggregates of olivine, diopside, Fe, Ni-metal, Fe sulfides, nepheline and Ca phosphate (Itoh & Tomeoka, 2003). Itoh & Tomeoka (2003) suggest that they might have formed as consequence of aqueous alteration and subsequent dehydration of a CO-like precursor, but some of them are hypothesised to be fragments of chondrule pseudomorphs.

Metallic inclusions are a minor constituent of CO chondrites. McSween (1977) observed that taenite inclusions ($\gamma$Ni-Fe) have Ni-rich rims, while kamacite rims ($\alpha$Ni-Fe) are Ni poor, however their Ni content varies with degree of metamorphism, decreasing in taenite and increasing in kamacite. Based on the Fe-Ni phase diagram, this behaviour only occurs at temperatures below 450 °C. Therefore these metal inclusions only record the thermal response below 450 °C, nevertheless the petrological sequence of COs is maintained (McSween, 1977).

Matrix is another fundamental component of COs and it can often occures as interchondrule matrix, which is the focus of the present work, and as fine grained rims (FGRs). Interchondrules matrix in CO 3.0 chondrites is also very fine grained ($< 2\mu$m), and in the least equilibrated of the COs such as ALHA 77307 (not studied in this work) and DOM 08006 it is dominated by Fe-bearing amorphous silicates (Hutchison, 2004; Alexander et al., 2018) where olivine, pyroxene, oxides, sulphides and metal grains are set. The matrix is considered to be a reservoir of FeO, containing up to 25 - 30 wt% (McSween, 1977) which is supplied to inclusions by diffusion during thermal equilibration. Metamorphism also redistributes FeO, MgO and MnO, and its effects are more visible in fine-grained inclusions as they are the first ones to be affected by high temperatures. During metamorphism, the matrix of COs becomes depleted in

FeO and enriched in MgO and the high petrologic subtypes have matrix FeO/MgO ratios which are similar to those of the inclusions. The matrices of Kainsaz (3.2), Felix (3.3), Ornans (3.4) and Lancé (3.5) have a very similar FeO/MgO ratio to each other (McSween & Richardson, 1977). MnO redistribution shows a correlation with FeO in amoeboid inclusions, which suggests that these two elements were fractionated together in the divalent state, rather than FeO being produced *in situ* by metal oxidation as Mn is likely present as an oxide. FeO-rich olivines are not present in the matrix of CO3.0, while their presence in higher petrologic subtypes suggest their secondary origin due to the crystallisation of the amorphous silicate and mobilisation of Mg and Fe. Moreover, matrix in very primitive chondrites such as CO3.0 is very rich in S and its abundance decreases with increasing metamorphism due to its mobilisation towards chondrule interiors (Grossman & Brearley, 2005). Fine grained rims are not igneous features constituted by a mixture of crystalline (e.g. silicates, oxides, sulphised, Fe,Ni metal and carbonates), amorphous grains and carbonaceous matter with grainsize $<5$ $\mu$m as well as presolar grains (Haenecour et al., 2018). FGRs envelope the majority of chondrules and CAIs, and they can display a variable thickness Brearley (1993). Their origin is still matter of debate, but one of the most recent theories about their formation was proposed by Bland et al. (2011), suggesting that FGRs accreted in the solar nebula around free floating chondrules, for then being compacted as consequence of low-intensity shocks or low-pressure impacts.

Some CO chondrites are among the most pristine available to study, therefore their matrix is a very precious source of information for further understanding the formation of the Solar System and the mineralogy of the protoplanetary disk, indeed it contains very primitve materials such as amorphous silicates, organic matter (OM) and presolar grains. *Amorphous silicates* are one of the most abundant phases in primitive unequilibrated carbonaceous chondrites (Brearley, 1993; McAdam et al., 2018). Their presence is ubiquitous in the matrix of primitive chondrites, and their presence is interpreted as a sign of pristinity of meteoritic material, as they are very reactive to secondary processes (Abreu & Brearley, 2010; Le Guillou et al., 2015). It is hypothesised that Fe-Mg amorphous silicates are the precursor material to olivine and pyroxene in more processed materials (Le Guillou et al., 2015). Fe-Mg amorphous silicates are also the

first phase to hydrate and alter to a serpentinite/saponite phase during aqueous alteration (Le Guillou et al., 2015). Fe-Mg amorphous silicates are reported to be relatively abundant (15 - 20 vol% (Alexander et al., 2018)) in less equilibrated CO chondrites by Brearley (1990) and Buseck & Hua (1993). The grain size of amorphous silicates is challenging to constrain and they are subject to compaction and lithification which could have played a role in the modification of their sizes. It is estimated that the maximum size of amorphous silicate grains is $< 0.4$ $\mu$m (Pontoppidan & Brearley, 2010) and at the transmission electron microscope (TEM) they have the appearance of fluffy aggregates with irregular outlines. Amorphous silicates are thought to have formed and been processed during astrophysical processes (Nuth et al., 2005) that took place in different environments such as:

- *Interstellar medium*: the solar nebula formed from ISM materials, which contained less than 1 % crystalline silicates. The formation of amorphous silicates in the ISM is thought to be the result of both non-equilibrium condensation and exposure to high energy radiation environments.

- *Solar nebula*: amorphous silicates can form in a Fe-Mg-Si-O system by disequilibrium condensation upon cooling of material that was vaporised during chondrule formation (Nuth et al., 2005).

- *Parent body*: amorphous silicates can form by aqueous alteration or shock metamorphism, but this second option is very unlikely as the amorphisation would be heterogeneous throughout the sample (Nuth et al., 2005).

The most widely accepted hypothesis is that amorphous silicates present in matrices of primitive meteorites formed in the solar nebula as result of disequilibrium condensation processes (Scott & Krot, 2005; Nuth et al., 2005; Abreu & Brearley, 2010). Amorphous silicates in the CO chondrites have similar textures and compositions as the Glass with Embedded Metal and Sulphide (GEMS) grains found in primitive interplanetary dust particles (IDPs). GEMS have a rounded shape with an average diameter of less than 0.5 $\mu$m (Bradley, 2007; Min & Flynn, 2010; Bradley, 2013), and are characterised by a low-Fe, Mg silicate glass which embeds nano inclusions of kamacite and pyrrhotite

(Bradley, 2007; Henning & Meeus, 2009). GEMS can be isotopically anomalous showing non solar O-isotopic composition which would demonstrate their interstellar origin (Keller & Messenger, 2007). A recent study, from Ishii et al. (2018), proposed that GEMS formation happens in two stages of grain aggregation which are mediated by organic carbon. The first generation of GEMS grains is coated with organic carbon, while the second generation is enclosed within a low-density organic carbon matrix. Organic matter present within matrix of COs, changes its maturity in function of the degree of thermal metamorphism (Bonal et al., 2007) becoming more homogenised in high petrologic subtypes samples. Moreover, within the most primitive COs it is possible to find also presolar grains, which are high temperature minerals and amorphous assemblages that formed in circumstellar environments and stellar ejecta (Haenecour et al., 2018). Among all, presolar silicates are the most sensitive to heating and weathering and therefore they can be used to provide constraints on accretion and compaction history of meteorites (Floss & Stadermann, 2012). Presolar grains have been described within matrix and FGRs in the most primitive COs such as ALHA77307, DOM 08006 (Nittler et al., 2018) and LAP 031117 (Haenecour et al., 2018).

Within this study, there are two samples that are frequently mentioned, Acfer 094 (C2-Ungrouped) and ALHA77307 (CO3.0). Acfer 094 is classified as a C2-Ungrouped. It was found in Algeria in 1990 and it has a mass of 82 g. It is considered an unusual meteorite as it has similarities with COs and CMs. It is characterised by abundant chondrules with a mean diameter of $\sim$130 $\mu$m. About 77 % of the chondrules are described as POP (more abundant) and PO, with the composition of the olivine very variable but generally $Fo_{<95}$, while pyroxene composition is $Fs_{<2}$ (Newton et al., 1995). Fe, Ni metal is the most abundant opaque phase described, containing between 4 and 7 wt% in Ni. Matrix is composed by forsteritic olivine $Fo_{99}$ and pyroxene $Fs_{1-16}$ with a $\sim$100 nm grainsize, while coarser olivine inclusions have a composition ranging between $Fo_{70-40}$ (Newton et al., 1995). Moreover, the matrix of Acfer 094 contains abundant Fe-bearing amorphous silicates which have been described as completely oxidised (Hopp & Vollmer, 2018).

ALHA77307 is classified as a CO3.0 and it has a total mass of 181.3 g. It is one of the most unequilibrated COs available to study, and it presents minimal aqueous

and thermal alteration (Jones, 1992). Chondrules in ALHA77307 can be subdivided in type IA with average olivine composition of $Fo_{99.1}$ and low-Ca pyroxene composition of $Fs_{1.07}$, and type II chondrules with average olivine composition of $Fo_{77}$ (Scott & Jones, 1990). Matrix in ALHA77307 in present in the forms of interchondrules matrix and fine grained rims surrounding the majority of the chondrules Brearley (1993). Matrix and rims are constituted of Fe-bearing amorphous silicates, olivine (with three different chemistries and grainsize $Fo_{95-98}$, $Fo_{82-28}$,and $Fo_{34-32}$), pyroxene, magnetite, kamacite, pentlandite, pyrrhotite, anhydrite and phyllosilicates Brearley (1993). Fine grained rims have a variable thickness of 10 - 30 $\mu$m and the interface between them and the surrounding matrix is often characterised by a layer of magnetite and sulphides (Brearley, 1993).

## 1.6 Petrologic subtypes in COs: a review

CO chondrites are all classified as type 3s, however they experienced thermal metamorphism and define a metamorphic sequence from 3.0 to 3.9 (McSween, 1977). A number of different approaches have been used to define the metamorphic sequence and constrain the thermal history of the CO parent body.

Jones & Rubie (1991) applied olivine diffusion modelling to examine the *in situ* equilibration of chondrule-matrix olivines. Their model take into consideration the Fe-Mg interdiffusion taking place between chondrules and matrix during parent body metamorphism. Jones & Rubie (1991) inferred that peak metamorphic temperatures for a uniform accretion of $\sim$ 500 °C with cooling rates of 10, 1 and 0.1 °/Ma would produce CO3 chondrites with petrologic subtypes 3.0 (unequilibrated), 3.4 and 4 (equilibrated) respectively. Moreover, they estimated that the range of peak temperatures between unequilibrate and equilibrated subtypes is of about 100 °C.

Schwinger et al. (2016) reported that the zoning of type I and type II chondrule olivine in Kainsaz and Lancé is mainly influenced by solid state diffusion and that in type II chondrule olivine up to CO3.2 there is only a minor influence due to diffusion during thermal metamorphism. Schwinger et al. (2016) estimated maximum peak metamorphic temperatures in the range of 380 to 575 °C for different petrologic

subtypes. However, the peak temperatures estimated on the basis of the Fe-Mg zoning for type I chondrule olivine are not consistent with temperature estimated for type II chondrule olivine, suggesting that there might have been an additional contribution of solar nebular processes for type I condrule olivine prior to accretion into the parent body.

Another effective method for the assessment of low petrologic subtypes is the study of Cr diffusion in olivines, which was explored by Grossman & Brearley (2005). This study showed that Cr distribution in FeO-rich olivine systematically changes with nucleation of a Cr-rich phase in relation to thermal metamorphism between subtype 3.0 and 3.2; Cr exolves from the olivine forming Cr-rich coatings around the grains, leading to a complete separation of chromite by subtype 3.2.

Greenwood & Franchi (2004) investigated under which conditions thermal metamorphism took place by looking at the whole rock oxygen and carbon isotopic composition of both CO3 falls and finds. They reported that the C and O isotopic compositions of CO3 finds are highly influenced by terrestrial weathering. For CO3 falls they reported an increase in $\Delta^{17}$O values within increasing metamorphic grade for subtypes between 3.1 and 3.4, however this trend was not observed in the higher petrologic subtypes. Greenwood & Franchi (2004) concluded that the increase in $\Delta^{17}$O values was caused by the the formation of phyllosilicates and progressive loss of primary phases due to the presence of an aqueous fluid phase during metamorphism. The bulk C abundance $\delta^{13}$C value of CO3 falls decrease with increasing thermal metamorphism and is connected to the changes in the nature of organic components.

Cloutis et al. (2012) investigated the bulk properties of COs through reflectance infrared (IR) spectroscopy, in order to understand spectral properties of the CO type, develop correlations between spectra and composition as well as trying to gather information for the determination of CO parent bodies. They found that the reflectance spectra of COs are characterised by features in the 1 $\mu$m and 2 $\mu$m regions. The 1 $\mu$m region is related to Fe-bearing amorphous phases and Fe-poor olivine, while the 2 $\mu$m absorption feature, characteristic of COs of subtype 3.1 or higher, is related to $Fe^{2+}$.

Thermoluminescence (TL) analyses were carried out by Sears et al. (1991) and (Sears, 2016) who further demonstrate that CO3 chondrites represent a metamorphic

sequence, like ordinary chondrites, and can be subdivided in petrologic subtypes. However, they suggested that CO chondrites experienced lower metamorphic temperatures, with a peak temperature of about 600 °C corrisponding to a petrologic subtype 3.5 for an ordinary chondrite.

The effects of thermal metamorphism in can also be defined by studying CAIs which can be classified into three main types on the basis of their mineralogy: melilite rich, spinel-pyroxene and hibonite-hercynite. Russell et al. (1998) reported that in CO3 chondrites, the relative abundance of these inclusions changes as a function of thermal metamorphism, with melilite-rich inclusion decreasing with thermal metamorphism and absent in subtypes above 3.5. Russell et al. (1998) concluded that thermal metamorphism introduced Fe to CAIs, which is reflected by the enrichment in Fe of the spinel present in melilite-rich and in spinel-pyroxene inclusions.

Another sensitive indicator of metamorphism in CO chondrites is Fe-Ni metal which is particularly useful for distinguishing between low and high petrologic subtypes. Fe-Ni metal in COs occurs in chondrules as well as isolated grains within the matrix. Ni-rich metal in petrologic subtypes lower than 3.1 are enriched in Co relative to the kamacite ($<$ 7.5 wt% Ni) present in the chondrules, while in petrologic subtypes between 3.15 and 3.9 it contains less Co than kamacite (Kimura et al., 2008). Kimura et al. (2008) reported that the abundance of Ni-rich metal grains in chondrule decreases in relation to thermal metamorphism. Moreover, Krot et al. (2014b) used Fe-Ni metal inclusions for determining peak metamorphic temperatures and cooling rates in CO3s, concluding that for Warrenton (3.7) the lower limit for the peak metamorphic temperature is $\sim$500 °C while for Felix (3.3) is about $\sim$ 50 °C lower, assuming cooling rates respectively of 3 and 5 °C/Myr respectively. Krot et al. (2014b) also concluded that $^{26}$Al decay was the major source of heat in COs and suggested that the radius of the CO3 parent body was at least $\sim$50 km.

Fine grained amoeboid olivine aggregates (AOAs) are sensitive indicators of parent-body aqueous and thermal alteration. With increasing petrologic subtype the olivine transforms from forsteritic to ferroan composition ($Fo_{35-40}$), due to the $Fe^{2+}$ and $Mg^{2+}$ exchange forming diffusive halos around low-FeO cores. Chizmadia et al. (2002) proposed that these systematic changes in olivine composition could be used as tool for

improving the classification of CO3 chondrites, inferring that the changes in low petrologic subtypes were due to aqueous or hydrothermal fluids, while for subtypes ≥3.3 the elemental exchange mainly occurred without the aid of fluids.

Bonal et al. (2007) investigated the effects of thermal metamorphism on the organic matter (OM) in the matrix of CO chondrites using Raman spectroscopy. They determined that the most metamorphosed meteorites such as Warrenton and Isna experienced a peak temperature of $\sim$ 300 °C.

Imae & Nakamuta (2018) carried out *in situ* X-ray diffraction (XRD) of polished thin sections of CO3 chondrites of different petrologic subtypes. They reported that the olivine (130) peaks change in relation to thermal metamorphism, with subtypes up to 3.5 showing doublet peaks due to the coexistence of ferroan olivines and magnesian olivines, while in subtypes from 3.6 onward they display just a single peak, position of which is consistent with ferroan olivine. Moreover, Imae & Nakamuta (2018) observed the presence of metastable primordial phases such as amorphous silicates and martensite. Being amorphous silicates are more resistant to thermal metamorphism than martensite, Imae & Nakamuta (2018) estimated metamorphic temperatures in the parent body to be around 325 - 637 °C on the basis of diffusion in olivine and Fe-Ni metal, cooling time of $10^6$ - $10^8$ yr using an onion shell model.

## 1.7 Aims and objectives

In this project, I study a set of highly primitive (unaltered) CO3 meteorites investigating the textural and chemical changes affecting the interchondrule matrix mineralogy and the organic matter of primitive CO chondrites. These aspects are important to investigate as they will allow to further comprehend parent body metamorphic processes for understanding the origin of dust and its components. The aims of this research are:

- improve the understanding of the mineralogical and textural changes affecting the matrix material from petrologic subtype 3.0 to 3.8, looking at the mineralogical variations of bulk samples through XRD, with particular focus on the changes in olivine chemistry, as well as through *in situ* analysis of matrix areas of down to nanometer scale;

- improve the understanding of the redox conditions in the disk and in the asteroidal parent body;
- investigate the distribution of the amorphous silicates and organic matter within the matrix and constrain their response to metamorphism;
- apply of advanced techniques such as XANES for the analysis of chondrite matrix material.

To meet these aims, I will study the matrix of CO chondrites using scanning electron microscopy (SEM), transmission electron microscopy (TEM) and synchrotron based scanning transmission X-ray microscopy (STXM). These analytical techniques are capable of providing the high spatial resolution and high sensitivity required to study meteorite matrix *in situ*. These analysis are supported by the investigation of changes that affected the bulk properties of the samples through the application XRD.

# Chapter 2

# Samples and Methodology

The CO chondrite in this study provide a systematic suite of samples that are ideal for studying changes in mineralogy and texture induced by thermal metamorphism, and by inference for studying parent body processes. I selected CO chondrites from across the petrologic range and characterised them from the bulk to the grain scale.

## 2.1 Samples

In this study I characterise 12 CO3 carbonaceous chondrites (Table 2.1) from across the entire petrologic range (3.0 – 3.8). Nine of the samples were sourced from the meteorite collection of the Natural History Museum in London and three were from the Astromaterials Acquisition and Curation Office at NASA.

In this study I am looking both at *falls*, meteorites associated with an observed fireball event, and *finds*, meteorites not connected to an observed fall (Weisberg et al., 2006). It is fundamental to preserve these materials as intact as possible and to minimize their weathering, which in tropical areas is particularly fast. However, if the climate is relatively dry, the weathering is slowed down and meteorites can be preserved for hundreds of years (Bland et al., 2006). In order to describe the degree of weathering experienced by the samples the Meteorite Working Group at the NASA Johnson Space Center in Houston created weathering categories for Antarctic finds. The weathering for Antarctic meteorites is defined with *A*: minor rustiness, with minor rust halos on metal particles and rust stains along fractures; *B*: moderate rustiness, minor rust halos on metal particles and extensive rust stains on internal fractures;

| Sample name | Sample number | Petrologic Subtype | Fall/Find | Weathering | Collection Location |
|---|---|---|---|---|---|
| Colony | BM 1983, M45 (P4485) | CO3.0 | Find | high | NHM London |
| DOM 08006 | DOM 08006 (69) | CO3.0 | Find | A/B | NASA |
| NWA 7892 | BM 2016, M5 (P21555) | CO3.05 | Find | n.a. | NHM London |
| MIL 090010 | | CO3.1 | Find | A/B | NASA |
| Kainsaz | BM 1999, M63 (P9527) | CO3.2 | Fall | n.a | NHM London |
| Felix | BM 1919,89 (P4814) | CO3.3 | Fall | n.a | NHM London |
| Ornans | BM 1985, M149 (P13343) | CO3.4 | Fall | n.a | NHM London |
| Lancé | BM 1985, M153 (P4436) | CO3.5 | Fall | n.a | NHM London |
| ALHA77003 | ALHA77003(141) | CO3.6 | Find | Ae | NASA |
| Moss | BM 2011, M1 | CO3.6 | Fall | n.a | NHM London |
| Warrenton | BM 53290 | CO3.7 | Fall | n.a | NHM London |
| Isna | | CO3.8 | Find | n.a | NHM London |

Table 2.1: *Summary of the CO chondrite meteorites analysed in the present study. The subtype classification used refers to Chizmadia et al. (2002).*

*C*: severe rustiness, metal particles have been severely stained by rust; *E*: evaporite minerals are visible to the naked eye.

Here I summarise the mineralogical and petrographic descriptions of each meteorite available in the literature (Figures 2.1 and 2.2).

### 2.1.1 Colony, CO3.0

The Colony meteorite was found in Oklahoma (USA) in 1975 (Graham, 1984), with a total recovered mass of 3,912 g. It is classified as 3.0, making it one of the least equilibrated CO chondrites (Rubin et al., 1985). However, it is highly weathered and is visibly rusty in hand specimen. Colony is a breccia, as was reported by Rubin et al. (1985), with angular clasts of chondritic material with different colour from the host matrix and very defined boundaries. The clasts contains chondrules and AOAs and the matrix appears more transparent.

*Mineralogy*: Olivine and low-Ca pyroxene are both contained in chondrules and matrix, kamacite (low-Ni and Co, high-Cr), including one observed grain of Co-rich kamacite, and AOAs with low FeO and MnO (Rubin et al., 1985). Also identified in Colony were ghelenite, spinel, forsterite, clinoenstatite, anorthite, troilite, isolated grains of metallic Fe, Ni and rare grains of taenite and Ni-rich taenite (Rubin et al., 1985).

*Chondrules and Refractory inclusions*: Chondrules in Colony have been described in detail by McSween (1977) and Rubin et al. (1985). They are well defined, with

| **Sample name and petro-logic subtype** | **Mineralogy** | **Chondrules and refractory inclusions** | **Matrix** |
|---|---|---|---|
| Colony<br>CO3.0 | Olivine, low-Ca pyroxene, kamacite, ghelenite, spinel, clinoenstatite, anorthite, troilite | *Chondrules*<br>Type I: porphyritic olivine $Fo_{(99.2-99.4)}$;<br>Type II: olivine $Fo_{(60-75)}$;<br>*CAIs*<br>Spinel-pyroxene (~98%) and melilite-rich (~2%). | Severely weathered, rich in FeO and $Cr_2O_3$, poor in MgO, MnO, $Na_2O$, $K_2O$, CaO and $SO_3$. |
| DOM 08006<br>CO3.0 | Olivine, pyroxene, sulphide, metal, magnetite, phyllosilicate and Fe-bearing amorphous silicates. | *Chondrules*<br>73% are FeO-poor; Type I: forsteritic olivine $Fo_{(100-99)}$, low-Ca $(En_{(96-99)}Fs_{(1-2)})$ $Wo_{(1-3)}$ high-Ca $Wo_{(15-45)}$ pyroxenes.<br>*CAIs*<br>Melilite-rich (80–86 %) and spinel-pyroxene (<6 %), pyroxene-anorthite-rich (~6 %), hibonite-bearing (<4.8%). | Highly unequilibrated amorphous silicates, olivine, pyroxene, metal and sulfides. |
| NWA 7892<br>CO3.05 | | *Chondrules*<br>Random olivine composition $Fo_{(99.7-43.2)}$, with chondrule ferroan olivine mean $Fo_{(69.3)}$, low-Ca pyroxene chondrules $Fs_{(0.8-41.3)}$.<br>*CAIs*<br>Spinel-pyroxene ( ~ 98 %) and melilite-rich (2 %). | |
| MIL 090010<br>CO3.1 | Olivine, pyroxene, sulphide, metal, magnetite, phyllosilicate and Fe-bearing amorphous silicates. | *Chondrules*<br>Olivine composition in the range $Fo_{(100-24)}$, pyroxene composition of $Fs_{(1-15)}$ and $Wo_{(0-6)}$.<br>*CAIs*<br>Melilite-rich (80–86%) and spinel-pyroxene (<6%), pyroxene-anorthite-rich (6%), hibonite-bearing (<4.8%). | Dark fine grained. |

Figure 2.1: *Summary table of samples analysed in the present work from CO3.0 to CO3.2.*

| **Sample name and petrologic subtype** | **Mineralogy** | **Chondrules and refractory inclusions** | **Matrix** |
|---|---|---|---|
| Kainsaz<br>CO3.2 | Silicates, Fe-Ni-metal and sulfides. | *Chondrules*<br>Porphyritic olivine-pyroxene chondrules (63%), with olivine and olivine-pyroxene chondrule composition of $Fo_{(99.1-88.5)}$ and $Fs_{(1.2-7.3)}$. $Cr_2O_3$ in the Fe-rich olivine is of about 0.1% | Fine grained olivines $Fo_{(80-50)}$ and pyroxene, such as enstatite and hedenbergite. |
| Felix<br>CO3.3 | Olivine, pyroxene, sulphide, metal, magnetite and chromite. | *Chondrules*<br>POP texture, Mg-rich olivine $Fo_{(99.3-78}$ and pyroxene $Wo_{(0.6-2.8)}En_{(99-91.4)}Fs_{(0.4-5.8)}$, some poikilitically enclosed by twinned clinoenstatite and more fayalitic $Fo_{(75)}$.<br>*CAIs*<br>Mainly melilite with Ti, Al-rich pyroxene and abundant spinel. | Average FeO / (FeO + MgO) ratio of 0.64. |
| Ornans<br>CO3.4 | Olivine, phyllosilicate, high-Ni taenite. | *Chondrules*<br>Type I $Fo_{(98-93)}$ and type II $Fo_{(74-58)}$. | |
| Lancé<br>CO3.5 | | *Chondrules*<br>Olivine $Fo_{(90-50)}$ and average composition of $Fo_{(79)}$. | Fine grained olivine $Fo_{(60-50)}$, minor phyllosilicates with very fine serpentine and saponite.<br>Average FeO / (FeO + MgO) ratio is 0.64. |
| ALHA77003<br>CO3.6 | Chondrules olivine $Fo_{(96-52)}$ w. a mean of $Fo_{(78)}$, pyroxene $Fs_{(2-25)}$ with a mean of $Fs_{(14)}$, average CaO content of 1%. | *Chondrules*<br>Type I: $Fo_{(88-84)}$; Type II: $Fo_{(64-58)}$. | Mixture of olivine $Fo_{(65-55)}$, sulfides, Fe-Ni metal, Fe oxides and small amounts of nepheline, spinel and high-Ca pyroxene. Average FeO / (FeO + MgO) is 0.63. |
| Moss<br>CO3.6 | Olivine, pyroxene, troilite and kamacite. | *Chondrules*<br>Olivine average composition of $Fo_{(80)}$. | Mildly recrystallized, sulfur-poor and olivine with a fayalitic composition |
| Warrenton<br>CO3.7 | | *Chondrules*<br>Type I average composition of $Fo_{(82)}$;<br>Type II average composition of $Fo_{(69)}$. | Fine-grained Fe-rich olivines $Fo_{(55-50)}$, taenite, plus poorly crystalline ferric oxide. Average FeO / (FeO + MgO) ratio is 0.54. |
| Isna<br>CO3.8 | Olivine $Fo_{(39)}$, pyroxene (mostly clinoenstatite), kamacite and taenite. | Chondrules<br>Type I $Fo_{(90-65)}$, type II $Fo_{(100-62)}$. | |

Figure 2.2: *Summary table of samples analysed in the present work from CO3.0 to CO3.2.*

the most abundant types being: unrecrystallised chondrules, porphyritic chondrules with olivine-pyroxene, barred olivine, cryptocrystalline and the very rare types such as radial pyroxene and granular olivine chondrules. The majority of the type I porphyritic chondrules in Colony are rich in metal (10-25 vol% metallic Fe-Ni) (McSween, 1977; Rubin et al., 1985) and have a uniform composition in olivine ($Fo_{99.2-99.4}$). In comparison, the composition of type II chondrules are more heterogeneous ($Fo_{60-75}$) (Scott & Jones, 1990). The abundance of CAIs is about 1% (Russell et al., 1998), with the majority of the CAIs containing spinel-pyroxene (∼98%) and just ∼2 % are melilite-rich (Zhang et al., 2020).

*Matrix*: The matrix of Colony constitutes about 29 vol% of the sample, is very fine grained, opaque, and appears unrecrystallised (McSween & Richardson, 1977; Rubin et al., 1985). The matrix is rich in FeO and $Cr_2O_3$, and poor in MgO, MnO, $Na_2O$, $K_2O$, CaO and $SO_3$ (McSween & Richardson, 1977; Rubin et al., 1985). The severe weathering of the sample might be responsible for the low abundance of $Na_2O$ and FeS (Rubin et al., 1985).

### 2.1.2 Dominion Range 08006, CO3.0

Dominion Range 08006 (DOM 08006) is considered to be one of the most pristine CO3.0 chondrites. It was found in Antarctica in 2008 with a total mass of 668 g and its weathering grade is A/B (Weisberg et al., 2010).

*Mineralogy*: The bulk modal mineralogy of DOM 08006 was reported by Alexander et al. (2018) as olivine 51 vol%, pyroxene 22 vol%, sulphide 3 vol%, metal 1 vol%, magnetite 6 vol%, phyllosilicate 2 vol% and Fe bearing amorphous silicates 15 vol%. Magnetite, sulfide and metal are mainly seen along chondrule exteriors or within chondrule inclusions. Metal grains in DOM 08006 (Davidson et al., 2014) have carbide inclusions similar to CO3.0, ALHA 77307 (Scott & Jones, 1990).

*Chondrules and Refractory inclusions*: DOM 08006 contains chondrules with an average diameter of 133 $\mu$m (Davidson et al., 2019). Over 73% of the chondrules are FeO-poor type I, which mainly consist of forsteritic olivine ($Fo_{100-99}$) and minor mounts of low-Ca ($En_{96-99}Fs_{1-2}Wo_{1-3}$) and high-Ca pyroxenes ($Wo_{15-45}$) (Davidson et al., 2019). Ferroan olivine in chondrules and in olivine fragment inclusions show very

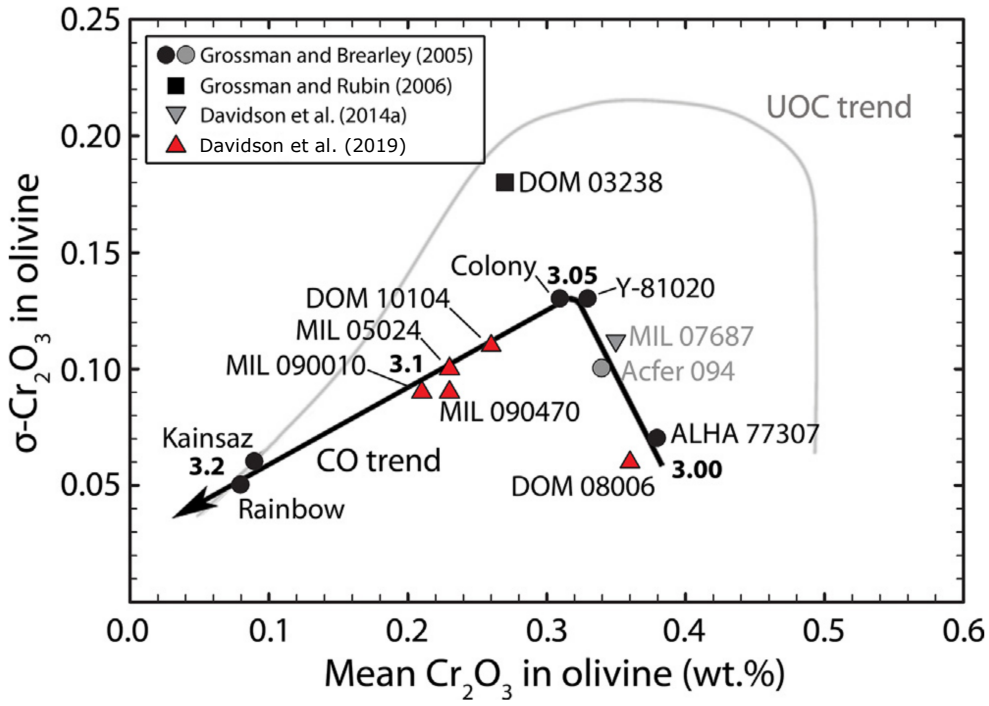


Figure 2.3: *Plot of the standard deviation ($\sigma$) versus the mean of the $Cr_2O_3$ content (weight percent) of ferroan olivine in CO3 chondrites, including Colony (CO3.0), DOM 08006 (CO3.6), MIL 090010 (CO3.1), Kainsaz (CO3.2) after Davidson et al. (2019).*

high $Cr_2O_3$ contents (Figure 2.3) which indicates that the sample is one of the most unequilibrated CO chondrites, if not the most primitive (Davidson et al., 2019). CAIs in DOM 08006 were described by Simon & Grossman (2015) and Zhang et al. (2020), with melilite-rich and spinel-pyroxene CAIs making up most of the CAIs population with abundances of 80-86 % and <6 % respectively. Pyroxene-anorthite-rich CAIs were also observed (∼6 %) as well as rare hibonite-bearing (<4.8 %) CAIs (Zhang et al., 2020).

*Matrix*: The matrix of DOM 08006 is dominated by highly unequilibrated amorphous silicates, olivine, pyroxene, metal and sulfides (pyrrothite and pentlandite) (Stroud et al., 2013; Davidson et al., 2014). The presence of Fe-(oxy)hydroxide needles in the matrix of DOM 08006 indicates very minor aqueous alteration that may have occurred on either the asteroid parent body or during its residence in Antarctica (Stroud et al., 2013; Krot et al., 2017; Davidson et al., 2014). Presolar grain abundances in the matrix of DOM 08006 (∼240 ppm) were reported to be higher than those in other primitive samples such as Acfer 094 and ALHA 77307 (Nittler et al., 2013; Haenecour et al., 2018; Nittler et al., 2018; Seifert et al., 2018). Moreover, the D/H and $^{15}N/^{14}N$

ratios are higher than in ALHA77307 which is an indicator that the matrix of DOM 08006 is rich in primitive organic matter (Davidson et al., 2014). XANES spectral features of IOM in DOM 08006 are typical of low level metamorphism (De Gregorio et al., 2015a).

### 2.1.3 Northwest Africa 7892, CO3.05

Northwest Africa 7892 (NWA 7892) was found in Morocco in 2012 with a total mass of 346 g (Ruzicka et al., 2015). There are no detailed reports of the mineralogy of NWA 7892 in the literature, however, the Meteoritical Bulletin does describe some aspects of the chondrules, while Zhang et al. (2020) described the CAIs.

*Chondrules and Refractory inclusions*: NWA 7892 has chondrules of various types such as porphyritic pyroxene, porphyritic olivine-pyroxene and porphyritic olivine. The chondrule size is between 50 and 300 $\mu$m. Irregular shaped and fragmented chondrules are also common (Ruzicka et al., 2015). Random chondrule olivine composition ranges between $Fo_{99.7-43.2}$, chondrule ferroan olivine mean $Fo_{69.3}$, low-Ca pyroxene chondrules have a composition in the range of $Fs_{0.8-41.3}$ (Ruzicka et al., 2015). The abundance of $Cr_2O_3$ in the Fe-rich olivine is about 0.39 wt% (Ruzicka et al., 2015), which is higher than in the most primitive COs such as ALHA 77307 and DOM 08006, indicating that NWA 7892 is a CO3.05. The majority of the CAIs are classified as spinel-pyroxene ($\sim$98 %) and just $\sim$2 % are melilite-rich (Zhang et al., 2020).

### 2.1.4 Miller Range 090010, CO3.1

Miller Range 090010 (MIL 090010) is classified as CO3.1 with a total mass of 2.49 kg. It was recovered in Antarctica in 2009 and its weathering grade is A/B (Ruzicka et al., 2015). Also, MIL 090010 is part of the MIL 07531 pairing group (Ruzicka et al., 2015).

*Mineralogy*: The modal mineralogy of MIL 090010 was reported by Alexander et al. (2018) as olivine 44 vol%, pyroxene 23 vol%, sulphide 2 vol%, metal 1 vol%, magnetite 7 vol%, phyllosilicate 1 vol% and Fe bearing amorphous silicates 21 vol%.

*Chondrules and Refractory inclusions*: The sample contains abundant small chondrules (up to 1.3 mm), with olivine composition in the range $Fo_{100-24}$, and a pyroxene composition of $Fs_{1-15}$ and $Wo_{0-5}$ (Ruzicka et al., 2015). CAIs are quite abundant

and they are up to 1 mm in size. Zhang et al. (2020) observed, like in DOM 08006, that melilite-rich and spinel-pyroxene CAI make up most of the CAIs population with abundances of 80-86 % and <6 %, respectively. Pyroxene-anorthite-rich CAIs were also observed (∼6 %) as well as rare hibonite-bearing (<4.8 %) CAIs (Zhang et al., 2020). AOAs are present up to 1 mm size as well as dark inclusions.

*Matrix*: Matrix in MIL 090010 has been reported as fine grained dark matrix (Ruzicka et al., 2015), but no further descriptions are available.

### 2.1.5 Kainsaz, CO3.2

Kainsaz was observed to fall in Russia in 1937 and has a recovered mass of 200 kg. Classified as a CO3.2, it is the least metamorphosed CO chondrite fall.

*Mineralogy*: Rubin et al. (1985) estimated that Kainsaz contains 89 vol% of silicates, 7 vol% of Fe-Ni-metal and about 4 vol% of sulfides.

*Chondrules and Refractory inclusions*: Porphyritic olivine-pyroxene chondrules are the most abundant (63 %) (Ebel et al., 2016), with olivine and olivine-pyroxene chondrule composition of $Fo_{99.1-88.5}$ and $Fs_{1.2-7.3}$. The abundance of $Cr_2O_3$ in the Fe-rich olivine is of about 0.1 wt% (Grossman & Brearley, 2005) meaning that the Cr exsolution in ferroan olivine is more advanced than in lower petrologic subtypes and therefore it was exposed to higher metamorphic temperatures (Figure 2.3). The CAI abundance is about 0.7 % (Russell et al., 1998). AOA abundance is ∼4.4% (Ebel et al., 2016), with angular or fragmented shapes (Chizmadia et al., 2002), and they have very low FeO concentrations (McSween, 1977).

*Matrix and fine-grained rims*: The matrix in Kainsaz was described as fresh and unaltered (Ahrens et al., 1973). It represents about 30 vol% of the sample, is heterogeneous, and consists of fine grained olivines ($Fo_{80-50}$) and pyroxene, such as enstatite and hedenbergite (Keller & Buseck, 1990; Alexander et al., 2007b), with an average FeO/(FeO + MgO) of 0.64 (Sears et al., 1991). The olivine composition in the fine grained rims is $Fo_{52-28}$ (Brearley, 1996).

### 2.1.6 Felix, CO3.3

Felix fell in the United States in 1900 and has a total mass of 3.2 kg. It is classified as a CO3.3 chondrite.

*Mineralogy*: The modal mineralogy of Felix was reported by Alexander et al. (2018) as: olivine 56 vol%, pyroxene 27 vol%, sulphide 3 vol%, metal 2 vol%, magnetite 3 vol% and chromite 1 vol%.

*Chondrules and Refractory inclusions*: The majority of chondrules show porphyritic texture with with olivine and/or pyroxene, the majority of the olivine is Mg-rich with composition in the range $Fo_{99.3-78}$ and pyroxene composition $Wo_{0.6-2.8}$ $En_{99-91.4}$ $Fs_{0.4-5.8}$, but some are poikilitically enclosed by twinned clinoenstatite and more fayalitic with an average composition of $Fo_{75}$ (Misawa & Nakamura, 1988). The CAIs abundance is about 1.5% (Russell et al., 1998), and they mainly constitute of melilite with Ti, Al-rich pyroxene and abundant spinel (Misawa & Nakamura, 1988).

*Matrix*: The matrix contains about 25.7% Fe (Wood, 1967), and has an average FeO/(FeO + MgO) ratio of 0.64 (Sears et al., 1991).

### 2.1.7 Ornans, CO3.4

Ornans was observed to fall in France in 1868 and has a total recovered mass of 6 kg. It is classified as CO 3.4 and it is the type specimen for the CO chondrites.

*Mineralogy*: Ornans shows the presence of olivine, phyllosilicate with a layer spacing of serpentine (Kerridge, 1964) and also contains high-Ni taenite instead of kamacite which is not common in other COs (McSween, 1977).

*Chondrules and Refractory inclusions*: Ornans contains both type I and type II chondrules with olivine compositions of $Fo_{98-93}$ and $Fo_{74-58}$, respectively (Scott & Jones, 1990). The abundance of CAIs is less than 1% (Russell et al., 1998).

*Matrix and fine-grained rims*: Rubin & Wasson (1988) described the matrix of Ornans as being composed of 81 % olivine ($Fo_{62}$), 10% quartz, 4% anorthite, 3% nepheline and 2% dicalcium silicate. The FeO/(FeO + MgO) ratio is 0.66 (Sears et al., 1991). Olivine in fine-grained chondrule rims have a variable composition of $Fo_{52-40}$ (Brearley, 1996).

### 2.1.8 Lancé, CO3.5

Lancé was observed to fall in France in 1872 and has a total recovered mass of 51.7 kg. It is classified as a CO3.5 chondrite.

*Chondrules and Refractory inclusions*: The olivine composition ranges from $Fo_{90}$ to $Fo_{50}$ and an average composition of $Fo_{79}$ (Sears et al., 1991). Type IA chondrules have a $Fo_{98-89}$ composition, while type II chondrules have a mean composition of $Fo_{64}$ (Scott & Jones, 1990). The CAI abundance is about 1% (Russell et al., 1998). An unusual ultrarefractory CAI rich in hibonite-hercynite was described by Fahey et al. (1994).

*Matrix*: Mainly composed of fine grained olivine $Fo_{60-50}$, minor phyllosilicates with very fine serpentine and saponite (Brearley, 1993) resulting from the weathering of the fine-grained olivine, and a $Fe^{3+}$-bearing phase such as ferrihydrite (Keller & Buseck, 1990). The average FeO/(FeO + MgO) ratio is 0.64 (Sears et al., 1991).

### 2.1.9 Allan Hills 77003, CO3.6

Allan Hills 77003 (ALHA77003) was found in Antarctica in 1977, and a total mass of 780 g was recovered (Grossman, 1994). It is classified as CO3.6 chondrite.

*Mineralogy*: Olivine and pyroxene are highly variable in composition; olivine ranges from $Fo_{96}$ to $Fo_{52}$ with a mean of $Fo_{78}$, while the pyroxene ranges from $Fs_2$ to $Fs_{25}$, with a mean of $Fs_{14}$ and an average CaO content of 1% (Grossman, 1994).

*Chondrules and Refractory inclusions*: Chondrules are usually between 0.1 and 0.6 mm in diameter, and commonly occur as granular aggregates of olivine and as polysynthetically twinned clinopyroxene; sometimes they contain glass between the olivine and the pyroxene (Grossman, 1994). Type IA chondrules have a composition of $Fo_{88-84}$, while type II chondrules have a composition of $Fo_{64-58}$ (Scott & Jones, 1990). The abundance of CAIs is estimated to be about 0.92% (Russell et al., 1998).

*Matrix*: The matrix contains a mixture of olivine $Fo_{65-55}$, sulfides, Fe-Ni metal, Fe oxides and small amounts of nepheline, spinel and high-Ca pyroxene (Ikeda, 1982; Housley, 1984). The average FeO/(FeO + MgO) is 0.63 (Sears et al., 1991).

### 2.1.10 Moss, CO3.6

Moss was observed to fall in Norway in 2006, and the total recovered mass is 3.76 kg (Connolly Jr. et al., 2007). It is classified as a CO3.6 chondrite.

*Mineralogy*: The main components in Moss are olivine, pyroxene, troilite and kamacite (Bilet & Roaldset, 2014).

*Chondrules and Refractory inclusions*: Moss was described by Greenwood et al. (2007) and Bilet & Roaldset (2014). Chondrules are smaller than 200 $\mu$m in size, with olivine grains with an average composition of $Fo_{80}$. Refractory inclusions contain spinel, Ca-pyroxene, nepheline and ilmenite. The AOAs contain relic cores of forsterite, but most of the olivine is converted into more Fe-rich components.

*Matrix*: The matrix is mildly recrystallized, sulfur-poor and olivine with a fayalitic composition (Bilet & Roaldset, 2014).

### 2.1.11 Warrenton, CO3.7

Warrenton was observed to fall in 1877 in the United States, and has total recovered mass of 1600 g. It is classified as a CO3.7 chondrite.

*Chondrules and Refractory inclusions*: Scott & Jones (1990) found that type IA chondrules have an average composition of $Fo_{82}$, while type II chondrules have an average composition of $Fo_{69}$. The CAI abundance is about 1% Russell et al. (1998).

*Matrix and fine-grained rims*: The matrix is composed of fine-grained Fe-rich olivines with a composition range of $Fo_{55-50}$, taenite, plus poorly crystalline ferric oxide leading Keller & Buseck (1990) to suggest that the matrix underwent some degree of oxidation. The FeO/(FeO + MgO) ratio is 0.54 (Sears et al., 1991). Brearley (1996) found that the composition of olivine in fine-grained chondrule rims ranged between $Fo_{54}$ and $Fo_{64}$

### 2.1.12 Isna, CO3.8

Isna was observed to fall in Egypt in 1970, and the total mass recovered is 23 kg (Clarke, 1975). It is classified as a CO3.8 chondrite.

*Mineralogy*: The olivine composition is about $Fo_{59}$. Pyroxene inclusions are mostly clinoenstatite, while kamacite and taenite are also present (Methot et al., 1975), with shock-modified textures, due to recrystallisation, fracturing and melting (Methot et al., 1975).

*Chondrules and Refractory inclusions*: Type IA chondrules have very heterogeneous compositions ($Fo_{90-65}$), as do type II chondrules with a composition of $Fo_{100-62}$ (Scott & Jones, 1990). The abundance of CAIs is 1.4% (Russell et al., 1998).

*Fine-grained rims*: Frequently, fine grained rims are present around the chondrules (Methot et al., 1975).

## 2.2 Bulk Analyses

X-ray radiation, or light, has wavelengths in the range of 0.01 to 10 nm and energies in the range of 100 eV to 100 KeV. Depending upon their energy they can be divided into hard ($>$ 5 keV) and soft ($<$ 5 keV) X-rays.

### 2.2.1 X-ray powder diffraction

X-ray powder diffraction (XRD) is a useful technique for identifing compounds by their diffraction patterns. I characterised the mineralogy of CO chondrites using two XRD instruments at the Natural History Museum in London. High resolution XRD was used to identify the minerals and monitor peak profiles, and position sensitive detector (PSD) XRD was used to determine the bulk modal mineralogy.

#### High resolution X-ray powder diffraction

The analyses were carried out using a Panalytical X'Pert Pro MPD Alpha 1 with a Bragg-Brentano geometry in reflection mode. The instrument is equipped with a Co X-ray tube (40 kV and 40 mA, Co-K$\alpha$ radiation, wavelength of 1.79 Å) and a X' Celerator RTMS (Real Time Multiple Strip) detector. Approximately 50 mg chips of each meteorite sample were ground using an agate mortar and pestle to a grain size of $\leq$ 25 $\mu$m to minimise potential grain size artifacts. Powders produced were also used for PSD-XRD measurements. For each meteorite $\sim$ 1-2 mg of powder was suspended in

three drops of acetone in an agate mortar. With the aid of a pipette a couple of drops of the suspension were then placed on a zero background silicon disk. Once the acetone had evaporated, it was estimated that 0.5 mg of powder was deposited as a thin smear on the silicon disk. At this point the sample was transferred to the instrument and XRD patterns were collected for 23 hours, with a scan range from 5 to 90 degrees 2Θ and a step size 0.02°. The instrument was calibrated using $LaB_6$, a cubic phase with diffraction peaks evenly spaced across the 2Θ range. The diffraction patterns were processed using X'Pert HighScore Plus and WinXPow software with mineral phases in the meteorites identified from their characteristic XRD patterns through comparison of peak position and intensity to reference patterns in the ICDD PDF 2 2004 database.

### Position sensitive detector X-ray diffraction

PSD-XRD analyses were performed on meteorite samples and mineral standards using an Enraf-Nonius (590) PDS 120 equipped with a curved position sensitive INEL 120 detector (Figure 2.4) in a fixed geometry that collects diffracted X-rays from 0 - 120 degrees 2Θ simultaneously. For PSD-XRD analyses approximately 50 mg chips of meteorites were powdered (grain size $\leq$ 25 $\mu$m) using an agate mortar and pestle. Both the standards and the meteorite powders were loaded into a sample well using the sharp edge of a spatula to create a high degree of randomness in crystal orientation and minimise the effect of preferred crystal alignments (Cressey & Schofield, 1996; Batchelder & Cressey, 1998). The only moving part during the analysis is the rotating sample holder, and consequently measurements of samples and standards are collected under identical conditions.

Meteorites and mineral standards were analysed using Cu K$\alpha_1$ radiation (wavelength 1.54059 Å) which was selected with a Ge 111 crystal monochromator. The size of the X-ray beam on the samples was restricted using post-monochromator slits to 0.24 x 2.00 mm. The instrument was calibrated using Ag-Behenate as an external standard for low angles and Si powder for high angles.

Following methods previously developed for the analysis of carbonaceous chondrites (Howard et al., 2009, 2010, 2011; King et al., 2015; King et al., 2017, 2019), each sample was measured for 16 hours in order to obtain a good signal-to-noise ratio. In order to

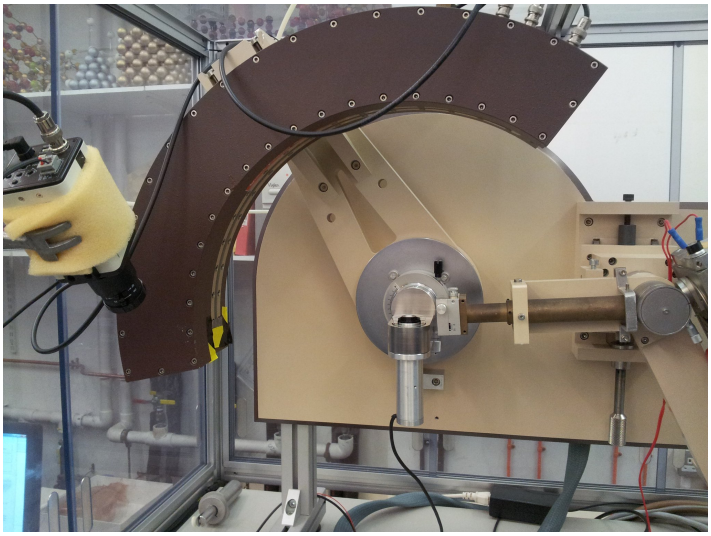

Figure 2.4: *Enraf-Nonius PSD 120 equipped with a INEL 120°curved position sensitive detector (PSD).*

quantify the modal mineralogy for each meteorite sample, powders of pure standards for each mineralogical phase identified with the scanning XRD were analysed for 30 minutes. Differences in the flux of the incident beam and the consistency of the packing were monitored throughout the experiment by analysing a polished Fe-metal block and a non-crystalline standard of Fe-(oxy)hydroxide, respectively.

Quantification of mineral abundances in the meteorites used a whole-pattern stripping procedure which was developed and described by Cressey & Schofield (1996), Batchelder & Cressey (1998) and Schofield et al. (2002) and it has been used to measure mineral abundances in >50 carbonaceous chondrites from several different classification groups.

Data were processed according to the following steps:

- Diffraction patterns of each mineral standard were scaled to the same measurement time as the meteorite sample (e.g. by 32 for a 16 hour measurement).
- The pattern of the mineral standard was reduced by a fit factor until its intensity matched that of the meteorite sample. Then, the pattern of the mineral standard was subtracted from the meteorite pattern, leaving a residual pattern (Figures 1 to 12, Appendix C).
- The process was repeated for each mineral standard until the residual meteorite pattern was reduced to zero counts and the sum of the fit factors was one. This

indicated that all the mineral phases present in the meteorite sample were taken into account.

- The fit factors of each mineral standard were corrected for relative differences in X-ray absorption to give their abundance in the meteorite sample. The correction for the bulk matrix absorption was described by Cressey & Schofield (1996) and Batchelder & Cressey (1998). The absorption coefficient is characteristic of every mineral and is related to density, chemical composition and the wavelength of the incident radiation. Typical values for the corrections are given in Howard et al. (2009).

The modal mineralogy was determined for phases with abundance $> 0.3$ vol% (see Tables 2, 3 and 4 in Appendix B for more more details). The absolute uncertainties were determined by varying the fit factor of the mineral phase until the fit "by-eye" was noticeably poorer, based on the fitting of the PSD-XRD data collected for the present work. This resulted in absolute uncertainties of 0.01 - 5.6 vol% for anhydrous minerals and 0.1 - 1.9 vol% for fine-grained poorly crystalline phases (see Appendix B). This method of measuring uncertainties directly has also been used by Schofield et al. (2002), King et al. (2015) and Lee et al. (2016) and was related to the calculated goodness-of-fit parameters by King et al. (2015).

## 2.3 Micro-scale analyses

### 2.3.1 Scanning electron microscopy

The scanning electron microscope (SEM) produces images by scanning the surface of a sample with an electron beam. SEM is a powerful technique often used for the identification and imaging of mineralogical phases, providing fundamental information about the petrology of a sample. SEM offers a variety of different imaging and mapping modes depending on the type of detectors installed on the instrument. In this study, for micrometer scale imaging and elemental characterisation of CO chondrites, a secondary electron detector (SE), a back scattered electron detector (BSE) and an energy-dispersive X-ray detector (EDX) were used.

*Secondary electron (SE)* imaging is based on low energy electrons that are emitted from the sample. SE emission is due to the inelastic scattering resulting from the interaction between the electron beam and the atomic valence bands of the atoms of the sample. Because of their low energy ($< 50$ eV), SE originate from a few nm below the surface. SE are attracted towards the detector by a positive electrical bias, and consequently accelerated by a high potential (usually 10 kV) towards a phosphor scintillator. Information about the topography of the sample surface is related to the incident angle at which the electrons reach the detector.

*Backscattered electron (BSE)* imaging uses high energy electrons that are scattered back from elastic interactions with the atoms of the sample. The only electrons collected by a BSE detector are those with a trajectory close to 180 degrees from the incident angle. Back scattered electrons carry information about the elemental composition of the sample. This information is strongly related to the backscatter coefficient which is responsible for generating different greyscales in BSE images.

*Energy dispersive X-ray (EDX)* analysis provides information about the chemical composition and elemental distribution within a sample. EDX results from the interaction between the electron beam and the sample. The incident electron excites and ejects an electron from a stable inner shell, creating an electronic vacancy. This vacancy leads an electron from a higher energy shell to fill the gap. The difference in energy between the higher energy shell and the lower energy shell leads to the release of an X-ray with a characteristic energy for each chemical element.

Samples used in this study for SEM analyses were in the form of polished thin sections (30 $\mu$m thick) and polished blocks. Specimens were carbon coated before the analysis to improve their conductivity in order to avoid the formation of artefacts and collection of the charge on the sample surface. In this study, a FEI Quanta 650 Field Emission Gun (FEG) SEM was used. The FEG enables a smaller electron beam diameter, more coherent beam and higher current density than with a thermionic emitter such as a tungsten filament. Therefore, the signal-to-noise ratio is improved as well as the spatial resolution and the life of the emitter. High resolution BSE images were used to identify suitable areas of matrix to analyse, which were selected (from 2 to 7 areas, depending on the sample) by looking for areas of fine grained matrix with

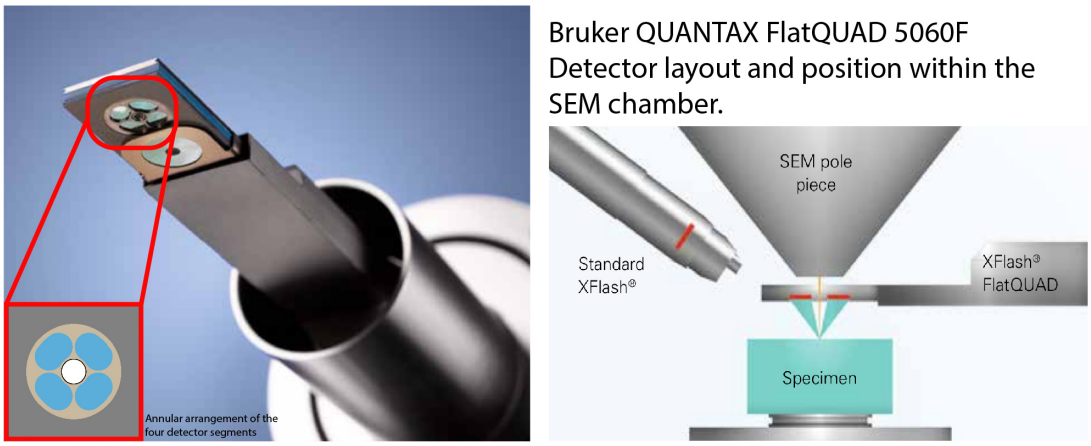


Figure 2.5: *Layout and position of the Bruker FlatQUAD 5060F detector used for the collection of EDX maps.*

a low number of inclusions. Fine grained rims around chondrules were not selected for this study. Subsequently, SE images of the selected matrix areas were collected at increasing magnifications.

The selected areas of interest were then mapped with a Bruker 5060F EDX detector (Figure 2.5), where the detector is placed between the microscope pole piece and the sample allowing mapping at very low electron voltage and consequently reaching a pixel resolution of a tenth of ∼10 nm. The Bruker Flat Quad 5060F is composed of four independent silicon drift detector chips (SDD) (Figure 2.5) which are arranged around a hole in the middle of the detector module that allows the electron beam to pass through. The four chips are equipped with separate signal processor channels in order to allow very high count rates per second (up to 4,000,000 cps). Focused Ion Beam (FIB) sections extracted from some of the matrix areas were also analysed with this instrument.

Images were processed with the Bruker Esprit 1.9 and 2.1 software, for selecting the chemical element of interest, adjusting the colours and intensities of the different chemical elements as well as for measuring the size of the grains through the "ruler" tool. Measurements were carried out in 2D.

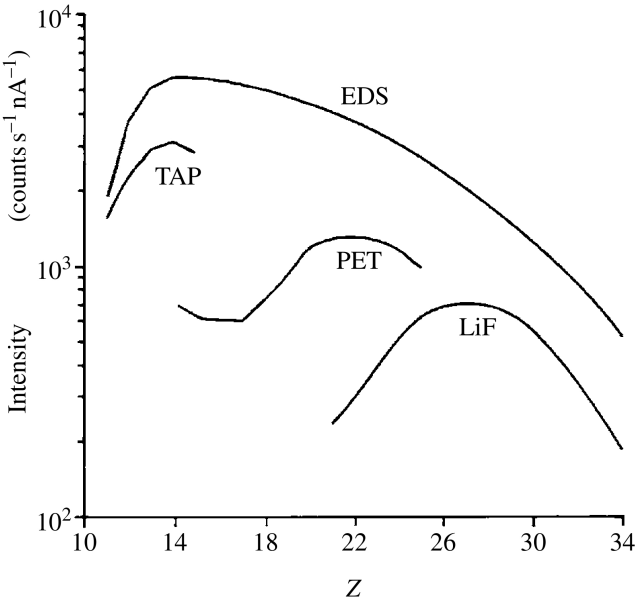


Figure 2.6: *Comparison in intensities of the Kα line of pure elements (Z: atomic number) as recorded by ED and WD detectors, with accelerating voltage of 20 kV. After Reed (2005).*

### 2.3.2 Electron probe microanalysis

The electron probe microanalyser (EPMA) is used to determine the chemical composition of solid materials. The sample is bombarded with a focused electron beam which consequently emits X-rays at wavelengths characteristic of the element being analysed. An X-ray spectrum has characteristic lines for each element, corresponding to characteristic wavelengths or photon energies. Comparing the intensities of the lines with those of standard materials, it is possible to determine the elemental concentration. The relative accuracy of the measurements is ± 1% and the detection limit is on the order of tens of ppm (Reed, 2005), while the spatial resolution is limited to 1 $\mu$m under normal conditions.

Most EPMA are equipped with both a wavelength dispersive spectrometer (WD) and an energy dispersive spectrometer (ED). In WD spectrometers the X-rays are dispersed by a diffractor, which can be a crystal, a pseudo crystal or a layered synthetic microstructure (used for light elements). The crystals have different layer spacings (or d-spacing) and enables different wavelengths to be selected: lithium fluoride (LiF, 2d= 4.026 ), pentaerythritol (PET, 2d= 8.742 ) and thallium acid phthalate (TAP, 2d= 25.9 ). This results in one wavelength being diffracted and passed to the detector.

The detector is a gas filled chamber, where the gas is ionized by the incoming X-rays, that have been focused by a Rowland Circle geometry, producing an electronic pulse generated within a voltage biased wire. It is necessary to select the most appropriate crystal in order to get the resolution and higher signal intensity required for the element of interest. The WD spectrometer is useful for elements heavier than boron (Z= 5). Therefore there are limitations in the analysis of H, Li and Be, which in principle can be calculated by difference and stoichiometry.

While an ED spectrometer records all X-ray energies simultaneously, a WD spectrometer records one X-ray energy at a time. For a given crystal, the efficiency of a WD spectrometer decreases with increasing wavelength (Figure 2.6) and this is due to the decrease of the solid angle with increasing Bragg angle. WD spectrometers have higher spectral resolution than ED spectrometers, but at the same time their count rates are lower than for ED spectrometers. Moreover, the peak-to-background ratio of a WD spectrometer is about ten times higher than for ED spectrometers, allowing for lower elemental detection limits (Reed, 2005). In contrast to ED spectrometers, WD spectrometers do not have a maximum count rate limit and therefore it is possible to increase the intensity by increasing the beam current.

Analyses can be carried out at different spot sizes, such as 1 $\mu$m focused beam for spot analysis of minerals, or with a defocused beam of 20 $\mu$m for bulk analyses. EPMA is a powerful technique for the acquisition of high quality chemical data and with high precision compared to an SEM.

The calculation of the errors for matrix material is very complex due to the nature and size of the material. The matrix of CO chondrites is mainly composed of anhydrous crystalline phases such as olivine, pyroxene, feldspar, sulfide, oxide but also by some partially hydrated phases such as amorphous silicates, Fe (oxy)-hydroxide and rare phyllosilicates.

As the matrix components have an average grainsize equal to smaller than 1 $\mu$m, and being that the analyses were carried out with a 10 $\mu$m defocused beam, they do not just reflect the chemistry of a single mineralogical phase, but they are an average of several grains. The totals for every point analysis are 10 – 15 % lower than a regular EPMA anlaysis (100 wt% oxide) because of porosity and hydrated phases. Consequently, the

standard deviation is not representative of the chemistry of a singular mineralogical phase but it can be used for determination of bulk ratios. Moreover, the standard ZAF matrix correction assumes that the material is homogeneous and since the material is highly heterogeneous in terms of chemistry and morphology, this further contributes to an increase in the uncertainty of each measurement.

The measurements were carried out with a calibration for silicate materials and the following standards were used for each element: Na on jadeite (JAD3, STD048), Si on fayalite (FAY, STD278), Mg on forsterite (FOR, STD277), K on potassium bromine (KBR3, STD075), Ca on wollastonite (WOL4, STD097), Cr on chromite (CRO2, STDIC), Ti on rutile (RUT, STD082), Fe on Fe oxide (FEO, STDIC), Mn on magnetite (MNT, STDIC), Co on cobalt(III) oxide (CO2, STD121), Ni on nickel dioxide (NIO2, STDIC), Al on corundum (COR4, STD028), V on vanadinite (VAN, STDIC), Zn on sphalerite (ZNS2, STDIC), P on scandium phosphate (SCP, STD217) and S on barite (BAR2, STDIC).

## 2.4 Nano-scale analyses

Six samples, covering most of the petrologic range, were selected for the extraction of ultra thin (about 100 nm thick) FIB sections transparent to electrons and X-rays. The FIB sections were extracted from 2 or 3 different matrix areas per sample; these areas were previously imaged and mapped using an SEM and also chemically characterised using an EPMA. The FIB sections were analysed using transmission electron microscopy (TEM) at the University of Glasgow, UK and by scanning transmission X-ray microscopy (STXM) at Diamond Light Source, UK.

### 2.4.1 Preparation of FIB sections

FIB-SEM is equipped with an ion gun that can produce an ion beam and an electron gun for an electron beam. The FIB sections were extracted using a FEI NOVA NANOLAB 200 and a dual-beam FIB system at the Kelvin Nanocharacterisation Centre, Univeristy of Glasgow, UK. This dual-beam instrument combines a FIB with an SEM, allowing the electron beam to image the sample and therefore avoid the problem

of sputtering the sample surface with material ejected and redeposited from its own surface (Wirth, 2010). The ion-milling process is controlled with the SEM and is very precise especially in the final stages of milling the FIB sections.

A FIB instrument is composed of: Vacuum system, Liquid Metal Ion Source (LMIS), Ion column, Detectors for imaging and a Gas injection system (GIS).

Vacuum system: this system is composed of a sample chamber, a sample stage and an ion column with LIMS, secondary electrons, ion detectors and gas injectors. The vacuum pump connected to the system evacuates the chamber to a pressure of about 1 x $10^{-6}$ Torr.

LIMS: The FIB process consists of sputtering atoms from the target material, the efficiency of which is related to the ion source. Best results are obtained with heavy ions, such as Ga, with an acceleration voltage of 30kV, and the ion source material needs to have a low melting point and a low vapour pressure. Ga meets all of these requirements as $Ga^+$ ions are heavy and its source material has a melting temperature of 29.8 °C. A $Ga^+$ ion source has a lifetime of about 1500 $\mu$A h. The LMIS consists of a Ga reservoir connected to a tungsten needle. The Ga is heated to its melting point which by surface tension flows to the tip of the tungsten needle ( $\sim$ 2-5 $\mu$m).

Ion Column: The $Ga^+$ ions are then accelerated down the ion column, pass through two lenses, the probe-forming lens and the objective lens, which focus the beam to the target. The LMIS is located in the upper part of the ion column together with the suppressor and the extractor cup and the first aperture.

Detectors: imaging and analyses are the same as with an SEM including SE and BSE detectors and an electron backscatter diffraction (EBSD) detector that was not used in this study.

Gas injection system (GIS): Injection systems consist of retractable tubes and the most common are Pt- and W- GISs. In order to protect the surface of the FIB section from the scanning ion beam, a Pt layer is deposited on the surface of the target material. Organic Pt-gas is decomposed to $Ga^+$ ions and deposited.

**Sample preparation**

FIB sections were extracted from 2 or 3 selected areas of interest for each of the following samples: DOM 08006, NWA 7892, MIL 090010, Kainsaz, Ornans and Moss.

Prior to the extraction of the foils, a 1.2 $\mu$m thick layer of Pt was deposited on the area of interest (Figure 2.7 a) in order to protect it from erosion during ion milling (Figure 2.7 b, c). The FIB sections were then produced by initially cutting a pair of trenches from the surface of the sample (thin section or polished block) with a 30kV $Ga^+$ ion beam (Figure 2.7 d, e). Once the foils were lifted, they had an initial thickness of about 1000 nm (Figure 2.7 f, g). Using an *in situ* micromanipulator (Omniprobe 100 micromanipulator) the FIB sections were then welded by Pt deposition to the tines of a copper holder (Figure 2.7 h). Subsequently, the FIB sections are polished to about 100 nm thick (Figure 2.7 i) using a 5kV $Ga^+$ ion beam (Lee, 2010) which helps to reduce the sample damage.

The preparation of the FIB sections can damage the sample. For example $Ga^+$ ions can redeposit below the surface of the target material which is called "ion implantation" which is a similar effect to radiation damage. This leads to structural damage of the target material including removal of atoms or the creation of atomic vacancies (Wirth, 2010). Silicate materials, such as pyroxene and quartz, are very sensitive to radiation damage, and the formation of dislocations between 500 and 1000 nm under the surface is quite common (Wirth, 2010). In contrast, olivine is less sensitive to $Ga^+$ irradiation damage. Redeposition of Ga ions and of sputtered target material can also affect the quality of the FIB section, causing a lower contrast in the TEM and potential modification of electron diffraction patterns. Na is one of the elements which is strongly affected by Ga redeposition, as its K line (1.041 keV) is very close to the Ga-L line (1.098 keV). Redeposition can be reduced by lowering the acceleration voltage and the beam size (Wirth, 2010). Overall, fine grained, porous, polyphase and polycrystalline material is the most challenging for TEM preparation, as different phases abrade differently during the milling process (Brenker, 2010). This is very important to consider when preparing FIB sections of matrix material.

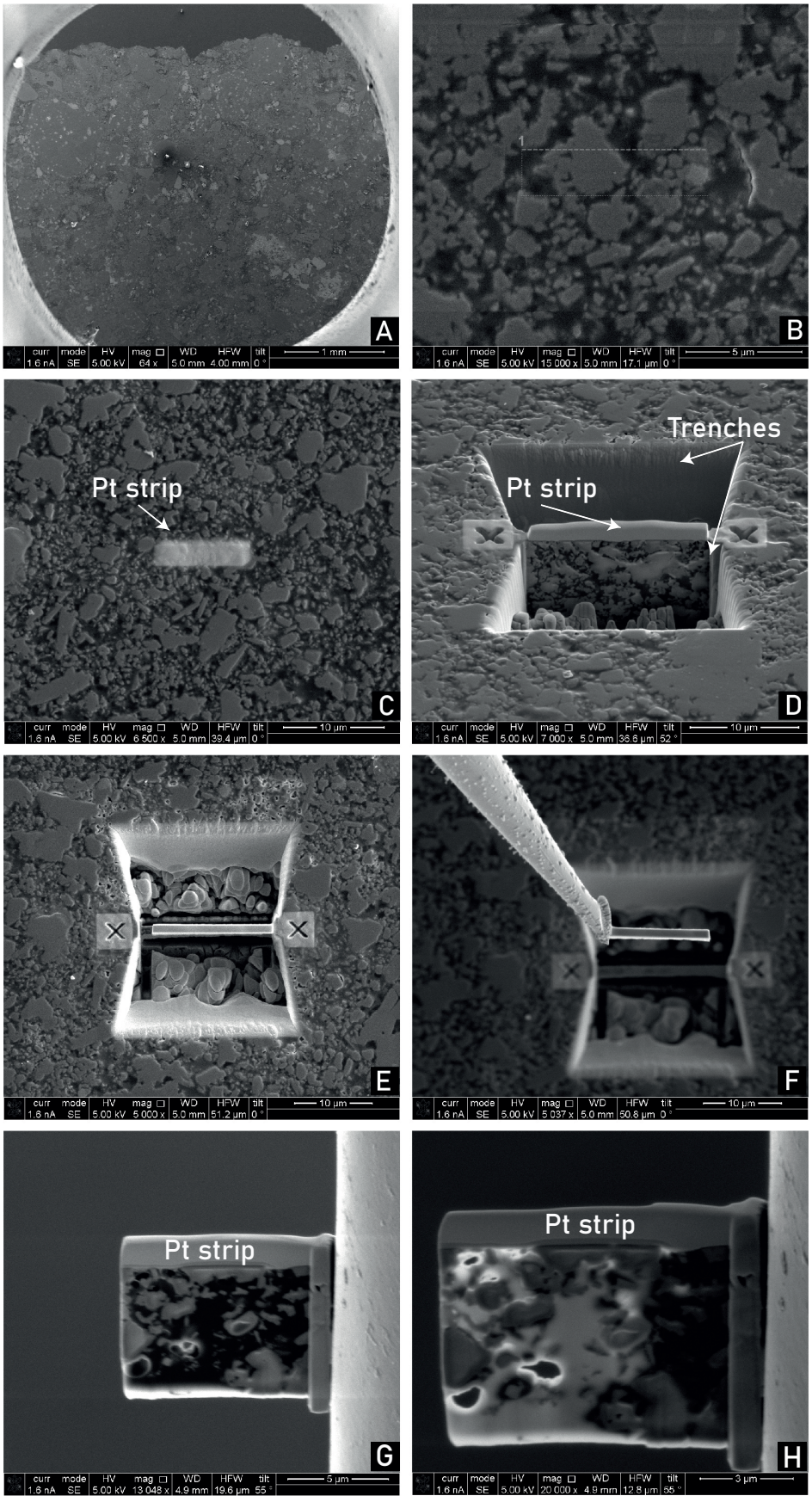


Figure 2.7: *Step by step FIB section preparation. a) and b) show the selection of the area where to extract the FIB section; c) a layer of Pt was deposited to protect the area of interest; d) and e) using a $Ga^+$ ion beam a pair of trenches are cut from the surface of the sample; f) FIB section, of about 1000 nm thickness, is lifted from the trench; g) the foil is welded to a copper holder; h) the foil is polished until reaching a thickness of about 100 nm.*

### 2.4.2 Scanning transmission X-ray microscopy

Since matrix material is very fine grained, synchrotron based STXM was selected for *in situ* analysis as it provides high spatial resolution, has high sensitivity to changes in elemental speciation and it has high energy resolution.

STXM is a combination of spectromicroscopy (imaging with spectral sensitivity) and microspectroscopy (extracting spectra from very small areas). STXM uses zone plates to focus a soft X-ray beam into a small spot on the sample, typically 10s nm. Zone plates are a set of radially symmetric rings, which alternate opaque and transparent zones, and diffract the light that hits them. The spacing between the zones allows the light to be diffracted and consequently to constructively interfere at the desired focus.

STXM analyses were carried out on Beamline I08 at Diamond Light Source (DLS), UK. The instrument uses soft X-rays, covering a photon energy range between 250 and 4200 eV, providing access to the K- and L-absorption edges of most of the major elements, combined with complementary X-ray imaging of the samples and X-ray absorption spectroscopy. It provides a monochromatic X-ray beam with a spot size down to 20 nm, depending on the zone plate in use. STXM allows the application of X-ray absorption near edge structure (XANES) spectroscopy, also known as near edge X-ray absorption fine structure (NEXAFS) spectroscopy.

Absorption spectroscopy is based on the absorption of X-rays in matter and is an element specific spectroscopic technique; the more energetic the X-rays, the more transparent the matter becomes to them. An absorption spectrum presents some discontinuities which are called *absorption edges*, and XANES utilises the fine structure just below, and up to 50 eV above the edge (Vincze et al., 2010). Absorption edges are characteristic for each element and correspond to the binding energies of different electron levels in that element. The absorption edges are obtained by changing the photon energy to an energy that is equal or above the binding energy of that characteristic electron energy level in that atom. The fine structure around the absorption edge depends on the local structure around the absorbing atom and the electronic states (e.g. oxidation state) of the target atoms (Vincze et al., 2010).

All the spectra were acquired using a multispectral imaging method called "Stacks"

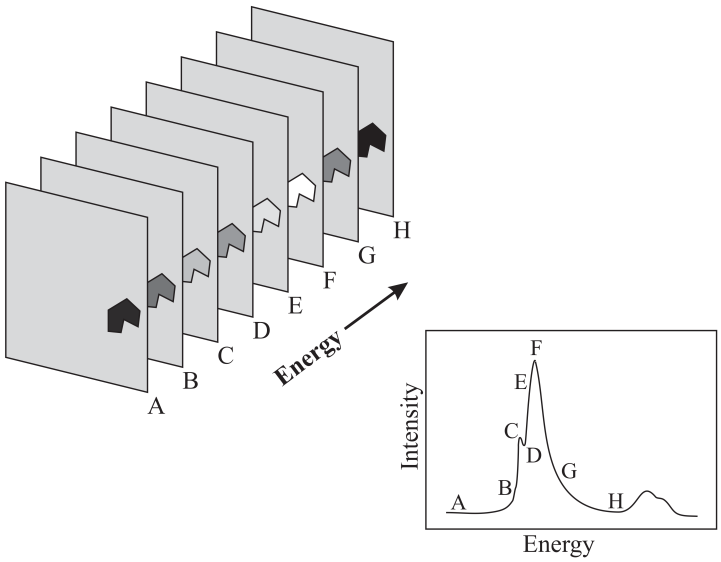


Figure 2.8: *A schematic of the STXM process, adapted from Smith et al. (2004). At every energy step in the scan a 2D map (image) is captured. Individual images in such a sequence record changes in intensity that represent changes in absorption that occur across the whole image at each different energy. A small region, common to each map/image, is shown varying in intensity as the energy of the incident X-ray beam changes. Subsequently, the pixels that define this region can be selected and their summed numerical intensities plotted at every step to yield spectral details.*

(Figure 2.8) which creates aligned hyper-spectral pixelated maps acquired over a range of energies that span the XANES region of interest (Smith et al., 2004; Jacobsen et al., 2000; Cody et al., 2008). Data collected consists of spectra from the sample *I(E)* and an $I_0$*(E)* spectrum, which correspond to a spectrum without the specimen. Because data were collected over a range of different energies, the XANES maps needed to be aligned as shifts at pixel scale in the $x$ and $y$ axes occur due to small changes in the focus. Once the stacks are aligned, the $I_0$*(E)* can be normalised from the measurement of the sample *I(E)* in order to obtain the absorption spectra, which can be analysed as optical density (OD) or as absorption. Spectra from single pixels and from areas of the map can be then extracted and plotted for the identification of their features.

In this study STXM was used for the study of C, N, O for the identification of functional groups characterising organic matter and Fe for the study of its oxidation state and the characterisation of the nature of the silicate components.

**C, N and O K-edges:**

Looking at the K-edges of C (edge ∼284.2 eV), N (edge ∼409.9 eV) and O (edge ∼543.1 eV) it is possible to characterise the nature of the organic molecules, identifying their functional groups, and to define their spatial relationship with the surrounding mineralogical phases. XANES maps were acquired throughout the FIB sections. For each element, the photon energy range used was selected depending on the photon energy of the K-edge and the energies of important spectral features. Moreover, the measurements were carried out with variable photon energy increments (ΔE) across the scan reflecting the complexity of the spectral regions:

- **C K-edge:** Photon energy range 278-310 eV
  278 - 282.5 eV with ΔE= 0.5 eV,
  282.6 - 292 eV with ΔE= 0.1 eV,
  292.2 - 296 eV with ΔE= 0.2 eV,
  296.5 - 310 eV with ΔE= 0.5 eV;

- **N K-edge:** Photon energy range 388-425 eV
  388 - 395 eV with ΔE= 0.5 eV,
  395.2 - 410 eV with ΔE= 0.2 eV,
  410.5 - 425 eV with ΔE= 0.5 eV

- **O K-edge:** Photon energy range 520-560 eV
  520 - 527 eV with ΔE= 1.0 eV,
  527.2 - 549.6 eV with ΔE= 0.4 eV,
  550 - 560 eV with ΔE= 1.0 eV

**Fe L-edge:**

The Fe L-edge allows the study of the Fe-bearing phases in order to determine the $Fe^{3+}$/ ΣFe ratios in amorphous and crystalline matrix phases and to monitor how this changes with increasing petrologic grade. In the case of the Fe L-edge the energy position of different features in XANES spectra increases as a function of the oxidation state.

- **Fe L-edges:** Photon energy range 700-730 eV

  700 - 706 eV with ΔE= 0.5 eV,

  706.1 - 715 eV with ΔE= 0.1 eV,

  715.2 - 720 eV with ΔE= 0.3 eV,

  720.1 - 726 eV with ΔE= 0.1 eV,

  726.5 - 730 eV with ΔE= 0.5 eV

The measurements were carried out over four different beamtimes, and were influenced by different operational procedures and beamline reliability, which resulted in some data being more prone to instrument related artefacts and stability. The measurements were made with reference to previous work done on similar materials by Cody et al. (2008), Bourdelle et al. (2013), Le Guillou et al. (2015) and Hopp & Vollmer (2018). In some cases the $I_0(E)$ spectrum was collected simultaneously with the spectra from the sample, while in other occasions it was collected separately if the region of interest was far from the edge of the sample or there was no convenient hole in the sample. For instrumental reasons, data were collected as a series of subfiles which were subsequently stitched together to produce a combined dataset ready for processing. Data were processed with the open source software *Mantis: Multivariate data analysis for spectromicroscopy* (Lerotic et al., 2014).

### 2.4.3 Transmission electron microscopy

The TEM (Figure 2.9) allows the study of samples at the micrometer and nanometre scale. High spatial resolution is possible as the TEM uses a focused beam of high energy electrons, and therefore high acceleration voltages which are in the range of 200 to 1250 kV. TEM analyses can be damaging for the sample, producing electron induced deterioration of the sample such as: radiolysis, which leads to breaking of bonds and therefore formation of defects, amorphization, sputtering of atoms from the surface of the sample and chemical changes; heating due to inelastic scattering of the electrons (Lee, 2010). Silicates, hydrous minerals, and carbonates are prone to beam damage especially, radiolysis and heating.

The FIB sections were imaged at the Kelvin Nanocharacterisation Centre (Univeristy of Glasgow) using an FEI Tecnai T20 instrument with a $LaB_6$ filament, beam

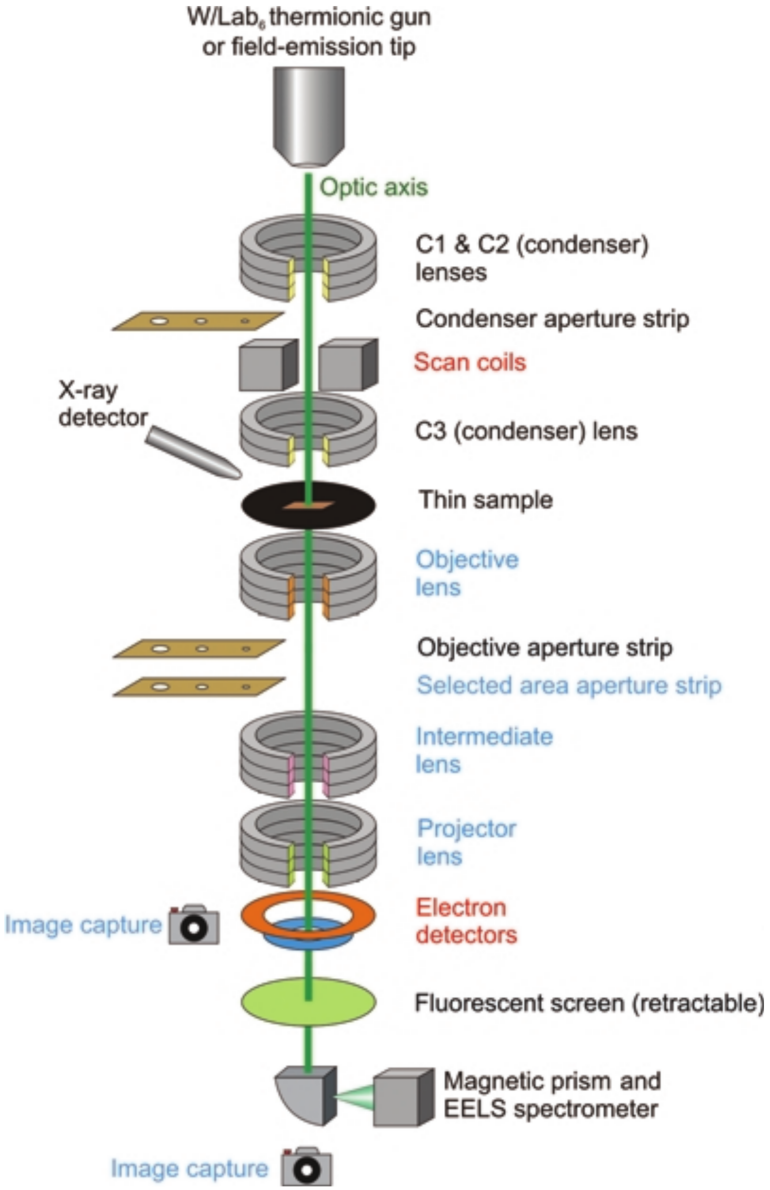


Figure 2.9: *Diagram adapted from Lee (2010) showing the locations of the main components in the microscope able to operate both in TEM and scanning transmission electron microscopy (STEM) modes. In black are the names of the components used in both modes, in blue the components used in TEM mode only, while in red the components for the STEM mode.*

size spot 3 and operated at 200 kV. TEM analysis can damage the samples, therefore STXM analysis were carried out first in order to keep the samples in a pristine state as possible and to avoid compromising measurements for organic matter. The FIB sections were studied by TEM in bright field mode. Imaging in bright field uses the direct beam which means that images were produced by unscattered and low angle forward-scattered electrons.

The TEM allowed analysis at the grain scale of the matrix component of the CO chondrites, identifying the Fe-bearing mineralogical phases recognised during STXM-XANES analysis, and the location of phyllosilicates, carbonates, carbonaceous phases and amorphous silicates. The composition and textural relationships of these phases were examined to assess how they evolved with increasing thermal metamorphism.

# Chapter 3

# Bulk Analyses

## 3.1 Introduction

This chapter examines the effects of thermal metamorphism on CO3 carbonaceous chondrites using X-ray techniques and electron microscopy. To date, there have been few systematic XRD studies of CO chondrites that take into consideration the whole metamorphic sequence. Imae & Nakamuta (2018) used XRD to analyse polished thin sections of CO chondrites, allowing complementary textural observations with SEM and EPMA. In contrast, here I investigated whole-rock CO chondrite powders (including chondrules, CAIs, AOAs and matrix), providing a more representative analysis of the bulk mineralogy and a lower risk of over or under representing phases. I used a combination of HR-XRD and PSD-XRD to quantify mineralogical trends and bulk modal mineralogy to better understand the thermal history of CO chondrites. A particular advantage of PSD-XRD for this work is the ability to quantify the abundance of amorphous silicates that are known to be present in the low petrologic type COs (McAdam et al., 2018; Alexander et al., 2018). PSD-XRD was previously used to study a wide range of ordinary (Dunn et al., 2010a,b) and carbonaceous chondrites including some low petrologic type COs (Alexander et al., 2018), CMs (Howard et al., 2009, 2011, 2015; King et al., 2017), CIs (King et al., 2015), CVs (Howard et al., 2010), CRs (Howard et al., 2015), CYs (King et al., 2019).

| Sample | Petrologic type | Olivine | Pyroxene | Feldspar | Nepheline | Sulfide | Magnetite | Kamacite | Calcite | Fe(oxy)hydroxide | Anhydrite | Phyllosilicate |
|---|---|---|---|---|---|---|---|---|---|---|---|---|
| Colony | 3.0 | X | X | X | | X | X | X | | X | | X |
| DOM 08006 | 3.0 | X | X | X | | X | X | X | | X | | |
| NWA 7892 | 3.05 | X | X | X | | X | X | X | X | X | | |
| MIL 090010 | 3.1 | X | X | X | | X | X | X | | X | | |
| Kainsaz | 3.2 | X | X | X | X | X | X | X | X | | | |
| Felix | 3.3 | X | X | X | X | X | X | X | | | | |
| Ornans | 3.4 | X | X | X | X | X | X | X | | | | |
| Lance | 3.5 | X | X | X | X | X | | X | | | | |
| Moss | 3.6 | X | X | X | X | X | | X | | X | | |
| ALHA77003 | 3.6 | X | X | X | X | X | | X | | X | | |
| Warrenton | 3.7 | X | X | X | X | X | | X | | X | | |
| Isna | 3.8 | X | X | X | X | X | | X | | X | X | |

Table 3.1: *Summary of minerals identified in 12 CO chondrites using HR XRD. Pyroxenes include enstatite, clinoenstatite, diopside, pigeonite, aegirine and augite; feldspars include albite, anorthite, labradorite; sulphides include troilite and pyrrhotite; Fe(oxy)hydroxides include goethite and akaganeite; phyllosilicates include tremolite, saponite and cronstedtite. For a more detailed overview of the specific minerals identified in each meteorite refer to Table 1 in Appendix A.*

## 3.2 High resolution X-ray powder diffraction

### 3.2.1 Experimental conditions

High resolution XRD provides well resolved diffraction features, which is very important for phase identification in complex mixtures. The resolution of the instrument was 0.02 degrees 2$\Theta$, and the X-ray source was Co $K_{\alpha 1}$ radiation, therefore avoiding background fluorescence generated by the presence of abundant Fe-bearing phases. Full details of the experimental conditions for HR XRD analyses are given in Chapter 3, however as a brief recap, 50 mg of each CO chondrite was ground in an agate pestle and mortar. Approximately 1-2 mg of the the powder was deposited onto a Si substrate for analysis using a Panalytical X'Pert Pro scanning diffractometer. XRD patterns were collected between 5 and 90 degrees $2\theta$. The diffraction patterns were analysed using X'Pert HighScore Plus and WinXPow utilising the ICDD PDF 2 2004 database.

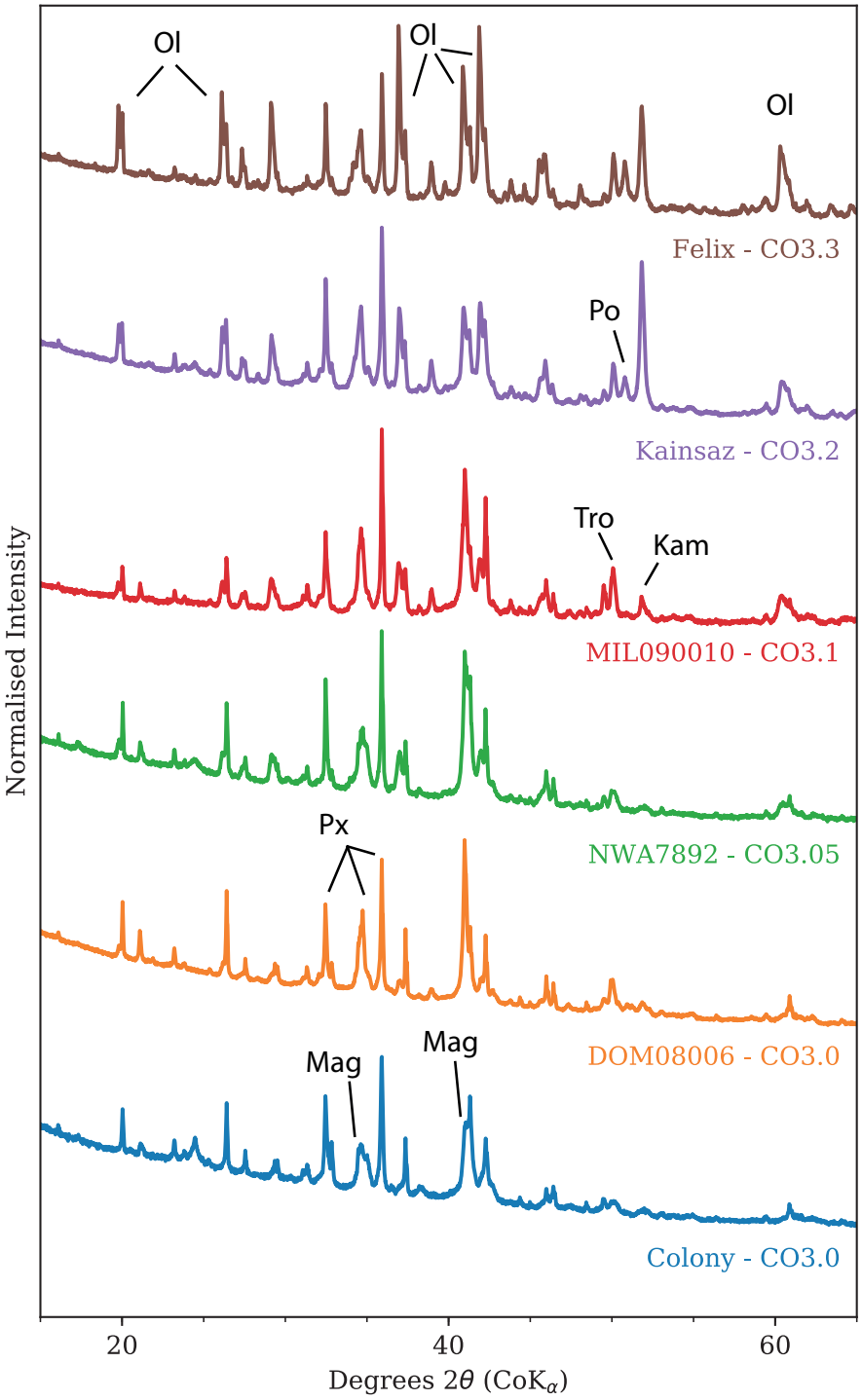


Figure 3.1: *High resolution XRD patterns of the CO samples with petrologic type from 3.0 to 3.3, showing variations in mineralogy throughout the metamorphic sequence. The following minerals are labelled: Ol: olivine, Po: pyrrhotite, Tro: troilite, Kam: kamacite, Px: pyroxene and Mag: magnetite.*

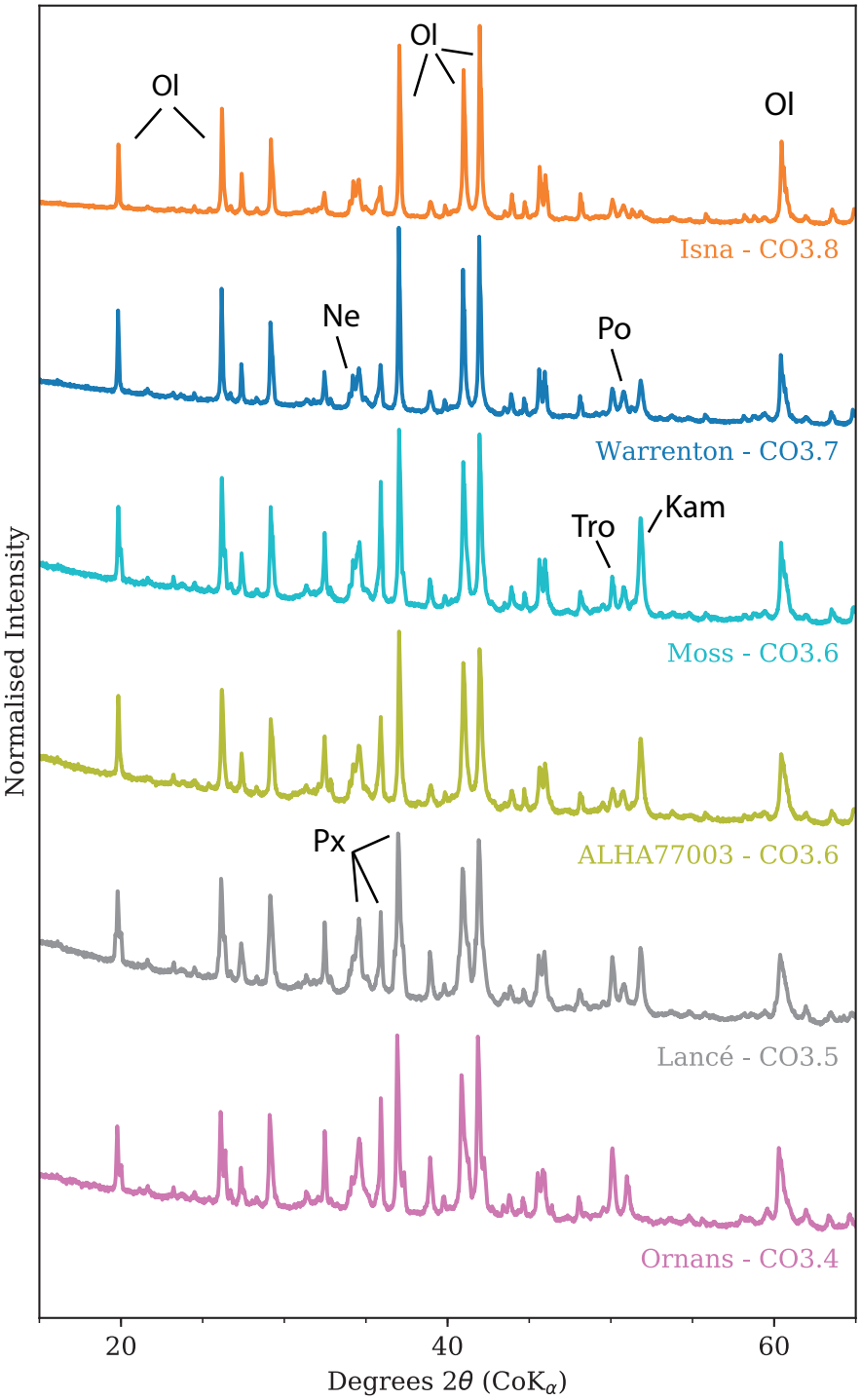


Figure 3.2: *High resolution XRD patterns of the CO samples with petrologic type from 3.4 to 3.8, showing variations in samples throughout the metamorphic sequence. The following minerals are labelled: Ol: olivine, Ne: nepheline, Po: pyrrhotite, Tro: troilite, Kam: kamacite, Px: pyroxene and Mag: magnetite.*

### 3.2.2 Results

Comparing the diffraction patterns of CO chondrite bulk powders collected with HR XRD with a database of diffraction patterns of mineral standards (Table 3.1, Figures 3.1 and 3.2) it was possible to interpret the mineral phases constituting the meteorite samples. The main phases detected in all samples are: olivine, pyroxene including enstatite, clinoenstatite, augite and diopside, feldspar including albite, anorthite and labradorite, troilite and kamacite (Table 3.1). Magnetite is present in samples ranging from 3.0 to 3.4, while nepheline is present in samples from 3.2 to 3.8. Pyrrhotite was detected in Kainsaz, ALHA77003, Moss and Isna. Phases such as goethite, akaganeite and cronstedtite, are the most common weathering products detected (Table 3.1). In some cases, phyllosilicates such as saponite and tremolite (in Colony), calcite (in NWA 7892 and Kainsaz) and anhydrite in Isna (Table 3.1) were detected.

Olivine is ubiquitous in all samples and changes its composition across the petrologic range looking at the shift of the (020) peak of the olivine (Figure 3.3) it was possible to infer that the olivine compositions range. Using the shift of the forsteritic ($Fo_{100-90}$) to more Fe-rich ($Fo_{50}$) depending on their petrologic subtype (Figures 3.3 and 3.4). For samples belonging to low petrologic type (3.00 to 3.1) such as Colony, DOM 08006, NWA 7892 and MIL 090010 the (020) olivine peak at 20.1 degrees 2$\Theta$ is intense, consistent with a forsteritic composition ($Mg_2SiO_4$). DOM 08006, NWA 7892 and MIL 090010 also display a second smaller peak at $\sim$ 19.8 degrees 2$\Theta$. The appearance of peaks at lower 2$\Theta$ angle is due to the presence of olivine with a more FeO-rich composition, suggesting the simultaneous existance of olivine with different chemical composition within the meteorites. In Kainsaz (CO3.2) and Felix (CO3.3) the peaks at 19.8 and 20.1 degrees 2$\Theta$ are both present and they have similar relative intensities, indicating that there is an increase in the amount of Fe-rich olivine relative to the forsteritic olivine compared to the lowest petrologic type samples (Figure 3.3). Ornans (CO3.4), Lancé (CO3.5) and Moss (CO3.6) show a decrease in intensity of the (020) forsterite peak at 20.1 degrees 2$\Theta$ and an increase in the intensity of the (020) olivine peak at 19.8 degrees 2$\Theta$, while ALHA77003 (CO3.6), Warrenton (CO3.7) and Isna (CO3.8) present only a diffraction peak of the Fe-rich olivine at $\sim$ 19.8 degrees 2$\Theta$ (Figures 3.3).

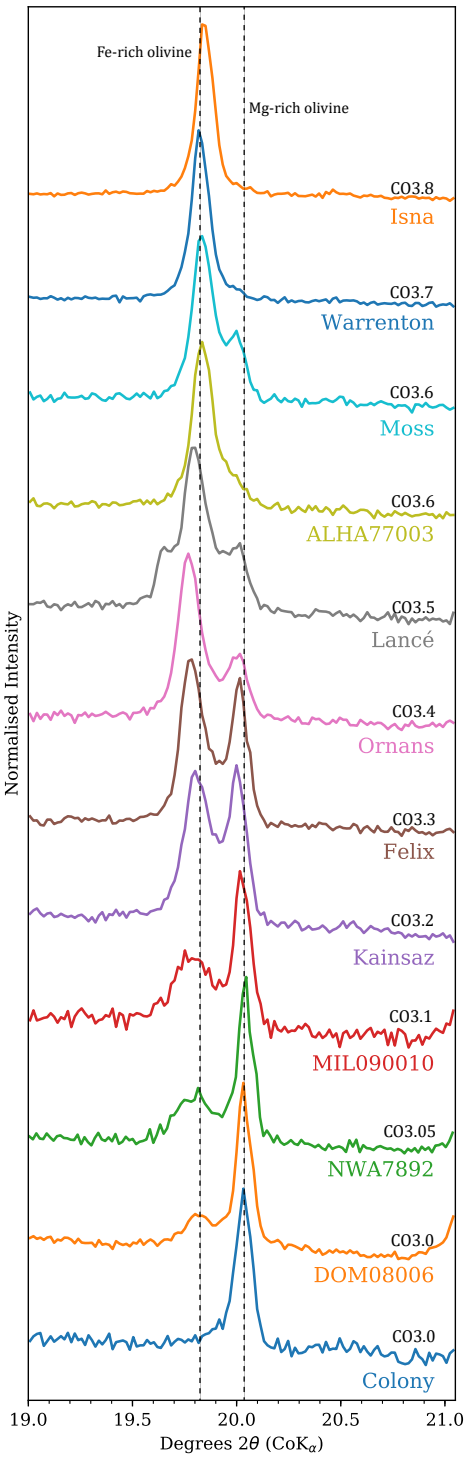


Figure 3.3: *With increasing petrologic type the composition of olivine changes from forsteritic to more fayalitic. This is reflected in a systematic decrease in intensity of the (020) fosteritic olivine peak at 20.1 degrees 2θ as well as a systematic increase in intensity of the (020) fayalitic olivine peak at 19.8 degrees 2θ towards higher petrologic subtypes.*

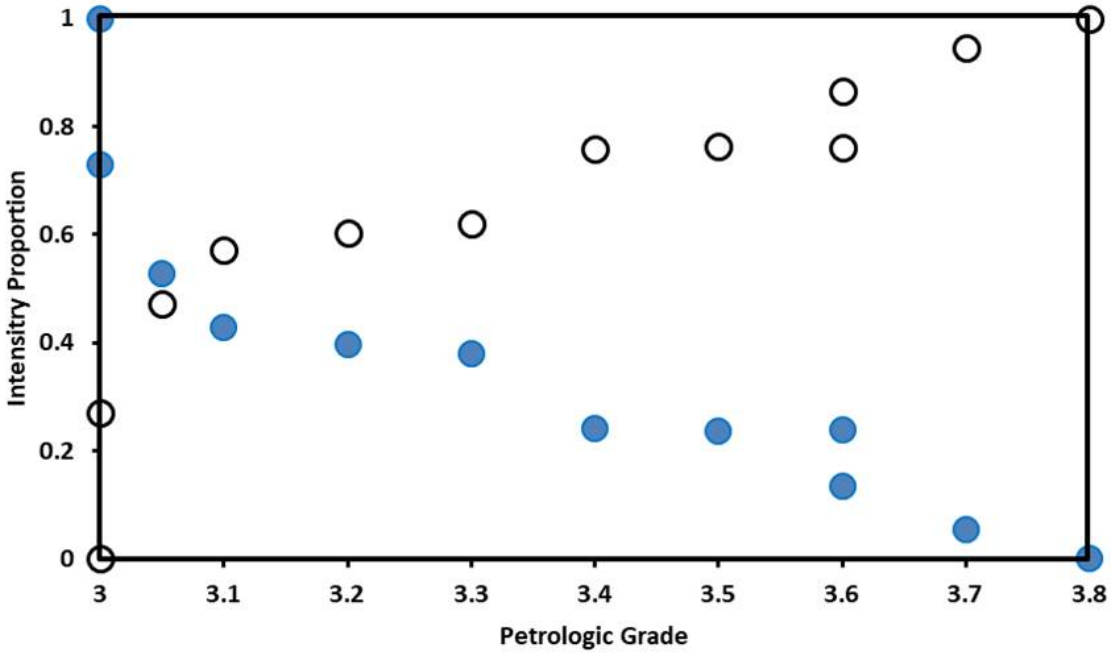


Figure 3.4: *Intensity proportion relative to the olivine (020) peak in association to the petrologic sub-type. Forsteritic olivine (blue) is the predominant type of olivine in low petrologic subtype CO chondrites, while Fe-rich olivine (white) is more abundant in higher subtypes.*

These observations are also demontrated in Figure 3.4, which illustrates the changes in olivine chemistry based on the intensity variations of the olivine (020) peak as a consequence of thermal metamorphism, leading to an increase in Fe-rich olivine (white) and a consequential decrease in forsteritic olivine (blue). Figure 3.4 illustrates how variations in the intensity proportion of the olivine (020) peak changes with thermal metamorphism. Low petrologic subtypes show a lower intensity proportion for Fe-rich olivine (white dots) compared to the high petrologic subtype samples (Figure 3.4). This is also demonstrated in Figure 3.3 where, for example, in Colony there is no (020) olivine peak at 19.8 degrees 2$\Theta$ but instead in DOM 08006 it is possible to see a small peak forming which with increasing petrologic subtypes becomes more intense. Simultaneously, the same happens for the (020) olivine peak at 20.1 degrees 2$\Theta$ but in the opposite direction.

The main peak of magnetite (311) occurs at $\sim$41.5 degrees 2$\Theta$ and overlaps with the (131) olivine peak, thus making its identification challenging (Figure 3.5). The relative intensity of other magnetite peaks is low, therefore if magnetite is only present in low abundances it would only be possible to observe its presence looking at its main

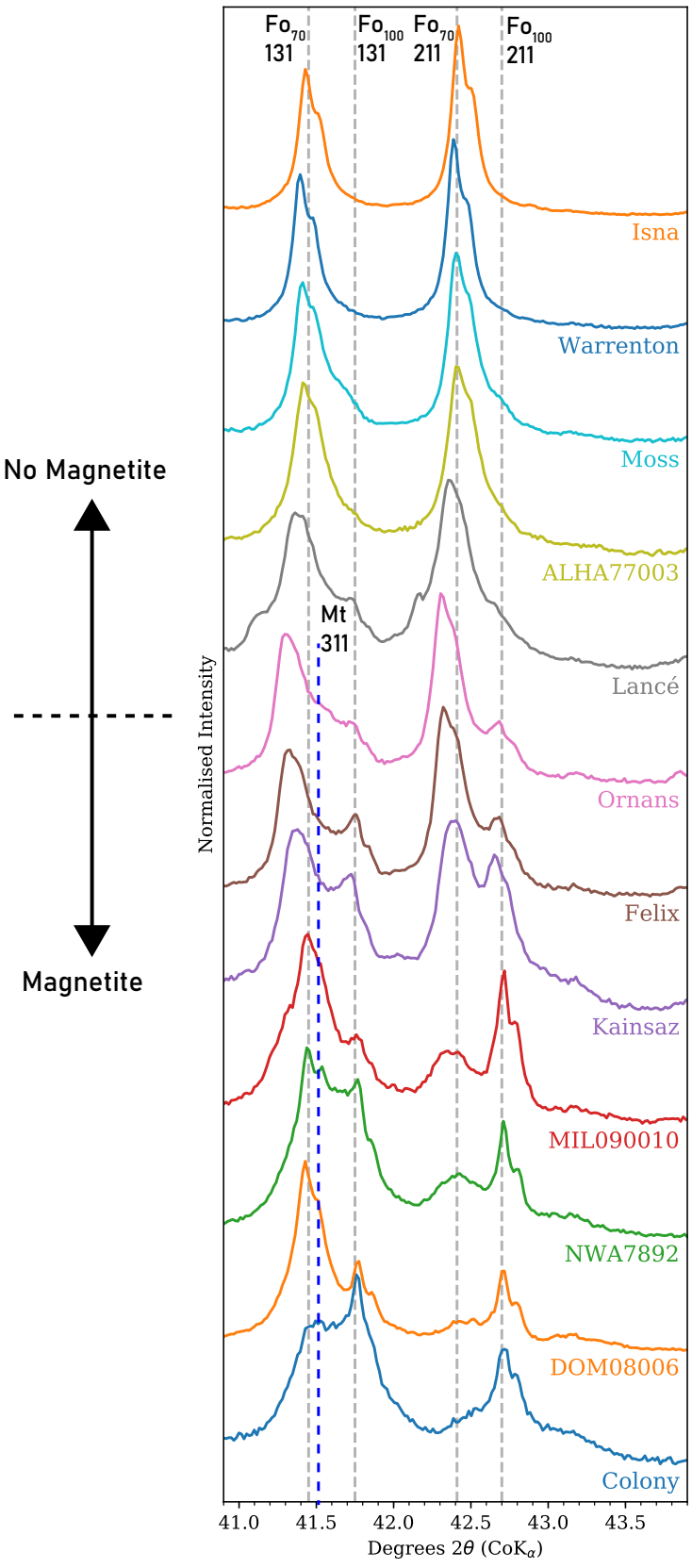


Figure 3.5: *XRD patterns of the studied samples between 41 and 43.5 degrees 2Θ in order of petrologic type: Colony (3.0), DOM 08006 (3.0), NWA 7892 (3.05), MIL 090010 (3.1), Kainsaz (3.2), Felix (3.3), Ornans (3.4), Lancé (3.5), Moss (3.6), ALHA77003 (3.6), Warrenton (3.7), Isna (3.8). The figure shows the changes in olivine composition and the influence of the magnetite main peaks on the olivine peak intensity.*

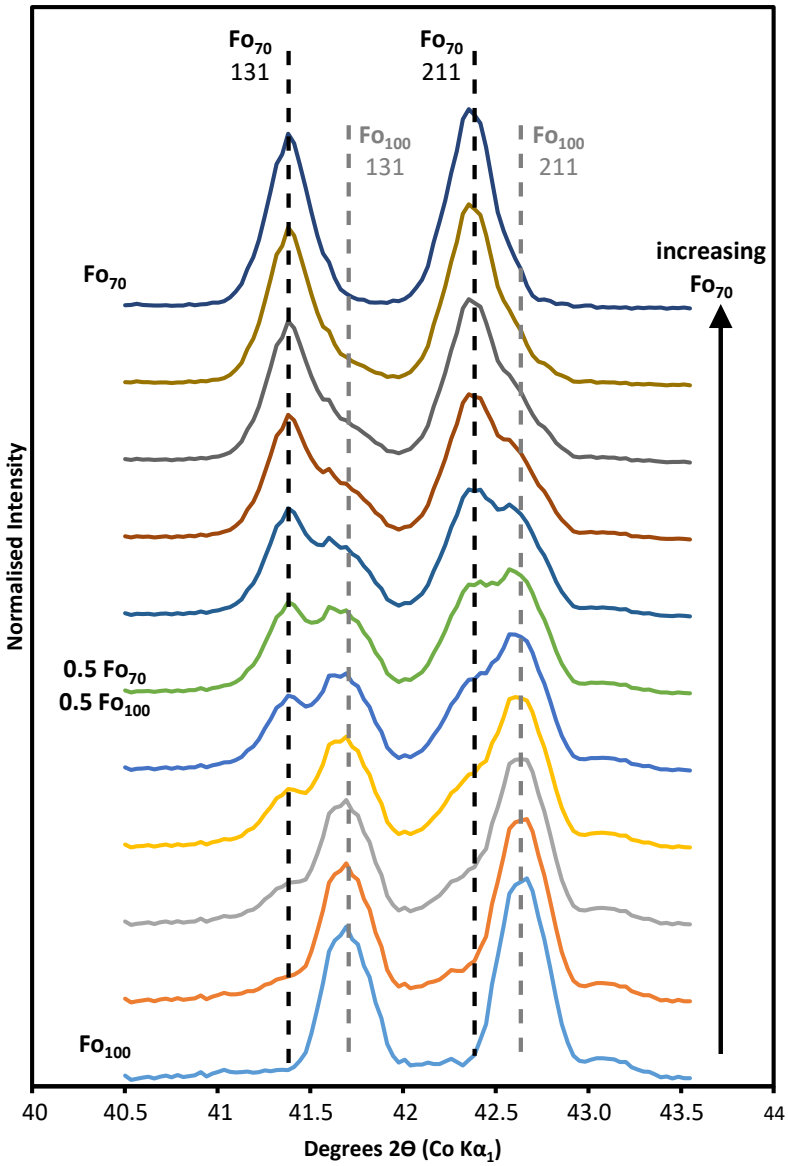


Figure 3.6: *A series of simulated diffraction patterns showing the variations associated with the olivine (131) and (211) peaks as forsterite ($Fo_{100}$) is transformed into $Fo_{70}$. The patterns are derived from a simple linear mixing model from the end member patterns at 10% intervals.*

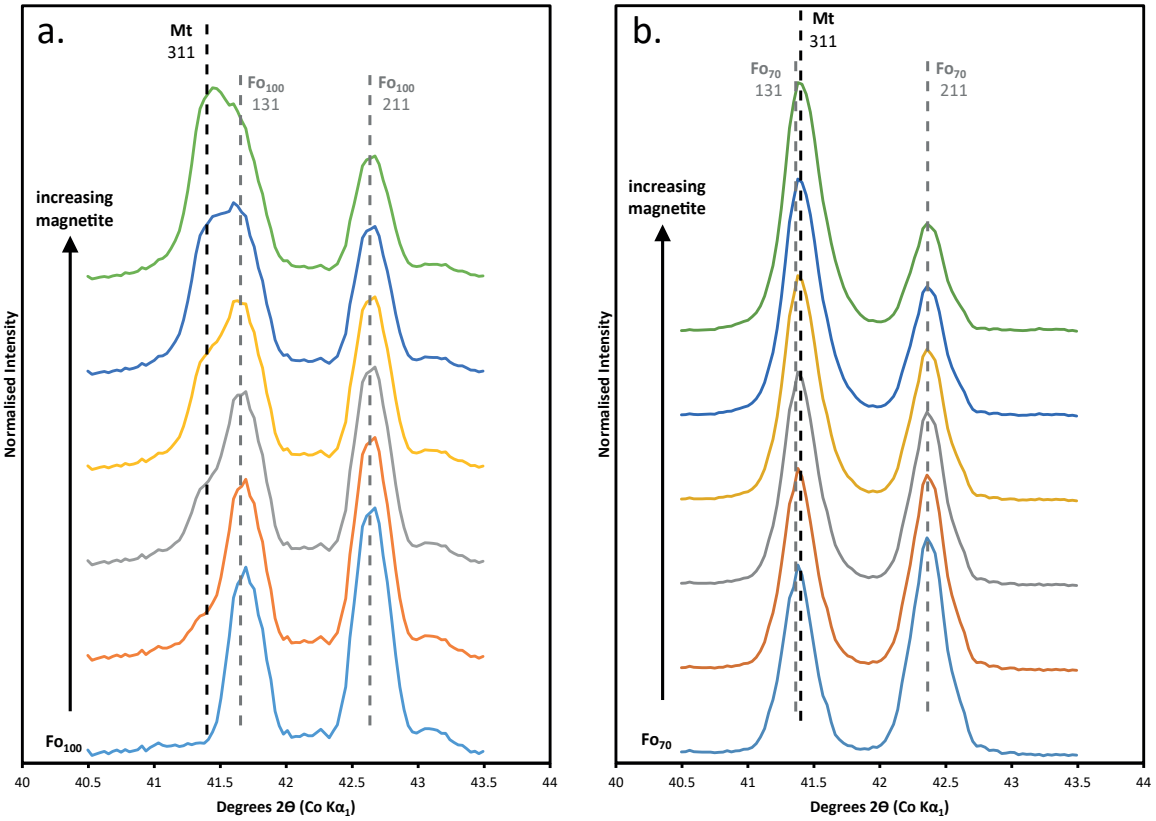


Figure 3.7: *a) Simulated diffraction patterns showing the effect of increasing amounts of magnetite on the diffraction pattern of forsterite between 40.5 and 43.5 degrees 2Θ. In forsterite the (211) peak is more intense than the (131) peak. Due to peak overlap from the magnetite (311) peak, the intensity of the forsterite (131) peak appears to become more intense than the forsterite (211) peak. The magnetite (311) peak can still be resolved from the forsterite (131) peak. b) Simulated diffraction patterns showing the effect of increasing amounts of magnetite on the diffraction pattern of $Fo_{70}$ between 40.5 and 43.5 degrees 2Θ. In $Fo_{70}$ the (211) peak is more intense than the 131 peak. Due to peak overlap from the magnetite (311) peak, the intensity of the forsterite (131) peak appears to become more intense than the forsterite (211) peak. In this system, the magnetite 311 peak can not be resolved from the forsterite (131) peak, and the presence of magnetite can only be inferred form the apparent intensity ratio between the $Fo_{70}$ (131) and (211) peaks.*

peak at ∼41.5 degrees 2Θ. However, it is possible to infer the presence of magnetite via changes in the apparent intensities of the olivine peaks.

This is shown in simulated patterns of Figures 3.6 and 3.7 obtained by addition of diffraction patterns. Figure 3.6 represents a linear mixing of $Fo_{70}$ and $Fo_{100}$ with 10% increments, while Figures 3.7a and b represent incremental mixing of magnetite with $Fo_{100}$ and $Fo_{70}$, respectively. These simulated XRD patterns indicate the changes expected for a sample firstly as forsterite is transformed into $Fo_{70}$, and secondly as increasing amounts of magnetite are present with either forsterite (Figure 3.7a) or Fe-rich olivine ($Fo_{70}$) (Figure 3.7b). In Figure 3.7b the magnetite (311) peak cannot be resolved from the $Fo_{70}$ (131) peak. The increasing presence of magnetite enhances the apparent intensity of the $Fo_{70}$ (131) peak making it appear more intense than the $Fo_{70}$ (211) peak. Thus the presence of magnetite in this system can only be inferred indirectly from the apparent intensity ratio between the olivine (131) and (211) peaks.

Figure 3.5 shows how the low petrologic subtype samples (3.00 to 3.1) are the ones contain magnetite. These samples show the contribution of magnetite at ∼41.5 degree 2Θ with the intensity of the olivine peak being almost twice the apparent intensity of the olivine peak at 42.7 degrees 2Θ (Figure 3.5). For samples of petrologic grade 3.2 to 3.4, there are two doublets of peaks related to the Fe-rich olivine; one doublet is at ∼41.5 and ∼41.7 degrees 2Θ, while the second doublet is located at ∼42.4 2Θ and at ∼42.6 degrees 2Θ. These doublets of peaks have about the same height between one another and they are comparable to the doublets of peaks that are simulated in Figure 3.6 with a composition of 0.6 $Fo_{70}$ and 0.4 $Fo_{100}$. Lancé, a CO 3.5, has a weak peak at 41.7 degrees 2Θ as well as at 42.6 degrees 2Θ, while from petrologic type 3.6 just the olivine diffraction peaks at 41.5 degrees 2Θ and at 42.4 degrees 2Θ are present. From these analyses, magnetite is not easily recognisable in COs samples with petrologic type between 3.2 and 3.8. This might mean either that magnetite is absent or it is present in very low concentration and its main peak cannot be recognised because of the high intensity of the olivine peak.

## 3.3 Position Sensitive Detector X-ray diffraction

Determination of mineralogical abundances through XRD is a useful tool for understanding the variations in mineralogy across a suite of samples due to thermal metamorphism. Following the identification of the main mineralogical phases through HR XRD, I determined the modal mineralogy of the whole suite of meteorite samples using PSD-XRD. Alexander et al. (2018) used PSD-XRD to investigate the bulk mineralogy of the most primitive COs, but here I have built upon this by characterising the entire metamorphic sequence.

### 3.3.1 Experimental conditions:

As described in detail in Chapter 2, PSD-XRD data were collected using a fixed geometry Enraf-Nonius (590) PDS 120 diffractometer equipped with an INEL curved position sensitive detector (PSD). Powders were loaded into sample wells in an identical manner to each other and to the mineral standards, and analysed by PSD-XRD. Phase quantification was achieved using a whole pattern profile stripping routine (see Chapter 2). Some of the samples analysed in this study contain a mixture of crystalline and amorphous Fe-bearing phases. In order to be able to quantify their contribution to the PSD-XRD patterns, the analyses were carried out using a Cu K$\alpha_1$ radiation as it causes Fe-bearing phases to fluoresce. The amount of fluorescence is proportional to the abundance of Fe, and can therefore be used to estimate the amount of Fe within the sample (Schofield et al., 2002). Amorphous phases do not produce coherent diffraction and sharp and intense diffraction peaks, rather only broad and low intensity features. However, if an amorphous phase contains Fe it will fluoresce and contribute to the overall intensity of the background. In this way it is possible to quantify the abundance of Fe-bearing amorphous phases in the CO chondrites.

| Sample | Petrologic type | Olivine | Pyroxene | Feldspar | Nepheline | Sulphide | Kamacite | Cocoite | Magnetite | Maghemite | Amorphous Fe-oxide | Amorphous silicates | Crossite/talc | Total |
|---|---|---|---|---|---|---|---|---|---|---|---|---|---|---|
| Colony | 3 | 30.7 (1.3) | 25.9 (1.1) | 0.5 (0.1) | – | 0.2 (0.04) | 0.1 (0.06) | 2.5 (0.1) | 2.7 (0.3) | 2.0 (0.6) | 4.9 (1.9) | 30.2 (1.8) | 0.2 (0.01) | 100.0 |
| DOM 08006 | 3 | 42.1 (1.7) | 32.3 (1.9) | 1.8 (0.1) | – | 2.3 (0.02) | 1.1 (0.05) | – | 3.4 (0.2) | – | – | 17.0 (1.3) | – | 100.0 |
| NWA 7892 | 3.05 | 55.8 (2.4) | 21.8 (1.1) | – | – | 1.6 (0.04) | 0.7 (0.04) | – | 6.7 (0.4) | – | 7.7 (0.9) | 5.7 (0.5) | – | 100.0 |
| MIL 090010 | 3.1 | 37.4 (1.0) | 35.6 (1.6) | – | – | 4.4 (0.1) | 0.5 (0.03) | – | 9.3 (0.5) | – | – | 12.9 (2.0) | – | 100.0 |
| Kainsaz | 3.2 | 48.7 (1.6) | 40.8 (2.0) | 4.2 (0.5) | – | 5.0 (0.2) | 1.3 (0.07) | – | – | – | – | – | – | 100.0 |
| Felix | 3.3 | 61.0 (2.2) | 23.8 (1.2) | – | 5.3 (0.2) | 8.2 (0.1) | 0.7 (0.01) | – | 0.9 (0.04) | – | – | – | – | 100.0 |
| Omans | 3.4 | 67.8 (2.5) | 18.3 (0.6) | – | 3.3 (0.3) | 10.4 (0.2) | 0.3 (0.04) | – | – | – | – | – | – | 100.0 |
| Lance | 3.5 | 54.8 (2.6) | 36.0 (0.9) | – | 3.1 (0.7) | 5.3 (0.1) | 0.8 (0.02) | – | – | – | – | – | – | 100.0 |
| Moss | 3.6 | 44.8 (4.0) | 36.1 (1.0) | 3.3 (0.2) | 6.5 (0.2) | 8.0 (0.1) | 1.4 (0.02) | – | – | – | – | – | – | 100.0 |
| ALHA77003 | 3.6 | 64.4 (5.6) | 27.2 (1.5) | 1.8 (0.1) | 2.4 (0.3) | 3.5 (0.1) | 0.4 (0.04) | 0.3 (0.1) | – | – | – | – | – | 100.0 |
| Warrenton | 3.7 | 45.6 (1.4) | 36.5 (1.8) | 2.3 (0.1) | 6.3 (0.3) | 7.7 (0.3) | 0.4 (0.03) | 1.2 (0.2) | – | – | – | – | – | 100.0 |
| Isna | 3.8 | 46.6 (1.5) | 33.9 (1.4) | 3.5 (0.2) | 6.5 (0.6) | 7.8 (0.4) | 0.4 (0.05) | 1.2 (0.3) | – | – | – | – | – | 100.0 |

Table 3.2: *Summary of the volume percent of minerals as determined by PSD-XRD. The uncertainties are provided in brackets. The – indicates that the mineralogical phase were below detection limit for PSD-XRD analysis. Pyroxenes include: enstatite, diopside and augite; feldspars include: anorthite; sulphides include: troilite and pyrrhotite. Detailed information about abundances, uncertainties and detection limits of each mineral phase can be found in Appendix B.*

### 3.3.2 Results

I have divided the samples into three groups based on their petrologic subtype. Results are described below with reference to Table 3.2. The uncertainties are in the range of 0.01 - 4 vol% for anhydrous minerals and 0.1 - 1.9 vol% for fine-grained poorly crystalline phases. Detailed information about uncertainties and detection limits of each mineral phase can be found in Appendix B.

#### CO3.00 to CO3.1

The low petrologic type COs Colony, DOM 08006 (Figures 3.8 and 3.9), NWA 7892 and MIL 090010 contain a mixture of crystalline and amorphous phases. A typical diffraction pattern of a low petrologic subtype is constituted by very sharp and intense olivine diffration peaks and weak pyroxene, kamacite and sulphide (troilite and pyrrothite) peaks (see DOM 08006 in Figure 3.8). The most abundant crystalline phases identified are: olivine $Fo_{100-50}$, pyroxene (enstatite and augite), troilite, kamacite and magnetite (Table 3.2). In addition, amorphous silicates were identified in all samples, while poorly crystalline Fe-oxide was identified in Colony and NWA 7892 (Table 3.2).

Amorphous silicates are characteristic of primitive samples and their abundance is respectively ∼30 vol% in Colony, 17 vol% in DOM 08006, 6 vol% in NWA 7892 and 13 vol% in MIL 090010. The olivine composition of the low petrologic type samples is a range between $Fo_{100}$ to $Fo_{50}$, and its total abundance is between ∼31 and ∼56 vol% (Table 3.2). Total pyroxene abundances are between ∼22 and ∼36 vol%, with enstatite the most abundant. The total abundance in sulphide ranged from ∼0.2 to ∼4.4 vol%, with MIL090010 containing ∼1 vol% in pyrrhotite. Low petrologic type samples show variable concentrations of magnetite ranging from ∼3 vol% in Colony up to 9.3 vol% in MIL 090010, while kamacite abundance ranges from 0.1 to 1.1 vol%. Feldspar was only detected in Colony (∼0.5 vol%) and DOM 08006 (∼1.8 vol%). In Colony, differently from the other samples, cronstedtite (0.2 vol%), goethite (∼3 vol%) and maghemite (2 vol%) were detected. Amorphous Fe-oxide is present in Colony and NWA 7892, with concentration of ∼5 and 8 vol%, respectively.

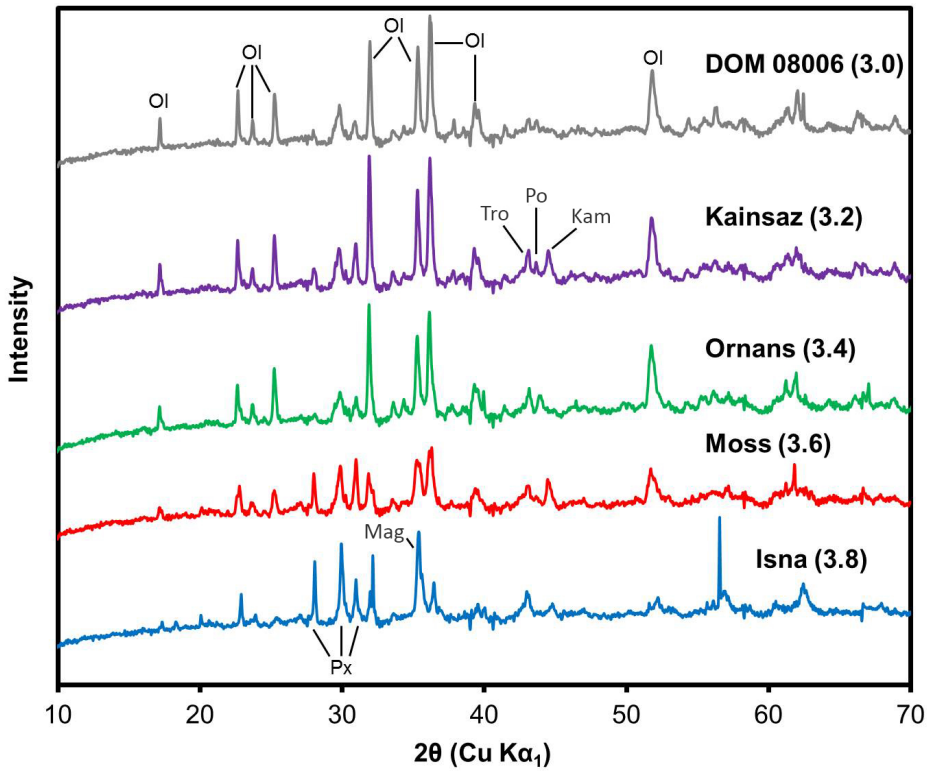


Figure 3.8: *X-ray diffraction patterns collected with PSD-XRD of selected samples. The figure shows changes of the XRD pattern in relation to the degree of metamorphism, and therefore variation within the samples mineralogy. Ol: olivine, Tro: troilite, Po: pyrrothite, Kam: kamacite/ Fe metal, Px: pyroxene and Mag: magnetite.*

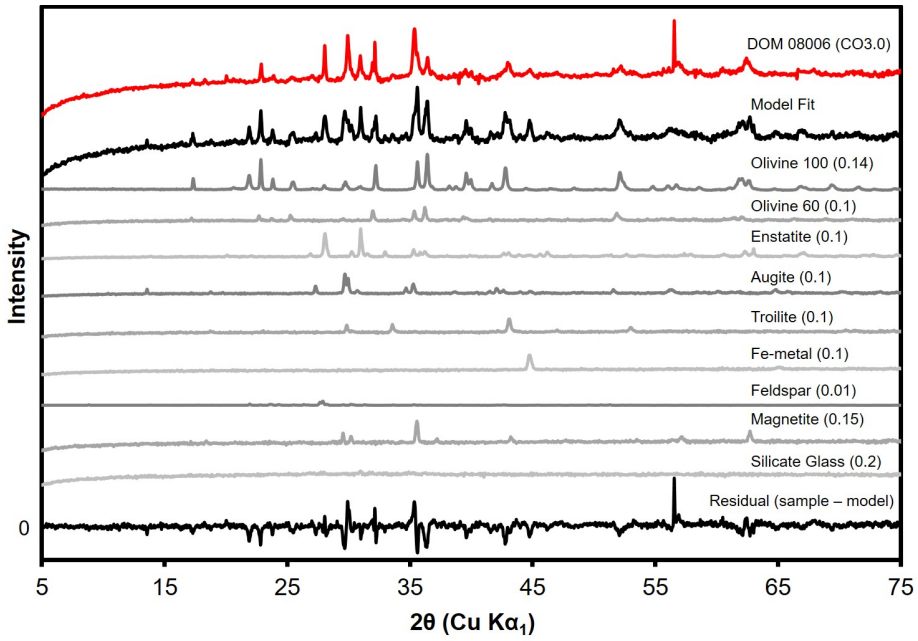


Figure 3.9: *PSD-XRD pattern of DOM 08006 and example of the sequential whole-pattern stripping procedure developed and described by Cressey & Schofield (1996) and Schofield et al. (2002) and fully described in Chapter 2. In brackets the scaling factors calculated for each mineral phase.*

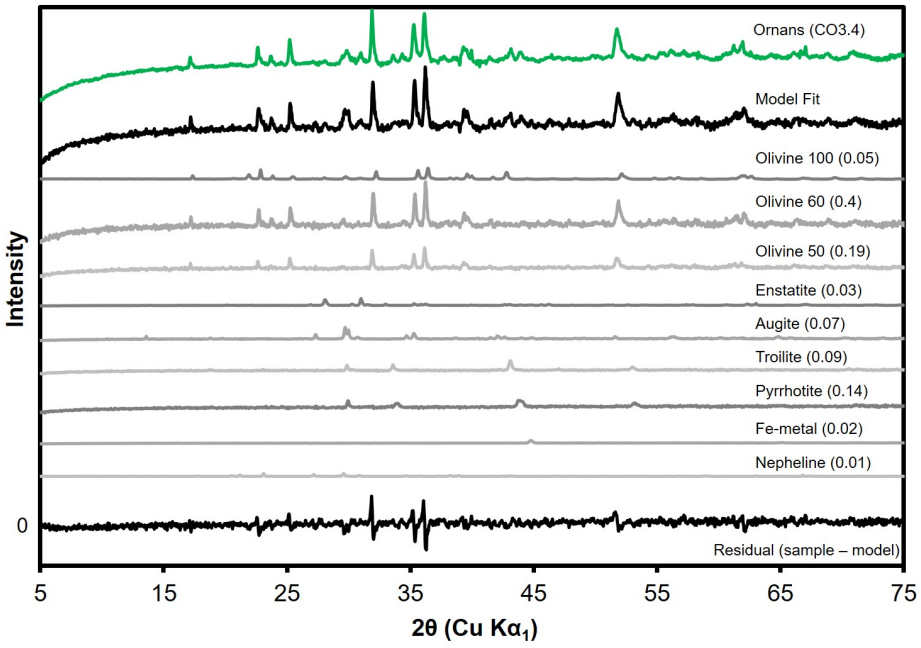


Figure 3.10: *PSD-XRD pattern of Ornans and example of the sequential whole-pattern stripping procedure developed and described by Cressey & Schofield (1996) and Schofield et al. (2002) and fully described in Chapter 2. In brackets the scaling factors calculated for each mineral phase.*

### CO3.2 to CO3.5

Intermediate petrologic type samples spanning between 3.2 and 3.5 such as Kainsaz, Felix, Ornans (Figures 3.8 and 3.10) and Lancé. Diffraction patterns with increasing thermal metamorphism shows enhanced peaks for sulphides and changes in intensity of the olivine peaks in relation to their changes in chemistry. The samples only contain crystalline phases including: olivine ($Fo_{100-40}$), pyroxene, nepheline, sulphide and kamacite (Figure 3.11 and Table 3.2). In these samples the olivine chemistry ranges between $Fo_{100}$ and $Fo_{40}$, with an increase in abundance of the more Fe-rich olivine relative to the low petrologic subtypes.

The total amount of olivine ranges between $\sim$ 49 and 68 vol% across the petrologic subtypes. The pyroxene abundance, which includes enstatite, augite and diopside, varies between 18.3 and 41 vol% across these samples. The total abundance in sulphide (troilite and pyrrhotite) ranges between 5 and 10 vol%. Kamacite is present at $\sim$ 1.3 vol% in Kainsaz, and between 0.3 and 0.8 vol% for the other samples. Nepheline begins to be detected from petrologic type 3.3 (Felix) and its abundance ranges between 3.1 and 5.2 vol%. Feldspar phases are quantifiable only in Kainsaz where their abundance

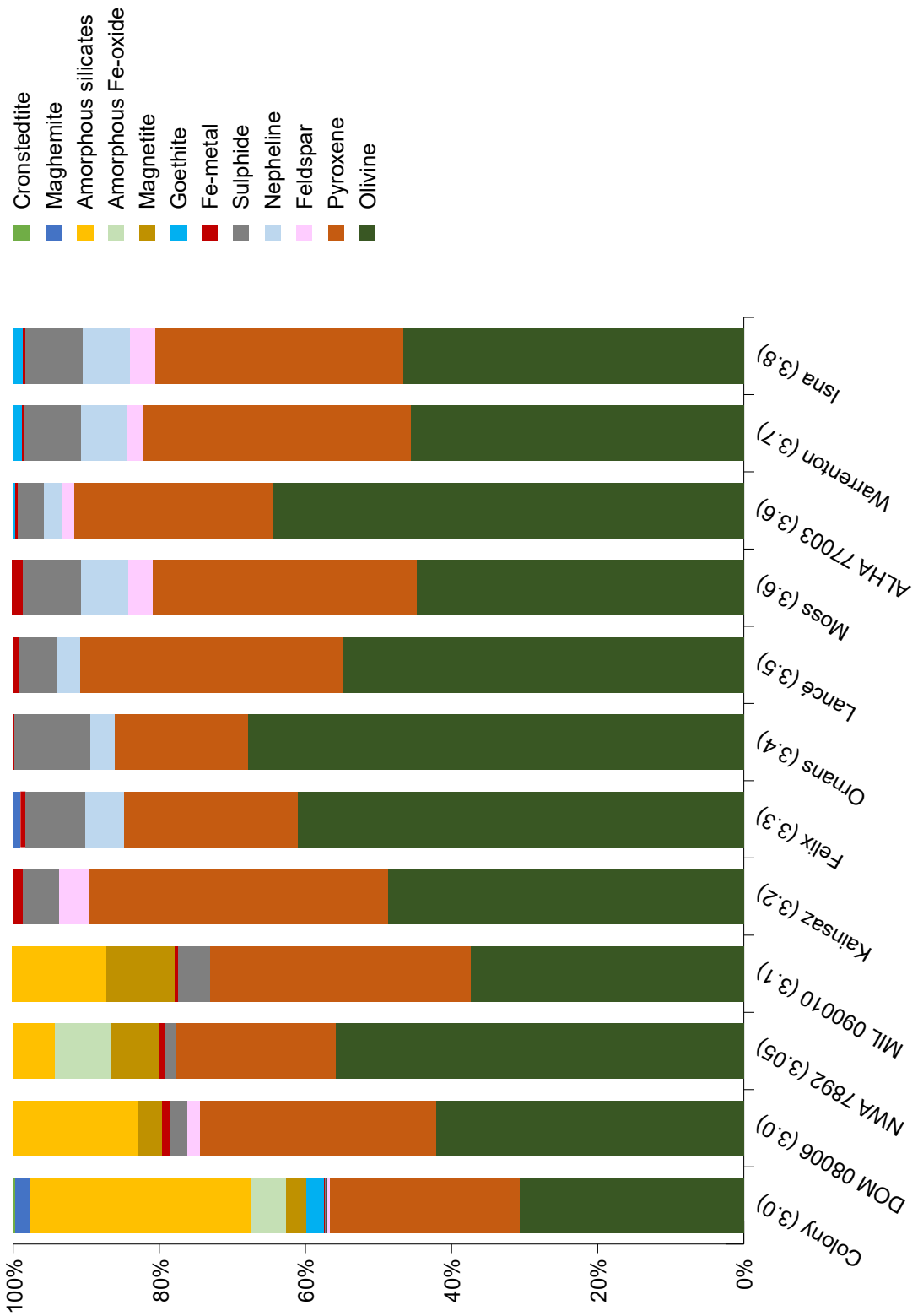


Figure 3.11: *Stacked columns showing the modal mineralogy of CO chondrites as determined by PSD-XRD. Pyroxene include: enstatite, diopside and augite; feldspar include: anorthite; sulphide include: troilite and pyrrhotite.*

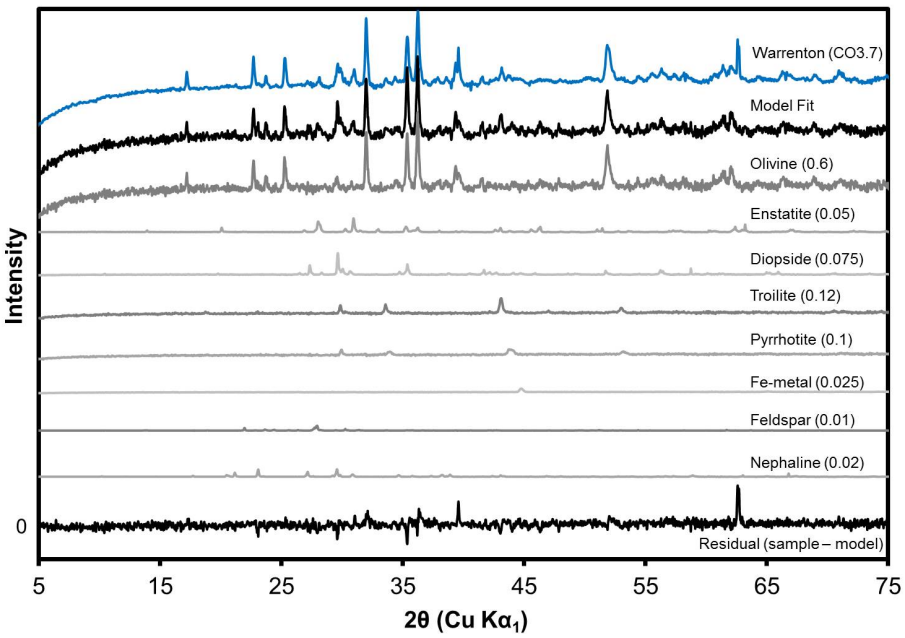


Figure 3.12: *PSD-XRD pattern of Warrenton and example of the sequential whole-pattern stripping procedure developed and described by Cressey & Schofield (1996) and Schofield et al. (2002) and fully described in Chapter 2. In brackets the scaling factors calculated for each mineral phase.*

is ∼ 4.2 vol%. A minor amount (∼1 vol%) of magnetite is present in Felix.

### CO3.6 to CO3.8

High petrologic type samples such as Moss, ALHA77003, Warrenton (3.8 and 3.12) and Isna are composed of crystalline phases including: olivine, pyroxene, feldspar, nepheline, sulphide, kamacite (Figure 3.11 and Table 3.2). The olivine chemistry ranges between $Fo_{100}$ and $Fo_{50}$, with most of the olivine being Fe-rich, and its abundance is 45 vol%, with the exception of ALHA77003 which is 64 vol%. Pyroxene (mix of augite, diopside and enstatite) abundance is between ∼27 and 37 vol%. The overall sulphide abundance is 3.5 vol% in ALHA77003, and ∼8 vol% in Moss, Warrenton and Isna. The nepheline abundance is ∼6 vol% in Moss, Warrenton and Isna, with the exception of ALHA77003 (2.4 vol%). The feldspar abundance ranges from 2 - 4 vol%, while the kamacite abundance is 0.4 vol%, with the exception of Moss which contains 1 vol%. Minor goethite was detected in ALHA77003, Warrenton and Isna (Table 3.2).

# Chapter 4

# In-situ analyses

The matrix of primitive meteorites preserves the original building blocks of the solar system and is an important tracer of the formation and evolution of asteroids (Brearley, 1993; Hezel & Palme, 2010; Haenecour et al., 2018). Therefore, it is important to study the matrix in detail and to unlock the information it contains about the mineralogy of the protoplanetary disk, as well as the chemical and physical processes that took place in the solar nebula and conditions on the first asteroids and planetesimals. In addition, the study of meteorites that have experienced some heating can show how the matrix is modified from its original state and track the thermal evolution of parent bodies. A major challenge with studying the matrix is its grain size ($< 1\mu$m), which sets many limitations in terms of analytical techniques that are suitable for its study. Therefore, an aim of this work is to apply correlated microscopic techniques in order to study the *in situ* mineralogy, crystal chemistry and OM within the matrix of CO chondrites. Matrix is difficult to separate from the rest of the meteorite components, therefore *in situ* analyses are the key to disentangling all the information held in it. In order to address important questions regarding modification of the matrix mineralogy and of the OM due to thermal metamorphism, in this chapter I will discuss the sampling strategy of the matrix material and the results of *in situ* analyses in the context of the existing literature.

## 4.1 Scanning electron microscopy

### 4.1.1 Experimental

A FEI Quanta 650 FEG-SEM was used to characterise the polished thin sections and polished blocks of the samples. BSE images illustrating the whole sample were collected at 15 kV with a working distance of 15 mm for each meteorite. BSE maps were used to identify areas suitable for analyses of the matrix. Images were processed using Bruker Esprit 1.9 and 2.1 software, for selecting the chemical element of interest, the colour keys and intensities of these elements as well as for measuring the size of the grains. Measurements were performed in 2D.

### 4.1.2 Results

SE images of thin sections and polished blocks show distinct variations in the matrix texture (Figure 4.1). Low petrologic subtypes CO3 chondrites, such as DOM 08006 (CO3.0) in Figure 4.1 A and B are characterised by an Fe-rich matrix constituted of abundant Fe-bearing amorphous silicates which act like a groundmass, giving the matrix a rather homogeneous and compact appearance, as well as small grains of Fe-metal, and silicates such as olivine and pyroxene embedded in it. Intermediate samples, such as Kainsaz (CO3.2), have a matrix that is more depleted in Fe compared to lower petrologic subtype samples (Figure 4.1 D) and show the presence of coarse mineral phases, while matrix in Moss (CO3.6) (Figure 4.1 G and H) is depleted in Fe but enriched in Mg and shows coarse silicates with a more defined habit, which formed as a consequence of the crystallisation of the amorphous silicates. The matrix in Moss looks more porous compared to Kainsaz and DOM08006. Among all the samples, the EDX map of Ornans stands out as it does not look to be part of the metamorphic sequence described here, since the matrix (Figure 4.1 F) does not seem as Fe depleted as Kainsaz. However, from the overlapping of the Fe and Mg EDX maps it looks like Mg and Fe are homogeneous throughout the phases in Figure 4.1 F which leads to infer that qualitatively Mg and Fe have the same abundance.

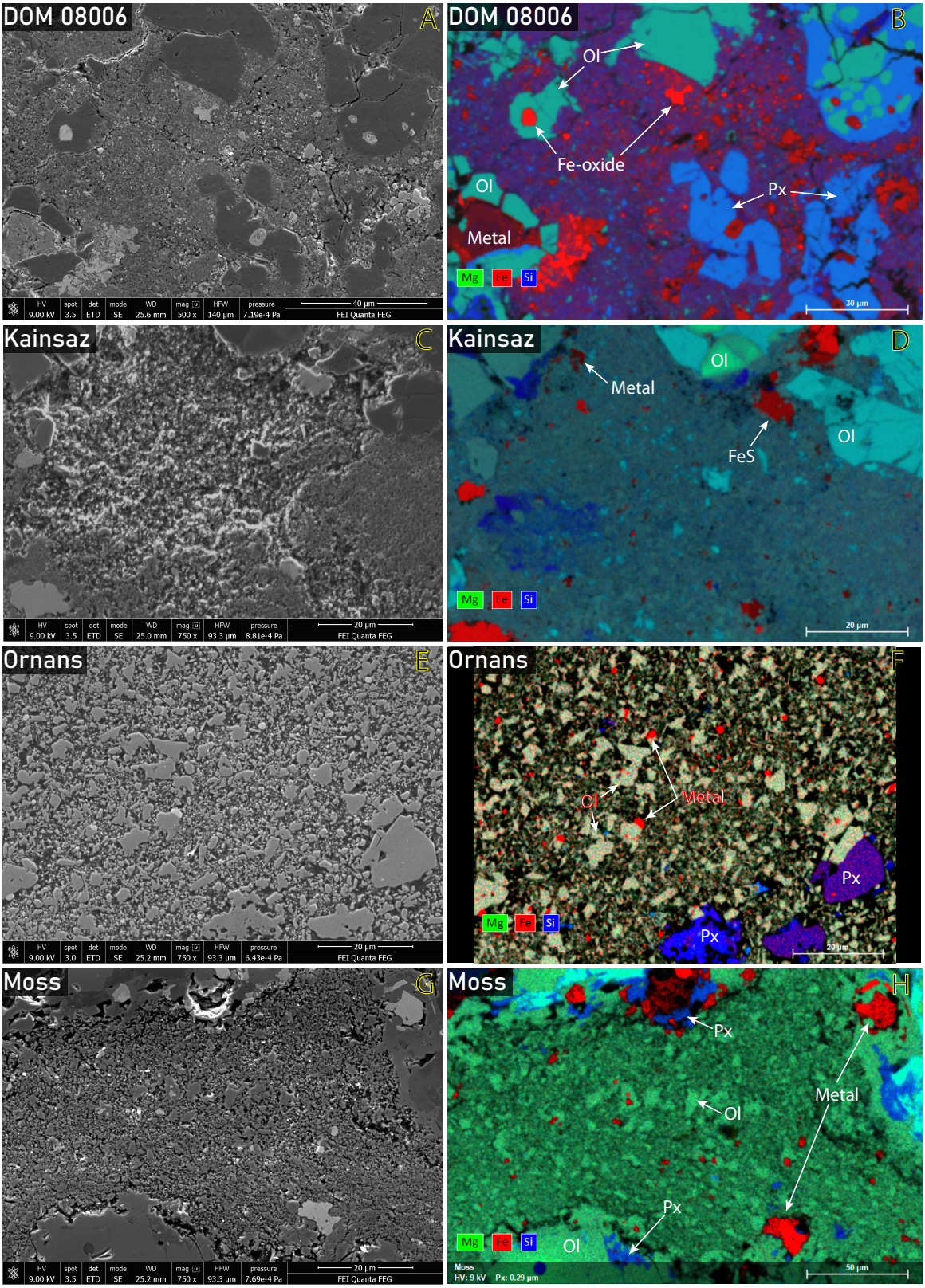


Figure 4.1: *SE images and EDX maps of areas of matrix in DOM 08006 (CO3.0), Kainsaz (CO3.2), Ornans (CO3.4) and Moss (CO3.6). The matrix in low petrologic types such as DOM 08006 is richer in Fe (red) and in this meteorite matrix is the main Fe reservoir. Fe and Mg (green) as result of heating present a diffusing exchange between matrix and chondrules, so the matrix in the more heated Moss is relatively depleted in Fe. With Px: pyroxene, Ol: olivine, FeS: Fe sulphide.*

## 4.2 Electron Microprobe Analyses

EPMA analyses were used to quantify how the concentrations of Fe, Si and Mg and the average elemental abundance of CO chondrite matrix varies with an increasing degree of metamorphism. This information enabled a more complete understanding of the chemical composition of the matrix, which reflects the history of the meteorite, including accretion, parent body processes and terrestrial weathering.

### 4.2.1 Experimental

The bulk chemical composition of matrix areas in each meteorite were determined using a CAMECA SX100 EPMA. The instrument is equipped with five WD spectrometers each fitted with multiple crystals for facilitating the simultaneous collection of X-rays. The crystals used in the CAMECA SX100 are: thallium acid phthalate (TAP), pentaerythritol (PET) and lithium fluoride (LIF). For each area of matrix, random points were analysed at 20 keV, with a 20 nA defocused beam of spot size of approximately 10$\mu$m. The instrument was calibrated with the use of silicate standards and the elements analysed were: Si, Ti, Al, Cr, Fe, Mn, Ni, Mg, Ca, Na, K, P, Co, V, Zn and S. Because of the grain-size of the matrix, inhomogeneity at the $\mu$m scale, porosity and volatiles in the sample, quantitative analysis is very challenging and the elemental totals are up to 15% lower than those that can be typically obtained by the analysis of coarse grained crystalline phases. The EPMA data provided the average bulk chemical composition of the matrix.

### 4.2.2 Results

Average chemical data are presented in Table 4.1 and show systematic chemical variations in relation to the petrologic subtype (for full EPMA dataset see Appendix D). Colony (CO3.6) was not considered in the present data-set because of its high Fe content due to terrestrial weathering. Elements such as Si, Ti, Al, Mn and Na show little variation in abundance across the metamorphic sequence. Ti is constantly present in the matrix with an abundance of about 0.04 - 0.06 wt%, while Mn is in the range 0.16-0.31 wt% across the across the metamorphic sequence. Na is generally between

| Sample | Si | Ti | Al | Cr | Fe |
|---|---|---|---|---|---|
| **DOM 08006** | 14.35 (2.37) | 0.05 (0.03) | 1.43 (0.50) | 0.23 (0.14) | 27.46 (6.16) |
| **NWA 7892** | 12.89 (2.38) | 0.04 (0.03) | 2.05 (0.68) | 0.22 (0.12) | 28.90 (6.56) |
| **MIL 090010** | 12.35 (2.62) | 0.04 (0.03) | 1.20 (0.62) | 0.19 (0.07) | 28.01 (7.47) |
| **Kainsaz** | 16.29 (2.95) | 0.06 (0.05) | 1.46 (1.58) | 0.37 (0.99) | 26.73 (7.68) |
| **Felix** | 12.85 (0.73) | 0.04 (0.01) | 1.23 (0.31) | 0.29 (0.10) | 28.86 (3.00) |
| **Ornans** | 12.13 (0.91) | 0.04 (0.02) | 1.82 (0.68) | 0.23 (0.10) | 25.97 (2.03) |
| **Lancé** | 13.76 (1.62) | 0.04 (0.02) | 1.14 (0.48) | 0.28 (0.14) | 31.34 (3.89) |
| **ALHA77003** | 15.10 (3.05) | 0.05 (0.04) | 1.16 (1.42) | 0.31 (0.32) | 28.35 (6.58) |
| **Moss** | 14.48 (1.02) | 0.05 (0.02) | 0.98 (0.33) | 0.32 (0.10) | 22.90 (1.90) |
| **Warrenton** | 13.64 (1.51) | 0.06 (0.02) | 1.37 (1.12) | 0.35 (0.14) | 21.45 (3.19) |

| Sample | Mn | Ni | Mg | Ca | Na |
|---|---|---|---|---|---|
| **DOM 08006** | 0.21 (0.13) | 1.87 (0.59) | 8.60 (4.38) | 0.79 (0.33) | 0.27 (0.09) |
| **NWA 7892** | 0.16 (0.05) | 1.10 (0.39) | 8.57 (4.04) | 1.39 (1.96) | 0.10 (0.05) |
| **MIL 090010** | 0.16 (0.07) | 2.03 (0.92) | 9.59 (5.66) | 1.14 (1.16) | 0.18 (0.09) |
| **Kainsaz** | 0.31 (0.11) | 0.87 (0.86) | 12.19 (2.83) | 1.08 (1.51) | 0.64 (0.73) |
| **Felix** | 0.23 (0.03) | 0.63 (0.54) | 9.98 (1.15) | 0.44 (0.67) | 0.14 (0.15) |
| **Ornans** | 0.19 (0.02) | 0.62 (0.92) | 9.58 (1.01) | 0.42 (0.38) | 0.37 (0.51) |
| **Lancé** | 0.24 (0.03) | 0.73 (0.65) | 11.85 (1.49) | 0.46 (0.97) | 0.23 (0.24) |
| **ALHA77003** | 0.21 (0.04) | 0.95 (0.75) | 14.32 (2.85) | 0.56 (1.39) | 0.22 (0.75) |
| **Moss** | 0.22 (0.02) | 0.48 (0.78) | 14.50 (0.97) | 0.43 (0.94) | 0.11 (0.20) |
| **Warrenton** | 0.17 (0.03) | 0.36 (0.59) | 13.01 (1.52) | 0.43 (0.99) | 0.36 (0.74) |

| Sample | K | P | Co | V | Zn |
|---|---|---|---|---|---|
| **DOM 08006** | 0.11 (0.04) | 0.16 (0.06) | 0.11 (0.03) | LOD | LOD |
| **NWA 7892** | 0.12 (0.04) | 0.19 (0.06) | 0.10 (0.03) | LOD | LOD |
| **MIL 090010** | 0.07 (0.07) | 0.13 (0.09) | 0.12 (0.05) | LOD | LOD |
| **Kainsaz** | 0.08 (0.06) | 0.13 (0.17) | 0.02 (0.04) | LOD | LOD |
| **Felix** | LOD | 0.13 (0.17) | LOD | LOD | LOD |
| **Ornans** | LOD | 0.09 (0.12) | 0.03 (0.04) | LOD | LOD |
| **Lancé** | LOD | 0.09 (0.13) | 0.04 (0.03) | LOD | LOD |
| **ALHA77003** | LOD | 0.07 (0.09) | 0.08 (0.04) | LOD | LOD |
| **Moss** | LOD | 0.11 (0.12) | LOD | LOD | LOD |
| **Warrenton** | 0.04 (0.09) | 0.09 (0.12) | LOD | LOD | LOD |

| Sample | S | O |
|---|---|---|
| **DOM 08006** | 1.23 (0.50) | 34.37 (3.02) |
| **NWA 7892** | 0.13 (0.04) | 32.00 (3.02) |
| **MIL 090010** | 0.63 (0.75) | 31.86 (4.32) |
| **Kainsaz** | 0.21 (0.47) | 37.24 (3.22) |
| **Felix** | 0.18 (0.44) | 31.63 (1.77) |
| **Ornans** | 0.09 (0.3) | 30.13 (1.91) |
| **Lancé** | 0.39 (0.82) | 34.89 (1.95) |
| **ALHA77003** | 0.33 (1.14) | 37.20 (3.17) |
| **Moss** | 0.14 (0.46) | 34.43 (1.68) |
| **Warrenton** | 0.23 (0.82) | 32.58 (2.88) |

Table 4.1: Average chemical composition of the CO meteorites analysed in this study. The abuncances are in wt% with LOD: Limit of Detection. Standard deviation for each measurement is provided in brackets. The average abundance for each element is based on the following number of data points (n) per sample: DOM 08006 $n$=146, NWA 7892 $n$=197, MIL 090010 $n$=73, Kainsaz $n$=209, Felix $n$=60, Ornans $n$=235, Lancé $n$=234, ALHA77003 $n$=289, Moss $n$=219 and Warrenton $n$=380.

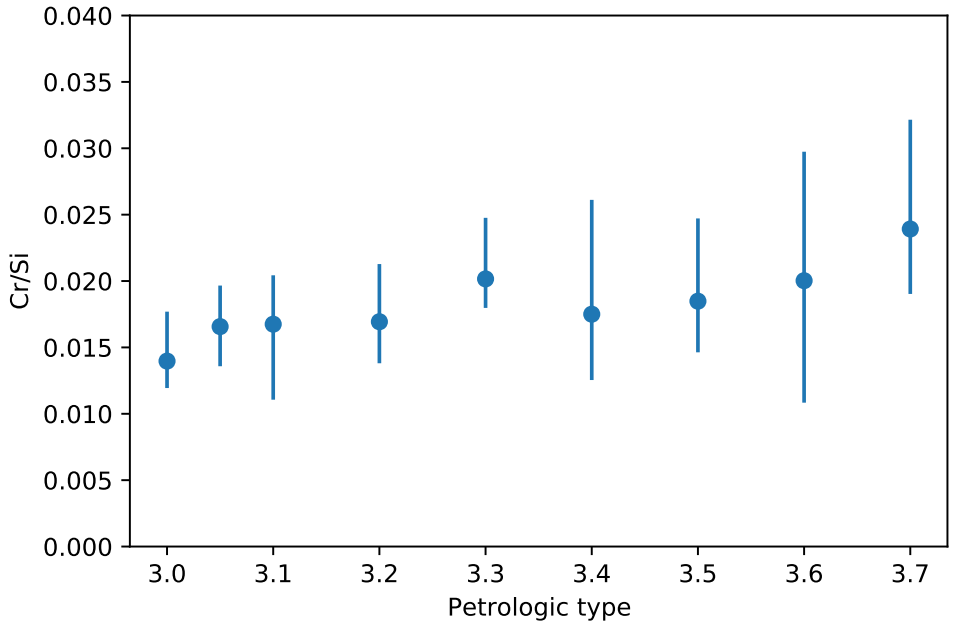


Figure 4.2: *Mean Cr/Si wt% content of the matrix relative to the petrologic type of CO3 chondrites.*

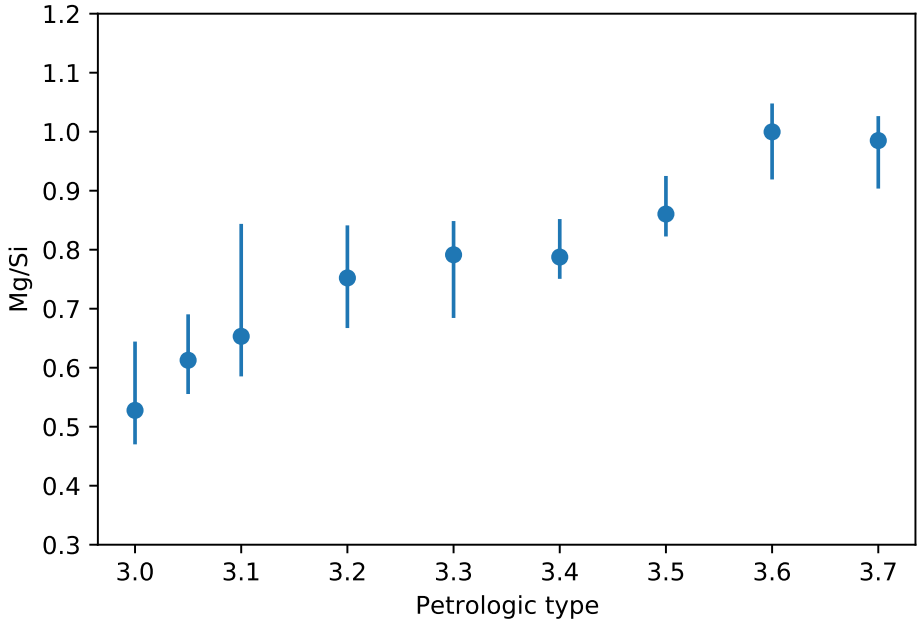


Figure 4.3: *Mean Mg/Si wt% content of the matrix relative to the petrologic type of CO3 chondrites.*

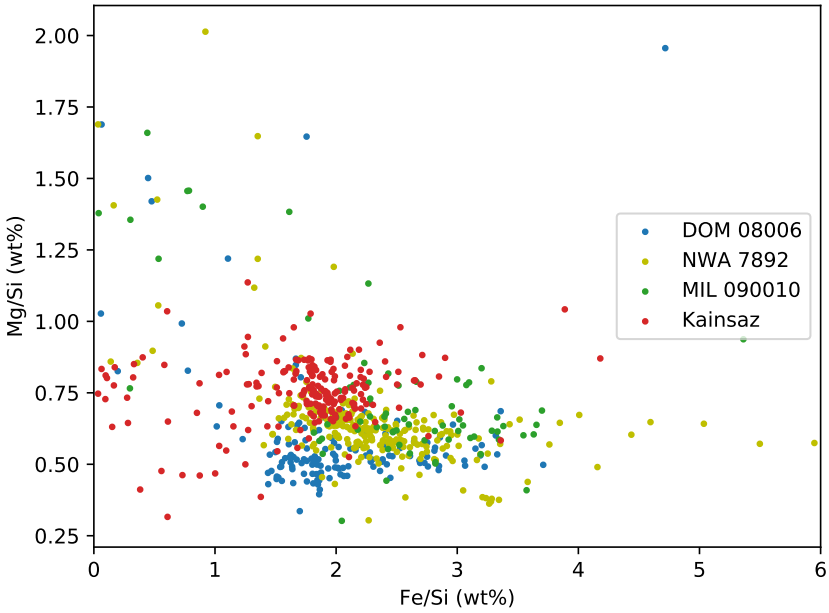


Figure 4.4: *Scatter plot of Fe and Mg wt% (normalised for Si) abundances in the matrix of the most primitive CO chondrites analysed in this work. The plot shows small variations in the amount of Fe and Mg within the matrices of DOM 08006, NWA 7892, MIL 090010 and Kainsaz.*

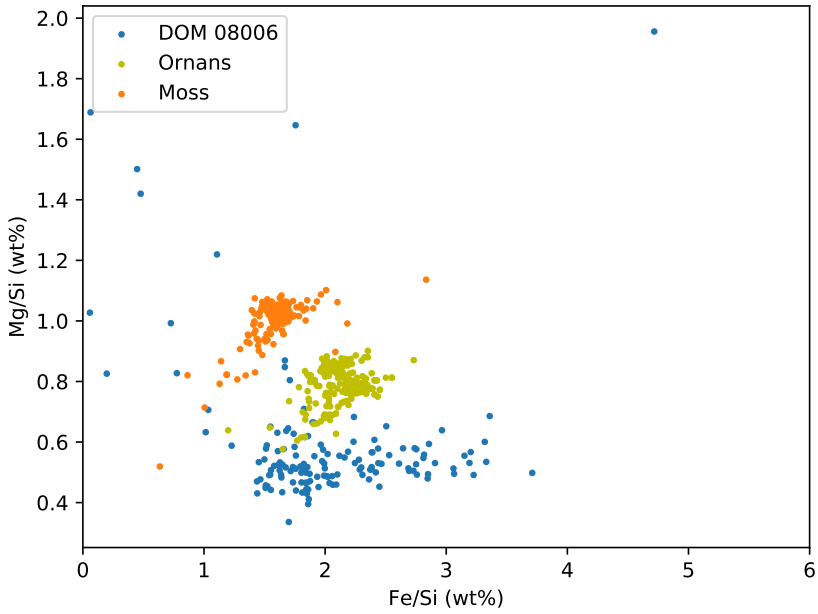


Figure 4.5: *Fe and Mg wt% (normalised for Si) for DOM 08006 (CO3.00), Ornans (CO3.4) and Moss (CO3.6). The scatter plot clearly shows how the concentration of Fe in the matrix decreases with petrologic type, while the Mg concentration increases.*

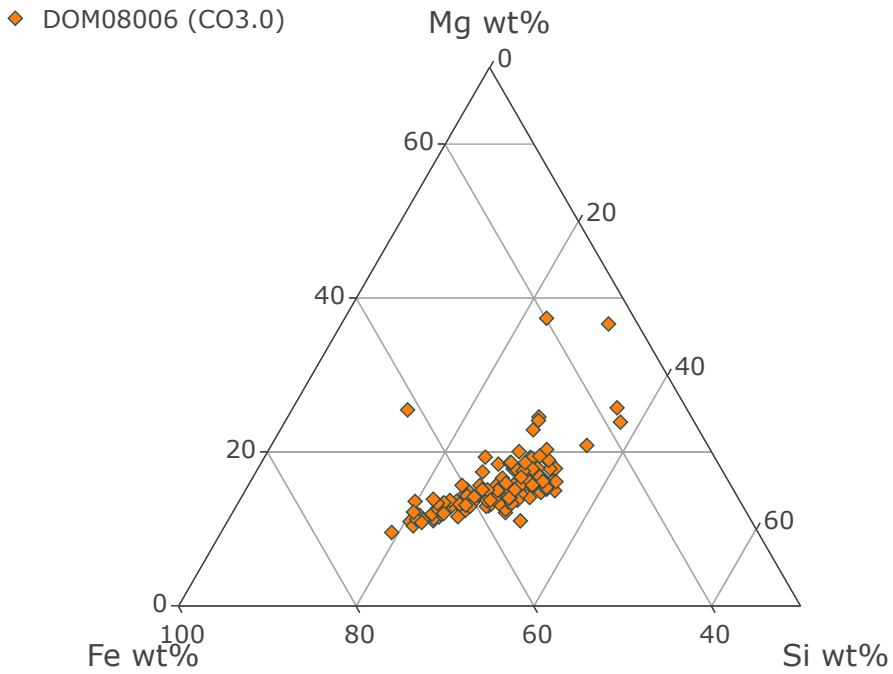


Figure 4.6: *Fe-Si-Mg ternary diagram of the matrix in DOM 08006, CO3.0. Data plotted are normalised to 100 and are in wt%.*

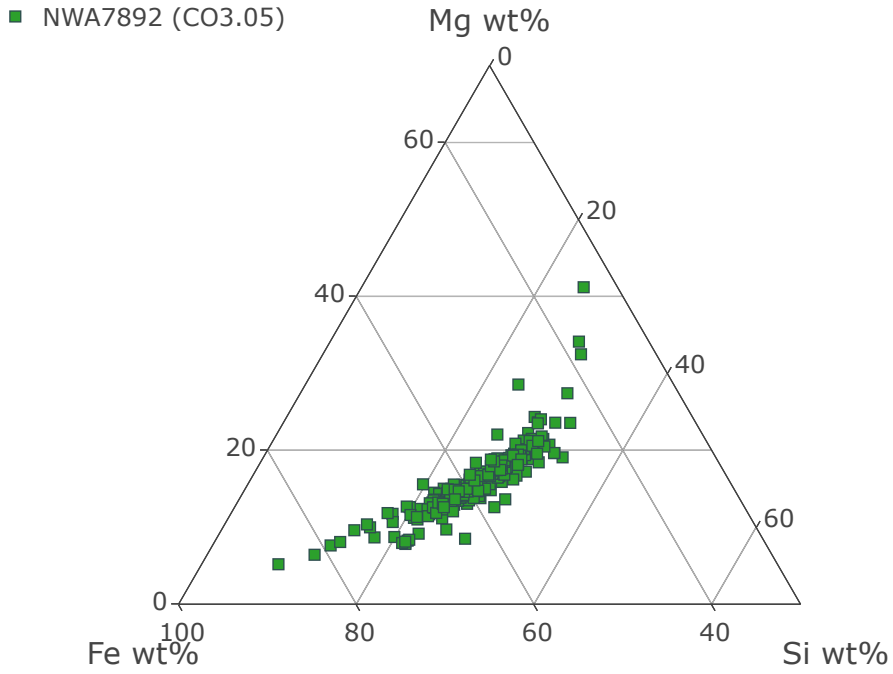


Figure 4.7: *Fe-Si-Mg ternary diagram of the matrix in NWA 7892, CO3.05. Data plotted are normalised to 100 and are in wt%.*

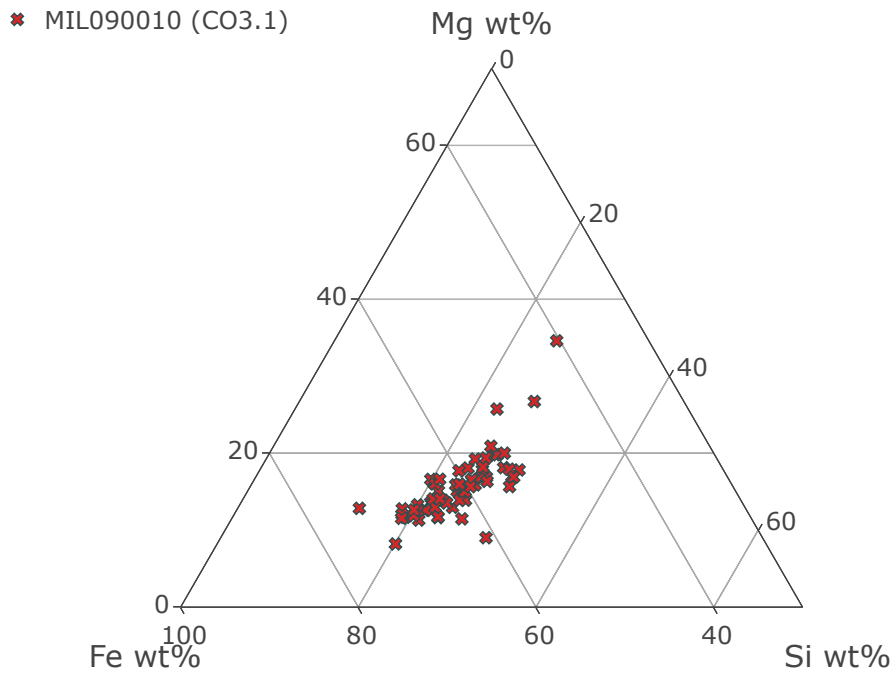


Figure 4.8: *Fe-Si-Mg ternary diagram of the matrix in MIL 090010, CO3.1. Data plotted are normalised to 100 and are in wt%.*

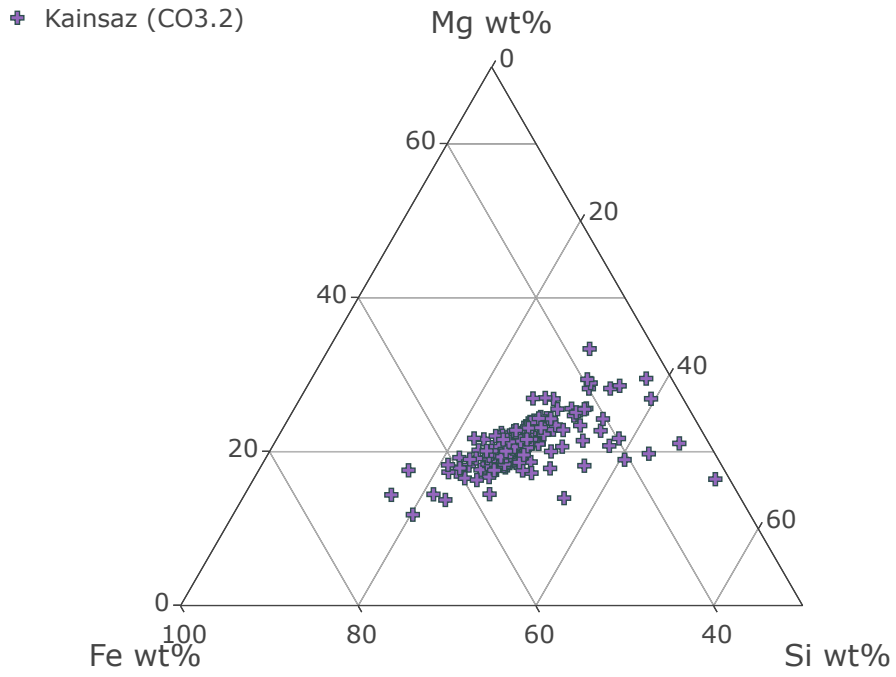


Figure 4.9: *Fe-Si-Mg ternary diagram of the matrix in Kainsaz, CO3.2. Data plotted are normalised to 100 and are in wt%.*

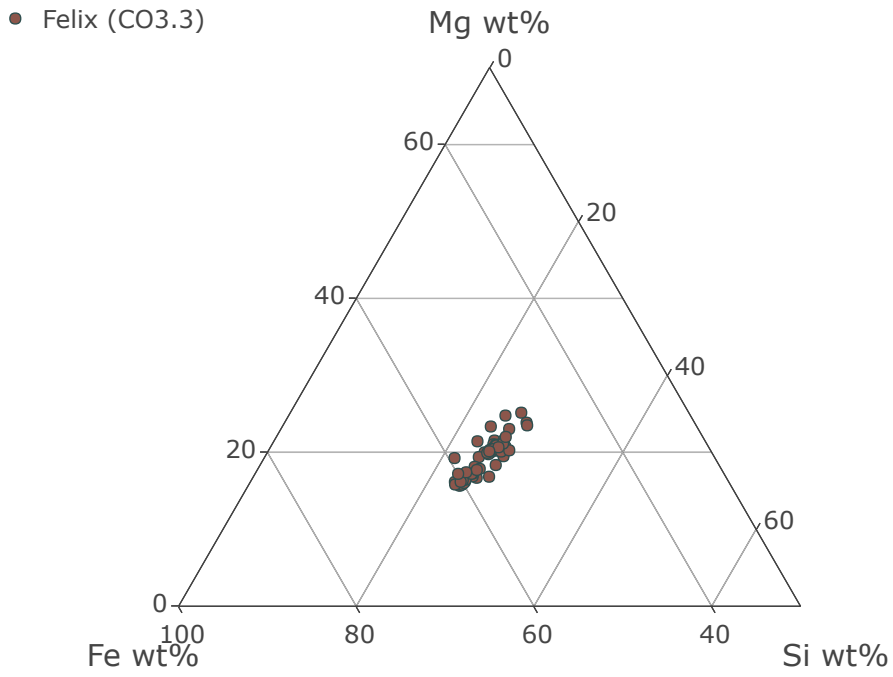


Figure 4.10: *Fe-Mg-Si ternary diagram of the matrix in Felix, CO3.3. Data plotted are normalised to 100 and are in wt%.*

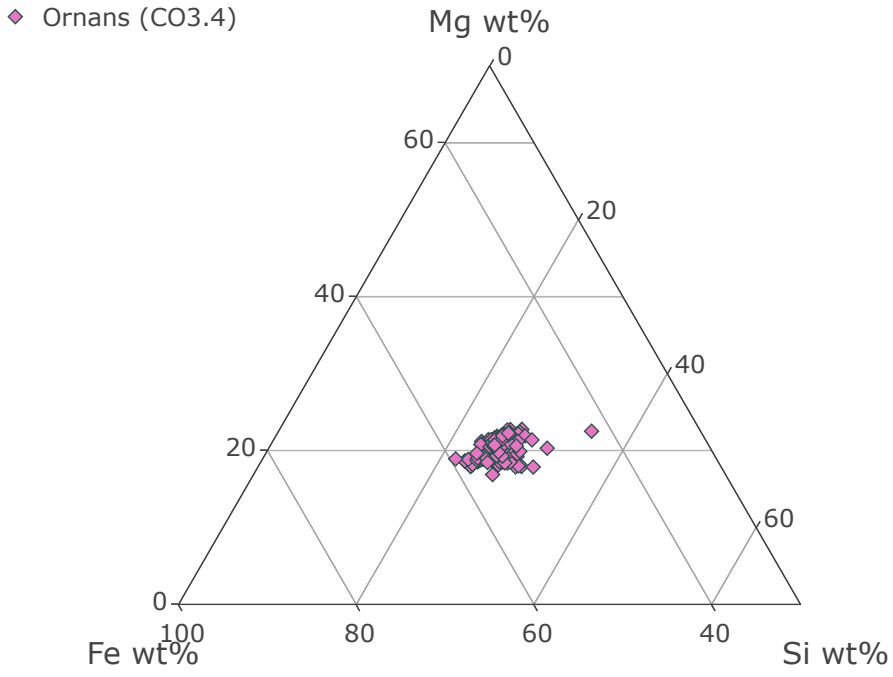


Figure 4.11: *Fe-Si-Mg ternary diagram of the matrix in Ornans, CO3.4. Data plotted are normalised to 100 and are in wt%.*

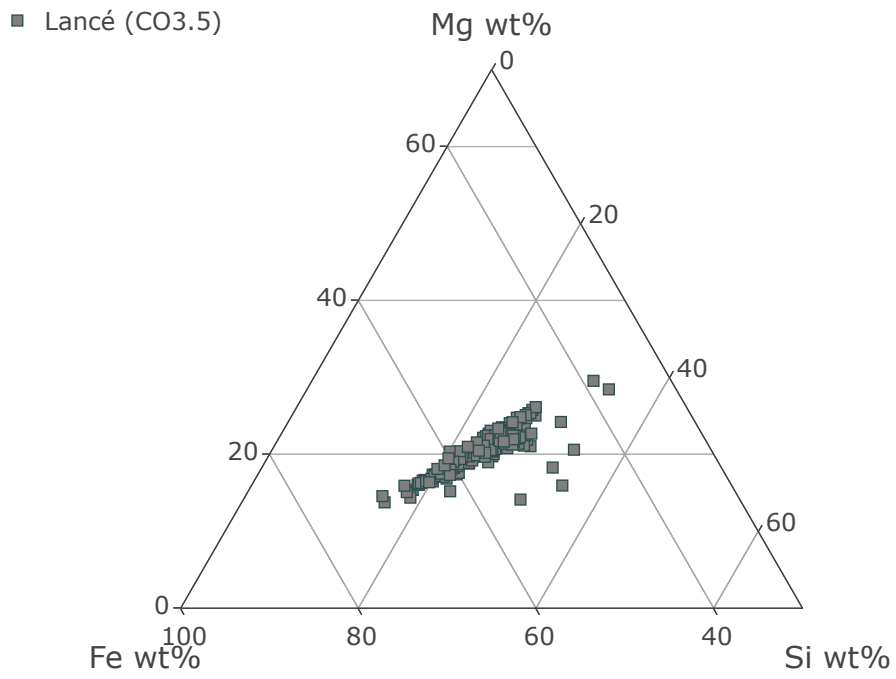


Figure 4.12: *Fe-Si-Mg ternary diagram of the matrix in Lancé, CO3.5. Data plotted are normalised to 100 and are in wt%.*

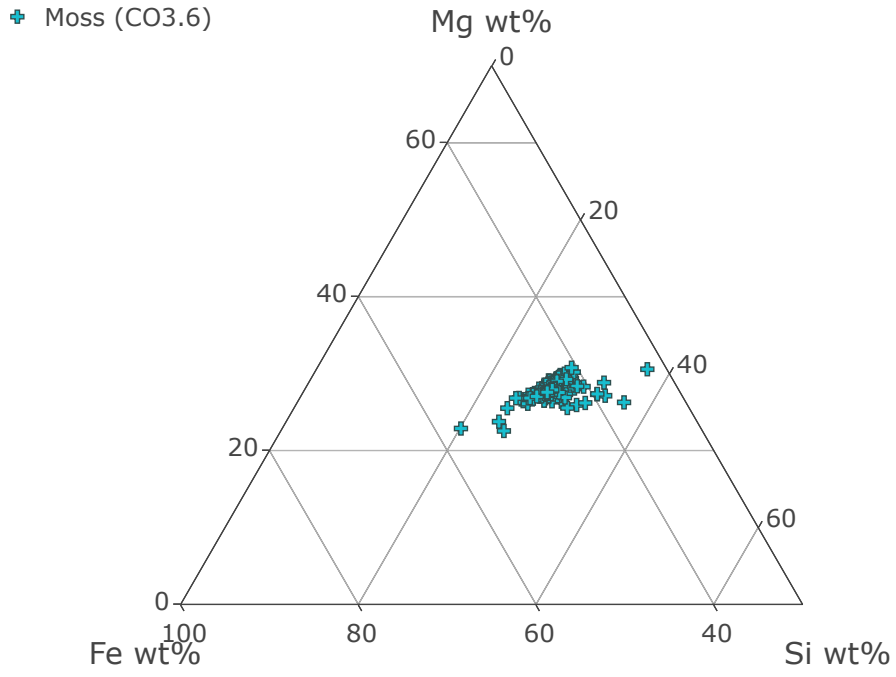


Figure 4.13: *Fe-Si-Mg ternary diagram of the matrix in Moss, CO3.6. Data plotted are normalised to 100 and are in wt%.*

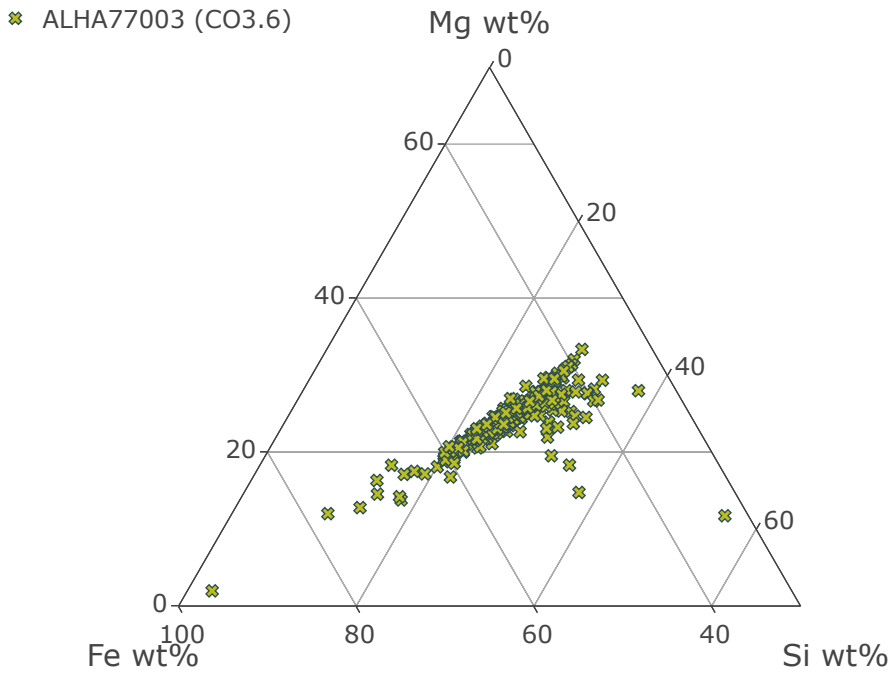


Figure 4.14: *Fe-Si-Mg ternary diagram of the matrix in ALHA77003, CO3.6. Data plotted are normalised to 100 and are in wt%.*

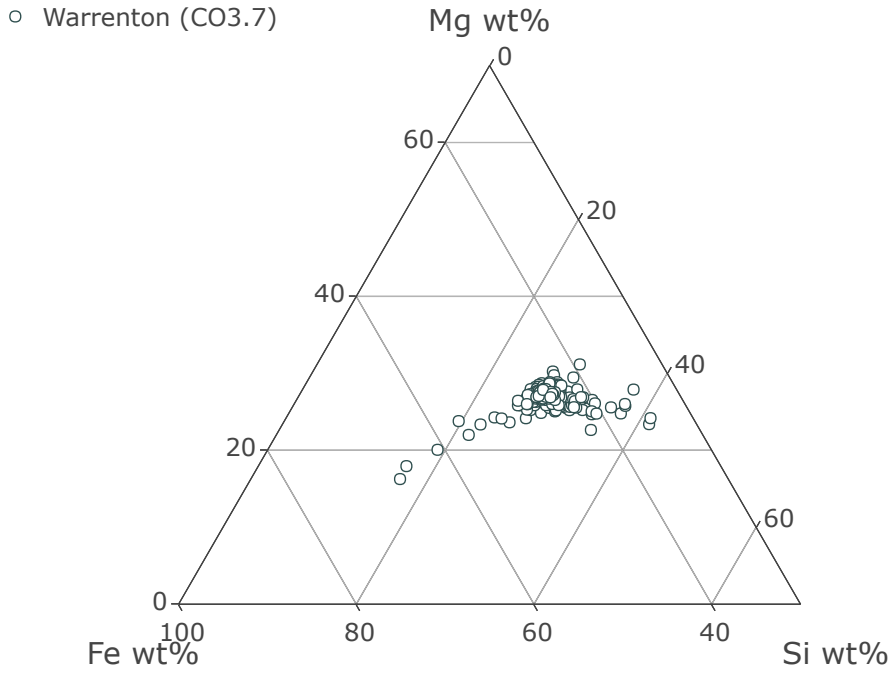


Figure 4.15: *Fe-Si-Mg ternary diagram of the matrix in Warrenton, CO3.7. Data plotted are normalised to 100 and are in wt%.*

0.10 and 0.23 wt% in most of the samples with the exception of Kainsaz (0.64 wt%), Ornans (0.37 wt%) and Warrenton (0.36 wt%) but with no relation to the petrologic subtype of the samples. However, systematic changes in abundance across the petrologic sequence do occur for Cr and Mg. Cr show an increase of about 0.13 wt% across the subtypes (Table 4.1), leading to highly metamorphosed samples having a more Cr rich matrix than the least-metamorphosed ones (Figure 4.2). At the same time, also Mg shows an increase of $\sim$ 5.9 wt% across the metamorphic sequence (Table 4.1), and it is also shown in Figure 4.3 for Mg values normalised for Si.

In contrast, Fe, Ni, and Ca show a decrease in their concentration in relation to increasing thermal metamorphism. Figures 4.4 and 4.5 show how Fe becomes depleted in the matrix of CO chondrites with increasing petrologic grade. Differences in Fe content in samples between 3.0 and 3.2 are relatively limited (Figure 4.4), with the samples having a broad range of Fe content between 1.5 and 4.0 wt%, whereas in higher petrologic types (>3.2) the Fe depletion becomes more evident (Figure 4.5). The concentration of Ni is highest in DOM 08006 and MIL 090010 ($\sim$2 wt%), whereas in Kainsaz it is 0.9 wt% before generally decreasing with petrologic type to 0.4 wt% in Warrenton. Ca is just above $\sim$ 1 wt% in NWA 7892, MIL 090010 and Kainsaz before falling below $\sim$ 0.5 wt% from subtype 3.3 onward, defining two groups, 3.0 - 3.2, and 3.3 - 3.8, rather than systematically decreasing with petrologic type.

Figures 4.6, 4.7, 4.8, 4.9 4.10, 4.11, 4.12, 4.13, 4.14, 4.15 show Fe, Si and Mg ternary diagrams for each CO chondrite analysed by EMPA. They illustrate how Fe abundance decreases (by $\sim$10 wt%) across the metamorphic sequence, while Mg increases. The presence of outliers from the main cluster are noticeable, which could possibly be related to the interaction of the beam with different mineralogical phases (e.g. metals, oxides). K, P, Co, V, Zn and S are present in the samples in such low amounts that often their abundance is below detection limit and therefore it is not reliable to make any conclusions concerning their variations with the COs matrix.

## 4.3 Transmission electron microscopy

### 4.3.1 Experimental

Transmission electron microscopy (TEM) was carried out only for selected samples within the petrologic range: DOM 08006 (CO3.00), NWA 7892 (CO3.05), MIL 090010 (CO3.1), Kainsaz (CO3.2), Ornans (CO3.4) and Moss (CO3.6). These samples were selected for the following reasons:

- In-depth characterisation of the pristine matrix in low petrologic type COs from 3.0 to 3.2
- Characterisation of the changes that are affecting the matrix of COs in relation to the degree of metamorphic alteration. Therefore samples were selected of petrologic types 3.4 and 3.6.

For each sample either 2 or 3 FIB sections were lifted from selected areas of matrix and prepared for TEM imaging. Each FIB section was attached to a different pin of the Cu TEM holder. The TEM analyses were carried out with an FEI T20 instrument operated at 200 kV, beam spot size 3; images were collected working in bright field, and diffraction patterns were obtained to characterise some components of the matrix and where possible identify specific minerals. FIB sections of DOM 08006, NWA 7892, MIL 090010, Kainsaz, Ornans and Moss were also imaged and EDX maps were collected with an FEI Quanta 650 FEG-SEM at 6 and 9 kV, with spot size 3 and a working distance of 13 mm. EDX maps of the FIB sections were used to support images collected using TEM, and used for determination of the mineralogy. The size of individual mineral grains was determined in 2D by measuring the longest axis. The porosity per area % for each FIB section was calculated using ImageJ, where it was possible to isolate specific greyscales setting the desired threshold. In this way, it was possible to differentiate between minerals, pores and resin as they have very distinct greyscales.

### 4.3.2 Descriptions

DOM 08006 (CO3.0) is the most primitive sample analysed in this work. TEM observations show that it is dominated by amorphous silicates and micro-crystalline phases

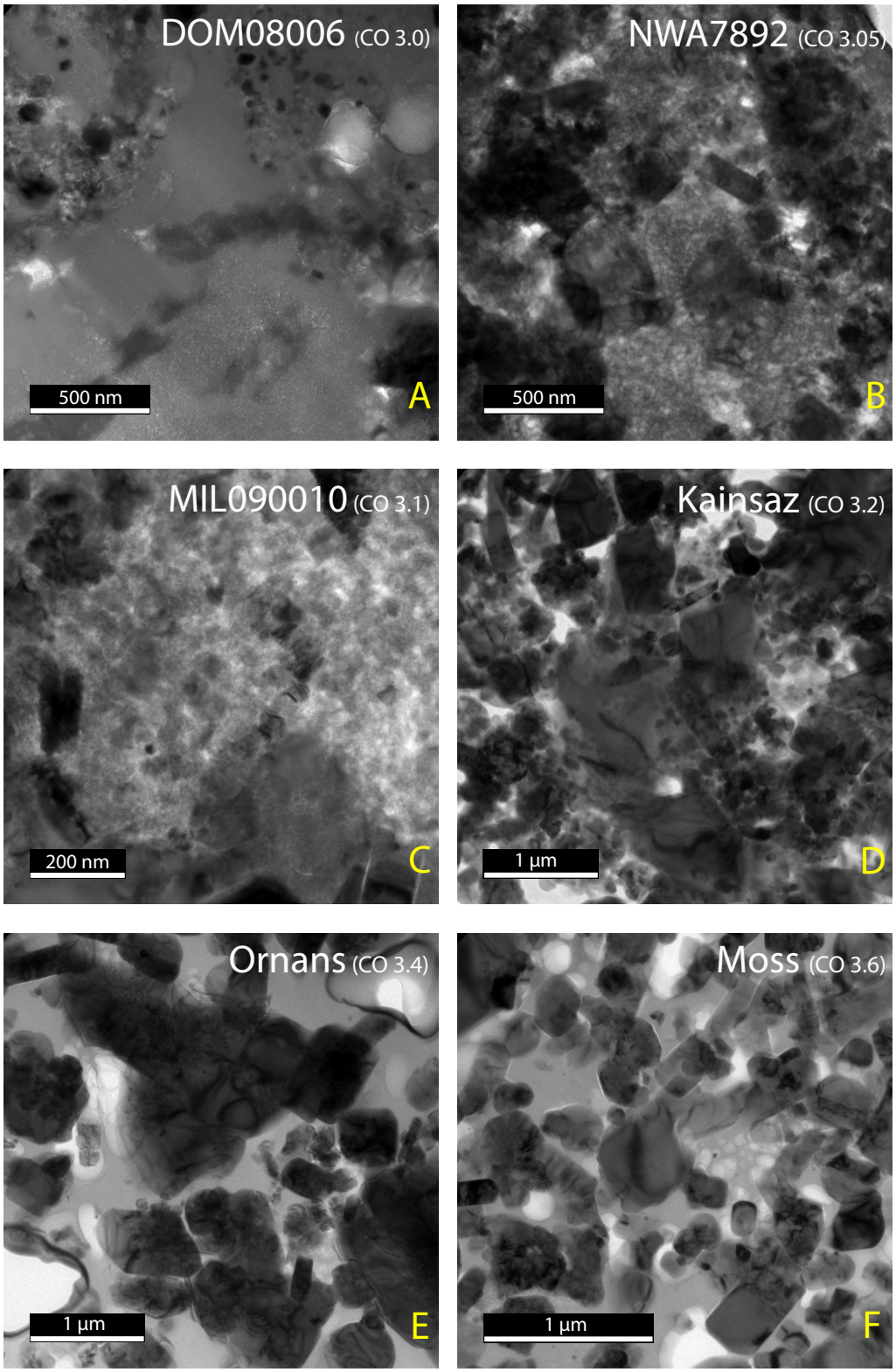


Figure 4.16: *Bright field TEM images of CO chondrites of varying petrologic type. The images highlight changes in texture with increasing thermal metamorphism. The samples are A) DOM 08006, CO3.0; B) NWA 7892, CO 3.05; C) MIL 090010, CO 3.1; D) Kainsaz, CO 3.2; E) Ornans, CO 3.4; F) Moss, CO 3.6.*

including sulphides, Fe-metal, Fe-oxide and traces of phyllosilicates (Figures 4.16a and 4.18) and it has an average porosity of ∼3 area %. The crystalline inclusions embedded in the amorphous matrix are generally very fine grained; for example sulphides have an average grain size of 150 nm, Fe-Mg silicate grains range between 130 nm and 450 nm while Fe-oxide can be slightly larger, ranging between 600 nm and 2.8 $\mu$m in size (Figures 4.17a and b). In some areas of the DOM 08006 FIB sections it is possible to observe dark boundaries as they are located in areas where there is a change in texture from smooth and homogeneous to microcrystalline (Figure 4.18d). In one of the FIB sections, I observed six examples of carbon nanoglobules (Figure 4.19), that appear to resemble the carbon nanoglobules that have been reported in other carbonaceous chondrites (Nakamura et al., 2002; Garvie & Buseck, 2004; Alexander et al., 2017), as they are often hollow and with a size ∼ 200 nm in size.

NWA 7892 (CO3.05) has a fluffy texture, described as consisting of very fine grained amorphous silicates and rich in nanometre size pores in which crystalline phases appear to be more abundant and larger than in DOM 08006 (Figure 4.20). FIB sections extracted from NWA 7892 show the presence of some euhedral minerals together with anhedral phases. Crystalline phases recognisable within the FIB sections of NWA 7892 include sulphides ranging from 150 to 500 nm in diametre, Fe-metal grains ranging from 130 nm to 340 nm diameter, Fe-Mg silicates with a grain size between 350 and 780 nm in diameter and Fe-oxide ranging from 270 nm to 800 nm diameter. Through EDX maps it was possible to see that nickel is present in submicron nuggets suggesting the presence of very small metal grains (Figure 4.17d). The presence of secondary phases, such as phyllosilicates, were recognised by measuring the distance between lamellae at the TEM, and carbonates recognised through SEM-EDX maps. Cross-cutting one of the FIB sections (Pin B) is a $CaCO_3$ vein 6.6 $\mu$m long and 1.3 $\mu$m wide (Figures 4.20a and 4.17c). In contrast to the more pristine sample DOM 08006, NWA 7892 has higher average porosity (∼ 4 area%), with pores varying in size depending on the FIB section (Figure 4.20a). This variation can be connected to the incipient crystallisation of the amorphous silicates.

MIL 090010 (CO3.1) has a similar texture to NWA 7892, an amorphous silicate ground mass, some phyllosilicates and the presence of euhedral crystals (4.16c). Fe-

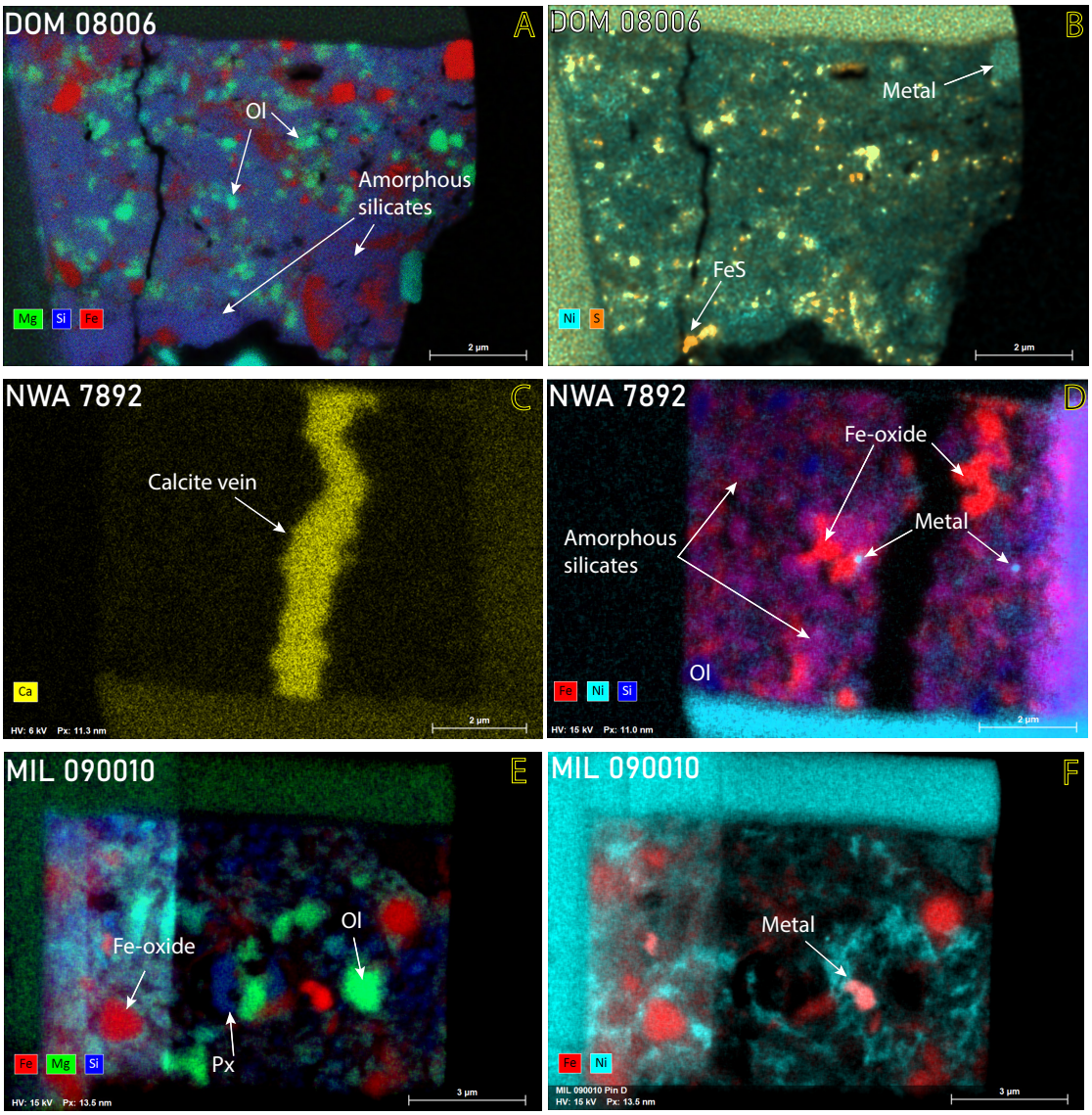


Figure 4.17: *SEM-EDX maps of FIB sections of: a) and b) DOM 08006 (CO3.0), c) and d) NWA 7892 (CO3.05), e) and f) MIL 090010 (CO3.1). For each EDX map are highlighted some mineralogical phases that were possible to recognise, with Ol: olivine and Px: pyroxene.*

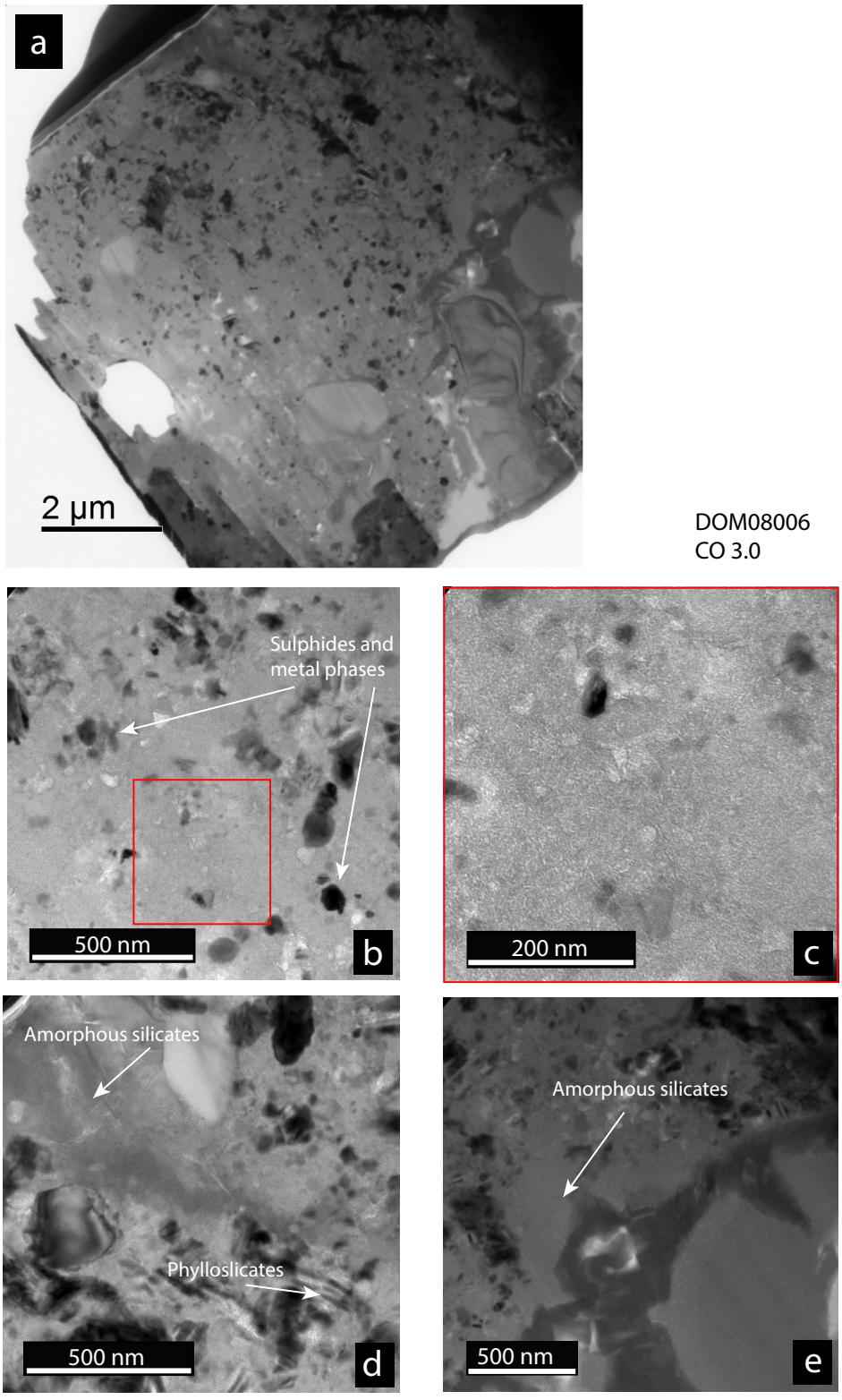


Figure 4.18: *a) Bright field TEM image of DOM 08006; b) shows a detail of the amorphous matrix containing small sulphide, oxide and metal grains; c) a close up of the amorphous matrix showing the presence of some micro-crystalline phases. d) shows the presence of elongated and layered mineral phases which are likely phyllosilicates and several larger silicate crystals; in e) is possible to see a dark boundary.*

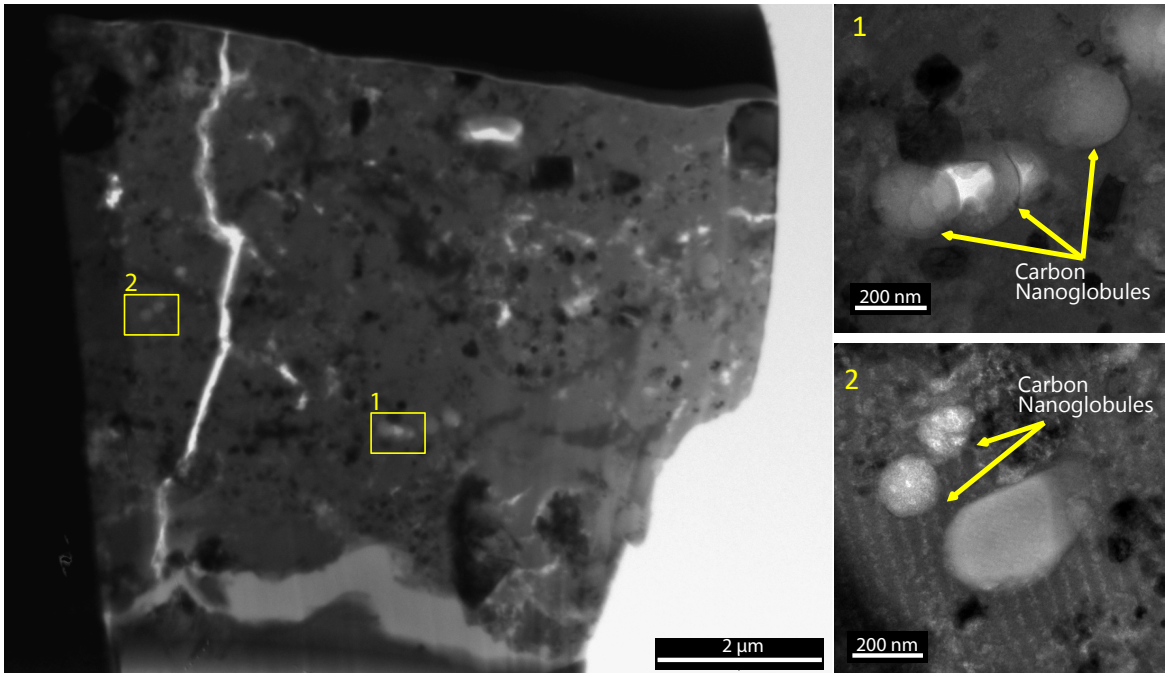


Figure 4.19: *Bright field TEM image of C nanoglobules in DOM 08006 (FIB section D).*

oxide crystals have sizes between 280 nm and 1 $\mu$m, Fe-metal is rare and it has a size of $\sim$270 nm, Fe-Mg silicates have sizes in the range of 300 nm to 1 $\mu$m, while sulphides range between 90 and 150 nm in size (Figures 4.17e and f). The average porosity measured for MIL 090010 is $\sim$ 1 area %. In one of the FIB sections (Pin D) there is an inclusion that resembles the texture of DOM 08006. In addition, in the FIB section of Pin C there is a very circular structure that is reminiscent of an agglomeration of dust particles (Figure 4.21).

In Kainsaz (CO3.2) the matrix has a texture mainly composed of euhedral minerals, there is no evidence either of amorphous silicates or phyllosilicates (Figure 4.16d). Fe-Mg silicate crystals have grain sizes between 200 nm and 1.3 $\mu$m, while metal grains are rare and have a size range of 1.3 to 1.6 $\mu$m Figure 4.22a and b). At the same time, the average porosity in Kainsaz is higher than for the lower petrologic samples as it is $\sim$ 8 area %.

Ornans (CO3.4) is composed of euhedral crystals, but overall the matrix material appears very porous (Figures 4.16e and 4.23a and b), indeed the average porosity increases to about 20 area %. Fe-Mg silicate crystals have sizes ranging from 1.1 $\mu$m to 2 $\mu$m, metal and sulfides have sizes of $\sim$1 $\mu$m. Amorphous silicates and phyllosilicates

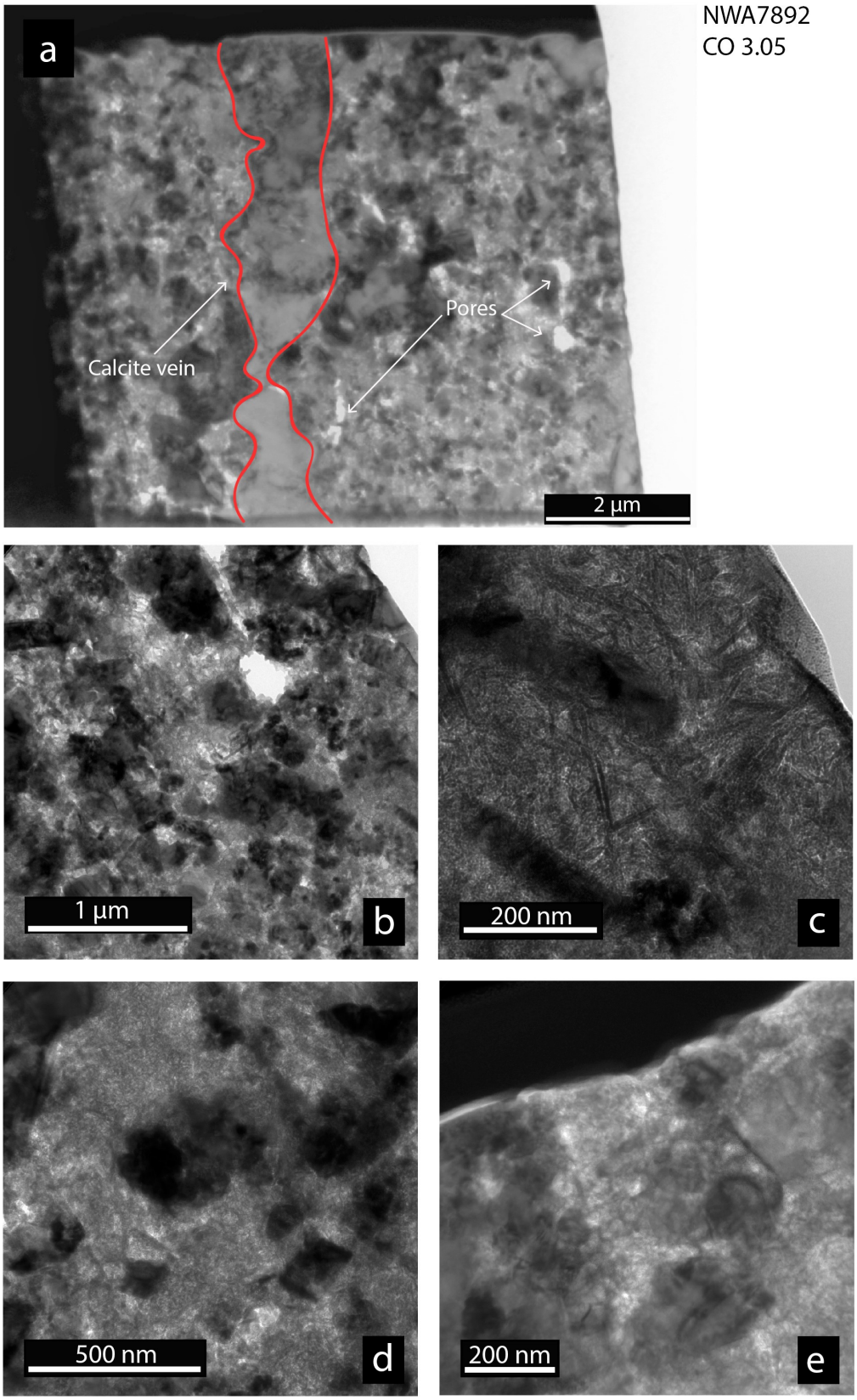


Figure 4.20: *a) Bright field TEM overview image of NWA 7892; b) shows sulphides, phyllosilicates and Fe-Mg silicates embedded in the amorphous matrix; c) a close up of the amorphous matrix showing the formation of elongated crystals and possibly phyllosilicates;, d) and e) show how crystalline material is replacing the amorphous silicates and sulphides are growing in size.*

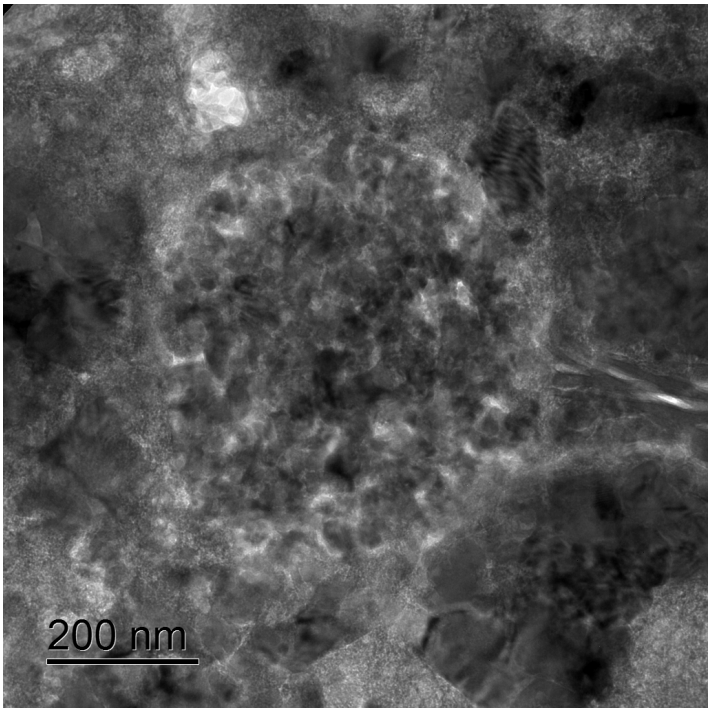


Figure 4.21: *Agglomeration of dust particles observed in bright field TEM in the matrix of MIL 090010 (CO3.1).*

are absent.

Moss (CO3.6) is characterised by well crystallised euhedral crystals, the absence of amorphous silicates, and a porosity of $\sim$ 25 area %. Fe-Mg silicate crystals range between 200 nm and 3.3 $\mu$m with an average size of 1.3 $\mu$m. In contrast to the lower petrologic type samples, Moss contains some Cr-rich grains that from EDS spectra seem to be chromite (no Al or Si in them), which form beside the olivine (Figure 4.24) as result of exolution from the olivine. These chromite inclusions range between 170 nm and 850 nm. Based on the SEM-EDX maps no magnetite crystals were identified, and only one sulphide was found in one of the FIB sections (Pin C) with a size of 985 nm.

## 4.4 Scanning Transmission X-ray microscopy

C, N and O K-edges are caused by the excitation of the 1s core shell electrons to their lowest unoccupied molecular orbitals such as $\pi^*$ or $\sigma^*$, while for the Fe $L_{2,3}$-edge they are produced by the 2p $\rightarrow$ 3d electron transitions (Cressey et al., 1993; Wasinger et al., 2003). Their spectra are obtained by measuring the absorption energy of a

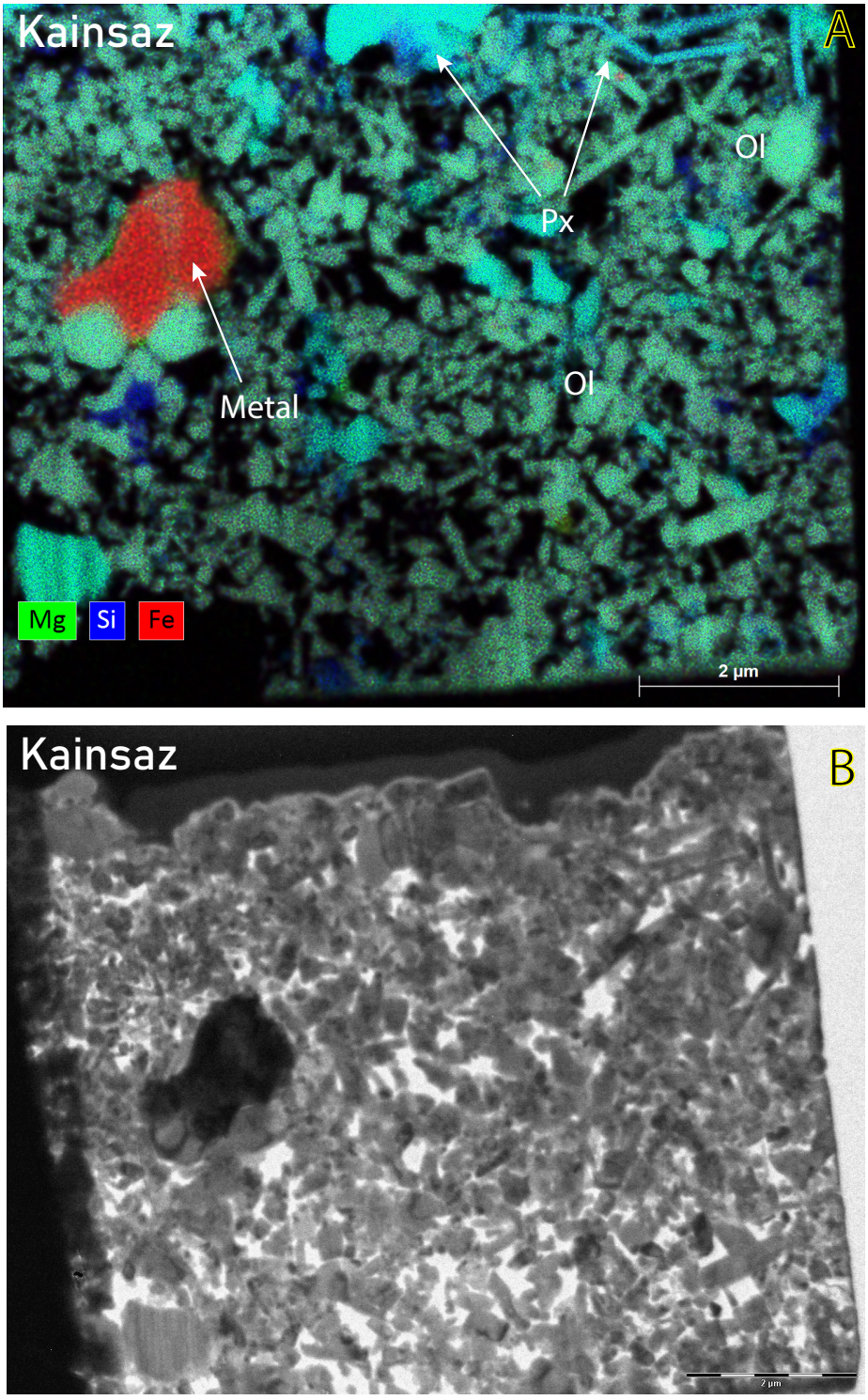


Figure 4.22: *A) SEM-EDX map and B) Bright field TEM image of a FIB section of Kainsaz (CO3.2), showing the presence of olivine (Ol), pyroxene (Px) and metal.*

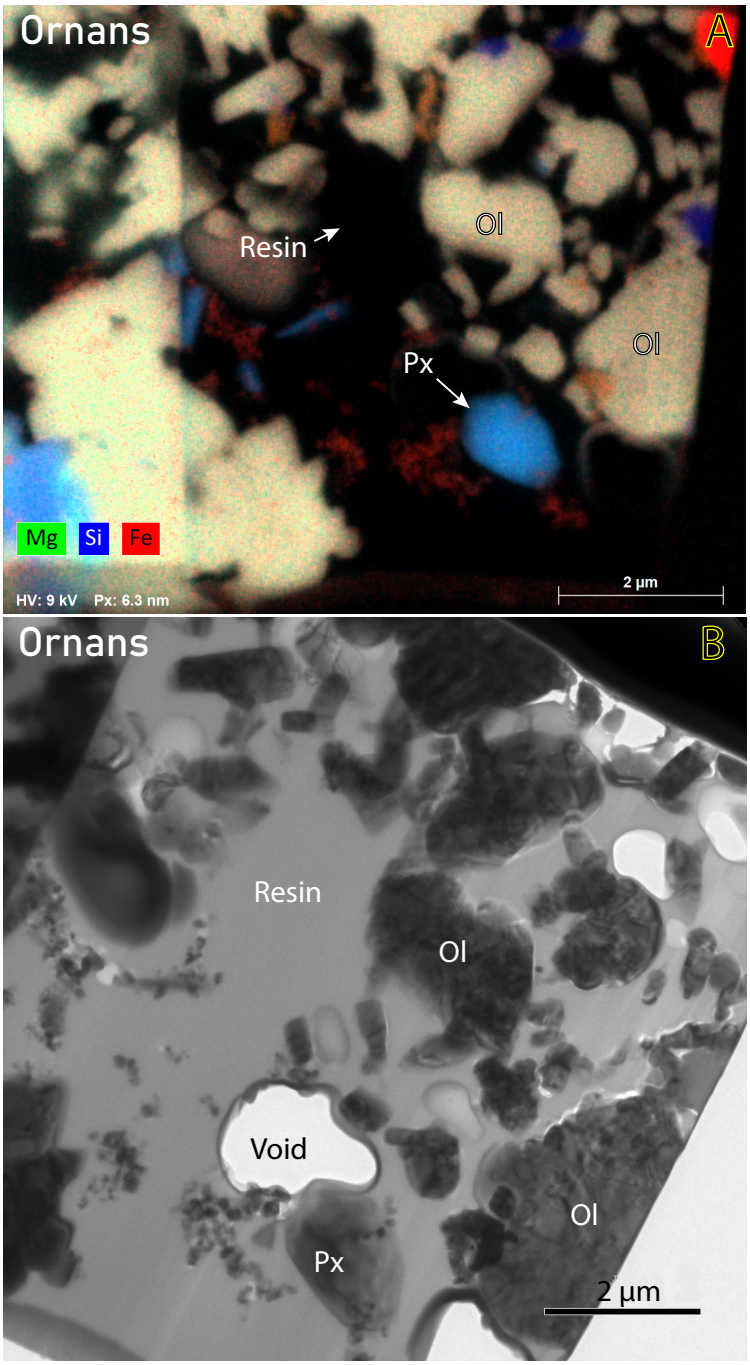


Figure 4.23: *A) SEM-EDX map and B) Bright field TEM image of a FIB section of Ornans (CO3.4),showing the presence of olivine (Ol), pyroxene (Px) and metal. Moreover, in B) is possible to notice how poorly consolidated the minerals are within the sample.*

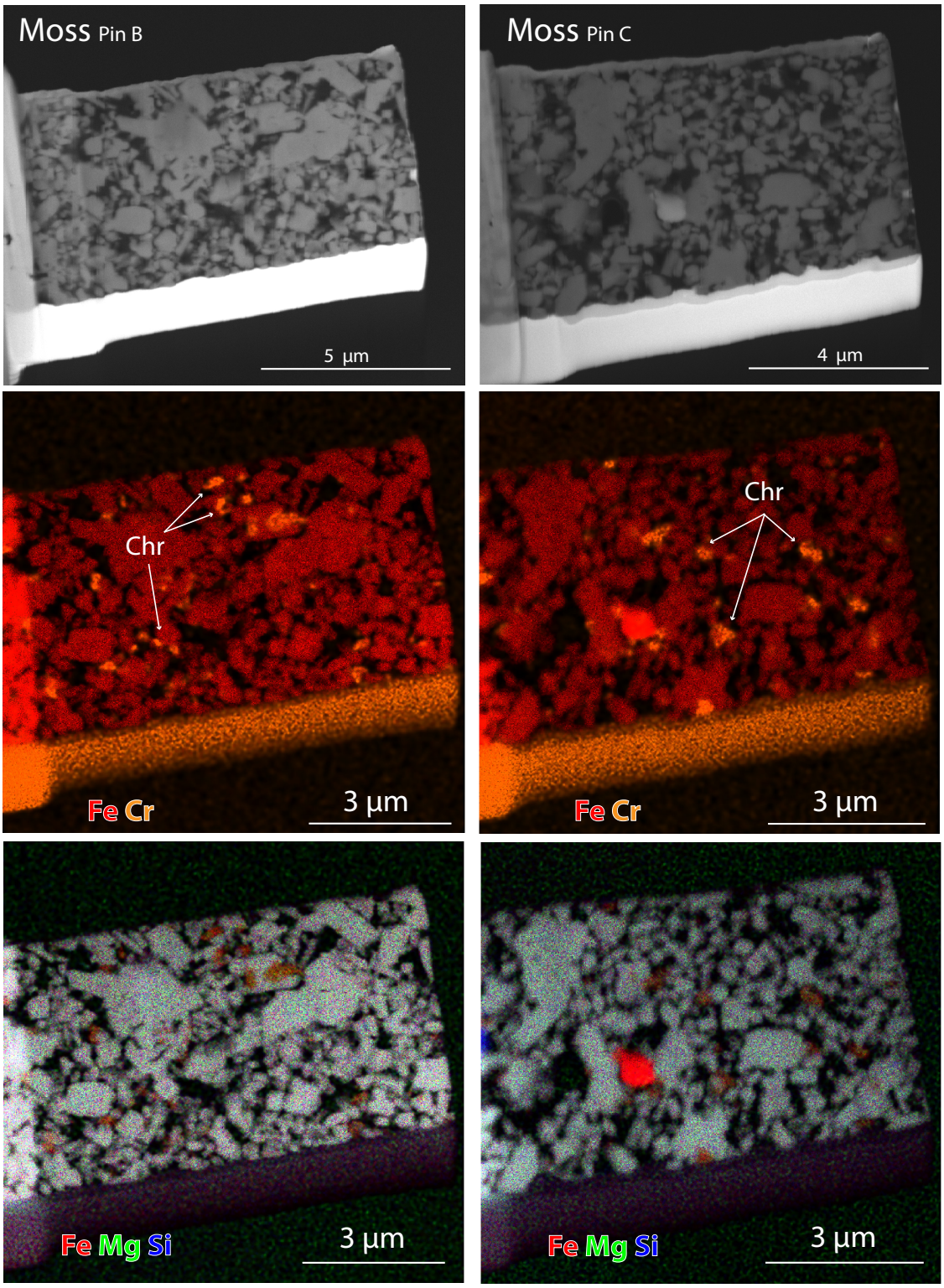


Figure 4.24: *SE images and SEM-EDX maps of FIB sections of Moss (CO3.6). In the Fe-Cr maps it is possible to see the chromite (Chr) grains that formed as result of diffusion from the olivine matrix.*

monochromated beam of X-rays when scanning the absorption edge of an element (Alexander et al., 2017).

### 4.4.1 XANES: Fe L-edge

Fe $L_3$-edge XANES provides information about the oxidation state of Fe, which can be very useful for determining important information about the environmental conditions during the formation of the solar system as well as parental body processes. For this study, the determination of the $Fe^{3+}/\Sigma Fe$ ratios in the amorphous and crystalline matrix silicates enables me to constrain the formation and evolution of amorphous silicates and therefore provide a basic understanding of the earliest stages of planet formation. The Fe $L_3$-edge is at different energies depending on the oxidation state of the Fe, $L_3$ at 708.7 eV for $Fe^{2+}$ and $L_3$ at 710.25 eV for $Fe^{3+}$; their relative intensities are respectively related to the abundance of $Fe^{2+}$ and $Fe^{3+}$ (Cressey et al., 1993; Schofield et al., 1995; Bourdelle et al., 2013; Le Guillou et al., 2015).

### 4.4.2 Experimental

Based on methods described in Chapter 2, the measurements were carried out between 700 - 730 eV with variable energy increments ($\Delta$E). The measurements were made of single region of interest (ROI) of approximately 4 x 4 $\mu$m with 100 x 100 pixels, 40 nm pixel sizes, 5 to 10 ms dwell time and photon energy increment of 0.1 eV immediately below and above the absorption edges. For each sample several ROIs were collected in order to map the entire sample, and spectra were extracted from each pixel of the ROI. The samples analysed were FIB sections of: DOM 08006, NWA 7892, MIL 090010, Kainsaz, Ornans and Moss. Reference standards such as San Carlos olivine and an Fe-(oxy)hydroxide were also measured, in order to calibrate the measurement as they are respectively $Fe^{2+}$ and $Fe^{3+}$ bearing minerals.

### 4.4.3 Results

Fe $L_3$-edge XANES of the selected samples clearly show variations between samples through the petrologic scale. Figure 4.25 shows typical Fe $L_3$-edge spectra extracted

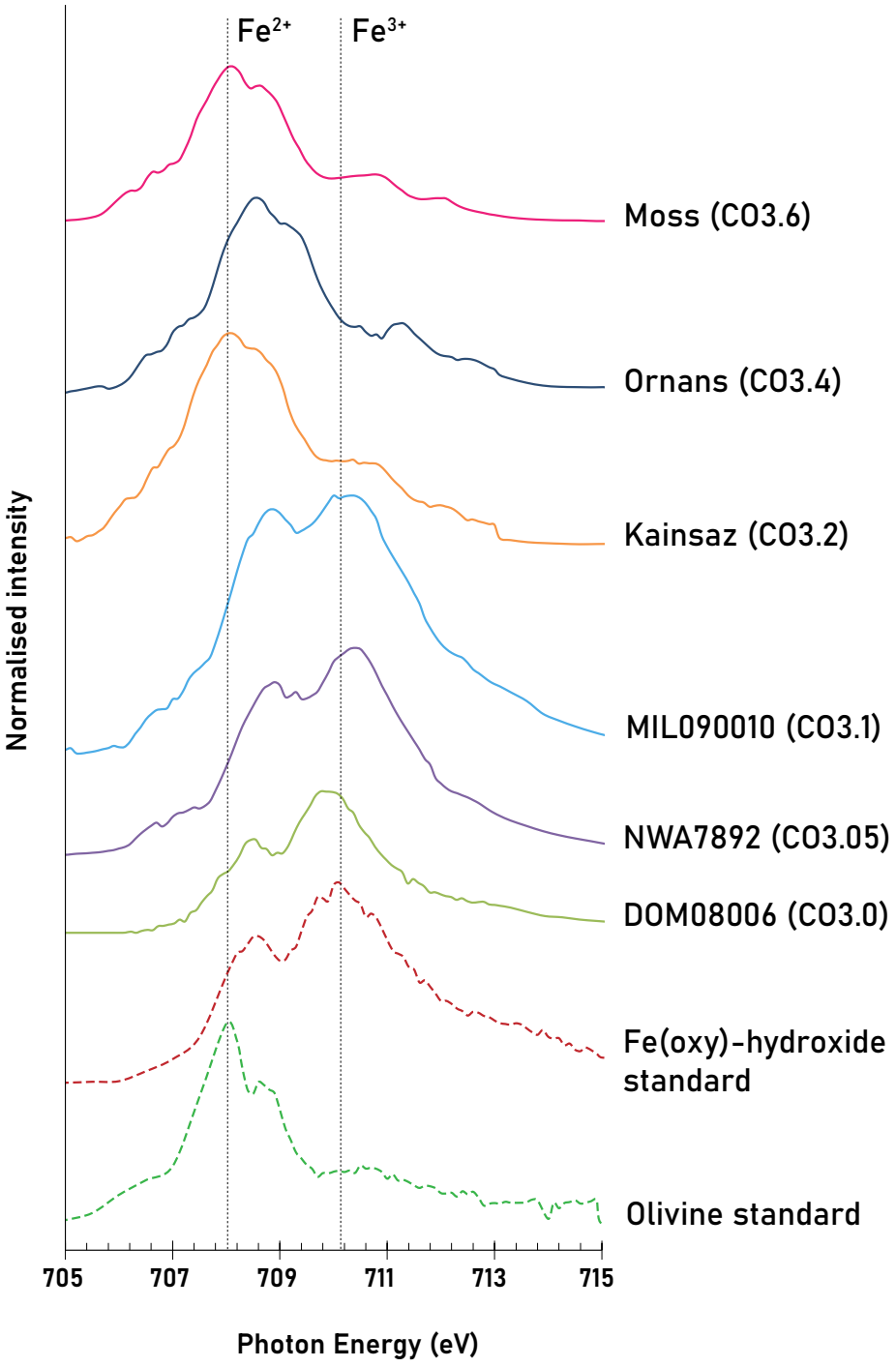


Figure 4.25: *Fe $L_3$-edge XANES spectra (705-715 eV) of San Carlos olivine and Fe-(oxy)hydroxide standards in relation to silicates in the CO chondrites DOM 08006, NWA 7892, MIL 090010, Kainsaz, Ornans and Moss. Highlighted are the differences in Fe oxidation state with reference to the characterisic spectral shapes of the $Fe^{2+}$ of the San Carlos olivine and of the $Fe^{3+}$ of the Fe-(oxy)hydroxide. The spectra of the silicates of CO3 samples show variations in the relative abundance of $Fe^{2+}$ and $Fe^{3+}$ with increasing metamorphism.*

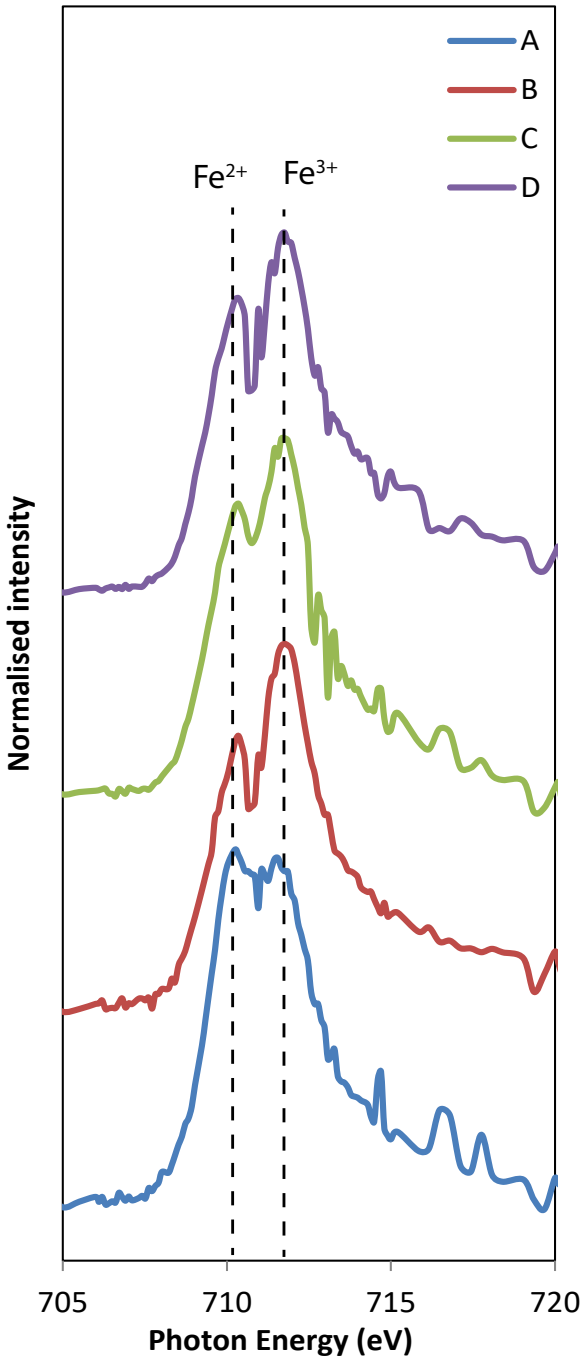


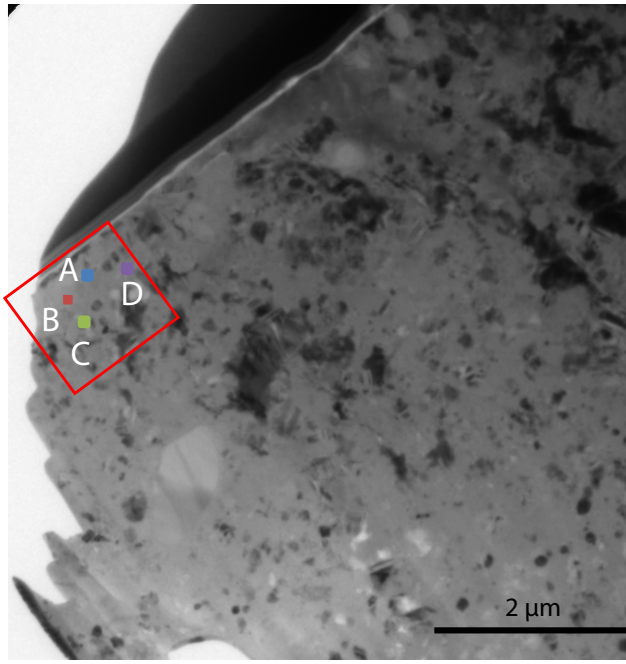


Figure 4.26: *Fe L-edge spectra extracted from the regions indicated on a FIB section of DOM 08006. The positions of the $Fe^{3+}$ and $Fe^{2+}$ peaks are indicated. The majority of spectra from DOM 08006 are dominated by $Fe^{3+}$ (spectra B, C and D), however in spectrum A can be inferred the presence of $Fe^{2+}$ as the spectrum is characterised by $Fe^{2+}$ and $Fe^{3+}$ having the same peak intensity.*

from silicates in DOM 08006, NWA 7892, MIL 090020, Kainsaz, Ornans and Moss compared to spectra for San Carlos olivine ($Fe^{2+}$) and an Fe-(oxy)hydroxide ($Fe^{3+}$). DOM 08006 is dominated by $Fe^{3+}$ (Figure 4.25), instead NWA 7892 and MIL 090010 shows variations in the relative intensities of $Fe^{3+}$ and $Fe^{2+}$ (Figure 4.25). In contrast, spectra from silicates in Kainsaz, Ornans and Moss (Figure 4.25) are more consistent with $Fe^{2+}$.

Based on comparison to the mineral standards and the methods of Cressey et al. (1993); Herd et al. (2001); van Aken & Liebscher (2002), I can qualitatively infer that silicates in the matrix of DOM 08006 are dominated by $Fe^{3+}$ (Figure 4.26), Kainsaz contains about 10% $Fe^{3+}$, and Moss is dominated by $Fe^{2+}$. The spatial variation in the spectra was much greater for DOM 08006, with some regions found to be less $Fe^{3+}$-rich than others (Figure4.26). Overall, with increasing petrologic type the intensity of the absorption peak relative to the $Fe^{2+}$ increases whereas the intensity absorption peak for the $Fe^{3+}$ decreases (Figure 4.25).

### 4.4.4 XANES: C, N, O K-edge

X-ray absorption near edge structure analyses of C, N and O K-edges are an excellent tool for the chemical and spatial characterisation of OM distributed within the matrix of primitive meteorites. In this study, the attention is focused on looking for traces of OM, and to relate its location within the matrix to the surrounding mineralogy in order to understand if organic matter is associated with particular minerals and/or textures.

Correlating the Fe L-edge study with organic speciation enables assessment of the redox condition in the disk environment, or parent body processing such as local aqueous alteration or larger scale metamorphism.

### 4.4.5 Experimental

Based on methods described in Chapter 2, the measurements were carried out between 278 - 310 eV for the C K-edge, 388 - 425 eV for the N K-edge and 520 - 560 eV for the O K-edge. Variable energy increments were selected to match the energies of important spectral features. FIB sections used for the study of the C, N and O K-edges are the

| Functional Group | Formula | Transition | Energy (eV) |
|---|---|---|---|
| | | Carbon | |
| Aromatic | C=C | 1s-$\pi^*$ | 285.2 |
| Ketones | C=O | 1s-$\pi^*$ | 286.0 - 286.4 |
| Carboxyl | COOH | 1s-$\pi^*$ | 288.5 |
| Carbonate | $CO_3$ | 1s-$\pi^*$ | 290.3 - 296 |
| | | Oxygen | |
| Carboxyl | COOH | 1s-$\pi^*$ | 532.0 |
| Alcohol, Ether | $CH_xO$ | 1s-3p/s$^*$ | 534.4 |

Table 4.2: *C and O-XANES transitions and associated functional groups considered in the present work, (Cody et al., 2008; Alexander et al., 2017).*

same as those used for the analysis of the Fe L-edge. In order to minimise the damage to the OM, Fe L-edge XANES were collected afterwards due to the higher energies involved. The measurements were made of single ROI of approximately 4x4 $\mu$m (100x100 px), 40 nm pixel size and 5 to 10 ms dwell time. For each sample I collected several ROIs in order to map the entire sample, and spectra were extracted for each pixel of the ROI. Spectra present different peaks each of which has a position characteristic of a specific bond criteria species or functional group (Table 4.2) while the intensity reflects the abundance of the species; these are both key factors for determining the nature of the OM.

### 4.4.6 Results: C K-edge

C K-edge XANES maps were collected from FIB sections of the following samples spanning most of the petrologic scale for COs: DOM 08006, NWA 7892, MIL 090010, Kainsaz, Ornans and Moss. Because of time and instrument software limitations it was not possible to collect just a single high resolution map for an entire FIB section, therefore I collected maps from several ROIs, which covered the majority of the surface of the FIB sections.

Looking at the C K-edge XANES maps collected for the most primitive samples such as DOM 08006 (CO3.0), NWA 7892 (CO3.05) and MIL 090010 (CO3.1), a spectral variability within the FIB sections of each sample was identified. The spectral variations identified can be grouped together based on distinct features that are related to discrete functional groups, with different relative intensities. For DOM 08006, NWA

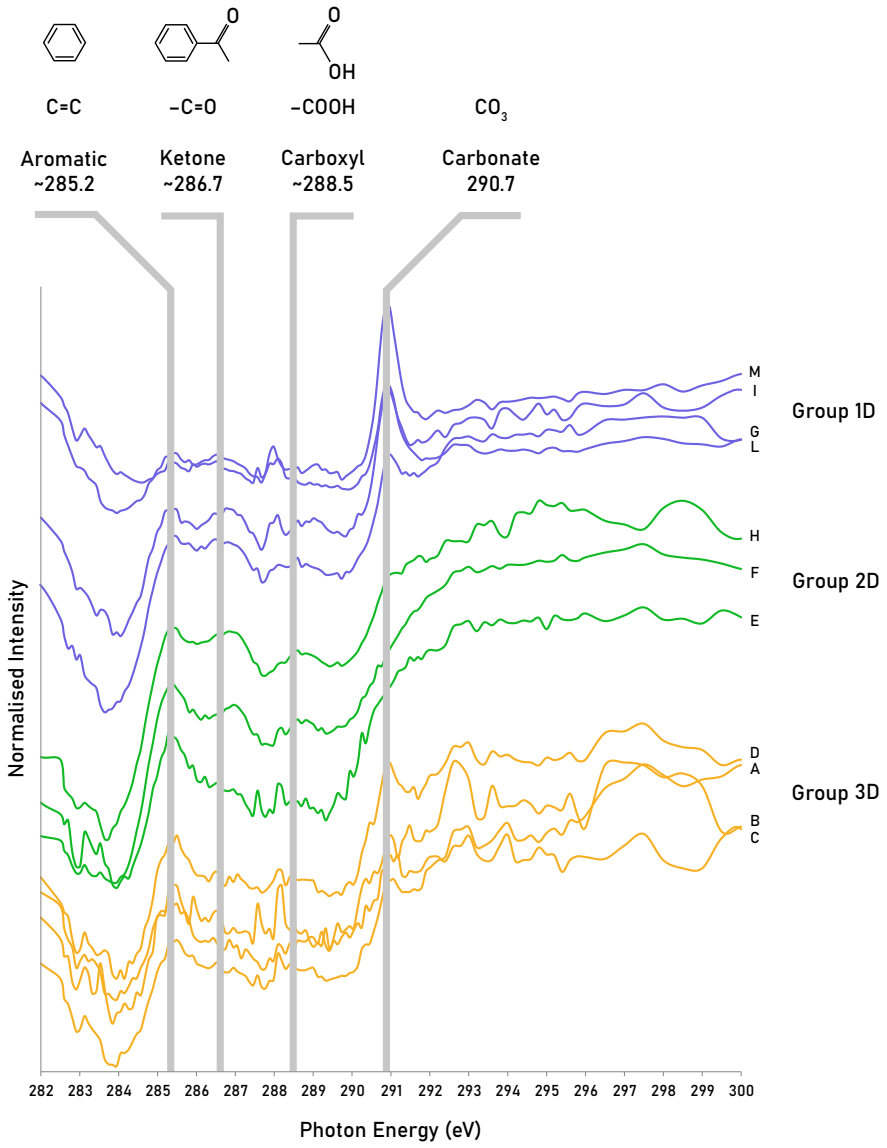


Figure 4.27: *C K-edge XANES spectra of DOM 08006, CO3.0. Example of spectral variability collected throughout a whole FIB section. Each group of spectra show distinct spectral features related to functional groups and relative intensities. Letter "D" in groups' name refers to DOM 08006; single spectra are labelled following the order in which they were extracted.*

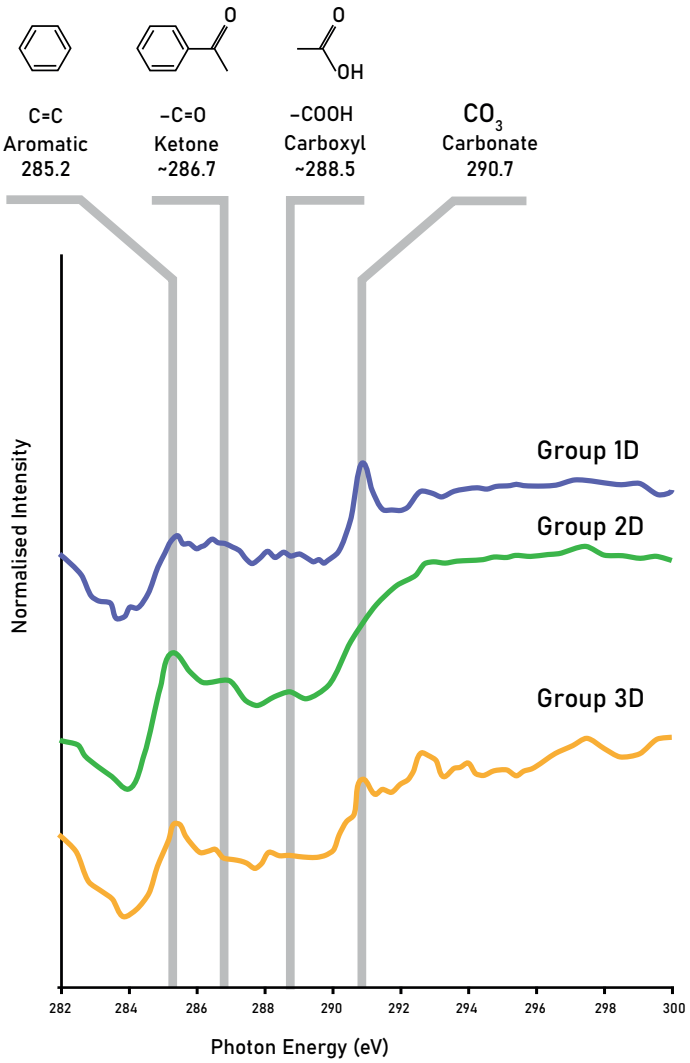


Figure 4.28: *C K-edge XANES spectra of DOM 08006, CO3.0. Spectra collected throughout the whole FIB section showed variations which can be can be represented by three main spectral groups: group 1D, group 2D and group 3D. Each group is characterised by distinct spectral features related to functional groups and relative intensities.*

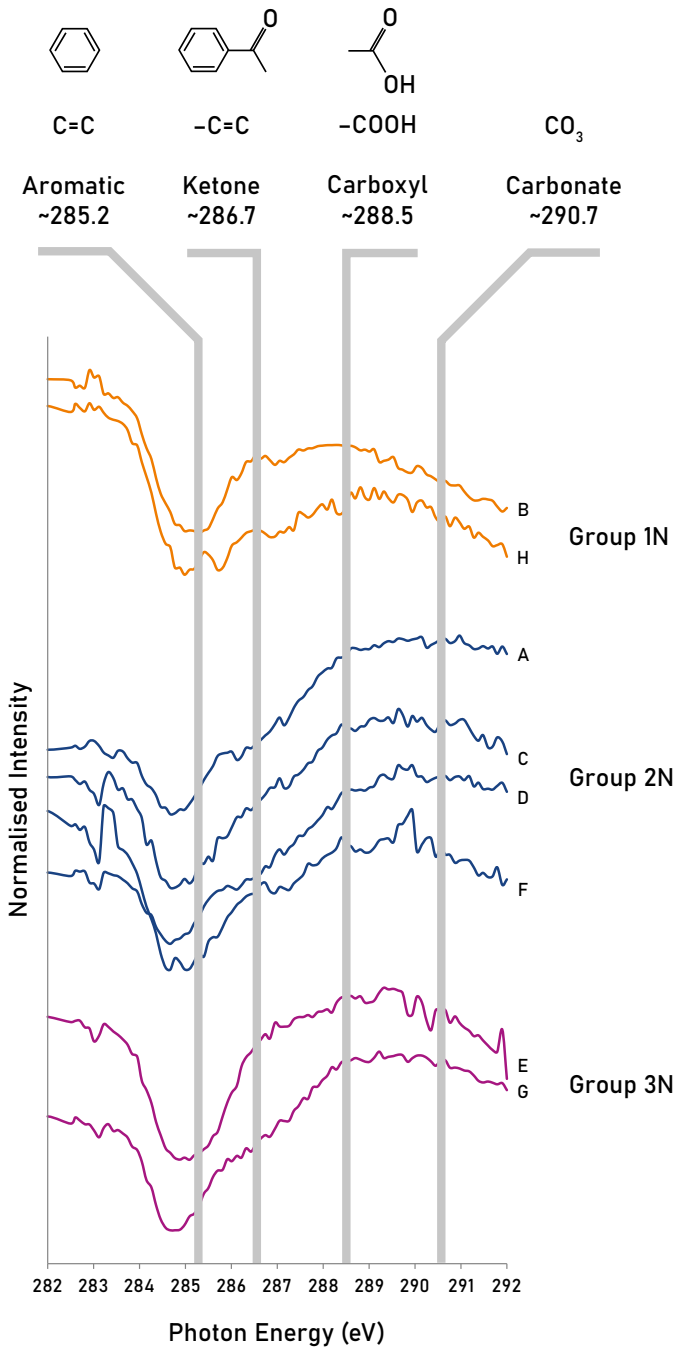


Figure 4.29: *C K-edge XANES spectra of NWA 7892, CO3.05. Spectra collected throughout the whole FIB section showed variations which can be can be represented by three main spectral groups: group 1N, group 2N and group 3N. Each group is characterised by distinct spectral features related to functional groups and relative intensities. Letter "N" in groups' name refers to NWA 7892; single spectra are labelled following the order in which they were extracted.*

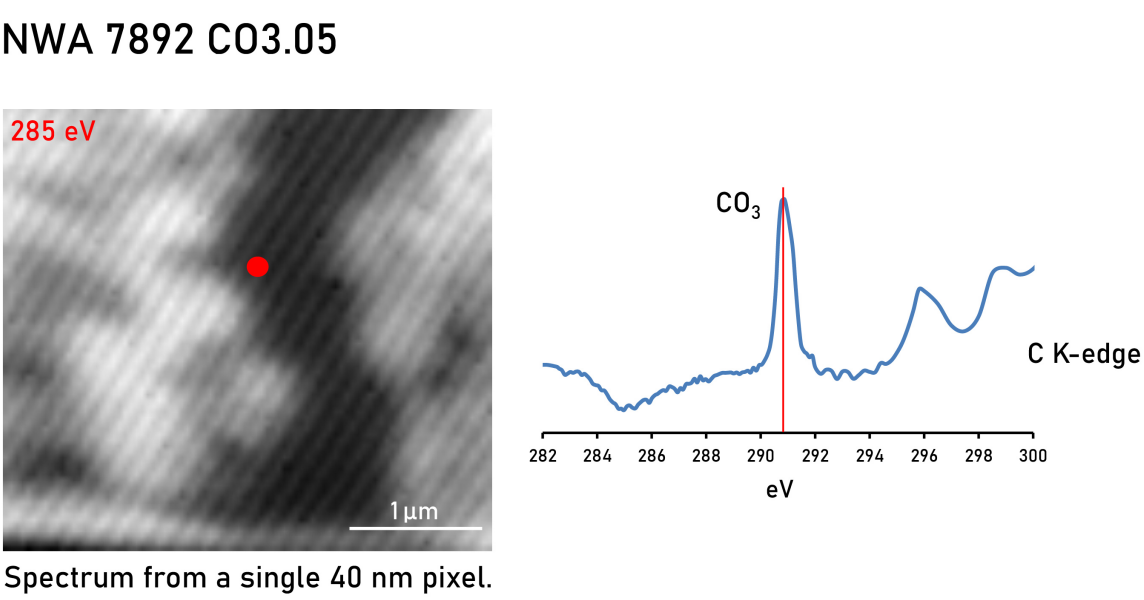


Figure 4.30: *C K-edge XANES spectra of the calcite vein (black) in NWA 7892 at 285 eV. The spectrum was extracted from a single 40 nm pixel, and its highlighted by the red dot.*

7892 and MIL 090010, all the spectra from across the samples could be summarised in three spectral groups. It is important to note that these three groups however are different between DOM 08006, NWA 7892 and MIL 090010.

DOM 08006 is the most primitive and pristine CO available for study and these aspects are also reflected in the variability of organic material found within its matrix. For each map collected, absorption spectra were extracted from single pixels and they show constant variations in the functional groups and their relative intensities. An example of how the data were extracted from each map and how the groups were determined is shown in Figure 4.27 for DOM 08006 (ROI 1 from Pin C). The spectra were extracted from hundreds of pixels throughout the ROI where a clear signal related to the presence of C was detected; in Figure 4.27 are shown the most representative spectra which show differences in their peaks and relative intensities in relation to their location within the region of interest. Group 1D (Figure 4.28), which corresponds to spectra G, I, L, and M in Figure 4.27, is characterised by weak absorption peaks at ~285.2 eV corresponding to aromatic C (C=C), and at ~286.7 eV related to ketone (C=O), at ~288.5 eV (carboxyl group, –COOH), and a distinct peak at 290.7 eV, corresponding to the 1s–$\pi^*$ bond of $CO_3$ (Table 4.2). In contrast, group 2D (Figure 4.28), which corresponds to spectra E, F and H in Figure 4.27, presents an intense

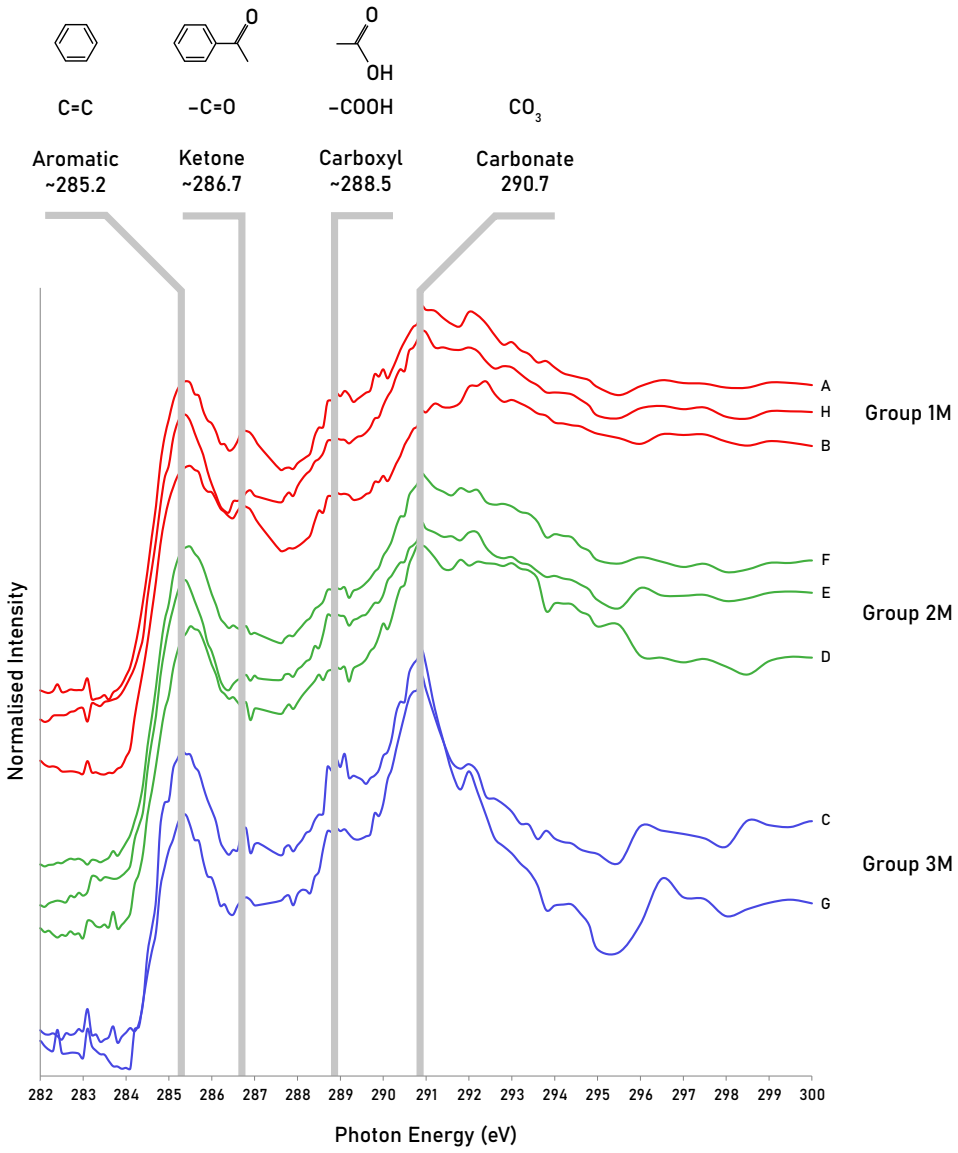


Figure 4.31: *C K-edge XANES spectra of MIL 090010, CO3.1. Example of spectral variability collected throughout a whole FIB section. Each group of spectra show distinct spectral features related to functional groups and relative intensities. Letter "M" in groups' name refers to MIL 090010; single spectra are labeled following the order in which they were extracted.*

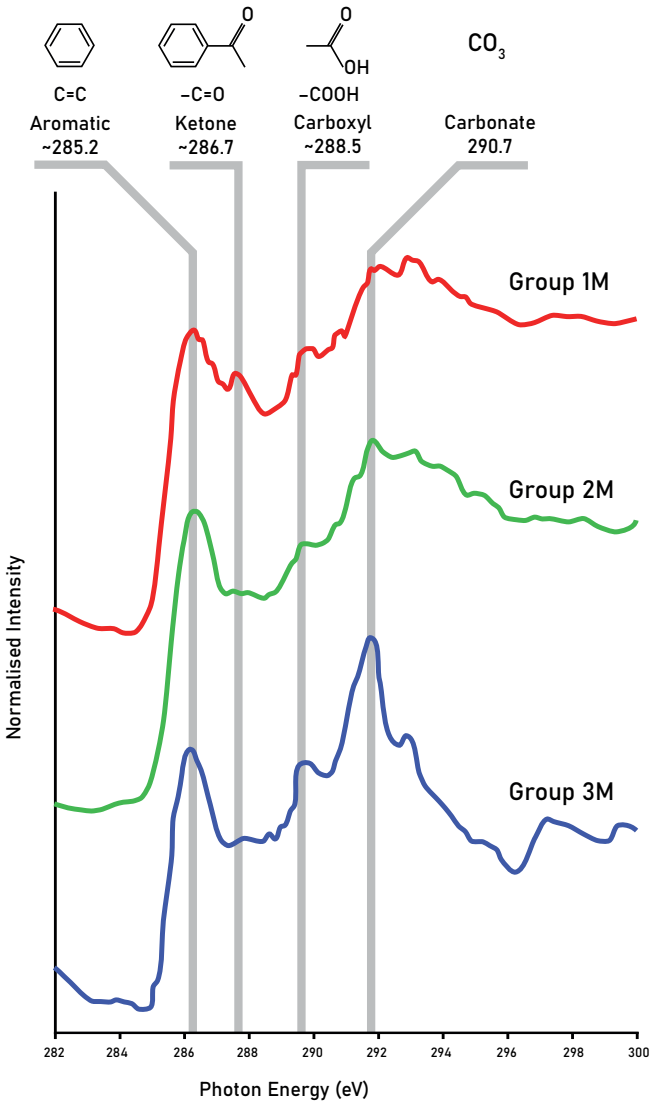


Figure 4.32: *C K-edge XANES spectra of MIL 090010, CO 3.1. Spectra collected throughout the whole FIB section showed variations which can be can be represented by three main spectral groups: group 1M, group 2M and group 3M. Each group is characterised by distinct spectral features related to functional groups and relative intensities.*

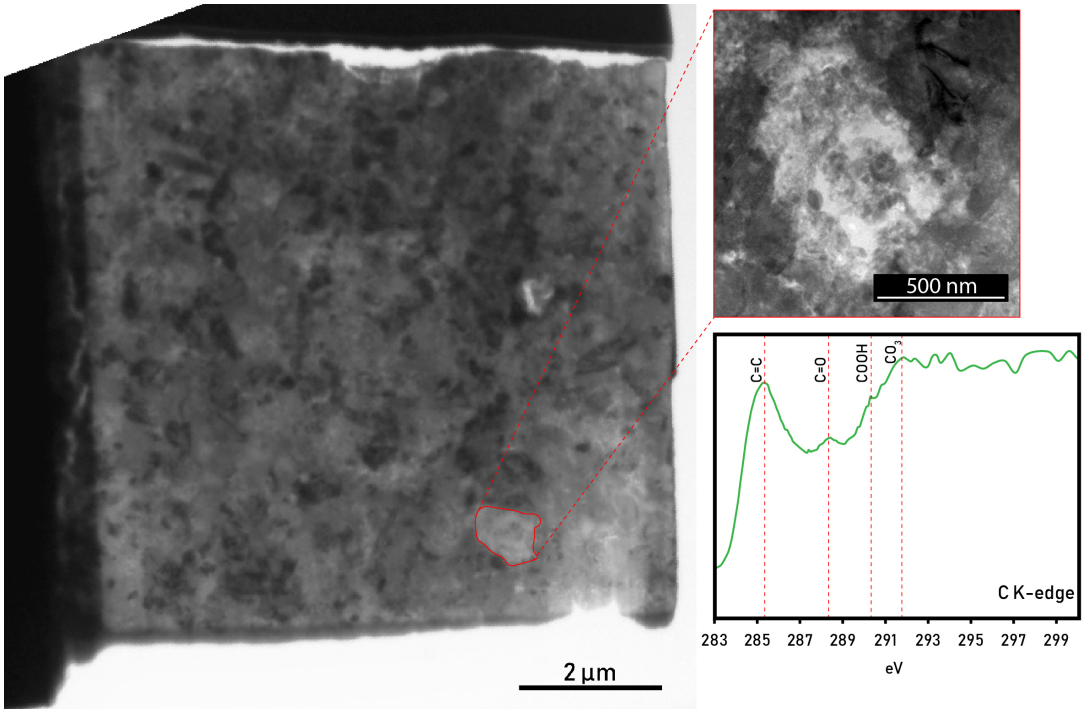


Figure 4.33: *C K-edge XANES spectra (from single pixels) of C-rich organic matter in MIL 090010.*

peak for C=C (∼285.2 eV) and C=O (∼286.7 eV), a broad COOH peak (288.5 eV), while the spectra do not have the $CO_3$ feature (290.7 eV). Group 3D, (Figure 4.28), which corresponds to spectra A, B, C and D in Figure 4.27, is characterised by sharp and intense C=C and $CO_3$ features, and a very weak COOH feature (∼288.5 eV).

NWA 7892 (CO3.05) shows variation in the spectra within the sample, which can be grouped into three main categories. Group 1N is characterised by spectra B and H (Figure 4.29) which presents a ketone feature at ∼286.7 eV (C=O), while carboxyl and carbonate features are absent (288.5 eV and 290.7 eV respectively). Group 2N (spectra A, C, D, F) presents a ketone feature at 286.7 eV that is weak for spectra A and F, but is stronger in C and D. The carboxyl (COOH) peak (288.5 eV) is recognisable, as is the carbonate peak at 290.7 eV. Group 3N (spectra E and G) has a very weak aromatic carbon peak (285.2 eV), as well as ketone (286.7 eV) and carboxyl (288.5 eV), while carbonate is absent (Figure 4.29). In addition, in NWA 7892 I identified a carbonate vein cutting across one of the FIB sections. Spectra from the vein have a very strong peak at 290.7 eV which is characteristic of the $CO_3$ (Figure 4.30). This observation is also supported by TEM and SEM-EDX data for this FIB section described earlier in the chapter.

MIL 090010 C K-edge spectra also can be divided into three groups (Figures 4.31 and 4.32) based on their distinct spectral characteristics. All groups show a strong aromatic C (C=C) absorption peak. However, the ketone C=O peak (286.7 eV) is intense in group 1M (corresponding to spectra A, B and H in Figure 4.31), absent in group 2M (spectra D, E and F in Figure 4.31) and weak in group 3M (spectra C and G in figure 4.31). While the carboxyl COOH peak (288.5 eV) is present in spectra from all the groups, it is more prominent in group 3M. The spectrum representing group 3M shows a distinct peak at 290.7 eV, which is related to $CO_3$. While these four functional groups are consistently observed throughout the samples, their relative intensities (and therefore abundance) changes in relation to their location and meteorite sample. Moreover, in MIL 090010 I found a particularly C-rich region in one of the FIB sections (Figure 4.33). This region has a characteristic C K-edge XANES spectrum that resembles the features previously discussed for group 1M.

C K-edge spectra from the matrix in Kainsaz (CO3.2) are different from the less metamorphosed samples in that they do not show any significant variations throughout the maps. Figure 4.34 shows a typical spectrum from Kainsaz, which is characterised by a very intense aromatic carbon (C=C) peak at ∼285.2 eV, while in comparison the features related to the ketone C=O (286.7 eV) and COOH (288.5 eV) are very weak, although still noticeable, and the carbonate feature is absent.

Moss (CO3.6) is a highly metamorphosed sample and does not show many strong C K-edge features (Figure 4.34). It is still possible to detect the aromatic carbon (C=C) peak at ∼285.2 eV, the ketone (286.7 eV) and the carboxyl (288.5 eV) features but they are not as easy to identify as in less metamorphosed samples.

### 4.4.7 Results: O K-edge

The O K-edge was mapped for NWA 7892, MIL 090010, Kainsaz, Ornans and Moss. O K-edge spectra from all of the samples show a pre-edge feature at ∼534 eV (Figure 4.35), which for organic material corresponds to the 1s-3p/s* of the alcohol group ($CH_xO$) (Table 4.2). This pre-edge feature changes in shape and rapidly decreases its intensity between MIL 090010 and Kainsaz, getting weaker towards more metamorphosed samples. There is a doublet feature on the main edge at 540 and 544 eV (Figure

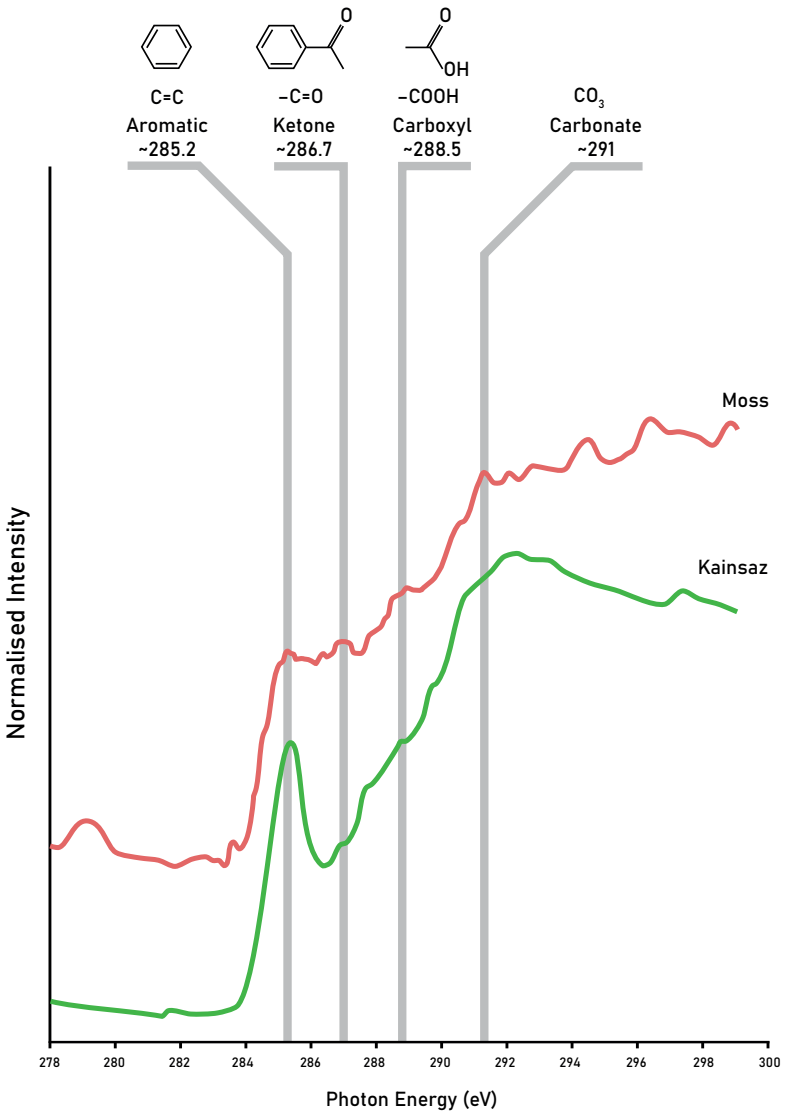


Figure 4.34: *C K-edge XANES spectra of Kainsaz (CO3.2) and Moss (CO3.6) extracted from single pixels. Highlighted are the main functional groups characterising the samples.*

4.35), which changes in shape like the pre-edge feature, going from a broad feature in MIL 090010 to a more resolved doublet in Moss. This feature is related to the chemical composition of the olivine grains within the samples (Garvie, 2010).

### 4.4.8 Results: N K-edge

N K-edge maps were acquired in DOM 08006, NWA 7892, MIL 090010, Kainsaz and Ornans. Considering that the average bulk N abundance in CO is of about 0.05 wt% (Pearson et al., 2006), and that in the present study spectra are extracted from single pixels of 40 nm is size, the N abundance is very low, as well as very diffuse within the samples, therefore no distinct absorption features sufficient for assigning functional groups were recognised within the matrix.

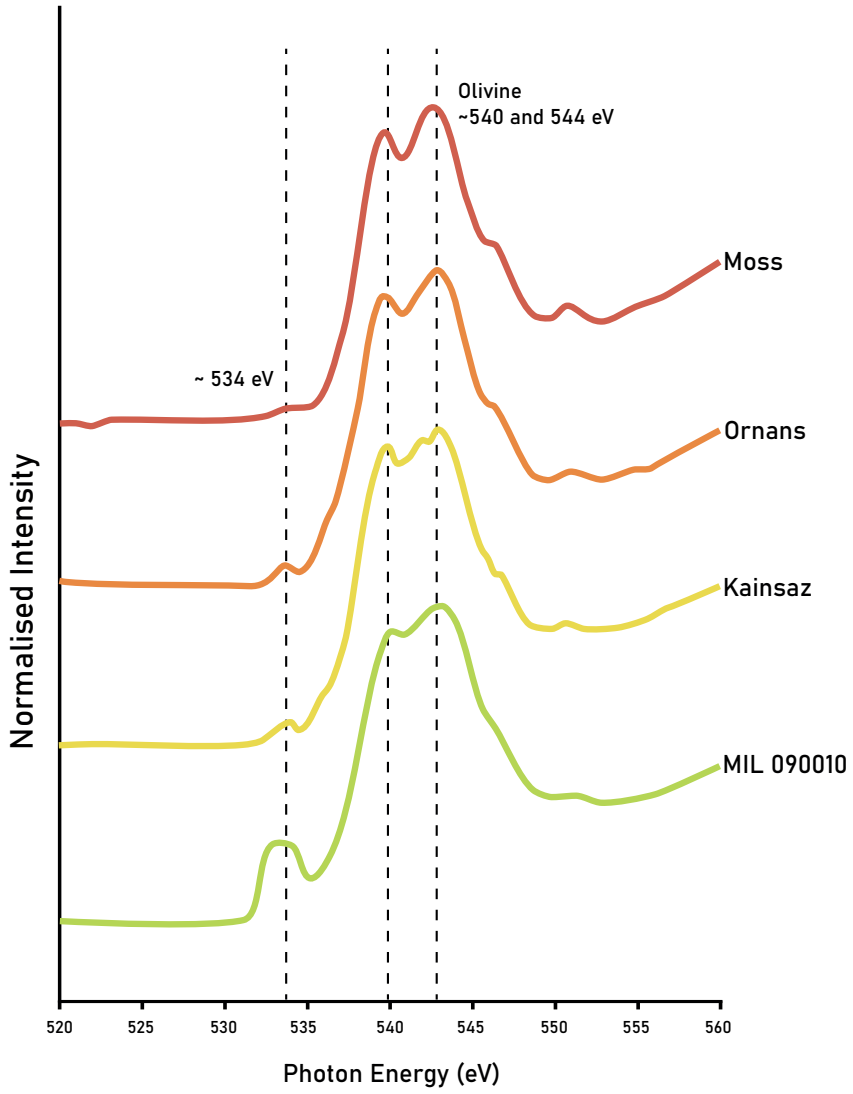


Figure 4.35: *O K-edge XANES spectra of samples MIL 090010 (CO 3.1), Kainsaz (CO 3.2), Ornans (CO 3.4) and Moss (CO 3.6) in order of petrologic type. The spectra, extracted from single pixels, show a variation in the feature intensity at ∼534 eV, 540 eV and 544 eV.*

# Chapter 5

# Discussion

Matrix is one of the first components of primitive carbonaceous chondrites to be affected by parent body alteration, and the combination of *in-situ* and bulk analyses can provide details about both its pristine nature and alteration history. This work is focused on investigating textural and chemical changes affecting the matrix mineralogy and the organic matter of primitive CO chondrites in relation to parent body metamorphic processes for understanding the origin of dust and its components.

## 5.1 Petrological Subtypes

Often the petrologic subtype assigned to CO chondrites varies in the literature depending on the analytical techniques applied. For example, the study of Bonal et al. (2007) applied Raman spectroscopy to study the OM maturity in relation to the thermal history of CO chondrites. Bonal et al. (2007) concluded that ALHA77307 should classified as 3.03, Colony as 3.1, Kainsaz, Felix, Ornans and Lancé as 3.6, while Warrenton and Isna should be classified as petrologic subtype 3.7. This petrologic classification is not in agreement with changes that affect the mineralogy of these samples as highlighted by the olivine mineralogy and chemistry seen in the present work as well as in Scott & Jones (1990) and Chizmadia et al. (2002). Studies looking at mineralogical changes provide petrologic classifications that are comparable between one another, while in Bonal et al. (2007) the study was focused on the analyses of organics which behave differently to thermal metamorphism than the mineralogy. In particular, the organics are very sensitive to even the smallest degree of aqueous alteration which would ho-

| | Present work | Bonal et al. (2007) | Chizmadia et al. (2002) | Sears et al. (1991) | Scott & Jones (1990) | McSween (1977) |
|---|---|---|---|---|---|---|
| Colony | 3.0 | 3.1 | 3.0 | 3.0 | 3.0 | – |
| DOM 08006 | 3.0 | – | – | – | – | – |
| NWA 7892 | 3.05 | – | – | – | – | – |
| MIL 090010 | 3.1 | – | – | – | – | – |
| Kainsaz | 3.2 | 3.6 | 3.2 | 3.2 | 3.1 | I |
| Felix | 3.3 | 3.6 | 3.3 | 3.4 | 3.2 | II |
| Ornans | 3.4 | 3.6 | 3.4 | 3.4 | 3.3 | II |
| Lancé | 3.5 | 3.6 | 3.5 | 3.4 | 3.4 | II |
| Moss | 3.6 | – | – | – | – | – |
| ALHA77003 | 3.6 | – | 3.6 | 3.4 | 3.5 | – |
| Warrenton | 3.7 | 3.7 | 3.7 | 3.6 | 3.6 | III |
| Isna | 3.8 | 3.7 | 3.8 | 3.7 | 3.7 | III |

Table 5.1: *Petrologic grades reported for the CO chondrites characterised in this study from different metamorphic classification schemes.*

mogenise their properties at lower temperatures but leaves the mineralogy essentially unchanged.

Other studies aiming to monitor the thermal history of CO3 chondrites include Sears et al. (1991) and Sears (2016), who used thermoluminescence (TL) properties of different mineralogical phases and meteorite components (matrix, refractory inclusions, chondrules, etc.). Sears et al. (1991) estimated the petrologic grade and therefore the degree of metamorphism (Table 5.1). Felix, Ornans and Lancé were defined as petrologic subtype 3.4, while Warrenton and Isna were respectively described as 3.6 and 3.7 (Table 5.1). Although CO chondrites are chemically similar (Ebel et al., 2016), they exhibit different degrees of equilibration of MgO and FeO in olivine and pyroxene due to different degrees of metamorphism (Jones & Rubie, 1990). The most accepted theory about the equilibration process (Fe-Mg exchange) is that it took place within the parent body due to metamorphic processes caused by $^{26}$Al isotopic decay (Jones & Rubie, 1991). While Grossman & Brearley (2005) on the basis of Cr distribution in Fe-rich chondrules olivine developed a new method for the assessment of primitive meteorites, which is particularly useful for the subdivision in subtypes especially for less metamorphosed samples ($< 3.2$); they also observed enrichments in Na and S in the matrix material of the least metamorphosed chondrites. In the matrix of samples analysed in the present work, I did not observe any enrichments in Na and S, but I observed an increase in Cr/Si ratio in function of the petrologic subtypes. Another method to estimate the metamorphic history of primitive CO3 chondrites was done by Kimura et al. (2008) looking at Co in Fe-Ni metal inclusions. Fe-Ni metal is very sensitive to temperature variations, and therefore a good proxy for identifying the

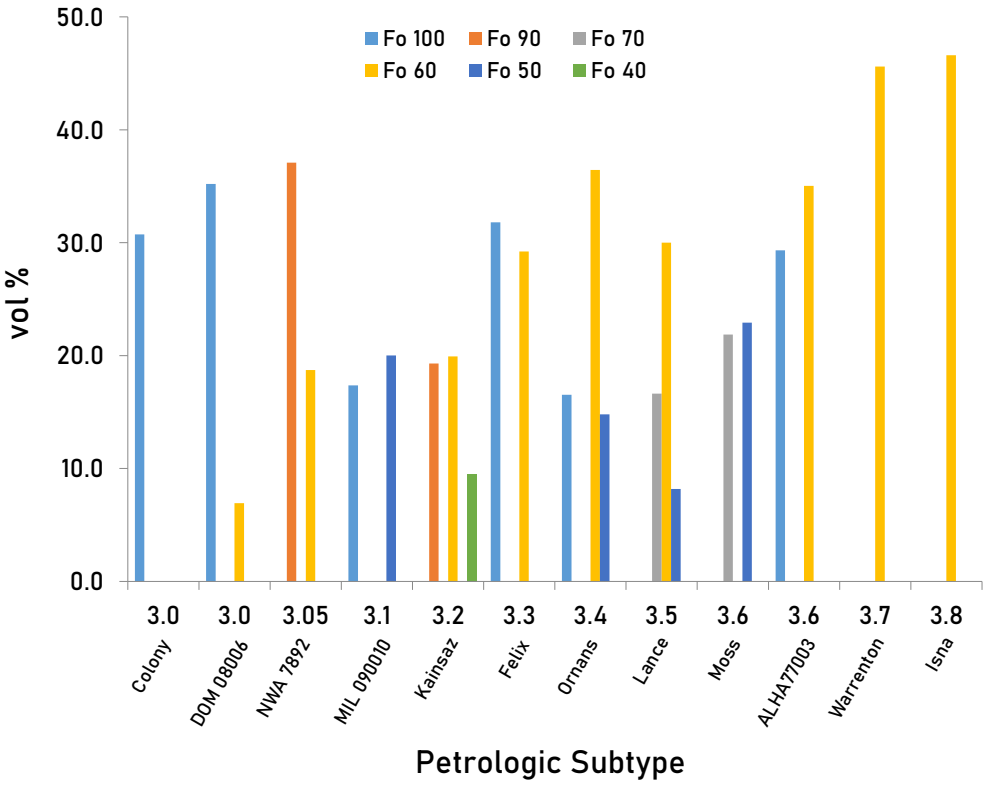


Figure 5.1: *Variations in olivine composition across the range of CO chondrites. The increase in $Fo_{60}$ with petrologic subtype has a strong positive correlation with increasing thermal metamorphism, and there is a concomitant negative correlation between the combined $Fo_{100}$ and $Fo_{90}$ with petrologic subtype (excluding the $Fo_{100}$ data point for ALHA77003).*

most primitive chondrites. Looking at the Co partitioning between kamacite and Ni-rich metal it is possible to determine peak metamorphic temperatures for samples with petrologic subtype between 3.05 and 3.2 in the range of 400 - 560 °C (Afiattalab & Wasson, 1980; Kimura et al., 2008). With the same method, it was estimated a temperature range of 400 - 550 °C for the CO3.05 Y-81020 by (Shibata & Matsueda, 1994), while Nagahara (1982) determined metamorphic temperature below 500 °C. These estimates are in agreement with TL measurements from Keck & Sears (1987).

The results obtained in the present work expand the petrologic subtype subdivision introduced by Chizmadia et al. (2002), who used EMPA to characterise amoeboid olivine inclusions with microprobe analyses, and this subdivision is the one that will be used throughout the whole study. Moreover, on the basis of the results obtained, it is possible to infer that low petrologic subtype COs do not show a quantifiable presence of phyllosilicates suggesting that alteration assisted by hydrothermal fluids in CO parent

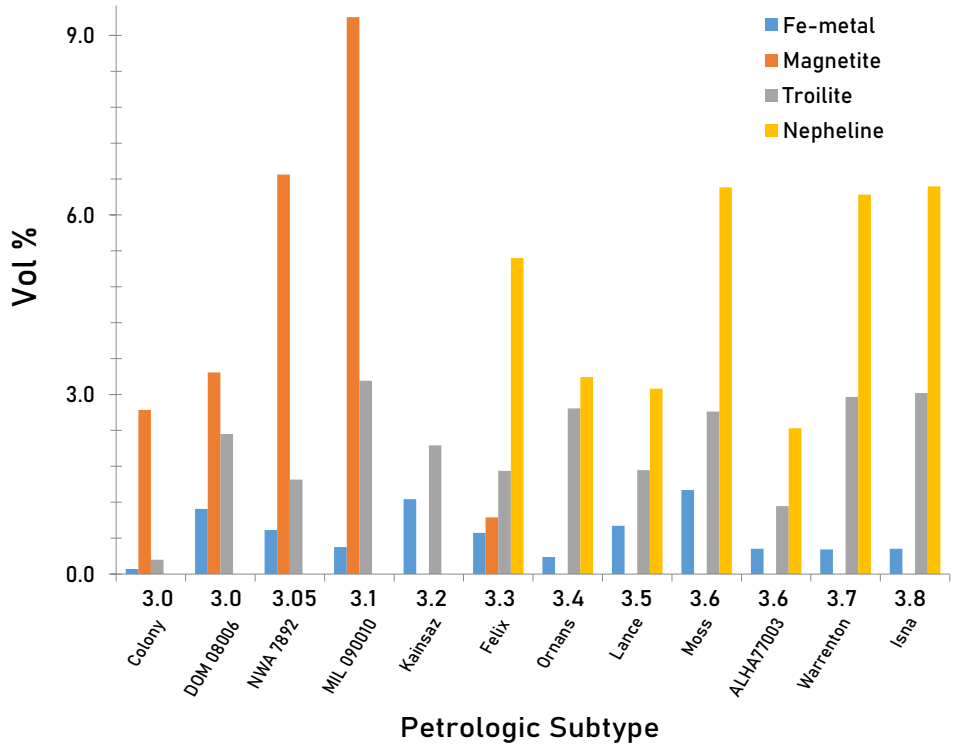


Figure 5.2: *Variations in abundance of kamacite, magnetite, troilite and nepheline as function of the petrologic grade.*

bodies was probably very minimal.

The present study has shown that PSD-XRD and high resolution XRD are excellent methods to combine for the determination of mineralogical changes in relation to thermal metamorphism in CO chondrites. These methods enabled the identification of modifications in the mineralogical abundances as well as changes in the chemical composition of the olivine based on its (020) peak. PSD-XRD and high resolution XRD were effective in the estimation of petrologic grades for primitive CO chondrites which are in agreement with other studies in the literature looking at mineralogical variations. Indeed, Figures 3.3 and 3.4 demonstrate how through XRD it is possible to quickly define the petrologic subtype of a CO chondrite, by taking into consideration the relative intensities of the (020) peaks of the Fe-poor and Fe-rich olivines.

Bonal et al. (2007) estimated the petrologic subtype of Colony as CO3.1, which on the basis of the chemical changes of the olivine it can be defined as CO3.0, and this classification is also valid for other CO3.0, even more pristine COs, such as DOM 08006 and NWA 7892 (Figure 3.3). Also while Bonal et al. (2007) group the petrologic subtype

of Kainsaz, Felix, Ornans and Lancé all together at 3.6, based on their mineralogy these meteorites show gradual changes and my observations suggest they should be classified as 3.2, 3.3, 3.4 and 3.5. This more incremental classification is further confirmed by the presence of a mixture of olivine that spans between $Fo_{90}$ and $Fo_{40}$ (Figure 3.3) the proportions of which vary gradually across the sequence (Figure 5.1, Table 3.2). Concerning Warrenton and Isna, the olivine chemistry matches with high petrologic subtype samples (Figure 3.3) and they are classified by Chizmadia et al. (2002) as 3.7 and 3.8. At this stage the samples are almost completely equilibrated, and as can be seen in Figures 3.3 and 3.4 there are still differences in the relative intensities of the olivine peaks between these two CO chondrites, and therefore I agree with the classification of Warrenton as 3.7 and Isna as 3.8. This was also confirmed by other studies such as Scott & Jones (1990), Sears et al. (1991) and Greenwood & Franchi (2004). Another distinctive or defining point within the CO chondrite petrological sequence identified from this study is the disappearance of magnetite at CO3.2 / CO3.3 and the appearance of nepheline at CO3.3 (Table 3.2 and Figure 5.2). This is discussed further in section 5.2.1.

## 5.2 Matrix mineralogy & chemistry

My data show that the least altered COs contain Fe-bearing amorphous silicates, in which are embedded Mg-rich olivine, pyroxene, Fe-Ni metal, magnetite and sulfides. This is consistent with previous descriptions of these meteorites e.g. by Brearley (1993). Other studies also described the presence of presolar grains (Nuth et al., 2005; Haenecour et al., 2018; Nittler et al., 2018) and organic matter (Bonal et al., 2007; De Gregorio et al., 2013; Alexander et al., 2017) although these are not likely to be identified using bulk XRD and were not observed in this study. However, with thermal metamorphism the matrix undergoes mineralogical, chemical and textural changes, which become more visible within samples of increasing petrologic subtype.

Primitive samples such as Colony (CO3.0), DOM 08006 (CO3.0), NWA 7892 (CO3.05) and MIL 090010 (CO3.1) are characterised by Fe-bearing amorphous silicates within their matrix. The amorphous nature of the matrix was ascertained using TEM analysis

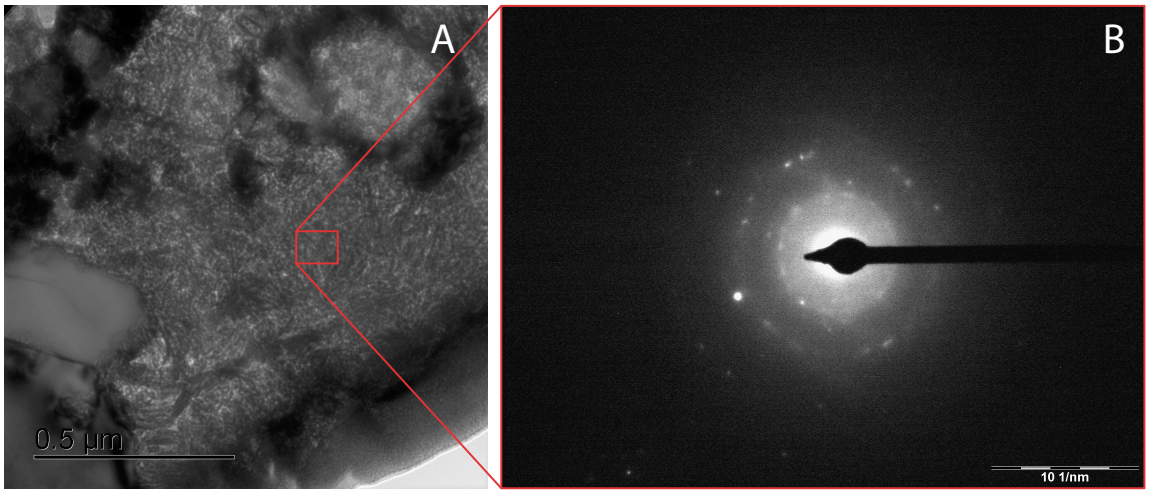


Figure 5.3: *a) Bright field TEM image of a detail of the matrix of NWA 7892 and b) TEM electron diffraction pattern showing the characteristic concentric rings of the amorphous silicates that compose the matrix of NWA 7892.*

as they were producing electron diffraction patterns with diffuse intensity variations and characteristic concentric rings (Figure 5.3). From the modal mineralogy (Table 3.2) the abundance of amorphous silicates ranged between 6 vol% and 30 vol%, with their abundance decreasing with petrologic subtype. This demonstrates that amorphous silicates are highly reactive and can therefore be used as an indicator of the progression of metamorphism. Similar abundances of amorphous silicates were also estimated through PSD-XRD by Alexander et al. (2017) for DOM 08006 and MIL 090010, however differently from their results, I did not detect any phyllosilicates.

The origin of the amorphous silicates is still not fully understood, with different theories including formation in the interstellar medium as the result of non-equilibrium condensation and exposure to high energy environments (Nuth et al., 2005), or that the amorphous material represents the glass with embedded metal and sulfide grains also known as GEMS which are very commonly found in IDPs (Keller & Messenger, 2011). However, a leading theory is that they are the product of disequilibrium condensation of lost evaporated material from chondrule formation (Brearley, 1993; Palme et al., 2015) which took place in the solar nebula. Chizmadia & Brearley (2008) suggested that amorphous silicates could be either the product of aqueously altered nebular phases that hydrated into a gel-like phase forming nonocrystalline phyllosilicates, or that they are primary materials of nebula origin that still retain a record of nebular processes

but underwent hydration during parent aqueous alteration.

Analysing various samples throughout the petrologic scale of COs, I observed that the Fe-bearing amorphous silicates contribute to the overall Fe content of the matrix, and when temperature increases they crystallise (Figure 4.16) into more Fe-rich olivine (Brearley, 1990; Jones & Rubie, 1991) as shown in Figure 5.1. However, the increasing abundance of $Fo_{60}$ and $Fo_{50}$ could also be influenced by the Fe redistribution due to the decomposition of magnetite (Figures 3.5 and 5.2). Data collected in this work are in agreement with Brearley (1990), McAdam et al. (2018) and Alexander et al. (2018) as they show that amorphous silicates are a likely precursor phase of olivine and are converted with thermal metamorphism and therefore increasing petrologic subtype. For example, in McAdam et al. (2018) the reflectance mid-IR spectra of low petrologic subtype COs are characterised by a feature at 21 $\mu$m, related to amorphous silicates, which disappears with thermal metamorphism, while features related to the olivine located at 12.7, 19.5 and 24 $\mu$m become stronger with increasing petrologic subtype.

The lack of amorphous silicates in COs of petrologic subtype higher than 3.1 gives insights on the sensitivity of this phase to changes in temperature, suggesting that they are affected by even mild metamorphism as well as aqueous alteration (Brearley, 1990; Greshake, 1997; Abreu & Brearley, 2010; McAdam et al., 2018). SEM-EDX maps and EMPA analyses (Figures 4.1 and Table 4.1) show how under the influence of thermal metamorphism the matrix is subjected to a depletion in Fe as a result of the equilibration process that took place between Fe-rich matrix and Mg-rich chondrules (Jones & Rubie, 1990). The enrichment in Mg content in the matrix (Figures 4.3 and 4.5), was of almost 6 wt % across the petrologic scale. These observations support the previous findings of McSween (1977); Jones & Rubie (1990); Grossman & Brearley (2005); Ebel et al. (2016). Moreover, spectra of the O K-edge XANES analysis show that there are changes affecting the doublet peaks at ~540 and ~ 544 eV (Figure 4.35). These variations could be related to the amorphous silicates that are crystallising, as in MIL 090010 in MIL 090010 where the spectrum has a shape consistent with forsteritic olivine, however the strong pre-edge feature at ~534 eV suggests that there may be some contribution from poorly crystalline or amorphous olivine (Takahashi et al., 2018). With increasing petrologic subtype the doublet becomes more defined

(Figure 4.35) and its shape matches with the O K-edge spectrum of Fe-rich olivine (Garvie, 2010), indicating chemical changes happening within the olivine. Since the alcohol/ether functional groups were not detected in C K-edge spectra of these samples, I would discard the option that the pre-edge feature is entirely related to an organic component, but I rather support the theory that the information that can be retrieved from O K-edge analysis reflects the crystallisation of the silicate from amorphous to Fe-rich olivine.

In other primitive COs such as NWA 7892 (CO3.05) and MIL 090010 (CO3.1), the transformation of amorphous silicates either into alteration products, or crystallising into olivine or pyroxene is more obvious and can be clearly seen in Figure 4.20. TEM analyses highlight that, due to parent body thermal metamorphism, samples from 3.2 onwards no longer contain an amorphous silicate component in the matrix (Figure 4.16). The main variation is related to the olivine chemistry in petrologic subtype above 3.2. Olivine is a major component of CO3 chondrites, found both in chondrules and matrix. Matrix olivine are $< 1$ $\mu$m in grainsize, very temperature sensitive, as they easily exchange Fe-Mg on heating, and they are an $Fe^{2+}$ reservoir (Jones & Rubie, 1990, 1991; Russell et al., 1998). During metamorphic processes in CO chondrites, there is equilibration between chondrules and matrix. This process consists of the migration of $Mg^{2+}$ from the chondrules to the matrix and of $Fe^{2+}$ from the matrix towards the chondrules (Jones & Rubie, 1990), leading to systematic variations in the Mg and Fe content of olivine. The first effects are seen in the transition between petrographic subtypes 3.1 and 3.2. The effects of this equilibration are very well recorded with high resolution XRD, for example in Figures 3.3 and 3.4 where the composition of the olivine systematically changes from forsteritic to more Fe-rich with increasing petrologic subtype. Samples from 3.00 to 3.1 present an intense forsterite peak at 20.1 degrees $2\Theta$ (Figure 3.3), meaning that the equilibration is yet to occur. It is estimated that the peak metamorphic temperature for samples belonging to subtype 3.0 is on the order of $\sim 200$°C as they do not show metamorphic effects at the micrometer scale (Brearley, 1993; Huss et al., 2006). With minor heating, a second peak at $\sim$ 19.8 degrees $2\Theta$ begins to form, which is the one related to Fe-rich olivine. This peak first appears in MIL 090010 as a very small peak.

In samples such as Kainsaz (CO3.2) and Felix (CO3.3) the intensity of the diffraction peak at ∼ 19.8 degrees 2Θ of the (020) Fe-rich olivine is equal to the (020) forsterite peak meaning that significant Fe-Mg exchange is taking place, and therefore olivine is becoming increasingly Fe-rich with thermal metamorphism (Figures 4.22, 4.23 and 4.24). At this point, for a sample like Kainsaz the estimated peak temperature is ∼ 300 °C (Huss & Lewis, 1994b; Huss et al., 2006). Samples ranging between 3.4 and 3.6, have both peaks at 19.8 and 20.1 degrees 2Θ, but the forsteritic olivine peak (20.1 degrees 2Θ) is about half the intensity of the Fe-rich olivine, indicating that Fe-rich olivine is becoming increasingly abundant. This is supported by the PSD-XRD results which show that these samples contain a mixture of olivine with different chemistries ranging between $Fo_{100}$ and $Fo_{40}$ (Figure 5.1). Kainsaz (CO3.2), Ornans (CO3.4) and Moss (CO3.6) are very different from the lower petrologic subtype COs as the matrix clearly show the effects of thermal metamorphism. It is mainly composed of crystalline euhedral minerals as the amorphous silicates have completely crystallised with the increase in temperature. Moreover, differently from what it was described by Rubin & Wasson (1988) XRD analysis showed no evidence of quartz in Ornans (CO3.4).

Samples from petrologic subtype 3.6 to 3.8 are characterised by a dominant Fe-rich olivine peak (19.8 degrees 2Θ) as the equilibration process is approaching completion (Figures 3.3 and 3.4). Moreover, the modal mineralogy shows that while the overall olivine abundance does not change much with petrologic subtype, but the composition of the olivine becomes increasingly Fe-rich until it is all approximately $Fo_{60}$ in petrologic subtype 3.8 (Figure 5.1). In addition, SEM-EDX maps of FIB sections of Moss show the presence of chromite crystallising on the edges of the matrix olivines (Figure 4.24). Moss is the highest petrologic subtype sample anylised using TEM in this study and the absence of chromite grains on the edges of matrix olivines in lower petrologic subtype samples leads to the assumption that their presence might likely be related to thermal metamorphism. The connection between Cr and metamorphism was shown in Figure 4.2, where there is an increase in Cr abundance within the matrix in relation to the petrologic subtype. Considering the high sensitivity of the matrix to temperature changes, these observations are in agreement with the recordings of Grossman & Brearley (2005). They noticed a loss in Cr from the olivine in relation to increasing

thermal metamorphism, with Cr exsolving from the chondrule olivine and forming a fine grained chromite precipitate around them.

### 5.2.1 Minor phases in the matrix

The abundance of kamacite in the suite of COs analysed here is generally below 1 vol% (Table 3.2 and Figure 5.2) with the exception of Kainsaz and Moss which have kamacite concentration $\leqslant$ 1.4 vol%. Troilite remains fairly constant at $\sim$ 2 vol% for most of the samples, but its abundance is over 3 vol% for the highest petrologic subtype samples Warrenton (3.7) and Isna (3.8). Magnetite is present in low petrologic subtype samples (between 3.0 and 3.1) as well as in Felix, which confirms the findings of Alexander et al. (2018) and Rubin & Li (2019). As well as stated by Rubin & Li (2019) the modal mineralogy calculated in the present work confirms that the major opaque inclusion in COs between 3.2 to 3.8 are troilite and kamacite, with the latter likely formed as secondary product of the magnetite reduction process. Independently of how magnetite formed, it is clear that magnetite disappears with thermal metamorphism (Table 3.2 and Figure 5.2). This was observed also by Rubin & Li (2019) and it confirms what was obtained with experimental studies and thermodynamic calculations by Zolotov et al. (2006) who demonstrated that during metamorphic processes affecting ordinary and carbonaceous chondrites, magnetite was reduced to fayalite and secondary kamacite as a consequence of changes in the $H_2/H_2O$ ratio in gas trapped within the asteroid. The reduction of magnetite is also responsible for the decrease in proportion of Ni-rich metal grains within ordinary chondrites as well as COs Rubin & Li (2019).

The modal mineralogy shows that nepheline is present with an abundance above detection limits of 1.6 vol% (Table 3 Appendix B) from petrologic subtype 3.3 upwards (Table 3.2 and Figure 5.2). Its presence can be attributed to metasomatic processes (Brearley, 2014; Brearley & Krot, 2013) which affected plagioclase-rich chondrules, anorthite and mesostasis in subtype I chondrules (Tomeoka & Itoh, 2004; Jones, 1997; Kurat & Kracher, 1980) and CAIs (Russell et al., 1998) There are several explanations as to why CAIs in high petrologic subtypes contain feldspathoids. Russell et al. (1998) suggest two main hypothesis to explain this phenomenon: the first one suggests heterogeneous accretion of the CO parent body leading to a higher abundance of Na-rich CAIs

in regions that experienced higher peak metamorphic temperatures. Alternatively the second hypothesis, suggests a metasomatic origin of nepheline (*nephelinisation*) due to Na-rich aqueous fluids, which is also supported by Tomeoka & Itoh (2004). Russell et al. (1998) suggest that Na was incorporated more easily within the CAIs that were located in hotter parts of the parent body, while (Tomeoka & Itoh, 2004) noticed that the nepheline is mainly present in the outer margins of type I chondrules, suggesting that the Na was supplied by the surrounding matrix in presence of fluids. Nepheline likely formed as hydrated nepheline during low temperature aqueous alteration in alkaline conditions, and subsequently dehydrated due to thermal metamorphism (Tomeoka & Itoh, 2004). The role of fluids will be discussed further in section 5.4.

## 5.3 Porosity and grainsize

The effect of thermal metamorphism can also be recorded in terms of changes in the grainsize and porosity of the matrix. The crystallisation of the Fe-bearing amorphous silicates into olivine (Brearley, 1990; McAdam et al., 2018; Alexander et al., 2018) at increasing metamorphic peak temperature is responsible for an increase in porosity at the sub-micron level. This can be observed in the TEM images (Figure 4.16), as the formation of new minerals takes up less volume than the amorphous silicates. I observed changes in microporosity throughout the petrologic sequence, with low petrologic subtype samples (3.0 and 3.1) having an average porosity of $\sim$ 2 area % compared to higher petrologic subtypes which range between $\sim$8 and $\sim$ 25 area %. However, in the case of DOM 08006 (CO3.0), the degree of porosity was harder to determine because of the presence of C nanoglobules that can be confused for porosity. Amorphous silicates being anhedral, take up all the space available among other phases. Amorphous silicates crystallise into olivine grains that have euhedral shapes and therefore create intergranular space which influences the compaction of the matrix material. The compaction of the matrix is very important as it can vary within the chondrite and influence the degree of fluid filtration at the nanometre scale, which is of particular importance in a fluid-limited system such as the one characterising CO3 chondrites (Bland et al., 2009; Brearley & Krot, 2013).

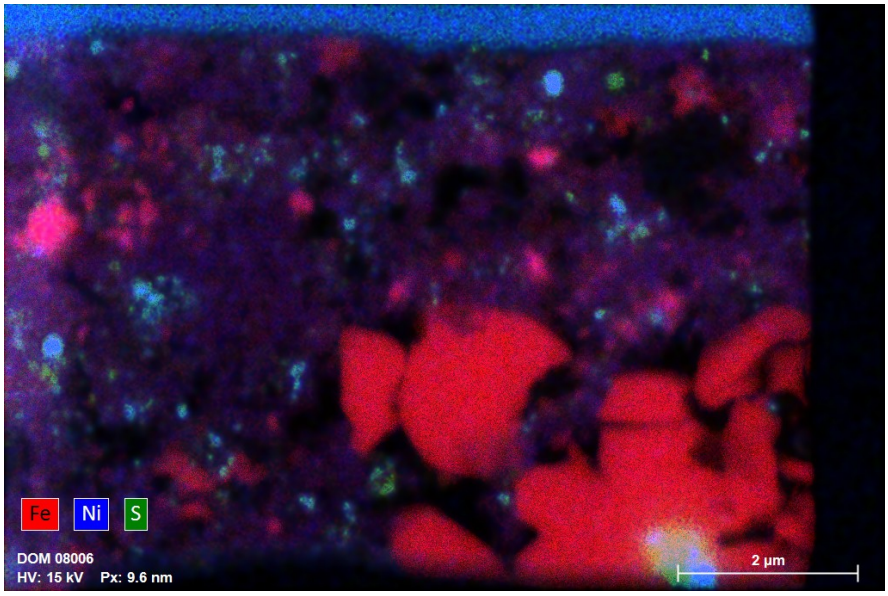


Figure 5.4: *SEM-EDX map of a FIB section of DOM 08006 showing the distribution of Fe, Ni and S within the matrix.*

Significant changes in matrix grain size can be seen throughout the metamorphic sequence of COs, where in CO3.0 the average grainsize of the matrix constituents is approximately 150 nm increasing up to $\sim$ 1 - 1.4 $\mu$m in CO3.6 (Figure 4.16). A similar matrix grain size distribution was identified for Acfer 094 (Bland et al., 2009) with rare grains of about 1 $\mu$m. As a consequence to changes in grainsize and porosity, also the permeability of the meteorites is affected by thermal metamorphism. Bland et al. (2009) showed that the finer the matrix particles, the lower is the permeability of the sample limiting the flow of acqueous fluids that could have been present in the CO parent body(s).

## 5.4 Fluids

It is known that DOM 08006 is one of the most unequilibrated COs available for study, as it is rich in amorphous silicates and presolar grains (Nittler et al., 2018) and I observed from TEM analysis very rare phyllosilicates within its matrix (Figure 4.18d). These characteristics resemble features that were described by Abreu & Brearley (2010) in the most primitive CR3 chondrites, QUE 99177 and MET 00426. The matrix of these two meteorites differs from most CR chondrites in consisting of abundant amorphous silicates and presolar grains, and very few phyllosilicates, and is comparable

to the matrix of vey unequilibrated meteorites such as Acfer 094 (C2-Ungrouped) and ALHA77307 (CO3.0) (Floss & Stadermann, 2009).

Le Guillou & Brearley (2014b) describe the amorphous silicates in MET 00426 as hydrated phases, containing up to about 10 wt% in water. They are metastable phases that when in contact with water-rich fluids, even at low temperature, can crystallise into phyllosilicates (Chizmadia et al., 2006; Chizmadia & Brearley, 2008; Le Guillou & Brearley, 2014b), while with thermal metamorphism the amorphous silicates crystallise into olivine (Brearley, 1990; Jones & Rubie, 1991). In the matrix of DOM 08006 (Figure 4.18d) and NWA 7892 (Figure 4.20c) I found evidence of oxidised amorphous silicates. Fe L-edge XANES shows that amorphous silicates are dominated by $Fe^{3+}$, despite some variation in the Fe oxidation state within the sample (Figure 4.26) likely related to the presence of various fine-grained mineralogical phases embedded within the amorphous matrix, which provide a contribution from $Fe^{2+}$. I also observed the occurance of rare phyllosilicate lamellae (Figure 4.18d), suggesting that in these primitive meteorites there might have been hydration of the amorphous silicates. Also the presence of magnetite in the low petrologic subtype samples can be an indicator of aqueous fluid assisted thermal metamorphism (Rubin & Li, 2019).

While DOM 08006, NWA 7892 and MIL 090010 are dominated by high $Fe^{3+}/\Sigma Fe$, in higher petrologic subtype samples there is a decrease in the $Fe^{3+}/\Sigma Fe$. The crystalline silicates are all $Fe^{2+}$-rich, which might be because the environmental conditions became increasingly reduced with thermal metamorphism (Figure 4.25) due to the removal of oxidising $H_2O$ and the initial presence of reducing agents such as H and C (Menzies et al., 2005). However, XRD data do not show a quantifiable amount of phyllosilicate, and therefore it opens the possibility of magnetite being a nebular product which formed under oxidising conditions and condensed in fine grained crystals (Brearley, 1993). This paradox could be resolved if the magnetite and small amount of phyllosilicates present in a CO3.0 as primitive and pristine as DOM 08006 also have a nebula origin as was suggested by Chizmadia & Brearley (2008). Moreover, EDX maps of FIB sections of DOM 08006 show that Ni-Fe metal/Fe-Ni sulfide grains embedded within the amorphous silicates are very common (Figure 5.4), and this would likely be completely oxidised and altered if fluids were moving within the parent body, therefore

arguing against parent body hydrothermal alteration.

These observations open questions about about where and when hydration of the amorphous silicates took place. A possible scenario is that they could have become hydrated due to interaction with water vapour in the nebula (Leroux, 2006) and therefore before accretion into an asteroid. Alternatively, they might have become hydrated in the parent body through fluid interaction (Ciesla et al., 2003; Chizmadia & Brearley, 2008), or through terrestrial weathering processes on Earth. The scenario of hydration in the parent body is the most widely accepted, especially for CM and CR chondrites as they contain a high abundance of phyllosilicates and other secondary phases that are typical products of low temperature aqueous alteration (Le Guillou & Brearley, 2014b).

Based on my observations, I suggest that the amorphous silicates in petrologic subtypes 3.0, 3.05 and 3.1 were hydrated within the nebula. If the amorphous silicates condensed in the solar nebula it is predicted that they should be rich in $Fe^{2+}$ due to the reducing environment (e.g. Hopp & Vollmer (2018)), however an $Fe^{3+}$ oxidation state is consistent with them being described as hydrated phases by Le Guillou & Brearley (2014b). Even low levels of parent body processing would have oxidised the amorphous silicates. This finding is in agreement with the model proposed by Hopp & Vollmer (2018) for $Fe^{3+}$-rich amorphous silicates in Acfer 094, and in aqueously altered CR chondrites (Le Guillou et al., 2015). In addition, I note that DOM 08006 is an Antarctic find of weathering grade A/B (Davidson et al., 2014; Alexander et al., 2018). Terrestrial alteration may explain why the silicates in DOM 08006 show greater variation in the $Fe^{3+}/\Sigma Fe$ ratios compared to the relatively minor differences observed between grains in Acfer 094 (Hopp & Vollmer, 2018). However, the weathering grade for DOM 08006 is low and therefore is unlikely that the oxidation can be completely attributed to weathering. Other weathering products that were noticed in the samples are calcite in NWA 7892 and anhydrite in Isna. These are weathering products that are typical of dry environments (Lee & Bland, 2004). It is likely that any small variation in the Fe L-edge XANES spectra, and hence the $Fe^{3+}/\Sigma Fe$ ratio, are related to mineral inclusions within the amorphous silicate that contain reduced Fe.

## 5.5 Organic matter in COs

Organic carbon constitutes up to 2 wt% of carbonaceous chondrites (Busemann et al., 2006) and it can be present as SOM and IOM, which is the most abundant form (Alexander et al., 2017). OM is unlikely to survive to the high temperatures associated with chondrule and CAI formation, therefore almost all of it is found within the matrix material (Remusat, 2015) and because of its high sensitivity it was subject to aqueous and/or thermal processing on the parent body.

Most of the studies of IOM are based on organic material extracted from meteorites through an acid digestion processes (De Gregorio et al., 2013; Alexander et al., 2017). The isolation process can potentially lead to a modification of the IOM as well as in a loss of C that is present in the form of SOM and carbonates (Alexander et al., 2015). A further consequence of the chemical digestion of meteorite matrix, is the loss of all spatial information, limiting efforts to understand the relationship between the OM and the matrix mineralogy. For these reasons, in this study *in situ* C, N, O K-edges XANES were applied to investigate the chemistry and distribution of OM in COs of different petrologic subtype.

In this study, *in situ* analyses of the very primitive COs DOM 08006 and MIL 090010 show the presence of diffusely distributed C-rich regions which have characteristic functional group chemistries that have been previously reported in the analyses of their bulk samples (De Gregorio et al., 2015a). The absorption spectra are generally characterised by the presence of aromatic C, ketone, and carboxyl, with carbonate occasionally present in some areas. The carbonate feature detected in some of the spectra can be related to carbonaceous sub-grains similar to those observed in CIs (Garvie & Buseck, 2006), Tagish Lake (Zega et al., 2010), CRs (Le Guillou & Brearley, 2014b) and IDPs (Flynn et al., 2003). However, it could also be related to terrestrial weathering, which is the case for NWA 7892, that includes a calcite vein cross-cutting one of the FIB sections (Figure 4.30). The relative intensities in the C K-edge XANES spectra of the OM vary depending on their location within the sample, perhaps suggesting that what is present in the sample can be in the form of inter-grain carbonaceous material and distinct carbonaceous sub-grains which was also discussed by Alexander et al. (2017).

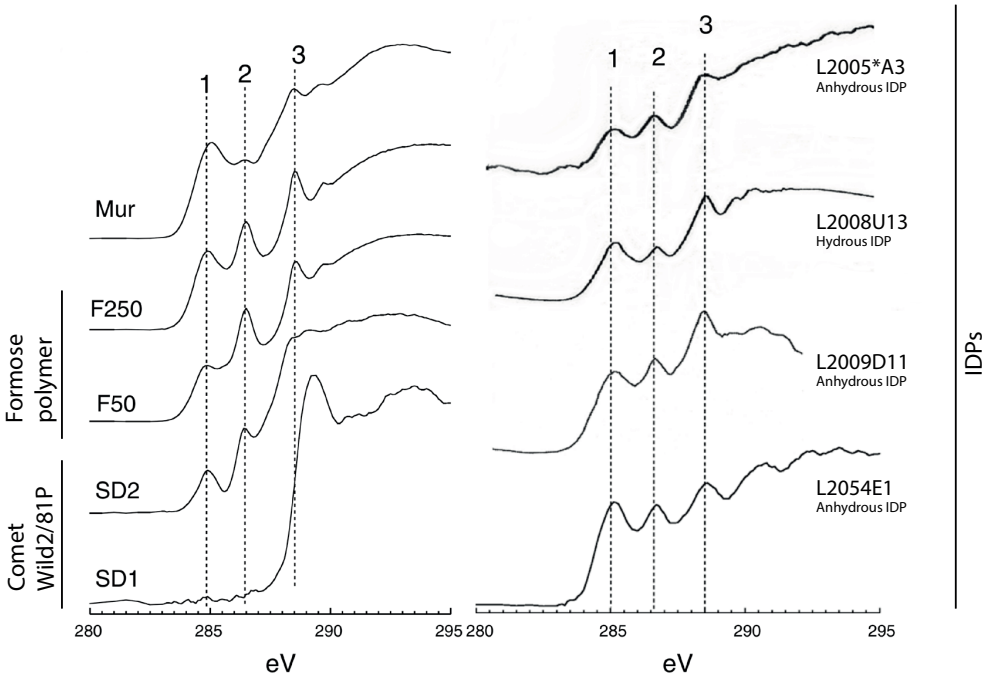


Figure 5.5: *Comparison of C K-edge XANES spectra of organic matter from Murchison (Mur), Formose polymer standards (F250 and F50), Comet Wild2/81P and IDPs after Cody et al. (2011). All the spectra present features corresponding to aromatic carbon (1), ketone (2) and carboxyl (3) which are also characteristic of low petrologic subtype COs studied in the present work.*

Bulk spectra of extracted IOM have similar features to *in situ* measurements, but they do not show such wide variation in the functional group chemistry (De Gregorio et al., 2013). However, the OM in the most pristine samples DOM 08006, NWA 7892 and MIL 090010 shows lots of variation that are characteristic of their low petrologic subtype. The C K-edge spectra from the low petrologic subtype CO chondrites present similar features (Figure 5.5) to those in other pristine extra-terrestrial samples such as IDPs (Flynn et al., 2003) and cometary materials returned by the Stardust mission (Cody et al., 2008), meaning that these materials contain organic matter that is constituted by the same type of functional groups.

Based on the evidence obtained through correlated analysis of the C K-edge XANES with TEM images and SEM-EDX maps of DOM 08006, NWA 7892, MIL 090010, Kainsaz, Ornans and Moss it was not possible to define if there were any obvious preferential mineralogical phases associated with the OM. In the literature there is evidence of association of OM with phyllosilicates in MET 00426 (CR3) (Le Guillou & Brearley, 2014b) as well as in Murchison (CM2), Ivuna (CI), Orgueil (CI) and Tagish Lake (C2-

Ungrouped) (Pearson et al., 2002), and in the proximity of enstatite needles or plates in QUE 99177 (CR3) (Alexander et al., 2017). Moreover, OM can also be present within the matrix material in the form of nanoglobules (Nakamura et al., 2002; Garvie & Buseck, 2004), similar to those I observed in DOM 08006 (Figure 4.19). Nanoglobules were also found in IDPs (Garvie & Buseck, 2004; Nakamura-Messenger et al., 2006) and samples from comet 8P/Wild2 (De Gregorio et al., 2010), and this further strengthen the pristine nature of DOM 08006 and link between primitive materials such as IDPs and the components of chondrite matrices (Klock et al., 1989; Alexander et al., 2017).

In low petrologic subtype samples I observed several C K-edge spectral variations in the functional groups. These differences could be associated to different OM precursor materials, or, if in common, they might not have been homogeneous at the nanometre scale (Alexander et al., 2017). Variations in chemical signatures of OM across the sample could also be due alteration processes form aqueous activity or thermal metamorphism. The effect of water may influence the kinetics of reactions while the most significant modifications that affected OM were likely due to thermal metamorphism, as it favored the carbonisation and oxidation processes (Alexander et al., 2017). One of the main examples is the progressive transformation of the OM in Tagish Lake. Tagish Lake comprises different lithologies and these are also reflected in the properties of the IOM. Alexander et al. (2017) observed that OM in Tagish Lake shifts from being very aliphatic-rich (typical of CI/CR- like IOM) to aliphatic-poor OM typical of CO chondrites likely due to hydrothermal activity.

The heterogeneous distribution of the carbonaceous material and the presence of rare phyllosilicates within the matrix of DOM 08006, NWA 7892 and MIL 090010 might be related to hydrothermal fluids that were mobilising the organics within the parent body (Le Guillou & Brearley, 2014b), with the chemistry of the fluids and minerals acting as catalysts (Alexander et al., 2017). Alexander et al. (2017) reports that the first evidence of thermal metamorphism on COs is the coarsening of matrix minerals, which can be seen already in petrologic subtype 3.05. The effect of temperature on OM is noticeable with increasing thermal metamorphism as its abundance decreases with increasing temperature (Alexander et al., 2007b, 2017). In higher petrologic subtypes the OM becomes homogenised with aromatic C (C=C) being the main feature, while

features associated with ketone and carboxyle aromatic groups become weaker and they almost disappear. These observations are consistent with studies such as Alexander et al. (2007b) and Alexander et al. (2017). More specifically, in Kainsaz (CO3.2) there is an intensification of the aromatic C peak (C=C) at 285 eV (Figure 4.34), which is an indicator that metamorphic processes influence the aromatisation of the OM (De Gregorio et al., 2015b). While in Moss (CO3.6) the aromatic C feature as well the ketone and the carboxyl features are still perceivable but they are very faint and difficult to distinguish (Figure 4.34). This suggests that in higher petrologic grade samples OM (Figure 4.34) persists in lower abundance as they tend to be destroyed because of its sensitivity to heating. This observation is in agreement with previous work from Alexander et al. (2007a, 2017) which affirms that these results are particularly true for for COs and CVs up to petrologic subtypes 3.6 - 3.8. However, in contrast to the study of Cody et al. (2008) in Moss I did not observe a strengthening of the C=C peak, instead there was a broadening of the feature, which is barely visible (in Moss) compared to the same feature in Kainsaz (Figure 4.34).

Thermal metamorphism also influences the O K-edge spectra, with changes in the intensity and shape of the pre-edge, and of the doublet peak on the absorption edge (Figure 4.35). The pre-edge feature in MIL 090010 is very broad, likely made up of two sharper components centred at slightly different energies. One component is related to amorphous or poorly crystalline olivine and the other may be an absorption peak from alcohol/ether (Figure 4.35). While the pre-edge feature of poorly crystalliine olivine persists up to high petrologic grades, the pre-edge feature associated with alcohol/ether can be seen to have disappeared by grade 3.2 (Figure 4.35).

## 5.6 Implications

Based on my results, I suggest that CO meteorites formed from an anhydrous parent body where limited aqueous alteration took place because the main source of water was from hydrated Fe-bearing amorphous silicates rather than the melting of water ice, suggesting that the CO parent body(s) might have accreted in a region of the proto-planetary disk that did not contain much ice. The amorphous silicates were

hydrated in the nebula forming a gel-like material with some partially crystallised into phyllosilicates. The water carried from the amorphous silicates contributed to oxidation of the Fe to $Fe^{3+}$, that I see recorded in the most pristine CO chondrites. Magnetite was also detected within the most primitive CO chondrites, and since only a few phyllosilicates are present, and there is no evidence of altered Fe-Ni metal or sulphides, this suggests that alteration was very limited and that all of these phases might have a nebular origin as also suggested by Vollmer et al. (2020). Low petrologic subtype COs show that submicron scale porosity is low, which is due to the amorphous silicates that act as a groundmass and therefore the limited fluid circulation which contributed the heterogeneous distribution and nature of the organic material in the least altered samples. However, with increased temperature the water contained in the amorphous silicates was released and localised in specific locations within the CO parent body(s) as the submicron porosity increased due to the crystallisation of the amorphous silicates into olivine. The release of water led to metasomatism and formation of nepheline and feldspars in chondrules, CAIs, and AOAs; these effects were seen with the appearance of nepheline from subtype 3.4 owords, with abundances up to 6.5 vol%. The release of aqueous fluids combined with heating likely homogenised the OM present in higher petrologic subtype sample.

Considering the range of subtypes that characterise CO3 chondrites, and the range of temperature at which every subtype was exposed during metamorphic processes I would assume that the asteroidal parent body(s) might have had an onion shell like structure, with COs parent body(s) reaching at least 50 Km in radius (Krot et al., 2014b). The high petrologic subtype COs would be concentrated in the inner part of the perent body(s) while the least metamorphosed samples on the surface, with the heating derived form the decay of $^{26}Al$ as it has been modelled for ordinary chondrites (Bennett & McSween, 1996). This would explain the gradual changes that we can see reflected in the meteorite samples in terms of mineralogy, texture and organic matter.

## 5.7 Summary

Overall, *in-situ* and bulk analyses provided a very detailed insight into the history of the COs asteroidal parent body(s) and its formation. Here listed are the main findings of the present analyses followed by their interpretation in connection with the larger scale context:

- XRD is a quick and effective technique to determine the petrologic subtype of COs looking at variations happening with increasing metamorphism such as changes in olivine chemistry, disappearance of amorphous silicates and magnetite, and increase in nepheline content. The petrologic sequence determined in the present work is consistent with the scale of Chizmadia et al. (2002) based on the compositions of AOAs.

- Thermal metamorphism affects the texture of the matrix material. I observed gradual crystallisation of the amorphous silicates, which were present as a groundmass, into olivine and the coarsening of the latter towards higher petrologic subtypes. As a consequence of this process, the porosity of the COs changed from $\sim$ 2 area % in CO3.0 to $\sim$ 25 area % in CO3.6.

- *In situ* Fe L-edge XANES measurements reveal variations in the Fe oxidation state, which changes from low petrologic subtype samples dominated by $Fe^{3+}$, associated with amorphous silicates, into $Fe^{2+}$ associated with crystalline silicate minerals. The oxidised nature of the amorphous silicates leads to the hypotheses that they might be hydrated phases and therefore a source of water for metamosomatic processes.

- *In situ* C K-edge XANES revealed variations in the organic material speciation within the matrix of low petrologic subtype samples. These samples are characterised by four main C functional groups such as aromatic (C=C), ketone (C=O), carboxyl (-COOH) and carbonate ($CO_3$). These variations became more homogenised with increasing thermal metamorphism.

# Chapter 6

# Conclusions

The CO3 chondrites form a metamorphic sequence, from 3.0 to 3.8, allowing an in depth study of the metamorphic history of this primitive meteorite group. CO3 chondrites are known to be chemically similar throughout the metamorphic sequence and have undergone minimal aqueous alteration. This means that their metamorphic history is not masked by other alteration processes, making them the ideal suite of materials for this study. This work is focused on the characterisation of matrix material in CO3 carbonaceous chondrites, with the aim to study the nature of the matrix mineralogy/organics in the most pristine CO meteorites and characterise how they changed with thermal metamorphism.

## 6.1 Final remarks

In order to characterise the nature of the pristine matrix and changes with thermal metamorphism I carried out both bulk and *in-situ* analyses of the CO chondrites. Most of the CO chondrites studied in this work are falls (7 samples out of 12), but some desert finds were also analysed, especially for the lower petrologic subtypes. XRD was used to analyse bulk CO chondrite powders and showed how their mineralogy changes with increasing thermal metamorphism. *In-situ* analyses were used to obtain mineralogical and chemical information about the matrix down to the nanometre scale. For example, SEM imaging, EDX maps and EPMA analyses of matrix areas in CO chondrites showed how element distributions and abundances varied in meteorites of different petrologic grade. These analyses were used to identify and characterise areas of matrix from which

FIB sections were extracted for investigation by TEM and synchrotron based STXM. STXM allowed the application of element specific XANES for the determination of Fe oxidation states within crystalline and amorphous phases, and the characterisation of organic matter through the determination of functional group chemistry (analysing C, N and O K-edges). TEM imaging offered a complementary technique to STXM and XANES and provided insights concerning the mineralogy and texture of the samples at sub-micron level.

The combined bulk and *in-situ* analyses provided a detailed insight into the formation and thermal history of the CO chondrite asteroid parent body. Low petrologic subtype COs are very unequilibrated materials and thermal metamorphism played an important role in the Fe and Mg exchange between matrix and chondrules, leading to variations in olivine chemistry. Olivine in the most unequilibrated samples is predominately forsteritic and gradually becomes increasingly Fe-rich towards the high petrologic subtypes, with $Fo_{60}$ being the most abundant olivine chemistry with increasing metamorphism, reaching up to 46.6 vol% in Isna. It was also demonstrated that XRD is an efficient and reliable method that can be applied for the determination of CO petrologic subtype. By monitoring variations in olivine abundances and peak intensity, XRD is especially strong in situations where changes to the petrologic grade may be too subtle for other techniques less sensitive to bulk properties.

Magnetite is present in the low petrologic subtype COs (3.0 to 3.1) up to 9.3 vol%, but it decomposes with thermal metamorphism forming fayalite and secondary kamacite. In this study I observed at the nanometre scale that thermal metamorphism contributes to the migration of Cr towards the edges of the matrix olivine grains (observed in chondrules by Grossman & Brearley (2005)) forming distinct chromite nuggets outside the olivine grain. However, this observation was made just in Moss (CO3.6), and it would be interesting to further explore this aspect looking at 3.7 and 3.8 COs to understand if this is a phenomenon, likely related to thermal metamorphism, occurring in all high petrologic subtype CO samples or if it is a unique characteristic of Moss, as this will give more insights on the effect of temperature on matrix material.

Amorphous silicates are characteristic phases only in the matrix of the least altered COs (3.0 to 3.1), as they are very sensitive to heating and aqueous alteration. Their

origin is still poorly understood and the most accepted theory about their formation is that they formed in the interstellar nebula as a result of disequilibrium condensation, however there is also the possibility that the amorphous material represents the glass with embedded metal and sulfide grains also known as GEMS. Thermal metamorphism contributes to their crystallisation into olivine, which also affects the sub-micron porosity of the samples, increasing from ∼2 area % in CO3.0 up to ∼25 area % in CO3.6, as the matrix grains become coarser but they occupy less volume. Overall, thermal metamorphism affects the texture of the samples by progressively increasing the porosity and the average grainsize of the minerals, which is very noticeable with TEM analysis. Thermal metamorphism also led to variations in the Fe oxidation state of amorphous and crystalline silicates, changing from low petrologic subtype samples dominated by $Fe^{3+}$, to high petrologic subtype samples being dominated by $Fe^{2+}$. This change in Fe oxidation state can be explained by changes in redox conditions within the parent body with increasing thermal metamorphism as the environment became more reducing due to the presence of reducing agents such as H and C (Menzies et al., 2005).

Low petrologic subtype COs are rich in amorphous silicates, which are known to be carriers of water and could have hydrated in the nebula. This may help explain why the Fe present in the amorphous silicates is $Fe^{3+}$ and suggests that low petrologic subtype COs were exposed to oxidising conditions. The water contained in the amorphous silicates could have been released during metamorphism, contributing to the presence of water fluids within the parent body(s). The presence of fluids, although limited, together with the temperature increase lead to metasomatic processes that contributed to the formation of nepheline (up to 6.5 wt% in CO3.8) at the expense of mesostasis and feldspars in chondrules, CAIs and AOIs.

Organic matter was found in the matrix of DOM 08006, NWA 7892, MIL 090010, Kainsaz, Ornans and Moss. For DOM 08006, NWA 7892 and MIL 090010, I observed variations in the functional groups across the samples supporting the hypothesis that these samples are pristine and that heating did not strongly modify the organic matter. With increasing petrologic subtype the functional groups become more homogenised across the samples and the intensity of the spectral features becomes weaker, suggesting that the OM is modified and destroyed by thermal metamorphism. Moreover, the

spectra of OM observed within these samples present similarities to spectra obtained from bulk analysis of the same samples, although with *in situ* analysis it was possible to detect more variations in the functional group across the same sample, as well as presenting similarities to spectra of OM found in IDPs and other extra-terrestrial materials (e.g. Stardust samples).

## 6.2 Future work

It was not possible to further explore many aspects of my project due to time, here are some interesting points that would be good to further develop:

- Analysis of more CO chondrites through XRD, to improve the subtype classification as well as to assign a specific petrologic subtype to many COs which on the Meteoritical Bulletin are simply classified as CO3.
- To further investigate the nature of the amorphous silicates, for example measuring the amount of $H_2O$ contained in them similar to previous studies by (Le Guillou & Brearley, 2014b).
- Further TEM analysis for a better determination of the matrix mineralogy at nanometer level, as well as chemical maps. These analyses would help an in depth observation of any existing relationship between mineralogy and organic matter.
- TEM analysis of high petrologic subtype COs for more extensive investigations of the Cr nuggets forming outside matrix olivine grains.

# Bibliography

Abreu, N. M., & Brearley, A. J. (2010). Early solar system processes recorded in the matrices of two highly pristine CR3 carbonaceous chondrites, MET 00426 and QUE 99177. Geochim. Cosmochim. Acta, *74*, 1146–1171.

Afiattalab, F., & Wasson, J. T. (1980). Composition of the metal phases in ordinary chondrites: implications regarding classification and metamorphism. Geochim. Cosmochim. Acta, *44*(3), 431,445–443,446.

Ahrens, L. H., Willis, J. P., & Erlank, A. J. (1973). The Chemical Composition of Kainsaz and Efremovka. *Meteoritics*, *8*.

Alexander, C. M. O., Boss, A. P., Keller, L. P., Nuth, J. A., & Weinberger, A. (2007a). Astronomical and Meteoritic Evidence for the Nature of Interstellar Dust and Its Processing in Protoplanetary Disks. In B. Reipurth, D. Jewitt, & K. Keil (Eds.) *Protostars and Planets V*, (p. 801).

Alexander, C. M. O., Fogel, M., Yabuta, H., & Cody, G. D. (2007b). The origin and evolution of chondrites recorded in the elemental and isotopic compositions of their macromolecular organic matter. *Geochimica et Cosmochimica Acta*, *71*, 4380–4403.

Alexander, C. M. O., Bowden, R., Fogel, M. L., & Howard, K. T. (2015). Carbonate abundances and isotopic compositions in chondrites. *Meteoritics and Planetary Science*, *50*(4), 810–833.

Alexander, C. M. O., Cody, G. D., De Gregorio, B. T., Nittler, L. R., & Stroud, R. M. (2017). The nature, origin and modification of insoluble organic matter in chondrites, the major source of Earth's C and N. *Chemie der Erde / Geochemistry*, *77*, 227–256.

Alexander, C. M. O., Greenwood, R. C., Bowden, R., Gibson, J. M., Howard, K. T., & Franchi, I. A. (2018). A mutli-technique search for the most primitive CO chondrites. *Geochimica et Cosmochimica Acta*, *221*, 406–420.

Amelin, Y., Krot, A. N., Hutcheon, I. D., & Ulyanov, A. A. (2002). Lead Isotopic Ages of Chondrules and Calcium-Aluminum-Rich Inclusions. *Science*, *297*(5587), 1678–1683.

Apai, D., Connolly, H. C., Jr., & Lauretta, D. S. (2010). *Thermal Processing in Protoplanetary Nebulae*, (pp. 230–262).

Apai, D., & Lauretta, D. S. (2010). *Planet Formation and Protoplanetary Dust*, (pp. 1–26).

Asphaug, E., Agnor, C. B., & Williams, Q. (2006). Hit-and-run planetary collisions. Nature, *439*, 155–160.

Batchelder, M., & Cressey, G. (1998). Rapid, accurate phase quantification of clay-bearing samples using a position-sensitive x-ray detector. *Clays and Clay Minerals*, *46*(2), 183–194. URL `https://doi.org/10.1346/CCMN.1998.0460209`

Bennett, I., Marvin E., & McSween, J., Harry Y. (1996). Revised model calculations for the thermal histories of ordinary chondrite parent bodies. *Meteoritics and Planetary Science*, *31*(6), 783–792.

Berlin, J., Jones, R. H., & Brearley, A. J. (2011). Fe-Mn systematics of type IIA chondrules in unequilibrated CO, CR, and ordinary chondrites. *Meteoritics and Planetary Science*, *46*(4), 513–533.

Bilet, M., & Roaldset, E. (2014). The meteorite Moss - a rare carbonaceous chondrite. In T. J. Jopek, F. J. M. Rietmeijer, J. Watanabe, & I. P. Williams (Eds.) *Meteoroids 2013*, (p. 69).

Bland, P. A., Zolensky, M. E., Benedix, G. K., & Sephton, M. A. (2006). *Weathering of Chondritic Meteorites*, (p. 853).

Bland, P. A., Jackson, M. D., Coker, R. F., Cohen, B. A., Webber, J. B. W., Lee, M. R., Duffy, C. M., Chater, R. J., Ardakani, M. G., McPhail, D. S., McComb, D. W., & Benedix, G. K. (2009). Why aqueous alteration in asteroids was isochemical: High porosity $\neq$ high permeability. *Earth and Planetary Science Letters*, *287*(3-4), 559–568.

Bland, P. A., Howard, L. E., Prior, D. J., Wheeler, J., Hough, R. M., & Dyl, K. A. (2011). Earliest rock fabric formed in the Solar System preserved in a chondrule rim. *Nature Geoscience*, *4*(4), 244–247.

Bonal, L., Bourot-Denise, M., Quirico, E., Montagnac, G., & Lewin, E. (2007). Organic matter and metamorphic history of CO chondrites. Geochim. Cosmochim. Acta, *71*(6), 1605–1623.

Bonal, L., Quirico, E., Bourot-Denise, M., & Montagnac, G. (2006). Determination of the petrologic type of CV3 chondrites by Raman spectroscopy of included organic matter. Geochim. Cosmochim. Acta, *70*(7), 1849–1863.

Boss, A. P., & Goswami, J. N. (2006). *Presolar Cloud Collapse and the Formation and Early Evolution of the Solar System*, (pp. 171–186).

Boss, A. P., & Keiser, S. A. (2015). Triggering Collapse of the Presolar Dense Cloud Core and Injecting Short-lived Radioisotopes with a Shock Wave. IV. Effects of Rotational Axis Orientation. ApJ, *809*(1), 103.

Bourdelle, F., Benzerara, K., Beyssac, O., Cosmidis, J., Neuville, D. R., Brown, G. E., & Paineau, E. (2013). Quantification of the ferric/ferrous iron ratio in silicates by scanning transmission X-ray microscopy at the Fe $L_{2,3}$ edges. *Contributions to Mineralogy and Petrology*, *166*, 423–434.

Bradley, J. (2007). 1.26 - interplanetary dust particles. In H. D. Holland, & K. K. Turekian (Eds.) *Treatise on Geochemistry*, (pp. 1 – 24). Oxford: Pergamon.
URL `http://www.sciencedirect.com/science/article/pii/B008043751601152X`

Bradley, J. P. (2013). How and where did GEMS form? Geochim. Cosmochim. Acta, *107*, 336–340.

Brearley, A. J. (1990). Matrix Mineralogy of the Unequilibrated CO3 Chondrite, ALH A77307: Evidence for Disequilibrium Condensation Processes and Implications for the Origin of Chondrite Matrices. In *Lunar and Planetary Science Conference*, vol. 21 of *Lunar and Planetary Science Conference*.

Brearley, A. J. (1993). Matrix and fine-grained rims in the unequilibrated CO3 chondrite, ALHA77307 - Origins and evidence for diverse, primitive nebular dust components. Geochim. Cosmochim. Acta, *57*, 1521–1550.

Brearley, A. J. (1996). Compositional and Mineralogical Trends in Fine-Grained Chondrule Rims in CO Chondrites. In *Lunar and Planetary Science Conference*, vol. 27 of *Lunar and Planetary Science Conference*.

Brearley, A. J., & Jones, R. H. (1998). Chondritic meteorites. *Reviews in mineralogy and geochemistry*, *36*(1), 3–1.

Brearley, A. J. (2003). Nebular versus Parent-body Processing. *Treatise on Geochemistry*, *1*, 711.

Brearley, A. J., & Krot, A. N. (2013). *Metasomatism in the Early Solar System: The Record from Chondritic Meteorites*, (pp. 659–789). Berlin, Heidelberg: Springer Berlin Heidelberg.

Brearley, A. J. (2014). *Nebular Versus Parent Body Processing*, vol. 1, (pp. 309–334).

Brenker, F. E. (2010). Nanopetrology of pyroxenes: reconstruction of geodynamic parameters using TEM techniques. In *Nanoscopic Approaches in Earth and Planetary Sciences*. Mineralogical Society of Great Britain and Ireland.
URL `https://doi.org/10.1180/EMU-notes.8.2`

Burbine, T. H. (2016). *Meteorites, Minerals, and Isotopes*, (p. 66–132). Cambridge Planetary Science. Cambridge University Press.

Buseck, P. R., & Hua, X. (1993). Matrices of carbonaceous chondrite meteorites. *Annual Review of Earth and Planetary Sciences*, *21*, 255–305.

Busemann, H., Young, A. F., O'D. Alexand er, C. M., Hoppe, P., Mukhopadhyay, S., & Nittler, L. R. (2006). Interstellar Chemistry Recorded in Organic Matter from Primitive Meteorites. *Science*, *312*(5774), 727–730.

Chizmadia, L. J., Rubin, A. E., & Wasson, J. T. (2002). Mineralogy and petrology of amoeboid olivine inclusions in CO3 chondrites: Relationship to parent-body aqueous alteration. *Meteoritics and Planetary Science*, *37*(12), 1781–1796.

Chizmadia, L. J., Nuth, I., J. A., & Rietmeijer, F. J. M. (2006). Experimental Aqueous Alteration of Amorphous Silicate Smokes. In S. Mackwell, & E. Stansbery (Eds.) *37th Annual Lunar and Planetary Science Conference*, Lunar and Planetary Science Conference, (p. 2187).

Chizmadia, L. J., & Brearley, A. J. (2008). Mineralogy, aqueous alteration, and primitive textural characteristics of fine-grained rims in the Y-791198 CM2 carbonaceous chondrite: TEM observations and comparison to ALHA81002. Geochim. Cosmochim. Acta, *72*(2), 602–625.

Ciesla, F. J., Lauretta, D. S., Cohen, B. A., & Hood, L. L. (2003). A nebular origin for chondritic fine-grained phyllosilicates. *Science*, *299*(5606), 549–552.
URL https://science.sciencemag.org/content/299/5606/549

Clarke, R. S., Jr. (1975). Meteoritical Bulletin, No. 53. *Meteoritics*, *10*.

Cloutis, E. A., Hudon, P., Hiroi, T., Gaffey, M. J., & Mann, P. (2012). Spectral reflectance properties of carbonaceous chondrites - 5: CO chondrites. Icarus, *220*(2), 466–486.

Cody, G., Alexander, C., Yabuta, H., Kilcoyne, A., Araki, T., Ade, H., Dera, P., Fogel, M., Militzer, B., & Mysen, B. (2008). Organic thermometry for chondritic parent bodies. *Earth and Planetary Science Letters*, *272*(1), 446 – 455.
URL http://www.sciencedirect.com/science/article/pii/S0012821X08003294

Cody, G. D., Ade, H., O'D. Alexander, C. M., Araki, T., Butterworth, A., Fleckenstein, H., Flynn, G., Gilles, M. K., Jacobsen, C., Kilcoyne, A. L. D., Messenger, K., Sandford, S. A., Tyliszczak, T., Westphal, A. J., Wirick, S., & Yabuta, H. (2008). Quantitative organic and light-element analysis of comet 81P/Wild 2 particles using C-, N-, and O-$\mu$-XANES. *Meteoritics and Planetary Science*, *43*, 353–365.

Cody, G. D., Heying, E., Alexander, C. M. O., Nittler, L. R., Kilcoyne, A. L. D., Sandford, S. A., & Stroud, R. M. (2011). Establishing a molecular relationship between chondritic and cometary organic solids. *Proceedings of the National Academy of Sciences*, *108*(48), 19171–19176.
URL https://www.pnas.org/content/108/48/19171

Connolly Jr., H. C., Zipfel, J., Folco, L., Smith, C., Jones, R. H., Benedix, G., Righter, K., Yamaguchi, A., Aoudjehane, H. C., & Grossman, J. N. (2007). The meteoritical bulletin, no. 91, 2007 march. *Meteoritics & Planetary Science*, *42*(3), 413–466.
URL https://onlinelibrary.wiley.com/doi/abs/10.1111/j.1945-5100.2007.tb00242.x

Cressey, G., Henderson, C. M. B., & van der Laan, G. (1993). Use of l-edge x-ray absorption spectroscopy to characterize multiple valence states of 3d transition metals; a new probe

for mineralogical and geochemical research. *Physics and Chemistry of Minerals*, *20*(2), 111–119.
URL https://doi.org/10.1007/BF00207204

Cressey, G., & Schofield, P. F. (1996). Rapid whole-pattern profile-stripping method for the quantification of multiphase samples. *Powder Diffraction*, *11*, 35–39.

Davidson, J., Nittler, L. R., Alexander, C. M. O., & Stroud, R. M. (2014). Petrography of Very Primitive CO3 Chondrites: Dominion Range 08006, Miller Range 07687, and Four Others. In *Lunar and Planetary Science Conference*, vol. 45 of *Lunar and Planetary Inst. Technical Report*, (p. 1384).

Davidson, J., Alexander, C. M. O., Stroud, R. M., Busemann, H., & Nittler, L. R. (2019). Mineralogy and petrology of Dominion Range 08006: A very primitive CO3 carbonaceous chondrite. Geochim. Cosmochim. Acta, *265*, 259–278.

Davis, A. M., & Richter, F. M. (2014). *Condensation and Evaporation of Solar System Materials*, vol. 1, (pp. 335–360).

De Gregorio, B. T., Stroud, R. M., Nittler, L. R., Alexander, C. M. O. D., Kilcoyne, A. L. D., & Zega, T. J. (2010). Isotopic anomalies in organic nanoglobules from Comet 81P/Wild 2: Comparison to Murchison nanoglobules and isotopic anomalies induced in terrestrial organics by electron irradiation. Geochim. Cosmochim. Acta, *74*(15), 4454–4470.

De Gregorio, B. T., Stroud, R. M., Nittler, L. R., Alexander, C. M. O., Bassim, N. D., Cody, G. D., Kilcoyne, A. L. D., Sandford, S. A., Milam, S. N., Nuevo, M., & Zega, T. J. (2013). Isotopic and chemical variation of organic nanoglobules in primitive meteorites. *Meteoritics and Planetary Science*, *48*, 904–928.

De Gregorio, B. T., Stroud, R. M., Burgess, K. D., Davidson, J., Nittler, L. R., & Alexander, C. M. O. (2015a). Chemical Heterogeneity of Organic Matter in Minimally-Heated CO Chondrites. In *78th Annual Meeting of the Meteoritical Society*, vol. 78, (p. 5128).

De Gregorio, B. T., Stroud, R. M., Davidson, J., Nittler, L. R., Alexander, C. M. O., Burgess, K., & Kilcoyne, A. L. D. (2015b). Chemical Heterogeneity of Organic Matter in Minimally-Heated CO Chondrites. In *Lunar and Planetary Science Conference*, (p. 2951).

DeMeo, F. E., Alexander, C. M. O., Walsh, K. J., Chapman, C. R., & Binzel, R. P. (2015). *The Compositional Structure of the Asteroid Belt*, (pp. 13–41).

Dodd, R. T. (1969). Metamorphism of the ordinary chondrites: A review. Geochim. Cosmochim. Acta, *33*(2), 161,IN1,165–164,IN5,203.

Dunn, T. L., Cressey, G., McSween, J., Harry Y. _jr., & McCoy, T. J. (2010a). Analysis of ordinary chondrites using powder X-ray diffraction: 1. Modal mineral abundances. *Meteoritics and Planetary Science*, *45*(1), 123–134.

Dunn, T. L., McSween, J., Harry Y. _jr., McCoy, T. J., & Cressey, G. (2010b). Analysis of ordinary chondrites using powder X-ray diffraction: 2. Applications to ordinary chondrite parent-body processes. *Meteoritics and Planetary Science*, *45*(1), 135–156.

Ebel, D. S. (2006). *Condensation of Rocky Material in Astrophysical Environments*, (p. 253).

Ebel, D. S., Brunner, C., Konrad, K., Leftwich, K., Erb, I., Lu, M., Rodriguez, H., Crapster-Pregont, E. J., Friedrich, J. M., & Weisberg, M. K. (2016). Abundance, major element composition and size of components and matrix in CV, CO and Acfer 094 chondrites. Geochim. Cosmochim. Acta, *172*, 322–356.

Fahey, A. J., Zinner, E., Kurat, G., & Kracher, A. (1994). Hibonite-hercynite inclusion HH-1 from the Lancé (CO3) meteorite: The history of an ultrarefractory CAI. Geochim. Cosmochim. Acta, *58*(21), 4779–4793.

Floss, C., & Stadermann, F. J. (2009). High Abundances of Circumstellar and Interstellar C-Anomalous Phases in the Primitive CR3 Chondrites QUE 99177 and MET 00426. ApJ, *697*(2), 1242–1255.

Floss, C., & Stadermann, F. J. (2012). Presolar silicate and oxide abundances and compositions in the ungrouped carbonaceous chondrite Adelaide and the K chondrite Kakangari: The effects of secondary processing. *Meteoritics and Planetary Science*, *47*(6), 992–1009.

Flynn, G. J., Keller, L. P., Feser, M., Wirick, S., & Jacobsen, C. (2003). The origin of organic matter in the solar system: evidence from the interplanetary dust particles. *Geochimica et Cosmochimica Acta*, *67*, 4791–4806.

Gail, H. P. (1998). Chemical reactions in protoplanetary accretion disks. IV. Multicomponent dust mixture. A&A, *332*, 1099–1122.

Gail, H. P. (2003). *Formation and Evolution of Minerals in Accretion Disks and Stellar Outflows*, (pp. 55–120).

Garvie, L. A. J., & Buseck, P. R. (2004). Nanosized carbon-rich grains in carbonaceous chondrite meteorites. *Earth and Planetary Science Letters*, *224* (3-4), 431–439.

Garvie, L. A. J., & Buseck, P. R. (2006). Carbonaceous materials in the acid residue from the Orgueil carbonaceous chondrite meteorite. *Meteoritics and Planetary Science*, *41* (4), 633–642.

Garvie, L. A. J. (2010). Can electron energy-loss spectroscopy (EELS) be used to quantify hydrogen in minerals from the O K edge? *American Mineralogist*, *95* (1), 92–97.

Gilmour, I. (2003). 1.10 - structural and isotopic analysis of organic matter in carbonaceous chondrites. In H. D. Holland, & K. K. Turekian (Eds.) *Treatise on Geochemistry*, (pp. 269 – 290). Oxford: Pergamon.
URL `http://www.sciencedirect.com/science/article/pii/B0080437516011464`

Grady, M. M., & Wright, I. (2006). *Types of extraterrestrial material available for study*, (p. 3).

Graham, A. L. (1984). Meteoritical Bulletin, No. 62. *Meteoritics*, *19*.

Greenwood, R. C., & Franchi, I. A. (2004). Alteration and metamorphism of CO3 chondrites: Evidence from oxygen and carbon isotopes. *Meteoritics and Planetary Science*, *39* (11), 1823–1838.

Greenwood, R. C., Pearson, V. K., Verchovsky, A. B., Johnson, D., Franchi, I. A., Roaldset, E., Raade, G., & Bartoschewitz, R. (2007). The Moss (CO3) Meteorite: An Integrated Isotopic, Organic and Mineralogical Study. In *Lunar and Planetary Science Conference*, (p. 2267).

Greshake, A. (1997). The primitive matrix components of the unique carbonaceous chondrite ACFER 094: A TEM study. Geochim. Cosmochim. Acta, *61* (2), 437–452.

Grossman, L. (1972). Condensation in the primitive solar nebula. Geochim. Cosmochim. Acta, *36*, 597–619.

Grossman, J. N. (1994). The Meteoritical Bulletin, no. 76, 1994 January: The U.S. Antarctic Meteorite Collection. *Meteoritics*, *29*, 100–143.

Grossman, J. N., & Score, R. (1996). The Meteoritical Bulletin, No. 79, 1996 July: Recently classified specimens in the United States Antarctic Meteorite Collection (1994-1996). *Meteoritics and Planetary Science Supplement*, *31*, A161–A174.

Grossman, J. N., & Brearley, A. J. (2005). The onset of metamorphism in ordinary and carbonaceous chondrites. *Meteoritics and Planetary Science*, *40*, 87.

Haenecour, P., Floss, C., Zega, T. J., Croat, T. K., Wang, A., Jolliff, B. L., & Carpenter, P. (2018). Presolar silicates in the matrix and fine-grained rims around chondrules in primitive CO3.0 chondrites: Evidence for pre-accretionary aqueous alteration of the rims in the solar nebula. Geochim. Cosmochim. Acta, *221*, 379–405.

Henning, T., & Meeus, G. (2009). Dust Processing and Mineralogy in Protoplanetary Accretion Disks. *ArXiv e-prints*.

Herd, C. D. K., Papike, J. J., & Brearley, A. J. (2001). Oxygen fugacity of martian basalts from electron microprobe oxygen and TEM-EELS analyses of Fe-Ti oxides. *American Mineralogist*, *86*(9), 1015–1024.

Hezel, D. C., & Palme, H. (2010). The chemical relationship between chondrules and matrix and the chondrule matrix complementarity. *Earth and Planetary Science Letters*, *294*, 85–93.

Hopp, T., & Vollmer, C. (2018). Chemical composition and iron oxidation state of amorphous matrix silicates in the carbonaceous chondrite acfer 094. *Meteoritics & Planetary Science*, *53*(2), 153–166.
URL `https://onlinelibrary.wiley.com/doi/abs/10.1111/maps.12991`

Housley, R. M. (1984). An SEM study of preterrestrial alteration effects in ALHA 77003. *Meteoritics*, *19*(4), 242–243.

Howard, K. T., Benedix, G. K., Bland, P. A., & Cressey, G. (2009). Modal mineralogy of CM2 chondrites by X-ray diffraction (PSD-XRD). Part 1: Total phyllosilicate abundance and the degree of aqueous alteration. Geochim. Cosmochim. Acta, *73*, 4576–4589.

Howard, K. T., Benedix, G. K., Bland, P. A., & Cressey, G. (2010). Modal mineralogy of CV3 chondrites by X-ray diffraction (PSD-XRD). Geochim. Cosmochim. Acta, *74*, 5084–5097.

Howard, K. T., Benedix, G. K., Bland, P. A., & Cressey, G. (2011). Modal mineralogy of CM chondrites by X-ray diffraction (PSD-XRD): Part 2. Degree, nature and settings of aqueous alteration. Geochim. Cosmochim. Acta, *75*, 2735–2751.

Howard, K. T., Alexander, C. M. O. D., Schrader, D. L., & Dyl, K. A. (2015). Classification of hydrous meteorites (CR, CM and C2 ungrouped) by phyllosilicate fraction: PSD-XRD modal mineralogy and planetesimal environments. Geochim. Cosmochim. Acta, *149*, 206–222.

Huss, G. R., & Lewis, R. S. (1994a). Noble Gases in Presolar Diamonds. I.: Three Distinct Components and Their Implications for Diamond Origins. *Meteoritics*, *29*(6), 791.

Huss, G. R., & Lewis, R. S. (1994b). Noble Gases in Presolar Diamonds. II.: Component Abundances Reflect Thermal Processing. *Meteoritics*, *29*(6), 811.

Huss, G. R., Rubin, A. E., & Grossman, J. N. (2006). *Thermal Metamorphism in Chondrites*, (pp. 567–586).

Hutchison, R. (1996). Hot Accretion of the Ordinary Chondrites: The Rocks Don't Lie. In *Lunar and Planetary Science Conference*, vol. 27, (p. 579).

Hutchison, R. (2004). *Meteorites*.

Ikeda, Y. (1982). Petrology of the ALH-77003 chondrite (C3). *National Institute Polar Research Memoirs*, *25*, 34–65.

Imae, N., & Nakamuta, Y. (2018). A new mineralogical approach for CO3 chondrite characterization by X-ray diffraction: Identification of primordial phases and thermal history. *Meteoritics and Planetary Science*, *53*(2), 232–248.

Ishii, H. A., Bradley, J. P., Bechtel, H. A., Brownlee, D. E., Bustillo, K. C., Ciston, J., Cuzzi, J. N., Floss, C., & Joswiak, D. J. (2018). Multiple generations of grain aggregation in different environments preceded solar system body formation. *Proceedings of the National Academy of Science*, *115*, 6608–6613.

Itoh, D., & Tomeoka, K. (2003). Dark inclusions in CO3 chondrites: new indicators of parent-body processes. Geochim. Cosmochim. Acta, *67*(1), 153–169.

Jacobsen, Wirick, Flynn, & Zimba (2000). Soft x-ray spectroscopy from image sequences with sub-100 nm spatial resolution. *Journal of Microscopy*, *197*(2), 173–184. URL https://onlinelibrary.wiley.com/doi/abs/10.1046/j.1365-2818.2000.00640.x

Jones, R. H., & Rubie, D. C. (1990). Thermal Metamorphism in CO3 Chondrites: Application of Olivine Diffusion Modelling to Post-Accretionary Metamorphism. In *Lunar and Planetary Science Conference*, vol. 21 of *Lunar and Planetary Inst. Technical Report*.

Jones, R. H., & Rubie, D. C. (1991). Thermal histories of CO3 chondrites: Application of olivine diffusion modelling to parent body metamorphism. *Earth and Planetary Science Letters*, *106*(1-4), 73–86.

Jones, R. H. (1992). On the relationship between isolated and chondrule olivine grains in the carbonaceous chondrite ALHA 77307. Geochim. Cosmochim. Acta, *56*(9), 3593–3593.

Jones, R. H. (1997). Alteration of Plagioclase-rich Chondrules in CO3 Chondrites: Evidence for Late-stage Sodium and Iron Metasomatism in a Nebular Environment. In M. E. Zolensky, A. N. Krot, & E. R. D. Scott (Eds.) *Parent-Body and Nebular Modification of Chondritic Materials*, (p. 30).

Kallemeyn, G. W., Rubin, A. E., & Wasson, J. T. (1991). The compositional classification of chondrites. V - The Karoonda (CK) group of carbonaceous chondrites. Geochim. Cosmochim. Acta, *55*, 881–892.

Keck, B. D., & Sears, D. W. G. (1987). Chemical and physical studies of type 3 chondrites—VIII: Thermoluminescence and metamorphism in the CO chondrites. Geochim. Cosmochim. Acta, *51*(11), 3013–3021.

Keller, L. P., & Buseck, P. R. (1990). Matrix mineralogy of the Lancé CO3 carbonaceous chondrite: A transmission electron microscope study. *Geochimica et Cosmochimica Acta*, *54*, 1155–1163.

Keller, L. P., & Messenger, S. (2007). Amorphous Silicates in Early Solar System and Presolar Materials. In *Chronology of Meteorites and the Early Solar System*, (pp. 88–89).

Keller, L. P., & Messenger, S. (2011). On the origins of GEMS grains. Geochim. Cosmochim. Acta, *75*(18), 5336–5365.

Kemper, F., Vriend, W. J., & Tielens, A. G. G. M. (2004). The Absence of Crystalline Silicates in the Diffuse Interstellar Medium. ApJ, *609*(2), 826–837.

Kerridge, J. F. (1964). Low-temperature Minerals from the Fine-grained Matrix of Some Carbonaceous Meteorites. In H. E. Whipple, & W. A. Cassidy (Eds.) *Cosmic Dust*, vol. 119, (p. 41).

Kimura, M., Grossman, J. N., & Weisberg, M. K. (2008). Fe-Ni metal in primitive chondrites: Indicators of classification and metamorphic conditions for ordinary and CO chondrites. *Meteoritics and Planetary Science*, *43*(7), 1161–1177.

King, A. J., Schofield, P. F., Howard, K. T., & Russell, S. S. (2015). Modal mineralogy of CI and CI-like chondrites by X-ray diffraction. Geochim. Cosmochim. Acta, *165*, 148–160.

King, A. J., Schofield, P. F., & Russell, S. S. (2017). Type 1 aqueous alteration in cm carbonaceous chondrites: Implications for the evolution of water-rich asteroids. *Meteoritics and Planetary Science*, (pp. 1–19).
URL `http://dx.doi.org/10.1111/maps.12872`

King, A., Bates, H., Krietsch, D., Busemann, H., Clay, P., Schofield, P., & Russell, S. (2019). The yamato-type (cy) carbonaceous chondrite group: Analogues for the surface of asteroid ryugu? *Geochemistry*.
URL `http://www.sciencedirect.com/science/article/pii/S0009281919300236`

Klock, W., Thomas, K. L., McKay, D. S., & Palme, H. (1989). Unusual olivine and pyroxene composition in interplanetary dust and unequilibrated ordinary chondrites. Nature, *339*(6220), 126–128.

Krot, A. N., Keil, K., Scott, E. R. D., Goodrich, C. A., & Weisberg, M. K. (2014a). *Classification of Meteorites and Their Genetic Relationships*, vol. 1, (pp. 1–63).

Krot, T. V., Scott, E. R. D., & Goldstein, J. I. (2014b). Thermal Histories of CO3 Chondrites: Constraints on Parent Body Size and Time of Accretion. In *77th Annual Meeting of the Meteoritical Society*, vol. 1800 of *LPI Contributions*, (p. 5108).

Krot, A. N., Nagashima, K., & Simon, S. B. (2017). Mineralogically-Controlled Oxygen-Isotope Exchange in Refractory Inclusions from CO Carbonaceous Chondrites During Fluid-Rock Interaction. In *80th Annual Meeting of the Meteoritical Society*, vol. 1987 of *LPI Contributions*, (p. 6056).

Kurat, G., & Kracher, A. (1980). Basalts in the Lancé carbonaceous chondrite. *Zeitschrift Naturforschung Teil A*, *35*, 180–190.

Lambrechts, M., & Johansen, A. (2012). Rapid growth of gas-giant cores by pebble accretion. A&A, *544*, A32.

Lauretta, D. S., Fegley, J., Bruce, Lodders, K., & Kremser, D. T. (1996). The kinetics and mechanism of iron sulfide formation in the solar nebula. *Antarctic Meteorite Research*, *9*, 111.

Le Guillou, C., & Brearley, A. (2014a). Relationships between organics, water and early stages of aqueous alteration in the pristine CR3.0 chondrite MET 00426. *Geochimica et Cosmochimica Acta*, *131*, 344–367.

Le Guillou, C., & Brearley, A. (2014b). Relationships between organics, water and early stages of aqueous alteration in the pristine CR3.0 chondrite MET 00426. Geochim. Cosmochim. Acta, *131*, 344–367.

Le Guillou, C., Changela, H. G., & Brearley, A. J. (2015). Widespread oxidized and hydrated amorphous silicates in CR chondrites matrices: Implications for alteration conditions and $H_2$ degassing of asteroids. *Earth and Planetary Science Letters*, *420*, 162–173.

Lee, M. R., & Bland, P. A. (2004). Mechanisms of weathering of meteorites recovered from hot and cold deserts and the formation of phyllosilicates. Geochim. Cosmochim. Acta, *68*(4), 893–916.

Lee, M. (2010). Transmission electron microscopy (tem) of earth and planetary materials: a review. *Mineralogical Magazine*, *74*(1), 1–27.
URL `http://eprints.gla.ac.uk/25484/`

Lee, M. R., Lindgren, P., King, A. J., Greenwood, R. C., Franchi, I. A., & Sparkes, R. (2016). Elephant Moraine 96029, a very mildly aqueously altered and heated CM carbonaceous chondrite: Implications for the drivers of parent body processing. Geochim. Cosmochim. Acta, *187*, 237–259.

Lerotic, M., Mak, R., Wirick, S., Meirer, F., & Jacobsen, C. (2014). *MANTiS*: a program for the analysis of X-ray spectromicroscopy data. *Journal of Synchrotron Radiation*, *21*(5), 1206–1212.
URL `https://doi.org/10.1107/S1600577514013964`

Leroux, H. (2006). Amorphous Silicate Hydration in the Protoplanetary Disk: An Experimental Approach. *Meteoritics and Planetary Science Supplement*, *41*, 5190.

McAdam, M. M., Sunshine, J. M., Howard, K. T., Alexander, C. M., McCoy, T. J., & Bus, S. J. (2018). Spectral evidence for amorphous silicates in least-processed CO meteorites and their parent bodies. Icarus, *306*, 32–49.

McSween, J., H. Y. (1977). Carbonaceous chondrites of the Ornans type: A metamorphic sequence. Geochim. Cosmochim. Acta, *41*(4), 477–491.

McSween, J., H. Y., & Richardson, S. M. (1977). The composition of carbonaceous chondrite matrix. Geochim. Cosmochim. Acta, *41*(8), 1145–1161.

Menzies, O. N., Bland, P. A., Berry, F. J., & Cressey, G. (2005). A M^ssbauer spectroscopy and X-ray diffraction study of ordinary chondrites: Quantification of modal mineralogy and implications for redox conditions during metamorphism. *Meteoritics and Planetary Science*, *40*, 1023.

Methot, R. L., Noonan, A. F., Jarosewich, E., Al-Far, D. M., & Degasparis, A. A. (1975). Mineralogy, petrology and chemistry of the Isna /C3/ meteorite. *Meteoritics*, *10*, 121–130.

Min, M., & Flynn, G. (2010). *Dust Composition in Protoplanetary Disks*, (pp. 161–190).

Misawa, K., & Nakamura, N. (1988). Highly fractionated rare-earth elements in ferromagnesian chondrules from the Felix (CO3) meteorite. Nature, *334*(6177), 47–50.

Nagahara, H. (1982). Ni-Fe Metals in Chondrites and Their Parental Body. In *15th ISAS Lunar and Planetary Symposium*, (p. 313).

Nakamura, K., Zolensky, M. E., Tomita, S., Nakashima, S., & Tomeoka, K. (2002). Hollow organic globules in the Tagish Lake meteorite as possible products of primitive organic reactions. *International Journal of Astrobiology*, *1*(3), 179–189.

Nakamura, T., Noguchi, T., Tanaka, M., Zolensky, M. E., Kimura, M., Tsuchiyama, A., Nakato, A., Ogami, T., Ishida, H., Uesugi, M., Yada, T., Shirai, K., Fujimura, A., Okazaki, R., Sandford, S. A., Ishibashi, Y., Abe, M., Okada, T., Ueno, M., Mukai, T., Yoshikawa, M., & Kawaguchi, J. (2011). Itokawa Dust Particles: A Direct Link Between S-Type Asteroids and Ordinary Chondrites. *Science*, *333*(6046), 1113.

Nakamura-Messenger, K., Messenger, S., Keller, L. P., Clemett, S. J., & Zolensky, M. E. (2006). Organic Globules in the Tagish Lake Meteorite: Remnants of the Protosolar Disk. *Science*, *314*(5804), 1439–1442.

Newton, J., Bischoff, A., Arden, J. W., Franchi, I. A., Geiger, T., Greshake, A., & Pillinger, C. T. (1995). Acfer 094, a uniquely primitive carbonaceous chondrite from the Sahara. *Meteoritics*, *30*(1), 47–56.

Nittler, L. R., Alexander, C. M. O., & Stroud, R. M. (2013). High Abundance of Presolar Materials in CO3 Chondrite Dominion Range 08006. In *Lunar and Planetary Science Conference*, (p. 2367).

Nittler, L. R., Alexander, C. M. O., Davidson, J., Riebe, M. E. I., Stroud, R. M., & Wang, J. (2018). High abundances of presolar grains and $^{15}$N-rich organic matter in CO3.0 chondrite Dominion Range 08006. Geochim. Cosmochim. Acta, *226*, 107–131.

Nuth, J. A., III., Brearley, A. J., & Scott, E. R. D. (2005). Microcrystals and Amorphous Material in Comets and Primitive Meteorites: Keys to Understanding Processes in the Early Solar System. In A. N. Krot, E. R. D. Scott, & B. Reipurth (Eds.) *Chondrites and the Protoplanetary Disk*, vol. 341 of *Astronomical Society of the Pacific Conference Series*, (p. 675).

Palme, H., Hezel, D. C., & Ebel, D. S. (2015). The origin of chondrules: Constraints from matrix composition and matrix-chondrule complementarity. *Earth and Planetary Science Letters*, *411*, 11 – 19.
URL `http://www.sciencedirect.com/science/article/pii/S0012821X14007250`

Pearson, V. K., Sephton, M. A., Kearsley, A. T., Bland, P. A., Franchi, I. A., & Gilmour, I. (2002). Clay mineral-organic matter relationships in the early solar system. *Meteoritics and Planetary Science*, *37*(12), 1829–1833.

Pearson, V. K., Sephton, M. A., Franchi, I. A., Gibson, J. M., & Gilmour, I. (2006). Carbon and nitrogen in carbonaceous chondrites: Elemental abundances and stable isotopic compositions. *Meteoritics and Planetary Science*, *41*(12), 1899–1918.

Pollack, J. B., Hollenbach, D., Beckwith, S., Simonelli, D. P., Roush, T., & Fong, W. (1994). Composition and Radiative Properties of Grains in Molecular Clouds and Accretion Disks. ApJ, *421*, 615.

Pontoppidan, K. M., & Brearley, A. J. (2010). *Dust Particle Size Evolution*, (pp. 191–229).

Reed, S. J. B. (2005). *Electron Microprobe Analysis and Scanning Electron Microscopy in Geology*. Cambridge University Press, 2 ed.

Remusat, L. (2015). Organics in primitive meteorites. *EMU Notes in Mineralogy*, *15*, 33–65.

Rubin, A. E., James, J. A., Keck, B. D., Weeks, K. S., Sears, D. W. G., & Jarosewich, E. (1985). The Colony Meteorite and Variations in CO3 Chondrite Properties. *Meteoritics*, *20*, 175.

Rubin, A. E., & Wasson, J. T. (1988). Chondrules and matrix in the Ornans CO3 meteorite: Possible precursor components. Geochim. Cosmochim. Acta, *52*(2), 425–432.

Rubin, A. E., & Brearley, A. J. (1996). A Critical Evaluation of the Evidence for Hot Accretion. Icarus, *124*(1), 86–96.

Rubin, A. E. (1998). Correlated petrologic and geochemical characteristics of CO3 chondrites. *Meteoritics and Planetary Science*, *33*.

Rubin, A. E., & Li, Y. (2019). Formation and destruction of magnetite in co3 chondrites and other chondrite groups. *Geochemistry*.
URL http://www.sciencedirect.com/science/article/pii/S0009281919300315

Russell, S. S., Huss, G. R., Fahey, A. J., Greenwood, R. C., Hutchison, R., & Wasserburg, G. J. (1998). An Isotopic and Petrologic Study of Calcium-Aluminum-Rich Inclusions from CO3 Meteorites. *Geochemica and Cosmochimica Acta*, *62*, 689–714.

Russell, S. S. (2007). The formation of the solar system. *Journal of the Geological Society*, *164*(3), 481–492.
URL http://jgs.geoscienceworld.org/content/164/3/481

Ruzicka, A., Grossman, J., Bouvier, A., Herd, C. D. K., & Agee, C. (2015). The meteoritical bulletin, no. 101. *Meteoritics & Planetary Science*, *50*(9), 1661–1661.
URL https://onlinelibrary.wiley.com/doi/abs/10.1111/maps.12490

Ruzicka, A., Grossman, J., Bouvier, A., Herd, C. D. K., & Agee, C. B. (2015). The meteoritical bulletin, no. 102. *Meteoritics & Planetary Science*, *50*(9), 1662–1662.
URL https://onlinelibrary.wiley.com/doi/abs/10.1111/maps.12491

Schofield, P. F., Henderson, C. M. B., Cressey, G., & van der Laan, G. (1995). $2p$ X-ray Absorption Spectroscopy in the Earth Sciences. *Journal of Synchrotron Radiation*, *2*(2), 93–98.
URL `https://doi.org/10.1107/S0909049595000598`

Schofield, P. F., Knight, K. S., Covey-Crump, S. J., Cressey, G., & Stretton, I. C. (2002). Accurate quantification of the modal mineralogy of rocks when image analysis is difficult. *Mineralogical Magazine*, *66*(1), 189–200.
URL `ingentaconnect.com/content/minsoc/mag/2002/00000066/00000001/art00012`

Schwinger, S., Dohmen, R., & Schertl, H. P. (2016). Modeling of Type II Chondrule Compositions in CO3 Chondrites — Constrains on the Conditions of Chondrule Formation and Thermal Metamorphism. In *79th Annual Meeting of the Meteoritical Society*, vol. 79, (p. 6165).

Scott, E. R. D., & Jones, R. H. (1990). Disentangling nebular and asteroidal features of CO3 carbonaceous chondrite meteorites. *Geochimica et Cosmochimica Acta*, *54*, 2485–2502.

Scott, E. R. D., & Krot, A. N. (2005). Thermal Processing of Silicate Dust in the Solar Nebula: Clues from Primitive Chondrite Matrices. ApJ, *623*(1), 571–578.

Scott, E. R. D., & Krot, A. N. (2014). *Chondrites and Their Components*, vol. 1, (pp. 65–137).

Sears, D. W. G., Batchelor, J. D., Lu, J., & Keck, B. D. (1991). Metamorphism of CO and CO-like chondrites and comparisons with type 3 ordinary chondrites. *Antarctic Meteorite Research*, *4*, 319.

Sears, D. W. G. (2016). The CO chondrites: Major recent Antarctic finds, their thermal and radiation history, and describing the metamorphic history of members of the class. Geochim. Cosmochim. Acta, *188*, 106–124.

Seifert, L. S., Haenecour, P. H., Zega, T. Z., & Floss, C. F. (2018). TEM Analysis of Presolar Silicate Grain in the Dominion Range 08006, CO Chondrite. In *Lunar and Planetary Science Conference*, vol. 49 of *Lunar and Planetary Inst. Technical Report*, (p. 2980).

Semenov, D., Chakraborty, S., & Thiemens, M. (2010). *Chemical and Isotopic Evolution of the Solar Nebula and Protoplanetary Disks*, (pp. 97–127).

Shibata, Y., & Matsueda, H. (1994). Chemical composition of Fe-Ni metal and phosphate minerals in Yamato-82094 carbonaceous chondrite. *Antarctic Meteorite Research*, *7*, 110.

Simon, S. B., & Grossman, L. (2015). Refractory inclusions in the pristine carbonaceous chondrites DOM 08004 and DOM 08006. *Meteoritics and Planetary Science*, *50*(6), 1032–1049.

Smith, A. D., Schofield, P. F., Cressey, G., Cressey, B. A., & Read, P. D. (2004). The development of X-ray photo-emission electron microscopy (XPEEM) for valence-state imaging of mineral intergrowths. *Mineralogical Magazine*, *68*(6), 859–869.
URL https://doi.org/10.1180/0026461046860228

Stroud, R. M., Nittler, L. R., & Alexander, C. M. O. (2013). Analytical Electron Microscopy of a CAI-Like Presolar Grain and Associated Fine-Grained Matrix Materials in the Dominion Range 08006 CO3 Meteorite. In *Lunar and Planetary Science Conference*, (p. 2315).

Takahashi, O., Tamenori, Y., Suenaga, T., Ikeda-Fukazawa, T., Matsuno, J., & Tsuchiyama, A. (2018). XANES spectra of forsterite in crystal, surface, and amorphous states. *AIP Advances*, *8*(2), 025107.

Tomeoka, K., & Itoh, D. (2004). Sodium-metasomatism in chondrules in CO3 chondrites: Relationship to parent body thermal metamorphism. *Meteoritics and Planetary Science*, *39*(8), 1359–1373.

van Aken, P. A., & Liebscher, B. (2002). Quantification of ferrous/ferric ratios in minerals: new evaluation schemes of Fe $L_{23}$ electron energy-loss near-edge spectra. *Physics and Chemistry of Minerals*, *29*(3), 188–200.

van Boekel, R., Min, M., Leinert, C., Waters, L. B. F. M., Richichi, A., Chesneau, O., Dominik, C., Jaffe, W., Dutrey, A., Graser, U., Henning, T., de Jong, J., Köhler, R., de Koter, A., Lopez, B., Malbet, F., Morel, S., Paresce, F., Perrin, G., Preibisch, T., Przygodda, F., Schöller, M., & Wittkowski, M. (2004). The building blocks of planets within the 'terrestrial' region of protoplanetary disks. *Nature*, *432*, 479–482.

Vincze, L., Silversmit, G., Vekemans, B., Terzano, R., & Brenker, F. (2010). Synchrotron radiation micro-and nanospectroscopy. *European Mineralogical Union Notes in Mineralogy*, *8*, 169–237.

Vollmer, C., Pelka, M., Leitner, J., & Janssen, A. (2020). Amorphous silicates as a record of solar nebular and parent body processes—A transmission electron microscope study of fine-grained rims and matrix in three Antarctic CR chondrites. *Meteoritics and Planetary Science*, *55*(7), 1491–1508.

Walsh, K. J., Morbidelli, A., Raymond, S. N., O'Brien, D. P., & Mandell, A. M. (2011). A low mass for Mars from Jupiter's early gas-driven migration. Nature, *475*(7355), 206–209.

Walsh, K. J., Morbidelli, A., Raymond, S. N., O'Brien, D. P., & Mandell, A. M. (2012). Populating the asteroid belt from two parent source regions due to the migration of giant planets—"the grand tack". *Meteoritics & Planetary Science*, *47*(12), 1941–1947.
URL https://onlinelibrary.wiley.com/doi/abs/10.1111/j.1945-5100.2012.01418.x

Wasinger, E. C., de Groot, F. M. F., Hedman, B., Hodgson, K. O., & Solomon, E. I. (2003). L-edge x-ray absorption spectroscopy of non-heme iron sites: Experimental determination of differential orbital covalency. *Journal of the American Chemical Society*, *125*(42), 12894–12906. PMID: 14558838.
URL https://doi.org/10.1021/ja034634s

Weisberg, M. K., McCoy, T. J., & Krot, A. N. (2006). *Systematics and Evaluation of Meteorite Classification*, (pp. 19–52).

Weisberg, M. K., Smith, C., Herd, C., Haack, H., Yamaguchi, A., Chennaoui Aoudjehane, H., Welzenbach, L., & Grossman, J. N. (2010). The meteoritical bulletin, no. 98, september 2010. *Meteoritics & Planetary Science*, *45*(9), 1530–1551.
URL https://onlinelibrary.wiley.com/doi/abs/10.1111/j.1945-5100.2010.01119.x

Wirth, R. (2010). Focused ion beam (FIB): site-specific sample preparation, nano-analysis, nano-characterization and nano-machining. In *Nanoscopic Approaches in Earth and Planetary Sciences*. Mineralogical Society of Great Britain and Ireland.
URL https://doi.org/10.1180/EMU-notes.8.1

Wood, J. A. (1967). Chondrites: Their metallic minerals, thermal histories, and parent planets. Icarus, *6*, 1–49.

Zega, T. J., Alexander, C. M. O. D., Busemann, H., Nittler, L. R., Hoppe, P., Stroud, R. M., & Young, A. F. (2010). Mineral associations and character of isotopically anomalous organic

material in the Tagish Lake carbonaceous chondrite. Geochim. Cosmochim. Acta, *74*(20), 5966–5983.

Zhang, M., Bonato, E., King, A. J., Russell, S. S., Tang, G., & Lin, Y. (2020). Petrology and oxygen isotopic compositions of calcium-aluminum-rich inclusions in primitive CO3.0-3.1 chondrites. *Meteoritics and Planetary Science*, *55*(4), 911–935.

Zinner, E. K. (2003). Presolar Grains. *Treatise on Geochemistry*, *1*, 711.

Zolensky, M. E., Abreu, N. M., Velbel, M. A., Rubin, A., Chaumard, N., Noguchi, T., & Michikami, T. (2018). Chapter 2 - physical, chemical, and petrological characteristics of chondritic materials and their relationships to small solar system bodies. In N. Abreu (Ed.) *Primitive Meteorites and Asteroids*, (pp. 59 – 204). Elsevier.
URL `http://www.sciencedirect.com/science/article/pii/B9780128133255000021`

Zolotov, M. Y., Mironenko, M. V., & Shock, E. L. (2006). Thermodynamic constraints on fayalite formation on parent bodies of chondrites. *Meteoritics and Planetary Science*, *41*(11), 1775–1796.

# Appendix

## A Comprehensive list of minerals identified by HR-XRD

| **Sample** | **Classification** | **Mineralogical assemblages*** |
|---|---|---|
| Colony | CO 3.0 | Forsterite, Enstatite, Augite, Troilite, Kamacite, Anorthite, Magnetite, Maghemite, Goethite, Smectite, *Clinoenstatite, Diopside, Albite, Tremolite, Saponite* |
| DOM 08006 | CO 3.0 | Forsterite, Olivine, Enstatite, Augite, Troilite, Kamacite, Anorthite, Magnetite, Akaganeite, *Clinoenstatite, Goethite* |
| NWA 7892 | CO 3.05 | Forsterite, Olivine, Enstatite, Augite, Troilite, Kamacite, Magnetite, *Clinoenstatite, Diopside, Anorthite, Albite, Calcite, Goethite* |
| MIL 090010 | CO 3.1 | Forsterite, Olivine, Enstatite, Augite, Troilite, Pyrrhotite, Kamacite, Magnetite, *Clinoenstatite, Pigeonite, Diopside, Albite, Anorthite, Labradorite, Akagaenite* |
| Kainsaz | CO 3.2 | Forsterite, Olivine, Enstatite, Augite, Troilite, Pyrrhotite, Kamacite, Anorthite, *Clinoenstatite, Nepheline, Magnetite, Calcite, Goethite, Cronstedtite* |
| Felix | CO 3.3 | Forsterite, Olivine, Enstatite, Augite, Troilite, Pyrrhotite, Kamacite, Nepheline, Magnetite, *Clinoenstatite, Aegirine, Diospide, Albite, Labradorite* |
| Ornans | CO 3.4 | Forsterite, Olivine, Enstatite, Augite, Troilite, Pyrrhotite, Kamacite, Nepheline, *Clinoenstatite, Aegirine, Anorthite, Labradorite, Magnetite* |
| Lance | CO 3.5 | Forsterite, Olivine, Enstatite, Augite, Diopside, Troilite, Pyrrhotite, Kamacite, Nepheline, *Clinoenstatite, Anorthite* |
| Moss | CO 3.6 | Forsterite, Olivine, Enstatite, Augite, Troilite, Pyrrhotite, Kamacite, Anorthite, Nepheline, *Clinoenstatite, Diopside, Labradorite, Goethite* |
| ALHA77003 | CO 3.6 | Forsterite, Olivine, Enstatite, Augite, Troilite, Pyrrhotite, Kamacite, Anorthite, Nepheline, Goethtie, *Clinoenstatite, Labradorite, Akaganeite* |
| Warrenton | CO 3.7 | Forsterite, Olivine, Enstatite, Augite, Diopside, Troilite, Pyrrhotite, Kamacite, Anorthite, Nepheline, Goethtie, *Clinoenstatite, Labradorite* |
| Isna | CO 3.8 | Olivine, Enstatite, Augite, Diopside, Troilite, Kamacite, Pyrrhotite, Anorthite, Nepheline, Goethite, *Clinoenstatite, Anhydrite* |

Table 1: *Comprehensive list of mineral present determined through high-resolution XRD for 12 CO carbonaceous chondrites. * Minerals in italics are those that were indicated with a low certainty from high resolution XRD data that are potential trace phases but whose presence was not confirmed by PSD-XRD or other methods used in this study.*

# B Comprehensive modal mineralogy of the set of CO3 chondrites determined by PSD-XRD: abundances, uncertainties and detection limits

Comprehensive summary table of the modal mineralogy determined by PSD-XRD

| | Colony (3.0) | | | DOM 08006 (3.0) | | |
|---|---|---|---|---|---|---|
| | vol% | vol% unc | det limits | vol% | vol% unc | det limits |
| **Fo 100** | 30.7 | 1.3 | – | 35.2 | 1.6 | – |
| **Fo 90** | – | – | – | – | – | – |
| **Fo 70** | – | – | – | – | – | – |
| **Fo 60** | – | – | – | 6.9 | 0.7 | – |
| **Fo 50** | – | – | – | – | – | – |
| **Fo 40** | – | – | – | – | – | – |
| **Enstatite** | 23.2 | 0.7 | – | 21.7 | 1.7 | – |
| **Augite** | 2.7 | 0.8 | – | 10.6 | 0.9 | – |
| **Diopside** | – | – | 1.0 | – | – | 0.3 |
| **Troilite** | 0.2 | 0.1 | – | 2.3 | 0.0 | – |
| **Pyrrhotite** | – | – | 0.3 | – | – | 0.4 |
| **Kamacite** | 0.1 | 0.0 | – | 1.1 | 0.1 | – |
| **Anorthite** | 0.5 | 0.1 | – | 1.8 | 0.1 | – |
| **Nepheline** | – | – | 0.9 | – | – | 0.6 |
| **Goethite** | 2.5 | 0.1 | – | – | – | 0.4 |
| **Magnetite** | 2.7 | 0.3 | – | 3.4 | 0.2 | – |
| **Amorphous FeO** | 4.9 | 0.7 | – | – | – | 0.8 |
| **Maghemite** | 2.0 | 0.2 | – | – | – | – |
| **Amorphous silicates** | 30.2 | 1.8 | – | 17.0 | 1.3 | – |
| **Cronstedtite** | 0.2 | 0.0 | – | – | – | 0.2 |
| **Antigorite** | – | – | 0.9 | – | – | 0.9 |
| **Smectite** | – | – | 2.1 | – | – | 1.5 |
| **Calcite** | – | – | 0.2 | – | – | 0.1 |
| **Gypsum** | – | – | 0.4 | – | – | 0.2 |
| **Anhydrite** | – | – | 0.5 | – | – | 0.5 |
| **Totals** | 100.0 | | | 100.0 | | |

| | NWA 7892 (3.05) | | | MIL 090010 (3.1) | | |
|---|---|---|---|---|---|---|
| | vol% | vol% unc | det limits | vol% | vol% unc | det limits |
| **Fo 100** | – | – | – | 17.4 | 0.7 | – |
| **Fo 90** | 37.1 | 2.3 | – | – | – | – |
| **Fo 70** | – | – | – | – | – | – |
| **Fo 60** | 18.7 | 0.8 | – | – | – | – |
| **Fo 50** | – | – | – | 20.0 | 0.7 | – |
| **Fo 40** | – | – | – | – | – | – |
| **Enstatite** | 14.7 | 0.6 | – | 21.0 | 1.1 | – |
| **Augite** | 7.1 | 0.9 | – | 14.6 | 1.2 | – |
| **Diopside** | – | – | 0.9 | – | – | 0.9 |
| **Troilite** | 1.6 | 0.04 | – | 3.2 | 0.06 | – |
| **Pyrrhotite** | – | – | 0.6 | 1.1 | 0.1 | – |
| **Kamacite** | 0.7 | 0.04 | – | 0.5 | 0.03 | – |
| **Anorthite** | – | – | 1.2 | – | – | 0.6 |
| **Nepheline** | – | – | 1.6 | – | – | 1.2 |
| **Labradorite** | – | – | – | – | – | – |
| **Goethite** | – | – | 0.4 | – | – | 0.4 |
| **Magnetite** | 6.7 | 0.4 | – | 9.3 | 0.5 | – |
| **Amorphous FeO** | 7.7 | 0.9 | – | – | – | 1 |
| **Maghemite** | – | – | – | – | – | – |
| **Amorphous silicates** | 5.7 | 0.5 | – | 12.9 | 2 | – |
| **Cronstedtite** | – | – | 0.3 | – | – | 0.3 |
| **Antigorite** | – | – | 1.1 | – | – | 1.1 |
| **Smectite** | – | – | 2.8 | – | – | 2.8 |
| **Calcite** | – | – | 0.4 | – | – | 0.4 |
| **Gypsum** | – | – | 0.3 | – | – | 0.6 |
| **Anhydrite** | – | – | 0.4 | – | – | 0.4 |
| **Totals** | 100.0 | | | 100.0 | | |

Table 2: *Abundances, uncertanties and detection limits (vol%) of the mineralogical phases quantified in COs from 3.0 to 3.1.*

| | Kainsaz (3.2) | | | Felix (3.3) | | |
|---|---|---|---|---|---|---|
| | vol% | vol% unc | det limits | vol% | vol% unc | det limits |
| **Fo 100** | – | – | – | 31.8 | 0.9 | – |
| **Fo 90** | 19.3 | 0.7 | – | – | – | – |
| **Fo 70** | – | – | – | – | – | – |
| **Fo 60** | 19.9 | 1.3 | – | 29.2 | 2 | – |
| **Fo 50** | – | – | – | – | – | – |
| **Fo 40** | 9.5 | 0.5 | – | – | – | – |
| **Enstatite** | 27.5 | 1.7 | – | 16.0 | 1 | – |
| **Augite** | 13.4 | 1 | – | 7.8 | 0.6 | – |
| **Diopside** | – | – | 0.8 | – | – | 1.4 |
| **Troilite** | 2.2 | 0.05 | – | 1.7 | 0.05 | – |
| **Pyrrhotite** | 2.8 | 0.2 | – | 6.5 | 0.1 | – |
| **Kamacite** | 1.3 | 0.07 | – | 0.7 | 0.01 | – |
| **Anorthite** | 4.2 | 0.5 | – | – | – | 1 |
| **Nepheline** | – | – | 1.4 | 5.3 | 0.2 | – |
| **Labradorite** | – | – | – | – | – | – |
| **Goethite** | – | – | 0.4 | – | – | 0.3 |
| **Magnetite** | – | – | 0.6 | 0.9 | 0.04 | – |
| **Amorphous FeO** | – | – | 0.9 | – | – | 0.8 |
| **Maghemite** | – | – | – | – | – | – |
| **Amorphous silicates** | – | – | 2.8 | – | – | 2.6 |
| **Cronstedtite** | – | – | 0.2 | – | – | 0.9 |
| **Antigorite** | – | – | 1 | – | – | 0.9 |
| **Smectite** | – | – | 3.2 | – | – | 5.8 |
| **Calcite** | – | – | 0.4 | – | – | 0.3 |
| **Gypsum** | – | – | 0.6 | – | – | 0.5 |
| **Anhydrite** | – | – | 0.3 | – | – | 0.3 |
| **Totals** | 100.0 | | | 100.0 | | |

| | Ornans (3.4) | | | Lance (3.5) | | |
|---|---|---|---|---|---|---|
| | vol% | vol% unc | det limits | vol% | vol% unc | det limits |
| **Fo 100** | 16.5 | 0.7 | – | – | – | – |
| **Fo 90** | – | – | – | – | – | – |
| **Fo 70** | – | – | – | 16.6 | 1.7 | – |
| **Fo 60** | 36.4 | 2.3 | – | 30.0 | 1.8 | – |
| **Fo 50** | 14.8 | 0.7 | – | 8.2 | 0.7 | – |
| **Fo 40** | – | – | – | – | – | – |
| **Enstatite** | 8.6 | 0.4 | – | 18.8 | 0.8 | – |
| **Augite** | 9.7 | 0.4 | – | 10.5 | 0.4 | – |
| **Diopside** | – | – | 2.6 | 6.7 | 0.3 | – |
| **Troilite** | 2.8 | 0.05 | – | 1.7 | 0.03 | – |
| **Pyrrhotite** | 7.6 | 0.2 | – | 3.6 | 0.1 | – |
| **Kamacite** | 0.3 | 0.04 | – | 0.8 | 0.02 | – |
| **Anorthite** | – | – | 1.2 | – | – | 1.1 |
| **Nepheline** | 3.3 | 0.3 | – | 3.1 | 0.7 | – |
| **Labradorite** | – | – | – | – | – | – |
| **Goethite** | – | – | 0.4 | – | – | 0.4 |
| **Magnetite** | – | – | 0.7 | – | – | 0.7 |
| **Amorphous FeO** | – | – | 1 | – | – | 0.9 |
| **Maghemite** | – | – | – | – | – | – |
| **Amorphous silicates** | – | – | 3.2 | – | – | 2 |
| **Cronstedtite** | – | – | 0.3 | – | – | 0.3 |
| **Antigorite** | – | – | 1.1 | – | – | 1 |
| **Smectite** | – | – | 5.4 | – | – | 5.1 |
| **Calcite** | – | – | 0.4 | – | – | 0.4 |
| **Gypsum** | – | – | 0.8 | – | – | 0.8 |
| **Anhydrite** | – | – | 0.4 | – | – | 0.4 |
| **Totals** | 100.0 | | | 100.0 | | |

Table 3: *Abundances, uncertanties and detection limits (vol%) of the mineralogical phases quantified in COs from 3.2 to 3.5.*

| | Moss (3.6) | | | ALHA77003 (3.6) | | |
|---|---|---|---|---|---|---|
| | vol% | vol% unc | det limits | vol% | vol% unc | det limits |
| **Fo 100** | – | – | – | 29.3 | 4.7 | – |
| **Fo 90** | – | – | – | – | – | – |
| **Fo 70** | 21.9 | 3.3 | – | – | – | – |
| **Fo 60** | – | – | – | 35.0 | 3 | – |
| **Fo 50** | 22.9 | 2.3 | – | – | – | – |
| **Fo 40** | – | – | – | – | – | – |
| **Enstatite** | 22.4 | 0.9 | – | 16.9 | 1.3 | – |
| **Augite** | 13.7 | 0.4 | – | 10.3 | 0.7 | – |
| **Diopside** | – | – | 2.6 | – | – | 2.6 |
| **Troilite** | 2.7 | 0.08 | – | 1.1 | 0.07 | – |
| **Pyrrhotite** | 5.3 | 0.1 | – | 2.4 | 0.1 | – |
| **Kamacite** | 1.4 | 0.02 | – | 0.4 | 0.04 | – |
| **Anorthite** | 3.3 | 0.2 | – | 1.8 | 0.1 | – |
| **Nepheline** | 6.5 | 0.2 | – | 2.4 | 0.3 | – |
| **Labradorite** | – | – | – | – | – | – |
| **Goethite** | – | – | 0.4 | 0.3 | 0.1 | – |
| **Magnetite** | – | – | 0.8 | – | – | 0.9 |
| **Amorphous FeO** | – | – | 1 | – | – | 1.1 |
| **Maghemite** | – | – | – | – | – | – |
| **Amorphous silicates** | – | – | 2.1 | – | – | 2.8 |
| **Cronstedtite** | – | – | 0.3 | – | – | 0.4 |
| **Antigorite** | – | – | 1.1 | – | – | 1.3 |
| **Smectite** | – | – | 5.3 | – | – | 4.1 |
| **Calcite** | – | – | 0.4 | – | – | 0.6 |
| **Gypsum** | – | – | 0.8 | – | – | 0.6 |
| **Anhydrite** | – | – | 0.4 | – | – | 0.3 |
| **Totals** | 100.0 | | | 100.0 | | |

| | Warrenton (3.7) | | | Isna (3.8) | | |
|---|---|---|---|---|---|---|
| | vol% | vol% unc | det limits | vol% | vol% unc | det limits |
| **Fo 100** | – | – | – | – | – | – |
| **Fo 90** | – | – | – | – | – | – |
| **Fo 70** | – | – | – | – | – | – |
| **Fo 60** | 45.6 | 1.4 | – | 46.6 | 1.5 | – |
| **Fo 50** | – | – | – | – | – | – |
| **Fo 40** | – | – | – | – | – | – |
| **Enstatite** | 13.7 | 1.5 | – | 8.4 | 1.2 | – |
| **Augite** | 10.7 | 0.9 | – | 12.3 | 0.6 | – |
| **Diopside** | 12.0 | 0.6 | – | 13.2 | 0.4 | – |
| **Troilite** | 3.0 | 0.1 | – | 3.0 | 0.2 | – |
| **Pyrrhotite** | 4.7 | 0.3 | – | 4.8 | 0.3 | – |
| **Kamacite** | 0.4 | 0.03 | – | 0.4 | 0.05 | – |
| **Anorthite** | 2.3 | 0.1 | – | 3.5 | 0.2 | – |
| **Nepheline** | 6.3 | 0.3 | – | 6.5 | 0.6 | – |
| **Labradorite** | – | – | – | – | – | – |
| **Goethite** | 1.2 | 0.2 | – | 1.2 | 0.3 | – |
| **Magnetite** | – | – | 0.6 | – | – | 1.1 |
| **Amorphous FeO** | – | – | 1 | – | – | 1.9 |
| **Maghemite** | – | – | – | – | – | – |
| **Amorphous silicates** | – | – | 2.6 | – | – | 3.2 |
| **Cronstedtite** | – | – | 0.3 | – | – | 0.4 |
| **Antigorite** | – | – | 1 | – | – | 1.1 |
| **Smectite** | – | – | 5.2 | – | – | 7 |
| **Calcite** | – | – | 0.8 | – | – | 0.4 |
| **Gypsum** | – | – | 0.8 | – | – | 0.8 |
| **Anhydrite** | – | – | 0.4 | – | – | 0.4 |
| **Totals** | 100.0 | | | 100.0 | | |

Table 4: *Abundances, uncertanties and detection limits (vol%) of the mineralogical phases quantified in COs from 3.6 to 3.6.*

# C PSD-XRD: model fits and residual patterns

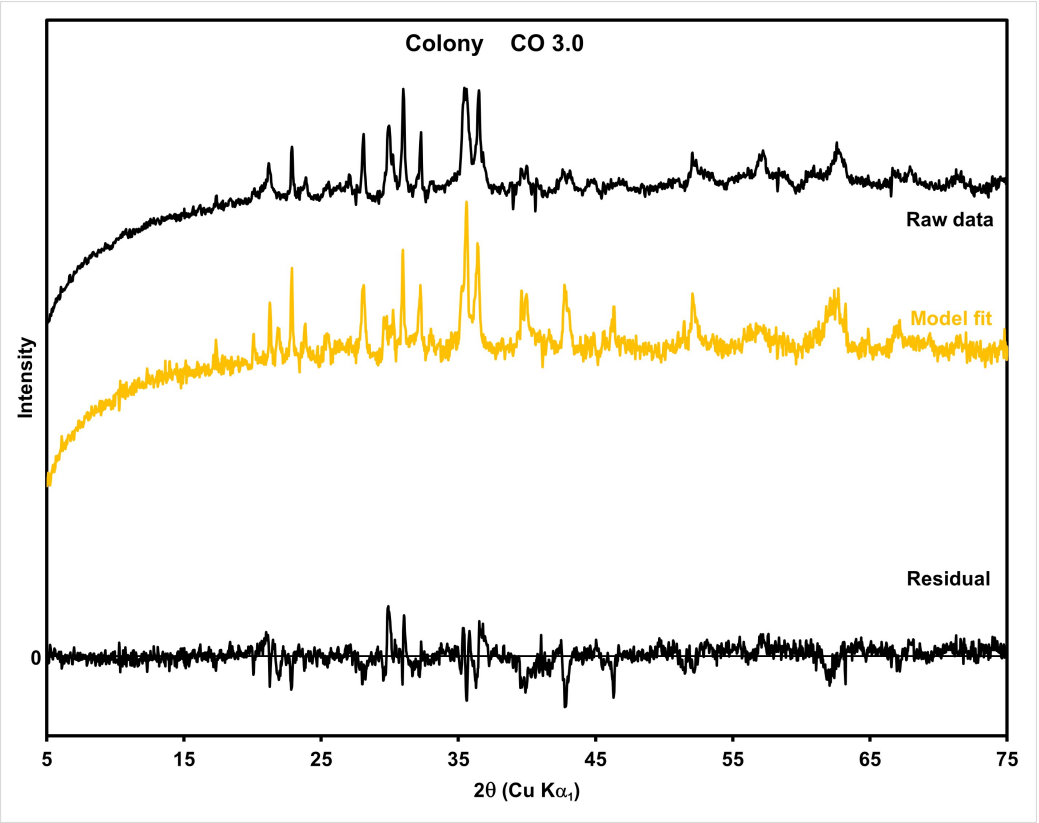


Figure 1: *Colony raw data, model fit and residual pattern*

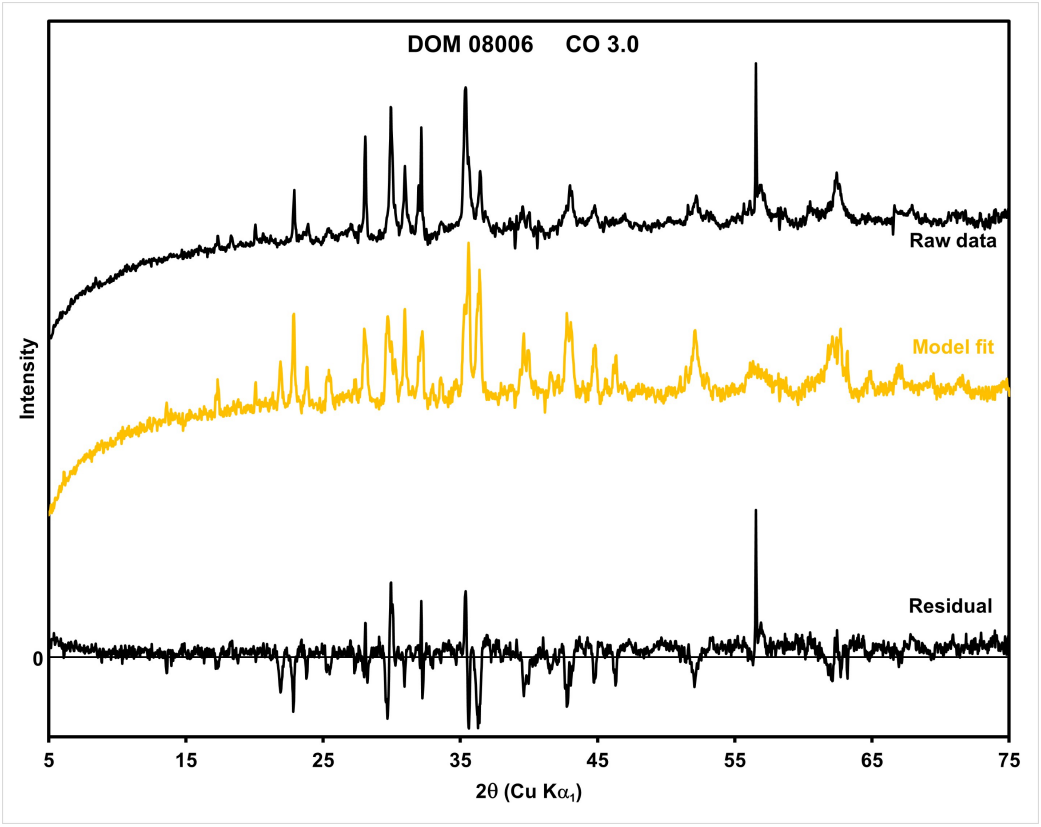


Figure 2: *DOM 08006 raw data, model fit and residual pattern.*

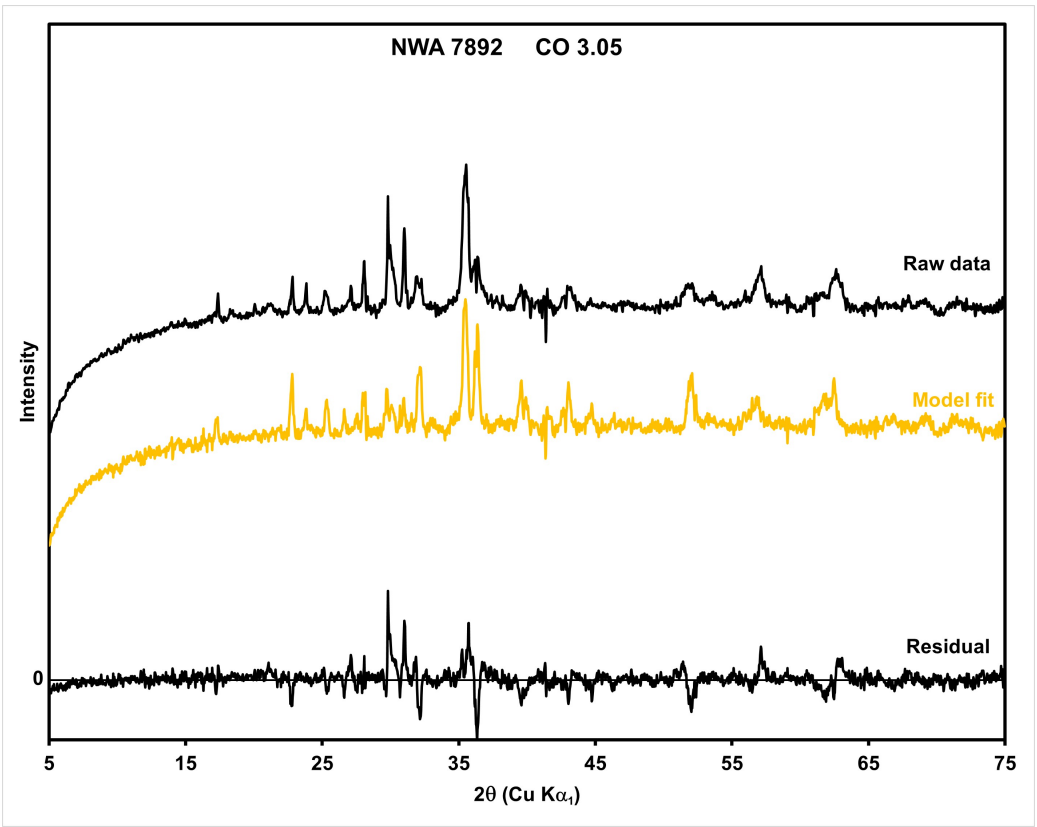


Figure 3: *NWA 7892 raw data, model fit and residual pattern.*

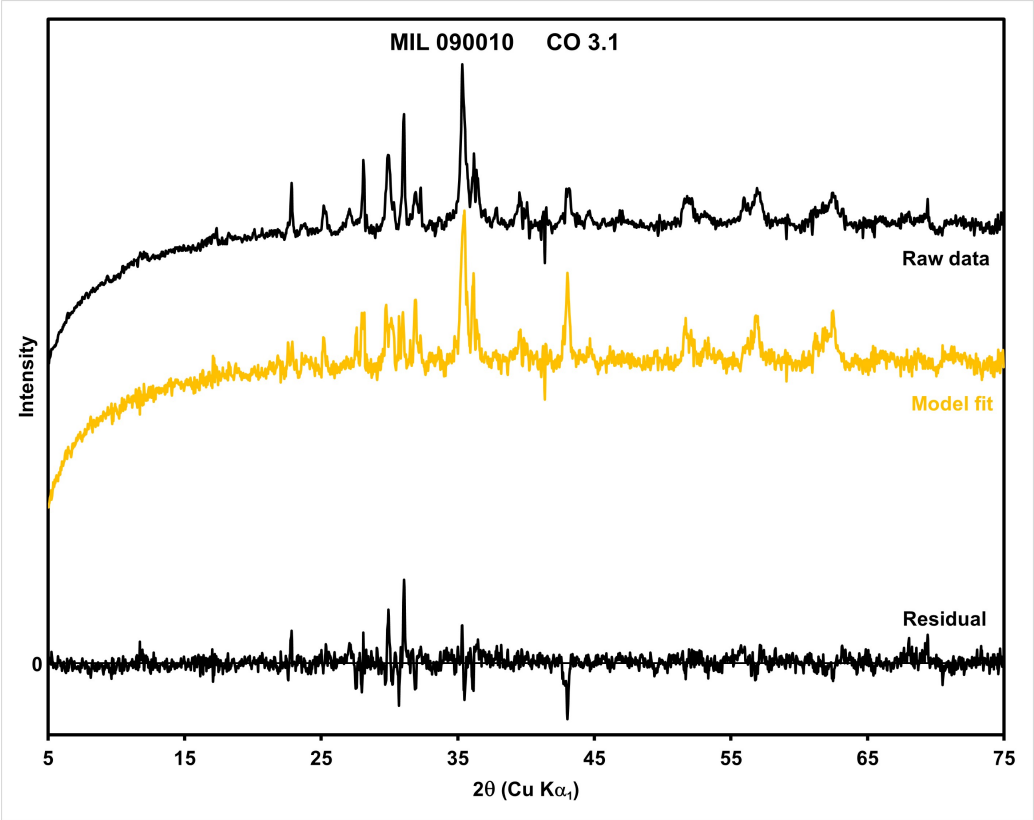


Figure 4: *Colony raw data, model fit and residual pattern.*

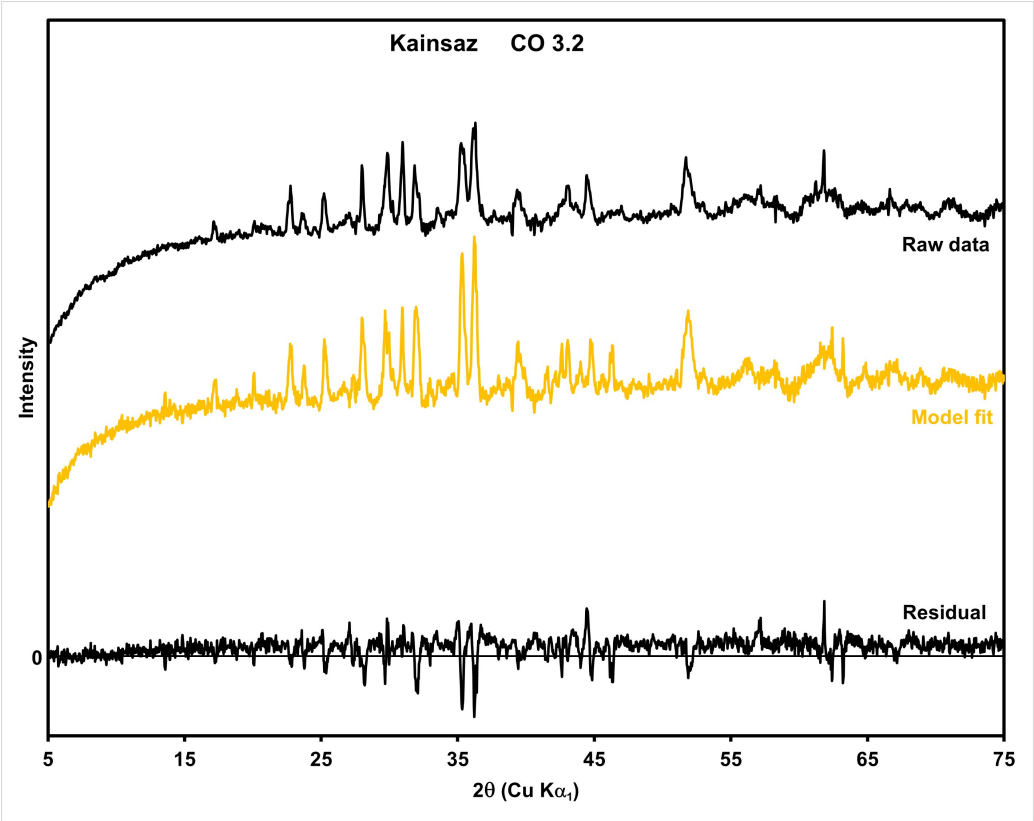


Figure 5: *Kainsaz raw data, model fit and residual pattern.*

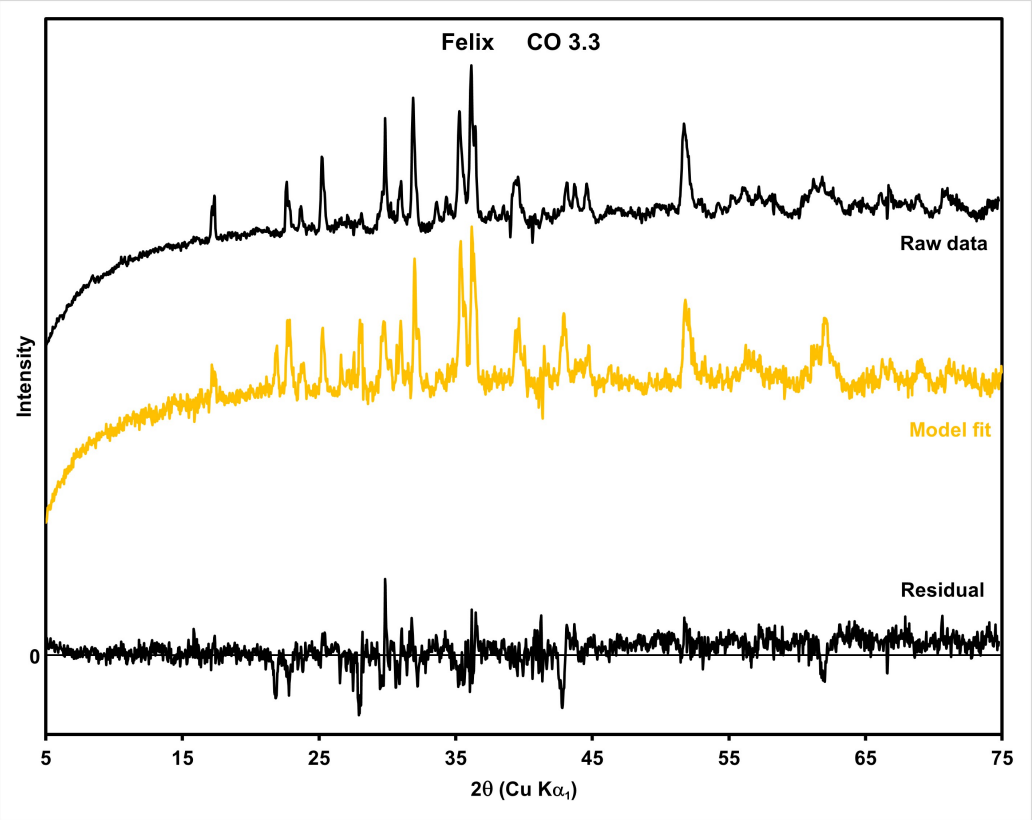


Figure 6: *Felix raw data, model fit and residual pattern.*

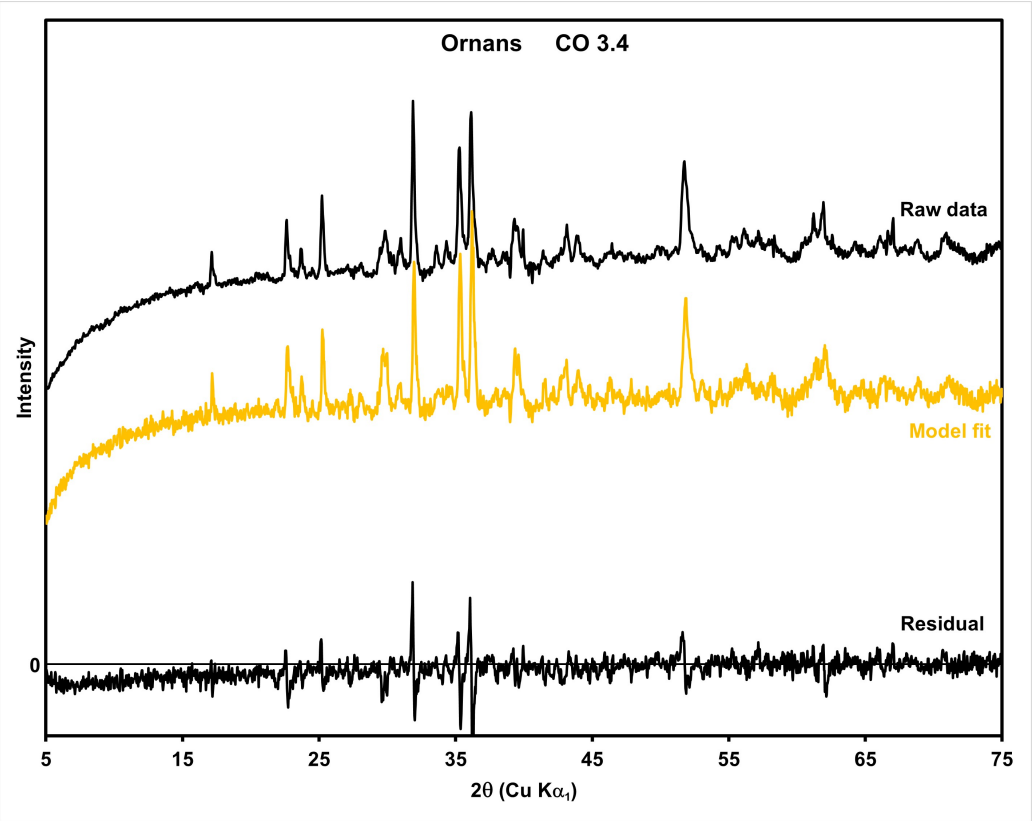


Figure 7: *Ornans raw data, model fit and residual pattern.*

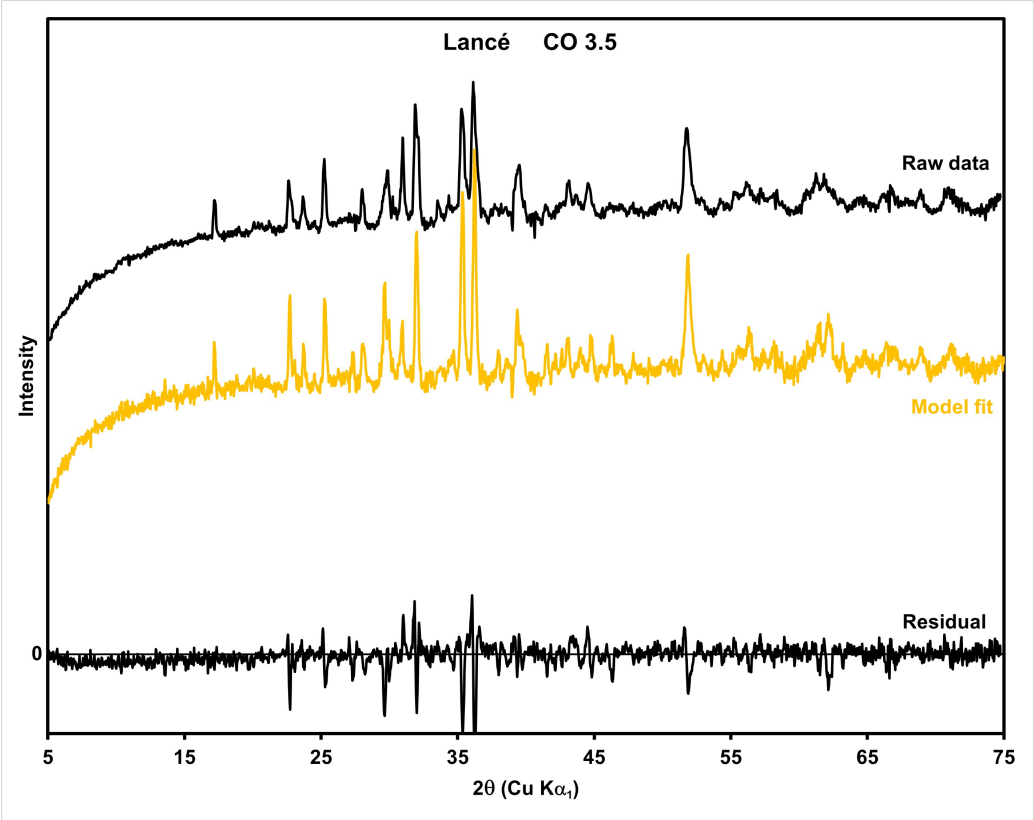


Figure 8: *Lancé raw data, model fit and residual pattern.*

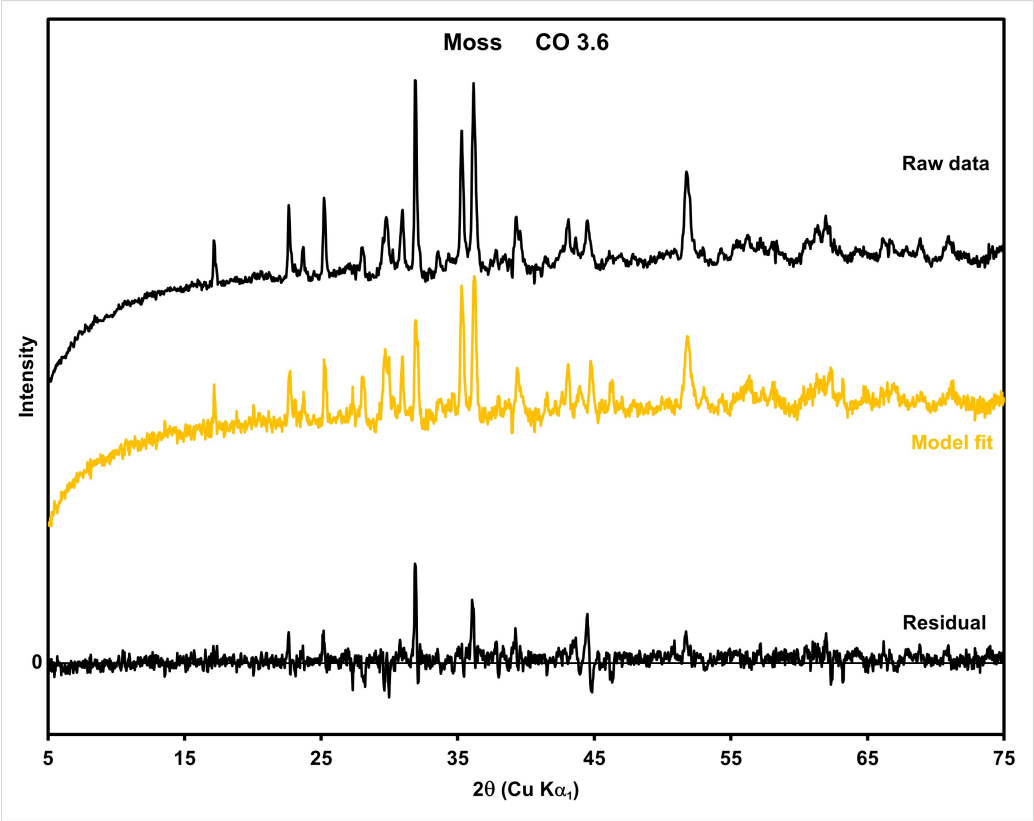


Figure 9: *Moss (CO3.6) raw data, model fit and residual pattern.*

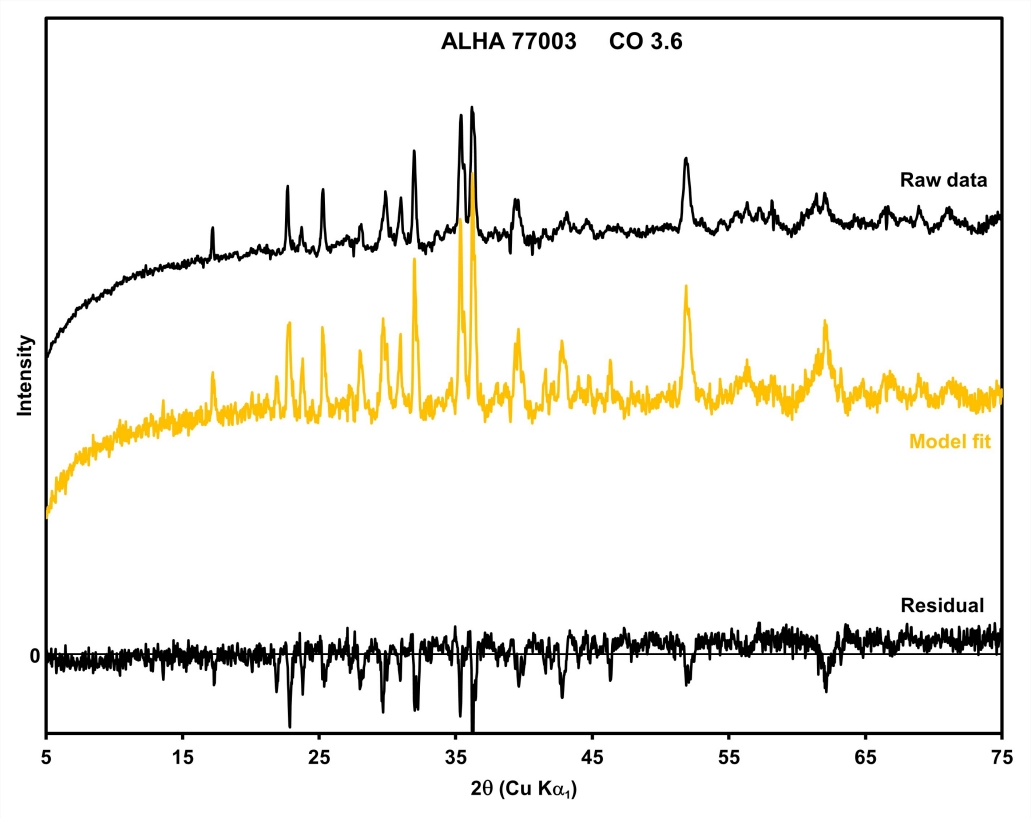


Figure 10: *ALHA77003 (CO3.6) raw data, model fit and residual pattern.*

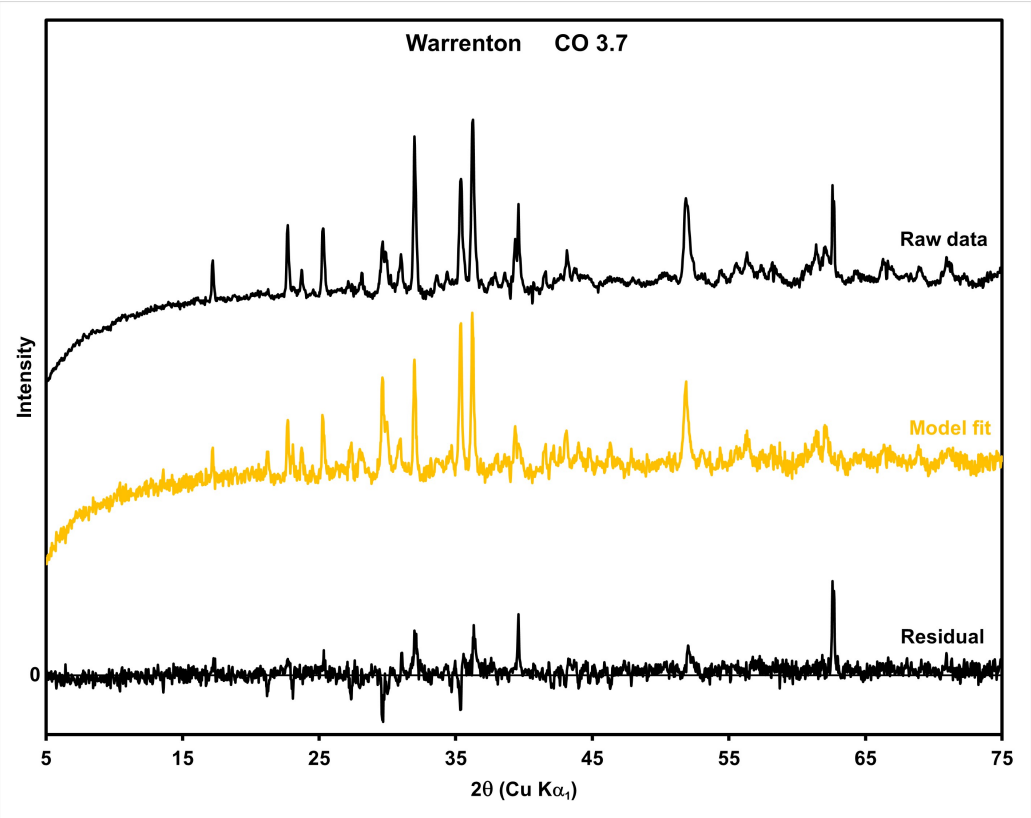


Figure 11: *Warrenton (CO3.7) raw data, model fit and residual pattern.*

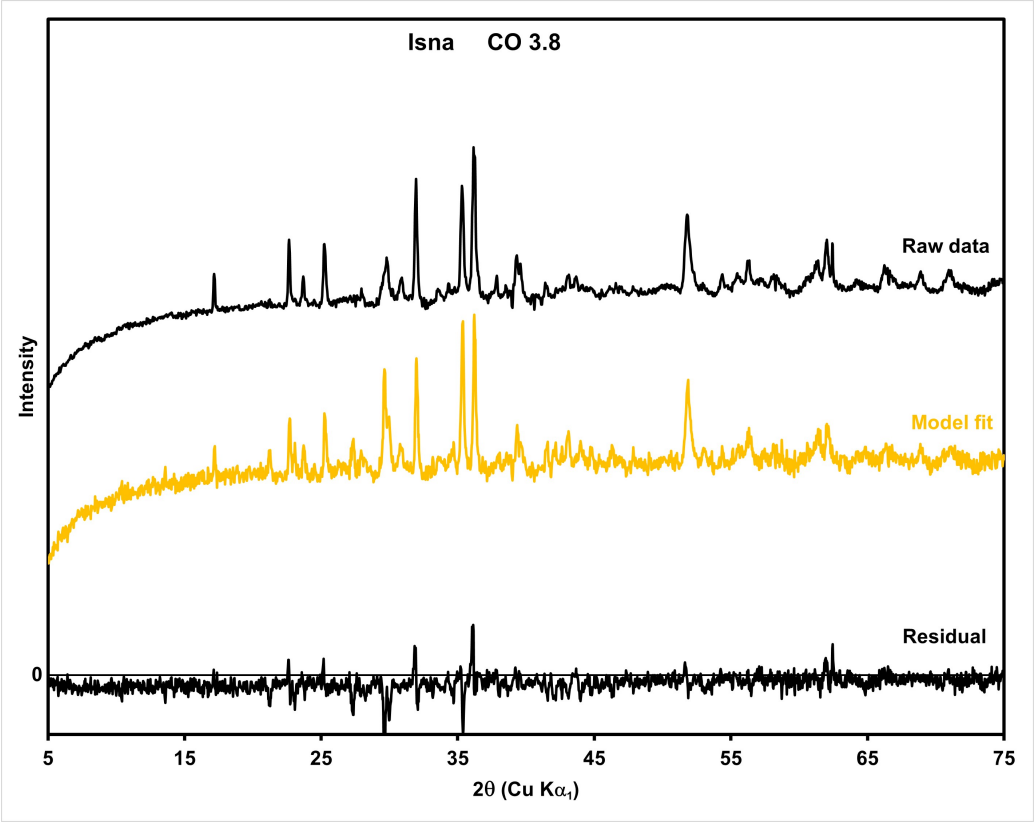


Figure 12: *Isna (CO3.8) raw data, model fit and residual pattern.*

# D Data tables for EPMA analyses of the matrix

Data tables for EPMA analyses of matrix areas of the CO chondrites analysed in this work. Data are in wt%.

| Sample | Area | Si | Ti | Al | Cr | Fe | Mn | Ni | Mg | Ca | Na | K | P | Co | V | Zn | S | O | Total |
|---|---|---|---|---|---|---|---|---|---|---|---|---|---|---|---|---|---|---|---|
| DOM08006 | 1a | 14.96 | 0.06 | 1.95 | 0.18 | 25.36 | 0.20 | 1.82 | 9.66 | 0.84 | 0.26 | 0.13 | 0.09 | 0.10 | 0.01 | 0.01 | 1.37 | 35.75 | 92.76 |
| DOM08006 | 1a | 10.96 | 0.07 | 1.24 | 0.22 | 35.09 | 0.15 | 1.71 | 6.21 | 0.61 | 0.23 | 0.09 | 0.11 | 0.10 | 0.00 | 0.02 | 1.40 | 31.01 | 89.21 |
| DOM08006 | 1a | 13.60 | 0.06 | 1.83 | 0.19 | 26.96 | 0.20 | 1.99 | 7.82 | 0.68 | 0.24 | 0.10 | 0.19 | 0.11 | 0.01 | 0.00 | 1.47 | 33.58 | 89.03 |
| DOM08006 | 1a | 13.56 | 0.04 | 1.69 | 0.19 | 32.64 | 0.14 | 1.74 | 8.23 | 0.67 | 0.27 | 0.10 | 0.10 | 0.09 | 0.00 | 0.01 | 1.26 | 34.78 | 95.52 |
| DOM08006 | 1a | 14.94 | 0.06 | 2.03 | 0.18 | 22.75 | 0.16 | 1.63 | 6.78 | 3.03 | 0.26 | 0.10 | 0.13 | 0.08 | 0.01 | 0.03 | 1.06 | 33.54 | 86.76 |
| DOM08006 | 1a | 15.53 | 0.04 | 2.43 | 0.19 | 28.02 | 0.14 | 1.81 | 7.24 | 0.80 | 0.34 | 0.16 | 0.12 | 0.09 | 0.00 | 0.02 | 1.17 | 35.71 | 93.82 |
| DOM08006 | 1a | 12.64 | 0.03 | 1.90 | 0.14 | 30.11 | 0.14 | 1.80 | 6.44 | 0.59 | 0.29 | 0.10 | 0.13 | 0.12 | 0.00 | 0.02 | 0.90 | 31.48 | 86.84 |
| DOM08006 | 1a | 12.96 | 0.05 | 1.99 | 0.15 | 31.36 | 0.13 | 1.85 | 6.48 | 0.62 | 0.34 | 0.14 | 0.14 | 0.13 | 0.01 | 0.03 | 1.02 | 32.58 | 89.96 |
| DOM08006 | 1a | 14.05 | 0.03 | 1.78 | 0.18 | 28.41 | 0.16 | 2.00 | 6.82 | 0.62 | 0.31 | 0.13 | 0.15 | 0.12 | 0.00 | 0.00 | 1.01 | 33.03 | 88.79 |
| DOM08006 | 1a | 14.91 | 0.04 | 1.89 | 0.20 | 26.79 | 0.18 | 1.81 | 7.75 | 0.68 | 0.32 | 0.15 | 0.15 | 0.12 | 0.01 | 0.03 | 0.94 | 34.17 | 90.13 |
| DOM08006 | 1a | 14.51 | 0.04 | 1.76 | 0.21 | 27.16 | 0.16 | 1.75 | 7.18 | 0.69 | 0.26 | 0.12 | 0.18 | 0.10 | 0.00 | 0.02 | 1.16 | 33.65 | 88.96 |
| DOM08006 | 1a | 15.75 | 0.05 | 1.93 | 0.18 | 25.81 | 0.18 | 2.07 | 7.61 | 0.70 | 0.30 | 0.14 | 0.18 | 0.11 | 0.01 | 0.03 | 1.20 | 35.29 | 91.54 |
| DOM08006 | 1a | 12.97 | 0.05 | 1.52 | 0.16 | 26.77 | 0.17 | 1.84 | 5.96 | 0.74 | 0.27 | 0.12 | 0.19 | 0.09 | 0.00 | 0.03 | 1.16 | 30.81 | 82.85 |
| DOM08006 | 1a | 14.71 | 0.04 | 2.19 | 0.22 | 27.27 | 0.14 | 1.79 | 7.61 | 0.88 | 0.49 | 0.15 | 0.17 | 0.09 | 0.01 | 0.02 | 1.84 | 35.75 | 93.37 |
| DOM08006 | 1a | 15.44 | 0.04 | 1.96 | 0.22 | 25.45 | 0.16 | 1.60 | 8.11 | 0.92 | 0.39 | 0.16 | 0.20 | 0.06 | 0.00 | 0.03 | 1.44 | 35.55 | 91.74 |
| DOM08006 | 1a | 19.19 | 0.06 | 1.34 | 0.41 | 19.46 | 0.55 | 1.31 | 12.13 | 1.11 | 0.27 | 0.10 | 0.12 | 0.07 | 0.00 | 0.00 | 0.71 | 39.16 | 96.01 |
| DOM08006 | 1a | 14.93 | 0.04 | 1.72 | 0.20 | 27.11 | 0.18 | 2.27 | 7.61 | 0.67 | 0.28 | 0.12 | 0.17 | 0.12 | 0.01 | 0.03 | 1.38 | 34.81 | 91.63 |
| DOM08006 | 1a | 12.47 | 0.04 | 1.61 | 0.93 | 35.12 | 0.15 | 2.15 | 6.96 | 1.20 | 0.36 | 0.08 | 0.14 | 0.14 | 0.01 | 0.00 | 0.93 | 33.60 | 95.90 |
| DOM08006 | 1a | 12.46 | 0.03 | 1.89 | 0.17 | 35.47 | 0.11 | 1.24 | 5.98 | 0.66 | 0.34 | 0.13 | 0.07 | 0.10 | 0.00 | 0.03 | 1.20 | 32.77 | 92.65 |
| DOM08006 | 1a | 13.91 | 0.04 | 1.90 | 0.22 | 33.90 | 0.15 | 1.36 | 8.05 | 0.80 | 0.33 | 0.16 | 0.12 | 0.10 | 0.00 | 0.01 | 1.19 | 35.53 | 97.78 |
| DOM08006 | 1a | 15.58 | 0.03 | 2.03 | 0.16 | 28.82 | 0.14 | 1.44 | 6.69 | 0.68 | 0.36 | 0.19 | 0.14 | 0.11 | 0.00 | 0.01 | 0.64 | 34.36 | 91.38 |
| DOM08006 | 1a | 14.88 | 0.05 | 1.77 | 0.20 | 27.14 | 0.22 | 1.72 | 7.81 | 0.69 | 0.26 | 0.13 | 0.14 | 0.09 | 0.00 | 0.02 | 0.96 | 34.13 | 90.19 |
| DOM08006 | 1a | 9.04 | 0.01 | 0.04 | 0.29 | 42.65 | 0.22 | 1.81 | 17.68 | 0.07 | 0.01 | 0.00 | 0.10 | 0.07 | 0.00 | 0.00 | 0.24 | 35.43 | 107.65 |
| DOM08006 | 1a | 12.37 | 0.04 | 0.75 | 0.19 | 20.77 | 0.18 | 2.87 | 7.88 | 0.50 | 0.11 | 0.06 | 0.13 | 0.12 | 0.00 | 0.02 | 1.16 | 29.03 | 76.16 |
| DOM08006 | 1a | 13.96 | 0.06 | 1.33 | 0.19 | 23.95 | 0.17 | 3.26 | 7.04 | 0.75 | 0.20 | 0.08 | 0.16 | 0.14 | 0.01 | 0.01 | 1.38 | 32.36 | 85.06 |
| DOM08006 | 1a | 14.78 | 0.04 | 1.32 | 0.20 | 25.62 | 0.16 | 3.66 | 7.64 | 0.62 | 0.20 | 0.10 | 0.13 | 0.16 | 0.00 | 0.01 | 1.44 | 34.26 | 90.36 |
| DOM08006 | 1a | 19.95 | 0.01 | 0.04 | 0.24 | 1.27 | 0.39 | 0.12 | 33.69 | 0.07 | 0.00 | 0.01 | 0.01 | 0.00 | 0.00 | 0.00 | 0.03 | 45.66 | 101.49 |
| DOM08006 | 2a | 13.78 | 0.04 | 1.72 | 0.16 | 27.53 | 0.18 | 1.91 | 7.07 | 0.75 | 0.28 | 0.12 | 0.18 | 0.13 | 0.00 | 0.03 | 1.03 | 32.69 | 87.60 |
| DOM08006 | 2a | 10.33 | 0.02 | 1.53 | 0.12 | 34.41 | 0.17 | 2.92 | 5.52 | 0.58 | 0.26 | 0.08 | 0.23 | 0.14 | 0.00 | 0.03 | 2.87 | 32.51 | 91.71 |
| DOM08006 | 2a | 12.63 | 0.04 | 1.27 | 0.15 | 23.03 | 0.15 | 1.58 | 6.67 | 0.60 | 0.28 | 0.09 | 0.22 | 0.10 | 0.00 | 0.01 | 1.02 | 29.28 | 77.13 |
| DOM08006 | 2a | 10.55 | 0.02 | 1.25 | 0.12 | 34.04 | 0.21 | 1.53 | 5.18 | 0.69 | 0.25 | 0.08 | 0.19 | 0.11 | 0.00 | 0.02 | 0.96 | 28.94 | 84.13 |
| DOM08006 | 2a | 11.47 | 0.06 | 1.75 | 0.13 | 31.65 | 0.17 | 2.13 | 5.65 | 1.04 | 0.27 | 0.10 | 0.31 | 0.14 | 0.00 | 0.03 | 1.14 | 30.82 | 86.84 |
| DOM08006 | 2a | 13.70 | 0.03 | 1.27 | 0.22 | 25.47 | 0.14 | 1.60 | 8.49 | 0.66 | 0.21 | 0.09 | 0.11 | 0.10 | 0.01 | 0.01 | 1.08 | 32.37 | 85.54 |
| DOM08006 | 2a | 13.65 | 0.04 | 1.47 | 0.23 | 30.66 | 0.18 | 2.00 | 7.24 | 0.74 | 0.23 | 0.12 | 0.11 | 0.11 | 0.01 | 0.00 | 1.52 | 33.99 | 92.30 |
| DOM08006 | 2a | 12.29 | 0.03 | 1.19 | 0.14 | 32.09 | 0.14 | 1.82 | 6.50 | 0.83 | 0.19 | 0.08 | 0.12 | 0.11 | 0.00 | 0.00 | 1.30 | 31.70 | 88.53 |
| DOM08006 | 2a | 11.71 | 0.02 | 1.32 | 0.14 | 33.38 | 0.16 | 1.85 | 5.78 | 0.81 | 0.29 | 0.11 | 0.09 | 0.13 | 0.00 | 0.02 | 1.39 | 31.20 | 88.41 |
| DOM08006 | 2a | 11.32 | 0.03 | 1.43 | 0.17 | 35.65 | 0.21 | 1.51 | 6.28 | 0.70 | 0.26 | 0.09 | 0.11 | 0.13 | 0.00 | 0.00 | 0.93 | 31.03 | 89.85 |
| DOM08006 | 2a | 13.81 | 0.03 | 1.95 | 0.20 | 31.74 | 0.18 | 1.51 | 7.13 | 0.94 | 0.35 | 0.13 | 0.16 | 0.09 | 0.00 | 0.02 | 0.99 | 34.07 | 93.29 |
| DOM08006 | 2a | 12.25 | 0.20 | 2.34 | 1.55 | 28.94 | 0.19 | 1.92 | 5.84 | 1.17 | 0.31 | 0.09 | 0.15 | 0.11 | 0.03 | 0.00 | 1.34 | 32.43 | 88.85 |
| DOM08006 | 2a | 10.80 | 0.06 | 1.59 | 0.14 | 33.04 | 0.20 | 2.06 | 5.54 | 0.69 | 0.25 | 0.10 | 0.22 | 0.14 | 0.01 | 0.00 | 1.21 | 30.09 | 86.15 |
| DOM08006 | 2a | 16.64 | 0.06 | 0.91 | 0.28 | 27.75 | 0.29 | 0.17 | 14.46 | 1.18 | 0.40 | 0.03 | 0.21 | 0.03 | 0.01 | 0.02 | 0.64 | 39.40 | 102.47 |
| DOM08006 | 2a | 16.15 | 0.14 | 0.75 | 0.42 | 26.93 | 0.28 | 0.21 | 13.69 | 1.40 | 0.29 | 0.02 | 0.16 | 0.03 | 0.00 | 0.00 | 0.10 | 37.24 | 97.80 |
| DOM08006 | 2a | 16.08 | 0.16 | 1.06 | 0.34 | 27.47 | 0.27 | 0.53 | 12.93 | 1.48 | 0.38 | 0.01 | 0.14 | 0.03 | 0.01 | 0.01 | 0.63 | 37.99 | 99.51 |
| DOM08006 | 2a | 14.89 | 0.12 | 1.16 | 0.34 | 22.52 | 0.85 | 1.72 | 8.61 | 0.85 | 0.15 | 0.05 | 0.24 | 0.08 | 0.00 | 0.00 | 0.87 | 33.11 | 85.55 |
| DOM08006 | 2a | 20.44 | 0.10 | 0.51 | 0.52 | 15.86 | 0.96 | 0.67 | 16.91 | 1.07 | 0.06 | 0.01 | 0.09 | 0.03 | 0.00 | 0.00 | 0.34 | 41.28 | 98.87 |
| DOM08006 | 2a | 18.95 | 0.12 | 0.39 | 0.48 | 13.76 | 0.70 | 0.60 | 18.81 | 0.86 | 0.04 | 0.01 | 0.07 | 0.04 | 0.01 | 0.00 | 0.28 | 39.81 | 94.92 |
| DOM08006 | 2a | 17.70 | 0.16 | 0.10 | 0.34 | 8.44 | 0.82 | 0.28 | 25.13 | 0.24 | 0.02 | 0.00 | 0.04 | 0.02 | 0.01 | 0.00 | 0.12 | 40.15 | 93.58 |
| DOM08006 | 2a | 16.37 | 0.04 | 1.67 | 0.22 | 23.77 | 0.24 | 1.78 | 8.73 | 0.89 | 0.25 | 0.13 | 0.10 | 0.09 | 0.00 | 0.02 | 0.96 | 35.45 | 90.72 |
| DOM08006 | 2a | 17.71 | 0.05 | 1.77 | 0.21 | 21.75 | 0.24 | 1.91 | 10.41 | 0.86 | 0.31 | 0.18 | 0.12 | 0.12 | 0.01 | 0.01 | 0.97 | 37.68 | 94.31 |

Continued on next page

| Sample | Area | Si | Ti | Al | Cr | Fe | Mn | Ni | Mg | Ca | Na | K | P | Co | V | Zn | S | O | Total |
|---|---|---|---|---|---|---|---|---|---|---|---|---|---|---|---|---|---|---|---|
| DOM08006 | 2a | 17.02 | 0.04 | 2.08 | 0.21 | 24.50 | 0.15 | 2.17 | 7.32 | 0.78 | 0.37 | 0.17 | 0.09 | 0.12 | 0.00 | 0.00 | 1.30 | 36.40 | 92.72 |
| DOM08006 | 2a | 13.56 | 0.05 | 1.40 | 0.16 | 30.99 | 0.23 | 1.68 | 6.90 | 0.66 | 0.29 | 0.12 | 0.11 | 0.10 | 0.00 | 0.02 | 0.94 | 32.72 | 89.93 |
| DOM08006 | 2a | 13.93 | 0.03 | 1.50 | 0.19 | 29.14 | 0.23 | 2.02 | 6.40 | 0.69 | 0.31 | 0.14 | 0.14 | 0.12 | 0.01 | 0.05 | 1.25 | 33.00 | 89.14 |
| DOM08006 | 2a | 16.15 | 0.04 | 1.66 | 0.22 | 25.08 | 0.20 | 2.19 | 8.19 | 0.81 | 0.35 | 0.15 | 0.11 | 0.12 | 0.00 | 0.03 | 1.44 | 36.06 | 92.82 |
| DOM08006 | 2a | 15.88 | 0.04 | 1.84 | 0.22 | 25.84 | 0.16 | 2.40 | 8.46 | 0.82 | 0.32 | 0.12 | 0.11 | 0.15 | 0.00 | 0.01 | 1.68 | 36.70 | 94.75 |
| DOM08006 | 2a | 16.37 | 0.05 | 1.70 | 0.20 | 24.00 | 0.16 | 2.26 | 7.80 | 0.79 | 0.33 | 0.16 | 0.10 | 0.14 | 0.00 | 0.02 | 1.29 | 35.54 | 90.93 |
| DOM08006 | 2a | 16.63 | 0.05 | 1.83 | 0.22 | 23.91 | 0.15 | 2.44 | 7.82 | 0.94 | 0.36 | 0.17 | 0.11 | 0.15 | 0.01 | 0.04 | 1.43 | 36.30 | 92.57 |
| DOM08006 | 2a | 16.61 | 0.04 | 1.80 | 0.22 | 25.56 | 0.18 | 2.40 | 8.15 | 0.76 | 0.40 | 0.16 | 0.12 | 0.14 | 0.01 | 0.06 | 1.39 | 36.84 | 94.85 |
| DOM08006 | 2a | 14.61 | 0.05 | 1.46 | 0.16 | 23.60 | 0.20 | 1.83 | 7.67 | 0.73 | 0.33 | 0.15 | 0.14 | 0.11 | 0.00 | 0.03 | 1.10 | 32.73 | 84.91 |
| DOM08006 | 2a | 16.44 | 0.05 | 1.61 | 0.18 | 24.64 | 0.20 | 1.86 | 8.92 | 0.70 | 0.31 | 0.15 | 0.10 | 0.10 | 0.00 | 0.03 | 1.25 | 36.23 | 92.78 |
| DOM08006 | 2a | 14.86 | 0.04 | 1.60 | 0.20 | 27.65 | 0.16 | 2.11 | 6.59 | 0.71 | 0.31 | 0.17 | 0.13 | 0.14 | 0.00 | 0.03 | 2.81 | 36.22 | 93.74 |
| DOM08006 | 2a | 16.31 | 0.03 | 1.68 | 0.21 | 25.30 | 0.20 | 2.08 | 7.21 | 0.71 | 0.35 | 0.17 | 0.12 | 0.12 | 0.00 | 0.03 | 1.13 | 35.14 | 90.78 |
| DOM08006 | 2a | 16.77 | 0.04 | 1.86 | 0.21 | 25.30 | 0.17 | 2.39 | 7.52 | 0.76 | 0.38 | 0.17 | 0.14 | 0.15 | 0.00 | 0.03 | 1.42 | 36.62 | 93.93 |
| DOM08006 | 2a | 17.55 | 0.06 | 1.64 | 0.25 | 18.17 | 0.19 | 1.72 | 12.39 | 0.84 | 0.27 | 0.13 | 0.12 | 0.09 | 0.01 | 0.01 | 0.97 | 37.60 | 92.03 |
| DOM08006 | 2a | 15.92 | 0.05 | 1.97 | 0.24 | 25.86 | 0.20 | 2.17 | 8.07 | 0.70 | 0.38 | 0.16 | 0.18 | 0.12 | 0.01 | 0.02 | 1.21 | 35.95 | 93.21 |
| DOM08006 | 2a | 15.71 | 0.05 | 1.72 | 0.17 | 23.72 | 0.15 | 1.99 | 7.18 | 0.64 | 0.33 | 0.17 | 0.18 | 0.13 | 0.01 | 0.03 | 1.10 | 33.97 | 87.23 |
| DOM08006 | 2a | 15.38 | 0.07 | 1.78 | 0.18 | 25.31 | 0.16 | 2.00 | 6.68 | 0.81 | 0.35 | 0.16 | 0.17 | 0.12 | 0.00 | 0.03 | 1.11 | 33.88 | 88.19 |
| DOM08006 | 2a | 14.68 | 0.05 | 1.94 | 0.40 | 29.89 | 0.12 | 2.20 | 6.82 | 0.70 | 0.35 | 0.16 | 0.18 | 0.14 | 0.01 | 0.03 | 1.25 | 34.95 | 93.87 |
| DOM08006 | 2a | 14.43 | 0.07 | 2.04 | 0.23 | 29.15 | 0.21 | 1.82 | 8.09 | 0.92 | 0.30 | 0.15 | 0.16 | 0.10 | 0.01 | 0.02 | 1.30 | 35.32 | 94.31 |
| DOM08006 | 2a | 14.99 | 0.04 | 2.84 | 0.17 | 26.01 | 0.18 | 1.83 | 7.00 | 1.35 | 0.53 | 0.15 | 0.16 | 0.11 | 0.01 | 0.01 | 1.05 | 34.92 | 91.37 |
| DOM08006 | 2a | 13.97 | 0.05 | 1.65 | 0.17 | 23.74 | 0.25 | 1.66 | 4.69 | 0.97 | 0.35 | 0.13 | 0.17 | 0.11 | 0.00 | 0.04 | 0.87 | 30.00 | 78.82 |
| DOM08006 | 2a | 14.61 | 0.07 | 2.05 | 0.26 | 28.87 | 0.20 | 1.88 | 7.85 | 0.82 | 0.29 | 0.15 | 0.17 | 0.10 | 0.00 | 0.03 | 1.29 | 35.29 | 93.93 |
| DOM08006 | 2a | 12.81 | 0.04 | 1.54 | 0.28 | 30.54 | 0.17 | 1.91 | 6.63 | 0.66 | 0.30 | 0.14 | 0.22 | 0.11 | 0.00 | 0.01 | 1.48 | 32.73 | 89.57 |
| DOM08006 | 2a | 14.04 | 0.05 | 1.52 | 0.22 | 26.12 | 0.25 | 1.64 | 5.55 | 1.14 | 0.39 | 0.12 | 0.17 | 0.11 | 0.00 | 0.03 | 1.41 | 32.12 | 84.86 |
| DOM08006 | 2a | 14.88 | 0.06 | 1.60 | 0.19 | 27.76 | 0.26 | 2.00 | 6.12 | 0.89 | 0.31 | 0.13 | 0.17 | 0.14 | 0.00 | 0.01 | 1.17 | 33.62 | 89.31 |
| DOM08006 | 2a | 15.57 | 0.04 | 1.66 | 0.20 | 27.38 | 0.15 | 2.10 | 6.85 | 0.70 | 0.27 | 0.15 | 0.15 | 0.13 | 0.01 | 0.04 | 1.11 | 34.61 | 91.12 |
| DOM08006 | 2a | 14.10 | 0.06 | 1.41 | 0.20 | 27.28 | 0.21 | 2.12 | 6.84 | 0.81 | 0.31 | 0.12 | 0.17 | 0.13 | 0.00 | 0.03 | 1.45 | 33.30 | 88.55 |
| DOM08006 | 2a | 15.44 | 0.06 | 1.59 | 0.21 | 25.86 | 0.20 | 2.03 | 7.97 | 0.83 | 0.28 | 0.12 | 0.15 | 0.12 | 0.00 | 0.03 | 1.46 | 35.28 | 91.62 |
| DOM08006 | 2a | 12.84 | 0.04 | 1.68 | 0.19 | 35.31 | 0.15 | 1.68 | 6.76 | 0.64 | 0.33 | 0.12 | 0.13 | 0.14 | 0.00 | 0.00 | 1.05 | 33.47 | 94.52 |
| DOM08006 | 2a | 13.26 | 0.04 | 1.42 | 0.17 | 36.18 | 0.16 | 1.78 | 6.69 | 0.59 | 0.27 | 0.12 | 0.15 | 0.15 | 0.01 | 0.01 | 1.08 | 33.99 | 96.07 |
| DOM08006 | 2a | 14.94 | 0.05 | 1.59 | 0.20 | 28.02 | 0.15 | 2.19 | 7.04 | 0.69 | 0.29 | 0.14 | 0.16 | 0.12 | 0.00 | 0.00 | 1.36 | 34.54 | 91.49 |
| DOM08006 | 2a | 14.92 | 0.06 | 1.93 | 0.17 | 27.35 | 0.17 | 1.67 | 9.20 | 0.56 | 0.29 | 0.14 | 0.13 | 0.11 | 0.00 | 0.02 | 0.79 | 34.98 | 92.50 |
| DOM08006 | 2a | 14.51 | 0.06 | 1.67 | 0.21 | 28.89 | 0.17 | 2.11 | 7.09 | 0.73 | 0.27 | 0.14 | 0.17 | 0.13 | 0.00 | 0.02 | 1.35 | 34.43 | 91.96 |
| DOM08006 | 3b | 10.28 | 0.05 | 0.81 | 0.27 | 34.53 | 0.49 | 3.94 | 7.05 | 1.59 | 0.12 | 0.02 | 0.14 | 0.15 | 0.00 | 0.02 | 0.68 | 30.25 | 90.39 |
| DOM08006 | 3b | 14.84 | 0.04 | 2.27 | 0.20 | 27.39 | 0.13 | 2.01 | 6.59 | 0.73 | 0.31 | 0.13 | 0.21 | 0.15 | 0.00 | 0.03 | 1.53 | 34.86 | 91.43 |
| DOM08006 | 3b | 14.68 | 0.04 | 2.26 | 0.20 | 28.55 | 0.16 | 2.00 | 6.62 | 0.72 | 0.32 | 0.14 | 0.17 | 0.13 | 0.01 | 0.04 | 1.30 | 34.62 | 91.95 |
| DOM08006 | 3b | 15.52 | 0.05 | 1.96 | 0.26 | 27.28 | 0.39 | 1.46 | 7.94 | 0.77 | 0.27 | 0.13 | 0.12 | 0.11 | 0.01 | 0.00 | 0.91 | 35.13 | 92.32 |
| DOM08006 | 3b | 14.54 | 0.04 | 2.25 | 0.20 | 26.35 | 0.18 | 2.14 | 6.30 | 0.73 | 0.30 | 0.18 | 0.24 | 0.16 | 0.01 | 0.02 | 1.23 | 33.66 | 88.55 |
| DOM08006 | 3b | 15.84 | 0.03 | 2.21 | 0.20 | 25.50 | 0.17 | 1.77 | 9.03 | 0.68 | 0.33 | 0.16 | 0.14 | 0.12 | 0.01 | 0.00 | 1.18 | 36.32 | 93.69 |
| DOM08006 | 3b | 13.51 | 0.04 | 1.82 | 0.21 | 29.18 | 0.18 | 2.03 | 7.41 | 0.74 | 0.28 | 0.13 | 0.18 | 0.14 | 0.00 | 0.04 | 1.11 | 33.35 | 90.37 |
| DOM08006 | 3b | 15.25 | 0.05 | 2.22 | 0.18 | 28.02 | 0.12 | 1.95 | 7.10 | 0.72 | 0.35 | 0.17 | 0.16 | 0.15 | 0.00 | 0.03 | 1.16 | 35.18 | 92.82 |
| DOM08006 | 3b | 13.93 | 0.11 | 0.86 | 0.20 | 22.00 | 0.14 | 1.86 | 7.26 | 0.52 | 0.17 | 0.08 | 0.16 | 0.11 | 0.00 | 0.02 | 1.54 | 31.27 | 80.23 |
| DOM08006 | 3b | 13.06 | 0.05 | 0.88 | 0.22 | 31.85 | 0.16 | 2.19 | 6.92 | 0.57 | 0.25 | 0.08 | 0.13 | 0.13 | 0.00 | 0.04 | 1.50 | 32.91 | 90.95 |
| DOM08006 | 3b | 14.97 | 0.08 | 0.95 | 0.22 | 24.82 | 0.18 | 2.02 | 8.63 | 0.68 | 0.26 | 0.13 | 0.14 | 0.11 | 0.00 | 0.03 | 1.51 | 34.33 | 89.08 |
| DOM08006 | 3b | 13.60 | 0.14 | 0.93 | 0.23 | 23.76 | 0.16 | 1.91 | 7.94 | 0.73 | 0.24 | 0.08 | 0.13 | 0.10 | 0.00 | 0.03 | 1.34 | 31.72 | 83.03 |
| DOM08006 | 3b | 13.32 | 0.08 | 1.62 | 0.22 | 31.84 | 0.19 | 1.59 | 7.54 | 0.76 | 0.28 | 0.11 | 0.09 | 0.16 | 0.01 | 0.02 | 1.37 | 34.00 | 93.20 |
| DOM08006 | 3b | 15.80 | 0.07 | 1.36 | 0.25 | 23.99 | 0.23 | 2.31 | 9.31 | 0.96 | 0.27 | 0.10 | 0.14 | 0.12 | 0.01 | 0.02 | 2.01 | 36.79 | 93.72 |
| DOM08006 | 3b | 14.23 | 0.07 | 1.49 | 0.20 | 28.64 | 0.18 | 1.99 | 6.94 | 0.81 | 0.26 | 0.10 | 0.15 | 0.14 | 0.00 | 0.03 | 1.17 | 33.47 | 89.86 |
| DOM08006 | 3b | 11.09 | 0.08 | 0.97 | 0.17 | 35.41 | 0.18 | 1.79 | 5.89 | 0.61 | 0.22 | 0.07 | 0.14 | 0.11 | 0.00 | 0.02 | 3.92 | 34.61 | 95.27 |
| DOM08006 | 3b | 13.52 | 0.04 | 1.54 | 0.22 | 30.20 | 0.20 | 1.83 | 8.12 | 0.78 | 0.28 | 0.10 | 0.14 | 0.13 | 0.01 | 0.01 | 1.19 | 33.91 | 92.24 |
| DOM08006 | 3b | 16.14 | 0.04 | 1.32 | 0.22 | 24.95 | 0.18 | 2.27 | 7.94 | 0.73 | 0.23 | 0.11 | 0.16 | 0.13 | 0.01 | 0.02 | 1.27 | 35.28 | 90.99 |
| DOM08006 | 3b | 11.79 | 0.03 | 1.35 | 0.15 | 32.47 | 0.18 | 1.56 | 6.80 | 0.71 | 0.27 | 0.08 | 0.14 | 0.14 | 0.00 | 0.03 | 1.16 | 31.34 | 88.20 |
| DOM08006 | 3b | 12.63 | 0.04 | 1.11 | 0.23 | 31.94 | 0.31 | 1.83 | 7.03 | 0.83 | 0.24 | 0.07 | 0.12 | 0.13 | 0.00 | 0.03 | 1.48 | 32.73 | 90.75 |
| DOM08006 | 3b | 16.45 | 0.06 | 0.94 | 0.41 | 25.46 | 0.54 | 1.21 | 10.71 | 1.16 | 0.20 | 0.05 | 0.11 | 0.10 | 0.01 | 0.00 | 0.71 | 36.41 | 94.52 |
| DOM08006 | 3b | 12.75 | 0.03 | 1.66 | 0.16 | 31.21 | 0.18 | 1.80 | 5.77 | 0.74 | 0.30 | 0.12 | 0.13 | 0.11 | 0.01 | 0.03 | 1.20 | 31.80 | 88.00 |
| DOM08006 | 3b | 13.77 | 0.06 | 1.04 | 0.26 | 28.92 | 0.39 | 1.73 | 6.79 | 1.00 | 0.29 | 0.10 | 0.15 | 0.11 | 0.00 | 0.02 | 0.95 | 32.28 | 87.85 |
| DOM08006 | 3b | 13.07 | 0.03 | 1.47 | 0.20 | 31.18 | 0.21 | 1.70 | 7.40 | 0.81 | 0.29 | 0.13 | 0.17 | 0.13 | 0.01 | 0.00 | 1.19 | 33.13 | 91.12 |
| DOM08006 | 3b | 12.65 | 0.04 | 1.62 | 0.18 | 34.01 | 0.17 | 1.51 | 6.49 | 0.78 | 0.31 | 0.14 | 0.13 | 0.14 | 0.01 | 0.02 | 1.09 | 32.74 | 92.04 |

Continued on next page

| Sample | Area | Si | Ti | Al | Cr | Fe | Mn | Ni | Mg | Ca | Na | K | P | Co | V | Zn | S | O | Total |
|---|---|---|---|---|---|---|---|---|---|---|---|---|---|---|---|---|---|---|---|
| DOM08006 | 3b | 11.62 | 0.04 | 1.47 | 0.15 | 35.61 | 0.19 | 1.47 | 5.75 | 0.65 | 0.28 | 0.11 | 0.10 | 0.14 | 0.00 | 0.00 | 1.05 | 31.21 | 89.85 |
| DOM08006 | 3b | 12.41 | 0.06 | 1.62 | 0.15 | 36.07 | 0.14 | 1.33 | 6.58 | 0.62 | 0.27 | 0.12 | 0.05 | 0.15 | 0.00 | 0.00 | 0.96 | 32.67 | 93.19 |
| DOM08006 | 3b | 12.11 | 0.04 | 1.30 | 0.38 | 32.02 | 0.22 | 2.01 | 7.02 | 0.67 | 0.22 | 0.10 | 0.17 | 0.13 | 0.01 | 0.02 | 1.46 | 32.39 | 90.28 |
| DOM08006 | 3b | 13.01 | 0.05 | 0.89 | 0.24 | 26.62 | 0.14 | 1.70 | 8.96 | 0.54 | 0.17 | 0.06 | 0.18 | 0.09 | 0.01 | 0.04 | 1.53 | 32.64 | 86.87 |
| DOM08006 | 3b | 12.46 | 0.03 | 1.06 | 0.20 | 31.20 | 0.20 | 1.77 | 8.12 | 0.69 | 0.19 | 0.08 | 0.14 | 0.12 | 0.00 | 0.04 | 2.07 | 33.76 | 92.13 |
| DOM08006 | 3b | 9.90 | 0.03 | 1.03 | 0.16 | 36.73 | 0.26 | 2.11 | 4.93 | 0.56 | 0.21 | 0.06 | 0.12 | 0.10 | 0.00 | 0.01 | 1.58 | 29.56 | 87.36 |
| DOM08006 | 3b | 13.41 | 0.04 | 1.50 | 0.24 | 30.56 | 0.22 | 1.69 | 7.26 | 0.70 | 0.34 | 0.12 | 0.14 | 0.13 | 0.01 | 0.01 | 1.19 | 33.24 | 90.80 |
| DOM08006 | 3b | 13.53 | 0.07 | 1.56 | 0.18 | 31.22 | 0.18 | 1.72 | 6.65 | 0.62 | 0.30 | 0.12 | 0.13 | 0.12 | 0.00 | 0.01 | 1.10 | 33.00 | 90.52 |
| DOM08006 | 3b | 13.50 | 0.04 | 1.50 | 0.17 | 33.29 | 0.19 | 1.65 | 7.13 | 0.65 | 0.32 | 0.12 | 0.11 | 0.11 | 0.01 | 0.03 | 1.24 | 34.00 | 94.05 |
| DOM08006 | 4a | 26.01 | 0.10 | 0.71 | 0.43 | 5.13 | 0.14 | 0.34 | 21.48 | 0.77 | 0.04 | 0.04 | 0.02 | 0.01 | 0.01 | 0.01 | 0.13 | 46.81 | 102.15 |
| DOM08006 | 4a | 25.40 | 0.08 | 0.35 | 0.38 | 1.47 | 0.10 | 0.09 | 26.09 | 0.39 | 0.01 | 0.00 | 0.01 | 0.00 | 0.01 | 0.00 | 0.02 | 47.33 | 101.71 |
| DOM08006 | 4a | 15.89 | 0.04 | 1.73 | 0.24 | 27.95 | 0.15 | 1.94 | 8.83 | 0.82 | 0.35 | 0.15 | 0.17 | 0.10 | 0.00 | 0.03 | 1.26 | 36.78 | 96.40 |
| DOM08006 | 4a | 15.87 | 0.03 | 0.76 | 0.17 | 17.57 | 0.12 | 1.55 | 19.36 | 0.61 | 0.17 | 0.09 | 0.14 | 0.07 | 0.00 | 0.03 | 1.19 | 39.40 | 97.12 |
| DOM08006 | 4a | 14.72 | 0.04 | 1.24 | 0.22 | 29.32 | 0.18 | 2.22 | 7.79 | 0.81 | 0.27 | 0.10 | 0.19 | 0.11 | 0.00 | 0.04 | 1.38 | 34.96 | 93.56 |
| DOM08006 | 4a | 14.83 | 0.04 | 1.26 | 0.24 | 27.08 | 0.15 | 2.35 | 7.46 | 0.76 | 0.31 | 0.12 | 0.22 | 0.12 | 0.00 | 0.02 | 1.66 | 34.75 | 91.37 |
| DOM08006 | 4a | 14.79 | 0.05 | 1.33 | 0.20 | 27.26 | 0.15 | 2.37 | 7.38 | 0.83 | 0.24 | 0.14 | 0.23 | 0.13 | 0.00 | 0.03 | 1.36 | 34.34 | 90.84 |
| DOM08006 | 4a | 15.70 | 0.03 | 1.41 | 0.24 | 25.70 | 0.15 | 2.35 | 7.72 | 0.83 | 0.32 | 0.14 | 0.24 | 0.12 | 0.01 | 0.01 | 1.43 | 35.37 | 91.77 |
| DOM08006 | 4a | 14.98 | 0.04 | 1.33 | 0.22 | 27.02 | 0.14 | 2.23 | 7.47 | 0.93 | 0.35 | 0.10 | 0.22 | 0.11 | 0.00 | 0.02 | 1.19 | 34.30 | 90.65 |
| DOM08006 | 4a | 13.01 | 0.00 | 0.26 | 0.14 | 22.85 | 0.21 | 0.45 | 21.43 | 2.87 | 0.08 | 0.03 | 0.08 | 0.03 | 0.00 | 0.00 | 2.43 | 40.87 | 104.73 |
| DOM08006 | 4a | 13.43 | 0.03 | 0.88 | 0.19 | 24.52 | 0.14 | 1.87 | 9.53 | 0.72 | 0.23 | 0.09 | 0.22 | 0.10 | 0.01 | 0.01 | 1.93 | 33.63 | 87.52 |
| DOM08006 | 4a | 13.47 | 0.03 | 1.00 | 0.19 | 26.45 | 0.15 | 1.97 | 7.96 | 0.66 | 0.23 | 0.11 | 0.24 | 0.09 | 0.00 | 0.02 | 1.31 | 32.41 | 86.30 |
| DOM08006 | 4a | 12.45 | 0.03 | 0.82 | 0.27 | 27.87 | 0.16 | 2.00 | 8.51 | 0.63 | 0.18 | 0.07 | 0.23 | 0.09 | 0.01 | 0.02 | 2.22 | 33.23 | 88.78 |
| DOM08006 | 4a | 12.61 | 0.03 | 0.95 | 0.18 | 24.11 | 0.16 | 2.24 | 6.98 | 0.70 | 0.26 | 0.10 | 0.24 | 0.10 | 0.00 | 0.01 | 1.19 | 29.98 | 79.83 |
| DOM08006 | 4a | 14.44 | 0.05 | 1.06 | 0.20 | 23.20 | 0.15 | 2.08 | 9.11 | 0.74 | 0.25 | 0.09 | 0.30 | 0.09 | 0.00 | 0.00 | 1.18 | 33.36 | 86.31 |
| DOM08006 | 4a | 13.42 | 0.03 | 1.04 | 0.19 | 25.61 | 0.16 | 2.15 | 8.91 | 0.74 | 0.24 | 0.09 | 0.26 | 0.12 | 0.01 | 0.01 | 1.43 | 33.06 | 87.46 |
| DOM08006 | 4a | 14.24 | 0.04 | 1.07 | 0.26 | 24.78 | 0.18 | 2.43 | 8.93 | 0.82 | 0.30 | 0.10 | 0.27 | 0.12 | 0.01 | 0.03 | 1.97 | 34.81 | 90.36 |
| DOM08006 | 4a | 13.41 | 0.02 | 1.14 | 0.16 | 28.40 | 0.16 | 1.77 | 7.44 | 0.69 | 0.26 | 0.11 | 0.20 | 0.11 | 0.01 | 0.02 | 0.90 | 31.97 | 86.75 |
| DOM08006 | 4a | 12.53 | 0.03 | 1.20 | 0.18 | 35.23 | 0.15 | 1.86 | 6.86 | 0.72 | 0.30 | 0.12 | 0.26 | 0.12 | 0.01 | 0.02 | 0.94 | 32.82 | 93.36 |
| DOM08006 | 4a | 13.33 | 0.04 | 1.24 | 0.18 | 31.62 | 0.15 | 1.95 | 6.78 | 0.76 | 0.29 | 0.10 | 0.27 | 0.11 | 0.00 | 0.03 | 1.11 | 32.97 | 90.92 |
| DOM08006 | 4a | 12.57 | 0.03 | 1.09 | 0.18 | 34.42 | 0.13 | 2.04 | 7.29 | 0.74 | 0.28 | 0.11 | 0.21 | 0.10 | 0.00 | 0.02 | 1.07 | 32.98 | 93.28 |
| DOM08006 | 4a | 11.70 | 0.04 | 1.04 | 0.18 | 33.42 | 0.18 | 1.82 | 6.94 | 0.71 | 0.26 | 0.11 | 0.23 | 0.13 | 0.01 | 0.00 | 1.05 | 31.36 | 89.16 |
| DOM08006 | 4a | 13.59 | 0.04 | 0.95 | 0.23 | 25.76 | 0.18 | 2.14 | 9.03 | 0.75 | 0.25 | 0.07 | 0.24 | 0.10 | 0.00 | 0.03 | 2.34 | 34.66 | 90.35 |
| DOM08006 | 4a | 13.09 | 0.03 | 1.04 | 0.19 | 28.66 | 0.16 | 2.32 | 7.44 | 0.85 | 0.30 | 0.11 | 0.26 | 0.12 | 0.01 | 0.00 | 1.45 | 32.74 | 88.77 |
| DOM08006 | 4a | 13.16 | 0.02 | 1.06 | 0.16 | 35.45 | 0.13 | 2.62 | 6.64 | 0.89 | 0.30 | 0.11 | 0.21 | 0.12 | 0.01 | 0.00 | 1.07 | 33.71 | 95.67 |
| DOM08006 | 4a | 11.61 | 0.01 | 0.74 | 0.15 | 34.41 | 0.15 | 2.24 | 7.42 | 0.68 | 0.22 | 0.06 | 0.23 | 0.12 | 0.00 | 0.00 | 1.66 | 32.53 | 92.23 |
| DOM08006 | 4a | 13.13 | 0.04 | 0.82 | 0.15 | 29.51 | 0.17 | 2.56 | 10.23 | 0.81 | 0.20 | 0.07 | 0.23 | 0.10 | 0.00 | 0.03 | 1.25 | 34.34 | 93.65 |
| DOM08006 | 4a | 10.86 | 0.02 | 0.80 | 0.15 | 36.04 | 0.11 | 2.83 | 6.52 | 0.69 | 0.20 | 0.09 | 0.22 | 0.10 | 0.00 | 0.00 | 2.34 | 32.76 | 93.72 |
| DOM08006 | 4a | 14.74 | 0.05 | 1.31 | 0.18 | 27.27 | 0.16 | 2.82 | 6.86 | 0.96 | 0.30 | 0.14 | 0.26 | 0.14 | 0.00 | 0.02 | 1.27 | 34.01 | 90.49 |
| DOM08006 | 4a | 19.37 | 0.01 | 0.42 | 0.21 | 8.67 | 0.29 | 0.81 | 29.09 | 0.34 | 0.08 | 0.03 | 0.10 | 0.03 | 0.01 | 0.01 | 0.39 | 45.38 | 105.25 |
| DOM08006 | 4a | 14.00 | 0.04 | 1.09 | 0.32 | 28.81 | 0.15 | 3.15 | 6.82 | 1.02 | 0.28 | 0.12 | 0.31 | 0.12 | 0.01 | 0.00 | 1.35 | 33.74 | 91.34 |

| Sample | Area | Si | Ti | Al | Cr | Fe | Mn | Ni | Mg | Ca | Na | K | P | Co | V | Zn | S | O | Total |
|---|---|---|---|---|---|---|---|---|---|---|---|---|---|---|---|---|---|---|---|
| NWA 7892 | 1a | 11.54 | 0.03 | 1.81 | 0.19 | 34.06 | 0.17 | 0.93 | 6.95 | 0.76 | 0.08 | 0.08 | 0.17 | 0.10 | 0.00 | 0.05 | 0.17 | 30.36 | 87.45 |
| NWA 7892 | 1a | 12.07 | 0.06 | 2.13 | 0.20 | 31.37 | 0.12 | 1.02 | 6.40 | 0.91 | 0.07 | 0.11 | 0.18 | 0.12 | 0.01 | 0.01 | 0.12 | 30.17 | 85.07 |
| NWA 7892 | 1a | 10.91 | 0.04 | 2.41 | 0.17 | 34.66 | 0.12 | 1.17 | 6.44 | 0.77 | 0.11 | 0.13 | 0.13 | 0.11 | 0.01 | 0.04 | 0.11 | 29.95 | 87.28 |
| NWA 7892 | 1a | 9.71 | 0.02 | 1.61 | 0.16 | 40.37 | 0.15 | 0.97 | 4.76 | 0.73 | 0.13 | 0.06 | 0.18 | 0.10 | 0.01 | 0.00 | 0.12 | 28.38 | 87.46 |
| NWA 7892 | 1a | 23.34 | 0.03 | 0.65 | 0.36 | 8.38 | 0.14 | 0.22 | 19.95 | 0.48 | 0.01 | 0.01 | 0.04 | 0.03 | 0.01 | 0.00 | 0.02 | 43.29 | 96.96 |
| NWA 7892 | 1a | 10.64 | 0.03 | 1.73 | 0.18 | 36.52 | 0.13 | 1.01 | 6.81 | 0.86 | 0.08 | 0.09 | 0.15 | 0.11 | 0.00 | 0.02 | 0.14 | 29.85 | 88.35 |
| NWA 7892 | 1a | 13.11 | 0.03 | 1.93 | 0.22 | 28.01 | 0.16 | 1.09 | 11.63 | 0.79 | 0.08 | 0.11 | 0.16 | 0.12 | 0.00 | 0.02 | 0.11 | 33.57 | 91.14 |
| NWA 7892 | 1a | 11.68 | 0.03 | 2.33 | 0.16 | 32.82 | 0.14 | 1.24 | 6.05 | 0.87 | 0.11 | 0.13 | 0.17 | 0.12 | 0.01 | 0.03 | 0.15 | 30.13 | 86.17 |
| NWA 7892 | 1a | 11.77 | 0.05 | 2.96 | 0.16 | 29.97 | 0.12 | 1.63 | 6.20 | 0.97 | 0.15 | 0.17 | 0.20 | 0.14 | 0.01 | 0.02 | 0.13 | 30.26 | 84.91 |
| NWA 7892 | 1a | 11.44 | 0.02 | 1.76 | 0.13 | 32.09 | 0.16 | 1.23 | 7.69 | 1.50 | 0.09 | 0.10 | 0.20 | 0.11 | 0.00 | 0.02 | 0.14 | 30.46 | 87.14 |
| NWA 7892 | 1a | 12.48 | 0.05 | 2.53 | 0.17 | 29.75 | 0.12 | 1.39 | 6.86 | 0.99 | 0.11 | 0.14 | 0.19 | 0.11 | 0.00 | 0.02 | 0.14 | 31.00 | 86.05 |
| NWA 7892 | 1a | 11.61 | 0.09 | 3.34 | 0.11 | 29.86 | 0.07 | 1.86 | 4.46 | 2.04 | 0.31 | 0.23 | 0.17 | 0.15 | 0.01 | 0.03 | 0.12 | 29.75 | 84.21 |
| NWA 7892 | 1a | 16.42 | 0.02 | 2.11 | 0.20 | 22.44 | 0.10 | 1.11 | 11.98 | 1.15 | 0.11 | 0.13 | 0.17 | 0.09 | 0.02 | 0.01 | 0.08 | 36.22 | 92.36 |

Continued on next page

| Sample | Area | Si | Ti | Al | Cr | Fe | Mn | Ni | Mg | Ca | Na | K | P | Co | V | Zn | S | O | Total |
|---|---|---|---|---|---|---|---|---|---|---|---|---|---|---|---|---|---|---|---|
| NWA 7892 | 1a | 12.37 | 0.02 | 2.60 | 0.15 | 29.08 | 0.12 | 1.61 | 6.22 | 1.56 | 0.14 | 0.15 | 0.22 | 0.14 | 0.01 | 0.04 | 0.16 | 30.67 | 85.26 |
| NWA 7892 | 1a | 12.68 | 0.05 | 2.34 | 0.17 | 30.81 | 0.15 | 1.47 | 7.30 | 0.87 | 0.10 | 0.13 | 0.18 | 0.13 | 0.01 | 0.01 | 0.15 | 31.62 | 88.17 |
| NWA 7892 | 1a | 11.25 | 0.05 | 1.96 | 0.14 | 33.13 | 0.14 | 1.56 | 5.87 | 1.09 | 0.11 | 0.12 | 0.17 | 0.13 | 0.01 | 0.01 | 0.18 | 29.52 | 85.44 |
| NWA 7892 | 1a | 14.11 | 0.19 | 1.45 | 0.14 | 19.97 | 0.12 | 0.90 | 12.87 | 3.16 | 0.06 | 0.05 | 0.16 | 0.08 | 0.02 | 0.02 | 0.10 | 33.72 | 87.12 |
| NWA 7892 | 1a | 13.28 | 0.06 | 2.17 | 0.22 | 28.76 | 0.14 | 1.28 | 7.44 | 1.06 | 0.08 | 0.13 | 0.16 | 0.12 | 0.00 | 0.04 | 0.14 | 31.67 | 86.75 |
| NWA 7892 | 1a | 10.54 | 0.05 | 1.62 | 0.10 | 37.75 | 0.19 | 1.17 | 4.62 | 0.68 | 0.11 | 0.09 | 0.13 | 0.11 | 0.00 | 0.01 | 0.16 | 28.52 | 85.85 |
| NWA 7892 | 1a | 12.18 | 0.04 | 1.76 | 0.22 | 32.74 | 0.17 | 1.16 | 5.64 | 0.83 | 0.09 | 0.11 | 0.16 | 0.11 | 0.01 | 0.03 | 0.15 | 29.89 | 85.29 |
| NWA 7892 | 1a | 12.00 | 0.06 | 1.54 | 0.23 | 26.17 | 0.14 | 1.05 | 7.65 | 0.82 | 0.04 | 0.10 | 0.17 | 0.09 | 0.01 | 0.02 | 0.17 | 28.92 | 79.18 |
| NWA 7892 | 1a | 13.22 | 0.04 | 2.04 | 0.23 | 29.97 | 0.15 | 0.98 | 8.96 | 0.77 | 0.09 | 0.11 | 0.14 | 0.10 | 0.00 | 0.02 | 0.11 | 32.54 | 89.47 |
| NWA 7892 | 1a | 12.50 | 0.02 | 2.17 | 0.22 | 30.51 | 0.15 | 1.19 | 7.30 | 0.90 | 0.11 | 0.13 | 0.16 | 0.11 | 0.01 | 0.01 | 0.17 | 31.12 | 86.78 |
| NWA 7892 | 1a | 12.69 | 0.06 | 1.71 | 0.22 | 29.31 | 0.15 | 1.11 | 8.36 | 0.88 | 0.08 | 0.13 | 0.18 | 0.10 | 0.01 | 0.01 | 0.18 | 31.30 | 86.48 |
| NWA 7892 | 1a | 12.69 | 0.02 | 1.78 | 0.23 | 29.10 | 0.15 | 1.25 | 7.49 | 0.90 | 0.06 | 0.11 | 0.20 | 0.11 | 0.01 | 0.01 | 0.16 | 30.76 | 85.03 |
| NWA 7892 | 1a | 13.87 | 0.04 | 1.90 | 0.22 | 30.45 | 0.20 | 1.06 | 8.62 | 0.92 | 0.11 | 0.10 | 0.14 | 0.09 | 0.01 | 0.01 | 0.13 | 33.21 | 91.08 |
| NWA 7892 | 1a | 12.65 | 0.04 | 1.95 | 0.18 | 30.73 | 0.16 | 1.16 | 7.96 | 0.83 | 0.11 | 0.12 | 0.14 | 0.11 | 0.01 | 0.01 | 0.15 | 31.50 | 87.81 |
| NWA 7892 | 1a | 12.04 | 0.03 | 1.71 | 0.22 | 31.84 | 0.15 | 1.13 | 6.92 | 0.87 | 0.07 | 0.10 | 0.18 | 0.12 | 0.01 | 0.00 | 0.14 | 30.26 | 85.79 |
| NWA 7892 | 1a | 11.51 | 0.00 | 1.78 | 0.23 | 33.07 | 0.14 | 1.06 | 6.97 | 0.86 | 0.07 | 0.11 | 0.18 | 0.09 | 0.01 | 0.01 | 0.17 | 30.11 | 86.37 |
| NWA 7892 | 1a | 12.76 | 0.01 | 1.86 | 0.22 | 30.26 | 0.15 | 1.10 | 7.26 | 1.06 | 0.08 | 0.12 | 0.15 | 0.12 | 0.00 | 0.02 | 0.17 | 31.07 | 86.41 |
| NWA 7892 | 1a | 11.87 | 0.01 | 2.58 | 0.27 | 32.64 | 0.12 | 1.46 | 6.46 | 0.95 | 0.13 | 0.15 | 0.18 | 0.11 | 0.00 | 0.02 | 0.13 | 30.90 | 87.98 |
| NWA 7892 | 1a | 12.34 | 0.02 | 1.88 | 0.19 | 30.79 | 0.14 | 1.18 | 7.84 | 0.86 | 0.07 | 0.12 | 0.19 | 0.10 | 0.01 | 0.04 | 0.15 | 31.08 | 87.00 |
| NWA 7892 | 1a | 12.21 | 0.04 | 2.21 | 0.22 | 29.16 | 0.20 | 1.34 | 7.13 | 1.18 | 0.14 | 0.10 | 0.19 | 0.11 | 0.01 | 0.03 | 0.13 | 30.51 | 84.91 |
| NWA 7892 | 1a | 12.56 | 0.03 | 1.85 | 0.21 | 30.94 | 0.12 | 1.19 | 7.08 | 0.89 | 0.08 | 0.13 | 0.18 | 0.13 | 0.00 | 0.00 | 0.13 | 30.83 | 86.35 |
| NWA 7892 | 1a | 13.19 | 0.02 | 1.84 | 0.23 | 29.06 | 0.15 | 1.13 | 8.78 | 0.82 | 0.09 | 0.12 | 0.12 | 0.11 | 0.01 | 0.03 | 0.14 | 32.02 | 87.86 |
| NWA 7892 | 1a | 12.09 | 0.04 | 1.82 | 0.22 | 31.99 | 0.11 | 1.29 | 7.00 | 0.85 | 0.07 | 0.11 | 0.20 | 0.12 | 0.01 | 0.03 | 0.17 | 30.61 | 86.73 |
| NWA 7892 | 1a | 14.05 | 0.07 | 1.95 | 0.22 | 27.51 | 0.14 | 1.31 | 9.06 | 0.89 | 0.08 | 0.10 | 0.17 | 0.13 | 0.00 | 0.04 | 0.13 | 32.99 | 88.84 |
| NWA 7892 | 1a | 12.36 | 0.01 | 1.94 | 0.21 | 30.81 | 0.14 | 1.56 | 7.92 | 0.91 | 0.06 | 0.09 | 0.23 | 0.14 | 0.00 | 0.02 | 0.21 | 31.48 | 88.09 |
| NWA 7892 | 1a | 13.24 | 0.05 | 1.39 | 0.16 | 33.08 | 0.18 | 1.14 | 7.77 | 1.16 | 0.13 | 0.07 | 0.19 | 0.10 | 0.01 | 0.00 | 0.13 | 32.38 | 91.18 |
| NWA 7892 | 1a | 15.96 | 0.08 | 0.69 | 0.10 | 28.01 | 0.25 | 0.26 | 12.58 | 1.76 | 0.11 | 0.03 | 0.17 | 0.05 | 0.01 | 0.00 | 0.03 | 36.38 | 96.47 |
| NWA 7892 | 1a | 8.55 | 0.02 | 1.75 | 0.18 | 37.94 | 0.11 | 1.54 | 5.16 | 1.10 | 0.06 | 0.07 | 0.25 | 0.17 | 0.01 | 0.01 | 0.23 | 27.31 | 84.46 |
| NWA 7892 | 1a | 12.58 | 0.05 | 3.37 | 0.20 | 27.47 | 0.12 | 2.12 | 6.40 | 1.17 | 0.19 | 0.18 | 0.27 | 0.18 | 0.01 | 0.02 | 0.13 | 31.32 | 85.78 |
| NWA 7892 | 1a | 12.53 | 0.05 | 2.54 | 0.19 | 29.61 | 0.14 | 1.71 | 7.10 | 0.96 | 0.10 | 0.12 | 0.23 | 0.14 | 0.01 | 0.01 | 0.14 | 31.32 | 86.90 |
| NWA 7892 | 2a | 5.01 | 0.00 | 0.80 | 1.64 | 49.95 | 0.07 | 0.51 | 3.01 | 0.64 | 0.05 | 0.02 | 0.20 | 0.09 | 0.01 | 0.01 | 0.16 | 24.43 | 86.60 |
| NWA 7892 | 2a | 9.22 | 0.05 | 1.17 | 0.22 | 42.37 | 0.10 | 0.59 | 5.97 | 0.66 | 0.04 | 0.09 | 0.10 | 0.08 | 0.02 | 0.00 | 0.10 | 28.54 | 89.32 |
| NWA 7892 | 2a | 6.89 | 0.01 | 1.23 | 0.21 | 46.42 | 0.09 | 0.74 | 3.66 | 1.07 | 0.05 | 0.05 | 0.27 | 0.10 | 0.01 | 0.01 | 0.19 | 26.11 | 87.11 |
| NWA 7892 | 2a | 9.86 | 0.05 | 1.62 | 0.19 | 37.93 | 0.11 | 0.89 | 6.36 | 1.40 | 0.05 | 0.10 | 0.17 | 0.10 | 0.01 | 0.02 | 0.16 | 29.21 | 88.23 |
| NWA 7892 | 2a | 10.85 | 0.03 | 1.86 | 0.21 | 35.28 | 0.11 | 1.21 | 5.83 | 0.85 | 0.08 | 0.11 | 0.17 | 0.11 | 0.01 | 0.02 | 0.14 | 29.29 | 86.16 |
| NWA 7892 | 2a | 12.08 | 0.05 | 2.56 | 0.21 | 32.18 | 0.14 | 1.40 | 7.81 | 0.89 | 0.11 | 0.14 | 0.17 | 0.11 | 0.01 | 0.03 | 0.17 | 31.90 | 89.96 |
| NWA 7892 | 2a | 8.57 | 0.02 | 1.66 | 0.18 | 43.16 | 0.10 | 0.87 | 5.50 | 0.71 | 0.08 | 0.06 | 0.12 | 0.09 | 0.01 | 0.03 | 0.12 | 28.28 | 89.56 |
| NWA 7892 | 2a | 11.85 | 0.01 | 1.83 | 0.20 | 35.23 | 0.13 | 0.93 | 7.98 | 0.73 | 0.07 | 0.11 | 0.12 | 0.10 | 0.00 | 0.01 | 0.16 | 31.63 | 91.09 |
| NWA 7892 | 2a | 12.01 | 0.03 | 1.76 | 0.21 | 33.17 | 0.15 | 0.93 | 7.47 | 0.78 | 0.07 | 0.12 | 0.14 | 0.11 | 0.00 | 0.00 | 0.11 | 30.81 | 87.87 |
| NWA 7892 | 2a | 10.49 | 0.03 | 1.84 | 0.20 | 29.99 | 0.12 | 0.97 | 6.32 | 5.18 | 0.08 | 0.08 | 0.24 | 0.09 | 0.00 | 0.02 | 0.17 | 29.46 | 85.28 |
| NWA 7892 | 2a | 12.78 | 0.04 | 1.01 | 0.21 | 25.53 | 0.22 | 0.60 | 8.70 | 6.35 | 0.06 | 0.03 | 0.20 | 0.07 | 0.00 | 0.01 | 0.12 | 31.87 | 87.80 |
| NWA 7892 | 2a | 9.22 | 0.03 | 0.99 | 0.15 | 32.41 | 0.13 | 0.59 | 6.05 | 6.91 | 0.05 | 0.04 | 0.22 | 0.08 | 0.02 | 0.03 | 0.15 | 28.27 | 85.34 |
| NWA 7892 | 2a | 9.24 | 0.03 | 1.31 | 0.18 | 34.75 | 0.14 | 0.73 | 5.26 | 5.26 | 0.07 | 0.06 | 0.22 | 0.08 | 0.00 | 0.02 | 0.15 | 28.11 | 85.61 |
| NWA 7892 | 2a | 13.23 | 0.06 | 2.85 | 0.21 | 29.21 | 0.14 | 1.41 | 6.94 | 1.78 | 0.22 | 0.16 | 0.20 | 0.14 | 0.00 | 0.03 | 0.10 | 32.37 | 89.05 |
| NWA 7892 | 2a | 13.78 | 0.07 | 2.21 | 0.38 | 27.31 | 0.18 | 1.14 | 8.86 | 0.99 | 0.11 | 0.14 | 0.16 | 0.10 | 0.01 | 0.02 | 0.10 | 32.76 | 88.32 |
| NWA 7892 | 2a | 13.31 | 0.03 | 2.36 | 0.23 | 27.34 | 0.16 | 1.20 | 8.83 | 1.54 | 0.12 | 0.16 | 0.14 | 0.11 | 0.01 | 0.02 | 0.11 | 32.48 | 88.15 |
| NWA 7892 | 2a | 11.17 | 0.01 | 1.54 | 0.20 | 37.47 | 0.16 | 0.84 | 6.38 | 1.02 | 0.09 | 0.09 | 0.12 | 0.09 | 0.01 | 0.02 | 0.17 | 30.30 | 89.68 |
| NWA 7892 | 2a | 12.97 | 0.01 | 2.25 | 0.23 | 28.13 | 0.16 | 1.12 | 7.48 | 1.58 | 0.12 | 0.15 | 0.17 | 0.10 | 0.00 | 0.01 | 0.12 | 31.37 | 85.97 |
| NWA 7892 | 2a | 12.96 | 0.05 | 2.12 | 0.21 | 28.22 | 0.14 | 1.07 | 8.50 | 1.16 | 0.10 | 0.13 | 0.14 | 0.10 | 0.01 | 0.01 | 0.12 | 31.71 | 86.75 |
| NWA 7892 | 2a | 11.24 | 0.04 | 1.94 | 0.21 | 27.92 | 0.15 | 0.97 | 6.49 | 4.90 | 0.09 | 0.12 | 0.18 | 0.10 | 0.00 | 0.01 | 0.16 | 29.75 | 84.27 |
| NWA 7892 | 2a | 12.36 | 0.03 | 1.90 | 0.19 | 33.02 | 0.16 | 1.05 | 7.03 | 0.84 | 0.08 | 0.10 | 0.15 | 0.10 | 0.00 | 0.03 | 0.13 | 31.12 | 88.29 |
| NWA 7892 | 2a | 13.03 | 0.03 | 2.05 | 0.31 | 29.62 | 0.20 | 1.09 | 7.87 | 0.90 | 0.09 | 0.14 | 0.14 | 0.09 | 0.00 | 0.01 | 0.11 | 31.64 | 87.32 |
| NWA 7892 | 2a | 8.58 | 0.00 | 0.79 | 0.08 | 17.07 | 0.06 | 0.59 | 3.70 | 19.58 | 0.06 | 0.05 | 0.33 | 0.04 | 0.00 | 0.00 | 0.13 | 26.49 | 77.55 |
| NWA 7892 | 2a | 11.78 | 0.04 | 2.15 | 0.29 | 29.47 | 0.12 | 1.19 | 6.40 | 3.86 | 0.09 | 0.09 | 0.23 | 0.11 | 0.00 | 0.03 | 0.13 | 30.62 | 86.60 |
| NWA 7892 | 2a | 12.17 | 0.03 | 1.88 | 0.23 | 30.08 | 0.14 | 1.07 | 7.06 | 0.90 | 0.10 | 0.11 | 0.17 | 0.10 | 0.00 | 0.02 | 0.14 | 30.14 | 84.34 |
| NWA 7892 | 2a | 13.95 | 0.06 | 2.03 | 0.26 | 28.25 | 0.23 | 1.09 | 9.07 | 0.94 | 0.11 | 0.11 | 0.15 | 0.10 | 0.00 | 0.03 | 0.11 | 33.11 | 89.60 |
| NWA 7892 | 2a | 12.39 | 0.08 | 2.00 | 0.24 | 31.49 | 0.14 | 1.05 | 7.21 | 0.87 | 0.10 | 0.11 | 0.18 | 0.11 | 0.00 | 0.03 | 0.14 | 31.03 | 87.17 |
| NWA 7892 | 2a | 13.89 | 0.01 | 1.08 | 0.19 | 34.17 | 0.30 | 0.79 | 8.59 | 0.89 | 0.08 | 0.06 | 0.11 | 0.09 | 0.01 | 0.00 | 0.13 | 33.37 | 93.76 |

Continued on next page

| Sample | Area | Si | Ti | Al | Cr | Fe | Mn | Ni | Mg | Ca | Na | K | P | Co | V | Zn | S | O | Total |
|---|---|---|---|---|---|---|---|---|---|---|---|---|---|---|---|---|---|---|---|
| NWA 7892 | 2a | 13.26 | 0.04 | 2.07 | 0.30 | 28.46 | 0.21 | 1.02 | 8.32 | 0.97 | 0.10 | 0.14 | 0.16 | 0.10 | 0.00 | 0.02 | 0.13 | 31.97 | 87.27 |
| NWA 7892 | 2a | 13.11 | 0.05 | 1.93 | 0.37 | 33.58 | 0.16 | 1.15 | 7.61 | 0.81 | 0.11 | 0.11 | 0.16 | 0.11 | 0.00 | 0.03 | 0.12 | 32.65 | 92.06 |
| NWA 7892 | 2a | 12.80 | 0.03 | 2.72 | 0.21 | 28.82 | 0.12 | 1.52 | 7.16 | 1.36 | 0.17 | 0.17 | 0.17 | 0.13 | 0.00 | 0.03 | 0.13 | 31.62 | 87.16 |
| NWA 7892 | 2a | 13.39 | 0.03 | 2.51 | 0.38 | 28.23 | 0.15 | 1.46 | 9.00 | 0.97 | 0.11 | 0.13 | 0.19 | 0.12 | 0.01 | 0.02 | 0.13 | 33.07 | 89.90 |
| NWA 7892 | 2a | 12.99 | 0.03 | 3.00 | 0.22 | 29.19 | 0.13 | 1.58 | 7.54 | 1.10 | 0.22 | 0.18 | 0.18 | 0.12 | 0.01 | 0.03 | 0.14 | 32.43 | 89.09 |
| NWA 7892 | 2a | 14.35 | 0.06 | 2.57 | 0.25 | 24.49 | 0.17 | 1.30 | 10.63 | 1.40 | 0.15 | 0.15 | 0.15 | 0.12 | 0.00 | 0.01 | 0.11 | 34.25 | 90.16 |
| NWA 7892 | 2a | 13.89 | 0.05 | 2.00 | 0.16 | 30.52 | 0.12 | 1.07 | 9.19 | 0.78 | 0.11 | 0.15 | 0.12 | 0.10 | 0.01 | 0.03 | 0.17 | 33.66 | 92.13 |
| NWA 7892 | 2a | 11.75 | 0.04 | 2.07 | 0.20 | 33.68 | 0.15 | 0.96 | 7.60 | 0.81 | 0.09 | 0.09 | 0.13 | 0.10 | 0.00 | 0.01 | 0.13 | 31.08 | 88.89 |
| NWA 7892 | 2a | 13.63 | 0.04 | 2.13 | 0.25 | 28.03 | 0.16 | 1.09 | 9.72 | 0.92 | 0.08 | 0.14 | 0.14 | 0.10 | 0.00 | 0.02 | 0.11 | 33.15 | 89.71 |
| NWA 7892 | 2a | 7.59 | 0.01 | 1.22 | 0.13 | 45.15 | 0.08 | 0.65 | 4.36 | 1.22 | 0.04 | 0.07 | 0.11 | 0.08 | 0.00 | 0.00 | 0.08 | 26.59 | 87.38 |
| NWA 7892 | 2a | 12.80 | 0.03 | 2.41 | 0.24 | 31.04 | 0.15 | 1.31 | 7.99 | 0.97 | 0.11 | 0.14 | 0.17 | 0.11 | 0.01 | 0.04 | 0.14 | 32.35 | 90.01 |
| NWA 7892 | 2a | 11.89 | 0.04 | 2.25 | 0.26 | 31.38 | 0.12 | 1.25 | 7.97 | 0.89 | 0.10 | 0.11 | 0.19 | 0.11 | 0.00 | 0.04 | 0.17 | 31.26 | 88.03 |
| NWA 7892 | 2a | 15.07 | 0.03 | 2.50 | 0.29 | 25.49 | 0.20 | 1.33 | 10.61 | 1.11 | 0.12 | 0.14 | 0.16 | 0.13 | 0.00 | 0.00 | 0.11 | 35.18 | 92.47 |
| NWA 7892 | 2a | 13.19 | 0.06 | 2.26 | 0.26 | 29.72 | 0.23 | 1.23 | 8.27 | 1.02 | 0.07 | 0.12 | 0.21 | 0.10 | 0.01 | 0.03 | 0.14 | 32.52 | 89.44 |
| NWA 7892 | 2a | 13.77 | 0.03 | 2.28 | 0.25 | 28.02 | 0.15 | 1.10 | 8.80 | 0.95 | 0.10 | 0.14 | 0.14 | 0.10 | 0.00 | 0.02 | 0.11 | 32.83 | 88.79 |
| NWA 7892 | 2a | 13.26 | 0.05 | 2.57 | 0.27 | 29.30 | 0.19 | 1.27 | 8.06 | 0.95 | 0.11 | 0.17 | 0.17 | 0.11 | 0.00 | 0.04 | 0.12 | 32.54 | 89.18 |
| NWA 7892 | 2a | 13.16 | 0.02 | 2.43 | 0.24 | 29.43 | 0.15 | 1.22 | 7.87 | 0.94 | 0.10 | 0.14 | 0.17 | 0.11 | 0.01 | 0.03 | 0.11 | 32.12 | 88.25 |
| NWA 7892 | 2a | 12.17 | 0.07 | 2.36 | 0.26 | 33.08 | 0.12 | 1.18 | 7.64 | 0.91 | 0.12 | 0.13 | 0.17 | 0.12 | 0.01 | 0.01 | 0.14 | 31.90 | 90.39 |
| NWA 7892 | 2a | 12.77 | 0.03 | 3.00 | 0.20 | 29.81 | 0.12 | 1.52 | 6.64 | 1.10 | 0.18 | 0.19 | 0.19 | 0.13 | 0.00 | 0.02 | 0.11 | 31.68 | 87.69 |
| NWA 7892 | 2a | 11.26 | 0.00 | 3.24 | 0.07 | 34.33 | 0.15 | 1.54 | 4.60 | 0.89 | 0.22 | 0.19 | 0.16 | 0.13 | 0.00 | 0.05 | 0.15 | 30.02 | 87.00 |
| NWA 7892 | 2a | 10.66 | 0.04 | 3.85 | 0.09 | 34.95 | 0.10 | 1.88 | 3.94 | 1.01 | 0.31 | 0.24 | 0.17 | 0.14 | 0.01 | 0.02 | 0.12 | 29.80 | 87.33 |
| NWA 7892 | 2a | 12.47 | 0.04 | 2.04 | 0.23 | 32.05 | 0.15 | 1.19 | 7.73 | 0.88 | 0.09 | 0.13 | 0.17 | 0.13 | 0.00 | 0.03 | 0.15 | 31.69 | 89.17 |
| NWA 7892 | 2a | 11.03 | 0.03 | 2.05 | 0.18 | 32.12 | 0.14 | 1.37 | 6.79 | 2.57 | 0.08 | 0.08 | 0.24 | 0.14 | 0.00 | 0.03 | 0.19 | 30.27 | 87.31 |
| NWA 7892 | 2a | 13.56 | 0.06 | 1.86 | 0.28 | 29.99 | 0.35 | 1.15 | 9.07 | 0.96 | 0.07 | 0.10 | 0.19 | 0.10 | 0.00 | 0.02 | 0.13 | 33.16 | 91.05 |
| NWA 7892 | 2a | 11.95 | 0.00 | 2.20 | 0.25 | 32.50 | 0.14 | 1.32 | 7.43 | 0.96 | 0.09 | 0.12 | 0.19 | 0.12 | 0.00 | 0.03 | 0.16 | 31.26 | 88.72 |
| NWA 7892 | 2a | 11.20 | 0.04 | 2.05 | 0.20 | 32.95 | 0.12 | 1.31 | 6.89 | 1.37 | 0.08 | 0.11 | 0.18 | 0.11 | 0.00 | 0.02 | 0.12 | 30.13 | 86.88 |
| NWA 7892 | 2a | 11.12 | 0.00 | 0.15 | 0.25 | 10.24 | 0.24 | 0.09 | 22.39 | 0.14 | 0.00 | 0.00 | 0.03 | 0.01 | 0.00 | 0.00 | 0.01 | 30.79 | 75.46 |
| NWA 7892 | 2a | 19.88 | 0.03 | 0.71 | 0.18 | 0.69 | 0.04 | 0.00 | 33.58 | 0.50 | 0.00 | 0.01 | 0.00 | 0.00 | 0.00 | 0.00 | 0.00 | 45.91 | 101.53 |
| NWA 7892 | 2a | 12.98 | 0.01 | 0.13 | 0.14 | 17.56 | 0.33 | 0.08 | 21.39 | 0.19 | 0.00 | 0.01 | 0.03 | 0.02 | 0.00 | 0.00 | 0.01 | 34.35 | 87.23 |
| NWA 7892 | 2a | 21.58 | 0.04 | 0.24 | 0.22 | 3.53 | 0.07 | 0.09 | 30.34 | 0.27 | 0.01 | 0.01 | 0.03 | 0.01 | 0.00 | 0.02 | 0.01 | 46.13 | 102.60 |
| NWA 7892 | 2a | 16.08 | 0.04 | 1.39 | 0.42 | 8.41 | 0.08 | 0.96 | 22.93 | 0.84 | 0.04 | 0.06 | 0.18 | 0.06 | 0.01 | 0.00 | 0.07 | 38.28 | 89.85 |
| NWA 7892 | 3a | 13.02 | 0.05 | 1.99 | 0.23 | 32.16 | 0.16 | 1.31 | 7.25 | 1.02 | 0.09 | 0.11 | 0.21 | 0.11 | 0.00 | 0.03 | 0.15 | 32.13 | 90.02 |
| NWA 7892 | 3a | 12.55 | 0.05 | 2.90 | 0.20 | 30.67 | 0.13 | 1.72 | 7.04 | 1.11 | 0.16 | 0.16 | 0.21 | 0.16 | 0.01 | 0.04 | 0.16 | 32.02 | 89.29 |
| NWA 7892 | 3a | 8.31 | 0.01 | 1.68 | 0.12 | 45.69 | 0.09 | 1.05 | 4.75 | 1.07 | 0.10 | 0.10 | 0.22 | 0.11 | 0.00 | 0.03 | 0.11 | 28.52 | 91.96 |
| NWA 7892 | 3a | 13.01 | 0.02 | 2.27 | 0.25 | 30.09 | 0.16 | 1.22 | 8.23 | 1.09 | 0.10 | 0.14 | 0.23 | 0.11 | 0.01 | 0.02 | 0.15 | 32.46 | 89.56 |
| NWA 7892 | 3a | 11.89 | 0.01 | 2.02 | 0.19 | 32.06 | 0.13 | 1.56 | 6.17 | 1.39 | 0.14 | 0.12 | 0.22 | 0.14 | 0.00 | 0.02 | 0.15 | 30.32 | 86.53 |
| NWA 7892 | 3a | 16.63 | 0.01 | 0.88 | 0.37 | 22.02 | 0.15 | 0.65 | 18.59 | 0.58 | 0.03 | 0.06 | 0.11 | 0.07 | 0.00 | 0.00 | 0.06 | 39.17 | 99.38 |
| NWA 7892 | 3a | 14.07 | 0.07 | 1.97 | 0.22 | 29.91 | 0.18 | 1.28 | 9.50 | 0.92 | 0.10 | 0.12 | 0.16 | 0.09 | 0.01 | 0.02 | 0.13 | 34.02 | 92.77 |
| NWA 7892 | 3a | 9.59 | 0.03 | 1.97 | 0.30 | 38.43 | 0.13 | 1.31 | 6.45 | 1.04 | 0.15 | 0.12 | 0.18 | 0.09 | 0.00 | 0.00 | 0.12 | 29.42 | 89.33 |
| NWA 7892 | 3a | 18.98 | 0.06 | 1.26 | 0.60 | 10.09 | 0.15 | 0.37 | 20.04 | 1.04 | 0.05 | 0.04 | 0.10 | 0.03 | 0.01 | 0.01 | 0.04 | 39.93 | 92.80 |
| NWA 7892 | 3a | 9.64 | 0.00 | 1.09 | 0.07 | 21.87 | 0.12 | 0.93 | 2.93 | 14.93 | 0.08 | 0.06 | 0.36 | 0.05 | 0.00 | 0.01 | 0.24 | 27.30 | 79.68 |
| NWA 7892 | 3a | 11.01 | 0.05 | 2.49 | 0.14 | 20.74 | 0.10 | 2.14 | 5.01 | 8.54 | 0.25 | 0.18 | 0.32 | 0.14 | 0.00 | 0.01 | 0.34 | 29.21 | 80.67 |
| NWA 7892 | 3a | 13.85 | 0.04 | 2.38 | 0.22 | 27.57 | 0.13 | 1.68 | 8.45 | 1.02 | 0.10 | 0.18 | 0.19 | 0.14 | 0.01 | 0.01 | 0.14 | 32.97 | 89.08 |
| NWA 7892 | 3a | 13.22 | 0.05 | 2.29 | 0.21 | 30.36 | 0.13 | 1.63 | 7.72 | 1.02 | 0.17 | 0.17 | 0.18 | 0.13 | 0.01 | 0.01 | 0.20 | 32.58 | 90.08 |
| NWA 7892 | 3a | 12.77 | 0.01 | 2.14 | 0.22 | 32.28 | 0.15 | 1.43 | 7.48 | 0.89 | 0.15 | 0.15 | 0.14 | 0.13 | 0.00 | 0.00 | 0.14 | 32.02 | 90.10 |
| NWA 7892 | 3a | 13.42 | 0.04 | 1.81 | 0.22 | 29.27 | 0.16 | 1.32 | 7.77 | 0.92 | 0.10 | 0.17 | 0.15 | 0.13 | 0.01 | 0.00 | 0.14 | 31.81 | 87.44 |
| NWA 7892 | 3a | 11.32 | 0.02 | 2.08 | 0.14 | 35.80 | 0.13 | 1.38 | 5.83 | 1.31 | 0.12 | 0.11 | 0.17 | 0.13 | 0.00 | 0.03 | 0.14 | 30.39 | 89.10 |
| NWA 7892 | 3a | 11.29 | 0.03 | 1.47 | 0.13 | 37.04 | 0.19 | 0.96 | 8.92 | 0.89 | 0.09 | 0.09 | 0.09 | 0.11 | 0.00 | 0.00 | 0.16 | 31.84 | 93.30 |
| NWA 7892 | 3a | 12.85 | 0.04 | 2.12 | 0.24 | 32.73 | 0.16 | 1.25 | 7.48 | 0.92 | 0.09 | 0.11 | 0.15 | 0.11 | 0.00 | 0.03 | 0.12 | 32.19 | 90.59 |
| NWA 7892 | 3a | 11.59 | 0.00 | 2.40 | 0.15 | 34.78 | 0.15 | 1.65 | 7.00 | 0.87 | 0.17 | 0.15 | 0.16 | 0.13 | 0.00 | 0.01 | 0.15 | 31.37 | 90.73 |
| NWA 7892 | 3a | 13.55 | 0.01 | 2.45 | 0.28 | 29.10 | 0.16 | 1.38 | 8.39 | 1.00 | 0.11 | 0.16 | 0.17 | 0.11 | 0.00 | 0.02 | 0.12 | 32.95 | 89.96 |
| NWA 7892 | 3a | 13.78 | 0.05 | 1.99 | 0.26 | 29.67 | 0.16 | 1.21 | 8.49 | 0.91 | 0.10 | 0.12 | 0.17 | 0.11 | 0.01 | 0.02 | 0.15 | 32.99 | 90.19 |
| NWA 7892 | 3a | 26.22 | 0.06 | 0.72 | 0.36 | 3.65 | 0.10 | 0.07 | 22.53 | 0.51 | 0.00 | 0.00 | 0.00 | 0.00 | 0.01 | 0.00 | 0.01 | 46.88 | 101.12 |
| NWA 7892 | 3a | 12.85 | 0.04 | 2.06 | 0.21 | 30.36 | 0.17 | 1.12 | 9.73 | 0.88 | 0.09 | 0.12 | 0.15 | 0.10 | 0.01 | 0.02 | 0.14 | 32.90 | 90.95 |
| NWA 7892 | 3a | 22.83 | 0.11 | 1.10 | 0.31 | 11.08 | 0.12 | 0.46 | 20.48 | 0.60 | 0.00 | 0.04 | 0.05 | 0.03 | 0.01 | -0.01 | 0.04 | 44.43 | 101.68 |
| NWA 7892 | 3a | 12.01 | 0.03 | 1.97 | 0.16 | 36.17 | 0.18 | 1.03 | 6.78 | 0.74 | 0.10 | 0.12 | 0.13 | 0.10 | 0.00 | -0.02 | 0.12 | 31.41 | 91.03 |
| NWA 7892 | 3a | 14.20 | 0.20 | 4.91 | 0.24 | 24.38 | 0.19 | 0.97 | 8.03 | 2.97 | 0.07 | 0.11 | 0.16 | 0.10 | 0.08 | 0.00 | 0.10 | 35.03 | 91.74 |
| NWA 7892 | 3a | 13.33 | 0.06 | 2.06 | 0.26 | 30.03 | 0.17 | 1.16 | 8.26 | 0.97 | 0.09 | 0.12 | 0.16 | 0.11 | 0.01 | 0.02 | 0.17 | 32.53 | 89.51 |

Continued on next page

| Sample | Area | Si | Ti | Al | Cr | Fe | Mn | Ni | Mg | Ca | Na | K | P | Co | V | Zn | S | O | Total |
|---|---|---|---|---|---|---|---|---|---|---|---|---|---|---|---|---|---|---|---|
| NWA 7892 | 3a | 12.99 | 0.02 | 2.22 | 0.24 | 30.92 | 0.16 | 1.26 | 8.60 | 0.89 | 0.10 | 0.12 | 0.17 | 0.10 | 0.00 | 0.03 | 0.15 | 32.70 | 90.67 |
| NWA 7892 | 3a | 12.92 | 0.07 | 1.63 | 0.23 | 30.99 | 0.15 | 1.35 | 8.48 | 1.03 | 0.07 | 0.10 | 0.19 | 0.09 | 0.00 | 0.00 | 0.17 | 32.18 | 89.65 |
| NWA 7892 | 4a | 11.22 | 0.02 | 1.91 | 0.18 | 33.23 | 0.19 | 1.41 | 5.74 | 1.68 | 0.12 | 0.15 | 0.18 | 0.11 | 0.01 | 0.00 | 0.16 | 29.56 | 85.87 |
| NWA 7892 | 4a | 12.54 | 0.04 | 3.13 | 0.19 | 28.53 | 0.12 | 1.88 | 6.58 | 2.10 | 0.22 | 0.18 | 0.23 | 0.16 | 0.00 | 0.00 | 0.20 | 31.83 | 87.93 |
| NWA 7892 | 4a | 10.28 | 0.03 | 2.19 | 0.12 | 27.86 | 0.12 | 1.45 | 5.87 | 6.39 | 0.17 | 0.12 | 0.25 | 0.11 | 0.01 | 0.01 | 0.22 | 29.33 | 84.53 |
| NWA 7892 | 4a | 12.46 | 0.03 | 2.88 | 0.11 | 31.62 | 0.14 | 2.05 | 6.05 | 1.07 | 0.33 | 0.19 | 0.20 | 0.16 | 0.00 | 0.00 | 0.24 | 31.71 | 89.24 |
| NWA 7892 | 4a | 14.32 | 0.01 | 2.68 | 0.21 | 26.03 | 0.18 | 1.84 | 8.17 | 1.23 | 0.16 | 0.15 | 0.21 | 0.13 | 0.02 | 0.00 | 0.17 | 33.34 | 88.85 |
| NWA 7892 | 4a | 11.62 | 0.06 | 2.73 | 0.18 | 33.47 | 0.11 | 1.74 | 6.45 | 2.07 | 0.17 | 0.13 | 0.24 | 0.15 | 0.00 | 0.02 | 0.17 | 31.67 | 90.98 |
| NWA 7892 | 4a | 10.62 | 0.01 | 2.08 | 0.15 | 30.95 | 0.11 | 1.95 | 5.99 | 2.66 | 0.09 | 0.11 | 0.29 | 0.14 | 0.01 | 0.03 | 0.20 | 29.23 | 84.62 |
| NWA 7892 | 4a | 11.70 | 0.01 | 2.09 | 0.17 | 31.08 | 0.14 | 1.69 | 7.26 | 2.81 | 0.14 | 0.11 | 0.23 | 0.14 | 0.01 | 0.02 | 0.23 | 31.35 | 89.18 |
| NWA 7892 | 4a | 14.51 | 0.03 | 2.68 | 0.21 | 26.22 | 0.13 | 1.81 | 8.17 | 1.19 | 0.16 | 0.15 | 0.23 | 0.13 | 0.00 | 0.01 | 0.20 | 33.66 | 89.49 |
| NWA 7892 | 4a | 13.83 | 0.03 | 2.90 | 0.20 | 28.66 | 0.14 | 1.82 | 7.39 | 1.16 | 0.20 | 0.17 | 0.22 | 0.14 | 0.01 | 0.04 | 0.18 | 33.23 | 90.32 |
| NWA 7892 | 4a | 14.47 | 0.03 | 2.03 | 0.18 | 27.83 | 0.20 | 1.13 | 9.93 | 0.86 | 0.14 | 0.11 | 0.15 | 0.10 | 0.00 | 0.01 | 0.10 | 34.06 | 91.33 |
| NWA 7892 | 4a | 12.85 | 0.05 | 2.62 | 0.20 | 28.61 | 0.15 | 1.71 | 7.15 | 1.22 | 0.17 | 0.15 | 0.24 | 0.14 | 0.00 | 0.03 | 0.21 | 31.76 | 87.26 |
| NWA 7892 | 4a | 12.04 | 0.02 | 2.67 | 0.23 | 26.83 | 0.16 | 1.52 | 7.55 | 1.14 | 0.11 | 0.15 | 0.16 | 0.12 | 0.00 | 0.04 | 0.13 | 30.28 | 83.15 |
| NWA 7892 | 4a | 15.54 | 0.06 | 2.03 | 0.27 | 25.94 | 0.27 | 1.34 | 9.64 | 2.21 | 0.11 | 0.08 | 0.16 | 0.10 | 0.02 | 0.00 | 0.13 | 35.27 | 93.17 |
| NWA 7892 | 5a | 13.20 | 0.05 | 1.97 | 0.19 | 26.71 | 0.18 | 0.85 | 7.82 | 0.96 | 0.10 | 0.15 | 0.24 | 0.09 | 0.00 | 0.01 | 0.12 | 30.96 | 83.60 |
| NWA 7892 | 5a | 13.22 | 0.07 | 2.27 | 0.28 | 25.90 | 0.19 | 0.95 | 7.39 | 1.10 | 0.15 | 0.16 | 0.23 | 0.09 | 0.01 | 0.01 | 0.11 | 30.86 | 82.99 |
| NWA 7892 | 5a | 13.76 | 0.02 | 2.72 | 0.20 | 23.70 | 0.15 | 1.03 | 9.18 | 0.92 | 0.15 | 0.15 | 0.27 | 0.09 | 0.01 | 0.03 | 0.13 | 32.40 | 84.91 |
| NWA 7892 | 5a | 12.84 | 0.03 | 2.20 | 0.24 | 25.68 | 0.20 | 1.00 | 7.69 | 0.88 | 0.13 | 0.15 | 0.28 | 0.10 | 0.01 | 0.03 | 0.13 | 30.49 | 82.08 |
| NWA 7892 | 5a | 11.95 | 0.06 | 2.21 | 0.20 | 27.37 | 0.17 | 0.99 | 7.00 | 0.81 | 0.11 | 0.15 | 0.27 | 0.10 | 0.01 | 0.01 | 0.12 | 29.44 | 80.97 |
| NWA 7892 | 5a | 12.76 | 0.03 | 2.19 | 0.20 | 25.27 | 0.17 | 0.95 | 8.10 | 0.79 | 0.11 | 0.17 | 0.24 | 0.11 | 0.01 | 0.02 | 0.13 | 30.41 | 81.66 |
| NWA 7892 | 5a | 11.59 | 0.06 | 1.73 | 0.20 | 27.65 | 0.18 | 0.90 | 7.27 | 0.72 | 0.08 | 0.14 | 0.23 | 0.10 | 0.00 | 0.01 | 0.12 | 28.73 | 79.71 |
| NWA 7892 | 5a | 12.71 | 0.03 | 1.99 | 0.19 | 27.95 | 0.22 | 0.90 | 7.27 | 0.77 | 0.11 | 0.14 | 0.22 | 0.10 | 0.01 | 0.02 | 0.12 | 30.33 | 83.08 |
| NWA 7892 | 5a | 12.83 | 0.03 | 2.22 | 0.20 | 25.84 | 0.17 | 0.89 | 7.71 | 0.86 | 0.11 | 0.19 | 0.24 | 0.09 | 0.00 | 0.01 | 0.12 | 30.40 | 81.91 |
| NWA 7892 | 5a | 14.00 | 0.02 | 2.20 | 0.22 | 25.69 | 0.18 | 0.84 | 7.68 | 0.79 | 0.11 | 0.19 | 0.21 | 0.09 | 0.00 | 0.04 | 0.09 | 31.55 | 83.90 |
| NWA 7892 | 5a | 13.36 | 0.08 | 3.66 | 0.22 | 25.05 | 0.20 | 0.63 | 9.34 | 0.89 | 0.06 | 0.14 | 0.18 | 0.07 | 0.01 | 0.04 | 0.09 | 32.99 | 87.01 |
| NWA 7892 | 5a | 14.80 | 0.04 | 1.98 | 0.23 | 22.60 | 0.17 | 0.80 | 9.78 | 0.80 | 0.07 | 0.15 | 0.18 | 0.09 | 0.01 | 0.01 | 0.09 | 32.70 | 84.50 |
| NWA 7892 | 5a | 12.98 | 0.05 | 2.33 | 0.20 | 26.71 | 0.16 | 0.99 | 8.22 | 1.02 | 0.09 | 0.15 | 0.25 | 0.09 | 0.00 | 0.02 | 0.13 | 31.37 | 84.76 |
| NWA 7892 | 5a | 12.87 | 0.03 | 2.92 | 0.20 | 27.75 | 0.17 | 1.25 | 7.20 | 0.87 | 0.13 | 0.16 | 0.29 | 0.12 | 0.01 | 0.04 | 0.16 | 31.54 | 85.71 |
| NWA 7892 | 5a | 12.15 | 0.06 | 2.05 | 0.24 | 29.63 | 0.21 | 1.06 | 6.91 | 1.00 | 0.12 | 0.12 | 0.29 | 0.10 | 0.01 | 0.00 | 0.12 | 30.27 | 84.34 |
| NWA 7892 | 5a | 12.51 | 0.01 | 1.97 | 0.20 | 29.85 | 0.17 | 0.89 | 7.27 | 0.76 | 0.09 | 0.13 | 0.24 | 0.10 | 0.01 | 0.02 | 0.13 | 30.66 | 85.01 |
| NWA 7892 | 5a | 13.53 | 0.04 | 1.84 | 0.19 | 28.30 | 0.18 | 0.88 | 7.95 | 0.78 | 0.08 | 0.13 | 0.23 | 0.10 | 0.01 | 0.02 | 0.11 | 31.67 | 86.04 |
| NWA 7892 | 5a | 11.81 | 0.03 | 2.34 | 0.21 | 30.27 | 0.19 | 1.06 | 7.29 | 0.96 | 0.08 | 0.12 | 0.27 | 0.11 | 0.01 | 0.00 | 0.15 | 30.50 | 85.40 |
| NWA 7892 | 5a | 11.57 | 0.03 | 2.29 | 0.24 | 30.19 | 0.16 | 1.07 | 6.47 | 0.80 | 0.09 | 0.15 | 0.30 | 0.11 | 0.00 | 0.00 | 0.15 | 29.61 | 83.23 |
| NWA 7892 | 5a | 15.36 | 0.02 | 0.90 | 0.17 | 20.78 | 0.15 | 0.37 | 18.72 | 0.40 | 0.02 | 0.07 | 0.09 | 0.06 | 0.00 | 0.01 | 0.04 | 37.20 | 94.36 |
| NWA 7892 | 5a | 15.12 | 0.07 | 3.14 | 0.19 | 21.21 | 0.17 | 1.40 | 8.57 | 2.37 | 0.24 | 0.18 | 0.30 | 0.11 | 0.01 | 0.02 | 0.13 | 33.99 | 87.22 |
| NWA 7892 | 5a | 15.25 | 0.08 | 3.19 | 0.21 | 22.48 | 0.18 | 1.35 | 9.22 | 1.20 | 0.19 | 0.15 | 0.26 | 0.10 | 0.02 | 0.01 | 0.11 | 34.40 | 88.40 |
| NWA 7892 | 5a | 15.03 | 0.08 | 3.20 | 0.23 | 24.12 | 0.18 | 1.34 | 8.85 | 1.24 | 0.20 | 0.16 | 0.30 | 0.11 | 0.01 | 0.01 | 0.13 | 34.51 | 89.70 |
| NWA 7892 | 5a | 15.55 | 0.08 | 3.24 | 0.21 | 22.97 | 0.18 | 1.31 | 9.42 | 1.24 | 0.18 | 0.17 | 0.26 | 0.08 | 0.01 | 0.04 | 0.11 | 35.08 | 90.13 |
| NWA 7892 | 5a | 10.38 | 0.03 | 3.73 | 0.13 | 33.12 | 0.11 | 1.33 | 5.56 | 1.23 | 0.23 | 0.19 | 0.20 | 0.11 | 0.01 | 0.04 | 0.16 | 29.92 | 86.48 |
| NWA 7892 | 5a | 12.75 | 0.03 | 1.83 | 0.21 | 29.66 | 0.19 | 0.63 | 7.89 | 1.05 | 0.08 | 0.15 | 0.17 | 0.08 | 0.01 | 0.00 | 0.07 | 31.03 | 85.83 |
| NWA 7892 | 5a | 15.07 | 0.05 | 1.58 | 0.21 | 24.97 | 0.20 | 0.56 | 10.45 | 0.72 | 0.07 | 0.14 | 0.15 | 0.08 | 0.01 | 0.02 | 0.06 | 33.60 | 87.94 |
| NWA 7892 | 5a | 14.06 | 0.02 | 1.68 | 0.24 | 25.18 | 0.22 | 0.55 | 10.60 | 0.81 | 0.06 | 0.13 | 0.18 | 0.07 | 0.01 | 0.02 | 0.09 | 32.81 | 86.73 |
| NWA 7892 | 5a | 14.55 | 0.03 | 1.69 | 0.24 | 23.15 | 0.20 | 0.69 | 10.31 | 0.73 | 0.06 | 0.14 | 0.18 | 0.08 | 0.01 | 0.03 | 0.11 | 32.65 | 84.85 |
| NWA 7892 | 5a | 13.60 | 0.04 | 1.75 | 0.25 | 27.55 | 0.22 | 0.83 | 9.41 | 0.94 | 0.08 | 0.12 | 0.20 | 0.06 | 0.01 | 0.02 | 0.10 | 32.43 | 87.61 |
| NWA 7892 | 5a | 14.14 | 0.03 | 1.78 | 0.24 | 27.59 | 0.19 | 0.79 | 9.00 | 0.73 | 0.09 | 0.13 | 0.19 | 0.07 | 0.00 | 0.02 | 0.09 | 32.68 | 87.76 |
| NWA 7892 | 5a | 14.31 | 0.04 | 2.33 | 0.25 | 25.06 | 0.16 | 1.02 | 9.46 | 1.23 | 0.08 | 0.15 | 0.22 | 0.09 | 0.01 | 0.01 | 0.12 | 33.30 | 87.84 |
| NWA 7892 | 5a | 14.41 | 0.04 | 2.11 | 0.26 | 26.08 | 0.26 | 0.92 | 9.04 | 1.09 | 0.08 | 0.14 | 0.21 | 0.09 | 0.01 | 0.02 | 0.13 | 33.17 | 88.06 |
| NWA 7892 | 5b | 12.77 | 0.07 | 3.22 | 0.22 | 26.82 | 0.16 | 1.30 | 7.31 | 0.90 | 0.13 | 0.19 | 0.27 | 0.12 | 0.01 | 0.01 | 0.16 | 31.54 | 85.20 |
| NWA 7892 | 5b | 13.53 | 0.02 | 2.83 | 0.20 | 27.28 | 0.17 | 1.08 | 8.03 | 0.90 | 0.12 | 0.16 | 0.24 | 0.12 | 0.01 | 0.03 | 0.13 | 32.45 | 87.30 |
| NWA 7892 | 5b | 11.84 | 0.02 | 2.18 | 0.17 | 33.42 | 0.17 | 0.83 | 6.09 | 0.67 | 0.09 | 0.13 | 0.23 | 0.08 | 0.01 | 0.02 | 0.17 | 30.29 | 86.41 |
| NWA 7892 | 5b | 12.73 | 0.00 | 2.33 | 0.23 | 29.30 | 0.20 | 0.81 | 7.89 | 0.92 | 0.09 | 0.14 | 0.23 | 0.09 | 0.01 | 0.05 | 0.14 | 31.53 | 86.69 |
| NWA 7892 | 5b | 12.88 | 0.03 | 2.18 | 0.19 | 28.71 | 0.22 | 0.80 | 8.05 | 0.82 | 0.07 | 0.15 | 0.23 | 0.07 | 0.00 | 0.05 | 0.13 | 31.43 | 86.01 |
| NWA 7892 | 5b | 12.91 | 0.03 | 2.03 | 0.26 | 29.60 | 0.17 | 0.78 | 7.66 | 0.79 | 0.06 | 0.10 | 0.22 | 0.09 | 0.01 | 0.02 | 0.16 | 31.35 | 86.24 |
| NWA 7892 | 5b | 13.56 | 0.06 | 2.17 | 0.26 | 27.27 | 0.17 | 0.87 | 9.16 | 0.81 | 0.07 | 0.14 | 0.25 | 0.09 | 0.01 | 0.03 | 0.14 | 32.61 | 87.67 |
| NWA 7892 | 5b | 13.42 | 0.02 | 0.54 | 0.14 | 26.58 | 0.26 | 0.27 | 15.98 | 0.58 | 0.03 | 0.04 | 0.09 | 0.06 | 0.00 | 0.00 | 0.03 | 34.57 | 92.61 |
| NWA 7892 | 5b | 12.59 | 0.02 | 1.95 | 0.18 | 30.12 | 0.15 | 0.75 | 8.40 | 0.62 | 0.06 | 0.11 | 0.18 | 0.07 | 0.01 | 0.03 | 0.11 | 31.31 | 86.66 |

Continued on next page

| Sample | Area | Si | Ti | Al | Cr | Fe | Mn | Ni | Mg | Ca | Na | K | P | Co | V | Zn | S | O | Total |
|---|---|---|---|---|---|---|---|---|---|---|---|---|---|---|---|---|---|---|---|
| NWA 7892 | 5b | 14.14 | 0.04 | 2.38 | 0.25 | 25.08 | 0.20 | 0.89 | 9.89 | 0.77 | 0.08 | 0.15 | 0.20 | 0.07 | 0.00 | 0.01 | 0.11 | 33.18 | 87.44 |
| NWA 7892 | 5b | 12.08 | 0.05 | 2.22 | 0.18 | 31.96 | 0.17 | 0.79 | 7.12 | 0.79 | 0.10 | 0.14 | 0.24 | 0.08 | 0.01 | 0.02 | 0.13 | 30.89 | 86.97 |
| NWA 7892 | 5b | 12.43 | 0.01 | 2.30 | 0.19 | 30.32 | 0.17 | 0.81 | 7.30 | 0.78 | 0.11 | 0.14 | 0.22 | 0.08 | 0.01 | 0.00 | 0.14 | 30.97 | 85.98 |
| NWA 7892 | 5b | 13.01 | 0.06 | 2.76 | 0.21 | 25.04 | 0.17 | 1.31 | 8.54 | 0.98 | 0.13 | 0.17 | 0.26 | 0.10 | 0.01 | 0.01 | 0.13 | 31.66 | 84.55 |
| NWA 7892 | 5b | 15.19 | 0.06 | 1.04 | 0.27 | 25.04 | 0.22 | 0.70 | 10.25 | 2.54 | 0.16 | 0.03 | 0.34 | 0.09 | 0.01 | 0.01 | 0.19 | 34.39 | 90.53 |
| NWA 7892 | 5b | 14.84 | 0.05 | 0.90 | 0.23 | 25.39 | 0.26 | 0.91 | 12.94 | 0.85 | 0.06 | 0.04 | 0.30 | 0.08 | 0.01 | 0.01 | 0.19 | 35.04 | 92.10 |
| NWA 7892 | 5b | 15.05 | 0.07 | 0.87 | 0.40 | 25.09 | 0.24 | 0.45 | 12.42 | 0.95 | 0.10 | 0.05 | 0.24 | 0.06 | 0.01 | 0.02 | 0.11 | 34.64 | 90.77 |
| NWA 7892 | 5b | 15.12 | 0.06 | 0.72 | 0.22 | 24.81 | 0.26 | 0.55 | 12.63 | 0.92 | 0.09 | 0.02 | 0.27 | 0.05 | 0.01 | 0.01 | 0.15 | 34.65 | 90.54 |
| NWA 7892 | 5b | 14.87 | 0.06 | 2.26 | 0.28 | 23.94 | 0.24 | 0.84 | 10.82 | 0.91 | 0.08 | 0.12 | 0.25 | 0.08 | 0.02 | 0.01 | 0.13 | 34.37 | 89.28 |
| NWA 7892 | 5b | 13.58 | 0.03 | 1.63 | 0.28 | 28.57 | 0.20 | 0.62 | 9.78 | 0.76 | 0.05 | 0.11 | 0.22 | 0.09 | 0.01 | 0.02 | 0.14 | 32.79 | 88.88 |
| NWA 7892 | 5b | 13.52 | 0.05 | 2.14 | 0.29 | 28.28 | 0.19 | 0.77 | 8.89 | 0.78 | 0.09 | 0.15 | 0.24 | 0.09 | 0.01 | 0.02 | 0.13 | 32.61 | 88.25 |
| NWA 7892 | rim | 12.70 | 0.02 | 1.50 | 0.25 | 26.32 | 0.16 | 0.62 | 8.58 | 0.72 | 0.06 | 0.16 | 0.15 | 0.10 | 0.01 | 0.03 | 0.11 | 30.06 | 81.55 |
| NWA 7892 | rim | 12.42 | 0.06 | 2.04 | 0.19 | 24.15 | 0.15 | 0.86 | 7.40 | 0.84 | 0.09 | 0.19 | 0.17 | 0.10 | 0.00 | 0.00 | 0.11 | 28.98 | 77.75 |
| NWA 7892 | rim | 11.47 | 0.03 | 1.30 | 0.18 | 31.28 | 0.16 | 0.49 | 7.50 | 0.56 | 0.07 | 0.12 | 0.11 | 0.08 | 0.00 | 0.01 | 0.10 | 29.00 | 82.46 |
| NWA 7892 | rim | 13.16 | 0.02 | 1.33 | 0.24 | 28.28 | 0.22 | 0.46 | 7.32 | 0.65 | 0.09 | 0.13 | 0.12 | 0.07 | 0.00 | 0.00 | 0.09 | 30.03 | 82.21 |
| NWA 7892 | rim | 12.63 | 0.02 | 1.35 | 0.25 | 26.42 | 0.16 | 0.48 | 7.96 | 0.74 | 0.05 | 0.12 | 0.17 | 0.07 | 0.00 | 0.01 | 0.10 | 29.45 | 79.98 |
| NWA 7892 | rim | 12.46 | 0.02 | 1.43 | 0.20 | 26.39 | 0.14 | 0.58 | 8.16 | 0.67 | 0.07 | 0.17 | 0.14 | 0.07 | 0.00 | 0.02 | 0.10 | 29.39 | 80.01 |
| NWA 7892 | rim | 11.47 | 0.02 | 1.49 | 0.21 | 26.17 | 0.17 | 0.59 | 6.89 | 0.68 | 0.05 | 0.16 | 0.14 | 0.09 | 0.01 | 0.00 | 0.12 | 27.46 | 75.72 |
| NWA 7892 | rim | 12.09 | 0.01 | 1.44 | 0.22 | 25.21 | 0.14 | 0.53 | 7.91 | 0.66 | 0.08 | 0.16 | 0.16 | 0.07 | 0.00 | 0.01 | 0.10 | 28.48 | 77.27 |
| NWA 7892 | rim | 12.78 | 0.04 | 1.40 | 0.24 | 23.93 | 0.14 | 0.52 | 8.47 | 0.67 | 0.05 | 0.16 | 0.12 | 0.07 | 0.01 | 0.01 | 0.10 | 29.22 | 77.93 |
| NWA 7892 | rim | 12.72 | 0.01 | 1.47 | 0.24 | 24.56 | 0.16 | 0.53 | 8.08 | 0.67 | 0.07 | 0.18 | 0.12 | 0.05 | 0.00 | 0.01 | 0.09 | 29.11 | 78.07 |
| NWA 7892 | rim | 13.73 | 0.02 | 1.20 | 0.20 | 22.89 | 0.15 | 0.43 | 11.25 | 0.55 | 0.05 | 0.15 | 0.10 | 0.07 | 0.01 | 0.00 | 0.09 | 31.49 | 82.38 |
| NWA 7892 | rim | 12.61 | 0.06 | 1.80 | 0.21 | 23.99 | 0.12 | 0.62 | 8.78 | 0.69 | 0.10 | 0.20 | 0.13 | 0.10 | 0.00 | 0.02 | 0.08 | 29.63 | 79.14 |
| NWA 7892 | rim | 12.61 | 0.03 | 1.81 | 0.19 | 25.61 | 0.20 | 0.79 | 8.62 | 0.79 | 0.09 | 0.14 | 0.21 | 0.07 | 0.01 | 0.00 | 0.14 | 30.24 | 81.55 |
| NWA 7892 | rim | 13.29 | 0.02 | 1.31 | 0.23 | 21.21 | 0.17 | 0.46 | 8.95 | 0.64 | 0.04 | 0.17 | 0.11 | 0.06 | 0.00 | 0.00 | 0.08 | 29.14 | 75.88 |
| NWA 7892 | rim | 11.55 | 0.01 | 1.09 | 0.15 | 32.75 | 0.18 | 0.42 | 6.74 | 0.51 | 0.05 | 0.13 | 0.08 | 0.09 | 0.01 | 0.00 | 0.12 | 28.74 | 82.62 |
| NWA 7892 | rim | 12.20 | 0.09 | 1.47 | 0.23 | 25.27 | 0.12 | 0.57 | 8.75 | 0.63 | 0.07 | 0.17 | 0.12 | 0.07 | 0.01 | 0.00 | 0.11 | 29.22 | 79.10 |
| NWA 7892 | rim | 12.44 | 0.02 | 1.76 | 0.21 | 24.20 | 0.13 | 0.71 | 7.87 | 0.72 | 0.08 | 0.16 | 0.17 | 0.09 | 0.00 | 0.01 | 0.11 | 28.95 | 77.63 |
| NWA 7892 | rim | 12.35 | 0.05 | 1.59 | 0.22 | 24.37 | 0.13 | 0.68 | 8.33 | 0.68 | 0.06 | 0.14 | 0.19 | 0.09 | 0.00 | 0.00 | 0.11 | 29.07 | 78.06 |
| NWA 7892 | rim | 13.67 | 0.03 | 1.35 | 0.28 | 23.60 | 0.15 | 0.56 | 10.04 | 0.74 | 0.08 | 0.11 | 0.16 | 0.09 | 0.01 | 0.00 | 0.11 | 31.24 | 82.22 |
| NWA 7892 | rim | 11.85 | 0.03 | 1.46 | 0.21 | 27.00 | 0.12 | 0.56 | 7.40 | 0.65 | 0.05 | 0.15 | 0.16 | 0.08 | 0.00 | 0.01 | 0.10 | 28.41 | 78.24 |
| NWA 7892 | rim | 10.85 | 0.01 | 1.53 | 0.23 | 28.23 | 0.12 | 0.72 | 6.83 | 0.71 | 0.08 | 0.14 | 0.17 | 0.11 | 0.00 | 0.01 | 0.24 | 27.60 | 77.58 |
| NWA 7892 | rim | 12.78 | 0.02 | 1.33 | 0.24 | 24.02 | 0.16 | 0.62 | 9.70 | 0.74 | 0.04 | 0.13 | 0.18 | 0.11 | 0.01 | 0.00 | 0.13 | 30.14 | 80.35 |
| NWA 7892 | rim | 12.96 | 0.03 | 1.58 | 0.26 | 23.35 | 0.14 | 0.70 | 9.08 | 0.77 | 0.06 | 0.15 | 0.17 | 0.11 | 0.00 | 0.00 | 0.12 | 30.00 | 79.48 |
| NWA 7892 | rim | 12.00 | 0.04 | 1.86 | 0.22 | 24.57 | 0.13 | 0.82 | 7.72 | 0.94 | 0.08 | 0.16 | 0.21 | 0.12 | 0.00 | 0.00 | 0.15 | 28.80 | 77.82 |
| NWA 7892 | rim | 14.23 | 0.05 | 1.55 | 0.29 | 22.36 | 0.19 | 0.66 | 9.43 | 0.96 | 0.08 | 0.11 | 0.20 | 0.11 | 0.00 | 0.01 | 0.12 | 31.49 | 81.84 |
| NWA 7892 | rim | 13.34 | 0.02 | 1.46 | 0.27 | 22.53 | 0.15 | 0.57 | 9.30 | 0.73 | 0.04 | 0.13 | 0.16 | 0.08 | 0.00 | 0.01 | 0.11 | 30.13 | 79.03 |
| NWA 7892 | rim | 12.63 | 0.02 | 1.45 | 0.22 | 22.78 | 0.13 | 0.59 | 8.48 | 0.66 | 0.07 | 0.12 | 0.15 | 0.07 | 0.00 | 0.01 | 0.09 | 28.77 | 76.24 |
| NWA 7892 | rim | 12.00 | 0.02 | 1.60 | 0.24 | 23.84 | 0.15 | 0.66 | 7.67 | 0.75 | 0.06 | 0.16 | 0.19 | 0.10 | 0.00 | 0.01 | 0.12 | 28.13 | 75.70 |
| NWA 7892 | rim | 11.72 | 0.04 | 1.53 | 0.19 | 26.28 | 0.14 | 0.66 | 7.59 | 0.73 | 0.06 | 0.11 | 0.17 | 0.09 | 0.01 | 0.01 | 0.12 | 28.35 | 77.80 |
| NWA 7892 | rim | 11.78 | 0.02 | 1.59 | 0.21 | 24.95 | 0.14 | 0.67 | 7.32 | 0.77 | 0.06 | 0.14 | 0.19 | 0.11 | 0.01 | 0.00 | 0.12 | 27.95 | 76.03 |
| NWA 7892 | rim | 12.88 | 0.02 | 2.28 | 0.16 | 21.01 | 0.10 | 0.91 | 8.24 | 0.78 | 0.10 | 0.19 | 0.17 | 0.10 | 0.01 | 0.00 | 0.12 | 29.34 | 76.41 |
| NWA 7892 | rim | 11.86 | 0.00 | 1.36 | 0.20 | 28.56 | 0.15 | 0.72 | 7.13 | 0.73 | 0.07 | 0.12 | 0.17 | 0.11 | 0.00 | 0.02 | 0.14 | 28.74 | 80.08 |
| NWA 7892 | rim | 13.91 | 0.03 | 1.38 | 0.20 | 22.78 | 0.12 | 0.71 | 9.87 | 0.66 | 0.04 | 0.10 | 0.19 | 0.11 | 0.00 | 0.01 | 0.14 | 31.22 | 81.47 |
| NWA 7892 | rim | 11.76 | 0.04 | 1.64 | 0.22 | 29.71 | 0.14 | 0.77 | 7.13 | 0.71 | 0.07 | 0.15 | 0.19 | 0.10 | 0.01 | 0.00 | 0.14 | 29.26 | 82.04 |
| NWA 7892 | rim | 11.59 | 0.05 | 1.69 | 0.23 | 29.61 | 0.19 | 0.95 | 6.50 | 0.76 | 0.07 | 0.10 | 0.23 | 0.10 | 0.00 | 0.00 | 0.16 | 28.84 | 81.07 |
| NWA 7892 | rim | 11.99 | 0.04 | 1.74 | 0.22 | 32.92 | 0.19 | 0.99 | 6.74 | 0.83 | 0.07 | 0.13 | 0.23 | 0.11 | 0.01 | 0.02 | 0.15 | 30.48 | 86.86 |
| NWA 7892 | rim | 12.45 | 0.02 | 1.65 | 0.27 | 26.67 | 0.17 | 0.80 | 7.94 | 0.76 | 0.07 | 0.13 | 0.23 | 0.08 | 0.00 | 0.01 | 0.14 | 29.82 | 81.21 |
| NWA 7892 | rim | 11.76 | 0.02 | 1.47 | 0.23 | 26.29 | 0.16 | 0.64 | 6.58 | 0.72 | 0.07 | 0.13 | 0.18 | 0.07 | 0.01 | 0.02 | 0.12 | 27.69 | 76.16 |
| NWA 7892 | rim | 12.67 | 0.04 | 1.56 | 0.26 | 26.37 | 0.14 | 0.64 | 8.59 | 0.74 | 0.07 | 0.14 | 0.18 | 0.09 | 0.00 | 0.01 | 0.13 | 30.20 | 81.83 |
| NWA 7892 | rim | 12.57 | 0.02 | 1.41 | 0.28 | 26.97 | 0.15 | 0.57 | 8.01 | 0.72 | 0.05 | 0.14 | 0.20 | 0.08 | 0.00 | 0.00 | 0.11 | 29.70 | 80.98 |
| NWA 7892 | rim | 12.51 | 0.05 | 1.63 | 0.24 | 25.50 | 0.14 | 0.61 | 8.42 | 0.77 | 0.05 | 0.14 | 0.16 | 0.08 | 0.01 | 0.01 | 0.14 | 29.70 | 80.16 |
| NWA 7892 | rim | 13.19 | 0.02 | 1.57 | 0.24 | 24.11 | 0.15 | 0.64 | 9.00 | 0.78 | 0.05 | 0.15 | 0.17 | 0.08 | 0.01 | 0.00 | 0.13 | 30.39 | 80.68 |
| NWA 7892 | rim | 13.13 | 0.03 | 1.64 | 0.24 | 25.91 | 0.14 | 0.63 | 8.98 | 0.81 | 0.06 | 0.16 | 0.16 | 0.07 | 0.00 | 0.02 | 0.14 | 30.92 | 83.04 |
| NWA 7892 | rim | 12.70 | 0.05 | 1.62 | 0.23 | 25.40 | 0.15 | 0.68 | 8.38 | 0.79 | 0.06 | 0.13 | 0.17 | 0.08 | 0.00 | 0.02 | 0.14 | 29.88 | 80.48 |
| NWA 7892 | rim | 12.35 | 0.02 | 1.35 | 0.25 | 23.25 | 0.21 | 0.52 | 8.52 | 0.72 | 0.04 | 0.12 | 0.17 | 0.07 | 0.01 | 0.01 | 0.11 | 28.61 | 76.33 |
| NWA 7892 | rim | 12.88 | 0.05 | 1.71 | 0.22 | 22.97 | 0.14 | 0.67 | 8.31 | 0.80 | 0.06 | 0.17 | 0.14 | 0.08 | 0.00 | 0.00 | 0.11 | 29.34 | 77.65 |
| NWA 7892 | rim | 13.86 | 0.02 | 1.41 | 0.23 | 25.10 | 0.24 | 0.53 | 8.61 | 0.70 | 0.06 | 0.15 | 0.14 | 0.05 | 0.01 | 0.00 | 0.09 | 30.90 | 82.10 |

Continued on next page

| Sample | Area | Si | Ti | Al | Cr | Fe | Mn | Ni | Mg | Ca | Na | K | P | Co | V | Zn | S | O | Total |
|---|---|---|---|---|---|---|---|---|---|---|---|---|---|---|---|---|---|---|---|
| NWA 7892 | rim | 12.55 | 0.04 | 1.38 | 0.17 | 29.15 | 0.18 | 0.54 | 7.99 | 0.68 | 0.09 | 0.13 | 0.11 | 0.07 | 0.01 | 0.00 | 0.10 | 30.09 | 83.28 |
| NWA 7892 | rim | 12.63 | 0.06 | 1.58 | 0.26 | 26.96 | 0.16 | 0.61 | 8.65 | 0.73 | 0.09 | 0.14 | 0.16 | 0.10 | 0.01 | 0.02 | 0.13 | 30.38 | 82.67 |
| NWA 7892 | rim | 11.32 | 0.03 | 1.48 | 0.22 | 30.68 | 0.19 | 0.55 | 6.06 | 0.66 | 0.08 | 0.12 | 0.14 | 0.07 | 0.00 | 0.02 | 0.11 | 28.01 | 79.74 |
| NWA 7892 | rim | 12.41 | 0.04 | 1.72 | 0.23 | 24.87 | 0.14 | 0.68 | 7.88 | 0.80 | 0.08 | 0.16 | 0.18 | 0.08 | 0.01 | 0.02 | 0.12 | 29.17 | 78.59 |
| NWA 7892 | rim | 12.88 | 0.01 | 1.45 | 0.25 | 27.11 | 0.17 | 0.60 | 9.11 | 0.69 | 0.08 | 0.13 | 0.15 | 0.09 | 0.00 | 0.00 | 0.12 | 30.79 | 83.63 |
| NWA 7892 | rim | 12.76 | 0.04 | 1.40 | 0.24 | 27.47 | 0.16 | 0.60 | 9.31 | 0.70 | 0.05 | 0.10 | 0.17 | 0.09 | 0.01 | 0.00 | 0.11 | 30.87 | 84.08 |
| NWA 7892 | rim | 14.57 | 0.07 | 1.28 | 0.27 | 21.81 | 0.18 | 0.51 | 11.23 | 0.77 | 0.07 | 0.13 | 0.14 | 0.09 | 0.01 | 0.00 | 0.08 | 32.44 | 83.65 |
| NWA 7892 | rim | 11.59 | 0.03 | 1.44 | 0.23 | 27.97 | 0.15 | 0.56 | 8.00 | 0.65 | 0.06 | 0.13 | 0.14 | 0.10 | 0.01 | 0.01 | 0.12 | 28.79 | 79.98 |
| NWA 7892 | rim | 12.50 | 0.00 | 0.20 | 0.29 | 40.47 | 0.41 | 0.19 | 4.77 | 0.21 | 0.07 | 0.01 | 0.24 | 0.07 | 0.00 | 0.00 | 0.06 | 29.99 | 89.48 |
| NWA 7892 | rim | 12.20 | 0.00 | 0.23 | 0.35 | 39.82 | 0.40 | 0.19 | 4.42 | 0.22 | 0.10 | 0.01 | 0.24 | 0.07 | 0.00 | 0.01 | 0.05 | 29.28 | 87.59 |
| NWA 7892 | rim | 12.86 | 0.00 | 0.21 | 0.27 | 41.26 | 0.42 | 0.21 | 4.95 | 0.28 | 0.11 | 0.02 | 0.26 | 0.07 | 0.00 | 0.00 | 0.04 | 30.79 | 91.75 |
| NWA 7892 | rim | 12.17 | 0.02 | 0.35 | 0.33 | 40.70 | 0.38 | 0.27 | 4.57 | 0.28 | 0.12 | 0.04 | 0.25 | 0.07 | 0.00 | 0.00 | 0.08 | 29.83 | 89.46 |
| NWA 7892 | rim | 11.76 | 0.02 | 0.20 | 0.42 | 38.63 | 0.36 | 0.22 | 4.46 | 0.23 | 0.14 | 0.02 | 0.24 | 0.09 | 0.01 | 0.00 | 0.07 | 28.53 | 85.40 |

| Sample | Area | Si | Ti | Al | Cr | Fe | Mn | Ni | Mg | Ca | Na | K | P | Co | V | Zn | S | O | Total |
|---|---|---|---|---|---|---|---|---|---|---|---|---|---|---|---|---|---|---|---|
| MIL090010 | 1a | 12.10 | 0.05 | 1.48 | 0.21 | 31.57 | 0.22 | 2.82 | 6.51 | 0.41 | 0.24 | 0.22 | 0.18 | 0.17 | 0.00 | 0.00 | 0.30 | 30.42 | 86.90 |
| MIL090010 | 1a | 12.23 | 0.00 | 1.04 | 0.22 | 31.80 | 0.19 | 2.17 | 7.82 | 0.31 | 0.23 | 0.08 | 0.17 | 0.12 | 0.00 | 0.00 | 0.27 | 30.75 | 87.40 |
| MIL090010 | 1a | 12.65 | 0.03 | 1.17 | 0.20 | 30.35 | 0.22 | 2.16 | 8.43 | 0.44 | 0.24 | 0.14 | 0.22 | 0.13 | 0.00 | 0.01 | 0.29 | 31.52 | 88.20 |
| MIL090010 | 1a | 12.29 | 0.02 | 1.21 | 0.21 | 30.71 | 0.22 | 2.48 | 7.60 | 0.51 | 0.20 | 0.11 | 0.17 | 0.14 | 0.01 | 0.00 | 0.34 | 30.81 | 87.03 |
| MIL090010 | 1a | 10.32 | 0.04 | 1.04 | 0.30 | 34.39 | 0.16 | 2.22 | 6.34 | 0.37 | 0.21 | 0.09 | 0.14 | 0.14 | 0.01 | 0.00 | 0.30 | 28.43 | 84.50 |
| MIL090010 | 1a | 11.84 | 0.03 | 1.83 | 0.17 | 28.76 | 0.17 | 2.30 | 6.55 | 1.57 | 0.22 | 0.19 | 0.33 | 0.14 | 0.01 | 0.02 | 0.31 | 30.12 | 84.56 |
| MIL090010 | 1a | 13.31 | 0.17 | 2.98 | 0.19 | 24.17 | 0.14 | 2.49 | 8.13 | 2.31 | 0.24 | 0.32 | 0.31 | 0.14 | 0.02 | 0.03 | 0.29 | 32.97 | 88.21 |
| MIL090010 | 1a | 11.80 | 0.02 | 1.20 | 0.24 | 29.76 | 0.19 | 2.31 | 6.70 | 0.49 | 0.21 | 0.16 | 0.28 | 0.14 | 0.00 | 0.01 | 0.28 | 29.40 | 83.19 |
| MIL090010 | 1a | 12.11 | 0.02 | 1.31 | 0.19 | 29.93 | 0.17 | 2.56 | 7.44 | 0.74 | 0.24 | 0.22 | 0.09 | 0.16 | 0.00 | 0.00 | 0.25 | 30.24 | 85.67 |
| MIL090010 | 1a | 12.75 | 0.04 | 1.21 | 0.25 | 28.04 | 0.23 | 2.73 | 8.28 | 0.46 | 0.20 | 0.08 | 0.15 | 0.17 | 0.00 | 0.01 | 0.31 | 31.02 | 85.93 |
| MIL090010 | 1a | 10.21 | 0.04 | 0.86 | 0.21 | 36.21 | 0.23 | 1.83 | 6.14 | 0.55 | 0.15 | 0.05 | 0.15 | 0.14 | 0.00 | 0.00 | 0.36 | 28.56 | 85.69 |
| MIL090010 | 1a | 10.96 | 0.04 | 1.11 | 0.18 | 33.40 | 0.21 | 2.38 | 6.97 | 0.39 | 0.17 | 0.13 | 0.17 | 0.14 | 0.01 | 0.01 | 0.37 | 29.51 | 86.15 |
| MIL090010 | 1a | 11.50 | 0.06 | 1.34 | 0.18 | 32.37 | 0.20 | 2.30 | 7.09 | 0.65 | 0.18 | 0.16 | 0.23 | 0.14 | 0.01 | 0.01 | 0.35 | 30.27 | 87.04 |
| MIL090010 | 1a | 12.62 | 0.05 | 1.03 | 0.22 | 29.48 | 0.21 | 2.11 | 7.95 | 0.45 | 0.18 | 0.07 | 0.16 | 0.14 | 0.01 | 0.00 | 0.32 | 30.72 | 85.72 |
| MIL090010 | 1a | 12.44 | 0.02 | 1.06 | 0.22 | 28.36 | 0.20 | 2.58 | 8.30 | 0.38 | 0.16 | 0.06 | 0.17 | 0.14 | 0.00 | 0.01 | 0.34 | 30.57 | 85.01 |
| MIL090010 | 1a | 10.47 | 0.04 | 1.13 | 0.16 | 32.87 | 0.17 | 2.73 | 6.25 | 0.40 | 0.20 | 0.10 | 0.14 | 0.16 | 0.00 | 0.00 | 0.31 | 28.30 | 83.43 |
| MIL090010 | 1a | 9.58 | 0.00 | 0.95 | 0.15 | 35.44 | 0.17 | 1.86 | 6.59 | 0.93 | 0.20 | 0.09 | 0.24 | 0.11 | 0.01 | 0.00 | 0.42 | 28.31 | 85.05 |
| MIL090010 | 1a | 12.70 | 0.03 | 0.98 | 0.22 | 28.98 | 0.17 | 2.32 | 9.06 | 1.07 | 0.17 | 0.08 | 0.34 | 0.13 | 0.01 | 0.00 | 0.32 | 31.88 | 88.46 |
| MIL090010 | 1a | 12.06 | 0.05 | 0.89 | 0.21 | 29.08 | 0.25 | 2.13 | 8.17 | 1.30 | 0.17 | 0.06 | 0.56 | 0.12 | 0.00 | 0.01 | 0.32 | 30.85 | 86.23 |
| MIL090010 | 1a | 10.96 | 0.02 | 1.14 | 0.15 | 30.90 | 0.16 | 2.04 | 5.51 | 2.58 | 0.17 | 0.13 | 0.23 | 0.12 | 0.01 | 0.01 | 0.38 | 28.67 | 83.18 |
| MIL090010 | 1a | 12.59 | 0.03 | 1.60 | 0.25 | 27.43 | 0.19 | 2.95 | 7.82 | 1.14 | 0.18 | 0.27 | 0.14 | 0.17 | 0.00 | 0.00 | 0.63 | 31.51 | 86.90 |
| MIL090010 | 1a | 11.53 | 0.02 | 0.69 | 0.25 | 29.00 | 0.14 | 2.15 | 8.94 | 0.57 | 0.12 | 0.02 | 0.12 | 0.12 | 0.00 | 0.01 | 1.86 | 31.95 | 87.49 |
| MIL090010 | 1a | 12.67 | 0.05 | 0.73 | 0.26 | 27.17 | 0.17 | 1.88 | 9.85 | 0.74 | 0.13 | 0.02 | 0.14 | 0.10 | 0.00 | 0.02 | 0.32 | 31.09 | 85.34 |
| MIL090010 | 1a | 13.06 | 0.00 | 0.74 | 0.28 | 27.60 | 0.20 | 1.76 | 10.04 | 0.63 | 0.11 | 0.01 | 0.12 | 0.09 | 0.00 | 0.02 | 0.30 | 31.65 | 86.61 |
| MIL090010 | 1a | 12.30 | 0.01 | 0.91 | 0.27 | 27.88 | 0.15 | 2.71 | 9.66 | 1.05 | 0.15 | 0.01 | 0.15 | 0.12 | 0.01 | 0.02 | 0.60 | 31.68 | 87.68 |
| MIL090010 | 1a | 12.98 | 0.03 | 0.70 | 0.21 | 31.55 | 0.18 | 1.53 | 10.61 | 1.00 | 0.15 | 0.03 | 0.10 | 0.11 | 0.00 | 0.00 | 5.26 | 40.51 | 104.95 |
| MIL090010 | 1a | 16.95 | 0.01 | 0.47 | 0.12 | 13.31 | 0.07 | 1.03 | 24.70 | 0.09 | 0.07 | 0.06 | 0.05 | 0.05 | 0.00 | 0.00 | 0.10 | 40.46 | 97.54 |
| MIL090010 | 1a | 10.44 | 0.03 | 1.23 | 0.20 | 32.34 | 0.15 | 2.15 | 8.21 | 0.68 | 0.22 | 0.14 | 0.36 | 0.13 | 0.01 | 0.00 | 0.37 | 29.84 | 86.50 |
| MIL090010 | 1a | 10.56 | 0.02 | 1.26 | 0.18 | 31.77 | 0.17 | 2.67 | 6.51 | 0.74 | 0.20 | 0.14 | 0.14 | 0.14 | -0.01 | 0.00 | 0.30 | 28.46 | 83.25 |
| MIL090010 | 1a | 10.81 | 0.01 | 1.27 | 0.18 | 33.60 | 0.18 | 2.63 | 6.40 | 0.67 | 0.24 | 0.12 | 0.16 | 0.15 | 0.01 | 0.00 | 0.28 | 29.18 | 85.89 |
| MIL090010 | 1a | 12.76 | 0.01 | 1.11 | 0.28 | 25.86 | 0.17 | 2.87 | 9.66 | 0.79 | 0.16 | 0.08 | 0.13 | 0.16 | 0.00 | 0.00 | 0.26 | 31.25 | 85.55 |
| MIL090010 | 1a | 11.57 | 0.03 | 1.12 | 0.16 | 29.65 | 0.17 | 3.06 | 7.62 | 0.45 | 0.19 | 0.10 | 0.15 | 0.13 | 0.00 | 0.00 | 0.29 | 29.60 | 84.29 |
| MIL090010 | 1a | 11.66 | 0.01 | 1.11 | 0.18 | 30.95 | 0.18 | 2.46 | 8.04 | 0.47 | 0.20 | 0.10 | 0.18 | 0.11 | 0.00 | 0.01 | 0.31 | 30.25 | 86.22 |
| MIL090010 | 1a | 10.67 | 0.03 | 1.12 | 0.23 | 31.53 | 0.12 | 2.03 | 7.50 | 2.04 | 0.18 | 0.10 | 0.13 | 0.13 | 0.01 | 0.00 | 0.61 | 29.85 | 86.28 |
| MIL090010 | 1a | 9.31 | 0.02 | 1.23 | 0.16 | 34.02 | 0.09 | 2.14 | 5.94 | 2.25 | 0.17 | 0.14 | 0.18 | 0.13 | 0.01 | 0.00 | 0.35 | 27.82 | 83.96 |
| MIL090010 | 1a | 12.60 | 0.03 | 1.70 | 0.18 | 25.20 | 0.08 | 2.59 | 8.37 | 3.33 | 0.16 | 0.13 | 0.17 | 0.13 | 0.00 | 0.01 | 0.35 | 31.63 | 86.66 |
| MIL090010 | 2a | 13.33 | 0.04 | 0.76 | 0.10 | 29.76 | 0.20 | 2.06 | 11.39 | 0.48 | 0.41 | 0.04 | 0.06 | 0.12 | 0.00 | 0.01 | 0.44 | 33.70 | 92.90 |
| MIL090010 | 2a | 6.07 | 0.01 | 0.47 | 0.24 | 32.55 | 0.11 | 6.84 | 5.69 | 0.26 | 0.32 | 0.03 | 0.02 | 0.42 | 0.00 | 0.00 | 1.49 | 25.01 | 79.53 |
| MIL090010 | 2a | 10.31 | 0.04 | 0.46 | 0.21 | 33.00 | 0.18 | 2.99 | 8.62 | 0.38 | 0.27 | 0.03 | 0.01 | 0.19 | 0.01 | 0.00 | 0.91 | 29.96 | 87.57 |
| MIL090010 | 2a | 10.64 | 0.03 | 0.86 | 0.09 | 32.72 | 0.16 | 2.19 | 8.27 | 0.32 | 0.57 | 0.06 | 0.04 | 0.16 | 0.00 | 0.00 | 2.75 | 32.96 | 91.82 |

Continued on next page

| Sample | Area | Si | Ti | Al | Cr | Fe | Mn | Ni | Mg | Ca | Na | K | P | Co | V | Zn | S | O | Total |
|---|---|---|---|---|---|---|---|---|---|---|---|---|---|---|---|---|---|---|---|
| MIL090010 | 2a | 10.64 | 0.03 | 0.92 | 0.20 | 31.91 | 0.14 | 2.27 | 8.48 | 0.27 | 0.15 | 0.01 | 0.09 | 0.11 | 0.00 | 0.01 | 1.10 | 30.40 | 86.73 |
| MIL090010 | 2a | 11.42 | 0.03 | 1.34 | 0.17 | 28.19 | 0.11 | 2.89 | 6.99 | 2.49 | 0.17 | 0.02 | 0.10 | 0.18 | 0.01 | 0.01 | 0.94 | 30.45 | 85.51 |
| MIL090010 | 2a | 11.12 | 0.03 | 1.35 | 0.16 | 32.57 | 0.19 | 2.49 | 6.52 | 0.28 | 0.23 | 0.02 | 0.08 | 0.16 | 0.00 | 0.00 | 0.60 | 29.56 | 85.36 |
| MIL090010 | 2a | 12.24 | 0.05 | 1.41 | 0.18 | 29.40 | 0.15 | 1.73 | 7.73 | 1.37 | 0.35 | 0.06 | 0.09 | 0.14 | 0.00 | 0.02 | 0.62 | 31.11 | 86.65 |
| MIL090010 | 2a | 10.15 | 0.03 | 1.47 | 0.11 | 32.42 | 0.16 | 3.00 | 5.43 | 0.35 | 0.21 | 0.09 | 0.07 | 0.16 | 0.00 | 0.01 | 0.83 | 28.28 | 82.77 |
| MIL090010 | 2a | 9.80 | 0.00 | 0.59 | 0.11 | 35.01 | 0.12 | 1.83 | 4.01 | 2.43 | 0.13 | 0.02 | 0.07 | 0.12 | 0.01 | 0.00 | 2.75 | 30.21 | 87.21 |
| MIL090010 | 2a | 11.41 | 0.02 | 0.71 | 0.21 | 27.56 | 0.15 | 2.45 | 5.05 | 2.97 | 0.12 | 0.01 | 0.11 | 0.12 | 0.01 | 0.00 | 0.74 | 28.19 | 79.83 |
| MIL090010 | 2a | 10.64 | 0.04 | 0.92 | 0.20 | 30.00 | 0.12 | 2.34 | 5.40 | 2.94 | 0.19 | 0.01 | 0.12 | 0.15 | 0.01 | 0.00 | 1.01 | 28.83 | 82.92 |
| MIL090010 | 2a | 9.20 | 0.03 | 1.00 | 0.17 | 30.23 | 0.15 | 2.20 | 5.68 | 0.22 | 0.21 | 0.01 | 0.10 | 0.12 | 0.00 | 0.02 | 0.63 | 25.79 | 75.76 |
| MIL090010 | 2a | 10.06 | 0.04 | 1.19 | 0.17 | 33.50 | 0.16 | 2.14 | 6.68 | 0.35 | 0.13 | 0.02 | 0.09 | 0.11 | 0.00 | 0.02 | 0.72 | 28.66 | 84.04 |
| MIL090010 | 2a | 12.10 | 0.06 | 1.15 | 0.21 | 27.61 | 0.15 | 2.03 | 8.83 | 0.76 | 0.12 | 0.00 | 0.09 | 0.14 | 0.01 | 0.00 | 0.52 | 30.55 | 84.33 |
| MIL090010 | 2a | 14.57 | 0.08 | 2.04 | 0.20 | 27.43 | 0.19 | 0.95 | 8.59 | 0.48 | 0.43 | 0.21 | 0.08 | 0.08 | 0.00 | 0.00 | 0.23 | 33.24 | 88.80 |
| MIL090010 | 2a | 17.25 | 0.03 | 0.82 | 0.22 | 15.51 | 0.10 | 0.46 | 24.17 | 0.43 | 0.04 | 0.03 | 0.03 | 0.03 | 0.02 | 0.04 | 0.49 | 42.01 | 101.68 |
| MIL090010 | 2a | 12.23 | 0.01 | 1.44 | 0.24 | 33.39 | 0.20 | 0.80 | 7.14 | 0.26 | 0.26 | 0.08 | 0.08 | 0.10 | 0.00 | 0.00 | 0.42 | 30.84 | 87.49 |
| MIL090010 | 2a | 10.47 | 0.02 | 1.37 | 0.15 | 35.01 | 0.17 | 1.62 | 6.14 | 0.38 | 0.20 | 0.03 | 0.08 | 0.14 | 0.01 | 0.00 | 0.46 | 28.86 | 85.11 |
| MIL090010 | 2a | 14.10 | 0.03 | 0.54 | 0.12 | 28.86 | 0.15 | 1.02 | 4.26 | 5.61 | 0.13 | 0.01 | 0.10 | 0.11 | 0.00 | 0.00 | 0.40 | 31.05 | 86.49 |
| MIL090010 | 2a | 14.73 | 0.00 | 0.56 | 0.15 | 26.08 | 0.23 | 0.55 | 14.88 | 0.28 | 0.10 | 0.02 | 0.04 | 0.07 | 0.00 | 0.01 | 0.15 | 35.27 | 93.12 |
| MIL090010 | 2a | 10.48 | 0.02 | 0.98 | 0.17 | 35.43 | 0.16 | 1.08 | 6.64 | 0.24 | 0.10 | 0.00 | 0.09 | 0.10 | 0.00 | 0.03 | 0.56 | 28.88 | 84.96 |
| MIL090010 | 2a | 10.96 | 0.02 | 0.98 | 0.20 | 33.07 | 0.15 | 1.25 | 7.20 | 1.34 | 0.12 | 0.01 | 0.10 | 0.13 | 0.01 | 0.00 | 0.57 | 29.67 | 85.78 |
| MIL090010 | 2a | 10.09 | 0.01 | 1.10 | 0.17 | 36.64 | 0.15 | 1.72 | 6.10 | 1.19 | 0.14 | 0.02 | 0.10 | 0.19 | 0.00 | 0.01 | 1.18 | 30.06 | 88.87 |
| MIL090010 | 2a | 23.21 | 0.09 | 0.93 | 0.52 | 6.91 | 0.15 | 0.69 | 17.77 | 2.45 | 0.18 | 0.04 | 0.09 | 0.04 | 0.01 | 0.01 | 0.19 | 42.95 | 96.23 |
| MIL090010 | 2a | 13.05 | 0.06 | 2.04 | 0.28 | 25.17 | 0.37 | 2.26 | 8.35 | 1.53 | 0.22 | 0.08 | 0.07 | 0.09 | 0.01 | 0.01 | 1.13 | 32.82 | 87.54 |
| MIL090010 | 2a | 11.66 | 0.11 | 1.52 | 0.25 | 30.23 | 0.43 | 1.90 | 7.97 | 1.08 | 0.13 | 0.04 | 0.07 | 0.09 | 0.01 | 0.00 | 1.83 | 32.72 | 90.04 |
| MIL090010 | 2a | 13.58 | 0.05 | 1.43 | 0.22 | 25.28 | 0.23 | 2.14 | 7.90 | 3.04 | 0.17 | 0.04 | 0.13 | 0.12 | 0.01 | 0.00 | 0.71 | 32.53 | 87.58 |
| MIL090010 | 2a | 13.25 | 0.03 | 1.01 | 0.18 | 25.03 | 0.10 | 1.99 | 7.11 | 4.39 | 0.15 | 0.02 | 0.14 | 0.12 | 0.00 | 0.00 | 0.56 | 31.38 | 85.46 |
| MIL090010 | 2a | 11.03 | 0.07 | 1.09 | 0.16 | 31.77 | 0.22 | 2.03 | 7.01 | 0.43 | 0.14 | 0.02 | 0.08 | 0.11 | 0.00 | 0.00 | 0.51 | 29.11 | 83.78 |
| MIL090010 | 2a | 17.92 | 0.02 | 0.22 | 0.07 | 7.91 | 0.03 | 0.39 | 29.74 | 0.13 | 0.01 | 0.00 | 0.01 | 0.03 | 0.00 | 0.00 | 0.14 | 42.90 | 99.52 |
| MIL090010 | 2a | 13.91 | 0.04 | 0.57 | 0.14 | 22.44 | 0.08 | 1.13 | 19.24 | 0.20 | 0.05 | 0.01 | 0.05 | 0.09 | 0.00 | 0.01 | 0.47 | 36.77 | 95.20 |
| MIL090010 | 2a | 17.95 | 0.19 | 3.25 | 0.06 | 9.59 | 0.04 | 0.46 | 21.88 | 4.12 | 0.04 | 0.00 | 0.05 | 0.04 | 0.00 | 0.00 | 0.20 | 42.81 | 100.68 |
| MIL090010 | 2a | 11.69 | 0.03 | 1.17 | 0.21 | 31.12 | 0.15 | 2.19 | 9.22 | 0.29 | 0.17 | 0.02 | 0.09 | 0.17 | 0.01 | 0.00 | 0.52 | 31.21 | 88.26 |
| MIL090010 | 2a | 18.51 | 0.13 | 2.95 | 0.06 | 5.58 | 0.02 | 0.46 | 25.09 | 2.95 | 0.03 | 0.00 | 0.03 | 0.02 | 0.01 | 0.01 | 0.12 | 43.50 | 99.47 |
| MIL090010 | 2a | 11.41 | 0.03 | 0.80 | 0.20 | 25.86 | 0.13 | 1.92 | 12.92 | 0.22 | 0.10 | 0.00 | 0.05 | 0.10 | 0.02 | 0.00 | 0.81 | 31.73 | 86.30 |
| MIL090010 | 2a | 15.17 | 0.06 | 1.32 | 0.07 | 11.71 | 0.03 | 0.71 | 22.09 | 1.12 | 0.04 | 0.00 | 0.03 | 0.06 | 0.01 | 0.01 | 0.26 | 37.54 | 90.23 |
| MIL090010 | 2a | 20.02 | 0.09 | 4.06 | 0.04 | 0.79 | 0.01 | 0.03 | 27.60 | 3.39 | 0.04 | 0.00 | 0.04 | 0.00 | 0.01 | 0.00 | 0.01 | 46.34 | 102.47 |

| Sample | Area | Si | Ti | Al | Cr | Fe | Mn | Ni | Mg | Ca | Na | K | P | Co | V | Zn | S | O | Total |
|---|---|---|---|---|---|---|---|---|---|---|---|---|---|---|---|---|---|---|---|
| Kainsaz | 1a | 17.02 | 0.09 | 3.95 | 0.23 | 18.60 | 0.17 | 1.06 | 9.33 | 4.38 | 2.48 | 0.15 | 0.11 | 0.02 | 0.00 | 0.02 | 0.09 | 37.81 | 95.50 |
| Kainsaz | 1a | 26.90 | 0.33 | 1.45 | 0.62 | 0.93 | 0.15 | 0.01 | 20.09 | 4.60 | 0.05 | 0.00 | 0.00 | 0.01 | 0.02 | 0.00 | 0.01 | 47.88 | 103.05 |
| Kainsaz | 1a | 15.89 | 0.04 | 1.28 | 0.25 | 30.11 | 0.35 | 0.51 | 11.15 | 0.45 | 0.75 | 0.12 | 0.12 | 0.00 | 0.00 | 0.00 | 0.09 | 36.34 | 97.44 |
| Kainsaz | 1a | 15.54 | 0.05 | 1.24 | 0.22 | 30.47 | 0.33 | 1.00 | 10.75 | 0.47 | 0.83 | 0.14 | 0.13 | 0.01 | 0.01 | 0.01 | 0.08 | 35.94 | 97.22 |
| Kainsaz | 1a | 15.72 | 0.04 | 1.30 | 0.27 | 29.73 | 0.38 | 0.54 | 10.61 | 0.47 | 0.81 | 0.16 | 0.10 | 0.01 | 0.01 | 0.00 | 0.07 | 35.73 | 95.95 |
| Kainsaz | 1a | 15.78 | 0.04 | 1.39 | 0.24 | 30.09 | 0.37 | 0.11 | 10.59 | 0.38 | 0.94 | 0.18 | 0.14 | 0.00 | 0.01 | 0.00 | 0.09 | 35.92 | 96.28 |
| Kainsaz | 1a | 15.24 | 0.04 | 1.28 | 0.22 | 31.72 | 0.38 | 1.09 | 10.05 | 0.40 | 0.62 | 0.11 | 0.12 | 0.02 | 0.00 | 0.03 | 0.10 | 35.44 | 96.84 |
| Kainsaz | 1a | 15.16 | 0.03 | 1.05 | 0.20 | 31.89 | 0.36 | 0.85 | 10.11 | 0.45 | 0.51 | 0.09 | 0.10 | 0.01 | 0.01 | 0.01 | 0.11 | 35.13 | 96.09 |
| Kainsaz | 1a | 14.99 | 0.04 | 1.27 | 0.23 | 31.51 | 0.36 | 1.52 | 10.12 | 0.39 | 0.73 | 0.15 | 0.11 | 0.02 | 0.00 | 0.01 | 0.07 | 35.24 | 96.75 |
| Kainsaz | 1a | 15.05 | 0.03 | 1.40 | 0.24 | 33.19 | 0.34 | 1.11 | 10.46 | 0.42 | 0.70 | 0.16 | 0.12 | 0.07 | 0.01 | 0.02 | 0.07 | 36.06 | 99.44 |
| Kainsaz | 1a | 14.75 | 0.04 | 1.26 | 0.30 | 33.18 | 0.33 | 0.74 | 10.48 | 0.68 | 0.63 | 0.08 | 0.14 | 0.06 | 0.01 | 0.03 | 1.27 | 37.42 | 101.40 |
| Kainsaz | 1a | 15.61 | 0.10 | 1.69 | 0.24 | 30.54 | 0.35 | 0.43 | 10.28 | 0.58 | 0.93 | 0.15 | 0.10 | 0.01 | 0.00 | 0.03 | 0.06 | 36.02 | 97.12 |
| Kainsaz | 1a | 16.29 | 0.14 | 2.21 | 0.24 | 27.77 | 0.34 | 0.50 | 10.10 | 1.82 | 0.94 | 0.17 | 0.13 | 0.01 | 0.01 | 0.01 | 0.11 | 37.01 | 97.80 |
| Kainsaz | 1a | 17.02 | 0.07 | 2.14 | 0.62 | 25.79 | 0.61 | 0.31 | 9.29 | 3.04 | 1.37 | 0.15 | 0.15 | 0.01 | 0.00 | 0.01 | 0.93 | 38.70 | 100.22 |
| Kainsaz | 1a | 15.46 | 0.03 | 1.22 | 0.20 | 28.72 | 0.33 | 0.30 | 10.05 | 0.38 | 0.62 | 0.12 | 0.14 | 0.00 | 0.00 | 0.03 | 0.13 | 34.60 | 92.31 |
| Kainsaz | 1a | 14.22 | 0.03 | 1.10 | 0.20 | 35.83 | 0.29 | 0.45 | 9.92 | 0.35 | 0.48 | 0.09 | 0.13 | 0.12 | 0.00 | 0.02 | 0.06 | 34.92 | 98.21 |
| Kainsaz | 1a | 15.53 | 0.04 | 0.98 | 0.25 | 28.79 | 0.35 | 0.45 | 10.90 | 0.78 | 0.49 | 0.07 | 0.12 | 0.00 | 0.01 | 0.01 | 0.07 | 35.12 | 93.96 |
| Kainsaz | 1a | 15.54 | 0.04 | 1.32 | 0.18 | 29.26 | 0.32 | 0.24 | 10.42 | 0.42 | 0.60 | 0.11 | 0.11 | 0.00 | 0.01 | 0.01 | 0.09 | 35.06 | 93.74 |
| Kainsaz | 1a | 14.56 | 0.03 | 1.24 | 0.20 | 31.28 | 0.33 | 2.23 | 10.35 | 0.38 | 0.57 | 0.10 | 0.11 | 0.02 | 0.01 | 0.02 | 0.08 | 34.92 | 96.42 |

Continued on next page

| Sample | Area | Si | Ti | Al | Cr | Fe | Mn | Ni | Mg | Ca | Na | K | P | Co | V | Zn | S | O | Total |
|---|---|---|---|---|---|---|---|---|---|---|---|---|---|---|---|---|---|---|---|
| Kainsaz | 1a | 13.92 | 0.03 | 1.08 | 0.23 | 32.08 | 0.32 | 3.53 | 9.86 | 0.34 | 0.50 | 0.10 | 0.10 | 0.04 | 0.01 | 0.00 | 0.06 | 34.24 | 96.45 |
| Kainsaz | 1a | 15.52 | 0.04 | 1.29 | 0.23 | 30.48 | 0.34 | 0.34 | 10.61 | 0.41 | 0.67 | 0.08 | 0.13 | 0.00 | 0.00 | 0.01 | 0.09 | 35.60 | 95.85 |
| Kainsaz | 1a | 17.61 | 0.05 | 1.06 | 0.28 | 26.91 | 0.30 | 0.46 | 13.19 | 0.79 | 0.40 | 0.08 | 0.10 | 0.01 | 0.01 | 0.02 | 0.08 | 38.52 | 99.88 |
| Kainsaz | 1a | 15.04 | 0.03 | 1.25 | 0.26 | 32.10 | 0.33 | 3.78 | 10.75 | 0.39 | 0.63 | 0.14 | 0.11 | 0.03 | 0.01 | 0.00 | 0.07 | 36.46 | 101.37 |
| Kainsaz | 1a | 15.55 | 0.04 | 1.02 | 0.26 | 30.81 | 0.39 | 1.79 | 11.06 | 0.40 | 0.51 | 0.10 | 0.09 | 0.01 | 0.00 | 0.00 | 0.07 | 36.06 | 98.16 |
| Kainsaz | 1a | 15.54 | 0.04 | 1.16 | 0.27 | 31.51 | 0.36 | 1.06 | 10.76 | 0.45 | 0.54 | 0.07 | 0.12 | 0.00 | 0.00 | 0.01 | 0.12 | 36.10 | 98.11 |
| Kainsaz | 1a | 14.12 | 0.04 | 1.35 | 0.28 | 30.34 | 0.33 | 2.40 | 9.91 | 0.47 | 0.63 | 0.13 | 0.13 | 0.02 | 0.01 | 0.02 | 0.09 | 34.17 | 94.46 |
| Kainsaz | 1a | 15.39 | 0.04 | 1.10 | 0.26 | 28.61 | 0.35 | 0.86 | 10.87 | 0.48 | 0.54 | 0.12 | 0.14 | 0.01 | 0.00 | 0.03 | 0.10 | 35.09 | 93.99 |
| Kainsaz | 1a | 16.47 | 0.05 | 1.11 | 0.29 | 26.58 | 0.35 | 0.52 | 12.33 | 0.87 | 0.56 | 0.09 | 0.13 | 0.00 | 0.01 | 0.03 | 0.09 | 36.77 | 96.25 |
| Kainsaz | 1a | 15.10 | 0.04 | 0.99 | 0.25 | 30.79 | 0.33 | 1.15 | 11.05 | 0.47 | 0.47 | 0.08 | 0.12 | 0.01 | 0.00 | 0.01 | 0.12 | 35.43 | 96.41 |
| Kainsaz | 1a | 18.55 | 0.04 | 1.49 | 0.30 | 24.91 | 0.30 | 0.23 | 14.32 | 1.35 | 0.56 | 0.06 | 0.15 | 0.02 | 0.01 | 0.01 | 0.12 | 40.47 | 102.89 |
| Kainsaz | 1a | 17.07 | 0.04 | 1.09 | 0.28 | 26.94 | 0.37 | 0.34 | 14.10 | 0.62 | 0.36 | 0.05 | 0.12 | 0.01 | 0.01 | 0.00 | 0.06 | 38.41 | 99.88 |
| Kainsaz | 1a | 16.01 | 0.05 | 1.14 | 0.23 | 29.82 | 0.33 | 0.21 | 11.79 | 0.45 | 0.49 | 0.08 | 0.12 | 0.01 | 0.01 | 0.02 | 0.09 | 36.53 | 97.41 |
| Kainsaz | 1a | 13.44 | 0.04 | 0.84 | 0.27 | 33.64 | 0.31 | 1.18 | 10.47 | 0.48 | 0.22 | 0.03 | 0.10 | 0.10 | 0.01 | 0.01 | 0.22 | 33.92 | 95.28 |
| Kainsaz | 1a | 15.37 | 0.04 | 1.02 | 0.28 | 30.58 | 0.35 | 0.25 | 11.50 | 0.47 | 0.27 | 0.04 | 0.12 | 0.01 | 0.01 | 0.02 | 0.10 | 35.68 | 96.11 |
| Kainsaz | 1a | 16.41 | 0.06 | 1.03 | 0.33 | 28.33 | 0.38 | 0.30 | 12.21 | 0.56 | 0.35 | 0.04 | 0.14 | 0.03 | 0.01 | 0.01 | 0.09 | 36.84 | 97.11 |
| Kainsaz | 1a | 18.97 | 0.03 | 0.41 | 0.21 | 23.98 | 0.34 | 0.06 | 14.79 | 2.53 | 0.17 | 0.02 | 0.06 | 0.00 | 0.00 | 0.00 | 0.04 | 40.01 | 101.61 |
| Kainsaz | 1a | 25.19 | 0.08 | 0.54 | 0.28 | 4.34 | 0.09 | 0.04 | 21.15 | 0.59 | 0.07 | 0.03 | 0.02 | 0.00 | 0.01 | 0.00 | 0.02 | 44.90 | 97.36 |
| Kainsaz | 1a | 20.94 | 0.07 | 0.52 | 0.50 | 12.67 | 0.29 | 0.19 | 21.68 | 0.63 | 0.09 | 0.02 | 0.03 | 0.01 | 0.01 | 0.01 | 0.05 | 43.05 | 100.75 |
| Kainsaz | 1a | 27.03 | 0.11 | 0.60 | 0.49 | 2.92 | 0.44 | 0.06 | 21.67 | 0.85 | 0.03 | 0.01 | 0.00 | 0.01 | 0.01 | 0.00 | 0.02 | 47.26 | 101.51 |
| Kainsaz | 1a | 19.73 | 0.09 | 6.38 | 0.33 | 22.73 | 0.18 | 0.88 | 12.48 | 2.96 | 3.02 | 0.53 | 0.01 | 0.18 | 0.01 | 0.02 | 0.04 | 45.87 | 115.44 |
| Kainsaz | 1a | 17.45 | 0.06 | 1.47 | 0.33 | 24.16 | 0.34 | 0.83 | 14.30 | 0.83 | 0.68 | 0.07 | 0.30 | 0.00 | 0.01 | 0.03 | 0.18 | 39.30 | 100.36 |
| Kainsaz | 1a | 16.60 | 0.05 | 1.00 | 0.29 | 26.03 | 0.30 | 0.65 | 13.69 | 0.55 | 0.44 | 0.05 | 0.12 | 0.00 | 0.01 | 0.03 | 0.08 | 37.38 | 97.27 |
| Kainsaz | 1a | 15.31 | 0.05 | 0.94 | 0.26 | 27.88 | 0.28 | 0.46 | 12.89 | 0.40 | 0.37 | 0.05 | 0.12 | 0.03 | 0.01 | 0.03 | 0.08 | 35.72 | 94.88 |
| Kainsaz | 1a | 15.10 | 0.05 | 1.05 | 0.29 | 32.23 | 0.36 | 0.91 | 11.59 | 0.83 | 0.58 | 0.06 | 0.19 | 0.08 | 0.01 | 0.00 | 0.10 | 36.50 | 99.94 |
| Kainsaz | 1a | 22.61 | 0.16 | 2.03 | 0.40 | 13.82 | 0.48 | 0.16 | 14.68 | 4.46 | 1.99 | 0.08 | 0.05 | 0.01 | 0.01 | 0.02 | 0.04 | 44.31 | 105.32 |
| Kainsaz | 1a | 15.90 | 0.04 | 1.62 | 0.17 | 31.41 | 0.34 | 0.36 | 10.35 | 0.61 | 1.23 | 0.22 | 0.10 | 0.00 | 0.00 | 0.00 | 0.06 | 36.62 | 99.05 |
| Kainsaz | 1a | 14.12 | 0.05 | 1.60 | 0.18 | 39.01 | 0.33 | 1.63 | 8.45 | 0.91 | 1.10 | 0.23 | 0.11 | 0.12 | 0.01 | 0.01 | 0.28 | 36.31 | 104.45 |
| Kainsaz | 1a | 16.17 | 0.05 | 1.08 | 0.27 | 30.59 | 0.36 | 0.46 | 11.13 | 0.51 | 0.59 | 0.11 | 0.11 | 0.02 | 0.00 | 0.00 | 0.10 | 36.59 | 98.13 |
| Kainsaz | 1a | 9.44 | 0.34 | 1.08 | 14.45 | 31.70 | 0.36 | 0.03 | 5.50 | 0.23 | 0.62 | 0.15 | 0.10 | 0.00 | 0.15 | 0.03 | 0.17 | 32.27 | 96.62 |
| Kainsaz | 1a | 15.03 | 0.05 | 1.25 | 0.27 | 32.41 | 0.34 | 2.82 | 10.44 | 0.62 | 0.51 | 0.11 | 0.10 | 0.03 | 0.01 | 0.01 | 0.10 | 36.18 | 100.29 |
| Kainsaz | 1a | 15.65 | 0.06 | 1.26 | 0.31 | 31.24 | 0.37 | 0.29 | 10.38 | 0.46 | 0.78 | 0.16 | 0.12 | 0.00 | 0.00 | 0.01 | 0.07 | 35.86 | 97.03 |
| Kainsaz | 1a | 15.88 | 0.05 | 1.06 | 0.24 | 28.23 | 0.31 | 0.33 | 12.23 | 0.37 | 0.43 | 0.06 | 0.10 | 0.00 | 0.00 | 0.01 | 0.12 | 36.12 | 95.55 |
| Kainsaz | 2a | 15.80 | 0.06 | 1.25 | 0.29 | 28.18 | 0.32 | 0.84 | 13.03 | 0.45 | 0.34 | 0.04 | 0.10 | 0.00 | 0.01 | 0.02 | 0.27 | 37.12 | 98.12 |
| Kainsaz | 2a | 15.73 | 0.04 | 1.07 | 0.26 | 28.38 | 0.28 | 0.19 | 12.76 | 0.36 | 0.35 | 0.05 | 0.14 | 0.01 | 0.01 | 0.02 | 0.09 | 36.28 | 96.01 |
| Kainsaz | 2a | 9.81 | 0.04 | 6.98 | 0.08 | 17.81 | 0.18 | 0.35 | 6.55 | 0.79 | 1.39 | 0.06 | 0.10 | 0.02 | 0.00 | 0.01 | 0.39 | 28.56 | 73.14 |
| Kainsaz | 2a | 16.39 | 0.10 | 2.02 | 0.08 | 24.98 | 0.27 | 0.13 | 10.35 | 1.84 | 1.70 | 0.01 | 0.28 | 0.01 | 0.01 | 0.00 | 0.06 | 36.45 | 94.68 |
| Kainsaz | 2a | 15.04 | 0.05 | 1.04 | 0.27 | 29.39 | 0.29 | 1.01 | 12.91 | 0.29 | 0.23 | 0.01 | 0.08 | 0.01 | 0.00 | 0.02 | 0.33 | 36.30 | 97.28 |
| Kainsaz | 2a | 15.80 | 0.05 | 1.06 | 0.42 | 28.40 | 0.32 | 0.14 | 13.70 | 0.43 | 0.19 | 0.01 | 0.11 | 0.00 | 0.01 | 0.04 | 0.25 | 37.24 | 98.17 |
| Kainsaz | 2a | 18.54 | 0.06 | 0.78 | 0.46 | 23.25 | 0.36 | 0.35 | 16.40 | 0.28 | 0.15 | 0.00 | 0.09 | 0.01 | 0.01 | 0.01 | 0.08 | 40.12 | 100.93 |
| Kainsaz | 2a | 15.34 | 0.05 | 1.07 | 0.26 | 29.28 | 0.31 | 0.19 | 12.23 | 0.33 | 0.41 | 0.06 | 0.13 | 0.01 | 0.01 | 0.03 | 0.10 | 35.79 | 95.61 |
| Kainsaz | 2a | 14.98 | 0.06 | 1.42 | 0.31 | 29.64 | 0.31 | 0.94 | 12.49 | 0.24 | 0.28 | 0.02 | 0.12 | 0.01 | 0.01 | 0.03 | 0.16 | 36.19 | 97.21 |
| Kainsaz | 2a | 13.98 | 0.05 | 1.35 | 0.29 | 31.15 | 0.31 | 1.52 | 11.17 | 0.34 | 0.25 | 0.04 | 0.11 | 0.02 | 0.00 | 0.04 | 0.08 | 34.58 | 95.28 |
| Kainsaz | 2a | 14.98 | 0.06 | 1.15 | 0.27 | 29.70 | 0.31 | 1.50 | 11.89 | 0.28 | 0.25 | 0.02 | 0.12 | 0.01 | 0.01 | 0.02 | 0.08 | 35.57 | 96.20 |
| Kainsaz | 2a | 12.55 | 0.04 | 1.16 | 0.35 | 33.17 | 0.27 | 0.98 | 9.95 | 0.28 | 0.28 | 0.03 | 0.13 | 0.01 | 0.00 | 0.01 | 2.40 | 35.90 | 97.50 |
| Kainsaz | 2a | 15.17 | 0.05 | 1.11 | 0.24 | 29.37 | 0.32 | 0.53 | 10.86 | 0.40 | 0.33 | 0.03 | 0.13 | 0.02 | 0.00 | 0.01 | 0.17 | 34.93 | 93.68 |
| Kainsaz | 2a | 15.55 | 0.05 | 1.18 | 0.23 | 27.37 | 0.31 | 0.47 | 11.05 | 0.37 | 0.45 | 0.08 | 0.12 | 0.01 | 0.01 | 0.03 | 0.09 | 34.87 | 92.24 |
| Kainsaz | 2a | 14.00 | 0.05 | 1.96 | 0.29 | 29.04 | 0.27 | 3.62 | 10.67 | 0.33 | 0.41 | 0.08 | 0.11 | 0.01 | 0.01 | 0.04 | 0.20 | 35.02 | 96.10 |
| Kainsaz | 2a | 15.12 | 0.04 | 1.34 | 0.21 | 28.25 | 0.32 | 0.36 | 10.33 | 0.33 | 0.58 | 0.09 | 0.14 | 0.01 | 0.00 | 0.01 | 0.08 | 34.28 | 91.48 |
| Kainsaz | 2a | 14.93 | 0.04 | 1.45 | 0.23 | 27.97 | 0.30 | 0.60 | 10.13 | 0.30 | 0.61 | 0.10 | 0.12 | 0.01 | 0.00 | 0.02 | 0.10 | 34.04 | 90.97 |
| Kainsaz | 2a | 15.33 | 0.04 | 1.34 | 0.22 | 28.91 | 0.32 | 0.42 | 10.50 | 0.38 | 0.50 | 0.11 | 0.15 | 0.01 | 0.01 | 0.00 | 0.10 | 34.89 | 93.22 |
| Kainsaz | 2a | 15.61 | 0.04 | 1.57 | 0.27 | 28.59 | 0.35 | 0.42 | 11.12 | 0.35 | 0.56 | 0.09 | 0.12 | 0.00 | 0.00 | 0.03 | 0.17 | 35.84 | 95.14 |
| Kainsaz | 2a | 15.61 | 0.04 | 1.35 | 0.24 | 27.46 | 0.28 | 0.20 | 11.12 | 0.35 | 0.47 | 0.09 | 0.12 | 0.00 | 0.00 | 0.03 | 0.12 | 35.13 | 92.63 |
| Kainsaz | 2a | 15.54 | 0.04 | 1.05 | 0.24 | 30.44 | 0.33 | 0.34 | 11.33 | 0.78 | 0.30 | 0.08 | 0.14 | 0.01 | 0.00 | 0.01 | 0.18 | 36.04 | 96.85 |
| Kainsaz | 2a | 14.17 | 0.03 | 1.56 | 0.28 | 31.25 | 0.32 | 1.40 | 10.56 | 0.26 | 0.51 | 0.06 | 0.10 | 0.01 | 0.00 | 0.02 | 0.26 | 34.88 | 95.68 |
| Kainsaz | 2a | 15.24 | 0.04 | 1.89 | 0.25 | 29.65 | 0.31 | 0.81 | 10.94 | 0.36 | 0.87 | 0.13 | 0.13 | 0.01 | 0.01 | 0.02 | 0.31 | 36.30 | 97.26 |
| Kainsaz | 2a | 15.78 | 0.04 | 1.92 | 0.30 | 28.45 | 0.32 | 0.37 | 11.75 | 0.32 | 0.62 | 0.10 | 0.12 | 0.00 | 0.00 | 0.03 | 0.11 | 36.63 | 96.87 |
| Kainsaz | 2a | 15.25 | 0.04 | 1.69 | 0.25 | 29.24 | 0.30 | 0.16 | 11.07 | 0.45 | 0.94 | 0.15 | 0.14 | 0.03 | -0.00 | 0.02 | 0.09 | 35.69 | 95.52 |

Continued on next page

| Sample | Area | Si | Ti | Al | Cr | Fe | Mn | Ni | Mg | Ca | Na | K | P | Co | V | Zn | S | O | Total |
|---|---|---|---|---|---|---|---|---|---|---|---|---|---|---|---|---|---|---|---|
| Kainsaz | 2a | 15.11 | 0.04 | 2.12 | 0.28 | 29.01 | 0.31 | 0.22 | 11.35 | 0.32 | 0.77 | 0.10 | 0.14 | 0.00 | 0.00 | 0.03 | 0.08 | 35.92 | 95.82 |
| Kainsaz | 2a | 15.21 | 0.05 | 2.46 | 0.27 | 28.09 | 0.30 | 0.52 | 11.22 | 0.35 | 0.93 | 0.12 | 0.16 | 0.01 | 0.00 | 0.02 | 0.27 | 36.46 | 96.45 |
| Kainsaz | 2a | 15.43 | 0.05 | 1.89 | 0.26 | 28.52 | 0.30 | 0.84 | 11.40 | 0.39 | 0.83 | 0.11 | 0.15 | 0.01 | 0.00 | 0.01 | 0.13 | 36.26 | 96.58 |
| Kainsaz | 2a | 14.21 | 0.04 | 1.27 | 0.24 | 31.31 | 0.27 | 1.27 | 11.80 | 0.34 | 0.53 | 0.07 | 0.14 | 0.02 | 0.00 | 0.03 | 2.15 | 38.37 | 102.07 |
| Kainsaz | 2a | 15.37 | 0.06 | 2.12 | 0.27 | 27.50 | 0.29 | 1.44 | 10.94 | 0.48 | 1.10 | 0.15 | 0.16 | 0.01 | 0.00 | 0.02 | 0.12 | 36.12 | 96.16 |
| Kainsaz | 2a | 15.13 | 0.04 | 1.54 | 0.25 | 29.30 | 0.31 | 0.72 | 11.17 | 0.40 | 0.81 | 0.08 | 0.13 | 0.00 | 0.00 | 0.03 | 0.10 | 35.57 | 95.59 |
| Kainsaz | 2a | 13.07 | 0.05 | 1.53 | 0.33 | 35.25 | 0.30 | 1.27 | 10.18 | 0.27 | 0.40 | 0.07 | 0.11 | 0.09 | 0.01 | 0.03 | 0.12 | 34.28 | 97.36 |
| Kainsaz | 2a | 15.37 | 0.05 | 1.43 | 0.36 | 28.83 | 0.33 | 1.01 | 11.75 | 0.48 | 0.67 | 0.07 | 0.15 | 0.03 | 0.01 | 0.03 | 0.13 | 36.20 | 96.92 |
| Kainsaz | 2a | 17.87 | 0.04 | 1.19 | 0.27 | 22.77 | 0.24 | 0.35 | 11.08 | 4.36 | 0.47 | 0.07 | 0.16 | 0.01 | 0.01 | 0.02 | 0.09 | 37.82 | 96.81 |
| Kainsaz | 2a | 18.22 | 0.04 | 0.98 | 0.23 | 22.64 | 0.21 | 0.30 | 16.61 | 0.49 | 0.30 | 0.02 | 0.09 | 0.01 | 0.00 | 0.01 | 0.07 | 39.85 | 100.07 |
| Kainsaz | 2a | 14.41 | 0.05 | 1.50 | 0.30 | 31.26 | 0.28 | 1.64 | 11.29 | 0.41 | 0.54 | 0.10 | 0.10 | 0.07 | 0.01 | 0.03 | 0.09 | 35.50 | 97.58 |
| Kainsaz | 2a | 15.41 | 0.05 | 1.43 | 0.31 | 27.79 | 0.29 | 2.89 | 12.47 | 0.44 | 0.61 | 0.05 | 0.13 | 0.03 | 0.00 | 0.03 | 0.09 | 36.77 | 98.79 |
| Kainsaz | 2a | 16.57 | 0.04 | 1.46 | 0.21 | 27.85 | 0.20 | 3.02 | 9.24 | 5.34 | 0.83 | 0.03 | 0.08 | 0.08 | 0.01 | 0.02 | 0.10 | 37.97 | 103.06 |
| Kainsaz | 2a | 15.48 | 0.13 | 1.74 | 0.25 | 27.52 | 0.27 | 0.05 | 13.47 | 0.64 | 0.29 | 0.03 | 0.12 | 0.01 | 0.01 | 0.05 | 0.05 | 36.85 | 96.95 |
| Kainsaz | 2a | 18.73 | 0.10 | 2.01 | 0.41 | 20.52 | 0.24 | 0.61 | 15.42 | 1.77 | 0.67 | 0.13 | 0.09 | 0.07 | 0.01 | 0.04 | 0.20 | 41.07 | 102.10 |
| Kainsaz | 2a | 25.45 | 0.12 | 1.16 | 0.54 | 4.21 | 0.30 | 0.12 | 19.74 | 1.94 | 0.21 | 0.06 | 0.02 | 0.00 | 0.01 | 0.01 | 0.07 | 45.68 | 99.63 |
| Kainsaz | 2a | 15.58 | 0.03 | 1.27 | 0.27 | 28.25 | 0.29 | 0.60 | 11.64 | 1.28 | 0.70 | 0.11 | 0.11 | 0.02 | 0.00 | 0.01 | 0.08 | 36.08 | 96.33 |
| Kainsaz | 3a | 15.39 | 0.03 | 1.09 | 0.20 | 28.50 | 0.31 | 0.45 | 11.36 | 0.37 | 0.52 | 0.10 | 0.13 | 0.01 | 0.00 | 0.01 | 0.20 | 35.30 | 93.96 |
| Kainsaz | 3a | 15.54 | 0.03 | 1.19 | 0.21 | 27.28 | 0.32 | 0.25 | 11.22 | 0.38 | 0.56 | 0.12 | 0.13 | 0.01 | 0.00 | 0.01 | 0.08 | 34.90 | 92.23 |
| Kainsaz | 3a | 15.93 | 0.03 | 1.12 | 0.26 | 27.65 | 0.28 | 0.97 | 13.78 | 0.32 | 0.30 | 0.06 | 0.13 | 0.01 | 0.00 | 0.01 | 0.14 | 37.25 | 98.23 |
| Kainsaz | 3a | 16.48 | 0.05 | 1.00 | 0.24 | 26.50 | 0.29 | 0.54 | 13.82 | 0.39 | 0.38 | 0.04 | 0.12 | 0.01 | 0.01 | 0.04 | 0.07 | 37.31 | 97.27 |
| Kainsaz | 3a | 13.77 | 0.05 | 0.98 | 0.25 | 33.11 | 0.27 | 0.72 | 11.84 | 0.30 | 0.40 | 0.07 | 0.12 | 0.09 | 0.00 | 0.02 | 0.19 | 35.00 | 97.18 |
| Kainsaz | 3a | 15.24 | 0.06 | 1.86 | 0.33 | 27.96 | 0.28 | 1.75 | 12.64 | 0.46 | 0.65 | 0.10 | 0.13 | 0.02 | 0.01 | 0.02 | 0.83 | 37.95 | 100.27 |
| Kainsaz | 3a | 16.37 | 0.07 | 3.01 | 0.27 | 22.25 | 0.25 | 0.52 | 12.66 | 0.61 | 1.58 | 0.20 | 0.11 | 0.01 | 0.00 | 0.05 | 0.16 | 37.66 | 95.80 |
| Kainsaz | 3a | 24.38 | 0.13 | 3.86 | 0.43 | 3.69 | 0.15 | 0.07 | 15.38 | 3.40 | 2.69 | 0.08 | 0.01 | 0.00 | 0.00 | 0.00 | 0.14 | 45.27 | 99.68 |
| Kainsaz | 3a | 26.52 | 0.11 | 2.79 | 0.45 | 2.52 | 0.23 | 0.04 | 19.30 | 2.20 | 1.45 | 0.13 | 0.02 | 0.01 | 0.01 | 0.01 | 0.03 | 47.98 | 103.80 |
| Kainsaz | 3a | 27.93 | 0.10 | 0.55 | 0.45 | 2.72 | 0.17 | 0.04 | 22.65 | 0.94 | 0.14 | 0.02 | 0.02 | 0.01 | 0.01 | 0.00 | 0.02 | 48.83 | 104.60 |
| Kainsaz | 3a | 14.88 | 0.09 | 3.55 | 0.23 | 24.56 | 0.26 | 0.17 | 10.49 | 1.01 | 4.13 | 0.07 | 0.40 | 0.01 | 0.01 | 0.03 | 1.24 | 38.58 | 99.71 |
| Kainsaz | 3a | 23.81 | 0.11 | 1.62 | 0.44 | 7.72 | 0.23 | 0.20 | 19.14 | 0.81 | 0.49 | 0.07 | 0.05 | 0.00 | 0.00 | 0.00 | 0.08 | 44.49 | 99.28 |
| Kainsaz | 3a | 20.07 | 0.08 | 0.81 | 0.44 | 25.53 | 0.17 | 0.43 | 18.98 | 1.55 | 0.11 | 0.02 | 0.14 | 0.09 | 0.01 | 0.00 | 3.45 | 49.86 | 121.73 |
| Kainsaz | 3a | 12.05 | 0.03 | 0.83 | 0.64 | 46.85 | 0.24 | 1.72 | 12.56 | 0.46 | 0.24 | 0.03 | 0.14 | 0.18 | 0.01 | 0.00 | 0.09 | 37.66 | 113.73 |
| Kainsaz | 3a | 16.20 | 0.04 | 1.02 | 0.23 | 25.30 | 0.26 | 0.46 | 15.23 | 0.29 | 0.35 | 0.04 | 0.12 | 0.01 | 0.00 | 0.00 | 0.10 | 37.52 | 97.16 |
| Kainsaz | 3a | 15.83 | 0.04 | 1.19 | 0.25 | 26.13 | 0.25 | 1.04 | 15.50 | 0.26 | 0.27 | 0.02 | 0.11 | 0.01 | 0.01 | 0.02 | 0.12 | 37.82 | 98.87 |
| Kainsaz | 3a | 13.60 | 0.03 | 0.63 | 0.25 | 24.33 | 0.29 | 0.28 | 13.97 | 0.57 | 0.22 | 0.00 | 0.08 | 0.03 | 0.01 | 0.02 | 0.08 | 33.07 | 87.47 |
| Kainsaz | 3a | 16.96 | 0.06 | 0.75 | 0.43 | 14.79 | 0.45 | 0.14 | 13.28 | 1.28 | 0.22 | 0.01 | 0.08 | 0.00 | 0.01 | 0.03 | 0.10 | 34.23 | 82.81 |
| Kainsaz | 3a | 17.51 | 0.05 | 0.45 | 0.39 | 4.93 | 0.25 | 0.10 | 11.28 | 3.90 | 0.14 | 0.00 | 0.05 | 0.01 | 0.00 | 0.00 | 0.03 | 31.21 | 70.32 |
| Kainsaz | 3a | 24.10 | 0.07 | 1.40 | 0.40 | 6.62 | 0.27 | 0.08 | 17.66 | 3.88 | 0.15 | 0.00 | 0.02 | 0.00 | 0.00 | 0.00 | 0.05 | 44.26 | 98.97 |
| Kainsaz | 3a | 15.71 | 0.06 | 1.70 | 0.30 | 29.00 | 0.32 | 0.81 | 11.06 | 0.53 | 0.92 | 0.14 | 0.11 | 0.01 | 0.01 | 0.03 | 0.09 | 36.34 | 97.13 |
| Kainsaz | 3a | 14.51 | 0.03 | 1.22 | 0.24 | 32.22 | 0.31 | 0.70 | 10.53 | 0.43 | 0.48 | 0.07 | 0.11 | 0.04 | 0.00 | 0.00 | 0.10 | 34.84 | 95.83 |
| Kainsaz | 3a | 14.19 | 0.05 | 1.65 | 0.24 | 28.28 | 0.33 | 0.83 | 9.56 | 0.45 | 0.64 | 0.12 | 0.13 | 0.01 | 0.01 | 0.02 | 0.13 | 33.31 | 89.94 |
| Kainsaz | 3a | 14.57 | 0.04 | 0.86 | 0.23 | 30.70 | 0.30 | 0.90 | 7.66 | 2.44 | 0.40 | 0.05 | 0.10 | 0.03 | 0.01 | 0.01 | 0.11 | 33.10 | 91.51 |
| Kainsaz | 3a | 12.17 | 0.02 | 1.08 | 0.20 | 36.88 | 0.30 | 1.01 | 8.29 | 0.39 | 0.48 | 0.08 | 0.08 | 0.07 | 0.00 | 0.03 | 0.45 | 32.45 | 93.98 |
| Kainsaz | 4a | 17.37 | 0.04 | 1.07 | 0.23 | 28.74 | 0.41 | 0.12 | 12.26 | 0.59 | 0.66 | 0.13 | 0.12 | 0.00 | 0.00 | 0.00 | 0.07 | 38.07 | 99.88 |
| Kainsaz | 4a | 15.31 | 0.03 | 1.35 | 0.16 | 33.05 | 0.42 | 0.39 | 9.69 | 0.75 | 0.74 | 0.13 | 0.33 | 0.01 | 0.00 | 0.01 | 0.07 | 35.94 | 98.39 |
| Kainsaz | 4a | 15.29 | 0.03 | 1.03 | 0.18 | 32.27 | 0.37 | 0.14 | 10.14 | 0.44 | 0.61 | 0.11 | 0.11 | 0.01 | 0.00 | 0.00 | 0.06 | 35.16 | 95.95 |
| Kainsaz | 4a | 20.24 | 0.06 | 0.88 | 0.92 | 20.27 | 0.74 | 0.23 | 9.47 | 4.30 | 1.04 | 0.08 | 0.26 | 0.02 | 0.01 | 0.01 | 0.16 | 39.31 | 97.99 |
| Kainsaz | 4a | 22.22 | 0.07 | 0.91 | 0.79 | 16.25 | 0.78 | 0.20 | 10.27 | 4.71 | 1.01 | 0.07 | 0.28 | 0.02 | 0.00 | 0.00 | 0.21 | 41.15 | 98.93 |
| Kainsaz | 4a | 16.05 | 0.03 | 0.65 | 0.27 | 29.41 | 0.33 | 0.87 | 11.84 | 0.36 | 0.24 | 0.03 | 0.10 | 0.00 | 0.00 | 0.01 | 0.10 | 36.07 | 96.35 |
| Kainsaz | 4a | 14.23 | 0.04 | 1.16 | 0.37 | 32.00 | 0.30 | 2.83 | 10.96 | 0.42 | 0.25 | 0.03 | 0.10 | 0.02 | 0.01 | 0.03 | 1.01 | 36.59 | 100.33 |
| Kainsaz | 4a | 14.20 | 0.04 | 1.45 | 0.25 | 28.96 | 0.29 | 4.17 | 10.30 | 1.07 | 0.40 | 0.06 | 0.12 | 0.01 | 0.01 | 0.04 | 0.28 | 35.09 | 96.75 |
| Kainsaz | 4a | 15.83 | 0.04 | 0.73 | 0.19 | 30.37 | 0.34 | 1.40 | 11.71 | 0.73 | 0.34 | 0.06 | 0.11 | 0.03 | 0.01 | 0.02 | 0.06 | 36.36 | 98.33 |
| Kainsaz | 4a | 15.10 | 0.05 | 0.87 | 0.24 | 32.43 | 0.34 | 1.42 | 11.44 | 0.38 | 0.33 | 0.04 | 0.11 | 0.05 | 0.00 | 0.02 | 0.10 | 36.00 | 98.91 |
| Kainsaz | 4a | 17.55 | 0.14 | 2.38 | 0.31 | 25.14 | 0.33 | 0.58 | 11.10 | 1.86 | 1.55 | 0.08 | 0.09 | 0.01 | 0.02 | 0.02 | 0.14 | 38.77 | 100.07 |
| Kainsaz | 4a | 14.39 | 0.03 | 0.83 | 0.29 | 32.21 | 0.33 | 3.96 | 11.05 | 0.45 | 0.39 | 0.04 | 0.12 | 0.05 | 0.01 | 0.00 | 0.25 | 35.83 | 100.22 |
| Kainsaz | 4a | 15.90 | 0.04 | 1.06 | 0.22 | 29.49 | 0.31 | 0.33 | 11.75 | 0.47 | 0.42 | 0.10 | 0.13 | 0.01 | 0.00 | 0.02 | 0.06 | 36.18 | 96.51 |
| Kainsaz | 4a | 15.07 | 0.04 | 0.68 | 0.23 | 31.86 | 0.32 | 1.30 | 12.20 | 0.28 | 0.21 | 0.03 | 0.10 | 0.03 | 0.01 | 0.01 | 0.07 | 35.94 | 98.35 |
| Kainsaz | 4a | 18.64 | 0.03 | 0.56 | 0.23 | 25.69 | 0.27 | 1.30 | 7.19 | 6.50 | 0.23 | 0.02 | 0.09 | 0.02 | 0.01 | 0.02 | 0.09 | 37.33 | 98.21 |
| Kainsaz | 4a | 14.85 | 0.04 | 0.92 | 0.27 | 30.77 | 0.30 | 3.34 | 11.19 | 1.08 | 0.21 | 0.02 | 0.11 | 0.02 | 0.01 | 0.03 | 0.57 | 36.59 | 100.32 |

Continued on next page

| Sample | Area | Si | Ti | Al | Cr | Fe | Mn | Ni | Mg | Ca | Na | K | P | Co | V | Zn | S | O | Total |
|---|---|---|---|---|---|---|---|---|---|---|---|---|---|---|---|---|---|---|---|
| Kainsaz | 4a | 15.65 | 0.05 | 0.77 | 0.28 | 29.73 | 0.33 | 0.56 | 11.81 | 0.57 | 0.26 | 0.02 | 0.12 | 0.00 | 0.00 | 0.01 | 0.07 | 35.79 | 96.01 |
| Kainsaz | 4a | 15.00 | 0.04 | 0.92 | 0.30 | 29.45 | 0.29 | 1.58 | 12.35 | 0.32 | 0.29 | 0.04 | 0.12 | 0.02 | 0.00 | 0.03 | 0.09 | 35.70 | 96.54 |
| Kainsaz | 4a | 18.47 | 0.03 | 0.63 | 0.21 | 23.11 | 0.24 | 0.55 | 9.23 | 6.24 | 0.26 | 0.03 | 0.10 | 0.01 | 0.00 | 0.00 | 0.08 | 37.48 | 96.66 |
| Kainsaz | 4a | 16.33 | 0.04 | 0.75 | 0.26 | 28.05 | 0.31 | 1.41 | 12.12 | 1.43 | 0.24 | 0.01 | 0.12 | 0.01 | 0.00 | 0.01 | 0.07 | 36.82 | 97.97 |
| Kainsaz | 4a | 14.61 | 0.04 | 0.68 | 0.23 | 30.93 | 0.26 | 0.49 | 13.16 | 0.31 | 0.21 | 0.03 | 0.11 | 0.05 | 0.00 | 0.02 | 0.10 | 35.63 | 96.86 |
| Kainsaz | 4a | 14.08 | 0.04 | 0.81 | 0.25 | 33.24 | 0.25 | 0.71 | 13.03 | 0.32 | 0.20 | -0.01 | 0.07 | 0.08 | 0.00 | 0.02 | 0.11 | 35.75 | 98.96 |
| Kainsaz | 4a | 16.87 | 0.03 | 0.86 | 0.36 | 29.93 | 0.61 | 0.19 | 9.96 | 2.38 | 0.67 | 0.09 | 0.07 | 0.01 | 0.00 | 0.00 | 0.77 | 37.98 | 100.78 |
| Kainsaz | 4a | 15.13 | 0.02 | 0.83 | 0.16 | 35.13 | 0.40 | 0.79 | 9.79 | 0.60 | 0.55 | 0.10 | 0.10 | 0.02 | 0.00 | 0.02 | 0.57 | 36.34 | 100.56 |
| Kainsaz | 4a | 16.76 | 0.02 | 0.98 | 0.16 | 30.57 | 0.48 | 0.07 | 10.82 | 1.21 | 0.68 | 0.14 | 0.10 | 0.00 | 0.00 | 0.00 | 0.04 | 37.03 | 99.07 |
| Kainsaz | 4a | 19.91 | 0.03 | 0.78 | 0.38 | 22.68 | 1.16 | 0.02 | 13.62 | 1.70 | 0.53 | 0.10 | 0.08 | 0.00 | 0.00 | 0.01 | 0.02 | 40.39 | 101.41 |
| Kainsaz | 4a | 15.96 | 0.05 | 1.04 | 0.29 | 29.32 | 0.32 | 0.34 | 11.92 | 0.42 | 0.50 | 0.09 | 0.12 | 0.02 | 0.01 | 0.02 | 0.06 | 36.33 | 96.79 |
| Kainsaz | 4a | 16.00 | 0.05 | 1.22 | 0.22 | 28.14 | 0.30 | 0.54 | 12.70 | 0.56 | 0.45 | 0.05 | 0.14 | 0.00 | 0.00 | 0.00 | 0.27 | 37.09 | 97.74 |
| Kainsaz | 4a | 17.16 | 0.04 | 0.69 | 0.52 | 25.91 | 0.63 | 0.65 | 13.19 | 1.00 | 0.37 | 0.02 | 0.10 | 0.01 | 0.00 | 0.01 | 0.29 | 38.00 | 98.59 |
| Kainsaz | 4a | 15.80 | 0.03 | 0.78 | 0.18 | 31.41 | 0.36 | 0.40 | 11.36 | 0.42 | 0.37 | 0.05 | 0.13 | 0.02 | 0.00 | 0.01 | 0.07 | 36.08 | 97.47 |
| Kainsaz | 4a | 18.20 | 0.01 | 0.91 | 0.24 | 26.18 | 0.69 | 0.84 | 13.11 | 1.15 | 0.52 | 0.14 | 0.14 | 0.00 | 0.00 | 0.00 | 0.02 | 39.12 | 101.29 |
| Kainsaz | 4a | 15.40 | 0.03 | 0.77 | 0.17 | 31.70 | 0.35 | 0.37 | 11.28 | 0.35 | 0.37 | 0.04 | 0.09 | 0.01 | 0.00 | 0.01 | 0.07 | 35.55 | 96.55 |
| Kainsaz | 4a | 15.60 | 0.03 | 0.84 | 0.20 | 30.08 | 0.34 | 0.24 | 11.70 | 0.40 | 0.42 | 0.06 | 0.11 | 0.00 | 0.00 | 0.00 | 0.08 | 35.69 | 95.79 |
| Kainsaz | 4a | 15.48 | 0.05 | 0.72 | 0.23 | 29.21 | 0.31 | 0.74 | 12.61 | 0.34 | 0.28 | 0.03 | 0.12 | 0.01 | 0.01 | 0.00 | 0.06 | 35.87 | 96.06 |
| Kainsaz | 4a | 15.59 | 0.05 | 0.86 | 0.25 | 27.65 | 0.29 | 0.60 | 13.08 | 0.40 | 0.29 | 0.05 | 0.13 | 0.00 | 0.00 | 0.02 | 0.06 | 35.99 | 95.31 |
| Kainsaz | 4a | 15.90 | 0.04 | 0.76 | 0.28 | 26.55 | 0.30 | 0.70 | 13.78 | 0.38 | 0.24 | 0.02 | 0.13 | 0.01 | 0.01 | 0.00 | 0.05 | 36.40 | 95.55 |
| Kainsaz | 4a | 15.20 | 0.04 | 0.70 | 0.23 | 29.71 | 0.28 | 1.31 | 13.16 | 0.27 | 0.30 | 0.03 | 0.12 | 0.03 | 0.01 | 0.02 | 0.07 | 36.20 | 97.67 |
| Kainsaz | 4a | 15.96 | 0.05 | 1.09 | 0.23 | 28.92 | 0.32 | 0.14 | 12.09 | 0.54 | 0.66 | 0.10 | 0.13 | 0.00 | 0.00 | 0.02 | 0.08 | 36.42 | 96.74 |
| Kainsaz | 4a | 14.65 | 0.03 | 1.41 | 0.29 | 35.35 | 0.27 | 0.99 | 11.81 | 0.34 | 0.81 | 0.11 | 0.10 | 0.08 | 0.01 | 0.01 | 0.06 | 37.04 | 103.36 |
| Kainsaz | 4a | 15.81 | 0.04 | 1.08 | 0.27 | 28.69 | 0.35 | 1.05 | 11.97 | 0.39 | 0.59 | 0.08 | 0.13 | 0.01 | 0.01 | 0.02 | 0.06 | 36.26 | 96.81 |
| Kainsaz | 4a | 16.18 | 0.03 | 1.15 | 0.25 | 28.14 | 0.30 | 0.61 | 12.28 | 0.39 | 0.63 | 0.08 | 0.13 | 0.01 | 0.00 | 0.02 | 0.09 | 36.70 | 97.00 |
| Kainsaz | 4a | 15.97 | 0.04 | 1.49 | 0.22 | 27.69 | 0.30 | 0.17 | 12.03 | 0.40 | 1.03 | 0.20 | 0.15 | 0.02 | 0.00 | 0.02 | 0.13 | 36.59 | 96.45 |
| Kainsaz | 4a | 19.63 | 0.04 | 1.80 | 0.21 | 17.16 | 0.21 | 0.32 | 9.04 | 7.84 | 0.91 | 0.12 | 0.10 | 0.01 | 0.00 | 0.01 | 0.05 | 38.78 | 96.23 |
| Kainsaz | 4a | 12.07 | 0.02 | 0.50 | 2.25 | 30.55 | 0.22 | 3.67 | 11.82 | 3.42 | 0.60 | 0.02 | 2.41 | 0.08 | 0.01 | 0.02 | 0.06 | 37.67 | 105.40 |
| Kainsaz | 4a | 15.74 | 0.04 | 1.00 | 0.23 | 28.42 | 0.31 | 0.55 | 11.98 | 0.46 | 0.55 | 0.11 | 0.13 | 0.01 | 0.00 | 0.02 | 0.06 | 35.88 | 95.47 |
| Kainsaz | 4a | 15.47 | 0.04 | 1.05 | 0.25 | 29.56 | 0.34 | 0.68 | 11.70 | 0.35 | 0.62 | 0.09 | 0.12 | 0.01 | 0.01 | 0.00 | 0.07 | 35.79 | 96.13 |
| Kainsaz | 4a | 14.53 | 0.04 | 1.11 | 0.22 | 32.27 | 0.32 | 1.41 | 11.30 | 0.27 | 0.46 | 0.07 | 0.10 | 0.04 | 0.00 | 0.02 | 0.08 | 35.37 | 97.60 |
| Kainsaz | 4a | 15.16 | 0.04 | 1.12 | 0.27 | 33.37 | 0.28 | 0.98 | 12.20 | 0.37 | 0.68 | 0.08 | 0.10 | 0.07 | 0.01 | 0.01 | 0.07 | 37.02 | 101.82 |
| Kainsaz | 4a | 16.00 | 0.05 | 1.27 | 0.66 | 28.23 | 0.36 | 0.53 | 11.40 | 1.44 | 0.93 | 0.11 | 0.12 | 0.03 | 0.00 | 0.01 | 0.11 | 36.79 | 98.06 |
| Kainsaz | 5a | 15.61 | 0.18 | 8.80 | 0.40 | 16.15 | 0.13 | 0.85 | 8.81 | 5.08 | 2.19 | 0.13 | 0.13 | 0.00 | 0.04 | 0.18 | 0.06 | 39.76 | 98.51 |
| Kainsaz | 5a | 13.36 | 0.03 | 0.94 | 0.32 | 36.22 | 0.30 | 1.90 | 11.79 | 0.55 | 0.28 | 0.02 | 0.14 | 0.17 | 0.01 | 0.03 | 0.12 | 35.70 | 101.88 |
| Kainsaz | 5a | 20.51 | 0.30 | 7.40 | 0.13 | 7.84 | 0.08 | 0.06 | 8.44 | 8.95 | 5.52 | 0.03 | 0.05 | 0.02 | 0.02 | 0.02 | 0.05 | 43.72 | 103.16 |
| Kainsaz | 5a | 17.30 | 0.10 | 1.61 | 0.30 | 23.23 | 0.32 | 0.35 | 13.59 | 1.35 | 0.60 | 0.08 | 0.13 | 0.02 | 0.01 | 0.03 | 0.08 | 38.22 | 97.31 |
| Kainsaz | 5a | 14.73 | 0.05 | 1.13 | 0.26 | 29.54 | 0.27 | 2.28 | 11.11 | 1.43 | 0.43 | 0.04 | 0.14 | 0.07 | 0.01 | 0.02 | 0.12 | 35.54 | 97.17 |
| Kainsaz | 5a | 20.03 | 0.41 | 4.57 | 0.14 | 11.18 | 0.07 | 0.42 | 9.54 | 9.71 | 2.17 | 0.01 | 0.05 | 0.03 | 0.04 | 0.04 | 0.07 | 41.70 | 100.17 |
| Kainsaz | 5a | 14.31 | 0.41 | 18.70 | 0.54 | 8.71 | 0.05 | 0.12 | 4.52 | 4.71 | 6.62 | 0.02 | 0.03 | 0.00 | 0.09 | 0.37 | 0.03 | 43.42 | 102.65 |
| Kainsaz | 5a | 16.25 | 0.05 | 1.14 | 0.26 | 25.43 | 0.28 | 0.96 | 13.36 | 0.54 | 0.41 | 0.03 | 0.13 | 0.01 | 0.00 | 0.00 | 0.12 | 36.83 | 95.81 |
| Kainsaz | 5a | 11.04 | 0.04 | 0.78 | 0.18 | 46.14 | 0.21 | 1.25 | 9.60 | 0.31 | 0.46 | 0.07 | 0.10 | 0.31 | 0.01 | 0.00 | 0.06 | 33.93 | 104.46 |
| Kainsaz | 5a | 22.60 | 0.07 | 0.84 | 0.34 | 13.15 | 0.19 | 0.49 | 19.15 | 0.82 | 0.17 | 0.02 | 0.24 | 0.01 | 0.01 | 0.00 | 0.04 | 44.03 | 102.16 |
| Kainsaz | 5a | 22.30 | 0.07 | 2.56 | 0.46 | 8.99 | 0.13 | 0.04 | 19.49 | 1.00 | 0.66 | 0.12 | 0.01 | 0.01 | 0.02 | 0.00 | 0.07 | 44.19 | 100.11 |
| Kainsaz | 5a | 17.63 | 0.12 | 2.39 | 0.49 | 22.55 | 0.26 | 1.83 | 13.76 | 1.62 | 0.70 | 0.10 | 0.09 | 0.01 | 0.00 | 0.04 | 0.07 | 39.77 | 101.44 |
| Kainsaz | 5a | 15.46 | 0.05 | 1.16 | 0.35 | 28.86 | 0.31 | 0.60 | 12.46 | 0.65 | 0.31 | 0.04 | 0.14 | 0.02 | 0.01 | 0.03 | 0.25 | 36.51 | 97.20 |
| Kainsaz | 5a | 13.61 | 0.03 | 0.71 | 0.67 | 36.11 | 0.20 | 0.54 | 10.81 | 2.56 | 0.20 | 0.04 | 0.12 | 0.10 | 0.01 | 0.01 | 2.65 | 39.40 | 107.77 |
| Kainsaz | 5a | 12.43 | 0.03 | 0.98 | 0.28 | 35.43 | 0.25 | 2.11 | 10.03 | 0.90 | 0.37 | 0.05 | 0.49 | 0.17 | 0.00 | 0.01 | 0.09 | 33.92 | 97.55 |
| Kainsaz | 5a | 15.84 | 0.04 | 1.02 | 0.25 | 28.59 | 0.32 | 0.82 | 12.35 | 0.38 | 0.46 | 0.06 | 0.11 | 0.01 | 0.00 | 0.02 | 0.09 | 36.35 | 96.71 |
| Kainsaz | 5a | 14.43 | 0.04 | 1.12 | 0.29 | 36.27 | 0.30 | 0.63 | 11.88 | 0.51 | 0.51 | 0.04 | 0.18 | 0.14 | 0.00 | 0.03 | 0.09 | 36.86 | 103.32 |
| Kainsaz | 5a | 15.33 | 0.04 | 0.95 | 0.27 | 28.36 | 0.33 | 0.76 | 11.87 | 0.44 | 0.34 | 0.06 | 0.11 | 0.00 | 0.00 | 0.01 | 0.07 | 35.26 | 94.19 |
| Kainsaz | 5a | 14.59 | 0.04 | 0.92 | 0.23 | 29.04 | 0.29 | 3.94 | 11.79 | 0.55 | 0.25 | 0.02 | 0.26 | 0.03 | 0.01 | 0.01 | 0.16 | 35.72 | 97.85 |
| Kainsaz | 5a | 16.37 | 0.05 | 0.91 | 0.29 | 27.36 | 0.50 | 1.34 | 13.51 | 0.36 | 0.42 | 0.04 | 0.11 | 0.02 | 0.00 | 0.04 | 0.07 | 37.44 | 98.85 |
| Kainsaz | 5a | 15.77 | 0.04 | 1.03 | 0.24 | 28.29 | 0.28 | 0.19 | 12.91 | 0.38 | 0.46 | 0.06 | 0.15 | 0.00 | 0.01 | 0.00 | 0.07 | 36.39 | 96.27 |
| Kainsaz | 5a | 11.65 | 0.03 | 0.84 | 0.21 | 33.79 | 0.21 | 2.49 | 10.16 | 0.21 | 0.13 | 0.03 | 0.05 | 0.03 | 0.00 | 0.02 | 3.92 | 37.34 | 101.11 |
| Kainsaz | 5a | 15.57 | 0.04 | 1.04 | 0.28 | 25.93 | 0.29 | 1.83 | 12.72 | 0.44 | 0.47 | 0.08 | 0.12 | 0.03 | 0.00 | 0.00 | 0.23 | 36.06 | 95.11 |
| Kainsaz | 5a | 15.34 | 0.04 | 0.94 | 0.23 | 27.14 | 0.29 | 0.65 | 13.24 | 0.34 | 0.44 | 0.05 | 0.16 | 0.01 | 0.01 | 0.02 | 0.10 | 35.86 | 94.86 |
| Kainsaz | 5a | 13.36 | 0.04 | 0.98 | 0.29 | 27.95 | 0.27 | 3.49 | 11.70 | 0.29 | 0.26 | 0.02 | 0.12 | 0.03 | 0.01 | 0.02 | 0.14 | 33.58 | 92.55 |

Continued on next page

| Sample | Area | Si | Ti | Al | Cr | Fe | Mn | Ni | Mg | Ca | Na | K | P | Co | V | Zn | S | O | Total |
|---|---|---|---|---|---|---|---|---|---|---|---|---|---|---|---|---|---|---|---|
| Kainsaz | 5a | 15.54 | 0.05 | 1.25 | 0.33 | 28.03 | 0.30 | 1.27 | 13.15 | 0.53 | 0.32 | 0.02 | 0.18 | 0.02 | 0.00 | 0.04 | 0.14 | 36.91 | 98.08 |
| Kainsaz | 5a | 16.00 | 0.05 | 1.02 | 0.24 | 28.57 | 0.26 | 0.81 | 13.36 | 0.46 | 0.33 | 0.05 | 0.10 | 0.07 | 0.01 | 0.01 | 0.04 | 37.10 | 98.49 |
| Kainsaz | 5a | 14.82 | 0.05 | 1.91 | 0.29 | 26.42 | 0.30 | 1.34 | 11.35 | 0.64 | 0.35 | 0.06 | 0.11 | 0.00 | 0.00 | 0.02 | 0.10 | 34.95 | 92.72 |
| Kainsaz | 5a | 17.75 | 0.06 | 0.94 | 0.30 | 23.11 | 0.31 | 0.25 | 12.48 | 3.01 | 0.36 | 0.05 | 0.16 | 0.01 | 0.00 | 0.01 | 0.08 | 37.90 | 96.79 |
| Kainsaz | 5a | 14.93 | 0.04 | 0.66 | 0.22 | 26.71 | 0.26 | 1.34 | 10.13 | 2.13 | 0.21 | 0.01 | 0.10 | 0.02 | 0.00 | 0.02 | 0.05 | 33.64 | 90.48 |
| Kainsaz | 5a | 14.08 | 0.04 | 1.23 | 0.27 | 30.81 | 0.26 | 1.77 | 12.68 | 0.31 | 0.32 | 0.06 | 0.12 | 0.08 | 0.01 | 0.02 | 0.08 | 35.57 | 97.70 |
| Kainsaz | 5a | 15.59 | 0.05 | 0.82 | 0.28 | 26.31 | 0.30 | 0.44 | 13.46 | 0.38 | 0.26 | 0.04 | 0.11 | 0.01 | 0.01 | 0.01 | 0.07 | 35.77 | 93.90 |
| Kainsaz | 5a | 16.72 | 0.04 | 0.72 | 0.23 | 21.24 | 0.24 | 0.49 | 19.00 | 0.46 | 0.22 | 0.04 | 0.09 | 0.00 | 0.01 | 0.00 | 0.07 | 39.12 | 98.69 |
| Kainsaz | 5a | 19.36 | 0.08 | 2.40 | 0.35 | 16.47 | 0.66 | 0.20 | 13.16 | 2.40 | 1.37 | 0.32 | 0.09 | 0.00 | 0.01 | 0.01 | 0.12 | 39.84 | 96.83 |
| Kainsaz | 5a | 27.30 | 0.08 | 0.49 | 0.36 | 1.73 | 0.09 | 0.08 | 22.76 | 0.63 | 0.07 | 0.01 | 0.01 | 0.00 | 0.01 | 0.00 | 0.07 | 47.69 | 101.37 |
| Kainsaz | 5a | 24.74 | 0.08 | 0.79 | 0.32 | 8.19 | 0.15 | 0.10 | 21.04 | 0.54 | 0.15 | 0.03 | 0.04 | 0.01 | 0.01 | 0.00 | 0.06 | 45.77 | 101.99 |
| Kainsaz | 5a | 16.03 | 0.04 | 1.94 | 0.33 | 26.46 | 0.29 | 1.23 | 12.77 | 0.59 | 0.76 | 0.14 | 0.10 | 0.02 | 0.00 | 0.02 | 0.60 | 38.15 | 99.48 |
| Kainsaz | 5a | 14.54 | 0.03 | 1.37 | 0.29 | 33.11 | 0.30 | 2.05 | 11.98 | 0.58 | 0.41 | 0.07 | 0.10 | 0.11 | 0.01 | 0.04 | 0.28 | 36.94 | 102.20 |
| Kainsaz | 5a | 14.49 | 0.04 | 1.44 | 0.26 | 30.04 | 0.27 | 0.73 | 12.24 | 0.35 | 0.65 | 0.11 | 0.13 | 0.05 | 0.01 | 0.02 | 0.10 | 35.62 | 96.56 |
| Kainsaz | 5a | 14.87 | 0.04 | 1.35 | 0.29 | 28.68 | 0.28 | 1.11 | 12.84 | 0.35 | 0.43 | 0.08 | 0.14 | 0.04 | 0.01 | 0.03 | 0.09 | 36.01 | 96.64 |
| Kainsaz | 5a | 19.39 | 0.07 | 1.32 | 0.44 | 20.04 | 0.41 | 0.33 | 15.76 | 0.88 | 0.40 | 0.06 | 0.12 | 0.00 | 0.00 | 0.02 | 0.11 | 40.66 | 99.99 |
| Kainsaz | 5a | 16.23 | 0.06 | 1.23 | 0.36 | 24.53 | 0.35 | 2.33 | 13.97 | 0.48 | 0.34 | 0.05 | 0.09 | 0.01 | 0.01 | 0.00 | 0.11 | 37.36 | 97.50 |

| Sample | Area | Si | Ti | Al | Cr | Fe | Mn | Ni | Mg | Ca | Na | K | P | Co | V | Zn | S | O | Total |
|---|---|---|---|---|---|---|---|---|---|---|---|---|---|---|---|---|---|---|---|
| Felix | 2a | 11.86 | 0.04 | 1.40 | 0.24 | 32.81 | 0.20 | 0.92 | 10.65 | 0.34 | 0.10 | 0.01 | 0.07 | 0.01 | NaN | NaN | 3.24 | 36.74 | 98.63 |
| Felix | 2a | 12.26 | 0.04 | 1.59 | 0.26 | 29.77 | 0.22 | 2.22 | 11.47 | 0.23 | 0.15 | 0.00 | 0.09 | 0.02 | NaN | NaN | 0.60 | 33.43 | 92.33 |
| Felix | 2a | 12.76 | 0.05 | 2.23 | 0.29 | 27.63 | 0.22 | 0.40 | 11.08 | 0.26 | 0.13 | 0.00 | 0.11 | 0.00 | NaN | NaN | 0.12 | 32.53 | 87.80 |
| Felix | 2a | 13.89 | 0.04 | 1.17 | 0.51 | 26.10 | 0.20 | 0.64 | 13.44 | 0.54 | 0.11 | 0.01 | 0.15 | 0.00 | NaN | NaN | 0.18 | 34.40 | 91.37 |
| Felix | 2a | 15.76 | 0.04 | 1.01 | 0.73 | 28.30 | 0.28 | 0.09 | 13.80 | 0.93 | 0.09 | 0.00 | 0.23 | 0.00 | NaN | NaN | 0.02 | 37.25 | 98.55 |
| Felix | 2a | 14.78 | 0.04 | 1.02 | 0.69 | 26.36 | 0.30 | 0.03 | 12.64 | 0.96 | 0.17 | 0.04 | 0.17 | 0.00 | NaN | NaN | 0.06 | 34.81 | 92.06 |
| Felix | 2a | 12.15 | 0.05 | 1.08 | 0.26 | 24.26 | 0.18 | 0.36 | 10.90 | 0.31 | 0.24 | 0.03 | 0.12 | 0.00 | NaN | NaN | 0.08 | 29.72 | 79.72 |
| Felix | 2a | 12.96 | 0.04 | 1.05 | 0.26 | 26.01 | 0.21 | 0.27 | 9.58 | 0.27 | 0.15 | 0.01 | 0.08 | 0.00 | NaN | NaN | 0.09 | 30.15 | 81.14 |
| Felix | 2a | 12.35 | 0.04 | 1.46 | 0.24 | 26.80 | 0.20 | 0.47 | 10.43 | 0.29 | 0.12 | 0.01 | 0.13 | 0.01 | NaN | NaN | 0.22 | 30.90 | 83.67 |
| Felix | 2a | 13.68 | 0.04 | 1.35 | 0.27 | 27.38 | 0.22 | 0.22 | 9.95 | 0.39 | 0.15 | 0.02 | 0.12 | 0.00 | NaN | NaN | 0.13 | 32.01 | 85.91 |
| Felix | 2a | 12.22 | 0.04 | 1.37 | 0.23 | 27.77 | 0.22 | 2.24 | 9.99 | 0.27 | 0.12 | 0.00 | 0.11 | 0.02 | NaN | NaN | 0.08 | 30.89 | 85.57 |
| Felix | 2a | 12.83 | 0.04 | 1.33 | 0.24 | 27.73 | 0.21 | 0.60 | 10.49 | 0.29 | 0.12 | 0.01 | 0.11 | 0.00 | NaN | NaN | 0.08 | 31.43 | 85.51 |
| Felix | 2a | 13.09 | 0.03 | 1.12 | 0.21 | 27.73 | 0.22 | 0.53 | 10.35 | 0.33 | 0.10 | 0.00 | 0.13 | 0.00 | NaN | NaN | 0.10 | 31.48 | 85.42 |
| Felix | 2a | 13.03 | 0.04 | 1.26 | 0.26 | 28.33 | 0.23 | 0.96 | 10.62 | 0.28 | 0.09 | 0.01 | 0.11 | 0.01 | NaN | NaN | 0.08 | 31.97 | 87.29 |
| Felix | 2a | 13.09 | 0.04 | 1.11 | 0.27 | 28.65 | 0.22 | 0.18 | 10.41 | 0.27 | 0.10 | 0.01 | 0.10 | 0.00 | NaN | NaN | 0.58 | 32.37 | 87.41 |
| Felix | 2a | 12.80 | 0.05 | 1.12 | 0.33 | 28.23 | 0.22 | 2.13 | 10.45 | 0.31 | 0.06 | 0.00 | 0.17 | 0.00 | NaN | NaN | 0.06 | 31.84 | 87.78 |
| Felix | 2a | 12.84 | 0.04 | 1.12 | 0.24 | 26.61 | 0.21 | 0.34 | 10.51 | 0.23 | 0.07 | 0.00 | 0.10 | 0.00 | NaN | NaN | 0.06 | 30.78 | 83.12 |
| Felix | 2a | 11.62 | 0.03 | 0.87 | 0.19 | 24.02 | 0.18 | 0.20 | 9.44 | 0.34 | 0.06 | 0.00 | 0.16 | 0.00 | NaN | NaN | 0.11 | 27.86 | 75.09 |
| Felix | 2a | 12.47 | 0.10 | 1.63 | 0.23 | 26.59 | 0.21 | 0.22 | 10.38 | 0.35 | 0.07 | 0.00 | 0.10 | 0.00 | NaN | NaN | 0.04 | 30.75 | 83.15 |
| Felix | 2a | 12.86 | 0.03 | 0.86 | 0.20 | 26.53 | 0.21 | 0.15 | 10.38 | 0.24 | 0.06 | 0.00 | 0.08 | 0.00 | NaN | NaN | 0.05 | 30.34 | 81.99 |
| Felix | 2a | 12.64 | 0.04 | 1.34 | 0.24 | 27.96 | 0.23 | 0.94 | 10.00 | 0.41 | 0.10 | 0.01 | 0.15 | 0.01 | NaN | NaN | 0.07 | 31.16 | 85.30 |
| Felix | 2a | 13.19 | 0.04 | 0.96 | 0.26 | 27.91 | 0.23 | 0.25 | 10.60 | 0.36 | 0.08 | 0.00 | 0.15 | 0.00 | NaN | NaN | 0.06 | 31.60 | 85.69 |
| Felix | 2a | 12.66 | 0.04 | 1.01 | 0.26 | 29.70 | 0.21 | 0.36 | 10.19 | 0.31 | 0.06 | 0.01 | 0.13 | 0.00 | NaN | NaN | 0.79 | 32.34 | 88.06 |
| Felix | 2a | 12.73 | 0.04 | 1.05 | 0.21 | 26.73 | 0.21 | 0.55 | 10.34 | 0.25 | 0.08 | 0.01 | 0.08 | 0.00 | NaN | NaN | 0.04 | 30.54 | 82.86 |
| Felix | 2a | 12.73 | 0.04 | 0.95 | 0.23 | 27.01 | 0.23 | 0.59 | 10.50 | 0.25 | 0.05 | 0.00 | 0.08 | 0.00 | NaN | NaN | 0.04 | 30.64 | 83.34 |
| Felix | 2a | 12.61 | 0.04 | 1.11 | 0.22 | 27.17 | 0.21 | 0.54 | 10.21 | 0.25 | 0.06 | 0.00 | 0.09 | 0.00 | NaN | NaN | 0.34 | 30.95 | 83.80 |
| Felix | 2a | 11.73 | 0.04 | 1.00 | 0.20 | 23.46 | 0.18 | 0.06 | 9.20 | 0.27 | 0.09 | 0.01 | 0.09 | 0.00 | NaN | NaN | 0.06 | 27.57 | 73.96 |
| Felix | 2a | 11.82 | 0.04 | 1.17 | 0.23 | 24.15 | 0.19 | 0.15 | 9.05 | 0.29 | 0.13 | 0.00 | 0.10 | 0.00 | NaN | NaN | 0.36 | 28.44 | 76.12 |
| Felix | 2a | 12.85 | 0.04 | 1.15 | 0.23 | 26.19 | 0.21 | 0.37 | 10.75 | 0.25 | 0.07 | 0.01 | 0.10 | 0.00 | NaN | NaN | 0.04 | 30.85 | 83.11 |
| Felix | 2a | 11.78 | 0.04 | 0.93 | 0.22 | 22.91 | 0.18 | 0.80 | 8.82 | 0.24 | 0.07 | 0.00 | 0.09 | 0.00 | NaN | NaN | 0.07 | 27.36 | 73.50 |
| Felix | 2a | 12.62 | 0.03 | 1.04 | 0.26 | 25.73 | 0.21 | 0.39 | 10.29 | 0.28 | 0.09 | 0.00 | 0.09 | 0.00 | NaN | NaN | 0.05 | 30.09 | 81.17 |
| Felix | 2a | 12.94 | 0.03 | 0.91 | 0.26 | 27.05 | 0.22 | 1.40 | 10.41 | 0.26 | 0.07 | 0.01 | 0.10 | 0.00 | NaN | NaN | 0.05 | 31.08 | 84.79 |
| Felix | 2a | 11.28 | 0.04 | 1.16 | 0.30 | 25.57 | 0.18 | 0.60 | 11.23 | 0.20 | 0.06 | 0.00 | 0.06 | 0.00 | NaN | NaN | 0.98 | 30.63 | 82.29 |
| Felix | 2a | 12.15 | 0.04 | 1.16 | 0.25 | 25.30 | 0.20 | 0.04 | 12.34 | 0.21 | 0.07 | 0.01 | 0.09 | 0.00 | NaN | NaN | 0.37 | 31.23 | 83.46 |
| Felix | 2a | 12.21 | 0.03 | 1.29 | 0.26 | 24.68 | 0.18 | 0.06 | 10.41 | 0.19 | 0.06 | 0.00 | 0.07 | 0.00 | NaN | NaN | 0.27 | 29.79 | 79.50 |
| Felix | 3a | 13.71 | 0.06 | 1.63 | 0.25 | 31.60 | 0.26 | 0.35 | 9.08 | 0.34 | 0.54 | 0.06 | 0.08 | 0.00 | NaN | NaN | 0.02 | 32.89 | 90.87 |

Continued on next page

| Sample | Area | Si | Ti | Al | Cr | Fe | Mn | Ni | Mg | Ca | Na | K | P | Co | V | Zn | S | O | Total |
|---|---|---|---|---|---|---|---|---|---|---|---|---|---|---|---|---|---|---|---|
| Felix | 3a | 13.23 | 0.04 | 1.29 | 0.25 | 32.69 | 0.27 | 0.57 | 8.90 | 0.28 | 0.21 | 0.07 | 0.07 | 0.00 | NaN | NaN | 0.05 | 32.18 | 90.09 |
| Felix | 3a | 12.66 | 0.04 | 1.24 | 0.24 | 32.20 | 0.26 | 1.31 | 8.33 | 0.30 | 0.20 | 0.04 | 0.10 | 0.03 | NaN | NaN | 0.04 | 31.20 | 88.17 |
| Felix | 3a | 12.91 | 0.04 | 1.00 | 0.24 | 32.99 | 0.27 | 0.34 | 8.66 | 0.29 | 0.14 | 0.01 | 0.09 | 0.00 | NaN | NaN | 0.04 | 31.41 | 88.45 |
| Felix | 3a | 12.79 | 0.04 | 1.20 | 0.27 | 32.10 | 0.29 | 0.23 | 8.43 | 0.32 | 0.14 | 0.01 | 0.12 | 0.00 | NaN | NaN | 0.04 | 31.07 | 87.05 |
| Felix | 3a | 13.00 | 0.03 | 0.62 | 0.21 | 30.82 | 0.27 | 0.31 | 8.90 | 0.28 | 0.06 | 0.00 | 0.05 | 0.00 | NaN | NaN | 0.03 | 30.58 | 85.16 |
| Felix | 3a | 12.46 | 0.03 | 0.62 | 0.21 | 30.66 | 0.25 | 1.73 | 8.76 | 0.22 | 0.05 | 0.01 | 0.05 | 0.04 | NaN | NaN | 0.03 | 30.19 | 85.32 |
| Felix | 3a | 13.61 | 0.03 | 1.28 | 0.27 | 33.81 | 0.27 | 0.88 | 9.05 | 0.28 | 0.12 | 0.02 | 0.08 | 0.01 | NaN | NaN | 0.04 | 33.06 | 92.81 |
| Felix | 3a | 13.44 | 0.04 | 1.17 | 0.28 | 33.23 | 0.27 | 1.15 | 9.20 | 0.28 | 0.13 | 0.02 | 0.08 | 0.03 | NaN | NaN | 0.04 | 32.82 | 92.19 |
| Felix | 3a | 13.51 | 0.05 | 1.40 | 0.30 | 32.08 | 0.26 | 0.58 | 10.09 | 0.28 | 0.10 | 0.00 | 0.10 | 0.00 | NaN | NaN | 0.03 | 33.20 | 91.98 |
| Felix | 3a | 13.11 | 0.04 | 1.11 | 0.27 | 33.59 | 0.28 | 1.19 | 9.18 | 0.29 | 0.10 | 0.01 | 0.09 | 0.03 | NaN | NaN | 0.03 | 32.48 | 91.80 |
| Felix | 3a | 12.40 | 0.03 | 0.86 | 0.22 | 31.34 | 0.26 | 1.22 | 8.98 | 1.88 | 0.22 | 0.00 | 1.37 | 0.05 | NaN | NaN | 0.03 | 32.98 | 91.84 |
| Felix | 3a | 13.70 | 0.04 | 1.00 | 0.26 | 31.38 | 0.26 | 0.44 | 9.80 | 0.24 | 0.09 | 0.00 | 0.08 | 0.00 | NaN | NaN | 0.03 | 32.55 | 89.86 |
| Felix | 3a | 13.05 | 0.04 | 0.95 | 0.24 | 31.00 | 0.24 | 0.57 | 9.20 | 0.25 | 0.08 | 0.00 | 0.09 | 0.00 | NaN | NaN | 0.03 | 31.31 | 87.06 |
| Felix | 3a | 13.48 | 0.04 | 1.00 | 0.27 | 32.34 | 0.26 | 0.76 | 9.53 | 0.27 | 0.09 | 0.02 | 0.10 | 0.02 | NaN | NaN | 0.03 | 32.53 | 90.72 |
| Felix | 3a | 13.07 | 0.07 | 1.60 | 0.31 | 27.91 | 0.22 | 0.74 | 8.29 | 5.02 | 0.23 | 0.03 | 0.11 | 0.02 | NaN | NaN | 0.06 | 32.55 | 90.23 |
| Felix | 3a | 12.50 | 0.05 | 1.50 | 0.33 | 33.01 | 0.25 | 1.35 | 8.77 | 0.23 | 0.07 | 0.01 | 0.08 | 0.03 | NaN | NaN | 0.03 | 31.71 | 89.92 |
| Felix | 3a | 12.67 | 0.04 | 1.00 | 0.28 | 33.27 | 0.26 | 1.44 | 8.63 | 0.29 | 0.09 | 0.02 | 0.10 | 0.03 | NaN | NaN | 0.09 | 31.58 | 89.77 |
| Felix | 3a | 13.16 | 0.05 | 1.70 | 0.46 | 33.09 | 0.27 | 0.58 | 9.07 | 0.24 | 0.10 | 0.01 | 0.08 | 0.02 | NaN | NaN | 0.07 | 32.77 | 91.66 |
| Felix | 3a | 13.01 | 0.06 | 1.86 | 0.27 | 33.08 | 0.27 | 0.52 | 8.90 | 0.27 | 0.19 | 0.02 | 0.09 | 0.02 | NaN | NaN | 0.06 | 32.58 | 91.19 |
| Felix | 3a | 13.28 | 0.05 | 1.73 | 0.46 | 30.95 | 0.25 | 0.29 | 9.52 | 1.74 | 0.22 | 0.01 | 0.35 | 0.00 | NaN | NaN | 0.05 | 33.52 | 92.44 |
| Felix | 3a | 12.15 | 0.05 | 1.64 | 0.49 | 30.27 | 0.25 | 0.78 | 8.94 | 0.28 | 0.11 | 0.01 | 0.09 | 0.01 | NaN | NaN | 0.07 | 30.77 | 85.89 |
| Felix | 3a | 13.81 | 0.05 | 1.67 | 0.33 | 28.71 | 0.23 | 0.07 | 9.56 | 0.32 | 0.68 | 0.10 | 0.07 | 0.00 | NaN | NaN | 0.03 | 32.53 | 88.16 |
| Felix | 3a | 12.38 | 0.04 | 2.05 | 0.29 | 32.45 | 0.19 | 0.56 | 9.32 | 0.39 | 0.95 | 0.14 | 0.07 | 0.11 | NaN | NaN | 0.04 | 32.43 | 91.42 |
| Felix | 3a | 13.24 | 0.03 | 1.17 | 0.43 | 29.55 | 0.24 | 0.22 | 10.66 | 0.24 | 0.21 | 0.02 | 0.04 | 0.02 | NaN | NaN | 0.05 | 32.25 | 88.36 |
| Felix | 3a | 12.36 | 0.03 | 1.38 | 0.27 | 27.29 | 0.23 | 0.04 | 10.00 | 0.34 | 0.19 | 0.01 | 0.07 | 0.00 | NaN | NaN | 0.07 | 30.33 | 82.62 |

| Sample | Area | Si | Ti | Al | Cr | Fe | Mn | Ni | Mg | Ca | Na | K | P | Co | V | Zn | S | O | Total |
|---|---|---|---|---|---|---|---|---|---|---|---|---|---|---|---|---|---|---|---|
| Ornans | 1a | 10.69 | 0.05 | 1.79 | 0.28 | 24.49 | 0.17 | 0.71 | 8.27 | 0.27 | 0.11 | 0.00 | 0.07 | 0.04 | 0.01 | 0.01 | 0.04 | 26.95 | 73.95 |
| Ornans | 1a | 10.08 | 0.06 | 1.32 | 0.26 | 24.27 | 0.17 | 3.26 | 8.10 | 1.28 | 0.24 | 0.01 | 0.74 | 0.14 | 0.00 | 0.02 | 0.07 | 27.75 | 77.77 |
| Ornans | 1a | 10.65 | 0.06 | 1.67 | 0.38 | 24.31 | 0.18 | 0.61 | 8.14 | 0.54 | 0.14 | 0.01 | 0.14 | 0.04 | 0.01 | 0.02 | 0.07 | 26.96 | 73.93 |
| Ornans | 1a | 10.64 | 0.05 | 1.51 | 0.30 | 25.33 | 0.17 | 2.46 | 8.26 | 0.23 | 0.13 | 0.00 | 0.04 | 0.09 | 0.01 | 0.02 | 0.04 | 27.34 | 76.62 |
| Ornans | 1a | 12.06 | 0.05 | 1.60 | 0.27 | 25.19 | 0.20 | 0.24 | 8.37 | 0.89 | 0.12 | 0.00 | 0.06 | 0.02 | 0.00 | 0.03 | 0.05 | 28.74 | 77.89 |
| Ornans | 1a | 10.89 | 0.04 | 1.31 | 0.21 | 24.67 | 0.19 | 1.81 | 8.33 | 0.77 | 0.09 | 0.00 | 0.08 | 0.09 | 0.01 | 0.02 | 0.06 | 27.36 | 75.93 |
| Ornans | 1a | 10.59 | 0.05 | 1.70 | 0.29 | 23.90 | 0.18 | 0.94 | 8.30 | 0.68 | 0.15 | 0.00 | 0.24 | 0.05 | 0.01 | 0.03 | 0.13 | 27.23 | 74.47 |
| Ornans | 1a | 11.56 | 0.05 | 1.68 | 0.28 | 25.72 | 0.20 | 0.34 | 8.86 | 0.30 | 0.12 | 0.01 | 0.09 | 0.03 | 0.00 | 0.02 | 0.03 | 28.52 | 77.81 |
| Ornans | 1a | 11.44 | 0.15 | 2.37 | 0.24 | 24.11 | 0.18 | 0.62 | 8.19 | 1.22 | 0.21 | 0.01 | 0.11 | 0.04 | 0.02 | 0.03 | 0.03 | 28.66 | 77.63 |
| Ornans | 1a | 11.39 | 0.05 | 1.66 | 0.29 | 25.62 | 0.18 | 0.37 | 8.93 | 0.33 | 0.08 | 0.01 | 0.11 | 0.03 | 0.01 | 0.03 | 0.06 | 28.40 | 77.55 |
| Ornans | 1a | 11.32 | 0.04 | 1.51 | 0.23 | 25.59 | 0.19 | 0.18 | 8.75 | 0.93 | 0.18 | 0.01 | 0.39 | 0.02 | 0.01 | 0.02 | 0.03 | 28.57 | 77.97 |
| Ornans | 1a | 11.19 | 0.04 | 1.72 | 0.29 | 25.32 | 0.19 | 0.24 | 8.80 | 0.55 | 0.17 | 0.00 | 0.25 | 0.01 | 0.01 | 0.03 | 0.06 | 28.33 | 77.20 |
| Ornans | 1a | 11.17 | 0.04 | 1.57 | 0.26 | 25.01 | 0.19 | 0.14 | 8.66 | 0.36 | 0.15 | 0.00 | 0.08 | 0.03 | 0.01 | 0.02 | 0.03 | 27.59 | 75.31 |
| Ornans | 1a | 10.43 | 0.04 | 1.48 | 0.26 | 25.32 | 0.18 | 2.57 | 8.38 | 1.21 | 0.16 | 0.00 | 0.49 | 0.11 | 0.01 | 0.01 | 0.03 | 28.12 | 78.80 |
| Ornans | 1a | 10.83 | 0.04 | 1.30 | 0.21 | 25.14 | 0.20 | 0.92 | 8.31 | 0.47 | 0.12 | 0.01 | 0.17 | 0.05 | 0.00 | 0.00 | 0.01 | 27.09 | 74.87 |
| Ornans | 1a | 11.22 | 0.04 | 1.42 | 0.23 | 25.44 | 0.18 | 0.28 | 8.67 | 0.28 | 0.11 | 0.00 | 0.07 | 0.02 | 0.01 | 0.01 | 0.03 | 27.61 | 75.62 |
| Ornans | 1a | 11.40 | 0.05 | 1.68 | 0.25 | 25.84 | 0.19 | 0.53 | 8.74 | 0.54 | 0.13 | 0.00 | 0.22 | 0.03 | 0.01 | 0.03 | 0.04 | 28.62 | 78.30 |
| Ornans | 1a | 12.06 | 0.05 | 1.84 | 0.40 | 27.22 | 0.21 | 0.11 | 9.18 | 0.53 | 0.10 | 0.00 | 0.21 | 0.03 | 0.01 | 0.02 | 0.03 | 30.10 | 82.10 |
| Ornans | 1a | 11.94 | 0.04 | 1.63 | 0.25 | 27.68 | 0.19 | 1.23 | 9.16 | 0.25 | 0.14 | 0.00 | 0.06 | 0.06 | 0.00 | 0.04 | 0.03 | 29.83 | 82.53 |
| Ornans | 1a | 12.00 | 0.07 | 1.82 | 0.64 | 29.42 | 0.21 | 0.45 | 9.27 | 0.40 | 0.14 | 0.00 | 0.14 | 0.04 | 0.02 | 0.00 | 0.35 | 31.29 | 86.26 |
| Ornans | 1a | 11.91 | 0.05 | 1.56 | 0.23 | 28.99 | 0.22 | 0.84 | 8.94 | 0.45 | 0.12 | 0.00 | 0.05 | 0.04 | 0.00 | 0.02 | 0.03 | 29.94 | 83.39 |
| Ornans | 1a | 11.81 | 0.06 | 1.83 | 0.35 | 28.23 | 0.22 | 0.72 | 9.17 | 0.41 | 0.16 | 0.01 | 0.11 | 0.03 | 0.00 | 0.03 | 0.19 | 30.34 | 83.67 |
| Ornans | 1a | 12.13 | 0.04 | 1.55 | 0.21 | 27.43 | 0.21 | 0.52 | 9.36 | 0.37 | 0.17 | 0.01 | 0.06 | 0.04 | 0.01 | 0.00 | 0.03 | 29.90 | 82.04 |
| Ornans | 1a | 11.29 | 0.05 | 2.00 | 0.32 | 26.41 | 0.20 | 0.78 | 8.58 | 0.30 | 0.13 | 0.01 | 0.06 | 0.03 | 0.01 | 0.03 | 0.06 | 28.68 | 78.94 |
| Ornans | 1a | 11.69 | 0.06 | 2.28 | 0.26 | 28.15 | 0.21 | 0.17 | 8.85 | 0.29 | 0.08 | 0.00 | 0.06 | 0.01 | 0.01 | 0.04 | 0.10 | 29.91 | 82.17 |
| Ornans | 1a | 12.59 | 0.04 | 1.58 | 0.21 | 29.15 | 0.22 | 2.11 | 9.93 | 0.26 | 0.11 | 0.00 | 0.06 | 0.09 | 0.00 | 0.01 | 0.03 | 31.68 | 88.07 |
| Ornans | 1a | 12.25 | 0.03 | 1.94 | 0.25 | 28.27 | 0.21 | 0.09 | 9.38 | 0.30 | 0.10 | 0.00 | 0.07 | 0.02 | 0.00 | 0.02 | 0.04 | 30.51 | 83.48 |
| Ornans | 1a | 11.09 | 0.07 | 1.49 | 0.36 | 23.78 | 0.19 | 0.36 | 8.50 | 0.98 | 0.12 | 0.01 | 0.12 | 0.03 | 0.00 | 0.01 | 0.03 | 27.37 | 74.51 |

Continued on next page

| Sample | Area | Si | Ti | Al | Cr | Fe | Mn | Ni | Mg | Ca | Na | K | P | Co | V | Zn | S | O | Total |
|---|---|---|---|---|---|---|---|---|---|---|---|---|---|---|---|---|---|---|---|
| Ornans | 1a | 11.99 | 0.03 | 1.64 | 0.21 | 26.14 | 0.21 | 0.32 | 9.61 | 0.28 | 0.10 | 0.00 | 0.06 | 0.03 | 0.00 | 0.02 | 0.03 | 29.49 | 80.16 |
| Ornans | 1a | 12.94 | 0.03 | 1.68 | 0.20 | 29.06 | 0.22 | 0.15 | 10.34 | 0.27 | 0.09 | 0.00 | 0.05 | 0.02 | 0.00 | 0.01 | 0.04 | 31.87 | 86.97 |
| Ornans | 1a | 12.57 | 0.06 | 1.58 | 0.22 | 29.37 | 0.21 | 0.11 | 10.17 | 0.26 | 0.09 | 0.00 | 0.04 | 0.03 | 0.01 | 0.03 | 0.10 | 31.44 | 86.29 |
| Ornans | 1a | 12.26 | 0.03 | 1.83 | 0.21 | 27.27 | 0.19 | 0.27 | 9.77 | 0.27 | 0.12 | 0.00 | 0.07 | 0.02 | 0.00 | 0.04 | 0.08 | 30.45 | 82.88 |
| Ornans | 1a | 9.99 | 0.04 | 1.58 | 0.31 | 22.52 | 0.16 | 0.04 | 7.69 | 0.26 | 0.24 | 0.00 | 0.05 | 0.01 | 0.01 | 0.02 | 0.03 | 24.83 | 67.78 |
| Ornans | 1a | 11.52 | 0.04 | 1.51 | 0.41 | 26.88 | 0.21 | 0.20 | 8.96 | 0.58 | 0.25 | 0.00 | 0.35 | 0.02 | 0.00 | 0.02 | 0.06 | 29.29 | 80.30 |
| Ornans | 1a | 11.04 | 0.04 | 0.97 | 0.27 | 25.50 | 0.19 | 4.82 | 9.02 | 0.22 | 0.21 | 0.03 | 0.04 | 0.21 | 0.00 | 0.00 | 0.04 | 28.54 | 81.14 |
| Ornans | 1a | 11.49 | 0.04 | 0.91 | 0.21 | 26.36 | 0.21 | 0.99 | 9.12 | 1.03 | 0.16 | 0.02 | 0.56 | 0.06 | 0.00 | 0.00 | 0.03 | 29.16 | 80.35 |
| Ornans | 1a | 10.78 | 0.04 | 1.11 | 0.13 | 27.50 | 0.20 | 3.67 | 8.76 | 0.21 | 0.22 | 0.01 | 0.03 | 0.17 | 0.01 | 0.01 | 0.07 | 28.41 | 81.33 |
| Ornans | 1a | 11.48 | 0.04 | 1.80 | 0.21 | 26.35 | 0.19 | 0.18 | 9.03 | 0.24 | 0.10 | 0.00 | 0.06 | 0.02 | 0.00 | 0.05 | 0.04 | 28.69 | 78.48 |
| Ornans | 1a | 11.64 | 0.02 | 1.32 | 0.17 | 25.31 | 0.19 | 0.11 | 8.88 | 0.24 | 0.35 | 0.02 | 0.05 | 0.02 | 0.01 | 0.00 | 0.08 | 28.13 | 76.54 |
| Ornans | 1a | 11.22 | 0.03 | 1.84 | 0.23 | 24.30 | 0.19 | 0.08 | 8.74 | 0.23 | 0.30 | 0.02 | 0.07 | 0.00 | 0.00 | 0.03 | 0.02 | 27.67 | 74.97 |
| Ornans | 1a | 11.18 | 0.04 | 1.31 | 0.33 | 25.03 | 0.19 | 0.78 | 8.84 | 0.22 | 0.08 | 0.00 | 0.06 | 0.04 | 0.01 | 0.02 | 0.05 | 27.63 | 75.81 |
| Ornans | 1b | 10.69 | 0.05 | 1.79 | 0.28 | 24.49 | 0.17 | 0.71 | 8.27 | 0.27 | 0.11 | 0.00 | 0.07 | 0.04 | 0.01 | 0.01 | 0.04 | 26.95 | 73.95 |
| Ornans | 1b | 10.08 | 0.06 | 1.32 | 0.26 | 24.27 | 0.17 | 3.26 | 8.10 | 1.28 | 0.24 | 0.01 | 0.74 | 0.14 | 0.00 | 0.02 | 0.07 | 27.75 | 77.77 |
| Ornans | 1b | 10.65 | 0.06 | 1.67 | 0.38 | 24.31 | 0.18 | 0.61 | 8.14 | 0.54 | 0.14 | 0.01 | 0.14 | 0.04 | 0.01 | 0.02 | 0.07 | 26.96 | 73.93 |
| Ornans | 1b | 10.64 | 0.05 | 1.51 | 0.30 | 25.33 | 0.17 | 2.46 | 8.26 | 0.23 | 0.13 | 0.00 | 0.04 | 0.09 | 0.01 | 0.02 | 0.04 | 27.34 | 76.62 |
| Ornans | 1b | 12.06 | 0.05 | 1.60 | 0.27 | 25.19 | 0.20 | 0.24 | 8.37 | 0.89 | 0.12 | 0.00 | 0.06 | 0.02 | 0.00 | 0.03 | 0.05 | 28.74 | 77.89 |
| Ornans | 1b | 10.89 | 0.04 | 1.31 | 0.21 | 24.67 | 0.19 | 1.81 | 8.33 | 0.77 | 0.09 | 0.00 | 0.08 | 0.09 | 0.01 | 0.02 | 0.06 | 27.36 | 75.93 |
| Ornans | 1b | 10.59 | 0.05 | 1.70 | 0.29 | 23.90 | 0.18 | 0.94 | 8.30 | 0.68 | 0.15 | 0.00 | 0.24 | 0.05 | 0.01 | 0.03 | 0.13 | 27.23 | 74.47 |
| Ornans | 1b | 11.56 | 0.05 | 1.68 | 0.28 | 25.72 | 0.20 | 0.34 | 8.86 | 0.30 | 0.12 | 0.01 | 0.09 | 0.03 | 0.00 | 0.02 | 0.03 | 28.52 | 77.81 |
| Ornans | 1b | 11.44 | 0.15 | 2.37 | 0.24 | 24.11 | 0.18 | 0.62 | 8.19 | 1.22 | 0.21 | 0.01 | 0.11 | 0.04 | 0.02 | 0.03 | 0.03 | 28.66 | 77.63 |
| Ornans | 1b | 11.39 | 0.05 | 1.66 | 0.29 | 25.62 | 0.18 | 0.37 | 8.93 | 0.33 | 0.08 | 0.01 | 0.11 | 0.03 | 0.01 | 0.03 | 0.06 | 28.40 | 77.55 |
| Ornans | 1b | 11.32 | 0.04 | 1.51 | 0.23 | 25.59 | 0.19 | 0.18 | 8.75 | 0.93 | 0.18 | 0.01 | 0.39 | 0.02 | 0.01 | 0.02 | 0.03 | 28.57 | 77.97 |
| Ornans | 1b | 11.19 | 0.04 | 1.72 | 0.29 | 25.32 | 0.19 | 0.24 | 8.80 | 0.55 | 0.17 | 0.00 | 0.25 | 0.01 | 0.01 | 0.03 | 0.06 | 28.33 | 77.20 |
| Ornans | 1b | 11.17 | 0.04 | 1.57 | 0.26 | 25.01 | 0.19 | 0.14 | 8.66 | 0.36 | 0.15 | 0.00 | 0.08 | 0.03 | 0.01 | 0.02 | 0.03 | 27.59 | 75.31 |
| Ornans | 1b | 10.43 | 0.04 | 1.48 | 0.26 | 25.32 | 0.18 | 2.57 | 8.38 | 1.21 | 0.16 | 0.00 | 0.49 | 0.11 | 0.01 | 0.01 | 0.03 | 28.12 | 78.80 |
| Ornans | 1b | 10.83 | 0.04 | 1.30 | 0.21 | 25.14 | 0.20 | 0.92 | 8.31 | 0.47 | 0.12 | 0.01 | 0.17 | 0.05 | 0.00 | 0.00 | 0.01 | 27.09 | 74.87 |
| Ornans | 1b | 11.22 | 0.04 | 1.42 | 0.23 | 25.44 | 0.18 | 0.28 | 8.67 | 0.28 | 0.11 | 0.00 | 0.07 | 0.02 | 0.01 | 0.01 | 0.03 | 27.61 | 75.62 |
| Ornans | 1b | 11.40 | 0.05 | 1.68 | 0.25 | 25.84 | 0.19 | 0.53 | 8.74 | 0.54 | 0.13 | 0.00 | 0.22 | 0.03 | 0.01 | 0.03 | 0.04 | 28.62 | 78.30 |
| Ornans | 1b | 12.06 | 0.05 | 1.84 | 0.40 | 27.22 | 0.21 | 0.11 | 9.18 | 0.53 | 0.10 | 0.00 | 0.21 | 0.03 | 0.01 | 0.02 | 0.03 | 30.10 | 82.10 |
| Ornans | 1b | 11.94 | 0.04 | 1.63 | 0.25 | 27.68 | 0.19 | 1.23 | 9.16 | 0.25 | 0.14 | 0.00 | 0.06 | 0.06 | 0.00 | 0.04 | 0.03 | 29.83 | 82.53 |
| Ornans | 1b | 12.00 | 0.07 | 1.82 | 0.64 | 29.42 | 0.21 | 0.45 | 9.27 | 0.40 | 0.14 | 0.00 | 0.14 | 0.04 | 0.02 | 0.00 | 0.35 | 31.29 | 86.26 |
| Ornans | 1b | 11.91 | 0.05 | 1.56 | 0.23 | 28.99 | 0.22 | 0.84 | 8.94 | 0.45 | 0.12 | 0.00 | 0.05 | 0.04 | 0.00 | 0.02 | 0.03 | 29.94 | 83.39 |
| Ornans | 1b | 11.81 | 0.06 | 1.83 | 0.35 | 28.23 | 0.22 | 0.72 | 9.17 | 0.41 | 0.16 | 0.01 | 0.11 | 0.03 | 0.00 | 0.03 | 0.19 | 30.34 | 83.67 |
| Ornans | 1b | 12.13 | 0.04 | 1.55 | 0.21 | 27.43 | 0.21 | 0.52 | 9.36 | 0.37 | 0.17 | 0.01 | 0.06 | 0.04 | 0.01 | 0.00 | 0.03 | 29.90 | 82.04 |
| Ornans | 1b | 11.29 | 0.05 | 2.00 | 0.32 | 26.41 | 0.20 | 0.78 | 8.58 | 0.30 | 0.13 | 0.01 | 0.06 | 0.03 | 0.01 | 0.03 | 0.06 | 28.68 | 78.94 |
| Ornans | 1b | 11.69 | 0.06 | 2.28 | 0.26 | 28.15 | 0.21 | 0.17 | 8.85 | 0.29 | 0.08 | 0.00 | 0.06 | 0.01 | 0.01 | 0.04 | 0.10 | 29.91 | 82.17 |
| Ornans | 1b | 12.59 | 0.04 | 1.58 | 0.21 | 29.15 | 0.22 | 2.11 | 9.93 | 0.26 | 0.11 | 0.00 | 0.06 | 0.09 | 0.00 | 0.01 | 0.03 | 31.68 | 88.07 |
| Ornans | 1b | 12.25 | 0.03 | 1.94 | 0.25 | 28.27 | 0.21 | 0.09 | 9.38 | 0.30 | 0.10 | 0.00 | 0.07 | 0.02 | 0.00 | 0.02 | 0.04 | 30.51 | 83.48 |
| Ornans | 1b | 11.09 | 0.07 | 1.49 | 0.36 | 23.78 | 0.19 | 0.36 | 8.50 | 0.98 | 0.12 | 0.01 | 0.12 | 0.03 | 0.00 | 0.01 | 0.03 | 27.37 | 74.51 |
| Ornans | 1b | 11.99 | 0.03 | 1.64 | 0.21 | 26.14 | 0.21 | 0.32 | 9.61 | 0.28 | 0.10 | 0.00 | 0.06 | 0.03 | 0.00 | 0.02 | 0.03 | 29.49 | 80.16 |
| Ornans | 1b | 12.94 | 0.03 | 1.68 | 0.20 | 29.06 | 0.22 | 0.15 | 10.34 | 0.27 | 0.09 | 0.00 | 0.05 | 0.02 | 0.00 | 0.01 | 0.04 | 31.87 | 86.97 |
| Ornans | 1b | 12.57 | 0.06 | 1.58 | 0.22 | 29.37 | 0.21 | 0.11 | 10.17 | 0.26 | 0.09 | 0.00 | 0.04 | 0.03 | 0.01 | 0.03 | 0.10 | 31.44 | 86.29 |
| Ornans | 1b | 12.26 | 0.03 | 1.83 | 0.21 | 27.27 | 0.19 | 0.27 | 9.77 | 0.27 | 0.12 | 0.00 | 0.07 | 0.02 | 0.00 | 0.04 | 0.08 | 30.45 | 82.88 |
| Ornans | 1b | 9.99 | 0.04 | 1.58 | 0.31 | 22.52 | 0.16 | 0.04 | 7.69 | 0.26 | 0.24 | 0.00 | 0.05 | 0.01 | 0.01 | 0.02 | 0.03 | 24.83 | 67.78 |
| Ornans | 1b | 11.52 | 0.04 | 1.51 | 0.41 | 26.88 | 0.21 | 0.20 | 8.96 | 0.58 | 0.25 | 0.00 | 0.35 | 0.02 | 0.00 | 0.02 | 0.06 | 29.29 | 80.30 |
| Ornans | 1b | 11.04 | 0.04 | 0.97 | 0.27 | 25.50 | 0.19 | 4.82 | 9.02 | 0.22 | 0.21 | 0.03 | 0.04 | 0.21 | 0.00 | 0.00 | 0.04 | 28.54 | 81.14 |
| Ornans | 1b | 11.49 | 0.04 | 0.91 | 0.21 | 26.36 | 0.21 | 0.99 | 9.12 | 1.03 | 0.16 | 0.02 | 0.56 | 0.06 | 0.00 | 0.00 | 0.03 | 29.16 | 80.35 |
| Ornans | 1b | 10.78 | 0.04 | 1.11 | 0.13 | 27.50 | 0.20 | 3.67 | 8.76 | 0.21 | 0.22 | 0.01 | 0.03 | 0.17 | 0.01 | 0.01 | 0.07 | 28.41 | 81.33 |
| Ornans | 1b | 11.48 | 0.04 | 1.80 | 0.21 | 26.35 | 0.19 | 0.18 | 9.03 | 0.24 | 0.10 | 0.00 | 0.06 | 0.02 | 0.00 | 0.05 | 0.04 | 28.69 | 78.48 |
| Ornans | 1b | 11.64 | 0.02 | 1.32 | 0.17 | 25.31 | 0.19 | 0.11 | 8.88 | 0.24 | 0.35 | 0.02 | 0.05 | 0.02 | 0.01 | 0.00 | 0.08 | 28.13 | 76.54 |
| Ornans | 1b | 11.22 | 0.03 | 1.84 | 0.23 | 24.30 | 0.19 | 0.08 | 8.74 | 0.23 | 0.30 | 0.02 | 0.07 | 0.00 | 0.00 | 0.03 | 0.02 | 27.67 | 74.97 |
| Ornans | 1b | 11.18 | 0.04 | 1.31 | 0.33 | 25.03 | 0.19 | 0.78 | 8.84 | 0.22 | 0.08 | 0.00 | 0.06 | 0.04 | 0.01 | 0.02 | 0.05 | 27.63 | 75.81 |
| Ornans | 2a | 13.54 | 0.02 | 1.05 | 0.14 | 28.52 | 0.21 | 0.05 | 10.99 | 0.23 | 0.14 | 0.00 | 0.05 | 0.02 | 0.00 | 0.01 | 0.04 | 32.20 | 87.21 |
| Ornans | 2a | 12.39 | 0.04 | 1.89 | 0.20 | 27.58 | 0.18 | 0.06 | 9.93 | 0.27 | 0.26 | 0.01 | 0.05 | 0.01 | 0.02 | 0.04 | 0.26 | 31.11 | 84.30 |
| Ornans | 2a | 12.20 | 0.03 | 1.71 | 0.21 | 27.64 | 0.20 | 0.08 | 9.72 | 0.24 | 0.18 | 0.00 | 0.05 | 0.01 | 0.00 | 0.02 | 0.05 | 30.24 | 82.58 |
| Ornans | 2a | 12.20 | 0.03 | 2.13 | 0.25 | 26.59 | 0.21 | 1.19 | 8.98 | 0.28 | 0.75 | 0.07 | 0.06 | 0.05 | 0.00 | 0.03 | 0.03 | 30.38 | 83.23 |

Continued on next page

| Sample | Area | Si | Ti | Al | Cr | Fe | Mn | Ni | Mg | Ca | Na | K | P | Co | V | Zn | S | O | Total |
|---|---|---|---|---|---|---|---|---|---|---|---|---|---|---|---|---|---|---|---|
| Ornans | 2a | 13.45 | 0.03 | 3.25 | 0.17 | 23.80 | 0.18 | 0.10 | 8.14 | 0.33 | 2.23 | 0.24 | 0.06 | 0.01 | 0.00 | 0.01 | 0.03 | 31.65 | 83.68 |
| Ornans | 2a | 12.80 | 0.05 | 2.28 | 0.22 | 25.55 | 0.20 | 0.16 | 8.69 | 0.32 | 1.40 | 0.14 | 0.07 | 0.01 | 0.00 | 0.01 | 0.02 | 30.66 | 82.58 |
| Ornans | 2a | 11.95 | 0.04 | 2.16 | 0.23 | 26.49 | 0.21 | 2.07 | 8.88 | 0.26 | 0.74 | 0.06 | 0.05 | 0.08 | 0.01 | 0.02 | 0.03 | 30.24 | 83.52 |
| Ornans | 2a | 12.91 | 0.05 | 2.72 | 0.23 | 24.98 | 0.17 | 0.11 | 8.54 | 0.31 | 1.43 | 0.16 | 0.07 | 0.02 | 0.00 | 0.00 | 0.02 | 30.91 | 82.63 |
| Ornans | 2a | 12.84 | 0.02 | 2.08 | 0.20 | 25.65 | 0.19 | 0.37 | 8.88 | 0.30 | 0.87 | 0.10 | 0.06 | 0.01 | 0.01 | 0.01 | 0.03 | 30.52 | 82.14 |
| Ornans | 2a | 11.28 | 0.03 | 2.76 | 0.26 | 26.10 | 0.19 | 0.96 | 8.85 | 0.28 | 0.32 | 0.04 | 0.03 | 0.04 | 0.00 | 0.03 | 0.03 | 29.41 | 80.61 |
| Ornans | 2a | 12.12 | 0.03 | 1.74 | 0.20 | 26.14 | 0.19 | 1.26 | 8.89 | 0.49 | 0.69 | 0.05 | 0.04 | 0.05 | 0.01 | 0.01 | 0.03 | 29.78 | 81.72 |
| Ornans | 2a | 12.59 | 0.07 | 0.53 | 0.25 | 31.49 | 0.22 | 2.14 | 10.23 | 0.20 | 0.12 | 0.00 | 0.04 | 0.10 | 0.01 | 0.01 | 0.02 | 31.62 | 89.64 |
| Ornans | 2a | 11.80 | 0.04 | 1.99 | 0.26 | 27.50 | 0.21 | 0.21 | 9.39 | 0.23 | 0.12 | 0.02 | 0.05 | 0.01 | 0.01 | 0.03 | 0.03 | 29.80 | 81.70 |
| Ornans | 2a | 11.87 | 0.04 | 2.11 | 0.21 | 26.86 | 0.19 | 0.55 | 9.29 | 0.28 | 0.27 | 0.00 | 0.06 | 0.04 | 0.00 | 0.03 | 0.04 | 29.91 | 81.75 |
| Ornans | 2a | 12.39 | 0.02 | 1.74 | 0.24 | 28.27 | 0.22 | 0.41 | 9.65 | 0.32 | 0.15 | 0.00 | 0.05 | 0.03 | 0.01 | 0.03 | 0.04 | 30.75 | 84.32 |
| Ornans | 2a | 13.24 | 0.04 | 2.40 | 0.34 | 24.31 | 0.21 | 0.28 | 8.93 | 1.73 | 0.77 | 0.05 | 0.09 | 0.01 | 0.01 | 0.02 | 0.02 | 31.52 | 83.97 |
| Ornans | 2a | 11.94 | 0.05 | 1.62 | 0.19 | 28.14 | 0.20 | 0.45 | 9.24 | 0.24 | 0.32 | 0.02 | 0.05 | 0.02 | 0.02 | 0.03 | 0.03 | 29.85 | 82.41 |
| Ornans | 2a | 12.63 | 0.03 | 1.35 | 0.55 | 28.14 | 0.19 | 0.11 | 9.78 | 0.41 | 0.16 | 0.00 | 0.04 | 0.00 | 0.00 | 0.00 | 0.02 | 30.76 | 84.17 |
| Ornans | 2a | 12.86 | 0.02 | 1.42 | 0.31 | 28.36 | 0.22 | 0.18 | 10.11 | 0.28 | 0.18 | 0.01 | 0.08 | 0.02 | 0.00 | 0.00 | 0.03 | 31.29 | 85.37 |
| Ornans | 2a | 12.80 | 0.02 | 1.09 | 0.18 | 27.82 | 0.22 | 0.38 | 10.16 | 0.27 | 0.15 | 0.00 | 0.05 | 0.03 | 0.01 | 0.00 | 0.02 | 30.75 | 83.95 |
| Ornans | 2a | 13.49 | 0.02 | 0.90 | 0.15 | 29.39 | 0.23 | 0.32 | 10.65 | 0.27 | 0.18 | 0.01 | 0.09 | 0.03 | 0.00 | 0.00 | 0.04 | 32.20 | 87.97 |
| Ornans | 2a | 11.86 | 0.02 | 1.35 | 0.19 | 26.58 | 0.21 | 0.07 | 9.36 | 0.33 | 0.20 | 0.01 | 0.07 | 0.01 | 0.01 | 0.04 | 0.03 | 29.03 | 79.37 |
| Ornans | 2b | 13.08 | 0.03 | 1.46 | 0.20 | 28.43 | 0.22 | 0.16 | 10.31 | 0.28 | 0.10 | 0.01 | 0.06 | 0.02 | 0.01 | 0.02 | 0.02 | 31.63 | 86.04 |
| Ornans | 2b | 12.51 | 0.02 | 1.82 | 0.24 | 28.29 | 0.20 | 1.15 | 10.16 | 0.26 | 0.04 | 0.00 | 0.05 | 0.06 | 0.01 | 0.03 | 0.02 | 31.41 | 86.27 |
| Ornans | 2b | 13.20 | 0.03 | 1.00 | 0.30 | 27.73 | 0.21 | 0.04 | 10.25 | 0.56 | 0.08 | 0.00 | 0.04 | 0.01 | 0.00 | 0.00 | 0.01 | 31.18 | 84.64 |
| Ornans | 2b | 12.89 | 0.03 | 1.99 | 0.21 | 28.23 | 0.21 | 0.08 | 10.43 | 0.26 | 0.07 | 0.01 | 0.06 | 0.01 | 0.00 | 0.07 | 0.01 | 31.85 | 86.41 |
| Ornans | 2b | 13.09 | 0.02 | 1.54 | 0.17 | 26.82 | 0.22 | 0.08 | 10.01 | 0.28 | 0.64 | 0.03 | 0.04 | 0.02 | 0.00 | 0.00 | 0.03 | 31.18 | 84.17 |
| Ornans | 2b | 12.89 | 0.03 | 1.71 | 0.19 | 25.84 | 0.20 | 0.20 | 9.75 | 0.30 | 0.69 | 0.04 | 0.06 | 0.01 | 0.00 | 0.01 | 0.02 | 30.73 | 82.67 |
| Ornans | 2b | 12.33 | 0.04 | 2.42 | 0.24 | 24.76 | 0.18 | 0.07 | 9.40 | 0.85 | 0.25 | 0.00 | 0.07 | 0.01 | 0.00 | 0.02 | 0.02 | 30.25 | 80.91 |
| Ornans | 2b | 12.88 | 0.03 | 1.77 | 0.19 | 28.40 | 0.21 | 0.16 | 10.38 | 0.28 | 0.07 | 0.00 | 0.06 | 0.02 | 0.00 | 0.03 | 0.03 | 31.69 | 86.20 |
| Ornans | 2b | 12.39 | 0.03 | 1.27 | 0.13 | 27.18 | 0.20 | 0.85 | 9.98 | 0.23 | 0.06 | 0.00 | 0.02 | 0.03 | 0.01 | 0.04 | 0.05 | 30.21 | 82.68 |
| Ornans | 2b | 12.24 | 0.04 | 1.95 | 0.19 | 25.99 | 0.18 | 0.63 | 9.71 | 0.28 | 0.40 | 0.02 | 0.05 | 0.03 | 0.01 | 0.04 | 0.01 | 30.23 | 82.00 |
| Ornans | 2b | 12.89 | 0.03 | 1.62 | 0.17 | 28.39 | 0.22 | 0.47 | 10.08 | 0.45 | 0.21 | 0.02 | 0.04 | 0.02 | 0.00 | 0.02 | 0.05 | 31.59 | 86.27 |
| Ornans | 2b | 11.59 | 0.04 | 2.51 | 0.26 | 27.24 | 0.21 | 2.38 | 9.12 | 0.31 | 0.20 | 0.03 | 0.07 | 0.10 | 0.00 | 0.05 | 0.02 | 30.46 | 84.59 |
| Ornans | 2b | 12.52 | 0.03 | 1.81 | 0.19 | 27.30 | 0.21 | 0.43 | 9.68 | 0.27 | 0.29 | 0.01 | 0.04 | 0.04 | 0.00 | 0.01 | 0.03 | 30.68 | 83.54 |
| Ornans | 2b | 12.74 | 0.05 | 1.65 | 0.18 | 25.87 | 0.20 | 0.25 | 9.49 | 0.27 | 0.53 | 0.08 | 0.04 | 0.02 | 0.00 | 0.01 | 0.02 | 30.28 | 81.68 |
| Ornans | 2b | 12.66 | 0.05 | 1.68 | 0.17 | 25.72 | 0.18 | 0.12 | 9.28 | 0.31 | 0.71 | 0.06 | 0.06 | 0.01 | 0.00 | 0.00 | 0.02 | 30.09 | 81.12 |
| Ornans | 2b | 12.67 | 0.04 | 2.04 | 0.20 | 25.87 | 0.19 | 0.09 | 9.09 | 0.29 | 0.86 | 0.10 | 0.06 | 0.00 | 0.00 | 0.00 | 0.03 | 30.40 | 81.93 |
| Ornans | 2b | 12.42 | 0.05 | 3.18 | 0.29 | 25.59 | 0.18 | 0.19 | 8.56 | 0.35 | 1.56 | 0.14 | 0.07 | 0.02 | 0.01 | 0.03 | 0.41 | 31.64 | 84.69 |
| Ornans | 2b | 12.71 | 0.03 | 3.19 | 0.23 | 25.93 | 0.22 | 0.13 | 8.55 | 0.34 | 1.92 | 0.15 | 0.07 | 0.02 | 0.00 | 0.02 | 0.26 | 31.94 | 85.71 |
| Ornans | 2b | 12.99 | 0.06 | 3.56 | 0.36 | 23.82 | 0.18 | 0.08 | 8.01 | 0.96 | 2.02 | 0.26 | 0.52 | 0.01 | 0.00 | 0.01 | 0.13 | 32.35 | 85.32 |
| Ornans | 2b | 13.29 | 0.07 | 2.46 | 0.19 | 27.04 | 0.20 | 0.08 | 9.18 | 0.31 | 1.46 | 0.10 | 0.07 | 0.01 | 0.00 | 0.01 | 0.04 | 32.14 | 86.65 |
| Ornans | 2b | 12.52 | 0.04 | 2.27 | 0.23 | 26.73 | 0.21 | 1.57 | 9.13 | 0.28 | 1.27 | 0.09 | 0.06 | 0.08 | 0.00 | 0.02 | 0.04 | 31.30 | 85.84 |
| Ornans | 2b | 13.93 | 0.03 | 3.43 | 0.17 | 25.11 | 0.20 | 0.58 | 8.57 | 0.37 | 2.54 | 0.26 | 0.05 | 0.03 | 0.00 | 0.00 | 0.04 | 33.29 | 88.60 |
| Ornans | 2b | 13.40 | 0.03 | 2.34 | 0.16 | 25.51 | 0.20 | 0.15 | 8.84 | 0.32 | 1.32 | 0.18 | 0.05 | 0.01 | 0.00 | 0.00 | 0.02 | 31.41 | 83.94 |
| Ornans | 2b | 12.36 | 0.03 | 2.23 | 0.26 | 28.06 | 0.21 | 0.99 | 9.68 | 0.70 | 0.42 | 0.03 | 0.32 | 0.05 | 0.01 | 0.04 | 0.04 | 31.87 | 87.30 |
| Ornans | 2b | 12.04 | 0.03 | 1.76 | 0.23 | 26.68 | 0.20 | 0.62 | 9.06 | 0.26 | 0.47 | 0.04 | 0.06 | 0.02 | 0.00 | 0.02 | 0.11 | 29.78 | 81.38 |
| Ornans | 2b | 12.95 | 0.03 | 2.33 | 0.19 | 25.77 | 0.21 | 0.19 | 8.88 | 0.30 | 1.32 | 0.12 | 0.06 | 0.01 | 0.00 | 0.00 | 0.03 | 31.01 | 83.40 |
| Ornans | 2b | 12.94 | 0.05 | 2.64 | 0.18 | 25.43 | 0.17 | 0.69 | 8.65 | 0.30 | 1.75 | 0.15 | 0.04 | 0.04 | 0.00 | 0.01 | 0.02 | 31.29 | 84.35 |
| Ornans | 3a | 13.73 | 0.04 | 1.47 | 0.17 | 27.48 | 0.21 | 0.06 | 11.20 | 0.35 | 0.74 | 0.04 | 0.06 | 0.02 | 0.01 | 0.02 | 0.02 | 32.91 | 88.53 |
| Ornans | 3a | 11.11 | 0.04 | 2.44 | 0.20 | 26.14 | 0.15 | 4.00 | 10.01 | 0.23 | 0.12 | 0.00 | 0.06 | 0.16 | 0.00 | 0.02 | 0.03 | 30.47 | 85.18 |
| Ornans | 3a | 12.47 | 0.04 | 1.94 | 0.21 | 26.97 | 0.17 | 1.90 | 10.86 | 0.23 | 0.15 | 0.00 | 0.07 | 0.09 | 0.01 | 0.03 | 0.03 | 31.83 | 87.00 |
| Ornans | 3a | 12.39 | 0.03 | 1.94 | 0.18 | 26.40 | 0.18 | 0.15 | 10.48 | 0.25 | 0.15 | 0.00 | 0.07 | 0.01 | 0.01 | 0.03 | 0.24 | 31.13 | 83.64 |
| Ornans | 3a | 12.50 | 0.04 | 2.29 | 0.17 | 27.12 | 0.20 | 0.19 | 10.76 | 0.28 | 0.09 | 0.00 | 0.05 | 0.01 | 0.01 | 0.03 | 0.06 | 31.65 | 85.45 |
| Ornans | 3a | 13.29 | 0.04 | 1.25 | 0.16 | 26.25 | 0.21 | 0.10 | 11.63 | 0.27 | 0.10 | 0.02 | 0.05 | 0.02 | 0.00 | 0.01 | 0.02 | 31.86 | 85.28 |
| Ornans | 3a | 13.49 | 0.04 | 1.44 | 0.15 | 25.38 | 0.19 | 0.04 | 11.07 | 0.52 | 0.43 | 0.04 | 0.05 | 0.01 | 0.00 | 0.02 | 0.02 | 31.84 | 84.73 |
| Ornans | 3a | 12.76 | 0.04 | 1.50 | 0.17 | 25.66 | 0.20 | 0.36 | 10.90 | 0.26 | 0.26 | 0.00 | 0.05 | 0.02 | 0.01 | 0.02 | 0.02 | 30.97 | 83.20 |
| Ornans | 3a | 12.25 | 0.03 | 2.12 | 0.20 | 25.34 | 0.18 | 0.52 | 10.53 | 0.26 | 0.14 | 0.01 | 0.08 | 0.04 | 0.01 | 0.04 | 0.03 | 30.68 | 82.46 |
| Ornans | 3a | 12.67 | 0.04 | 1.40 | 0.16 | 25.46 | 0.19 | 0.23 | 11.05 | 0.25 | 0.22 | 0.02 | 0.07 | 0.02 | 0.00 | 0.01 | 0.03 | 30.80 | 82.62 |
| Ornans | 3a | 12.66 | 0.04 | 1.90 | 0.19 | 25.51 | 0.19 | 0.16 | 11.00 | 0.26 | 0.23 | 0.01 | 0.07 | 0.02 | 0.01 | 0.01 | 0.04 | 31.23 | 83.53 |
| Ornans | 3a | 12.58 | 0.02 | 1.59 | 0.20 | 26.63 | 0.20 | 0.08 | 10.72 | 0.25 | 0.17 | 0.00 | 0.07 | 0.02 | 0.00 | 0.03 | 0.02 | 30.92 | 83.50 |
| Ornans | 3a | 13.16 | 0.06 | 1.84 | 0.19 | 27.17 | 0.19 | 0.08 | 11.17 | 0.45 | 0.11 | 0.00 | 0.04 | 0.00 | 0.01 | 0.03 | 0.02 | 32.28 | 86.80 |

Continued on next page

| Sample | Area | Si | Ti | Al | Cr | Fe | Mn | Ni | Mg | Ca | Na | K | P | Co | V | Zn | S | O | Total |
|---|---|---|---|---|---|---|---|---|---|---|---|---|---|---|---|---|---|---|---|
| Ornans | 3a | 12.90 | 0.04 | 1.67 | 0.18 | 26.05 | 0.20 | 0.08 | 11.01 | 0.27 | 0.28 | 0.01 | 0.05 | 0.01 | 0.00 | 0.02 | 0.03 | 31.42 | 84.22 |
| Ornans | 3a | 12.41 | 0.04 | 1.75 | 0.13 | 24.46 | 0.19 | 0.05 | 10.47 | 0.25 | 0.25 | 0.03 | 0.06 | 0.02 | 0.00 | 0.02 | 0.04 | 30.10 | 80.27 |
| Ornans | 3a | 12.35 | 0.04 | 2.31 | 0.23 | 26.50 | 0.18 | 0.73 | 10.66 | 0.24 | 0.20 | 0.00 | 0.08 | 0.04 | 0.00 | 0.03 | 0.05 | 31.48 | 85.12 |
| Ornans | 3a | 12.68 | 0.03 | 2.05 | 0.19 | 25.80 | 0.17 | 0.22 | 10.84 | 0.26 | 0.18 | 0.01 | 0.06 | 0.00 | 0.00 | 0.03 | 0.04 | 31.34 | 83.90 |
| Ornans | 3a | 12.11 | 0.05 | 1.75 | 0.19 | 27.28 | 0.18 | 2.75 | 10.73 | 0.27 | 0.11 | 0.01 | 0.06 | 0.12 | 0.01 | 0.01 | 0.22 | 31.76 | 87.61 |
| Ornans | 3a | 12.27 | 0.04 | 1.79 | 0.19 | 25.07 | 0.19 | 0.24 | 10.50 | 0.26 | 0.22 | 0.00 | 0.07 | 0.01 | 0.01 | 0.03 | 0.04 | 30.25 | 81.18 |
| Ornans | 3a | 13.42 | 0.03 | 1.22 | 0.11 | 27.80 | 0.19 | 2.02 | 11.64 | 0.20 | 0.15 | 0.00 | 0.04 | 0.08 | 0.00 | 0.01 | 0.03 | 32.94 | 89.88 |
| Ornans | 3a | 12.70 | 0.03 | 1.19 | 0.13 | 26.78 | 0.18 | 1.07 | 10.81 | 0.21 | 0.16 | 0.00 | 0.04 | 0.05 | 0.01 | 0.00 | 0.12 | 31.13 | 84.61 |
| Ornans | 3a | 12.65 | 0.03 | 1.75 | 0.22 | 27.01 | 0.18 | 1.89 | 11.09 | 0.20 | 0.07 | 0.00 | 0.04 | 0.08 | 0.01 | 0.02 | 0.03 | 31.92 | 87.19 |
| Ornans | 3a | 12.68 | 0.03 | 2.05 | 0.26 | 26.52 | 0.19 | 0.65 | 10.80 | 0.24 | 0.10 | 0.02 | 0.06 | 0.04 | 0.00 | 0.03 | 0.05 | 31.65 | 85.37 |
| Ornans | 3a | 12.77 | 0.04 | 1.60 | 0.24 | 27.21 | 0.20 | 1.54 | 10.99 | 0.25 | 0.13 | 0.00 | 0.08 | 0.07 | 0.00 | 0.03 | 0.03 | 31.93 | 87.11 |
| Ornans | 3a | 12.26 | 0.03 | 1.65 | 0.16 | 25.64 | 0.20 | 0.31 | 10.15 | 0.21 | 0.16 | 0.00 | 0.05 | 0.02 | 0.01 | 0.02 | 0.13 | 30.12 | 81.12 |
| Ornans | 3a | 12.35 | 0.05 | 1.61 | 0.25 | 26.75 | 0.18 | 1.94 | 10.80 | 0.25 | 0.11 | 0.02 | 0.05 | 0.08 | 0.01 | 0.01 | 0.03 | 31.29 | 85.78 |
| Ornans | 3a | 11.41 | 0.03 | 2.14 | 0.30 | 26.55 | 0.17 | 5.51 | 10.04 | 0.38 | 0.11 | 0.00 | 0.03 | 0.21 | 0.01 | 0.04 | 0.03 | 31.18 | 88.14 |
| Ornans | 3a | 12.04 | 0.04 | 2.15 | 0.24 | 27.71 | 0.18 | 2.19 | 10.46 | 0.24 | 0.12 | 0.00 | 0.04 | 0.09 | 0.00 | 0.01 | 0.31 | 31.92 | 87.74 |
| Ornans | 3a | 12.91 | 0.05 | 1.60 | 0.19 | 27.18 | 0.20 | 0.09 | 10.93 | 0.21 | 0.24 | 0.01 | 0.06 | 0.02 | 0.01 | 0.02 | 0.03 | 31.62 | 85.37 |
| Ornans | 3a | 13.30 | 0.04 | 1.43 | 0.18 | 28.03 | 0.21 | 0.40 | 11.43 | 0.24 | 0.04 | 0.00 | 0.05 | 0.03 | 0.01 | 0.02 | 0.02 | 32.49 | 87.92 |
| Ornans | 3b | 12.58 | 0.06 | 2.03 | 0.38 | 25.33 | 0.18 | 0.06 | 11.11 | 0.33 | 0.35 | 0.00 | 0.07 | 0.00 | 0.00 | 0.02 | 0.02 | 31.37 | 83.89 |
| Ornans | 3b | 15.51 | 0.05 | 1.17 | 0.26 | 28.44 | 0.22 | 0.05 | 12.94 | 0.39 | 0.60 | 0.09 | 0.05 | 0.00 | 0.00 | 0.00 | 0.01 | 36.07 | 95.85 |
| Ornans | 3b | 13.02 | 0.04 | 1.61 | 0.16 | 26.56 | 0.19 | 0.14 | 10.97 | 0.27 | 0.15 | 0.04 | 0.05 | 0.03 | 0.01 | 0.01 | 0.03 | 31.59 | 84.87 |
| Ornans | 3b | 11.77 | 0.03 | 1.83 | 0.19 | 24.27 | 0.19 | 0.06 | 9.26 | 0.30 | 0.50 | 0.10 | 0.05 | 0.02 | 0.00 | 0.02 | 0.03 | 28.69 | 77.31 |
| Ornans | 3b | 13.08 | 0.04 | 2.02 | 0.21 | 25.26 | 0.18 | 0.11 | 10.28 | 0.32 | 0.95 | 0.09 | 0.08 | 0.03 | 0.01 | 0.01 | 0.02 | 31.53 | 84.22 |
| Ornans | 3b | 12.93 | 0.03 | 1.94 | 0.18 | 24.74 | 0.19 | 0.11 | 10.31 | 0.29 | 0.75 | 0.08 | 0.06 | 0.03 | 0.00 | 0.01 | 0.02 | 31.05 | 82.72 |
| Ornans | 3b | 12.65 | 0.04 | 1.81 | 0.24 | 26.13 | 0.19 | 0.57 | 10.76 | 0.28 | 0.22 | 0.01 | 0.08 | 0.02 | 0.00 | 0.02 | 0.04 | 31.30 | 84.36 |
| Ornans | 3b | 12.16 | 0.04 | 1.70 | 0.37 | 26.07 | 0.18 | 0.36 | 10.32 | 0.26 | 0.17 | 0.00 | 0.05 | 0.03 | 0.01 | 0.02 | 0.03 | 30.28 | 82.05 |
| Ornans | 3b | 12.97 | 0.03 | 1.52 | 0.16 | 27.71 | 0.21 | 0.17 | 11.05 | 0.27 | 0.14 | 0.00 | 0.07 | 0.02 | 0.00 | 0.05 | 0.02 | 31.84 | 86.23 |
| Ornans | 3b | 11.93 | 0.04 | 1.60 | 0.15 | 25.50 | 0.19 | 0.09 | 9.90 | 0.26 | 0.69 | 0.00 | 0.07 | 0.03 | 0.01 | 0.02 | 0.03 | 29.52 | 80.03 |
| Ornans | 3b | 12.97 | 0.03 | 1.38 | 0.12 | 26.73 | 0.21 | 0.12 | 10.93 | 0.23 | 0.17 | 0.02 | 0.04 | 0.01 | 0.00 | 0.01 | 0.05 | 31.30 | 84.32 |
| Ornans | 3b | 12.63 | 0.08 | 1.46 | 0.19 | 28.05 | 0.19 | 0.09 | 10.84 | 0.21 | 0.08 | 0.00 | 0.04 | 0.01 | 0.01 | 0.02 | 0.01 | 31.27 | 85.18 |
| Ornans | 3b | 12.66 | 0.02 | 0.78 | 0.17 | 26.55 | 0.20 | 0.04 | 10.54 | 0.19 | 0.07 | 0.01 | 0.03 | 0.01 | 0.00 | 0.01 | 0.02 | 30.00 | 81.30 |
| Ornans | 3b | 13.10 | 0.02 | 2.06 | 0.17 | 24.59 | 0.19 | 0.17 | 10.46 | 0.25 | 0.80 | 0.05 | 0.04 | 0.01 | 0.01 | 0.03 | 0.02 | 31.36 | 83.33 |
| Ornans | 3b | 10.59 | 0.02 | 1.47 | 0.15 | 19.62 | 0.14 | 0.06 | 8.72 | 0.20 | 0.41 | 0.04 | 0.06 | 0.01 | 0.00 | 0.00 | 0.02 | 25.22 | 66.73 |
| Ornans | 3b | 11.97 | 0.03 | 1.48 | 0.15 | 22.35 | 0.16 | 0.03 | 9.77 | 0.24 | 0.41 | 0.03 | 0.05 | 0.01 | 0.00 | 0.01 | 0.02 | 28.28 | 74.99 |
| Ornans | 3b | 11.35 | 0.03 | 1.41 | 0.10 | 23.25 | 0.16 | 0.05 | 8.87 | 0.21 | 0.40 | 0.05 | 0.02 | 0.00 | 0.01 | -0.01 | 0.12 | 27.27 | 73.29 |
| Ornans | 3b | 10.47 | 0.03 | 2.20 | 0.19 | 21.27 | 0.16 | 0.40 | 8.57 | 0.22 | 0.14 | 0.01 | 0.05 | 0.03 | 0.00 | 0.04 | 0.02 | 26.13 | 69.93 |
| Ornans | 3b | 12.19 | 0.05 | 1.77 | 0.36 | 27.18 | 0.17 | 0.07 | 10.11 | 0.21 | 0.20 | 0.03 | 0.03 | 0.00 | 0.01 | 0.01 | 0.11 | 30.54 | 83.04 |
| Ornans | 3b | 11.53 | 0.18 | 2.40 | 0.12 | 23.08 | 0.15 | 0.73 | 8.69 | 0.80 | 0.84 | 0.14 | 0.02 | 0.03 | 0.03 | 0.03 | 0.08 | 28.86 | 77.71 |
| Ornans | 3b | 8.72 | 0.09 | 8.51 | 0.12 | 19.12 | 0.12 | 0.04 | 6.30 | 0.37 | 1.61 | 0.23 | 0.03 | 0.02 | 0.05 | 0.14 | 0.04 | 28.23 | 73.74 |
| Ornans | 3b | 11.84 | 0.05 | 1.63 | 0.34 | 23.89 | 0.17 | 0.97 | 9.72 | 1.13 | 0.11 | 0.01 | 0.16 | 0.05 | 0.01 | 0.01 | 0.18 | 29.68 | 79.95 |
| Ornans | 3b | 11.79 | 0.04 | 2.09 | 0.35 | 24.94 | 0.19 | 0.14 | 9.94 | 0.27 | 0.10 | 0.00 | 0.06 | 0.01 | 0.00 | 0.03 | 0.02 | 29.53 | 79.50 |
| Ornans | 3b | 12.47 | 0.04 | 1.45 | 0.32 | 24.45 | 0.19 | 0.19 | 10.40 | 0.29 | 0.15 | 0.03 | 0.07 | 0.02 | 0.00 | 0.02 | 0.03 | 29.93 | 80.05 |
| Ornans | 3b | 12.14 | 0.04 | 1.67 | 0.23 | 26.46 | 0.18 | 2.15 | 10.52 | 0.27 | 0.09 | 0.00 | 0.06 | 0.09 | 0.01 | 0.02 | 0.11 | 31.02 | 85.06 |
| Ornans | 3b | 11.99 | 0.05 | 1.67 | 0.59 | 28.22 | 0.18 | 0.76 | 10.55 | 1.44 | 0.19 | 0.02 | 0.91 | 0.04 | 0.01 | 0.02 | 0.78 | 33.76 | 91.18 |
| Ornans | 3b | 13.57 | 0.02 | 1.11 | 0.13 | 26.09 | 0.16 | 0.47 | 9.87 | 2.73 | 0.09 | 0.00 | 0.03 | 0.03 | 0.00 | 0.01 | 1.13 | 33.54 | 88.98 |
| Ornans | 3b | 14.78 | 0.10 | 1.61 | 0.30 | 30.79 | 0.22 | 0.05 | 12.59 | 0.75 | 0.07 | 0.00 | 0.11 | 0.01 | 0.01 | 0.00 | 0.01 | 36.15 | 97.55 |
| Ornans | 3b | 12.68 | 0.05 | 1.10 | 0.20 | 28.02 | 0.20 | 3.11 | 11.09 | 0.29 | 0.09 | 0.01 | 0.03 | 0.13 | 0.00 | 0.02 | 0.03 | 32.05 | 89.10 |
| Ornans | 3b | 13.66 | 0.03 | 1.48 | 0.42 | 24.37 | 0.18 | 0.07 | 10.67 | 1.71 | 0.08 | 0.02 | 0.07 | 0.01 | 0.01 | 0.03 | 0.02 | 32.02 | 84.85 |
| Ornans | 3b | 12.58 | 0.05 | 1.89 | 0.28 | 26.50 | 0.19 | 0.27 | 10.73 | 0.33 | 0.08 | 0.00 | 0.06 | 0.02 | 0.00 | 0.02 | 0.03 | 31.25 | 84.28 |
| Ornans | 3b | 12.59 | 0.04 | 1.42 | 0.21 | 25.55 | 0.19 | 0.42 | 10.76 | 0.32 | 0.10 | 0.00 | 0.06 | 0.04 | 0.00 | 0.00 | 0.01 | 30.57 | 82.28 |
| Ornans | 3b | 11.99 | 0.04 | 1.36 | 0.24 | 24.27 | 0.17 | 0.64 | 10.23 | 0.26 | 0.06 | 0.01 | 0.05 | 0.02 | 0.00 | 0.02 | 0.03 | 29.17 | 78.56 |
| Ornans | 3b | 13.07 | 0.06 | 2.29 | 0.26 | 26.60 | 0.18 | 0.10 | 10.93 | 0.34 | 0.29 | 0.03 | 0.08 | 0.01 | 0.01 | 0.03 | 0.03 | 32.40 | 86.71 |
| Ornans | 3b | 13.27 | 0.08 | 1.78 | 0.36 | 26.39 | 0.20 | 0.93 | 10.98 | 0.84 | 0.08 | 0.01 | 0.06 | 0.03 | 0.01 | 0.02 | 0.02 | 32.52 | 87.58 |
| Ornans | 4a | 12.02 | 0.06 | 3.26 | 0.10 | 25.12 | 0.17 | 0.09 | 7.54 | 0.25 | 2.57 | 0.24 | 0.02 | 0.02 | 0.01 | 0.00 | 0.66 | 30.99 | 83.12 |
| Ornans | 4a | 12.88 | 0.03 | 4.10 | 0.18 | 21.26 | 0.15 | 0.04 | 7.42 | 0.30 | 3.27 | 0.32 | 0.03 | 0.03 | 0.00 | 0.00 | 0.69 | 31.86 | 82.56 |
| Ornans | 4a | 11.56 | 0.04 | 2.45 | 0.15 | 21.60 | 0.16 | 0.05 | 8.48 | 0.32 | 0.93 | 0.08 | 0.02 | 0.00 | 0.00 | 0.02 | 0.03 | 27.82 | 73.71 |
| Ornans | 4a | 12.16 | 0.04 | 2.98 | 0.20 | 24.55 | 0.16 | 0.03 | 9.25 | 0.31 | 0.71 | 0.09 | 0.04 | 0.01 | 0.01 | 0.01 | 0.27 | 30.66 | 81.48 |
| Ornans | 4a | 11.39 | 0.03 | 2.08 | 0.18 | 21.80 | 0.16 | 0.05 | 9.17 | 0.21 | 0.46 | 0.03 | 0.03 | 0.01 | 0.00 | 0.02 | 0.26 | 27.95 | 73.83 |
| Ornans | 4a | 12.76 | 0.03 | 1.83 | 0.14 | 23.84 | 0.18 | 0.04 | 9.09 | 2.42 | 0.29 | 0.01 | 0.05 | 0.01 | 0.01 | 0.03 | 0.12 | 30.44 | 81.29 |

Continued on next page

| Sample | Area | Si | Ti | Al | Cr | Fe | Mn | Ni | Mg | Ca | Na | K | P | Co | V | Zn | S | O | Total |
|---|---|---|---|---|---|---|---|---|---|---|---|---|---|---|---|---|---|---|---|
| Ornans | 4a | 12.65 | 0.03 | 1.47 | 0.16 | 25.74 | 0.19 | 0.06 | 9.93 | 0.28 | 0.40 | 0.06 | 0.04 | 0.02 | 0.00 | 0.02 | 0.09 | 30.25 | 81.39 |
| Ornans | 4a | 11.85 | 0.03 | 1.86 | 0.91 | 24.13 | 0.17 | 0.08 | 9.35 | 0.27 | 0.49 | 0.08 | 0.05 | 0.01 | 0.01 | 0.01 | 0.17 | 29.35 | 78.82 |
| Ornans | 4a | 12.58 | 0.06 | 3.11 | 0.36 | 25.30 | 0.18 | 0.15 | 9.04 | 1.17 | 1.58 | 0.20 | 0.23 | 0.02 | 0.01 | 0.01 | 0.12 | 32.14 | 86.26 |
| Ornans | 4a | 12.91 | 0.03 | 1.90 | 0.14 | 27.30 | 0.18 | 0.07 | 10.61 | 0.23 | 0.15 | 0.05 | 0.05 | 0.00 | 0.01 | 0.02 | 0.13 | 31.78 | 85.56 |
| Ornans | 4a | 12.68 | 0.04 | 1.71 | 0.12 | 25.91 | 0.18 | 0.51 | 10.68 | 0.24 | 0.13 | 0.00 | 0.03 | 0.04 | 0.00 | 0.03 | 0.02 | 30.92 | 83.24 |
| Ornans | 4a | 12.54 | 0.03 | 3.29 | 0.22 | 23.07 | 0.16 | 0.09 | 8.66 | 0.28 | 1.70 | 0.15 | 0.04 | 0.00 | 0.00 | 0.03 | 0.03 | 30.57 | 80.86 |
| Ornans | 4a | 12.59 | 0.03 | 2.50 | 0.17 | 27.14 | 0.18 | 0.68 | 10.21 | 0.26 | 0.35 | 0.06 | 0.04 | 0.04 | 0.01 | 0.05 | 0.30 | 32.17 | 86.78 |
| Ornans | 4a | 11.06 | 0.04 | 1.90 | 0.14 | 24.39 | 0.18 | 0.42 | 9.14 | 0.27 | 0.25 | 0.02 | 0.05 | 0.03 | 0.01 | 0.03 | 0.02 | 27.86 | 75.81 |
| Ornans | 4a | 12.31 | 0.03 | 1.26 | 0.12 | 25.96 | 0.18 | 0.06 | 10.24 | 0.78 | 0.15 | 0.00 | 0.35 | 0.01 | 0.01 | 0.03 | 0.04 | 30.36 | 81.89 |
| Ornans | 4a | 12.72 | 0.04 | 1.50 | 0.17 | 27.24 | 0.19 | 0.04 | 10.59 | 0.28 | 0.06 | 0.00 | 0.04 | 0.00 | 0.01 | 0.03 | 0.02 | 30.99 | 83.92 |
| Ornans | 4a | 14.12 | 0.14 | 1.75 | 0.18 | 16.94 | 0.15 | 0.08 | 9.02 | 2.93 | 0.88 | 0.07 | 0.03 | 0.00 | 0.00 | 0.03 | 0.05 | 30.31 | 76.68 |
| Ornans | 4a | 14.34 | 0.03 | 3.34 | 0.07 | 22.13 | 0.17 | 0.10 | 9.29 | 0.73 | 2.15 | 0.26 | 0.08 | 0.01 | 0.01 | 0.00 | 0.07 | 33.21 | 85.99 |
| Ornans | 4b | 11.71 | 0.03 | 1.28 | 0.08 | 24.73 | 0.19 | 0.04 | 9.96 | 0.16 | 0.10 | 0.03 | 0.03 | 0.01 | 0.01 | 0.01 | 0.02 | 28.43 | 76.82 |
| Ornans | 4b | 13.40 | 0.04 | 1.30 | 0.10 | 26.77 | 0.19 | 0.04 | 11.50 | 0.20 | 0.15 | 0.01 | 0.03 | 0.01 | 0.00 | 0.03 | 0.04 | 32.06 | 85.87 |
| Ornans | 4b | 12.94 | 0.05 | 1.70 | 0.14 | 28.28 | 0.20 | 0.11 | 11.03 | 0.24 | 0.13 | 0.03 | 0.04 | 0.02 | 0.01 | 0.00 | 0.03 | 32.07 | 87.02 |
| Ornans | 4b | 11.96 | 0.04 | 1.39 | 0.13 | 24.86 | 0.18 | 0.04 | 10.19 | 0.21 | 0.08 | 0.01 | 0.04 | 0.01 | 0.01 | 0.02 | 0.03 | 29.08 | 78.28 |
| Ornans | 4b | 11.22 | 0.04 | 2.13 | 0.10 | 24.23 | 0.17 | 0.08 | 9.63 | 0.24 | 0.10 | 0.00 | 0.05 | 0.01 | 0.01 | 0.05 | 0.01 | 28.33 | 76.40 |
| Ornans | 4b | 11.72 | 0.04 | 2.23 | 0.19 | 21.75 | 0.16 | 0.04 | 9.00 | 0.22 | 1.02 | 0.08 | 0.05 | 0.01 | 0.00 | 0.01 | 0.09 | 28.33 | 74.94 |
| Ornans | 4b | 12.24 | 0.04 | 1.72 | 0.21 | 23.90 | 0.18 | 0.12 | 9.61 | 0.66 | 0.71 | 0.07 | 0.27 | 0.02 | 0.00 | 0.00 | 0.03 | 29.80 | 79.58 |
| Ornans | 4b | 12.21 | 0.04 | 2.04 | 0.16 | 25.32 | 0.16 | 0.07 | 9.27 | 0.24 | 1.08 | 0.11 | 0.05 | 0.01 | 0.00 | 0.01 | 0.86 | 31.08 | 82.71 |
| Ornans | 4b | 13.39 | 0.03 | 2.90 | 0.16 | 22.80 | 0.16 | 0.07 | 9.84 | 0.47 | 1.37 | 0.15 | 0.13 | 0.01 | 0.00 | 0.01 | 0.11 | 32.05 | 83.65 |
| Ornans | 4b | 13.13 | 0.04 | 1.65 | 0.15 | 26.86 | 0.19 | 0.65 | 11.30 | 0.23 | 0.22 | 0.01 | 0.04 | 0.04 | 0.02 | 0.02 | 0.02 | 32.18 | 86.75 |
| Ornans | 4b | 12.17 | 0.03 | 1.44 | 0.10 | 24.14 | 0.17 | 0.06 | 10.25 | 0.20 | 0.26 | 0.03 | 0.04 | 0.01 | 0.01 | 0.01 | 0.02 | 29.21 | 78.15 |
| Ornans | 4b | 11.78 | 0.02 | 1.12 | 0.10 | 23.96 | 0.17 | 0.04 | 9.90 | 0.21 | 0.15 | 0.02 | 0.04 | 0.01 | 0.00 | 0.01 | 0.03 | 28.16 | 75.72 |
| Ornans | 4b | 12.81 | 0.03 | 1.14 | 0.07 | 26.40 | 0.18 | 2.55 | 10.69 | 0.17 | 0.76 | 0.06 | 0.02 | 0.10 | 0.01 | 0.00 | 0.24 | 31.78 | 87.01 |
| Ornans | 4b | 12.25 | 0.03 | 1.57 | 0.12 | 25.25 | 0.18 | 0.85 | 10.52 | 0.19 | 0.04 | 0.01 | 0.03 | 0.04 | 0.01 | 0.02 | 0.07 | 30.14 | 81.32 |
| Ornans | 4b | 12.76 | 0.03 | 1.42 | 0.14 | 25.41 | 0.18 | 0.04 | 10.93 | 0.19 | 0.11 | 0.01 | 0.04 | 0.01 | 0.00 | 0.01 | 0.02 | 30.64 | 81.94 |
| Ornans | 4b | 12.66 | 0.04 | 2.82 | 0.18 | 22.98 | 0.16 | 0.04 | 8.85 | 0.40 | 1.72 | 0.15 | 0.05 | 0.00 | 0.00 | 0.00 | 0.04 | 30.42 | 80.51 |
| Ornans | 4b | 12.89 | 0.04 | 1.10 | 0.45 | 35.21 | 0.19 | 0.05 | 11.22 | 0.56 | 0.54 | 0.02 | 0.15 | 0.01 | 0.01 | 0.00 | 4.21 | 40.36 | 107.01 |
| Ornans | 4b | 12.25 | 0.05 | 2.67 | 0.23 | 22.84 | 0.17 | 0.08 | 9.10 | 0.52 | 0.78 | 0.09 | 0.06 | 0.01 | 0.00 | 0.01 | 0.05 | 29.73 | 78.64 |
| Ornans | 4b | 12.33 | 0.05 | 2.15 | 0.19 | 26.57 | 0.19 | 0.04 | 10.06 | 0.28 | 0.14 | 0.01 | 0.05 | 0.03 | 0.01 | 0.01 | 0.04 | 30.69 | 82.84 |
| Ornans | 4b | 11.33 | 0.05 | 2.25 | 0.19 | 24.47 | 0.19 | 0.05 | 9.31 | 0.20 | 0.13 | 0.02 | 0.04 | 0.02 | 0.01 | 0.02 | 0.22 | 28.76 | 77.26 |
| Ornans | 4b | 11.01 | 0.02 | 1.78 | 0.17 | 23.62 | 0.18 | 0.03 | 9.05 | 0.21 | 0.08 | 0.02 | 0.04 | 0.00 | 0.00 | 0.04 | 0.06 | 27.28 | 73.59 |
| Ornans | 4b | 10.76 | 0.05 | 1.58 | 0.18 | 25.66 | 0.18 | 0.12 | 8.90 | 0.21 | 0.08 | 0.00 | 0.04 | 0.01 | 0.01 | 0.02 | 0.55 | 28.06 | 76.41 |

| Sample | Area | Si | Ti | Al | Cr | Fe | Mn | Ni | Mg | Ca | Na | K | P | Co | V | Zn | S | O | Total |
|---|---|---|---|---|---|---|---|---|---|---|---|---|---|---|---|---|---|---|---|
| Lancé | 1a | 12.28 | 0.06 | 1.62 | 0.36 | 34.26 | 0.24 | 1.08 | 10.04 | 0.22 | 0.20 | 0.01 | 0.08 | 0.07 | 0.00 | 0.03 | 0.19 | 33.01 | 93.77 |
| Lancé | 1a | 12.12 | 0.05 | 1.56 | 0.22 | 34.72 | 0.22 | 1.29 | 9.49 | 0.57 | 0.50 | 0.06 | 0.09 | 0.10 | 0.01 | 0.04 | 1.25 | 34.40 | 96.70 |
| Lancé | 1a | 13.15 | 0.04 | 1.40 | 0.22 | 33.16 | 0.25 | 1.11 | 10.72 | 0.23 | 0.36 | 0.05 | 0.07 | 0.05 | 0.00 | 0.03 | 0.15 | 33.85 | 94.84 |
| Lancé | 1a | 13.35 | 0.03 | 0.97 | 0.20 | 33.46 | 0.27 | 1.13 | 11.20 | 0.20 | 0.12 | 0.00 | 0.06 | 0.06 | 0.00 | 0.02 | 0.22 | 34.09 | 95.39 |
| Lancé | 1a | 13.28 | 0.04 | 0.79 | 0.18 | 33.56 | 0.25 | 0.92 | 11.00 | 0.21 | 0.08 | 0.01 | 0.06 | 0.06 | 0.00 | 0.00 | 0.12 | 33.52 | 94.09 |
| Lancé | 1a | 12.59 | 0.04 | 1.09 | 0.26 | 32.04 | 0.27 | 1.13 | 10.40 | 0.56 | 0.12 | 0.01 | 0.27 | 0.04 | 0.01 | 0.02 | 0.16 | 32.74 | 91.73 |
| Lancé | 1a | 13.02 | 0.04 | 1.12 | 0.24 | 32.50 | 0.26 | 1.72 | 11.18 | 0.18 | 0.10 | 0.00 | 0.06 | 0.08 | 0.00 | 0.01 | 0.14 | 33.60 | 94.27 |
| Lancé | 1a | 13.78 | 0.05 | 2.44 | 0.30 | 30.10 | 0.25 | 0.36 | 10.80 | 0.30 | 0.92 | 0.14 | 0.10 | 0.04 | 0.01 | 0.04 | 0.18 | 34.84 | 94.66 |
| Lancé | 1a | 13.80 | 0.06 | 2.01 | 0.23 | 30.71 | 0.25 | 0.26 | 10.42 | 0.37 | 1.18 | 0.17 | 0.09 | 0.04 | 0.01 | 0.03 | 0.11 | 34.36 | 94.10 |
| Lancé | 1a | 13.58 | 0.06 | 1.46 | 0.25 | 31.37 | 0.28 | 1.04 | 11.31 | 0.25 | 0.24 | 0.04 | 0.09 | 0.03 | 0.00 | 0.02 | 0.10 | 34.19 | 94.29 |
| Lancé | 1a | 13.77 | 0.07 | 2.06 | 0.31 | 29.89 | 0.26 | 0.30 | 10.93 | 0.30 | 0.69 | 0.11 | 0.11 | 0.03 | 0.00 | 0.02 | 0.09 | 34.30 | 93.23 |
| Lancé | 1a | 13.95 | 0.04 | 1.74 | 0.29 | 30.70 | 0.26 | 0.59 | 11.48 | 0.24 | 0.37 | 0.05 | 0.10 | 0.02 | 0.01 | 0.06 | 0.11 | 34.75 | 94.77 |
| Lancé | 1a | 13.86 | 0.07 | 2.12 | 0.25 | 30.28 | 0.28 | 1.18 | 11.29 | 0.25 | 0.59 | 0.09 | 0.10 | 0.03 | 0.01 | 0.03 | 0.31 | 35.27 | 96.00 |
| Lancé | 1a | 14.03 | 0.07 | 2.08 | 0.28 | 30.59 | 0.26 | 0.99 | 11.54 | 0.22 | 0.55 | 0.08 | 0.08 | 0.03 | 0.00 | 0.05 | 0.25 | 35.51 | 96.60 |
| Lancé | 1a | 13.93 | 0.04 | 1.92 | 0.32 | 30.10 | 0.27 | 0.17 | 12.14 | 0.17 | 0.13 | 0.00 | 0.08 | 0.00 | 0.00 | 0.06 | 0.17 | 34.97 | 94.47 |
| Lancé | 1a | 14.05 | 0.05 | 1.27 | 0.28 | 31.56 | 0.27 | 1.36 | 12.04 | 0.17 | 0.14 | 0.03 | 0.09 | 0.04 | 0.00 | 0.03 | 0.09 | 35.11 | 96.57 |
| Lancé | 1a | 14.38 | 0.04 | 1.32 | 0.23 | 30.75 | 0.26 | 0.46 | 12.61 | 0.17 | 0.14 | 0.03 | 0.06 | 0.03 | 0.01 | 0.01 | 0.12 | 35.39 | 95.99 |
| Lancé | 1a | 13.60 | 0.05 | 1.64 | 0.30 | 29.86 | 0.27 | 1.53 | 11.88 | 0.17 | 0.12 | 0.01 | 0.12 | 0.03 | 0.01 | 0.03 | 0.18 | 34.55 | 94.36 |
| Lancé | 1a | 13.31 | 0.05 | 1.60 | 0.26 | 33.08 | 0.25 | 0.40 | 11.39 | 0.18 | 0.14 | 0.01 | 0.07 | 0.06 | 0.00 | 0.02 | 0.10 | 34.29 | 95.22 |

Continued on next page

| Sample | Area | Si | Ti | Al | Cr | Fe | Mn | Ni | Mg | Ca | Na | K | P | Co | V | Zn | S | O | Total |
|---|---|---|---|---|---|---|---|---|---|---|---|---|---|---|---|---|---|---|---|
| Lancé | 1a | 13.26 | 0.05 | 1.49 | 0.23 | 32.49 | 0.28 | 0.52 | 11.29 | 0.18 | 0.15 | 0.01 | 0.09 | 0.05 | 0.00 | 0.04 | 0.11 | 33.97 | 94.20 |
| Lancé | 1a | 13.75 | 0.06 | 1.30 | 0.22 | 31.03 | 0.27 | 0.78 | 11.74 | 0.17 | 0.11 | 0.00 | 0.08 | 0.04 | 0.00 | 0.03 | 0.11 | 34.27 | 93.98 |
| Lancé | 1a | 13.63 | 0.06 | 1.65 | 0.19 | 31.17 | 0.24 | 0.65 | 11.39 | 0.30 | 0.45 | 0.05 | 0.06 | 0.04 | 0.01 | 0.03 | 0.17 | 34.45 | 94.54 |
| Lancé | 1a | 14.40 | 0.03 | 0.72 | 0.27 | 31.17 | 0.23 | 1.57 | 13.01 | 0.40 | 0.08 | 0.03 | 0.02 | 0.03 | 0.00 | 0.01 | 1.69 | 37.95 | 101.61 |
| Lancé | 1a | 13.28 | 0.04 | 1.13 | 0.25 | 31.98 | 0.25 | 1.15 | 11.70 | 0.19 | 0.06 | 0.03 | 0.09 | 0.03 | 0.01 | 0.01 | 1.12 | 35.44 | 96.75 |
| Lancé | 1a | 14.28 | 0.05 | 1.11 | 0.27 | 30.81 | 0.27 | 0.99 | 12.12 | 0.17 | 0.11 | 0.01 | 0.09 | 0.02 | 0.00 | 0.02 | 0.09 | 34.94 | 95.36 |
| Lancé | 1a | 13.03 | 0.07 | 1.32 | 0.80 | 28.90 | 0.26 | 0.57 | 10.97 | 2.05 | 0.31 | 0.01 | 1.51 | 0.02 | 0.00 | 0.01 | 0.06 | 35.14 | 95.02 |
| Lancé | 1a | 13.90 | 0.06 | 1.11 | 0.28 | 31.35 | 0.27 | 0.56 | 11.89 | 0.19 | 0.11 | 0.01 | 0.08 | 0.01 | 0.00 | 0.03 | 0.09 | 34.39 | 94.33 |
| Lancé | 1a | 14.60 | 0.05 | 1.09 | 0.30 | 31.15 | 0.25 | 0.40 | 12.60 | 0.17 | 0.14 | 0.03 | 0.06 | 0.04 | 0.00 | 0.01 | 0.08 | 35.51 | 96.47 |
| Lancé | 1a | 14.51 | 0.05 | 1.31 | 0.31 | 30.70 | 0.28 | 0.45 | 12.48 | 0.18 | 0.09 | 0.03 | 0.07 | 0.03 | 0.01 | 0.03 | 0.12 | 35.48 | 96.13 |
| Lancé | 1a | 14.00 | 0.04 | 1.36 | 0.27 | 31.04 | 0.27 | 1.24 | 12.23 | 0.21 | 0.12 | 0.03 | 0.08 | 0.04 | 0.00 | 0.04 | 0.37 | 35.48 | 96.80 |
| Lancé | 1a | 14.68 | 0.04 | 1.07 | 0.23 | 31.07 | 0.27 | 0.63 | 12.89 | 0.27 | 0.10 | 0.02 | 0.08 | 0.03 | 0.01 | 0.00 | 0.10 | 35.87 | 97.36 |
| Lancé | 1a | 14.77 | 0.04 | 1.05 | 0.24 | 31.44 | 0.25 | 0.36 | 12.90 | 0.23 | 0.12 | 0.01 | 0.07 | 0.04 | 0.00 | 0.01 | 0.11 | 35.97 | 97.59 |
| Lancé | 1b | 14.22 | 0.03 | 1.13 | 0.23 | 32.12 | 0.28 | 1.19 | 12.07 | 0.15 | 0.13 | 0.02 | 0.05 | 0.03 | 0.01 | 0.03 | 0.11 | 35.25 | 97.03 |
| Lancé | 1b | 13.96 | 0.05 | 1.92 | 0.30 | 30.74 | 0.27 | 0.76 | 11.82 | 0.20 | 0.23 | 0.03 | 0.10 | 0.03 | 0.00 | 0.03 | 0.08 | 35.10 | 95.63 |
| Lancé | 1b | 14.44 | 0.03 | 1.11 | 0.21 | 31.35 | 0.27 | 0.82 | 12.51 | 0.14 | 0.07 | 0.01 | 0.07 | 0.01 | 0.01 | 0.02 | 0.10 | 35.41 | 96.58 |
| Lancé | 1b | 13.19 | 0.05 | 2.15 | 0.36 | 31.31 | 0.25 | 3.16 | 11.65 | 0.26 | 0.12 | 0.01 | 0.16 | 0.05 | 0.00 | 0.06 | 0.07 | 35.18 | 98.01 |
| Lancé | 1b | 14.64 | 0.04 | 0.93 | 0.26 | 31.01 | 0.28 | 0.88 | 12.40 | 0.15 | 0.08 | 0.00 | 0.06 | 0.03 | 0.00 | 0.01 | 0.05 | 35.28 | 96.12 |
| Lancé | 1b | 12.58 | 0.05 | 1.31 | 0.30 | 31.80 | 0.22 | 1.62 | 11.20 | 0.22 | 0.12 | 0.00 | 0.09 | 0.05 | 0.01 | 0.02 | 0.94 | 34.34 | 94.87 |
| Lancé | 1b | 14.38 | 0.05 | 1.11 | 0.23 | 30.53 | 0.24 | 1.00 | 12.34 | 0.26 | 0.17 | 0.03 | 0.10 | 0.02 | 0.00 | 0.03 | 0.09 | 35.16 | 95.72 |
| Lancé | 1b | 14.65 | 0.04 | 1.09 | 0.29 | 31.49 | 0.27 | 0.44 | 12.63 | 0.18 | 0.09 | 0.02 | 0.08 | 0.03 | 0.00 | 0.05 | 0.10 | 35.73 | 97.19 |
| Lancé | 1b | 14.34 | 0.05 | 1.21 | 0.30 | 31.26 | 0.26 | 0.50 | 12.54 | 0.22 | 0.09 | 0.00 | 0.08 | 0.05 | 0.00 | 0.04 | 0.12 | 35.44 | 96.50 |
| Lancé | 1b | 14.47 | 0.05 | 1.17 | 0.22 | 31.94 | 0.26 | 1.78 | 12.74 | 0.31 | 0.26 | 0.06 | 0.07 | 0.03 | 0.00 | 0.01 | 0.31 | 36.56 | 100.24 |
| Lancé | 1b | 13.75 | 0.06 | 0.98 | 0.29 | 26.57 | 0.24 | 0.14 | 12.60 | 0.21 | 0.17 | 0.01 | 0.08 | 0.03 | 0.01 | 0.02 | 0.08 | 33.12 | 88.37 |
| Lancé | 1b | 13.48 | 0.06 | 1.04 | 0.29 | 26.17 | 0.23 | 0.17 | 12.48 | 0.19 | 0.14 | 0.01 | 0.09 | 0.03 | 0.01 | 0.02 | 0.09 | 32.67 | 87.16 |
| Lancé | 1b | 13.81 | 0.05 | 1.31 | 0.34 | 26.20 | 0.23 | 0.15 | 12.95 | 0.23 | 0.15 | 0.01 | 0.09 | 0.03 | 0.01 | 0.04 | 0.07 | 33.63 | 89.30 |
| Lancé | 1b | 12.84 | 0.05 | 1.86 | 0.30 | 27.39 | 0.21 | 1.06 | 12.37 | 0.31 | 0.20 | 0.01 | 0.11 | 0.08 | 0.01 | 0.05 | 0.12 | 33.36 | 90.34 |
| Lancé | 1b | 13.80 | 0.04 | 0.95 | 0.29 | 27.08 | 0.24 | 0.28 | 12.90 | 0.21 | 0.20 | 0.00 | 0.09 | 0.04 | 0.00 | 0.01 | 0.08 | 33.53 | 89.76 |
| Lancé | 1b | 14.30 | 0.03 | 0.97 | 0.27 | 28.38 | 0.23 | 0.46 | 13.13 | 0.30 | 0.16 | 0.00 | 0.12 | 0.04 | 0.01 | 0.01 | 0.07 | 34.73 | 93.23 |
| Lancé | 1b | 13.77 | 0.07 | 1.28 | 0.21 | 29.17 | 0.24 | 0.20 | 12.41 | 0.29 | 0.33 | 0.02 | 0.10 | 0.05 | 0.01 | 0.03 | 0.15 | 34.25 | 92.59 |
| Lancé | 1b | 13.03 | 0.06 | 1.76 | 0.32 | 27.98 | 0.22 | 1.06 | 12.03 | 0.22 | 0.20 | 0.00 | 0.12 | 0.03 | 0.01 | 0.04 | 0.25 | 33.61 | 90.95 |
| Lancé | 1b | 13.91 | 0.06 | 1.48 | 0.28 | 27.62 | 0.26 | 0.14 | 12.56 | 0.23 | 0.15 | 0.01 | 0.11 | 0.04 | 0.01 | 0.04 | 0.08 | 34.07 | 91.04 |
| Lancé | 1b | 13.34 | 0.05 | 1.87 | 0.30 | 28.53 | 0.23 | 1.87 | 11.87 | 0.31 | 0.26 | 0.04 | 0.11 | 0.04 | 0.00 | 0.02 | 0.07 | 34.09 | 93.02 |
| Lancé | 1b | 14.55 | 0.06 | 1.54 | 0.21 | 28.38 | 0.26 | 0.43 | 12.40 | 0.22 | 0.49 | 0.06 | 0.08 | 0.02 | 0.00 | 0.02 | 0.08 | 35.06 | 93.85 |
| Lancé | 1b | 14.03 | 0.06 | 1.91 | 0.29 | 27.55 | 0.24 | 0.24 | 11.92 | 0.24 | 0.45 | 0.05 | 0.12 | 0.00 | 0.00 | 0.03 | 0.08 | 34.30 | 91.53 |
| Lancé | 1b | 14.39 | 0.05 | 1.41 | 0.27 | 27.99 | 0.26 | 0.08 | 12.62 | 0.30 | 0.15 | 0.01 | 0.22 | 0.01 | 0.01 | 0.01 | 0.06 | 34.80 | 92.65 |
| Lancé | 2a | 11.54 | 0.03 | 0.81 | 0.24 | 36.90 | 0.21 | 0.79 | 10.18 | 0.27 | 0.35 | 0.10 | 0.01 | 0.03 | 0.00 | 0.00 | 7.16 | 42.55 | 111.18 |
| Lancé | 2a | 13.44 | 0.04 | 1.33 | 0.19 | 31.03 | 0.23 | 0.95 | 11.15 | 0.19 | 0.65 | 0.09 | 0.04 | 0.03 | 0.00 | 0.03 | 2.03 | 36.58 | 97.98 |
| Lancé | 2a | 14.00 | 0.06 | 0.98 | 0.24 | 27.32 | 0.25 | 0.29 | 12.04 | 0.22 | 0.14 | 0.01 | 0.07 | 0.01 | 0.00 | 0.01 | 0.07 | 33.21 | 88.93 |
| Lancé | 2a | 14.05 | 0.04 | 0.75 | 0.22 | 27.58 | 0.26 | 0.33 | 12.18 | 0.15 | 0.15 | 0.02 | 0.08 | 0.00 | 0.00 | 0.02 | 0.06 | 33.21 | 89.11 |
| Lancé | 2a | 14.24 | 0.03 | 0.75 | 0.26 | 29.55 | 0.27 | 0.53 | 12.61 | 0.15 | 0.10 | 0.02 | 0.09 | 0.01 | 0.00 | 0.01 | 0.63 | 35.19 | 94.43 |
| Lancé | 2a | 14.35 | 0.04 | 0.86 | 0.23 | 28.15 | 0.27 | 0.10 | 12.42 | 0.14 | 0.09 | 0.00 | 0.07 | 0.01 | 0.01 | 0.02 | 0.12 | 33.97 | 90.86 |
| Lancé | 2a | 15.05 | 0.02 | 0.40 | 0.17 | 29.11 | 0.28 | 0.18 | 13.16 | 0.12 | 0.09 | 0.00 | 0.04 | 0.02 | 0.01 | 0.00 | 0.05 | 34.94 | 93.65 |
| Lancé | 2a | 14.43 | 0.05 | 1.09 | 0.26 | 26.65 | 0.26 | 0.07 | 11.86 | 0.76 | 0.14 | 0.01 | 0.08 | 0.01 | 0.01 | 0.01 | 0.09 | 33.70 | 89.48 |
| Lancé | 2a | 14.83 | 0.04 | 0.72 | 0.25 | 29.64 | 0.29 | 0.27 | 12.75 | 0.18 | 0.13 | 0.02 | 0.09 | 0.01 | 0.00 | 0.02 | 0.08 | 35.08 | 94.41 |
| Lancé | 2a | 14.42 | 0.04 | 0.87 | 0.24 | 29.38 | 0.27 | 0.94 | 12.41 | 0.16 | 0.09 | 0.00 | 0.09 | 0.03 | 0.01 | 0.00 | 0.09 | 34.62 | 93.66 |
| Lancé | 2a | 15.82 | 0.03 | 0.54 | 0.54 | 31.26 | 0.30 | 0.34 | 13.67 | 0.15 | 0.04 | 0.00 | 0.03 | 0.02 | 0.01 | 0.00 | 0.12 | 37.21 | 100.07 |
| Lancé | 2a | 15.25 | 0.02 | 0.77 | 0.26 | 31.87 | 0.28 | 0.82 | 13.24 | 0.12 | 0.07 | 0.01 | 0.07 | 0.01 | 0.01 | 0.01 | 0.32 | 36.99 | 100.10 |
| Lancé | 2a | 15.66 | 0.02 | 0.62 | 0.46 | 30.97 | 0.30 | 0.16 | 13.44 | 0.21 | 0.08 | 0.01 | 0.07 | 0.01 | 0.01 | 0.00 | 0.07 | 36.78 | 98.87 |
| Lancé | 2a | 16.15 | 0.03 | 0.68 | 0.34 | 29.73 | 0.30 | 0.07 | 14.37 | 0.15 | 0.07 | 0.01 | 0.06 | 0.00 | 0.00 | 0.00 | 0.04 | 37.49 | 99.51 |
| Lancé | 2a | 16.39 | 0.02 | 0.57 | 0.33 | 28.42 | 0.29 | 0.09 | 14.97 | 0.13 | 0.06 | 0.01 | 0.03 | 0.00 | 0.00 | 0.01 | 0.04 | 37.61 | 98.95 |
| Lancé | 2a | 16.01 | 0.03 | 0.17 | 0.04 | 32.53 | 0.30 | 0.54 | 13.55 | 0.13 | 0.02 | 0.01 | 0.04 | 0.01 | 0.00 | 0.00 | 0.01 | 37.03 | 100.41 |
| Lancé | 2a | 15.53 | 0.03 | 0.13 | 0.02 | 33.59 | 0.30 | 0.10 | 13.04 | 0.10 | 0.08 | 0.01 | 0.02 | 0.01 | 0.01 | 0.00 | 0.02 | 36.30 | 99.28 |
| Lancé | 2a | 13.94 | 0.04 | 0.59 | 0.15 | 34.81 | 0.27 | 0.20 | 11.76 | 0.12 | 0.08 | 0.01 | 0.06 | 0.01 | 0.00 | 0.00 | 0.08 | 34.62 | 96.74 |
| Lancé | 2a | 15.05 | 0.01 | 0.04 | 0.01 | 34.32 | 0.28 | 0.07 | 12.82 | 0.06 | 0.03 | 0.00 | 0.02 | 0.01 | 0.00 | 0.00 | 0.14 | 35.83 | 98.67 |
| Lancé | 2a | 12.62 | 0.04 | 0.75 | 0.19 | 35.88 | 0.23 | 0.82 | 11.05 | 0.21 | 0.12 | 0.01 | 0.07 | 0.03 | 0.00 | 0.01 | 0.25 | 33.62 | 95.90 |
| Lancé | 2a | 12.33 | 0.02 | 1.08 | 0.23 | 36.43 | 0.24 | 0.40 | 10.71 | 0.20 | 0.08 | 0.03 | 0.07 | 0.02 | 0.01 | 0.04 | 0.56 | 33.88 | 96.36 |
| Lancé | 2a | 13.02 | 0.04 | 0.66 | 0.13 | 35.80 | 0.24 | 0.28 | 11.14 | 0.16 | 0.10 | 0.03 | 0.05 | 0.01 | 0.01 | 0.00 | 0.38 | 33.97 | 96.00 |

Continued on next page

| Sample | Area | Si | Ti | Al | Cr | Fe | Mn | Ni | Mg | Ca | Na | K | P | Co | V | Zn | S | O | Total |
|---|---|---|---|---|---|---|---|---|---|---|---|---|---|---|---|---|---|---|---|
| Lancé | 2a | 13.02 | 0.03 | 0.82 | 0.26 | 35.18 | 0.23 | 0.55 | 11.08 | 0.23 | 0.09 | 0.01 | 0.10 | 0.02 | 0.00 | 0.03 | 0.65 | 34.53 | 96.83 |
| Lancé | 2a | 12.74 | 0.03 | 0.73 | 0.21 | 36.53 | 0.23 | 0.38 | 10.79 | 0.11 | 0.05 | 0.00 | 0.08 | 0.04 | 0.00 | 0.00 | 0.08 | 33.31 | 95.31 |
| Lancé | 2a | 13.61 | 0.04 | 0.82 | 0.21 | 34.61 | 0.26 | 0.37 | 11.48 | 0.11 | 0.06 | 0.00 | 0.09 | 0.02 | 0.01 | 0.01 | 0.07 | 34.32 | 96.09 |
| Lancé | 2a | 13.84 | 0.03 | 0.43 | 0.19 | 34.31 | 0.27 | 0.86 | 11.98 | 0.13 | 0.03 | 0.01 | 0.02 | 0.03 | 0.00 | 0.01 | 0.49 | 35.13 | 97.77 |
| Lancé | 2a | 13.89 | 0.03 | 1.06 | 0.34 | 31.68 | 0.25 | 1.10 | 12.00 | 0.16 | 0.09 | 0.01 | 0.08 | 0.05 | 0.00 | 0.02 | 0.26 | 34.90 | 95.92 |
| Lancé | 2a | 15.56 | 0.02 | 0.21 | 0.13 | 31.73 | 0.27 | 0.86 | 13.15 | 0.29 | 0.07 | 0.00 | 0.05 | 0.04 | 0.01 | 0.00 | 0.17 | 36.52 | 99.08 |
| Lancé | 2a | 14.09 | 0.01 | 0.56 | 0.21 | 33.50 | 0.25 | 0.81 | 12.31 | 0.12 | 0.07 | 0.00 | 0.04 | 0.07 | 0.00 | 0.02 | 0.68 | 35.82 | 98.56 |
| Lancé | 2a | 11.73 | 0.04 | 0.99 | 0.24 | 36.89 | 0.23 | 0.24 | 9.59 | 0.23 | 0.23 | 0.03 | 0.08 | 0.07 | 0.00 | 0.01 | 0.10 | 31.86 | 92.59 |
| Lancé | 2a | 13.02 | 0.05 | 0.58 | 0.22 | 34.94 | 0.23 | 0.25 | 10.49 | 0.54 | 0.21 | 0.02 | 0.08 | 0.09 | 0.00 | 0.00 | 0.08 | 33.07 | 93.87 |
| Lancé | 2a | 12.32 | 0.04 | 0.48 | 0.18 | 36.24 | 0.24 | 0.47 | 10.00 | 0.21 | 0.20 | 0.03 | 0.07 | 0.19 | 0.00 | 0.00 | 0.16 | 32.27 | 93.09 |
| Lancé | 2a | 13.05 | 0.04 | 0.72 | 0.24 | 35.12 | 0.23 | 0.30 | 10.14 | 1.14 | 0.14 | 0.00 | 0.06 | 0.06 | 0.00 | 0.02 | 0.48 | 33.86 | 95.61 |
| Lancé | 2a | 15.89 | 0.06 | 2.14 | 0.29 | 27.60 | 0.25 | 0.48 | 11.60 | 0.71 | 1.30 | 0.20 | 0.06 | 0.04 | 0.01 | 0.00 | 0.12 | 36.98 | 97.72 |
| Lancé | 2a | 12.99 | 0.05 | 1.11 | 0.19 | 34.57 | 0.24 | 0.56 | 10.15 | 0.45 | 0.57 | 0.05 | 0.06 | 0.07 | 0.00 | 0.01 | 0.09 | 33.34 | 94.50 |
| Lancé | 2a | 12.92 | 0.04 | 0.96 | 0.28 | 30.79 | 0.23 | 1.27 | 10.93 | 0.18 | 0.19 | 0.04 | 0.09 | 0.07 | 0.00 | 0.01 | 0.12 | 32.62 | 90.73 |
| Lancé | 2a | 12.58 | 0.04 | 1.34 | 0.30 | 30.96 | 0.23 | 1.02 | 10.80 | 0.14 | 0.07 | 0.00 | 0.05 | 0.04 | 0.01 | 0.03 | 0.10 | 32.35 | 90.07 |
| Lancé | 2b | 10.73 | 0.04 | 1.11 | 0.22 | 38.50 | 0.22 | 0.52 | 8.95 | 0.64 | 0.21 | 0.02 | 0.41 | 0.02 | 0.00 | 0.02 | 1.04 | 32.90 | 95.54 |
| Lancé | 2b | 9.43 | 0.03 | 1.56 | 0.24 | 41.14 | 0.19 | 1.96 | 8.07 | 0.13 | 0.16 | 0.03 | 0.07 | 0.05 | 0.00 | 0.02 | 0.14 | 30.38 | 93.59 |
| Lancé | 2b | 11.11 | 0.03 | 0.91 | 0.23 | 39.85 | 0.18 | 0.36 | 8.55 | 1.09 | 0.13 | 0.03 | 0.06 | 0.03 | 0.00 | 0.00 | 0.12 | 31.53 | 94.20 |
| Lancé | 2b | 10.33 | 0.05 | 1.56 | 0.24 | 38.65 | 0.20 | 0.42 | 8.71 | 0.13 | 0.08 | 0.03 | 0.09 | 0.01 | 0.01 | 0.04 | 0.43 | 31.14 | 92.11 |
| Lancé | 2b | 10.94 | 0.03 | 1.07 | 0.21 | 38.34 | 0.22 | 0.29 | 9.42 | 0.14 | 0.13 | 0.00 | 0.08 | 0.01 | 0.00 | 0.01 | 0.16 | 31.31 | 92.34 |
| Lancé | 2b | 11.19 | 0.03 | 0.37 | 0.32 | 38.77 | 0.21 | 0.13 | 9.55 | 0.13 | 0.08 | 0.01 | 0.08 | 0.02 | 0.01 | 0.00 | 0.26 | 31.32 | 92.48 |
| Lancé | 2b | 11.44 | 0.01 | 0.60 | 0.20 | 38.91 | 0.22 | 1.34 | 10.01 | 0.10 | 0.09 | 0.02 | 0.07 | 0.03 | 0.00 | 0.02 | 0.14 | 32.22 | 95.42 |
| Lancé | 2b | 10.92 | 0.02 | 1.00 | 0.29 | 38.05 | 0.22 | 1.21 | 9.48 | 0.13 | 0.08 | 0.01 | 0.05 | 0.02 | 0.00 | 0.03 | 0.36 | 31.72 | 93.59 |
| Lancé | 2b | 12.83 | 0.03 | 0.82 | 0.21 | 35.79 | 0.22 | 0.20 | 11.31 | 0.16 | 0.05 | 0.01 | 0.07 | 0.02 | 0.00 | 0.01 | 0.09 | 33.60 | 95.42 |
| Lancé | 2b | 14.93 | 0.02 | 0.45 | 0.19 | 32.38 | 0.27 | 0.26 | 13.44 | 0.14 | 0.03 | 0.00 | 0.09 | 0.03 | 0.00 | 0.01 | 0.05 | 36.05 | 98.33 |
| Lancé | 2b | 14.68 | 0.02 | 0.47 | 0.17 | 32.72 | 0.24 | 0.17 | 12.36 | 0.85 | 0.02 | 0.01 | 0.04 | 0.03 | 0.01 | 0.00 | 0.07 | 35.39 | 97.25 |
| Lancé | 2b | 18.06 | 0.03 | 0.45 | 0.17 | 24.15 | 0.17 | 0.14 | 10.95 | 6.32 | 0.09 | 0.01 | 0.04 | 0.03 | 0.01 | 0.00 | 0.13 | 38.10 | 98.85 |
| Lancé | 2b | 12.04 | 0.03 | 0.42 | 0.09 | 36.38 | 0.21 | 0.52 | 10.63 | 0.27 | 0.11 | 0.00 | 0.14 | 0.09 | 0.01 | 0.00 | 0.14 | 32.34 | 93.42 |
| Lancé | 2b | 12.53 | 0.03 | 0.97 | 0.19 | 34.48 | 0.23 | 0.55 | 11.16 | 0.20 | 0.11 | 0.01 | 0.07 | 0.02 | 0.00 | 0.04 | 0.17 | 33.17 | 93.95 |
| Lancé | 2b | 16.22 | 0.05 | 0.98 | 0.52 | 28.94 | 0.29 | 0.04 | 12.65 | 0.91 | 0.50 | 0.09 | 0.09 | 0.01 | 0.00 | 0.00 | 0.02 | 37.04 | 98.35 |
| Lancé | 2b | 14.08 | 0.10 | 1.91 | 0.31 | 30.46 | 0.27 | 2.24 | 11.63 | 0.21 | 0.58 | 0.08 | 0.09 | 0.03 | 0.01 | 0.02 | 0.21 | 35.77 | 98.00 |
| Lancé | 2b | 13.60 | 0.07 | 1.66 | 0.36 | 37.78 | 0.24 | 1.42 | 11.46 | 0.22 | 0.65 | 0.08 | 0.07 | 0.13 | 0.02 | 0.02 | 0.27 | 36.88 | 104.93 |
| Lancé | 2b | 13.58 | 0.08 | 1.57 | 0.33 | 30.73 | 0.23 | 2.60 | 11.48 | 0.21 | 0.55 | 0.07 | 0.10 | 0.04 | 0.01 | 0.01 | 0.30 | 35.10 | 96.98 |
| Lancé | 2b | 14.53 | 0.07 | 1.59 | 0.19 | 29.11 | 0.28 | 0.31 | 11.46 | 0.28 | 0.85 | 0.14 | 0.07 | 0.01 | 0.00 | 0.01 | 0.12 | 34.87 | 93.88 |
| Lancé | 2b | 12.44 | 0.05 | 1.02 | 0.20 | 33.87 | 0.23 | 1.53 | 10.48 | 0.23 | 0.15 | 0.03 | 0.06 | 0.09 | 0.00 | 0.00 | 0.19 | 32.83 | 93.40 |
| Lancé | 2b | 11.96 | 0.06 | 0.94 | 0.20 | 34.56 | 0.23 | 0.82 | 10.08 | 0.31 | 0.23 | 0.01 | 0.07 | 0.04 | 0.01 | 0.02 | 0.20 | 32.05 | 91.80 |
| Lancé | 2b | 9.71 | 0.01 | 0.56 | 0.36 | 44.08 | 0.18 | 1.38 | 9.17 | 0.15 | 0.02 | 0.00 | 0.04 | 0.15 | 0.01 | 0.02 | 4.34 | 37.50 | 107.69 |
| Lancé | 2b | 11.34 | 0.02 | 0.86 | 0.31 | 38.03 | 0.20 | 0.23 | 9.88 | 0.13 | 0.06 | 0.00 | 0.07 | 0.02 | 0.01 | 0.03 | 0.19 | 31.82 | 93.20 |
| Lancé | 2b | 11.79 | 0.02 | 0.88 | 0.42 | 36.31 | 0.21 | 0.42 | 10.23 | 0.15 | 0.07 | 0.01 | 0.06 | 0.03 | 0.01 | 0.03 | 0.10 | 32.09 | 92.84 |
| Lancé | 2b | 12.31 | 0.03 | 0.81 | 0.34 | 32.73 | 0.22 | 1.51 | 10.74 | 0.29 | 0.03 | 0.00 | 0.04 | 0.07 | 0.00 | 0.02 | 0.21 | 32.37 | 91.73 |
| Lancé | 2b | 12.63 | 0.03 | 1.06 | 0.34 | 33.15 | 0.23 | 0.71 | 11.25 | 0.12 | 0.03 | 0.00 | 0.07 | 0.05 | 0.01 | 0.02 | 0.14 | 33.06 | 92.92 |
| Lancé | 2b | 12.69 | 0.03 | 0.76 | 0.20 | 35.80 | 0.24 | 0.50 | 10.86 | 0.16 | 0.09 | 0.03 | 0.04 | 0.04 | 0.00 | 0.02 | 0.31 | 33.49 | 95.26 |
| Lancé | 2b | 12.32 | 0.03 | 0.36 | 0.25 | 35.98 | 0.23 | 0.61 | 10.57 | 0.28 | 0.05 | 0.01 | 0.07 | 0.04 | 0.01 | 0.00 | 0.80 | 33.42 | 95.01 |
| Lancé | 2b | 13.76 | 0.03 | 0.36 | 0.24 | 34.88 | 0.24 | 0.49 | 11.32 | 0.65 | 0.07 | 0.00 | 0.02 | 0.05 | 0.00 | 0.00 | 2.77 | 38.23 | 103.10 |
| Lancé | 2b | 11.13 | 0.04 | 0.66 | 0.96 | 38.16 | 0.20 | 0.47 | 9.59 | 0.21 | 0.17 | 0.02 | 0.04 | 0.11 | 0.01 | 0.02 | 0.45 | 32.09 | 94.33 |
| Lancé | 2b | 13.83 | 0.02 | 0.56 | 0.21 | 34.69 | 0.25 | 0.50 | 11.64 | 0.25 | 0.06 | 0.00 | 0.05 | 0.07 | 0.00 | 0.00 | 0.20 | 34.69 | 97.03 |
| Lancé | 2b | 11.88 | 0.02 | 0.54 | 0.39 | 37.13 | 0.21 | 0.74 | 10.33 | 0.15 | 0.07 | 0.02 | 0.07 | 0.06 | 0.01 | 0.00 | 0.48 | 32.84 | 94.94 |
| Lancé | 2b | 11.65 | 0.02 | 0.49 | 0.28 | 38.57 | 0.21 | 0.42 | 9.93 | 0.14 | 0.06 | 0.02 | 0.07 | 0.03 | 0.00 | 0.01 | 0.75 | 32.93 | 95.59 |
| Lancé | 2b | 11.67 | 0.01 | 0.78 | 0.19 | 37.30 | 0.20 | 0.52 | 9.90 | 0.35 | 0.07 | 0.01 | 0.05 | 0.04 | 0.00 | 0.00 | 0.26 | 32.12 | 93.48 |
| Lancé | 2b | 12.76 | 0.02 | 0.90 | 0.14 | 35.83 | 0.23 | 0.30 | 10.79 | 0.32 | 0.23 | 0.06 | 0.04 | 0.04 | 0.00 | 0.01 | 0.21 | 33.52 | 95.38 |
| Lancé | 2b | 11.80 | 0.03 | 0.96 | 0.42 | 37.10 | 0.21 | 0.26 | 10.15 | 0.29 | 0.19 | 0.03 | 0.07 | 0.06 | 0.00 | 0.01 | 0.28 | 32.69 | 94.56 |
| Lancé | 2b | 12.62 | 0.02 | 1.03 | 0.26 | 36.06 | 0.24 | 0.27 | 10.88 | 0.23 | 0.15 | 0.00 | 0.07 | 0.05 | 0.00 | 0.00 | 0.30 | 33.76 | 95.92 |
| Lancé | 2b | 13.75 | 0.02 | 0.86 | 0.33 | 34.10 | 0.28 | 0.58 | 11.37 | 0.70 | 0.10 | 0.01 | 0.07 | 0.06 | 0.00 | 0.03 | 0.16 | 34.76 | 97.19 |
| Lancé | 2b | 14.34 | 0.00 | 0.18 | 0.20 | 34.07 | 0.26 | 0.51 | 12.33 | 0.26 | 0.04 | 0.00 | 0.05 | 0.09 | 0.00 | 0.00 | 0.17 | 35.15 | 97.65 |
| Lancé | 2b | 12.33 | 0.02 | 0.92 | 0.31 | 35.91 | 0.23 | 0.68 | 10.66 | 0.31 | 0.10 | 0.00 | 0.10 | 0.14 | 0.01 | 0.01 | 0.37 | 33.47 | 95.58 |
| Lancé | 2b | 10.36 | 0.02 | 0.22 | 0.28 | 40.19 | 0.18 | 0.62 | 9.57 | 0.17 | 0.06 | 0.00 | 0.05 | 0.23 | 0.00 | 0.01 | 5.54 | 38.70 | 106.22 |
| Lancé | 2b | 15.96 | 0.05 | 0.91 | 1.66 | 22.38 | 0.08 | 1.17 | 7.27 | 8.85 | 0.08 | 0.01 | 0.06 | 0.07 | 0.03 | 0.02 | 2.21 | 38.33 | 99.13 |
| Lancé | 2b | 12.14 | 0.03 | 1.46 | 0.31 | 32.95 | 0.21 | 0.82 | 10.40 | 0.22 | 0.20 | 0.05 | 0.04 | 0.05 | 0.00 | 0.01 | 0.51 | 32.87 | 92.26 |

Continued on next page

| Sample | Area | Si | Ti | Al | Cr | Fe | Mn | Ni | Mg | Ca | Na | K | P | Co | V | Zn | S | O | Total |
|---|---|---|---|---|---|---|---|---|---|---|---|---|---|---|---|---|---|---|---|
| Lancé | 2b | 13.18 | 0.03 | 0.75 | 0.19 | 33.56 | 0.24 | 0.33 | 11.50 | 0.20 | 0.06 | 0.02 | 0.06 | 0.05 | 0.00 | 0.01 | 0.15 | 33.57 | 93.91 |
| Lancé | 2b | 13.23 | 0.02 | 0.83 | 0.28 | 32.77 | 0.25 | 0.54 | 11.67 | 0.21 | 0.06 | 0.00 | 0.04 | 0.03 | 0.01 | 0.01 | 0.48 | 34.15 | 94.59 |
| Lancé | 3a | 15.05 | 0.06 | 1.27 | 0.36 | 27.64 | 0.25 | 0.64 | 14.00 | 0.18 | 0.22 | 0.03 | 0.11 | 0.04 | 0.00 | 0.00 | 0.08 | 36.29 | 96.22 |
| Lancé | 3a | 14.10 | 0.05 | 1.66 | 0.29 | 27.32 | 0.24 | 1.51 | 13.58 | 0.31 | 0.19 | 0.02 | 0.22 | 0.03 | 0.00 | 0.02 | 0.10 | 35.62 | 95.28 |
| Lancé | 3a | 15.02 | 0.04 | 0.92 | 0.22 | 26.75 | 0.23 | 0.96 | 14.51 | 0.16 | 0.08 | 0.01 | 0.07 | 0.04 | 0.01 | 0.00 | 0.10 | 35.94 | 95.03 |
| Lancé | 3a | 14.90 | 0.03 | 0.93 | 0.21 | 27.13 | 0.23 | 1.15 | 14.27 | 0.16 | 0.14 | 0.02 | 0.09 | 0.03 | 0.00 | 0.01 | 0.17 | 35.98 | 95.47 |
| Lancé | 3a | 14.46 | 0.05 | 0.96 | 0.26 | 25.98 | 0.23 | 0.25 | 13.74 | 0.20 | 0.14 | 0.00 | 0.11 | 0.03 | 0.00 | 0.02 | 0.06 | 34.47 | 90.96 |
| Lancé | 3a | 14.63 | 0.04 | 1.02 | 0.23 | 28.61 | 0.26 | 0.13 | 13.24 | 0.14 | 0.11 | 0.02 | 0.05 | 0.02 | 0.00 | 0.02 | 0.04 | 34.98 | 93.55 |
| Lancé | 3a | 15.45 | 0.07 | 1.26 | 0.34 | 27.94 | 0.24 | 0.25 | 11.62 | 1.86 | 0.17 | 0.02 | 0.07 | 0.00 | 0.00 | 0.04 | 0.06 | 35.71 | 95.10 |
| Lancé | 3a | 14.22 | 0.06 | 0.98 | 0.29 | 29.45 | 0.27 | 0.41 | 11.95 | 0.19 | 0.13 | 0.00 | 0.07 | 0.03 | 0.01 | 0.02 | 0.05 | 34.06 | 92.21 |
| Lancé | 3a | 14.18 | 0.01 | 0.31 | 0.41 | 33.17 | 0.28 | 0.30 | 12.17 | 0.23 | 0.13 | 0.04 | 0.04 | 0.05 | 0.01 | 0.00 | 1.02 | 36.06 | 98.40 |
| Lancé | 3a | 14.62 | 0.06 | 0.93 | 0.23 | 30.69 | 0.28 | 0.57 | 12.42 | 0.15 | 0.10 | 0.02 | 0.07 | 0.03 | 0.00 | 0.02 | 0.15 | 35.26 | 95.61 |
| Lancé | 3a | 13.94 | 0.05 | 1.25 | 0.34 | 31.09 | 0.27 | 0.87 | 11.58 | 0.30 | 0.12 | 0.02 | 0.07 | 0.05 | 0.01 | 0.05 | 0.20 | 34.61 | 94.81 |
| Lancé | 3a | 13.26 | 0.05 | 1.16 | 0.23 | 32.16 | 0.26 | 4.40 | 11.27 | 0.29 | 0.13 | 0.02 | 0.06 | 0.07 | 0.01 | 0.03 | 0.08 | 34.58 | 98.06 |
| Lancé | 3a | 14.44 | 0.06 | 0.66 | 0.16 | 32.93 | 0.29 | 0.51 | 12.22 | 0.17 | 0.07 | 0.03 | 0.09 | 0.05 | 0.01 | 0.02 | 0.15 | 35.32 | 97.18 |
| Lancé | 3a | 15.91 | 0.05 | 1.48 | 0.46 | 29.84 | 0.28 | 0.56 | 12.44 | 0.66 | 0.67 | 0.10 | 0.06 | 0.03 | 0.01 | 0.03 | 0.04 | 37.33 | 99.94 |
| Lancé | 3a | 14.83 | 0.05 | 1.49 | 0.23 | 26.95 | 0.24 | 0.35 | 12.12 | 0.66 | 0.47 | 0.09 | 0.09 | 0.02 | 0.00 | 0.03 | 0.08 | 34.92 | 92.61 |
| Lancé | 3a | 14.69 | 0.05 | 1.25 | 0.33 | 29.86 | 0.28 | 0.59 | 12.43 | 0.36 | 0.13 | 0.01 | 0.08 | 0.02 | 0.01 | 0.02 | 0.04 | 35.39 | 95.55 |
| Lancé | 3a | 22.43 | 0.05 | 0.42 | 0.24 | 15.38 | 0.17 | 0.09 | 17.69 | 1.44 | 0.13 | 0.01 | 0.04 | 0.01 | 0.01 | 0.01 | 0.01 | 42.89 | 101.00 |
| Lancé | 3a | 18.18 | 0.04 | 0.59 | 0.27 | 22.24 | 0.20 | 0.75 | 16.96 | 0.84 | 0.15 | 0.02 | 0.02 | 0.04 | 0.01 | 0.00 | 0.14 | 39.83 | 100.27 |
| Lancé | 3a | 18.95 | 0.06 | 1.08 | 0.31 | 20.95 | 0.22 | 0.24 | 15.86 | 0.83 | 0.73 | 0.04 | 0.09 | 0.01 | 0.00 | 0.02 | 0.03 | 40.07 | 99.50 |
| Lancé | 3a | 15.48 | 0.04 | 0.63 | 0.37 | 29.94 | 0.23 | 0.47 | 12.54 | 1.15 | 0.08 | 0.01 | 0.05 | 0.07 | 0.00 | 0.00 | 1.48 | 38.22 | 100.78 |
| Lancé | 3a | 12.66 | 0.02 | 1.07 | 0.17 | 35.62 | 0.23 | 0.63 | 11.56 | 0.12 | 0.11 | 0.01 | 0.05 | 0.08 | 0.01 | 0.03 | 3.14 | 38.43 | 103.95 |
| Lancé | 3a | 12.87 | 0.05 | 1.77 | 0.30 | 34.42 | 0.23 | 0.56 | 11.63 | 0.15 | 0.08 | 0.03 | 0.07 | 0.09 | 0.00 | 0.03 | 1.82 | 37.09 | 101.20 |
| Lancé | 3a | 13.45 | 0.05 | 2.43 | 0.23 | 30.81 | 0.23 | 0.99 | 10.85 | 0.45 | 1.07 | 0.16 | 0.15 | 0.10 | 0.00 | 0.02 | 0.22 | 35.07 | 96.28 |
| Lancé | 3a | 12.62 | 0.04 | 1.83 | 0.33 | 31.58 | 0.22 | 5.63 | 11.67 | 0.35 | 0.52 | 0.11 | 0.13 | 0.06 | 0.01 | 0.04 | 1.27 | 36.95 | 103.34 |
| Lancé | 3a | 14.35 | 0.07 | 1.48 | 0.25 | 30.12 | 0.26 | 0.69 | 12.20 | 0.28 | 0.38 | 0.07 | 0.10 | 0.04 | 0.01 | 0.02 | 0.14 | 35.34 | 95.77 |
| Lancé | 3a | 14.66 | 0.06 | 1.52 | 0.22 | 28.32 | 0.25 | 0.30 | 12.35 | 0.27 | 0.56 | 0.08 | 0.11 | 0.01 | 0.00 | 0.01 | 0.09 | 35.20 | 94.02 |
| Lancé | 3a | 13.12 | 0.06 | 1.59 | 0.49 | 35.45 | 0.24 | 0.65 | 11.70 | 0.72 | 0.27 | 0.05 | 0.10 | 0.13 | 0.00 | 0.02 | 0.71 | 36.36 | 101.64 |
| Lancé | 3a | 15.29 | 0.10 | 0.90 | 0.26 | 30.84 | 0.28 | 0.33 | 13.30 | 0.20 | 0.24 | 0.03 | 0.08 | 0.04 | 0.01 | 0.02 | 0.29 | 36.90 | 99.10 |
| Lancé | 3a | 15.27 | 0.09 | 1.20 | 0.23 | 29.55 | 0.27 | 0.23 | 13.11 | 0.18 | 0.28 | 0.07 | 0.08 | 0.02 | 0.01 | 0.02 | 0.07 | 36.28 | 96.97 |
| Lancé | 3a | 13.87 | 0.07 | 2.00 | 0.31 | 29.89 | 0.26 | 0.25 | 12.19 | 0.16 | 0.29 | 0.04 | 0.07 | 0.02 | 0.01 | 0.04 | 0.93 | 36.18 | 96.56 |
| Lancé | 3a | 14.22 | 0.07 | 1.21 | 0.64 | 31.39 | 0.27 | 0.35 | 11.94 | 0.33 | 0.24 | 0.05 | 0.14 | 0.04 | 0.00 | 0.02 | 0.26 | 35.46 | 96.62 |
| Lancé | 3a | 14.92 | 0.06 | 0.85 | 0.25 | 30.39 | 0.29 | 0.36 | 12.31 | 0.27 | 0.30 | 0.02 | 0.04 | 0.02 | 0.00 | 0.03 | 0.05 | 35.25 | 95.40 |
| Lancé | 3a | 15.93 | 0.12 | 0.79 | 0.43 | 30.41 | 0.29 | 0.11 | 13.08 | 0.34 | 0.23 | 0.05 | 0.04 | 0.03 | 0.01 | 0.01 | 0.02 | 36.89 | 98.76 |
| Lancé | 3b | 13.49 | 0.05 | 0.74 | 0.21 | 31.22 | 0.20 | 0.83 | 13.13 | 0.30 | 0.11 | 0.03 | 0.15 | 0.06 | 0.00 | 0.00 | 0.15 | 34.63 | 95.29 |
| Lancé | 3b | 13.16 | 0.07 | 1.01 | 0.28 | 32.23 | 0.20 | 0.51 | 12.34 | 0.16 | 0.20 | 0.01 | 0.10 | 0.10 | 0.01 | 0.00 | 0.26 | 34.31 | 94.95 |
| Lancé | 3b | 13.89 | 0.05 | 1.21 | 0.23 | 28.26 | 0.21 | 1.19 | 13.35 | 0.44 | 0.11 | 0.02 | 0.21 | 0.04 | 0.00 | 0.02 | 0.16 | 35.06 | 94.46 |
| Lancé | 3b | 13.66 | 0.07 | 0.90 | 0.28 | 29.27 | 0.23 | 1.09 | 12.95 | 0.14 | 0.08 | 0.02 | 0.08 | 0.06 | 0.01 | 0.01 | 0.15 | 34.27 | 93.28 |
| Lancé | 3b | 14.43 | 0.02 | 0.72 | 0.19 | 28.20 | 0.23 | 1.19 | 14.03 | 0.13 | 0.06 | 0.03 | 0.08 | 0.05 | 0.00 | 0.02 | 0.13 | 35.28 | 94.79 |
| Lancé | 3b | 13.26 | 0.03 | 0.59 | 0.20 | 31.69 | 0.20 | 0.51 | 12.79 | 0.29 | 0.09 | 0.02 | 0.06 | 0.09 | 0.01 | 0.03 | 0.15 | 33.93 | 93.92 |
| Lancé | 3b | 13.57 | 0.04 | 0.76 | 0.20 | 30.82 | 0.22 | 0.94 | 13.01 | 0.16 | 0.10 | 0.02 | 0.08 | 0.11 | 0.00 | 0.01 | 0.14 | 34.41 | 94.58 |
| Lancé | 3b | 13.81 | 0.03 | 1.05 | 0.35 | 30.56 | 0.23 | 0.39 | 13.20 | 0.19 | 0.11 | 0.01 | 0.07 | 0.07 | 0.01 | 0.02 | 0.12 | 34.88 | 95.10 |
| Lancé | 3b | 13.21 | 0.05 | 0.87 | 0.19 | 29.21 | 0.21 | 1.88 | 12.45 | 0.20 | 0.14 | 0.01 | 0.10 | 0.11 | 0.01 | 0.00 | 0.20 | 33.67 | 92.50 |
| Lancé | 3b | 13.47 | 0.05 | 1.01 | 0.24 | 29.58 | 0.22 | 1.58 | 12.57 | 0.15 | 0.10 | 0.00 | 0.08 | 0.14 | 0.01 | 0.02 | 0.22 | 34.21 | 93.64 |
| Lancé | 3b | 12.91 | 0.03 | 0.71 | 0.14 | 30.33 | 0.19 | 0.96 | 12.45 | 0.14 | 0.16 | 0.03 | 0.08 | 0.09 | 0.00 | 0.02 | 0.13 | 33.06 | 91.42 |
| Lancé | 3b | 12.70 | 0.04 | 0.85 | 0.18 | 29.12 | 0.18 | 1.72 | 12.54 | 0.18 | 0.14 | 0.01 | 0.09 | 0.12 | 0.00 | 0.00 | 0.16 | 32.96 | 90.99 |
| Lancé | 3b | 14.53 | 0.07 | 1.83 | 0.30 | 25.36 | 0.22 | 0.44 | 14.12 | 0.76 | 0.33 | 0.01 | 0.55 | 0.02 | 0.01 | 0.03 | 0.06 | 36.35 | 94.98 |
| Lancé | 3b | 14.57 | 0.05 | 1.56 | 0.25 | 26.93 | 0.23 | 1.21 | 13.90 | 0.18 | 0.16 | 0.02 | 0.11 | 0.03 | 0.01 | 0.03 | 0.13 | 35.88 | 95.26 |
| Lancé | 3b | 14.12 | 0.05 | 1.66 | 0.68 | 29.35 | 0.30 | 1.34 | 13.29 | 0.25 | 0.20 | 0.03 | 0.08 | 0.04 | 0.02 | 0.01 | 0.73 | 36.92 | 99.05 |
| Lancé | 3b | 22.32 | 0.07 | 1.41 | 0.44 | 13.87 | 0.17 | 0.01 | 18.08 | 1.05 | 0.80 | 0.08 | 0.02 | 0.00 | 0.01 | 0.02 | 0.01 | 43.64 | 102.01 |
| Lancé | 3b | 17.65 | 0.04 | 0.81 | 0.43 | 25.93 | 0.26 | 0.33 | 13.92 | 1.47 | 0.36 | 0.05 | 0.05 | 0.00 | 0.01 | 0.01 | 0.25 | 38.98 | 100.56 |
| Lancé | 3b | 15.14 | 0.06 | 1.10 | 0.23 | 29.69 | 0.28 | 0.30 | 13.13 | 0.19 | 0.19 | 0.04 | 0.09 | 0.01 | 0.01 | 0.01 | 0.06 | 36.07 | 96.61 |
| Lancé | 3b | 12.95 | 0.05 | 0.73 | 0.18 | 30.24 | 0.26 | 0.24 | 11.37 | 0.18 | 0.17 | 0.00 | 0.07 | 0.03 | 0.00 | 0.02 | 0.09 | 32.18 | 88.77 |
| Lancé | 3b | 14.00 | 0.04 | 1.07 | 0.25 | 27.93 | 0.24 | 0.94 | 12.93 | 0.19 | 0.11 | 0.04 | 0.09 | 0.04 | 0.01 | 0.02 | 0.11 | 34.31 | 92.31 |
| Lancé | 3b | 13.92 | 0.04 | 0.87 | 0.22 | 27.55 | 0.24 | 0.87 | 12.75 | 0.24 | 0.15 | 0.04 | 0.06 | 0.03 | -0.00 | 0.02 | 0.08 | 33.72 | 90.79 |
| Lancé | 3b | 12.74 | 0.05 | 1.09 | 0.25 | 29.51 | 0.21 | 2.56 | 12.21 | 0.12 | 0.13 | 0.00 | 0.07 | 0.09 | 0.00 | 0.03 | 0.16 | 33.34 | 92.55 |
| Lancé | 3b | 12.73 | 0.04 | 1.10 | 0.28 | 28.11 | 0.23 | 1.77 | 11.83 | 0.14 | 0.11 | 0.00 | 0.07 | 0.05 | 0.01 | 0.03 | 0.14 | 32.45 | 89.09 |

Continued on next page

| Sample | Area | Si | Ti | Al | Cr | Fe | Mn | Ni | Mg | Ca | Na | K | P | Co | V | Zn | S | O | Total |
|---|---|---|---|---|---|---|---|---|---|---|---|---|---|---|---|---|---|---|---|
| Lancé | 3b | 13.61 | 0.06 | 1.18 | 0.29 | 27.59 | 0.23 | 1.16 | 12.43 | 0.14 | 0.17 | 0.01 | 0.09 | 0.04 | 0.01 | 0.03 | 0.11 | 33.61 | 90.75 |
| Lancé | 3b | 13.27 | 0.04 | 0.94 | 0.20 | 30.06 | 0.24 | 0.92 | 12.22 | 0.15 | 0.15 | 0.02 | 0.08 | 0.07 | 0.01 | 0.02 | 0.12 | 33.48 | 91.99 |
| Lancé | 3b | 13.43 | 0.04 | 1.04 | 0.23 | 28.92 | 0.24 | 2.15 | 12.06 | 0.17 | 0.12 | 0.01 | 0.08 | 0.03 | 0.01 | 0.00 | 0.07 | 33.57 | 92.15 |
| Lancé | 3b | 14.08 | 0.05 | 0.97 | 0.25 | 31.38 | 0.28 | 0.26 | 11.77 | 0.22 | 0.17 | 0.05 | 0.09 | 0.03 | 0.00 | 0.00 | 0.10 | 34.36 | 94.05 |
| Lancé | 3b | 14.02 | 0.06 | 1.73 | 0.26 | 27.23 | 0.23 | 1.04 | 12.88 | 0.19 | 0.34 | 0.05 | 0.10 | 0.03 | 0.01 | 0.03 | 0.11 | 34.81 | 93.09 |
| Lancé | 3b | 13.84 | 0.06 | 1.48 | 0.24 | 27.83 | 0.24 | 1.01 | 12.51 | 0.18 | 0.19 | 0.05 | 0.10 | 0.04 | 0.01 | 0.03 | 0.13 | 34.28 | 92.21 |
| Lancé | 3b | 14.14 | 0.06 | 1.02 | 0.21 | 29.25 | 0.25 | 1.04 | 12.41 | 0.22 | 0.33 | 0.05 | 0.08 | 0.07 | 0.01 | 0.00 | 0.13 | 34.60 | 93.88 |
| Lancé | 3b | 13.04 | 0.04 | 1.32 | 0.28 | 30.61 | 0.23 | 0.95 | 11.70 | 0.22 | 0.19 | 0.01 | 0.09 | 0.09 | 0.00 | 0.01 | 0.13 | 33.49 | 92.41 |
| Lancé | 3b | 15.55 | 0.08 | 1.39 | 0.27 | 29.73 | 0.27 | 0.22 | 12.90 | 0.27 | 0.33 | 0.07 | 0.09 | 0.02 | 0.01 | 0.01 | 0.11 | 36.81 | 98.13 |
| Lancé | 3b | 16.07 | 0.07 | 1.19 | 0.17 | 30.12 | 0.27 | 0.24 | 13.20 | 0.22 | 0.69 | 0.05 | 0.05 | 0.01 | 0.01 | 0.01 | 0.06 | 37.47 | 99.92 |
| Lancé | 3b | 14.61 | 0.06 | 1.92 | 0.30 | 29.02 | 0.26 | 0.84 | 11.83 | 0.26 | 0.73 | 0.16 | 0.07 | 0.04 | 0.01 | 0.01 | 0.09 | 35.57 | 95.78 |
| Lancé | 3b | 14.59 | 0.07 | 1.23 | 0.28 | 31.01 | 0.26 | 0.56 | 12.67 | 0.16 | 0.20 | 0.05 | 0.07 | 0.05 | 0.01 | 0.01 | 0.10 | 35.75 | 97.07 |
| Lancé | 3b | 14.58 | 0.06 | 1.07 | 0.51 | 29.41 | 0.26 | 0.76 | 12.91 | 0.15 | 0.09 | 0.03 | 0.07 | 0.01 | 0.01 | 0.03 | 0.09 | 35.38 | 95.42 |
| Lancé | 3b | 15.33 | 0.06 | 1.35 | 0.31 | 29.73 | 0.26 | 0.44 | 13.06 | 0.24 | 0.41 | 0.06 | 0.05 | 0.02 | 0.00 | 0.01 | 0.19 | 36.76 | 98.27 |
| Lancé | 3b | 14.54 | 0.05 | 1.66 | 0.22 | 28.90 | 0.27 | 0.19 | 12.05 | 0.20 | 0.64 | 0.14 | 0.06 | 0.03 | 0.01 | 0.02 | 0.07 | 35.04 | 94.08 |
| Lancé | 4a | 12.41 | 0.04 | 1.04 | 0.21 | 34.14 | 0.20 | 0.24 | 11.94 | 0.19 | 0.09 | 0.02 | 0.06 | 0.08 | 0.00 | 0.02 | 0.10 | 33.32 | 94.10 |
| Lancé | 4a | 11.90 | 0.05 | 1.23 | 0.44 | 33.62 | 0.17 | 1.03 | 10.71 | 1.05 | 0.18 | 0.03 | 0.06 | 0.05 | 0.01 | 0.01 | 1.99 | 35.47 | 98.00 |
| Lancé | 4a | 12.94 | 0.04 | 1.20 | 0.25 | 32.03 | 0.19 | 0.96 | 12.35 | 0.23 | 0.20 | 0.01 | 0.07 | 0.04 | 0.01 | 0.02 | 0.26 | 34.24 | 95.03 |
| Lancé | 4a | 11.64 | 0.06 | 1.44 | 0.21 | 34.50 | 0.16 | 0.48 | 11.80 | 0.18 | 0.12 | 0.01 | 0.09 | 0.09 | 0.01 | 0.04 | 0.16 | 33.01 | 93.99 |
| Lancé | 4a | 13.77 | 0.05 | 1.74 | 0.23 | 29.45 | 0.20 | 0.68 | 12.80 | 0.23 | 0.40 | 0.06 | 0.10 | 0.03 | 0.01 | 0.01 | 0.18 | 35.14 | 95.09 |
| Lancé | 4a | 14.49 | 0.05 | 2.09 | 0.23 | 28.36 | 0.19 | 0.67 | 12.21 | 0.82 | 0.64 | 0.14 | 0.16 | 0.04 | 0.01 | 0.01 | 0.70 | 36.76 | 97.56 |
| Lancé | 4a | 14.78 | 0.04 | 1.14 | 0.25 | 28.24 | 0.23 | 0.25 | 14.22 | 0.17 | 0.08 | 0.02 | 0.07 | 0.02 | 0.01 | 0.03 | 0.06 | 35.88 | 95.48 |
| Lancé | 4a | 13.85 | 0.05 | 1.17 | 0.26 | 27.71 | 0.21 | 0.25 | 13.25 | 1.56 | 0.08 | 0.02 | 0.82 | 0.04 | 0.01 | 0.02 | 0.08 | 35.61 | 94.96 |
| Lancé | 4a | 14.79 | 0.05 | 1.66 | 0.25 | 29.05 | 0.25 | 0.60 | 12.69 | 0.25 | 0.61 | 0.08 | 0.06 | 0.03 | 0.00 | 0.01 | 0.15 | 36.04 | 96.59 |
| Lancé | 4a | 14.52 | 0.04 | 2.35 | 0.27 | 28.27 | 0.22 | 0.82 | 11.56 | 1.05 | 0.67 | 0.15 | 0.10 | 0.05 | 0.00 | 0.01 | 0.22 | 35.95 | 96.26 |
| Lancé | 4a | 13.32 | 0.03 | 2.02 | 0.21 | 30.64 | 0.21 | 0.85 | 11.12 | 0.32 | 0.68 | 0.11 | 0.10 | 0.03 | 0.01 | 0.03 | 0.25 | 34.40 | 94.33 |
| Lancé | 4a | 13.22 | 0.05 | 1.28 | 0.27 | 28.88 | 0.20 | 0.63 | 12.83 | 1.17 | 0.11 | 0.01 | 0.31 | 0.04 | 0.01 | 0.02 | 0.35 | 34.77 | 94.15 |
| Lancé | 4a | 15.54 | 0.04 | 1.02 | 0.15 | 23.26 | 0.10 | 0.50 | 8.68 | 7.03 | 0.28 | 0.04 | 0.06 | 0.04 | 0.00 | 0.02 | 0.25 | 34.63 | 91.64 |
| Lancé | 4a | 15.26 | 0.12 | 2.57 | 0.49 | 26.76 | 0.09 | 0.20 | 6.91 | 6.65 | 1.40 | 0.20 | 0.04 | 0.06 | 0.01 | 0.02 | 3.77 | 41.20 | 105.75 |
| Lancé | 4a | 15.28 | 0.05 | 1.27 | 0.18 | 29.78 | 0.23 | 0.30 | 12.68 | 0.62 | 0.75 | 0.12 | 0.03 | 0.04 | 0.01 | 0.00 | 0.17 | 36.52 | 98.01 |
| Lancé | 4a | 16.00 | 0.04 | 1.63 | 0.22 | 27.98 | 0.27 | 0.17 | 12.91 | 0.72 | 0.92 | 0.16 | 0.08 | 0.00 | 0.00 | 0.00 | 0.11 | 37.36 | 98.58 |
| Lancé | 4a | 14.64 | 0.03 | 1.14 | 0.34 | 30.27 | 0.25 | 0.32 | 12.43 | 0.63 | 0.29 | 0.03 | 0.04 | 0.07 | 0.00 | 0.01 | 1.34 | 37.32 | 99.14 |
| Lancé | 4a | 13.29 | 0.05 | 1.68 | 0.23 | 32.01 | 0.24 | 0.34 | 11.66 | 0.28 | 0.31 | 0.07 | 0.07 | 0.04 | 0.00 | 0.02 | 0.21 | 34.44 | 94.94 |
| Lancé | 4a | 12.03 | 0.04 | 1.79 | 0.22 | 34.12 | 0.20 | 0.61 | 10.12 | 0.44 | 0.75 | 0.14 | 0.06 | 0.04 | 0.00 | 0.03 | 0.67 | 33.64 | 94.89 |
| Lancé | 4a | 11.15 | 0.02 | 1.65 | 0.18 | 35.96 | 0.18 | 1.00 | 9.22 | 0.31 | 0.91 | 0.12 | 0.05 | 0.09 | 0.01 | 0.01 | 0.21 | 31.84 | 92.90 |
| Lancé | 4a | 11.99 | 0.04 | 1.50 | 0.32 | 32.74 | 0.15 | 0.58 | 8.02 | 2.82 | 0.43 | 0.09 | 0.06 | 0.07 | 0.02 | 0.03 | 3.35 | 36.45 | 98.66 |
| Lancé | 4a | 11.83 | 0.03 | 1.40 | 0.20 | 35.63 | 0.19 | 0.29 | 10.06 | 0.25 | 0.60 | 0.10 | 0.07 | 0.04 | 0.00 | 0.00 | 0.14 | 32.44 | 93.28 |
| Lancé | 4a | 11.73 | 0.06 | 0.71 | 0.21 | 36.67 | 0.20 | 0.56 | 10.70 | 0.12 | 0.09 | 0.02 | 0.06 | 0.08 | 0.00 | 0.00 | 0.15 | 32.30 | 93.65 |
| Lancé | 4a | 12.12 | 0.04 | 0.87 | 0.31 | 34.18 | 0.16 | 0.41 | 9.70 | 2.52 | 0.10 | 0.01 | 0.06 | 0.09 | 0.00 | 0.00 | 2.52 | 36.00 | 99.09 |
| Lancé | 4a | 11.62 | 0.06 | 1.04 | 0.48 | 34.73 | 0.18 | 0.55 | 10.57 | 0.61 | 0.07 | 0.02 | 0.07 | 0.09 | 0.01 | 0.03 | 0.86 | 33.23 | 94.20 |
| Lancé | 4a | 11.65 | 0.05 | 1.13 | 0.29 | 34.35 | 0.19 | 0.56 | 11.13 | 0.22 | 0.06 | 0.02 | 0.06 | 0.09 | 0.01 | 0.03 | 0.57 | 32.91 | 93.31 |
| Lancé | 4a | 11.70 | 0.04 | 2.75 | 0.27 | 30.62 | 0.21 | 1.62 | 11.24 | 1.40 | 0.36 | 0.03 | 0.94 | 0.04 | 0.01 | 0.03 | 0.56 | 35.36 | 97.18 |

| Sample | Area | Si | Ti | Al | Cr | Fe | Mn | Ni | Mg | Ca | Na | K | P | Co | V | Zn | S | O | Total |
|---|---|---|---|---|---|---|---|---|---|---|---|---|---|---|---|---|---|---|---|
| ALHA 77003 | 2a | 14.37 | 0.05 | 2.36 | 0.38 | 29.05 | 0.21 | 1.68 | 12.75 | 0.06 | 0.05 | 0.01 | 0.11 | 0.10 | 0.0 | 0.0 | 0.54 | 36.93 | 98.64 |
| ALHA 77003 | 2a | 16.83 | 0.02 | 0.63 | 0.09 | 27.74 | 0.26 | 0.23 | 16.39 | 0.13 | 0.14 | 0.01 | 0.00 | 0.03 | 0.0 | 0.0 | 0.07 | 38.86 | 101.41 |
| ALHA 77003 | 2a | 8.18 | 0.01 | 0.71 | 0.04 | 42.68 | 0.11 | 3.23 | 7.46 | 0.05 | 0.02 | 0.00 | 0.04 | 0.17 | 0.0 | 0.0 | 0.68 | 29.18 | 92.57 |
| ALHA 77003 | 2a | 12.25 | 0.03 | 1.26 | 0.18 | 33.90 | 0.19 | 2.26 | 11.61 | 0.06 | 0.02 | 0.00 | 0.09 | 0.12 | 0.0 | 0.0 | 0.69 | 34.42 | 97.07 |
| ALHA 77003 | 2a | 14.46 | 0.05 | 1.78 | 0.19 | 28.03 | 0.22 | 1.89 | 13.64 | 0.06 | 0.05 | 0.00 | 0.15 | 0.07 | 0.0 | 0.0 | 0.68 | 37.05 | 98.33 |
| ALHA 77003 | 2a | 14.53 | 0.05 | 1.53 | 0.24 | 28.68 | 0.23 | 1.67 | 14.15 | 0.08 | 0.02 | 0.00 | 0.12 | 0.09 | 0.0 | 0.0 | 0.61 | 37.24 | 99.23 |
| ALHA 77003 | 2a | 18.57 | 0.05 | 0.70 | 0.10 | 23.43 | 0.15 | 1.04 | 7.28 | 9.04 | 0.07 | 0.03 | 0.07 | 0.08 | 0.0 | 0.0 | 0.36 | 37.99 | 98.98 |
| ALHA 77003 | 2a | 13.43 | 0.04 | 1.26 | 0.15 | 31.73 | 0.22 | 1.08 | 12.69 | 0.06 | 0.02 | 0.01 | 0.09 | 0.09 | 0.0 | 0.0 | 0.53 | 35.29 | 96.69 |
| ALHA 77003 | 2a | 13.90 | 0.05 | 1.78 | 0.26 | 28.57 | 0.21 | 2.62 | 13.33 | 0.04 | 0.04 | 0.01 | 0.14 | 0.10 | 0.0 | 0.0 | 0.76 | 36.68 | 98.50 |
| ALHA 77003 | 2a | 14.01 | 0.04 | 1.72 | 0.29 | 28.50 | 0.23 | 1.92 | 13.42 | 0.27 | 0.03 | 0.01 | 0.26 | 0.09 | 0.0 | 0.0 | 0.64 | 36.67 | 98.08 |
| ALHA 77003 | 2a | 16.92 | 0.04 | 0.96 | 0.15 | 26.43 | 0.21 | 1.22 | 13.62 | 2.15 | 0.04 | 0.00 | 0.09 | 0.07 | 0.0 | 0.0 | 0.43 | 38.82 | 101.15 |

Continued on next page

| Sample | Area | Si | Ti | Al | Cr | Fe | Mn | Ni | Mg | Ca | Na | K | P | Co | V | Zn | S | O | Total |
|---|---|---|---|---|---|---|---|---|---|---|---|---|---|---|---|---|---|---|---|
| ALHA 77003 | 2a | 16.49 | 0.03 | 0.45 | 0.10 | 27.69 | 0.26 | 0.35 | 15.63 | 0.55 | 0.02 | 0.01 | 0.06 | 0.05 | 0.0 | 0.0 | 0.21 | 38.28 | 100.19 |
| ALHA 77003 | 2a | 14.71 | 0.05 | 1.04 | 0.15 | 30.23 | 0.24 | 1.13 | 13.61 | 0.05 | 0.02 | 0.00 | 0.08 | 0.09 | 0.0 | 0.0 | 0.52 | 36.71 | 98.63 |
| ALHA 77003 | 2a | 14.32 | 0.04 | 1.70 | 0.35 | 30.47 | 0.22 | 0.98 | 13.20 | 0.06 | 0.03 | 0.01 | 0.11 | 0.08 | 0.0 | 0.0 | 0.48 | 36.68 | 98.72 |
| ALHA 77003 | 2a | 15.45 | 0.06 | 0.96 | 0.24 | 28.86 | 0.24 | 0.74 | 14.28 | 0.05 | 0.02 | 0.00 | 0.11 | 0.06 | 0.0 | 0.0 | 0.34 | 37.24 | 98.65 |
| ALHA 77003 | 2a | 15.76 | 0.03 | 0.80 | 0.20 | 28.80 | 0.23 | 0.63 | 14.90 | 0.03 | 0.03 | 0.00 | 0.08 | 0.07 | 0.0 | 0.0 | 0.35 | 37.74 | 99.66 |
| ALHA 77003 | 2a | 13.99 | 0.08 | 1.50 | 0.40 | 30.64 | 0.22 | 1.41 | 11.94 | 0.07 | 0.09 | 0.01 | 0.12 | 0.08 | 0.0 | 0.0 | 0.69 | 35.87 | 97.11 |
| ALHA 77003 | 2a | 15.46 | 0.06 | 0.84 | 0.20 | 29.64 | 0.25 | 0.68 | 14.61 | 0.03 | 0.01 | 0.01 | 0.09 | 0.04 | 0.0 | 0.0 | 0.41 | 37.61 | 99.92 |
| ALHA 77003 | 2a | 11.89 | 0.05 | 1.54 | 0.41 | 35.21 | 0.19 | 1.28 | 10.87 | 0.03 | 0.04 | 0.00 | 0.09 | 0.11 | 0.0 | 0.0 | 0.47 | 33.67 | 95.87 |
| ALHA 77003 | 2a | 12.62 | 0.04 | 1.76 | 0.46 | 33.54 | 0.21 | 1.26 | 11.71 | 0.04 | 0.05 | 0.00 | 0.10 | 0.11 | 0.0 | 0.0 | 0.49 | 34.84 | 97.23 |
| ALHA 77003 | 2a | 12.91 | 0.05 | 1.06 | 0.22 | 33.95 | 0.22 | 1.47 | 11.71 | 0.04 | 0.03 | 0.00 | 0.10 | 0.11 | 0.0 | 0.0 | 0.50 | 34.62 | 96.99 |
| ALHA 77003 | 2a | 12.34 | 0.06 | 1.24 | 0.29 | 34.23 | 0.20 | 1.96 | 10.96 | 0.06 | 0.03 | 0.01 | 0.13 | 0.10 | 0.0 | 0.0 | 0.71 | 34.26 | 96.58 |
| ALHA 77003 | 2a | 13.34 | 0.08 | 1.66 | 0.42 | 31.95 | 0.22 | 1.54 | 11.72 | 0.10 | 0.06 | 0.00 | 0.12 | 0.08 | 0.0 | 0.0 | 0.72 | 35.58 | 97.58 |
| ALHA 77003 | 2a | 11.63 | 0.05 | 1.20 | 0.34 | 35.82 | 0.18 | 1.28 | 10.48 | 0.07 | 0.07 | 0.00 | 0.15 | 0.15 | 0.0 | 0.0 | 0.75 | 33.49 | 95.67 |
| ALHA 77003 | 2a | 15.58 | 0.08 | 0.64 | 0.27 | 29.80 | 0.24 | 0.47 | 14.77 | 0.15 | 0.09 | 0.01 | 0.16 | 0.06 | 0.0 | 0.0 | 0.36 | 37.81 | 100.48 |
| ALHA 77003 | 2a | 13.97 | 0.07 | 1.38 | 0.60 | 30.44 | 0.21 | 0.85 | 12.66 | 0.06 | 0.04 | 0.01 | 0.17 | 0.07 | 0.0 | 0.0 | 0.74 | 36.19 | 97.45 |
| ALHA 77003 | 2a | 14.18 | 0.07 | 1.33 | 0.48 | 30.57 | 0.20 | 0.92 | 12.96 | 0.06 | 0.04 | 0.01 | 0.13 | 0.07 | 0.0 | 0.0 | 0.78 | 36.60 | 98.39 |
| ALHA 77003 | 2a | 13.65 | 0.09 | 1.36 | 0.42 | 31.22 | 0.22 | 1.23 | 12.51 | 0.05 | 0.06 | 0.00 | 0.15 | 0.05 | 0.0 | 0.0 | 0.76 | 35.98 | 97.74 |
| ALHA 77003 | 2a | 13.75 | 0.07 | 0.86 | 0.39 | 32.09 | 0.20 | 0.80 | 12.70 | 0.04 | 0.03 | 0.01 | 0.12 | 0.08 | 0.0 | 0.0 | 0.50 | 35.45 | 97.10 |
| ALHA 77003 | 2a | 13.76 | 0.04 | 0.95 | 0.23 | 31.54 | 0.22 | 0.92 | 13.30 | 0.04 | 0.03 | 0.01 | 0.05 | 0.07 | 0.0 | 0.0 | 0.69 | 35.90 | 97.73 |
| ALHA 77003 | 2a | 15.31 | 0.01 | 0.65 | 0.04 | 32.23 | 0.20 | 5.33 | 14.98 | 0.32 | 0.33 | 0.04 | 0.14 | 0.11 | 0.0 | 0.0 | 0.19 | 39.39 | 109.25 |
| ALHA 77003 | 2a | 12.87 | 0.04 | 0.69 | 0.92 | 33.91 | 0.18 | 0.49 | 12.34 | 0.33 | 0.03 | 0.01 | 0.19 | 0.10 | 0.0 | 0.0 | 4.08 | 40.27 | 106.45 |
| ALHA 77003 | 2a | 13.72 | 0.07 | 2.23 | 0.39 | 30.36 | 0.20 | 0.86 | 12.75 | 0.03 | 0.05 | 0.00 | 0.12 | 0.07 | 0.0 | 0.0 | 0.78 | 36.60 | 98.23 |
| ALHA 77003 | 2a | 14.59 | 0.06 | 1.98 | 0.43 | 29.16 | 0.22 | 0.80 | 13.74 | 0.05 | 0.04 | 0.02 | 0.10 | 0.08 | 0.0 | 0.0 | 0.59 | 37.38 | 99.25 |
| ALHA 77003 | 2a | 14.74 | 0.01 | 0.11 | 0.03 | 29.47 | 0.17 | 1.16 | 15.80 | 0.04 | 0.00 | 0.01 | 0.00 | 0.09 | 0.0 | 0.0 | 0.42 | 36.79 | 98.83 |
| ALHA 77003 | 2a | 14.96 | 0.02 | 0.47 | 0.14 | 30.50 | 0.23 | 0.66 | 14.79 | 0.05 | 0.02 | 0.00 | 0.08 | 0.08 | 0.0 | 0.0 | 0.32 | 36.89 | 99.21 |
| ALHA 77003 | 2a | 11.92 | 0.05 | 2.05 | 0.64 | 34.47 | 0.18 | 0.95 | 11.62 | 0.04 | 0.02 | 0.00 | 0.09 | 0.11 | 0.0 | 0.0 | 0.48 | 34.47 | 97.10 |
| ALHA 77003 | 2a | 15.14 | 0.06 | 1.60 | 0.55 | 28.55 | 0.21 | 0.69 | 14.23 | 0.04 | 0.03 | 0.00 | 0.10 | 0.07 | 0.0 | 0.0 | 0.45 | 37.62 | 99.34 |
| ALHA 77003 | 2a | 14.66 | 0.08 | 1.18 | 0.26 | 29.24 | 0.20 | 0.72 | 13.44 | 0.06 | 0.04 | 0.01 | 0.13 | 0.07 | 0.0 | 0.0 | 0.60 | 36.54 | 97.23 |
| ALHA 77003 | 2a | 12.96 | 0.06 | 1.77 | 0.42 | 32.30 | 0.19 | 0.66 | 12.05 | 0.05 | 0.04 | 0.00 | 0.18 | 0.07 | 0.0 | 0.0 | 0.82 | 35.52 | 97.10 |
| ALHA 77003 | 2a | 11.89 | 0.06 | 1.25 | 0.34 | 35.42 | 0.17 | 0.96 | 11.38 | 0.06 | 0.04 | 0.02 | 0.16 | 0.09 | 0.0 | 0.0 | 0.71 | 34.14 | 96.69 |
| ALHA 77003 | 2a | 16.99 | 0.05 | 0.79 | 0.58 | 26.41 | 0.14 | 0.66 | 12.21 | 3.38 | 0.05 | 0.01 | 0.07 | 0.07 | 0.0 | 0.0 | 0.54 | 38.46 | 100.40 |
| ALHA 77003 | 2a | 13.59 | 0.06 | 0.95 | 0.63 | 31.56 | 0.19 | 0.70 | 13.69 | 0.05 | 0.04 | 0.01 | 0.36 | 0.10 | 0.0 | 0.0 | 1.08 | 37.11 | 100.12 |
| ALHA 77003 | 2a | 13.60 | 0.07 | 0.93 | 0.62 | 31.76 | 0.19 | 0.69 | 13.70 | 0.06 | 0.03 | 0.00 | 0.35 | 0.08 | 0.0 | 0.0 | 1.09 | 37.16 | 100.35 |
| ALHA 77003 | 2a | 13.47 | 0.07 | 1.73 | 0.72 | 30.79 | 0.18 | 0.58 | 13.22 | 0.06 | 0.03 | 0.01 | 0.16 | 0.05 | 0.0 | 0.0 | 0.91 | 36.64 | 98.65 |
| ALHA 77003 | 2a | 15.25 | 0.04 | 0.79 | 0.38 | 28.04 | 0.22 | 0.29 | 15.64 | 0.12 | 0.02 | 0.00 | 0.07 | 0.06 | 0.0 | 0.0 | 0.45 | 37.60 | 98.97 |
| ALHA 77003 | 2a | 13.98 | 0.07 | 1.01 | 0.26 | 31.24 | 0.19 | 0.43 | 13.41 | 0.04 | 0.03 | 0.03 | 0.08 | 0.06 | 0.0 | 0.0 | 0.86 | 36.38 | 98.06 |
| ALHA 77003 | 2a | 13.52 | 0.18 | 0.62 | 0.07 | 31.96 | 0.16 | 0.42 | 11.88 | 1.39 | 0.00 | 0.01 | 0.08 | 0.08 | 0.0 | 0.0 | 0.48 | 34.64 | 95.48 |
| ALHA 77003 | 2a | 14.83 | 0.05 | 0.35 | 0.07 | 31.74 | 0.19 | 0.33 | 14.03 | 0.14 | 0.00 | 0.00 | 0.08 | 0.08 | 0.0 | 0.0 | 0.39 | 36.51 | 98.80 |
| ALHA 77003 | 2a | 14.95 | 0.04 | 0.65 | 0.16 | 29.73 | 0.21 | 0.53 | 14.41 | 0.02 | 0.01 | 0.00 | 0.08 | 0.06 | 0.0 | 0.0 | 0.62 | 36.97 | 98.43 |
| ALHA 77003 | 2a | 15.71 | 0.04 | 0.56 | 0.20 | 28.82 | 0.22 | 0.38 | 15.14 | 0.01 | 0.02 | 0.01 | 0.06 | 0.06 | 0.0 | 0.0 | 0.36 | 37.56 | 99.16 |
| ALHA 77003 | 2a | 14.08 | 0.07 | 2.26 | 0.67 | 29.33 | 0.20 | 0.63 | 13.17 | 0.05 | 0.02 | 0.01 | 0.09 | 0.05 | 0.0 | 0.0 | 0.59 | 36.75 | 97.96 |
| ALHA 77003 | 2a | 14.51 | 0.07 | 1.92 | 0.48 | 28.39 | 0.21 | 0.76 | 13.75 | 0.04 | 0.02 | 0.00 | 0.10 | 0.08 | 0.0 | 0.0 | 0.65 | 37.11 | 98.08 |
| ALHA 77003 | 2a | 13.33 | 0.03 | 1.03 | 0.25 | 32.88 | 0.20 | 0.81 | 12.67 | 0.01 | 0.02 | 0.01 | 0.07 | 0.09 | 0.0 | 0.0 | 0.47 | 35.11 | 96.98 |
| ALHA 77003 | 2a | 14.21 | 0.05 | 1.14 | 0.28 | 30.82 | 0.23 | 0.92 | 13.45 | 0.03 | 0.02 | 0.00 | 0.11 | 0.08 | 0.0 | 0.0 | 0.45 | 36.22 | 98.00 |
| ALHA 77003 | 3a | 15.55 | 0.05 | 1.90 | 0.38 | 26.27 | 0.21 | 0.52 | 14.71 | 0.23 | 0.84 | 0.12 | 0.09 | 0.05 | 0.0 | 0.0 | 0.07 | 37.66 | 98.63 |
| ALHA 77003 | 3a | 14.91 | 0.06 | 1.10 | 0.32 | 28.38 | 0.22 | 0.91 | 15.06 | 0.27 | 0.07 | 0.00 | 0.15 | 0.07 | 0.0 | 0.0 | 0.06 | 36.94 | 98.52 |
| ALHA 77003 | 3a | 15.21 | 0.04 | 1.07 | 0.36 | 28.66 | 0.22 | 0.79 | 15.63 | 0.09 | 0.03 | 0.01 | 0.06 | 0.07 | 0.0 | 0.0 | 0.10 | 37.55 | 99.89 |
| ALHA 77003 | 3a | 14.33 | 0.06 | 1.23 | 0.38 | 29.40 | 0.21 | 1.25 | 14.51 | 0.15 | 0.05 | 0.03 | 0.10 | 0.09 | 0.0 | 0.0 | 0.07 | 36.36 | 98.22 |
| ALHA 77003 | 3a | 14.50 | 0.06 | 1.50 | 0.43 | 29.58 | 0.22 | 0.98 | 14.85 | 0.12 | 0.08 | 0.04 | 0.09 | 0.11 | 0.0 | 0.0 | 0.10 | 37.05 | 99.70 |
| ALHA 77003 | 3a | 14.88 | 0.05 | 0.78 | 0.48 | 29.16 | 0.23 | 0.55 | 14.76 | 0.20 | 0.06 | 0.01 | 0.09 | 0.08 | 0.0 | 0.0 | 0.03 | 36.48 | 97.84 |
| ALHA 77003 | 3a | 14.35 | 0.06 | 0.93 | 0.28 | 29.97 | 0.21 | 1.37 | 14.40 | 0.11 | 0.08 | 0.00 | 0.09 | 0.11 | 0.0 | 0.0 | 0.08 | 36.17 | 98.21 |
| ALHA 77003 | 3a | 14.85 | 0.07 | 1.17 | 0.37 | 29.09 | 0.23 | 0.71 | 14.58 | 0.14 | 0.07 | 0.00 | 0.08 | 0.09 | 0.0 | 0.0 | 0.09 | 36.70 | 98.24 |
| ALHA 77003 | 3a | 15.91 | 0.03 | 0.48 | 0.40 | 27.92 | 0.23 | 0.54 | 16.37 | 0.07 | 0.02 | 0.01 | 0.05 | 0.07 | 0.0 | 0.0 | 0.03 | 37.91 | 100.03 |
| ALHA 77003 | 3a | 12.16 | 0.10 | 4.41 | 4.08 | 28.65 | 0.21 | 0.81 | 11.41 | 0.26 | 0.37 | 0.06 | 0.11 | 0.09 | 0.0 | 0.0 | 0.04 | 36.20 | 98.96 |
| ALHA 77003 | 3a | 14.96 | 0.05 | 0.76 | 0.20 | 28.60 | 0.22 | 1.62 | 14.99 | 0.13 | 0.06 | 0.00 | 0.07 | 0.11 | 0.0 | 0.0 | 0.09 | 36.74 | 98.61 |
| ALHA 77003 | 3a | 14.42 | 0.07 | 1.43 | 0.39 | 29.03 | 0.23 | 1.32 | 14.50 | 0.13 | 0.10 | 0.00 | 0.09 | 0.12 | 0.0 | 0.0 | 0.10 | 36.59 | 98.51 |
| ALHA 77003 | 3a | 14.68 | 0.06 | 1.13 | 0.35 | 29.06 | 0.21 | 1.04 | 14.79 | 0.10 | 0.05 | 0.00 | 0.07 | 0.08 | 0.0 | 0.0 | 0.07 | 36.61 | 98.31 |
| ALHA 77003 | 3a | 14.01 | 0.07 | 1.08 | 0.37 | 30.75 | 0.21 | 1.41 | 13.87 | 0.19 | 0.09 | 0.00 | 0.08 | 0.10 | 0.0 | 0.0 | 0.09 | 35.90 | 98.22 |

Continued on next page

| Sample | Area | Si | Ti | Al | Cr | Fe | Mn | Ni | Mg | Ca | Na | K | P | Co | V | Zn | S | O | Total |
|---|---|---|---|---|---|---|---|---|---|---|---|---|---|---|---|---|---|---|---|
| ALHA 77003 | 3a | 13.73 | 0.07 | 1.49 | 0.49 | 30.81 | 0.20 | 1.18 | 13.60 | 0.17 | 0.10 | 0.00 | 0.09 | 0.08 | 0.0 | 0.0 | 0.09 | 35.78 | 97.88 |
| ALHA 77003 | 3a | 12.73 | 0.09 | 1.75 | 0.48 | 32.66 | 0.19 | 0.88 | 12.58 | 0.17 | 0.06 | 0.00 | 0.09 | 0.07 | 0.0 | 0.0 | 0.07 | 34.60 | 96.42 |
| ALHA 77003 | 3a | 15.14 | 0.03 | 0.69 | 0.17 | 29.99 | 0.23 | 0.35 | 15.09 | 0.07 | 0.04 | 0.00 | 0.03 | 0.05 | 0.0 | 0.0 | 0.05 | 36.83 | 98.77 |
| ALHA 77003 | 3a | 10.81 | 0.05 | 1.11 | 0.37 | 32.22 | 0.18 | 2.91 | 10.15 | 0.12 | 0.08 | 0.00 | 0.06 | 0.13 | 0.0 | 0.0 | 0.21 | 30.77 | 89.18 |
| ALHA 77003 | 3a | 14.08 | 0.04 | 1.24 | 0.28 | 30.77 | 0.21 | 0.73 | 14.18 | 0.13 | 0.04 | 0.00 | 0.06 | 0.06 | 0.0 | 0.0 | 0.09 | 35.99 | 97.89 |
| ALHA 77003 | 3a | 12.21 | 0.07 | 2.12 | 0.65 | 33.40 | 0.18 | 0.69 | 12.40 | 0.20 | 0.07 | 0.00 | 0.08 | 0.07 | 0.0 | 0.0 | 0.16 | 34.59 | 96.89 |
| ALHA 77003 | 3a | 13.76 | 0.08 | 0.85 | 0.24 | 30.26 | 0.21 | 2.05 | 13.87 | 0.15 | 0.07 | 0.00 | 0.08 | 0.10 | 0.0 | 0.0 | 0.16 | 35.48 | 97.36 |
| ALHA 77003 | 3a | 13.63 | 0.06 | 1.68 | 0.43 | 28.92 | 0.20 | 2.41 | 13.81 | 0.14 | 0.05 | 0.00 | 0.10 | 0.11 | 0.0 | 0.0 | 0.12 | 35.77 | 97.42 |
| ALHA 77003 | 3a | 15.19 | 0.05 | 0.57 | 0.14 | 28.89 | 0.23 | 1.05 | 15.49 | 0.11 | 0.03 | 0.02 | 0.07 | 0.08 | 0.0 | 0.0 | 0.06 | 37.00 | 98.99 |
| ALHA 77003 | 3a | 21.64 | 0.02 | 4.94 | 0.15 | 2.51 | 0.02 | 0.06 | 10.90 | 15.27 | 0.09 | 0.00 | 0.01 | 0.00 | 0.0 | 0.0 | 0.01 | 43.21 | 98.83 |
| ALHA 77003 | 3a | 14.25 | 0.07 | 0.91 | 0.28 | 30.39 | 0.21 | 1.10 | 14.28 | 0.20 | 0.14 | 0.00 | 0.10 | 0.13 | 0.0 | 0.0 | 0.06 | 36.05 | 98.16 |
| ALHA 77003 | 3a | 14.17 | 0.05 | 0.88 | 0.24 | 30.87 | 0.22 | 1.07 | 14.35 | 0.14 | 0.14 | 0.03 | 0.14 | 0.07 | 0.0 | 0.0 | 0.09 | 36.16 | 98.60 |
| ALHA 77003 | 3a | 14.12 | 0.05 | 0.89 | 0.33 | 30.73 | 0.22 | 0.97 | 14.18 | 0.16 | 0.08 | 0.02 | 0.06 | 0.07 | 0.0 | 0.0 | 0.61 | 36.65 | 99.15 |
| ALHA 77003 | 3a | 14.21 | 0.06 | 0.86 | 0.32 | 30.75 | 0.22 | 1.00 | 14.23 | 0.17 | 0.08 | 0.00 | 0.05 | 0.08 | 0.0 | 0.0 | 0.57 | 36.70 | 99.30 |
| ALHA 77003 | 3a | 15.85 | 0.04 | 0.74 | 0.34 | 28.28 | 0.23 | 0.61 | 15.66 | 0.48 | 0.05 | 0.00 | 0.04 | 0.07 | 0.0 | 0.0 | 0.10 | 37.99 | 100.50 |
| ALHA 77003 | 3a | 13.25 | 0.05 | 0.93 | 0.30 | 32.27 | 0.20 | 1.43 | 13.39 | 0.24 | 0.07 | 0.00 | 0.08 | 0.17 | 0.0 | 0.0 | 0.08 | 34.98 | 97.44 |
| ALHA 77003 | 3a | 13.38 | 0.08 | 0.62 | 0.24 | 32.34 | 0.20 | 1.52 | 13.60 | 0.18 | 0.06 | 0.01 | 0.07 | 0.09 | 0.0 | 0.0 | 0.10 | 35.01 | 97.49 |
| ALHA 77003 | 3a | 13.39 | 0.07 | 0.60 | 0.24 | 32.84 | 0.19 | 1.55 | 13.72 | 0.18 | 0.07 | 0.01 | 0.08 | 0.07 | 0.0 | 0.0 | 0.10 | 35.23 | 98.33 |
| ALHA 77003 | 4a | 17.27 | 0.05 | 1.29 | 0.42 | 25.81 | 0.30 | 0.65 | 15.61 | 0.59 | 0.48 | 0.10 | 0.04 | 0.07 | 0.0 | 0.0 | 0.07 | 39.57 | 102.29 |
| ALHA 77003 | 4a | 16.23 | 0.03 | 1.54 | 0.08 | 26.24 | 0.24 | 1.10 | 15.01 | 0.30 | 0.71 | 0.14 | 0.09 | 0.07 | 0.0 | 0.0 | 0.08 | 38.34 | 100.21 |
| ALHA 77003 | 4a | 18.49 | 0.07 | 0.79 | 0.33 | 22.11 | 0.23 | 0.51 | 15.94 | 1.20 | 0.24 | 0.03 | 0.04 | 0.05 | 0.0 | 0.0 | 0.05 | 39.71 | 99.78 |
| ALHA 77003 | 4a | 13.90 | 0.02 | 1.37 | 0.11 | 31.32 | 0.19 | 1.37 | 13.82 | 0.11 | 0.03 | 0.01 | 0.00 | 0.11 | 0.0 | 0.0 | 0.13 | 35.91 | 98.41 |
| ALHA 77003 | 4a | 15.15 | 0.01 | 0.27 | 0.10 | 30.30 | 0.23 | 0.90 | 15.68 | 0.10 | 0.02 | 0.02 | 0.02 | 0.10 | 0.0 | 0.0 | 0.08 | 37.10 | 100.08 |
| ALHA 77003 | 4a | 13.88 | 0.05 | 0.99 | 0.39 | 29.75 | 0.20 | 1.95 | 14.36 | 0.12 | 0.07 | 0.02 | 0.06 | 0.15 | 0.0 | 0.0 | 0.09 | 35.80 | 97.88 |
| ALHA 77003 | 4a | 13.87 | 0.04 | 0.79 | 0.30 | 30.49 | 0.19 | 1.32 | 14.36 | 0.13 | 0.07 | 0.01 | 0.06 | 0.12 | 0.0 | 0.0 | 0.18 | 35.74 | 97.68 |
| ALHA 77003 | 4a | 14.34 | 0.05 | 1.37 | 0.50 | 29.05 | 0.19 | 1.11 | 14.21 | 0.22 | 0.33 | 0.01 | 0.06 | 0.11 | 0.0 | 0.0 | 0.09 | 36.31 | 97.96 |
| ALHA 77003 | 4a | 15.57 | 0.06 | 0.91 | 0.26 | 27.53 | 0.19 | 0.97 | 14.83 | 0.96 | 0.08 | 0.00 | 0.07 | 0.07 | 0.0 | 0.0 | 0.08 | 37.34 | 98.94 |
| ALHA 77003 | 4a | 14.21 | 0.06 | 1.31 | 0.44 | 28.96 | 0.21 | 1.40 | 15.01 | 0.11 | 0.05 | 0.00 | 0.08 | 0.12 | 0.0 | 0.0 | 0.07 | 36.51 | 98.53 |
| ALHA 77003 | 4a | 14.38 | 0.05 | 0.75 | 0.25 | 30.58 | 0.20 | 0.62 | 15.53 | 0.11 | 0.04 | 0.02 | 0.05 | 0.08 | 0.0 | 0.0 | 0.09 | 36.69 | 99.43 |
| ALHA 77003 | 4a | 14.39 | 0.04 | 0.48 | 0.21 | 29.37 | 0.21 | 1.16 | 15.26 | 0.16 | 0.07 | 0.00 | 0.07 | 0.10 | 0.0 | 0.0 | 0.13 | 36.18 | 97.82 |
| ALHA 77003 | 4a | 16.17 | 0.03 | 0.28 | 0.15 | 26.82 | 0.20 | 0.36 | 17.35 | 0.09 | 0.04 | 0.02 | 0.06 | 0.06 | 0.0 | 0.0 | 0.04 | 38.23 | 99.88 |
| ALHA 77003 | 4a | 16.67 | 0.03 | 0.50 | 0.28 | 25.72 | 0.22 | 0.15 | 18.05 | 0.06 | 0.02 | 0.00 | 0.04 | 0.04 | 0.0 | 0.0 | 0.01 | 39.05 | 100.84 |
| ALHA 77003 | 4a | 17.26 | 0.00 | 0.00 | 0.01 | 23.90 | 0.18 | 0.26 | 19.37 | 0.08 | 0.00 | 0.00 | 0.00 | 0.04 | 0.0 | 0.0 | 0.03 | 39.48 | 100.63 |
| ALHA 77003 | 4a | 16.71 | 0.01 | 0.01 | 0.00 | 25.62 | 0.21 | 0.44 | 18.36 | 0.07 | 0.00 | 0.00 | 0.00 | 0.06 | 0.0 | 0.0 | 0.02 | 38.73 | 100.23 |
| ALHA 77003 | 4a | 14.41 | 0.06 | 1.06 | 0.26 | 29.89 | 0.19 | 0.63 | 15.18 | 0.12 | 0.07 | 0.01 | 0.07 | 0.09 | 0.0 | 0.0 | 0.07 | 36.59 | 98.70 |
| ALHA 77003 | 4a | 14.66 | 0.04 | 0.73 | 0.26 | 29.38 | 0.18 | 1.02 | 16.18 | 0.11 | 0.05 | 0.01 | 0.06 | 0.10 | 0.0 | 0.0 | 0.09 | 37.20 | 100.07 |
| ALHA 77003 | 4a | 19.11 | 0.02 | 0.01 | 0.03 | 12.07 | 0.07 | 0.02 | 27.42 | 0.21 | 0.00 | 0.00 | 0.00 | 0.02 | 0.0 | 0.0 | 0.01 | 43.44 | 102.45 |
| ALHA 77003 | 4a | 13.54 | 0.05 | 1.18 | 0.33 | 30.48 | 0.19 | 1.30 | 14.37 | 0.15 | 0.07 | 0.01 | 0.09 | 0.13 | 0.0 | 0.0 | 0.12 | 35.68 | 97.69 |
| ALHA 77003 | 4a | 14.23 | 0.08 | 1.62 | 0.42 | 28.75 | 0.18 | 0.85 | 15.12 | 0.14 | 0.07 | 0.01 | 0.10 | 0.08 | 0.0 | 0.0 | 0.08 | 36.73 | 98.45 |
| ALHA 77003 | 4a | 16.43 | 0.01 | 0.03 | 0.01 | 26.48 | 0.21 | 0.63 | 17.86 | 0.05 | 0.00 | 0.00 | 0.01 | 0.06 | 0.0 | 0.0 | 0.04 | 38.44 | 100.26 |
| ALHA 77003 | 4a | 17.23 | 0.02 | 0.16 | 0.16 | 24.18 | 0.24 | 0.07 | 18.94 | 0.04 | 0.01 | 0.01 | 0.00 | 0.03 | 0.0 | 0.0 | 0.01 | 39.40 | 100.52 |
| ALHA 77003 | 4a | 17.05 | 0.01 | 0.03 | 0.01 | 24.93 | 0.21 | 0.25 | 18.68 | 0.05 | 0.00 | 0.00 | 0.01 | 0.04 | 0.0 | 0.0 | 0.01 | 39.09 | 100.36 |
| ALHA 77003 | 4a | 16.15 | 0.02 | 0.11 | 0.03 | 26.17 | 0.18 | 0.38 | 17.88 | 0.05 | 0.01 | 0.01 | 0.00 | 0.07 | 0.0 | 0.0 | 0.03 | 38.03 | 99.12 |
| ALHA 77003 | 4a | 14.15 | 0.04 | 0.61 | 0.18 | 30.76 | 0.19 | 0.49 | 14.46 | 0.10 | 0.06 | 0.02 | 0.07 | 0.04 | 0.0 | 0.0 | 0.05 | 35.54 | 96.76 |
| ALHA 77003 | 4a | 16.06 | 0.05 | 1.16 | 0.32 | 27.11 | 0.23 | 0.99 | 14.74 | 0.69 | 0.29 | 0.04 | 0.07 | 0.08 | 0.0 | 0.0 | 0.08 | 37.95 | 99.90 |
| ALHA 77003 | 4a | 15.58 | 0.06 | 1.71 | 0.27 | 28.11 | 0.21 | 0.48 | 14.87 | 0.30 | 0.36 | 0.05 | 0.09 | 0.07 | 0.0 | 0.0 | 0.06 | 37.95 | 100.18 |
| ALHA 77003 | 4a | 15.32 | 0.05 | 0.60 | 0.18 | 28.65 | 0.24 | 0.66 | 15.55 | 0.11 | 0.04 | 0.01 | 0.06 | 0.07 | 0.0 | 0.0 | 0.06 | 37.05 | 98.64 |
| ALHA 77003 | 4a | 16.41 | 0.02 | 0.03 | 0.07 | 26.90 | 0.21 | 0.66 | 17.62 | 0.07 | 0.02 | 0.00 | 0.00 | 0.06 | 0.0 | 0.0 | 0.05 | 38.45 | 100.57 |
| ALHA 77003 | 4a | 16.20 | 0.02 | 0.08 | 0.19 | 27.29 | 0.23 | 0.58 | 16.80 | 0.08 | 0.01 | 0.00 | 0.00 | 0.07 | 0.0 | 0.0 | 0.02 | 37.80 | 99.35 |
| ALHA 77003 | 4a | 13.56 | 0.04 | 0.60 | 0.25 | 30.69 | 0.20 | 2.37 | 14.44 | 0.10 | 0.04 | 0.00 | 0.02 | 0.18 | 0.0 | 0.0 | 0.14 | 35.47 | 98.11 |
| ALHA 77003 | 4a | 19.41 | 0.03 | 13.49 | 0.08 | 10.79 | 0.10 | 0.09 | 6.06 | 4.37 | 5.39 | 0.02 | 0.00 | 0.02 | 0.0 | 0.0 | 0.01 | 44.94 | 104.80 |
| ALHA 77003 | 4a | 14.19 | 0.08 | 1.21 | 0.30 | 30.11 | 0.21 | 1.28 | 14.20 | 0.26 | 0.30 | 0.06 | 0.06 | 0.15 | 0.0 | 0.0 | 0.13 | 36.35 | 98.90 |
| ALHA 77003 | 4a | 17.02 | 0.02 | 0.02 | 0.01 | 26.85 | 0.25 | 0.33 | 17.88 | 0.03 | 0.01 | 0.00 | 0.04 | 0.04 | 0.0 | 0.0 | 0.01 | 39.15 | 101.66 |
| ALHA 77003 | 4a | 13.84 | 0.05 | 0.93 | 0.28 | 31.02 | 0.20 | 1.09 | 13.61 | 0.62 | 0.09 | 0.00 | 0.07 | 0.12 | 0.0 | 0.0 | 0.11 | 35.51 | 97.52 |
| ALHA 77003 | 4a | 17.50 | 0.02 | 1.74 | 0.18 | 23.27 | 0.23 | 0.02 | 16.95 | 0.41 | 0.64 | 0.03 | 0.01 | 0.02 | 0.0 | 0.0 | 0.01 | 39.90 | 100.92 |
| ALHA 77003 | 4a | 17.77 | 0.07 | 3.04 | 0.09 | 22.20 | 0.22 | 0.04 | 15.30 | 2.46 | 0.01 | 0.00 | 0.00 | 0.03 | 0.0 | 0.0 | 0.00 | 40.52 | 101.75 |
| ALHA 77003 | 4a | 17.73 | 0.10 | 3.09 | 0.10 | 22.05 | 0.21 | 0.02 | 15.16 | 2.55 | 0.01 | 0.00 | 0.00 | 0.03 | 0.0 | 0.0 | 0.01 | 40.47 | 101.53 |
| ALHA 77003 | 4a | 17.77 | 0.09 | 3.02 | 0.09 | 22.18 | 0.22 | 0.04 | 15.27 | 2.41 | 0.01 | 0.01 | 0.00 | 0.03 | 0.0 | 0.0 | 0.00 | 40.49 | 101.61 |

Continued on next page

| Sample | Area | Si | Ti | Al | Cr | Fe | Mn | Ni | Mg | Ca | Na | K | P | Co | V | Zn | S | O | Total |
|---|---|---|---|---|---|---|---|---|---|---|---|---|---|---|---|---|---|---|---|
| ALHA 77003 | 5a | 13.40 | 0.07 | 1.33 | 0.48 | 31.36 | 0.19 | 1.84 | 13.08 | 0.17 | 0.12 | 0.01 | 0.07 | 0.15 | 0.0 | 0.0 | 0.15 | 35.34 | 97.78 |
| ALHA 77003 | 5a | 20.59 | 0.10 | 0.64 | 0.30 | 18.67 | 0.17 | 0.89 | 15.25 | 3.52 | 0.16 | 0.02 | 0.01 | 0.06 | 0.0 | 0.0 | 0.04 | 41.47 | 101.88 |
| ALHA 77003 | 5a | 17.37 | 0.02 | 0.18 | 0.10 | 24.80 | 0.21 | 0.07 | 19.05 | 0.11 | 0.00 | 0.00 | 0.00 | 0.04 | 0.0 | 0.0 | 0.01 | 39.78 | 101.73 |
| ALHA 77003 | 5a | 17.35 | 0.02 | 0.22 | 0.10 | 24.87 | 0.20 | 0.08 | 19.06 | 0.10 | 0.00 | 0.00 | 0.01 | 0.03 | 0.0 | 0.0 | 0.00 | 39.83 | 101.87 |
| ALHA 77003 | 5a | 12.48 | 0.06 | 1.91 | 2.00 | 30.62 | 0.21 | 1.63 | 12.21 | 0.13 | 0.07 | 0.00 | 0.09 | 0.12 | 0.0 | 0.0 | 0.13 | 34.61 | 96.27 |
| ALHA 77003 | 5a | 17.18 | 0.09 | 1.03 | 0.45 | 24.79 | 0.26 | 0.83 | 15.21 | 1.58 | 0.12 | 0.01 | 0.03 | 0.08 | 0.0 | 0.0 | 0.08 | 39.03 | 100.78 |
| ALHA 77003 | 5a | 23.61 | 0.07 | 0.55 | 0.52 | 10.01 | 0.23 | 1.68 | 16.25 | 4.44 | 0.10 | 0.01 | 0.01 | 0.12 | 0.0 | 0.0 | 0.10 | 43.76 | 101.43 |
| ALHA 77003 | 5a | 13.91 | 0.05 | 0.72 | 0.28 | 30.91 | 0.20 | 1.96 | 14.20 | 0.12 | 0.05 | 0.00 | 0.05 | 0.10 | 0.0 | 0.0 | 0.16 | 35.84 | 98.55 |
| ALHA 77003 | 5a | 17.10 | 0.23 | 1.39 | 0.30 | 23.47 | 0.21 | 1.80 | 13.72 | 2.20 | 0.27 | 0.03 | 0.12 | 0.09 | 0.0 | 0.0 | 0.19 | 38.76 | 99.88 |
| ALHA 77003 | 5a | 25.00 | 0.05 | 0.49 | 0.42 | 11.45 | 0.33 | 0.28 | 20.01 | 0.80 | 0.02 | 0.00 | 0.00 | 0.05 | 0.0 | 0.0 | 0.01 | 46.13 | 105.04 |
| ALHA 77003 | 5a | 16.74 | 0.05 | 2.28 | 0.33 | 24.34 | 0.23 | 0.98 | 13.94 | 0.66 | 0.88 | 0.17 | 0.03 | 0.10 | 0.0 | 0.0 | 0.06 | 38.52 | 99.30 |
| ALHA 77003 | 5a | 1.51 | 0.03 | 1.10 | 0.74 | 51.39 | 0.01 | 5.71 | 1.06 | 0.52 | 0.25 | 0.01 | 0.21 | 0.32 | 0.0 | 0.0 | 2.21 | 23.99 | 89.05 |
| ALHA 77003 | 5a | 16.95 | 0.07 | 0.81 | 1.02 | 26.05 | 0.24 | 0.69 | 14.69 | 3.08 | 0.16 | 0.02 | 0.10 | 0.07 | 0.0 | 0.0 | 3.72 | 44.96 | 112.64 |
| ALHA 77003 | 5a | 18.38 | 0.06 | 1.77 | 0.11 | 22.00 | 0.20 | 0.18 | 14.68 | 2.44 | 0.57 | 0.08 | 0.01 | 0.03 | 0.0 | 0.0 | 0.02 | 39.92 | 100.45 |
| ALHA 77003 | 5a | 10.36 | 0.02 | 3.59 | 0.08 | 38.84 | 0.12 | 0.60 | 7.87 | 0.44 | 2.61 | 0.29 | 0.07 | 0.07 | 0.0 | 0.0 | 9.32 | 46.76 | 121.04 |
| ALHA 77003 | 5a | 16.47 | 0.01 | 0.11 | 0.11 | 28.35 | 0.27 | 0.49 | 16.81 | 0.07 | 0.06 | 0.01 | 0.18 | 0.05 | 0.0 | 0.0 | 0.03 | 38.66 | 101.69 |
| ALHA 77003 | 5a | 14.85 | 0.03 | 0.61 | 0.34 | 30.26 | 0.22 | 1.20 | 14.96 | 0.13 | 0.05 | 0.01 | 0.06 | 0.08 | 0.0 | 0.0 | 0.40 | 37.33 | 100.55 |
| ALHA 77003 | 5a | 14.82 | 0.02 | 0.81 | 0.11 | 28.83 | 0.21 | 1.51 | 14.78 | 0.17 | 0.25 | 0.03 | 0.05 | 0.10 | 0.0 | 0.0 | 0.18 | 36.66 | 98.54 |
| ALHA 77003 | 5a | 11.96 | 0.04 | 2.89 | 0.30 | 32.84 | 0.14 | 1.05 | 9.03 | 0.62 | 1.30 | 0.20 | 0.04 | 0.09 | 0.0 | 0.0 | 0.16 | 33.10 | 93.75 |
| ALHA 77003 | 5a | 13.44 | 0.06 | 0.80 | 0.05 | 31.65 | 0.17 | 0.66 | 12.98 | 1.10 | 0.02 | 0.01 | 0.01 | 0.09 | 0.0 | 0.0 | 0.08 | 34.53 | 95.64 |
| ALHA 77003 | 5a | 17.55 | 0.06 | 1.15 | 0.24 | 25.04 | 0.24 | 0.02 | 16.55 | 1.33 | 0.03 | 0.03 | 0.00 | 0.02 | 0.0 | 0.0 | 0.00 | 39.87 | 102.14 |
| ALHA 77003 | 5a | 14.17 | 0.04 | 0.43 | 0.16 | 31.73 | 0.23 | 0.64 | 13.80 | 0.24 | 0.03 | 0.01 | 0.02 | 0.06 | 0.0 | 0.0 | 0.06 | 35.29 | 96.89 |
| ALHA 77003 | 5a | 23.87 | 0.06 | 0.61 | 0.50 | 10.79 | 0.22 | 0.52 | 16.25 | 3.23 | 0.15 | 0.00 | 0.05 | 0.03 | 0.0 | 0.0 | 0.32 | 43.90 | 100.49 |
| ALHA 77003 | 5a | 12.91 | 0.01 | 0.42 | 0.20 | 32.83 | 0.18 | 2.06 | 13.00 | 0.21 | 0.02 | 0.00 | 0.12 | 0.09 | 0.0 | 0.0 | 0.58 | 34.91 | 97.55 |
| ALHA 77003 | 5a | 13.80 | 0.03 | 0.75 | 0.28 | 32.23 | 0.21 | 1.11 | 13.99 | 0.10 | 0.05 | 0.00 | 0.05 | 0.07 | 0.0 | 0.0 | 0.12 | 35.65 | 98.42 |
| ALHA 77003 | 5a | 18.04 | 0.05 | 0.27 | 0.12 | 24.24 | 0.25 | 0.17 | 16.30 | 2.00 | 0.10 | 0.01 | 0.19 | 0.03 | 0.0 | 0.0 | 0.04 | 39.82 | 101.62 |
| ALHA 77003 | 5a | 14.83 | 0.01 | 0.23 | 0.06 | 30.58 | 0.22 | 1.05 | 14.72 | 0.05 | 0.03 | 0.00 | 0.04 | 0.06 | 0.0 | 0.0 | 0.07 | 36.15 | 98.11 |
| ALHA 77003 | 5a | 16.17 | 0.03 | 0.50 | 0.19 | 27.85 | 0.24 | 0.42 | 15.99 | 0.10 | 0.04 | 0.00 | 0.04 | 0.06 | 0.0 | 0.0 | 0.03 | 37.83 | 99.50 |
| ALHA 77003 | 5a | 16.56 | 0.05 | 1.52 | 0.28 | 25.93 | 0.25 | 0.26 | 15.10 | 0.42 | 0.44 | 0.08 | 0.11 | 0.04 | 0.0 | 0.0 | 0.03 | 38.42 | 99.48 |
| ALHA 77003 | 5a | 15.06 | 0.01 | 0.04 | 0.03 | 28.32 | 0.12 | 0.76 | 17.34 | 0.18 | 0.01 | 0.00 | 0.00 | 0.07 | 0.0 | 0.0 | 0.08 | 37.19 | 99.22 |
| ALHA 77003 | 5a | 15.87 | 0.04 | 0.52 | 0.23 | 28.71 | 0.25 | 0.50 | 16.17 | 0.08 | 0.03 | 0.00 | 0.06 | 0.05 | 0.0 | 0.0 | 0.05 | 37.96 | 100.52 |
| ALHA 77003 | 5a | 14.17 | 0.05 | 1.48 | 0.46 | 29.87 | 0.22 | 1.30 | 14.14 | 0.09 | 0.07 | 0.00 | 0.08 | 0.09 | 0.0 | 0.0 | 0.09 | 36.32 | 98.42 |
| ALHA 77003 | 5a | 16.39 | 0.09 | 0.57 | 0.10 | 27.90 | 0.23 | 0.42 | 15.97 | 0.71 | 0.01 | 0.01 | 0.00 | 0.05 | 0.0 | 0.0 | 0.03 | 38.33 | 100.82 |
| ALHA 77003 | 5a | 11.81 | 0.03 | 0.59 | 0.51 | 34.73 | 0.20 | 1.91 | 10.91 | 0.23 | 0.09 | 0.00 | 0.27 | 0.17 | 0.0 | 0.0 | 0.22 | 32.79 | 94.44 |
| ALHA 77003 | 5a | 26.63 | 0.09 | 0.42 | 0.34 | 3.65 | 0.12 | 0.03 | 21.06 | 0.85 | 0.09 | 0.01 | 0.00 | 0.01 | 0.0 | 0.0 | 0.00 | 46.24 | 99.51 |
| ALHA 77003 | 5a | 14.13 | 0.04 | 0.46 | 0.15 | 32.08 | 0.21 | 1.13 | 13.49 | 0.22 | 0.08 | 0.03 | 0.07 | 0.08 | 0.0 | 0.0 | 0.09 | 35.41 | 97.66 |
| ALHA 77003 | 5a | 15.71 | 0.01 | 0.10 | 0.04 | 29.77 | 0.22 | 0.82 | 16.34 | 0.06 | 0.00 | 0.00 | 0.02 | 0.09 | 0.0 | 0.0 | 0.06 | 37.74 | 100.98 |
| ALHA 77003 | 5a | 15.87 | 0.01 | 0.09 | 0.04 | 29.96 | 0.23 | 0.74 | 16.41 | 0.06 | 0.00 | 0.00 | 0.01 | 0.07 | 0.0 | 0.0 | 0.05 | 37.98 | 101.54 |
| ALHA 77003 | 5a | 13.45 | 0.04 | 0.27 | 0.11 | 33.29 | 0.20 | 1.34 | 13.05 | 0.10 | 0.05 | 0.01 | 0.03 | 0.11 | 0.0 | 0.0 | 0.08 | 34.43 | 96.55 |
| ALHA 77003 | 5a | 14.59 | 0.05 | 0.51 | 0.23 | 30.17 | 0.22 | 1.51 | 14.21 | 0.23 | 0.07 | 0.00 | 0.06 | 0.11 | 0.0 | 0.0 | 0.07 | 36.03 | 98.06 |
| ALHA 77003 | 5a | 16.65 | 0.05 | 0.15 | 0.25 | 27.45 | 0.26 | 0.51 | 16.23 | 0.36 | 0.03 | 0.00 | 0.04 | 0.06 | 0.0 | 0.0 | 0.03 | 38.27 | 100.33 |
| ALHA 77003 | 5a | 12.29 | 0.08 | 1.07 | 0.40 | 31.62 | 0.19 | 0.89 | 12.60 | 1.88 | 0.15 | 0.00 | 1.23 | 0.08 | 0.0 | 0.0 | 0.10 | 35.40 | 97.98 |
| ALHA 77003 | 5a | 16.82 | 0.03 | 0.10 | 0.07 | 27.82 | 0.25 | 0.28 | 17.02 | 0.04 | 0.01 | 0.01 | 0.01 | 0.05 | 0.0 | 0.0 | 0.03 | 38.72 | 101.25 |
| ALHA 77003 | 5a | 14.47 | 0.03 | 0.27 | 0.06 | 31.46 | 0.21 | 1.05 | 14.51 | 0.08 | 0.04 | 0.00 | 0.02 | 0.07 | 0.0 | 0.0 | 0.11 | 35.95 | 98.35 |
| ALHA 77003 | 5a | 12.32 | 0.03 | 0.20 | 0.14 | 35.03 | 0.18 | 2.32 | 12.32 | 0.15 | 0.07 | 0.00 | 0.03 | 0.15 | 0.0 | 0.0 | 0.15 | 33.52 | 96.62 |
| ALHA 77003 | 5a | 12.83 | 0.07 | 1.16 | 0.43 | 32.38 | 0.22 | 1.55 | 12.57 | 0.11 | 0.07 | 0.02 | 0.06 | 0.12 | 0.0 | 0.0 | 0.12 | 34.29 | 95.99 |
| ALHA 77003 | 5a | 14.86 | 0.05 | 0.31 | 0.19 | 30.19 | 0.24 | 1.58 | 14.95 | 0.16 | 0.04 | 0.01 | 0.05 | 0.12 | 0.0 | 0.0 | 0.09 | 36.63 | 99.47 |
| ALHA 77003 | 5a | 13.89 | 0.03 | 0.08 | 0.09 | 30.90 | 0.21 | 2.25 | 14.52 | 0.07 | 0.00 | 0.00 | 0.01 | 0.12 | 0.0 | 0.0 | 0.11 | 35.29 | 97.59 |
| ALHA 77003 | 5a | 15.26 | 0.03 | 0.16 | 0.09 | 29.91 | 0.22 | 0.74 | 15.44 | 0.08 | 0.04 | 0.00 | 0.05 | 0.07 | 0.0 | 0.0 | 0.07 | 36.81 | 98.96 |
| ALHA 77003 | 5a | 15.21 | 0.04 | 0.45 | 0.21 | 29.47 | 0.21 | 0.73 | 15.03 | 0.09 | 0.06 | 0.00 | 0.06 | 0.07 | 0.0 | 0.0 | 0.07 | 36.71 | 98.41 |
| ALHA 77003 | 5a | 13.33 | 0.05 | 1.41 | 0.31 | 31.32 | 0.18 | 2.04 | 13.76 | 0.13 | 0.09 | 0.00 | 0.07 | 0.12 | 0.0 | 0.0 | 0.18 | 35.74 | 98.73 |
| ALHA 77003 | 5a | 12.70 | 0.06 | 1.76 | 0.28 | 31.39 | 0.19 | 1.99 | 12.46 | 0.12 | 0.10 | 0.02 | 0.07 | 0.11 | 0.0 | 0.0 | 0.20 | 34.50 | 95.95 |
| ALHA 77003 | 5a | 13.42 | 0.05 | 0.73 | 0.19 | 33.05 | 0.18 | 1.15 | 13.54 | 0.09 | 0.06 | 0.00 | 0.06 | 0.09 | 0.0 | 0.0 | 0.09 | 35.10 | 97.80 |
| ALHA 77003 | 5a | 13.40 | 0.06 | 0.60 | 0.20 | 32.77 | 0.18 | 1.05 | 13.24 | 0.10 | 0.08 | 0.00 | 0.07 | 0.06 | 0.0 | 0.0 | 0.07 | 34.67 | 96.56 |
| ALHA 77003 | 5a | 14.16 | 0.05 | 1.24 | 0.51 | 29.87 | 0.22 | 1.36 | 14.27 | 0.14 | 0.06 | 0.00 | 0.05 | 0.08 | 0.0 | 0.0 | 0.11 | 36.20 | 98.30 |
| ALHA 77003 | 5a | 14.61 | 0.06 | 1.08 | 0.26 | 29.39 | 0.20 | 1.07 | 13.65 | 0.79 | 0.18 | 0.02 | 0.05 | 0.09 | 0.0 | 0.0 | 0.12 | 36.16 | 97.73 |
| ALHA 77003 | 5a | 12.24 | 0.06 | 0.70 | 0.30 | 33.09 | 0.17 | 2.50 | 12.38 | 0.14 | 0.07 | 0.01 | 0.05 | 0.14 | 0.0 | 0.0 | 0.16 | 33.54 | 95.55 |
| ALHA 77003 | 6a | 14.55 | 0.08 | 1.01 | 0.29 | 29.49 | 0.24 | 1.94 | 13.97 | 0.10 | 0.18 | 0.03 | 0.10 | 0.09 | 0.0 | 0.0 | 0.09 | 36.30 | 98.46 |

Continued on next page

| Sample | Area | Si | Ti | Al | Cr | Fe | Mn | Ni | Mg | Ca | Na | K | P | Co | V | Zn | S | O | Total |
|---|---|---|---|---|---|---|---|---|---|---|---|---|---|---|---|---|---|---|---|
| ALHA 77003 | 6a | 8.42 | 0.01 | 0.10 | 0.05 | 41.34 | 0.15 | 1.91 | 9.71 | 0.13 | 0.10 | 0.00 | 0.00 | 0.14 | 0.0 | 0.0 | 0.27 | 29.03 | 91.37 |
| ALHA 77003 | 6a | 12.21 | 0.05 | 1.79 | 0.24 | 33.52 | 0.20 | 1.48 | 10.42 | 0.25 | 0.80 | 0.07 | 0.08 | 0.11 | 0.0 | 0.0 | 0.11 | 33.27 | 94.60 |
| ALHA 77003 | 6a | 16.36 | 0.01 | 0.07 | 0.04 | 29.01 | 0.29 | 0.26 | 15.12 | 0.57 | 0.03 | 0.00 | 0.02 | 0.06 | 0.0 | 0.0 | 0.02 | 37.45 | 99.30 |
| ALHA 77003 | 6a | 11.00 | 0.06 | 0.54 | 0.24 | 36.60 | 0.20 | 1.24 | 9.87 | 0.08 | 0.13 | 0.02 | 0.03 | 0.16 | 0.0 | 0.0 | 0.10 | 30.84 | 91.09 |
| ALHA 77003 | 6a | 25.58 | 0.08 | 0.53 | 0.32 | 6.93 | 0.13 | 0.03 | 19.77 | 2.10 | 0.15 | 0.00 | 0.00 | 0.00 | 0.0 | 0.0 | 0.00 | 45.75 | 101.36 |
| ALHA 77003 | 6a | 12.79 | 0.04 | 1.02 | 0.43 | 34.17 | 0.22 | 0.48 | 12.50 | 0.10 | 0.08 | 0.00 | 0.07 | 0.07 | 0.0 | 0.0 | 0.07 | 34.20 | 96.23 |
| ALHA 77003 | 6a | 14.10 | 0.03 | 0.21 | 0.10 | 33.34 | 0.22 | 0.81 | 13.87 | 0.05 | 0.07 | 0.01 | 0.06 | 0.09 | 0.0 | 0.0 | 0.07 | 35.55 | 98.58 |
| ALHA 77003 | 6a | 12.72 | 0.07 | 0.89 | 0.33 | 34.46 | 0.20 | 1.04 | 12.41 | 0.10 | 0.13 | 0.02 | 0.07 | 0.09 | 0.0 | 0.0 | 0.09 | 34.22 | 96.84 |
| ALHA 77003 | 6a | 14.78 | 0.02 | 0.39 | 0.15 | 29.83 | 0.24 | 1.72 | 14.70 | 0.06 | 0.07 | 0.00 | 0.10 | 0.08 | 0.0 | 0.0 | 0.08 | 36.35 | 98.57 |
| ALHA 77003 | 6a | 19.17 | 0.12 | 8.80 | 0.18 | 11.26 | 0.30 | 1.12 | 4.04 | 5.96 | 3.85 | 0.56 | 0.01 | 0.08 | 0.0 | 0.0 | 0.05 | 40.06 | 95.56 |
| ALHA 77003 | 6a | 16.51 | 0.06 | 0.56 | 0.16 | 25.97 | 0.21 | 1.13 | 12.72 | 3.98 | 0.14 | 0.01 | 0.05 | 0.08 | 0.0 | 0.0 | 0.07 | 37.44 | 99.08 |
| ALHA 77003 | 6a | 18.00 | 0.05 | 0.60 | 0.31 | 22.44 | 0.14 | 1.08 | 13.13 | 1.91 | 0.18 | 0.01 | 0.03 | 0.05 | 0.0 | 0.0 | 0.11 | 37.67 | 95.71 |
| ALHA 77003 | 6a | 11.80 | 0.06 | 1.78 | 0.81 | 34.03 | 0.20 | 0.89 | 11.67 | 0.09 | 0.11 | 0.01 | 0.07 | 0.09 | 0.0 | 0.0 | 0.11 | 33.52 | 95.23 |
| ALHA 77003 | 6a | 12.75 | 0.04 | 1.95 | 0.93 | 31.76 | 0.21 | 1.94 | 13.09 | 0.07 | 0.07 | 0.01 | 0.05 | 0.07 | 0.0 | 0.0 | 0.08 | 35.28 | 98.30 |
| ALHA 77003 | 6a | 16.99 | 0.06 | 1.69 | 0.33 | 25.02 | 0.23 | 0.07 | 15.93 | 0.59 | 0.47 | 0.11 | 0.09 | 0.03 | 0.0 | 0.0 | 0.19 | 39.62 | 101.43 |
| ALHA 77003 | 6a | 8.57 | 0.01 | 0.54 | 0.30 | 39.88 | 0.14 | 3.06 | 8.24 | 0.14 | 0.13 | 0.00 | 0.02 | 0.23 | 0.0 | 0.0 | 0.15 | 28.52 | 89.90 |
| ALHA 77003 | 6a | 11.50 | 0.02 | 1.00 | 0.30 | 34.61 | 0.17 | 1.76 | 11.50 | 0.17 | 0.30 | 0.04 | 0.09 | 0.10 | 0.0 | 0.0 | 0.85 | 33.77 | 96.19 |
| ALHA 77003 | 6a | 15.62 | 0.11 | 2.30 | 0.47 | 21.01 | 0.30 | 1.98 | 8.21 | 6.42 | 0.78 | 0.07 | 0.03 | 0.12 | 0.0 | 0.0 | 0.20 | 35.40 | 93.01 |
| ALHA 77003 | 6a | 12.73 | 0.06 | 0.62 | 0.16 | 34.46 | 0.21 | 0.60 | 12.66 | 0.09 | 0.10 | 0.00 | 0.06 | 0.08 | 0.0 | 0.0 | 0.12 | 33.94 | 95.88 |
| ALHA 77003 | 6a | 12.96 | 0.04 | 0.61 | 0.14 | 34.72 | 0.21 | 0.58 | 12.89 | 0.09 | 0.08 | 0.00 | 0.06 | 0.07 | 0.0 | 0.0 | 0.10 | 34.37 | 96.92 |
| ALHA 77003 | 6a | 16.06 | 0.04 | 0.56 | 0.39 | 29.01 | 0.25 | 0.48 | 15.50 | 0.14 | 0.08 | 0.00 | 0.03 | 0.04 | 0.0 | 0.0 | 0.05 | 37.93 | 100.55 |
| ALHA 77003 | 6a | 13.47 | 0.05 | 1.03 | 0.37 | 32.54 | 0.21 | 1.10 | 13.16 | 0.09 | 0.10 | 0.01 | 0.07 | 0.11 | 0.0 | 0.0 | 0.09 | 35.15 | 97.55 |
| ALHA 77003 | 6a | 16.24 | 0.00 | 0.00 | 0.01 | 28.86 | 0.24 | 0.26 | 16.70 | 0.02 | 0.01 | 0.00 | 0.00 | 0.05 | 0.0 | 0.0 | 0.01 | 37.95 | 100.38 |
| ALHA 77003 | 6a | 16.43 | 0.05 | 0.58 | 0.67 | 27.25 | 0.28 | 0.28 | 14.36 | 0.93 | 0.09 | 0.01 | 0.06 | 0.05 | 0.0 | 0.0 | 0.04 | 37.54 | 98.61 |
| ALHA 77003 | 6a | 14.76 | 0.05 | 0.45 | 0.15 | 31.88 | 0.23 | 0.75 | 13.97 | 0.10 | 0.11 | 0.01 | 0.06 | 0.09 | 0.0 | 0.0 | 0.06 | 36.19 | 98.87 |
| ALHA 77003 | 6a | 12.71 | 0.04 | 0.69 | 0.38 | 35.13 | 0.22 | 0.33 | 12.03 | 0.09 | 0.09 | 0.01 | 0.06 | 0.07 | 0.0 | 0.0 | 0.07 | 33.70 | 95.62 |
| ALHA 77003 | 6a | 13.14 | 0.04 | 0.95 | 0.23 | 34.57 | 0.22 | 0.40 | 12.05 | 0.15 | 0.31 | 0.03 | 0.11 | 0.06 | 0.0 | 0.0 | 0.07 | 34.40 | 96.73 |
| ALHA 77003 | 6a | 26.73 | 0.06 | 0.30 | 0.33 | 3.81 | 0.07 | 0.42 | 22.66 | 0.37 | 0.02 | 0.01 | 0.00 | 0.04 | 0.0 | 0.0 | 0.03 | 47.26 | 102.10 |
| ALHA 77003 | 6a | 14.76 | 0.07 | 0.89 | 0.40 | 29.57 | 0.28 | 1.36 | 13.91 | 0.27 | 0.22 | 0.04 | 0.13 | 0.09 | 0.0 | 0.0 | 0.10 | 36.46 | 98.55 |
| ALHA 77003 | 6a | 17.15 | 0.07 | 0.70 | 0.17 | 27.62 | 0.28 | 0.05 | 15.72 | 0.80 | 0.07 | 0.00 | 0.06 | 0.02 | 0.0 | 0.0 | 0.01 | 39.08 | 101.79 |
| ALHA 77003 | 6a | 13.24 | 0.05 | 1.37 | 0.36 | 33.56 | 0.23 | 0.86 | 13.39 | 0.10 | 0.09 | 0.00 | 0.08 | 0.07 | 0.0 | 0.0 | 0.11 | 35.60 | 99.12 |
| ALHA 77003 | 6a | 12.64 | 0.05 | 0.85 | 0.18 | 34.74 | 0.21 | 1.30 | 12.28 | 0.11 | 0.10 | 0.02 | 0.04 | 0.08 | 0.0 | 0.0 | 0.21 | 34.20 | 97.00 |
| ALHA 77003 | 6a | 9.48 | 0.27 | 2.04 | 1.35 | 36.27 | 0.13 | 1.90 | 7.57 | 1.61 | 0.76 | 0.12 | 0.41 | 0.14 | 0.0 | 0.0 | 0.18 | 31.11 | 93.33 |
| ALHA 77003 | 6a | 13.13 | 0.07 | 1.14 | 0.37 | 32.15 | 0.20 | 1.79 | 12.57 | 0.34 | 0.14 | 0.04 | 0.10 | 0.11 | 0.0 | 0.0 | 0.26 | 34.95 | 97.34 |
| ALHA 77003 | 6a | 16.14 | 0.06 | 0.93 | 0.31 | 27.76 | 0.25 | 0.62 | 15.51 | 0.14 | 0.19 | 0.08 | 0.05 | 0.06 | 0.0 | 0.0 | 0.04 | 38.07 | 100.19 |
| ALHA 77003 | 6a | 16.28 | 0.04 | 0.35 | 0.21 | 27.96 | 0.21 | 0.60 | 14.54 | 0.69 | 0.15 | 0.01 | 0.01 | 0.07 | 0.0 | 0.0 | 0.08 | 37.27 | 98.47 |
| ALHA 77003 | 6a | 13.59 | 0.05 | 1.23 | 0.44 | 33.64 | 0.21 | 0.43 | 13.95 | 0.06 | 0.10 | 0.01 | 0.07 | 0.05 | 0.0 | 0.0 | 2.95 | 40.39 | 107.18 |
| ALHA 77003 | 6a | 14.76 | 0.08 | 1.21 | 0.37 | 29.69 | 0.23 | 0.66 | 14.61 | 0.07 | 0.12 | 0.02 | 0.10 | 0.08 | 0.0 | 0.0 | 0.10 | 36.85 | 98.95 |
| ALHA 77003 | 6a | 11.97 | 0.07 | 0.26 | 0.05 | 35.23 | 0.18 | 1.77 | 12.32 | 0.11 | 0.09 | 0.01 | 0.05 | 0.15 | 0.0 | 0.0 | 0.17 | 33.10 | 95.52 |
| ALHA 77003 | 6a | 22.52 | 0.50 | 14.71 | 0.13 | 6.00 | 0.05 | 0.02 | 4.79 | 5.06 | 9.98 | 0.01 | 0.01 | 0.00 | 0.0 | 0.0 | 0.01 | 49.55 | 113.34 |
| ALHA 77003 | 6a | 9.74 | 0.04 | 0.72 | 0.26 | 38.22 | 0.15 | 2.30 | 9.90 | 0.10 | 0.14 | 0.00 | 0.05 | 0.21 | 0.0 | 0.0 | 0.14 | 30.45 | 92.43 |
| ALHA 77003 | 6a | 14.40 | 0.07 | 0.69 | 0.21 | 29.75 | 0.23 | 0.73 | 14.24 | 0.06 | 0.09 | 0.01 | 0.07 | 0.07 | 0.0 | 0.0 | 0.06 | 35.58 | 96.27 |
| ALHA 77003 | 6a | 14.00 | 0.05 | 0.88 | 0.15 | 29.40 | 0.21 | 1.66 | 14.10 | 0.05 | 0.08 | 0.00 | 0.06 | 0.13 | 0.0 | 0.0 | 0.11 | 35.38 | 96.26 |
| ALHA 77003 | 6a | 13.66 | 0.06 | 1.10 | 0.31 | 31.78 | 0.20 | 1.15 | 14.15 | 0.05 | 0.07 | 0.00 | 0.08 | 0.09 | 0.0 | 0.0 | 0.11 | 35.85 | 98.66 |
| ALHA 77003 | 6a | 10.72 | 0.03 | 1.15 | 0.23 | 39.02 | 0.15 | 0.48 | 10.55 | 0.22 | 0.14 | 0.01 | 0.04 | 0.09 | 0.0 | 0.0 | 0.19 | 32.16 | 95.20 |
| ALHA 77003 | 7a | 15.65 | 0.09 | 1.91 | 0.33 | 25.39 | 0.20 | 0.57 | 15.04 | 0.26 | 0.51 | 0.15 | 0.10 | 0.05 | 0.0 | 0.0 | 0.06 | 37.68 | 97.97 |
| ALHA 77003 | 7a | 17.37 | 0.02 | 0.04 | 0.07 | 25.60 | 0.25 | 0.22 | 18.11 | 0.11 | 0.00 | 0.00 | 0.00 | 0.03 | 0.0 | 0.0 | 0.02 | 39.34 | 101.18 |
| ALHA 77003 | 7a | 16.22 | 0.09 | 1.65 | 0.36 | 25.44 | 0.23 | 0.39 | 16.15 | 0.19 | 0.36 | 0.08 | 0.10 | 0.05 | 0.0 | 0.0 | 0.04 | 38.68 | 100.03 |
| ALHA 77003 | 7a | 15.52 | 0.10 | 2.61 | 0.25 | 25.22 | 0.21 | 0.67 | 14.69 | 0.21 | 1.00 | 0.12 | 0.10 | 0.07 | 0.0 | 0.0 | 0.05 | 38.02 | 98.85 |
| ALHA 77003 | 7a | 15.45 | 0.07 | 1.38 | 0.32 | 26.89 | 0.21 | 0.93 | 16.37 | 0.09 | 0.07 | 0.00 | 0.07 | 0.08 | 0.0 | 0.0 | 0.08 | 38.11 | 100.11 |
| ALHA 77003 | 7a | 27.91 | 0.13 | 0.41 | 0.10 | 1.09 | 0.07 | 0.02 | 23.58 | 0.52 | 0.01 | 0.01 | 0.00 | 0.00 | 0.0 | 0.0 | 0.00 | 48.36 | 102.21 |
| ALHA 77003 | 7a | 14.48 | 0.07 | 0.83 | 0.29 | 30.94 | 0.19 | 0.39 | 14.20 | 0.23 | 0.20 | 0.03 | 0.11 | 0.09 | 0.0 | 0.0 | 0.05 | 36.20 | 98.31 |
| ALHA 77003 | 7a | 24.78 | 0.09 | 0.39 | 0.29 | 8.31 | 0.17 | 0.00 | 19.45 | 1.58 | 0.06 | 0.00 | 0.01 | 0.00 | 0.0 | 0.0 | 0.01 | 44.68 | 99.81 |
| ALHA 77003 | 7a | 16.19 | 0.04 | 5.21 | 0.34 | 21.61 | 0.17 | 0.43 | 12.39 | 0.54 | 2.30 | 0.42 | 0.08 | 0.04 | 0.0 | 0.0 | 0.05 | 39.07 | 98.89 |
| ALHA 77003 | 7a | 16.08 | 0.02 | 1.48 | 0.28 | 26.36 | 0.26 | 0.26 | 16.24 | 0.10 | 0.26 | 0.05 | 0.10 | 0.03 | 0.0 | 0.0 | 0.03 | 38.48 | 100.03 |
| ALHA 77003 | 7a | 14.69 | 0.04 | 2.60 | 0.81 | 27.31 | 0.22 | 0.50 | 15.27 | 0.08 | 0.06 | 0.01 | 0.09 | 0.09 | 0.0 | 0.0 | 0.04 | 37.79 | 99.60 |
| ALHA 77003 | 7a | 6.66 | 0.01 | 1.86 | 0.54 | 47.62 | 0.08 | 1.22 | 7.41 | 0.11 | 0.43 | 0.00 | 0.06 | 0.06 | 0.0 | 0.0 | 14.13 | 49.80 | 129.97 |
| ALHA 77003 | 7a | 19.12 | 0.05 | 1.03 | 0.34 | 21.78 | 0.21 | 0.02 | 16.99 | 1.22 | 0.46 | 0.05 | 0.04 | 0.02 | 0.0 | 0.0 | 0.00 | 41.10 | 102.42 |

Continued on next page

| Sample | Area | Si | Ti | Al | Cr | Fe | Mn | Ni | Mg | Ca | Na | K | P | Co | V | Zn | S | O | Total |
|---|---|---|---|---|---|---|---|---|---|---|---|---|---|---|---|---|---|---|---|
| ALHA 77003 | 7a | 16.00 | 0.03 | 1.39 | 0.54 | 27.40 | 0.24 | 0.26 | 15.99 | 0.14 | 0.10 | 0.02 | 0.08 | 0.05 | 0.0 | 0.0 | 0.07 | 38.56 | 100.88 |
| ALHA 77003 | 7a | 14.05 | 0.03 | 0.92 | 0.37 | 29.74 | 0.22 | 0.72 | 14.63 | 0.07 | 0.10 | 0.00 | 0.05 | 0.12 | 0.0 | 0.0 | 0.06 | 35.68 | 96.77 |
| ALHA 77003 | 7a | 14.33 | 0.06 | 1.48 | 0.77 | 29.72 | 0.22 | 0.49 | 14.55 | 0.15 | 0.21 | 0.04 | 0.10 | 0.09 | 0.0 | 0.0 | 0.05 | 36.70 | 98.96 |
| ALHA 77003 | 7a | 15.27 | 0.06 | 2.71 | 0.90 | 26.70 | 0.22 | 0.92 | 16.15 | 0.17 | 0.18 | 0.01 | 0.18 | 0.05 | 0.0 | 0.0 | 0.05 | 39.33 | 102.90 |
| ALHA 77003 | 7a | 14.54 | 0.06 | 3.12 | 0.48 | 21.40 | 0.20 | 1.62 | 10.88 | 1.31 | 1.05 | 0.18 | 0.07 | 0.10 | 0.0 | 0.0 | 0.11 | 34.59 | 89.71 |
| ALHA 77003 | 7a | 17.33 | 0.01 | 0.03 | 0.10 | 25.83 | 0.23 | 0.03 | 18.38 | 0.06 | 0.00 | 0.00 | 0.01 | 0.02 | 0.0 | 0.0 | 0.00 | 39.44 | 101.49 |
| ALHA 77003 | 7a | 16.74 | 0.05 | 0.57 | 0.40 | 26.59 | 0.25 | 0.25 | 17.19 | 0.10 | 0.07 | 0.00 | 0.05 | 0.04 | 0.0 | 0.0 | 0.01 | 39.03 | 101.34 |
| ALHA 77003 | 7a | 13.77 | 0.05 | 1.16 | 0.24 | 29.84 | 0.21 | 0.67 | 14.02 | 0.15 | 0.11 | 0.02 | 0.10 | 0.08 | 0.0 | 0.0 | 0.11 | 35.31 | 95.85 |
| ALHA 77003 | 7a | 18.21 | 0.07 | 1.41 | 0.04 | 21.21 | 0.17 | 0.48 | 14.41 | 2.79 | 0.79 | 0.13 | 0.01 | 0.07 | 0.0 | 0.0 | 0.19 | 39.55 | 99.54 |
| ALHA 77003 | 7a | 15.19 | 0.05 | 0.84 | 0.34 | 27.93 | 0.22 | 0.40 | 15.05 | 0.62 | 0.07 | 0.00 | 0.08 | 0.07 | 0.0 | 0.0 | 0.03 | 36.76 | 97.64 |
| ALHA 77003 | 7a | 16.59 | 0.02 | 0.35 | 0.15 | 26.45 | 0.23 | 0.24 | 17.34 | 0.06 | 0.04 | 0.01 | 0.05 | 0.06 | 0.0 | 0.0 | 0.03 | 38.60 | 100.24 |
| ALHA 77003 | 7a | 16.01 | 0.07 | 0.63 | 0.43 | 27.02 | 0.25 | 0.21 | 16.08 | 0.08 | 0.08 | 0.03 | 0.07 | 0.04 | 0.0 | 0.0 | 0.02 | 37.70 | 98.72 |
| ALHA 77003 | 7a | 15.00 | 0.05 | 0.71 | 0.15 | 29.94 | 0.23 | 0.51 | 15.94 | 0.08 | 0.07 | 0.00 | 0.07 | 0.08 | 0.0 | 0.0 | 0.09 | 37.40 | 100.32 |
| ALHA 77003 | 7a | 17.15 | 0.03 | 0.11 | 0.07 | 26.46 | 0.25 | 0.08 | 17.96 | 0.03 | 0.03 | 0.00 | 0.02 | 0.03 | 0.0 | 0.0 | 0.01 | 39.26 | 101.49 |
| ALHA 77003 | 7a | 15.28 | 0.05 | 0.58 | 0.17 | 29.14 | 0.22 | 0.42 | 15.76 | 0.11 | 0.08 | 0.01 | 0.09 | 0.06 | 0.0 | 0.0 | 0.07 | 37.25 | 99.30 |
| ALHA 77003 | 7a | 14.60 | 0.04 | 0.67 | 0.25 | 29.54 | 0.21 | 0.83 | 14.99 | 0.15 | 0.07 | 0.01 | 0.07 | 0.10 | 0.0 | 0.0 | 0.10 | 36.35 | 97.98 |
| ALHA 77003 | 7a | 15.12 | 0.06 | 2.30 | 0.55 | 27.58 | 0.25 | 0.38 | 14.79 | 0.13 | 0.26 | 0.02 | 0.10 | 0.07 | 0.0 | 0.0 | 0.08 | 37.80 | 99.48 |
| ALHA 77003 | 7a | 15.12 | 0.07 | 1.66 | 0.37 | 25.75 | 0.23 | 1.52 | 15.34 | 0.16 | 0.29 | 0.06 | 0.06 | 0.06 | 0.0 | 0.0 | 0.06 | 37.25 | 98.00 |
| ALHA 77003 | 7a | 15.99 | 0.06 | 2.10 | 0.19 | 24.41 | 0.20 | 1.53 | 14.46 | 0.61 | 0.98 | 0.20 | 0.12 | 0.06 | 0.0 | 0.0 | 0.05 | 38.07 | 99.02 |
| ALHA 77003 | 7a | 16.54 | 0.08 | 0.97 | 0.17 | 25.95 | 0.24 | 0.25 | 16.38 | 0.16 | 0.33 | 0.04 | 0.06 | 0.05 | 0.0 | 0.0 | 0.04 | 38.54 | 99.80 |
| ALHA 77003 | 7a | 16.83 | 0.06 | 1.67 | 0.23 | 26.15 | 0.22 | 0.37 | 15.68 | 0.31 | 0.78 | 0.11 | 0.07 | 0.05 | 0.0 | 0.0 | 0.05 | 39.38 | 101.96 |
| ALHA 77003 | 7a | 15.20 | 0.06 | 0.67 | 0.34 | 27.55 | 0.24 | 0.23 | 14.85 | 0.12 | 0.09 | 0.02 | 0.04 | 0.05 | 0.0 | 0.0 | 0.59 | 36.95 | 97.01 |
| ALHA 77003 | 7a | 13.24 | 0.06 | 0.97 | 0.17 | 31.78 | 0.19 | 2.30 | 13.73 | 0.24 | 0.31 | 0.07 | 0.08 | 0.14 | 0.0 | 0.0 | 0.10 | 35.39 | 98.75 |
| ALHA 77003 | 7a | 14.32 | 0.08 | 1.70 | 0.47 | 29.66 | 0.22 | 0.59 | 14.41 | 0.15 | 0.09 | 0.03 | 0.08 | 0.09 | 0.0 | 0.0 | 0.07 | 36.66 | 98.65 |
| ALHA 77003 | 7a | 15.12 | 0.04 | 0.55 | 0.46 | 27.20 | 0.23 | 1.27 | 15.33 | 0.08 | 0.05 | 0.02 | 0.03 | 0.08 | 0.0 | 0.0 | 0.09 | 36.51 | 97.06 |
| ALHA 77003 | 7a | 16.12 | 0.06 | 1.48 | 1.06 | 26.21 | 0.27 | 0.17 | 16.48 | 0.05 | 0.02 | 0.00 | 0.03 | 0.03 | 0.0 | 0.0 | 0.01 | 38.78 | 100.77 |
| ALHA 77003 | 7a | 13.85 | 0.06 | 2.47 | 0.78 | 28.25 | 0.18 | 1.61 | 13.67 | 0.25 | 0.08 | 0.01 | 0.09 | 0.09 | 0.0 | 0.0 | 0.12 | 36.40 | 97.89 |
| ALHA 77003 | 7a | 9.32 | 0.06 | 1.90 | 0.69 | 42.04 | 0.14 | 1.13 | 11.50 | 0.09 | 0.09 | 0.01 | 0.05 | 0.12 | 0.0 | 0.0 | 7.11 | 43.44 | 117.69 |
| ALHA 77003 | 7a | 14.21 | 0.04 | 0.58 | 0.21 | 30.28 | 0.21 | 1.11 | 15.07 | 0.09 | 0.04 | 0.00 | 0.04 | 0.09 | 0.0 | 0.0 | 0.17 | 36.17 | 98.32 |
| ALHA 77003 | 7a | 12.97 | 0.05 | 1.00 | 0.23 | 32.32 | 0.21 | 0.81 | 13.56 | 0.10 | 0.07 | 0.01 | 0.08 | 0.07 | 0.0 | 0.0 | 0.13 | 34.66 | 96.27 |
| ALHA 77003 | 7a | 13.89 | 0.05 | 0.73 | 0.28 | 30.94 | 0.20 | 1.07 | 14.56 | 0.10 | 0.07 | 0.00 | 0.08 | 0.07 | 0.0 | 0.0 | 0.13 | 35.82 | 98.00 |
| ALHA 77003 | 7a | 13.24 | 0.08 | 1.15 | 0.28 | 30.95 | 0.18 | 1.01 | 13.65 | 0.15 | 0.07 | 0.03 | 0.11 | 0.07 | 0.0 | 0.0 | 0.12 | 34.90 | 95.99 |
| ALHA 77003 | 7a | 17.08 | 0.03 | 0.02 | 0.03 | 25.16 | 0.23 | 0.08 | 18.58 | 0.03 | 0.01 | 0.03 | 0.00 | 0.02 | 0.0 | 0.0 | 0.00 | 39.07 | 100.38 |
| ALHA 77003 | 7a | 15.84 | 0.03 | 0.05 | 0.02 | 26.54 | 0.21 | 1.01 | 17.78 | 0.04 | 0.01 | 0.00 | 0.00 | 0.06 | 0.0 | 0.0 | 0.04 | 37.87 | 99.51 |
| ALHA 77003 | 7a | 16.82 | 0.02 | 0.08 | 0.06 | 26.17 | 0.24 | 0.17 | 17.75 | 0.21 | 0.00 | 0.00 | 0.00 | 0.04 | 0.0 | 0.0 | 0.01 | 38.68 | 100.25 |
| ALHA 77003 | 7a | 13.79 | 0.05 | 2.86 | 0.27 | 25.56 | 0.20 | 1.11 | 11.53 | 0.38 | 2.07 | 0.11 | 0.03 | 0.12 | 0.0 | 0.0 | 0.15 | 34.87 | 93.09 |
| ALHA 77003 | 7a | 13.72 | 0.17 | 3.80 | 0.34 | 20.58 | 0.27 | 3.44 | 8.32 | 3.40 | 1.26 | 0.31 | 0.05 | 0.15 | 0.0 | 0.0 | 0.23 | 33.98 | 90.02 |
| ALHA 77003 | 7a | 26.89 | 0.05 | 0.21 | 0.35 | 2.94 | 0.16 | 0.06 | 20.78 | 2.65 | 0.08 | 0.00 | 0.00 | 0.00 | 0.0 | 0.0 | 0.00 | 46.70 | 100.87 |
| ALHA 77003 | 7a | 24.91 | 0.10 | 0.42 | 0.36 | 8.66 | 0.15 | 0.29 | 18.20 | 3.60 | 0.14 | 0.00 | 0.02 | 0.03 | 0.0 | 0.0 | 0.03 | 45.13 | 102.04 |
| ALHA 77003 | 7a | 27.75 | 0.05 | 0.32 | 0.23 | 1.39 | 0.15 | 0.06 | 22.50 | 0.88 | 0.02 | 0.00 | 0.00 | 0.01 | 0.0 | 0.0 | 0.01 | 47.68 | 101.04 |
| ALHA 77003 | 7a | 14.23 | 0.03 | 0.28 | 0.08 | 29.64 | 0.22 | 0.97 | 14.71 | 0.12 | 0.07 | 0.00 | 0.05 | 0.09 | 0.0 | 0.0 | 0.06 | 35.27 | 95.83 |
| ALHA 77003 | 7a | 14.59 | 0.10 | 0.89 | 0.32 | 28.45 | 0.23 | 0.56 | 14.88 | 0.15 | 0.09 | 0.01 | 0.12 | 0.07 | 0.0 | 0.0 | 0.06 | 36.15 | 96.65 |
| ALHA 77003 | 7a | 13.96 | 0.04 | 0.96 | 1.18 | 29.07 | 0.21 | 0.96 | 13.31 | 0.77 | 0.12 | 0.02 | 0.04 | 0.06 | 0.0 | 0.0 | 0.11 | 35.34 | 96.15 |
| ALHA 77003 | 7a | 16.72 | 0.01 | 0.17 | 0.25 | 26.08 | 0.25 | 0.05 | 17.93 | 0.10 | 0.02 | 0.02 | 0.03 | 0.04 | 0.0 | 0.0 | 0.01 | 38.80 | 100.47 |
| ALHA 77003 | 7a | 16.74 | 0.04 | 2.76 | 0.34 | 22.47 | 0.17 | 0.74 | 12.20 | 3.36 | 0.89 | 0.23 | 0.07 | 0.04 | 0.0 | 0.0 | 0.07 | 38.36 | 98.50 |
| ALHA 77003 | 7a | 17.22 | 0.02 | 0.01 | 0.02 | 22.73 | 0.19 | 0.04 | 19.99 | 0.09 | 0.00 | 0.00 | 0.00 | 0.04 | 0.0 | 0.0 | 0.01 | 39.43 | 99.78 |
| ALHA 77003 | 7a | 13.83 | 0.05 | 0.72 | 0.19 | 28.47 | 0.20 | 2.72 | 15.61 | 0.07 | 0.09 | 0.02 | 0.07 | 0.09 | 0.0 | 0.0 | 0.29 | 36.36 | 98.79 |

| Sample | Area | Si | Ti | Al | Cr | Fe | Mn | Ni | Mg | Ca | Na | K | P | Co | V | Zn | S | O | Total |
|---|---|---|---|---|---|---|---|---|---|---|---|---|---|---|---|---|---|---|---|
| Moss | 1a | 15.21 | 0.04 | 0.83 | 0.32 | 22.41 | 0.22 | 0.06 | 15.86 | 0.14 | 0.06 | 0.00 | 0.08 | 0.01 | 0.00 | 0.01 | 0.03 | 35.41 | 90.68 |
| Moss | 1a | 15.32 | 0.04 | 0.99 | 0.55 | 21.70 | 0.22 | 0.14 | 15.23 | 0.86 | 0.08 | 0.00 | 0.10 | 0.00 | 0.01 | 0.03 | 0.04 | 35.53 | 90.83 |
| Moss | 1a | 15.26 | 0.05 | 0.91 | 0.29 | 22.70 | 0.23 | 0.03 | 15.92 | 0.09 | 0.08 | 0.01 | 0.09 | 0.01 | 0.00 | 0.03 | 0.05 | 35.68 | 91.42 |
| Moss | 1a | 14.88 | 0.06 | 1.00 | 0.39 | 22.87 | 0.22 | 0.36 | 15.50 | 0.15 | 0.07 | 0.01 | 0.09 | 0.00 | 0.00 | 0.01 | 0.03 | 35.24 | 90.89 |
| Moss | 1a | 14.80 | 0.05 | 0.90 | 0.58 | 22.48 | 0.21 | 0.11 | 15.61 | 0.09 | 0.06 | 0.00 | 0.08 | 0.00 | 0.01 | 0.02 | 0.15 | 35.17 | 90.33 |
| Moss | 1a | 14.54 | 0.05 | 1.22 | 0.37 | 21.95 | 0.23 | 0.16 | 15.28 | 0.09 | 0.09 | 0.02 | 0.11 | 0.00 | 0.01 | 0.02 | 0.03 | 34.58 | 88.75 |

Continued on next page

| Sample | Area | Si | Ti | Al | Cr | Fe | Mn | Ni | Mg | Ca | Na | K | P | Co | V | Zn | S | O | Total |
|---|---|---|---|---|---|---|---|---|---|---|---|---|---|---|---|---|---|---|---|
| Moss | 1a | 14.61 | 0.06 | 1.43 | 0.35 | 21.68 | 0.21 | 0.10 | 15.27 | 0.43 | 0.09 | 0.02 | 0.33 | 0.00 | 0.01 | 0.03 | 0.04 | 35.19 | 89.85 |
| Moss | 1a | 15.13 | 0.04 | 0.63 | 0.22 | 22.82 | 0.21 | 0.05 | 15.93 | 0.09 | 0.05 | 0.00 | 0.09 | 0.01 | 0.00 | 0.01 | 0.33 | 35.70 | 91.31 |
| Moss | 1a | 14.63 | 0.05 | 1.00 | 0.32 | 22.27 | 0.21 | 0.81 | 15.67 | 0.09 | 0.06 | 0.01 | 0.06 | 0.01 | 0.01 | 0.01 | 0.02 | 34.90 | 90.13 |
| Moss | 1a | 15.34 | 0.04 | 0.53 | 0.19 | 22.74 | 0.24 | 0.02 | 16.13 | 0.07 | 0.06 | 0.01 | 0.06 | 0.00 | 0.01 | 0.03 | 0.03 | 35.46 | 90.97 |
| Moss | 1a | 15.16 | 0.04 | 0.75 | 0.26 | 22.50 | 0.22 | 0.03 | 15.92 | 0.08 | 0.07 | 0.00 | 0.08 | 0.01 | 0.01 | 0.04 | 0.04 | 35.33 | 90.53 |
| Moss | 1a | 15.52 | 0.05 | 0.92 | 0.29 | 21.97 | 0.22 | 0.05 | 15.50 | 0.67 | 0.07 | 0.01 | 0.09 | 0.00 | 0.00 | 0.01 | 0.03 | 35.69 | 91.08 |
| Moss | 1a | 19.38 | 0.04 | 0.59 | 0.21 | 12.32 | 0.11 | 0.02 | 10.06 | 9.96 | 0.08 | 0.00 | 0.07 | 0.00 | 0.01 | 0.01 | 0.03 | 37.07 | 89.96 |
| Moss | 1a | 17.45 | 0.03 | 0.45 | 0.11 | 20.73 | 0.21 | 0.03 | 14.34 | 3.30 | 0.06 | 0.01 | 0.05 | 0.00 | 0.00 | 0.01 | 0.03 | 37.26 | 94.07 |
| Moss | 1a | 15.43 | 0.04 | 0.90 | 0.31 | 21.03 | 0.22 | 0.03 | 14.73 | 1.12 | 0.07 | 0.02 | 0.07 | 0.00 | 0.00 | 0.03 | 0.04 | 34.98 | 89.03 |
| Moss | 1a | 14.69 | 0.06 | 0.76 | 0.24 | 20.80 | 0.21 | 0.02 | 15.04 | 0.27 | 0.07 | 0.01 | 0.07 | 0.00 | 0.00 | 0.00 | 0.04 | 33.78 | 86.07 |
| Moss | 1a | 15.51 | 0.04 | 0.57 | 0.31 | 23.55 | 0.22 | 0.04 | 16.31 | 0.07 | 0.05 | 0.01 | 0.06 | 0.02 | 0.01 | 0.00 | 0.16 | 36.29 | 93.22 |
| Moss | 1a | 15.52 | 0.04 | 0.72 | 0.40 | 21.84 | 0.22 | 0.20 | 15.32 | 0.48 | 0.09 | 0.00 | 0.09 | 0.00 | 0.01 | 0.01 | 0.04 | 35.40 | 90.38 |
| Moss | 1b | 15.30 | 0.05 | 1.02 | 0.29 | 20.93 | 0.20 | 0.08 | 14.56 | 1.10 | 0.07 | 0.01 | 0.07 | 0.00 | 0.01 | 0.03 | 0.05 | 34.84 | 88.65 |
| Moss | 1b | 14.56 | 0.04 | 0.91 | 0.40 | 22.03 | 0.22 | 0.02 | 15.06 | 0.27 | 0.06 | 0.01 | 0.06 | 0.00 | 0.00 | 0.01 | 0.30 | 34.56 | 88.51 |
| Moss | 1b | 14.21 | 0.05 | 0.93 | 0.30 | 21.95 | 0.21 | 0.67 | 14.99 | 0.07 | 0.06 | 0.00 | 0.08 | 0.01 | 0.00 | 0.01 | 0.03 | 33.80 | 87.38 |
| Moss | 1b | 14.50 | 0.07 | 1.29 | 0.60 | 22.35 | 0.22 | 0.13 | 14.90 | 0.24 | 0.10 | 0.00 | 0.12 | 0.01 | 0.01 | 0.01 | 0.04 | 34.67 | 89.27 |
| Moss | 1b | 12.25 | 0.04 | 1.06 | 0.54 | 26.74 | 0.17 | 0.30 | 12.14 | 0.94 | 0.13 | 0.01 | 0.09 | 0.07 | 0.01 | 0.00 | 1.25 | 33.40 | 89.14 |
| Moss | 1b | 17.28 | 0.06 | 0.68 | 0.28 | 19.72 | 0.21 | 0.03 | 14.98 | 2.44 | 0.10 | 0.01 | 0.08 | 0.00 | 0.00 | 0.00 | 0.03 | 37.19 | 93.07 |
| Moss | 1b | 16.66 | 0.04 | 0.70 | 0.23 | 18.82 | 0.16 | 1.60 | 13.20 | 4.02 | 0.08 | 0.00 | 0.06 | 0.00 | 0.01 | 0.00 | 0.02 | 36.05 | 91.66 |
| Moss | 1b | 15.55 | 0.05 | 0.80 | 0.28 | 22.77 | 0.25 | 0.07 | 16.02 | 0.36 | 0.06 | 0.02 | 0.09 | 0.01 | 0.01 | 0.01 | 0.02 | 36.08 | 92.44 |
| Moss | 1b | 15.16 | 0.07 | 2.13 | 0.29 | 20.86 | 0.23 | 0.06 | 14.04 | 0.31 | 1.17 | 0.13 | 0.10 | 0.00 | 0.00 | 0.00 | 0.05 | 35.41 | 90.01 |
| Moss | 1b | 15.27 | 0.05 | 1.08 | 0.36 | 22.95 | 0.23 | 0.03 | 15.94 | 0.09 | 0.14 | 0.01 | 0.08 | 0.00 | 0.00 | 0.03 | 0.05 | 35.98 | 92.29 |
| Moss | 1b | 15.25 | 0.03 | 1.04 | 0.40 | 23.76 | 0.23 | 0.04 | 16.22 | 0.10 | 0.07 | 0.00 | 0.08 | 0.00 | 0.01 | 0.02 | 0.35 | 36.77 | 94.37 |
| Moss | 1b | 14.68 | 0.06 | 1.08 | 0.35 | 22.56 | 0.23 | 0.43 | 15.56 | 0.09 | 0.08 | 0.00 | 0.11 | 0.00 | 0.00 | 0.02 | 0.03 | 35.05 | 90.35 |
| Moss | 1b | 15.16 | 0.05 | 0.92 | 0.29 | 23.23 | 0.25 | 0.61 | 16.10 | 0.10 | 0.07 | 0.01 | 0.09 | 0.01 | 0.00 | 0.04 | 0.03 | 35.99 | 92.92 |
| Moss | 1b | 14.70 | 0.08 | 1.21 | 0.43 | 22.20 | 0.23 | 0.14 | 15.55 | 0.12 | 0.09 | 0.02 | 0.12 | 0.01 | 0.01 | 0.03 | 0.04 | 35.09 | 90.06 |
| Moss | 1b | 16.14 | 0.05 | 1.06 | 0.32 | 20.95 | 0.20 | 0.34 | 14.64 | 1.87 | 0.10 | 0.00 | 0.08 | 0.01 | 0.01 | 0.01 | 0.03 | 36.25 | 92.05 |
| Moss | 1b | 16.02 | 0.03 | 0.69 | 0.26 | 22.34 | 0.22 | 0.05 | 16.59 | 0.52 | 0.11 | 0.02 | 0.04 | 0.00 | 0.01 | 0.02 | 0.04 | 36.76 | 93.71 |
| Moss | 1b | 15.83 | 0.07 | 0.72 | 0.30 | 23.46 | 0.24 | 0.05 | 16.83 | 0.07 | 0.05 | 0.01 | 0.08 | 0.00 | 0.01 | 0.02 | 0.03 | 36.96 | 94.74 |
| Moss | 1b | 14.67 | 0.07 | 1.22 | 0.43 | 22.83 | 0.22 | 0.78 | 15.59 | 0.08 | 0.09 | 0.02 | 0.10 | 0.02 | 0.01 | 0.02 | 0.06 | 35.43 | 91.64 |
| Moss | 1b | 15.17 | 0.05 | 0.94 | 0.34 | 23.16 | 0.22 | 0.52 | 15.64 | 0.37 | 0.18 | 0.01 | 0.07 | 0.01 | 0.01 | 0.00 | 0.06 | 35.85 | 92.59 |
| Moss | 1b | 19.21 | 0.10 | 0.62 | 0.28 | 16.61 | 0.17 | 0.04 | 15.77 | 3.38 | 0.10 | 0.00 | 0.07 | 0.01 | 0.01 | 0.01 | 0.02 | 39.34 | 95.72 |
| Moss | 1b | 15.79 | 0.07 | 0.46 | 0.40 | 22.50 | 0.23 | 0.06 | 15.28 | 0.88 | 0.07 | 0.00 | 0.05 | 0.00 | 0.00 | 0.00 | 0.06 | 35.73 | 91.55 |
| Moss | 1b | 13.93 | 0.07 | 1.06 | 0.28 | 21.27 | 0.22 | 0.11 | 14.37 | 0.11 | 0.10 | 0.01 | 0.10 | 0.00 | 0.01 | 0.02 | 0.06 | 32.94 | 84.63 |
| Moss | 1b | 13.96 | 0.05 | 0.81 | 0.35 | 21.53 | 0.22 | 0.17 | 14.45 | 0.11 | 0.05 | 0.01 | 0.10 | 0.00 | 0.00 | 0.00 | 0.10 | 32.96 | 84.88 |
| Moss | 1b | 14.44 | 0.05 | 0.97 | 0.30 | 21.19 | 0.21 | 0.66 | 14.25 | 0.79 | 0.04 | 0.00 | 0.07 | 0.01 | 0.00 | 0.00 | 0.04 | 33.68 | 86.71 |
| Moss | 1b | 14.82 | 0.05 | 0.88 | 0.23 | 22.55 | 0.22 | 0.08 | 15.43 | 0.11 | 0.07 | 0.00 | 0.08 | 0.00 | 0.00 | 0.02 | 0.03 | 34.73 | 89.30 |
| Moss | 1b | 14.14 | 0.07 | 1.23 | 0.36 | 22.54 | 0.21 | 0.43 | 14.83 | 0.10 | 0.10 | 0.00 | 0.12 | 0.00 | 0.00 | 0.01 | 0.09 | 34.17 | 88.40 |
| Moss | 1b | 14.35 | 0.07 | 1.25 | 0.34 | 22.56 | 0.24 | 0.03 | 14.94 | 0.06 | 0.08 | 0.01 | 0.10 | 0.01 | 0.01 | 0.01 | 0.03 | 34.28 | 88.37 |
| Moss | 1b | 14.57 | 0.06 | 0.77 | 0.49 | 22.38 | 0.25 | 0.05 | 15.15 | 0.09 | 0.07 | 0.00 | 0.09 | 0.00 | 0.01 | 0.02 | 0.05 | 34.27 | 88.30 |
| Moss | 1b | 13.86 | 0.05 | 0.96 | 0.33 | 23.33 | 0.21 | 2.10 | 14.74 | 0.15 | 0.06 | 0.00 | 0.13 | 0.01 | 0.00 | 0.02 | 0.06 | 34.20 | 90.22 |
| Moss | 1b | 13.03 | 0.06 | 1.35 | 0.35 | 19.85 | 0.19 | 0.24 | 13.43 | 0.15 | 0.07 | 0.01 | 0.10 | 0.00 | 0.01 | 0.02 | 0.06 | 31.20 | 80.11 |
| Moss | 1b | 13.03 | 0.04 | 1.29 | 0.36 | 22.60 | 0.21 | 2.18 | 13.88 | 0.12 | 0.07 | 0.02 | 0.13 | 0.00 | 0.01 | 0.01 | 0.05 | 32.77 | 86.75 |
| Moss | 1b | 15.03 | 0.04 | 0.46 | 0.42 | 24.64 | 0.22 | 2.66 | 16.29 | 0.10 | 0.02 | 0.00 | 0.03 | 0.01 | 0.00 | 0.01 | 0.14 | 36.62 | 96.69 |
| Moss | 1b | 14.27 | 0.05 | 0.55 | 0.21 | 20.25 | 0.18 | 0.01 | 15.34 | 0.34 | 0.03 | 0.00 | 0.06 | 0.00 | 0.00 | 0.01 | 0.04 | 33.12 | 84.47 |
| Moss | 1b | 15.18 | 0.06 | 1.24 | 0.33 | 23.21 | 0.23 | 0.08 | 16.10 | 0.08 | 0.09 | 0.01 | 0.10 | 0.00 | 0.01 | 0.02 | 0.02 | 36.18 | 92.95 |
| Moss | 1b | 15.48 | 0.04 | 0.75 | 0.27 | 23.63 | 0.23 | 0.18 | 16.49 | 0.35 | 0.06 | 0.01 | 0.19 | 0.00 | 0.00 | 0.01 | 0.06 | 36.70 | 94.46 |
| Moss | 1b | 12.53 | 0.03 | 1.19 | 0.71 | 35.50 | 0.18 | 0.40 | 14.23 | 0.56 | 0.10 | 0.03 | 0.11 | 0.12 | 0.01 | 0.03 | 4.15 | 42.05 | 111.93 |
| Moss | 1b | 14.37 | 0.06 | 1.39 | 0.49 | 23.59 | 0.21 | 2.51 | 15.27 | 0.47 | 0.05 | 0.00 | 0.12 | 0.02 | 0.00 | 0.02 | 0.03 | 35.85 | 94.45 |
| Moss | 1b | 14.75 | 0.05 | 1.29 | 0.37 | 23.97 | 0.22 | 1.06 | 15.87 | 0.14 | 0.08 | 0.01 | 0.14 | 0.00 | 0.01 | 0.03 | 0.31 | 36.57 | 94.87 |
| Moss | 1b | 16.89 | 0.05 | 0.63 | 0.38 | 25.35 | 0.13 | 0.80 | 15.88 | 2.81 | 0.16 | 0.02 | 0.56 | 0.08 | 0.01 | 0.00 | 2.63 | 43.86 | 110.24 |
| Moss | 1b | 15.22 | 0.06 | 0.73 | 0.29 | 23.47 | 0.23 | 0.08 | 16.05 | 0.08 | 0.04 | 0.00 | 0.09 | 0.00 | 0.00 | 0.03 | 0.03 | 35.74 | 92.13 |
| Moss | 1b | 16.47 | 0.03 | 0.25 | 0.15 | 25.33 | 0.25 | 0.12 | 17.45 | 0.62 | 0.05 | 0.00 | 0.49 | 0.00 | 0.01 | 0.00 | 0.06 | 38.91 | 100.19 |
| Moss | 1b | 16.45 | 0.01 | 0.07 | 0.07 | 25.28 | 0.24 | 0.03 | 17.45 | 0.04 | 0.00 | 0.01 | 0.02 | 0.00 | 0.00 | 0.01 | 0.01 | 37.70 | 97.39 |
| Moss | 1b | 13.83 | 0.05 | 0.56 | 0.77 | 24.38 | 0.22 | 1.68 | 14.46 | 0.13 | 0.06 | 0.00 | 0.15 | 0.01 | 0.01 | 0.03 | 0.04 | 34.01 | 90.39 |
| Moss | 1b | 14.76 | 0.06 | 0.77 | 0.60 | 23.81 | 0.24 | 0.76 | 15.51 | 0.20 | 0.10 | 0.00 | 0.15 | 0.01 | 0.01 | 0.01 | 0.07 | 35.54 | 92.59 |
| Moss | 2a | 13.42 | 0.07 | 1.02 | 0.40 | 22.04 | 0.23 | 0.12 | 14.11 | 0.11 | 0.06 | 0.00 | 0.08 | 0.00 | 0.00 | 0.00 | 0.06 | 32.38 | 84.10 |
| Moss | 2a | 12.87 | 0.05 | 0.75 | 0.36 | 23.84 | 0.21 | 0.19 | 13.75 | 0.10 | 0.06 | 0.01 | 0.08 | 0.00 | 0.00 | 0.01 | 1.07 | 33.31 | 86.67 |

Continued on next page

| Sample | Area | Si | Ti | Al | Cr | Fe | Mn | Ni | Mg | Ca | Na | K | P | Co | V | Zn | S | O | Total |
|---|---|---|---|---|---|---|---|---|---|---|---|---|---|---|---|---|---|---|---|
| Moss | 2a | 12.75 | 0.08 | 0.94 | 0.40 | 22.95 | 0.20 | 0.33 | 13.42 | 0.11 | 0.10 | 0.00 | 0.09 | 0.00 | 0.01 | 0.02 | 0.50 | 32.11 | 84.01 |
| Moss | 2a | 13.31 | 0.07 | 1.16 | 0.44 | 22.64 | 0.22 | 0.07 | 14.06 | 0.11 | 0.05 | 0.01 | 0.08 | 0.00 | 0.01 | 0.03 | 0.47 | 33.14 | 85.86 |
| Moss | 2a | 13.35 | 0.07 | 0.93 | 0.31 | 21.43 | 0.21 | 0.10 | 13.99 | 0.08 | 0.06 | 0.01 | 0.09 | 0.00 | 0.00 | 0.03 | 0.07 | 31.93 | 82.65 |
| Moss | 2a | 12.92 | 0.06 | 0.80 | 0.31 | 24.95 | 0.23 | 0.06 | 13.75 | 0.20 | 0.07 | 0.00 | 0.08 | 0.01 | 0.01 | 0.02 | 1.28 | 34.03 | 88.77 |
| Moss | 2a | 14.12 | 0.10 | 0.69 | 0.25 | 23.15 | 0.23 | 0.20 | 14.96 | 0.14 | 0.05 | 0.01 | 0.05 | 0.01 | 0.00 | 0.00 | 0.25 | 34.01 | 88.22 |
| Moss | 2a | 13.70 | 0.08 | 0.60 | 0.20 | 22.52 | 0.22 | 0.06 | 14.28 | 0.09 | 0.06 | 0.00 | 0.07 | 0.01 | 0.01 | 0.02 | 0.36 | 32.91 | 85.17 |
| Moss | 2a | 13.06 | 0.07 | 1.19 | 0.30 | 21.48 | 0.20 | 0.31 | 13.70 | 0.07 | 0.04 | 0.01 | 0.08 | 0.01 | 0.01 | 0.03 | 0.05 | 31.68 | 82.29 |
| Moss | 2a | 13.56 | 0.08 | 1.14 | 0.37 | 21.54 | 0.20 | 0.06 | 14.15 | 0.09 | 0.11 | 0.01 | 0.08 | 0.00 | 0.00 | 0.01 | 0.06 | 32.52 | 83.98 |
| Moss | 2a | 12.14 | 0.05 | 0.91 | 0.40 | 23.08 | 0.19 | 0.09 | 12.64 | 0.59 | 0.06 | 0.01 | 0.05 | 0.00 | 0.01 | 0.02 | 2.19 | 33.49 | 85.92 |
| Moss | 2a | 13.54 | 0.06 | 0.99 | 0.34 | 21.86 | 0.23 | 0.37 | 14.19 | 0.09 | 0.03 | 0.00 | 0.07 | 0.01 | 0.01 | 0.01 | 0.09 | 32.54 | 84.42 |
| Moss | 2a | 14.29 | 0.05 | 0.76 | 0.28 | 22.63 | 0.22 | 0.20 | 15.01 | 0.07 | 0.05 | 0.01 | 0.07 | 0.01 | 0.01 | 0.02 | 0.03 | 33.79 | 87.49 |
| Moss | 2a | 13.79 | 0.06 | 0.84 | 0.30 | 21.78 | 0.21 | 0.05 | 14.41 | 0.12 | 0.05 | 0.01 | 0.09 | 0.00 | 0.00 | 0.02 | 0.05 | 32.71 | 84.49 |
| Moss | 2a | 12.42 | 0.05 | 0.68 | 0.26 | 26.10 | 0.19 | 0.05 | 13.19 | 0.49 | 0.05 | 0.00 | 0.06 | 0.00 | 0.01 | 0.01 | 3.22 | 36.28 | 93.08 |
| Moss | 2a | 13.71 | 0.04 | 0.45 | 0.17 | 22.73 | 0.21 | 0.04 | 13.59 | 0.91 | 0.03 | 0.00 | 0.06 | 0.00 | 0.00 | 0.00 | 1.02 | 33.64 | 86.60 |
| Moss | 2a | 13.62 | 0.06 | 1.00 | 0.32 | 21.94 | 0.22 | 0.40 | 14.18 | 0.10 | 0.05 | 0.02 | 0.08 | 0.01 | 0.00 | 0.03 | 0.03 | 32.60 | 84.66 |
| Moss | 2a | 13.51 | 0.05 | 0.58 | 0.24 | 21.70 | 0.22 | 0.09 | 13.90 | 0.12 | 0.04 | 0.02 | 0.07 | 0.00 | 0.00 | 0.00 | 0.16 | 31.90 | 82.61 |
| Moss | 2a | 13.33 | 0.05 | 0.94 | 0.33 | 22.16 | 0.21 | 0.92 | 13.95 | 0.09 | 0.04 | 0.01 | 0.07 | 0.01 | 0.00 | 0.04 | 0.24 | 32.58 | 84.98 |
| Moss | 2a | 14.41 | 0.03 | 0.89 | 0.28 | 23.09 | 0.24 | 0.01 | 15.19 | 0.07 | 0.06 | 0.02 | 0.06 | 0.00 | 0.00 | 0.03 | 0.05 | 34.26 | 88.69 |
| Moss | 2a | 13.70 | 0.06 | 1.01 | 0.30 | 22.70 | 0.21 | 1.03 | 14.22 | 0.10 | 0.06 | 0.00 | 0.10 | 0.00 | 0.01 | 0.02 | 0.05 | 33.17 | 86.75 |
| Moss | 2a | 14.62 | 0.05 | 0.88 | 0.30 | 23.62 | 0.21 | 0.78 | 15.38 | 0.09 | 0.04 | 0.01 | 0.07 | 0.01 | 0.00 | 0.01 | 0.03 | 34.98 | 91.07 |
| Moss | 2a | 14.11 | 0.07 | 0.66 | 0.33 | 27.74 | 0.22 | 0.21 | 15.35 | 0.26 | 0.08 | 0.00 | 0.16 | 0.06 | 0.01 | 0.00 | 0.03 | 35.44 | 94.73 |
| Moss | 2a | 13.79 | 0.08 | 0.92 | 0.32 | 21.87 | 0.23 | 0.04 | 14.32 | 0.09 | 0.07 | 0.00 | 0.08 | 0.01 | 0.00 | 0.01 | 0.03 | 32.70 | 84.54 |
| Moss | 2a | 14.38 | 0.06 | 0.91 | 0.28 | 22.87 | 0.23 | 0.14 | 15.06 | 0.07 | 0.07 | 0.01 | 0.09 | 0.00 | 0.01 | 0.02 | 0.02 | 34.15 | 88.38 |
| Moss | 2a | 13.39 | 0.07 | 1.99 | 0.56 | 22.05 | 0.21 | 0.15 | 13.96 | 0.13 | 0.09 | 0.01 | 0.08 | 0.01 | 0.02 | 0.06 | 0.03 | 33.20 | 86.00 |
| Moss | 2a | 13.56 | 0.08 | 1.18 | 0.39 | 22.16 | 0.21 | 0.32 | 14.15 | 0.09 | 0.06 | 0.00 | 0.11 | 0.01 | 0.01 | 0.01 | 0.07 | 32.85 | 85.25 |
| Moss | 2a | 13.66 | 0.09 | 0.94 | 0.37 | 21.66 | 0.21 | 0.12 | 14.10 | 0.09 | 0.10 | 0.01 | 0.10 | 0.01 | 0.00 | 0.00 | 0.04 | 32.48 | 83.99 |
| Moss | 2a | 13.69 | 0.07 | 0.75 | 0.35 | 21.99 | 0.20 | 0.31 | 14.23 | 0.88 | 0.08 | 0.01 | 0.49 | 0.01 | 0.01 | 0.01 | 0.03 | 33.36 | 86.46 |
| Moss | 2a | 14.67 | 0.05 | 1.12 | 0.28 | 22.48 | 0.23 | 0.13 | 14.97 | 0.38 | 0.09 | 0.00 | 0.08 | 0.00 | 0.00 | 0.00 | 0.03 | 34.59 | 89.11 |
| Moss | 2a | 13.98 | 0.07 | 1.13 | 0.30 | 21.68 | 0.22 | 0.28 | 14.62 | 0.10 | 0.07 | 0.01 | 0.11 | 0.01 | 0.01 | 0.03 | 0.07 | 33.42 | 86.10 |
| Moss | 2a | 13.76 | 0.05 | 1.12 | 0.29 | 21.76 | 0.21 | 0.33 | 14.37 | 0.08 | 0.06 | 0.00 | 0.08 | 0.00 | 0.01 | 0.02 | 0.04 | 32.91 | 85.08 |
| Moss | 2a | 14.43 | 0.08 | 1.22 | 0.40 | 23.74 | 0.23 | 1.01 | 13.97 | 0.98 | 0.07 | 0.00 | 0.09 | 0.01 | 0.01 | 0.01 | 0.85 | 35.91 | 92.99 |
| Moss | 2b | 15.08 | 0.04 | 0.62 | 0.19 | 23.66 | 0.23 | 0.05 | 15.41 | 0.26 | 0.07 | 0.00 | 0.05 | 0.00 | 0.01 | 0.00 | 0.33 | 35.53 | 91.52 |
| Moss | 2b | 16.47 | 0.05 | 0.62 | 0.26 | 23.27 | 0.23 | 0.05 | 15.79 | 1.05 | 0.03 | 0.01 | 0.02 | 0.00 | 0.01 | 0.00 | 0.00 | 37.09 | 94.95 |
| Moss | 2b | 14.53 | 0.04 | 0.75 | 0.28 | 23.20 | 0.23 | 0.83 | 14.77 | 0.37 | 0.04 | 0.00 | 0.06 | 0.00 | 0.00 | 0.01 | 0.03 | 34.33 | 89.48 |
| Moss | 2b | 15.10 | 0.05 | 0.60 | 0.21 | 20.41 | 0.20 | 0.03 | 14.05 | 2.10 | 0.06 | 0.00 | 0.07 | 0.00 | 0.01 | 0.01 | 0.03 | 34.03 | 86.96 |
| Moss | 2b | 16.10 | 0.04 | 0.79 | 0.28 | 19.10 | 0.18 | 0.08 | 13.25 | 3.78 | 0.08 | 0.01 | 0.08 | 0.01 | 0.00 | 0.00 | 0.07 | 35.22 | 89.07 |
| Moss | 2b | 13.17 | 0.05 | 1.09 | 0.38 | 22.17 | 0.21 | 1.34 | 13.58 | 0.82 | 0.05 | 0.00 | 0.51 | 0.00 | 0.01 | 0.02 | 0.04 | 32.98 | 86.41 |
| Moss | 2b | 14.45 | 0.02 | 0.48 | 0.30 | 23.73 | 0.25 | 0.04 | 14.70 | 0.14 | 0.04 | 0.00 | 0.04 | 0.01 | 0.01 | 0.00 | 0.02 | 33.76 | 87.99 |
| Moss | 2b | 15.05 | 0.02 | 0.25 | 0.18 | 21.61 | 0.22 | 0.13 | 14.16 | 1.20 | 0.04 | 0.00 | 0.03 | 0.00 | 0.01 | 0.01 | 0.28 | 34.04 | 87.22 |
| Moss | 2b | 14.24 | 0.07 | 1.11 | 0.37 | 22.18 | 0.24 | 0.03 | 14.56 | 0.14 | 0.05 | 0.00 | 0.13 | 0.01 | 0.02 | 0.01 | 0.03 | 33.74 | 86.94 |
| Moss | 2b | 14.51 | 0.07 | 0.65 | 0.28 | 23.93 | 0.23 | 0.28 | 14.73 | 0.11 | 0.10 | 0.00 | 0.09 | 0.02 | 0.01 | 0.01 | 0.05 | 34.27 | 89.34 |
| Moss | 2b | 14.07 | 0.10 | 1.07 | 0.39 | 21.75 | 0.22 | 0.08 | 14.41 | 0.09 | 0.09 | 0.02 | 0.09 | 0.00 | 0.01 | 0.01 | 0.04 | 33.28 | 85.72 |
| Moss | 2b | 14.05 | 0.08 | 0.98 | 0.31 | 25.15 | 0.23 | 0.52 | 14.67 | 0.08 | 0.04 | 0.01 | 0.07 | 0.01 | 0.01 | 0.01 | 1.33 | 36.28 | 93.82 |
| Moss | 2b | 13.84 | 0.08 | 0.77 | 0.36 | 21.50 | 0.19 | 0.25 | 13.97 | 0.28 | 0.08 | 0.01 | 0.17 | 0.01 | 0.00 | 0.02 | 0.04 | 32.58 | 84.15 |
| Moss | 2b | 14.41 | 0.07 | 0.74 | 0.23 | 22.55 | 0.24 | 0.19 | 14.90 | 0.07 | 0.04 | 0.00 | 0.07 | 0.00 | 0.01 | 0.01 | 0.03 | 33.80 | 87.35 |
| Moss | 2b | 12.43 | 0.06 | 1.26 | 0.24 | 18.12 | 0.17 | 0.06 | 12.63 | 0.08 | 0.12 | 0.00 | 0.09 | 0.01 | 0.01 | 0.01 | 0.10 | 29.36 | 74.76 |
| Moss | 2b | 13.01 | 0.06 | 1.50 | 0.43 | 21.62 | 0.19 | 1.93 | 13.83 | 0.12 | 0.07 | 0.01 | 0.09 | 0.02 | 0.01 | 0.04 | 0.07 | 32.58 | 85.56 |
| Moss | 2b | 13.11 | 0.04 | 1.32 | 0.41 | 20.31 | 0.21 | 0.04 | 13.65 | 0.09 | 0.07 | 0.00 | 0.07 | 0.01 | 0.00 | 0.02 | 0.06 | 31.47 | 80.91 |
| Moss | 2b | 14.60 | 0.11 | 1.20 | 0.36 | 23.28 | 0.22 | 0.26 | 14.64 | 0.21 | 0.16 | 0.01 | 0.10 | 0.01 | 0.01 | 0.03 | 0.04 | 34.72 | 89.94 |
| Moss | 2b | 14.69 | 0.09 | 1.05 | 0.29 | 24.82 | 0.24 | 0.04 | 14.74 | 0.16 | 0.19 | 0.03 | 0.08 | 0.00 | 0.00 | 0.02 | 0.41 | 35.61 | 92.46 |
| Moss | 2b | 14.64 | 0.10 | 2.02 | 0.54 | 24.34 | 0.24 | 0.45 | 15.13 | 0.11 | 0.14 | 0.01 | 0.10 | 0.01 | 0.01 | 0.03 | 0.05 | 36.24 | 94.14 |
| Moss | 2b | 14.95 | 0.08 | 1.37 | 0.42 | 24.30 | 0.23 | 0.10 | 15.43 | 0.07 | 0.05 | 0.00 | 0.07 | 0.00 | 0.00 | 0.03 | 0.20 | 36.17 | 93.48 |
| Moss | 2b | 14.04 | 0.07 | 1.46 | 0.40 | 23.81 | 0.22 | 1.20 | 14.59 | 0.10 | 0.08 | 0.01 | 0.08 | 0.00 | 0.01 | 0.03 | 0.10 | 34.67 | 90.87 |
| Moss | 3a | 13.37 | 0.06 | 1.16 | 0.42 | 24.59 | 0.23 | 3.34 | 13.39 | 0.52 | 0.33 | 0.04 | 0.31 | 0.02 | 0.00 | 0.00 | 0.06 | 34.16 | 92.00 |
| Moss | 3a | 14.61 | 0.04 | 0.97 | 0.28 | 23.84 | 0.25 | 0.47 | 14.54 | 0.09 | 0.06 | 0.02 | 0.11 | 0.00 | 0.01 | 0.01 | 0.03 | 34.52 | 89.84 |
| Moss | 3a | 14.38 | 0.05 | 1.09 | 0.30 | 23.61 | 0.23 | 0.07 | 14.32 | 0.09 | 0.05 | 0.00 | 0.09 | 0.00 | 0.00 | 0.00 | 0.03 | 34.02 | 88.35 |
| Moss | 3a | 14.43 | 0.06 | 0.79 | 0.24 | 23.28 | 0.23 | 0.26 | 14.23 | 0.08 | 0.06 | 0.01 | 0.09 | 0.01 | 0.00 | 0.01 | 0.03 | 33.69 | 87.50 |
| Moss | 3a | 14.27 | 0.05 | 1.07 | 0.32 | 23.02 | 0.25 | 0.06 | 14.22 | 0.08 | 0.07 | 0.02 | 0.07 | 0.01 | 0.01 | 0.01 | 0.03 | 33.63 | 87.19 |

Continued on next page

| Sample | Area | Si | Ti | Al | Cr | Fe | Mn | Ni | Mg | Ca | Na | K | P | Co | V | Zn | S | O | Total |
|---|---|---|---|---|---|---|---|---|---|---|---|---|---|---|---|---|---|---|---|
| Moss | 3a | 12.54 | 0.03 | 1.03 | 0.34 | 25.19 | 0.18 | 6.04 | 13.82 | 1.22 | 0.13 | 0.00 | 0.75 | 0.02 | 0.01 | 0.01 | 0.03 | 34.96 | 96.30 |
| Moss | 3a | 15.33 | 0.04 | 0.65 | 0.19 | 23.90 | 0.24 | 0.28 | 15.38 | 0.09 | 0.06 | 0.00 | 0.12 | 0.00 | 0.00 | 0.00 | 0.02 | 35.52 | 91.81 |
| Moss | 3a | 13.81 | 0.05 | 0.93 | 0.27 | 21.74 | 0.21 | 0.15 | 13.62 | 0.09 | 0.12 | 0.01 | 0.10 | 0.00 | 0.01 | 0.01 | 0.04 | 32.30 | 83.46 |
| Moss | 3a | 13.30 | 0.04 | 1.35 | 0.56 | 21.14 | 0.22 | 0.17 | 13.33 | 0.24 | 0.22 | 0.04 | 0.14 | 0.00 | 0.01 | 0.02 | 0.04 | 32.02 | 82.84 |
| Moss | 3a | 15.50 | 0.04 | 1.28 | 0.54 | 23.47 | 0.28 | 0.13 | 14.55 | 0.71 | 0.35 | 0.05 | 0.08 | 0.01 | 0.01 | 0.00 | 0.05 | 36.09 | 93.13 |
| Moss | 3a | 14.76 | 0.05 | 0.90 | 0.18 | 21.46 | 0.24 | 0.04 | 13.79 | 0.49 | 0.47 | 0.04 | 0.07 | 0.00 | 0.01 | 0.00 | 0.02 | 33.53 | 86.05 |
| Moss | 3a | 14.33 | 0.05 | 0.79 | 0.23 | 23.11 | 0.22 | 0.17 | 14.31 | 0.08 | 0.07 | 0.01 | 0.09 | 0.01 | 0.01 | 0.00 | 0.03 | 33.54 | 87.03 |
| Moss | 3a | 13.53 | 0.05 | 0.79 | 0.56 | 23.31 | 0.21 | 0.95 | 13.78 | 0.68 | 0.10 | 0.01 | 0.51 | 0.00 | 0.01 | 0.01 | 0.02 | 33.49 | 88.02 |
| Moss | 3a | 14.47 | 0.04 | 1.04 | 0.31 | 23.43 | 0.24 | 0.19 | 14.34 | 0.10 | 0.07 | 0.01 | 0.11 | 0.00 | 0.01 | 0.02 | 0.02 | 34.10 | 88.50 |
| Moss | 3a | 14.87 | 0.04 | 0.83 | 0.24 | 23.77 | 0.25 | 0.04 | 14.77 | 0.08 | 0.06 | 0.00 | 0.09 | 0.00 | 0.01 | 0.02 | 0.03 | 34.65 | 89.74 |
| Moss | 3a | 13.89 | 0.04 | 1.11 | 0.45 | 23.70 | 0.24 | 1.11 | 14.03 | 0.67 | 0.12 | 0.00 | 0.31 | 0.01 | 0.01 | 0.01 | 0.04 | 34.22 | 89.95 |
| Moss | 3a | 14.48 | 0.06 | 1.90 | 0.31 | 21.45 | 0.21 | 0.56 | 12.85 | 0.38 | 1.11 | 0.12 | 0.08 | 0.01 | 0.01 | 0.00 | 0.04 | 33.92 | 87.48 |
| Moss | 3a | 14.33 | 0.04 | 0.91 | 0.29 | 23.70 | 0.24 | 0.39 | 14.21 | 0.08 | 0.09 | 0.00 | 0.11 | 0.00 | 0.01 | 0.02 | 0.03 | 33.87 | 88.32 |
| Moss | 3a | 14.31 | 0.04 | 0.84 | 0.25 | 24.25 | 0.23 | 1.55 | 14.43 | 0.08 | 0.06 | 0.00 | 0.07 | 0.01 | 0.00 | 0.00 | 0.04 | 34.33 | 90.49 |
| Moss | 3a | 15.66 | 0.04 | 0.48 | 0.15 | 24.49 | 0.26 | 0.23 | 15.62 | 0.22 | 0.05 | 0.00 | 0.06 | 0.00 | 0.01 | 0.00 | 0.02 | 36.01 | 93.28 |
| Moss | 3a | 14.88 | 0.04 | 0.71 | 0.26 | 23.83 | 0.25 | 0.04 | 14.86 | 0.08 | 0.04 | 0.01 | 0.07 | 0.01 | 0.01 | 0.02 | 0.02 | 34.60 | 89.71 |
| Moss | 3a | 14.55 | 0.05 | 1.19 | 0.32 | 23.53 | 0.23 | 0.06 | 14.57 | 0.09 | 0.07 | 0.00 | 0.09 | 0.00 | 0.00 | 0.02 | 0.03 | 34.46 | 89.26 |
| Moss | 3a | 14.18 | 0.06 | 1.06 | 0.35 | 23.45 | 0.23 | 0.10 | 14.22 | 0.12 | 0.08 | 0.01 | 0.10 | 0.00 | 0.00 | 0.03 | 0.03 | 33.74 | 87.76 |
| Moss | 3a | 12.62 | 0.05 | 1.50 | 0.25 | 19.86 | 0.21 | 0.05 | 11.65 | 0.17 | 0.45 | 0.05 | 0.10 | 0.00 | 0.01 | 0.00 | 0.04 | 29.72 | 76.73 |
| Moss | 3a | 13.70 | 0.06 | 1.59 | 0.36 | 21.92 | 0.21 | 0.10 | 13.41 | 0.12 | 0.24 | 0.03 | 0.10 | 0.00 | 0.01 | 0.03 | 0.03 | 32.76 | 84.67 |
| Moss | 3a | 13.66 | 0.04 | 1.00 | 0.28 | 23.61 | 0.23 | 1.84 | 13.84 | 0.07 | 0.07 | 0.01 | 0.07 | 0.03 | 0.00 | 0.03 | 0.04 | 33.27 | 88.09 |
| Moss | 3a | 14.00 | 0.04 | 0.98 | 0.23 | 22.89 | 0.25 | 0.20 | 13.92 | 0.09 | 0.07 | 0.00 | 0.09 | 0.02 | 0.01 | 0.00 | 0.03 | 33.05 | 85.87 |
| Moss | 3a | 13.59 | 0.07 | 1.00 | 0.29 | 25.05 | 0.22 | 3.95 | 14.13 | 0.10 | 0.07 | 0.01 | 0.09 | 0.03 | 0.01 | 0.01 | 0.01 | 34.38 | 93.00 |
| Moss | 3a | 14.15 | 0.05 | 0.94 | 0.30 | 23.22 | 0.22 | 0.61 | 14.22 | 0.13 | 0.09 | 0.01 | 0.11 | 0.00 | 0.00 | 0.00 | 0.04 | 33.65 | 87.74 |
| Moss | 3a | 14.26 | 0.05 | 0.99 | 0.29 | 23.29 | 0.25 | 0.11 | 14.19 | 0.09 | 0.06 | 0.01 | 0.12 | 0.00 | 0.01 | 0.02 | 0.06 | 33.71 | 87.50 |
| Moss | 3a | 13.78 | 0.05 | 0.78 | 0.26 | 24.59 | 0.23 | 2.47 | 14.00 | 0.28 | 0.07 | 0.00 | 0.23 | 0.02 | 0.01 | 0.00 | 0.04 | 34.04 | 90.84 |
| Moss | 3a | 14.79 | 0.04 | 0.71 | 0.25 | 23.72 | 0.23 | 0.10 | 14.63 | 0.10 | 0.07 | 0.01 | 0.08 | 0.00 | 0.00 | 0.00 | 0.03 | 34.37 | 89.13 |
| Moss | 3a | 15.71 | 0.04 | 2.65 | 0.31 | 21.12 | 0.22 | 0.11 | 12.88 | 0.84 | 1.69 | 0.18 | 0.04 | 0.00 | 0.01 | 0.00 | 0.05 | 36.14 | 92.00 |
| Moss | 3a | 14.74 | 0.04 | 2.48 | 0.27 | 20.95 | 0.21 | 0.15 | 12.23 | 0.46 | 1.72 | 0.18 | 0.06 | 0.01 | 0.01 | 0.01 | 0.04 | 34.28 | 87.83 |
| Moss | 3a | 14.92 | 0.04 | 0.72 | 0.26 | 24.17 | 0.24 | 0.24 | 14.92 | 0.15 | 0.02 | 0.00 | 0.08 | 0.01 | 0.00 | 0.02 | 0.02 | 34.88 | 90.70 |
| Moss | 3a | 14.54 | 0.05 | 0.87 | 0.30 | 23.39 | 0.25 | 0.08 | 14.52 | 0.09 | 0.05 | 0.01 | 0.10 | 0.00 | 0.00 | 0.00 | 0.04 | 34.11 | 88.39 |
| Moss | 3a | 13.99 | 0.04 | 0.93 | 0.28 | 24.03 | 0.23 | 1.57 | 14.17 | 0.17 | 0.05 | 0.02 | 0.12 | 0.00 | 0.01 | 0.00 | 0.03 | 33.94 | 89.60 |
| Moss | 3a | 14.18 | 0.05 | 0.82 | 0.26 | 24.45 | 0.23 | 2.19 | 14.39 | 0.08 | 0.08 | 0.01 | 0.09 | 0.02 | 0.01 | 0.00 | 0.03 | 34.41 | 91.27 |
| Moss | 3a | 14.52 | 0.05 | 0.88 | 0.27 | 23.61 | 0.25 | 0.26 | 14.45 | 0.09 | 0.05 | 0.02 | 0.08 | 0.00 | 0.00 | 0.03 | 0.04 | 34.12 | 88.72 |
| Moss | 3a | 14.17 | 0.05 | 0.91 | 0.25 | 23.20 | 0.23 | 0.13 | 14.08 | 0.07 | 0.08 | 0.02 | 0.09 | 0.00 | 0.01 | 0.03 | 0.03 | 33.36 | 86.70 |
| Moss | 3a | 13.78 | 0.04 | 1.19 | 0.32 | 22.68 | 0.23 | 0.46 | 13.80 | 0.08 | 0.08 | 0.00 | 0.10 | 0.01 | 0.01 | 0.03 | 0.04 | 32.98 | 85.84 |
| Moss | 3a | 14.02 | 0.06 | 1.05 | 0.32 | 22.90 | 0.23 | 0.59 | 14.04 | 0.10 | 0.07 | 0.00 | 0.10 | 0.01 | 0.00 | 0.03 | 0.04 | 33.40 | 86.98 |
| Moss | 3a | 13.53 | 0.05 | 1.31 | 0.33 | 23.32 | 0.21 | 1.71 | 13.79 | 0.12 | 0.08 | 0.02 | 0.10 | 0.01 | 0.01 | 0.02 | 0.04 | 33.32 | 87.94 |
| Moss | 3a | 14.69 | 0.03 | 0.90 | 0.21 | 22.15 | 0.22 | 0.50 | 13.69 | 0.92 | 0.06 | 0.01 | 0.07 | 0.01 | 0.01 | 0.02 | 0.03 | 33.74 | 87.24 |
| Moss | 3a | 14.99 | 0.03 | 0.79 | 0.20 | 19.11 | 0.20 | 0.07 | 12.10 | 2.92 | 0.08 | 0.00 | 0.08 | 0.00 | 0.01 | 0.00 | 0.05 | 32.79 | 83.43 |
| Moss | 3b | 12.84 | 0.04 | 0.91 | 0.53 | 21.25 | 0.20 | 0.10 | 12.27 | 0.16 | 0.05 | 0.00 | 0.06 | 0.00 | 0.01 | 0.03 | 0.00 | 30.20 | 78.65 |
| Moss | 3b | 13.95 | 0.07 | 1.10 | 0.30 | 22.54 | 0.23 | 0.22 | 13.82 | 0.18 | 0.08 | 0.03 | 0.13 | 0.01 | 0.00 | 0.01 | 0.00 | 33.08 | 85.76 |
| Moss | 3b | 14.66 | 0.07 | 0.89 | 0.22 | 24.89 | 0.23 | 1.47 | 14.64 | 0.17 | 0.26 | 0.02 | 0.13 | 0.01 | 0.01 | 0.01 | 0.00 | 35.37 | 93.04 |
| Moss | 3b | 13.90 | 0.04 | 1.25 | 0.35 | 23.72 | 0.21 | 1.90 | 14.33 | 0.11 | 0.08 | 0.00 | 0.09 | 0.01 | 0.01 | 0.02 | 0.00 | 34.17 | 90.17 |
| Moss | 3b | 13.33 | 0.05 | 1.06 | 0.31 | 22.34 | 0.21 | 1.16 | 13.43 | 0.07 | 0.07 | 0.01 | 0.08 | 0.00 | 0.00 | 0.00 | 0.00 | 32.13 | 84.23 |
| Moss | 3b | 14.51 | 0.05 | 0.87 | 0.22 | 22.96 | 0.25 | 0.07 | 14.21 | 0.09 | 0.17 | 0.01 | 0.09 | 0.00 | 0.01 | 0.00 | 0.00 | 33.72 | 87.23 |
| Moss | 3b | 14.96 | 0.05 | 1.07 | 0.34 | 24.18 | 0.24 | 0.08 | 14.90 | 0.08 | 0.07 | 0.00 | 0.08 | 0.01 | 0.01 | 0.04 | 0.00 | 35.23 | 91.33 |
| Moss | 3b | 14.88 | 0.07 | 1.06 | 0.37 | 24.32 | 0.25 | 0.22 | 14.78 | 0.15 | 0.10 | 0.02 | 0.10 | 0.00 | 0.01 | 0.01 | 0.00 | 35.20 | 91.53 |
| Moss | 3b | 14.99 | 0.06 | 0.90 | 0.28 | 24.30 | 0.24 | 0.16 | 14.93 | 0.09 | 0.07 | 0.00 | 0.10 | 0.00 | 0.01 | 0.00 | 0.00 | 35.19 | 91.32 |
| Moss | 3b | 13.69 | 0.05 | 1.14 | 0.32 | 22.87 | 0.24 | 0.31 | 13.89 | 1.63 | 0.18 | 0.00 | 1.21 | 0.01 | 0.01 | 0.02 | 0.00 | 34.99 | 90.55 |
| Moss | 3b | 14.35 | 0.06 | 1.16 | 0.31 | 23.75 | 0.25 | 0.56 | 14.38 | 0.08 | 0.09 | 0.00 | 0.10 | 0.00 | 0.00 | 0.02 | 0.00 | 34.29 | 89.39 |
| Moss | 3b | 14.77 | 0.05 | 0.99 | 0.25 | 24.91 | 0.23 | 1.46 | 14.96 | 0.11 | 0.16 | 0.01 | 0.09 | 0.02 | 0.01 | 0.01 | 0.00 | 35.59 | 93.62 |
| Moss | 3b | 14.80 | 0.05 | 1.19 | 0.30 | 23.99 | 0.23 | 0.10 | 14.64 | 0.21 | 0.04 | 0.02 | 0.10 | 0.00 | 0.00 | 0.03 | 0.00 | 34.97 | 90.65 |
| Moss | 3b | 14.63 | 0.05 | 1.07 | 0.28 | 23.90 | 0.23 | 0.14 | 14.55 | 0.08 | 0.08 | 0.01 | 0.09 | 0.02 | 0.01 | 0.02 | 0.00 | 34.55 | 89.72 |
| Moss | 3b | 15.28 | 0.04 | 0.60 | 0.23 | 24.46 | 0.23 | 0.25 | 15.46 | 0.07 | 0.06 | 0.00 | 0.04 | 0.00 | 0.01 | 0.01 | 0.00 | 35.53 | 92.25 |
| Moss | 3b | 15.36 | 0.04 | 0.80 | 0.31 | 23.69 | 0.24 | 0.08 | 14.94 | 0.40 | 0.05 | 0.00 | 0.07 | 0.00 | 0.01 | 0.00 | 0.00 | 35.40 | 91.40 |
| Moss | 3b | 18.12 | 0.05 | 0.83 | 0.61 | 18.21 | 0.22 | 0.25 | 12.94 | 4.22 | 0.15 | 0.02 | 0.04 | 0.00 | 0.01 | 0.00 | 0.00 | 37.40 | 93.08 |
| Moss | 3b | 14.80 | 0.06 | 0.79 | 0.30 | 24.82 | 0.24 | 0.89 | 14.90 | 0.08 | 0.03 | 0.00 | 0.09 | 0.00 | 0.01 | 0.01 | 0.00 | 35.18 | 92.20 |

Continued on next page

| Sample | Area | Si | Ti | Al | Cr | Fe | Mn | Ni | Mg | Ca | Na | K | P | Co | V | Zn | S | O | Total |
|---|---|---|---|---|---|---|---|---|---|---|---|---|---|---|---|---|---|---|---|
| Moss | 3b | 14.09 | 0.07 | 1.74 | 0.26 | 29.36 | 0.19 | 0.81 | 12.65 | 1.38 | 0.94 | 0.12 | 0.07 | 0.13 | 0.01 | 0.02 | 0.00 | 35.88 | 97.71 |
| Moss | 3b | 14.91 | 0.04 | 0.84 | 0.19 | 23.15 | 0.24 | 1.07 | 14.28 | 0.50 | 0.29 | 0.02 | 0.06 | 0.01 | 0.01 | 0.03 | 0.00 | 34.68 | 90.31 |
| Moss | 3b | 14.62 | 0.05 | 1.18 | 0.37 | 23.65 | 0.23 | 0.12 | 14.53 | 0.79 | 0.09 | 0.00 | 0.31 | 0.01 | 0.01 | 0.03 | 0.00 | 35.29 | 91.27 |
| Moss | 3b | 14.42 | 0.06 | 1.42 | 0.41 | 24.19 | 0.24 | 0.48 | 14.49 | 0.12 | 0.09 | 0.01 | 0.10 | 0.01 | 0.01 | 0.03 | 0.00 | 34.87 | 90.96 |
| Moss | 3b | 14.61 | 0.07 | 1.42 | 0.28 | 24.20 | 0.23 | 1.11 | 13.98 | 0.28 | 0.53 | 0.04 | 0.08 | 0.02 | 0.01 | 0.03 | 0.00 | 35.10 | 92.00 |
| Moss | 3b | 13.27 | 0.05 | 1.28 | 0.33 | 21.32 | 0.21 | 0.23 | 13.20 | 0.20 | 0.11 | 0.00 | 0.20 | 0.00 | 0.01 | 0.03 | 0.00 | 31.84 | 82.28 |
| Moss | 3b | 14.04 | 0.06 | 1.21 | 0.35 | 23.21 | 0.22 | 0.73 | 14.16 | 0.10 | 0.08 | 0.00 | 0.09 | 0.01 | 0.01 | 0.05 | 0.00 | 33.75 | 88.06 |
| Moss | 3b | 14.83 | 0.02 | 0.62 | 0.27 | 21.45 | 0.21 | 0.02 | 13.63 | 0.56 | 0.19 | 0.01 | 0.03 | 0.00 | 0.00 | 0.00 | 0.00 | 33.14 | 84.98 |
| Moss | 3b | 14.32 | 0.05 | 1.15 | 0.30 | 23.64 | 0.23 | 0.13 | 14.35 | 0.06 | 0.08 | 0.01 | 0.10 | 0.01 | 0.01 | 0.01 | 0.00 | 34.06 | 88.49 |
| Moss | 3b | 13.88 | 0.07 | 1.34 | 0.37 | 23.00 | 0.22 | 0.53 | 13.81 | 0.20 | 0.08 | 0.00 | 0.14 | 0.01 | 0.01 | 0.01 | 0.00 | 33.45 | 87.10 |
| Moss | 3b | 13.88 | 0.03 | 0.98 | 0.26 | 22.44 | 0.24 | 0.52 | 13.76 | 0.23 | 0.08 | 0.00 | 0.14 | 0.00 | 0.00 | 0.04 | 0.00 | 32.88 | 85.46 |
| Moss | 3b | 14.18 | 0.05 | 0.88 | 0.24 | 23.17 | 0.23 | 0.62 | 14.23 | 0.09 | 0.09 | 0.02 | 0.09 | 0.00 | 0.01 | 0.02 | 0.00 | 33.56 | 87.47 |
| Moss | 3b | 14.26 | 0.04 | 0.86 | 0.22 | 24.13 | 0.23 | 0.10 | 14.23 | 0.09 | 0.04 | 0.01 | 0.11 | 0.02 | 0.00 | 0.01 | 0.00 | 33.77 | 88.14 |
| Moss | 3b | 14.19 | 0.04 | 0.78 | 0.22 | 22.41 | 0.24 | 0.07 | 14.03 | 0.08 | 0.05 | 0.00 | 0.10 | 0.00 | 0.01 | 0.01 | 0.00 | 32.97 | 85.20 |
| Moss | 3b | 14.67 | 0.04 | 0.99 | 0.28 | 23.87 | 0.26 | 0.08 | 14.66 | 0.06 | 0.06 | 0.00 | 0.07 | 0.01 | 0.01 | 0.02 | 0.00 | 34.55 | 89.64 |
| Moss | 3b | 14.32 | 0.03 | 1.28 | 0.30 | 23.36 | 0.23 | 0.06 | 14.22 | 0.08 | 0.09 | 0.01 | 0.07 | 0.00 | 0.00 | 0.02 | 0.00 | 33.93 | 88.00 |
| Moss | 3b | 13.77 | 0.03 | 0.83 | 0.26 | 20.99 | 0.21 | 0.10 | 12.90 | 0.78 | 0.05 | 0.00 | 0.06 | 0.00 | 0.01 | 0.01 | 0.00 | 31.60 | 81.59 |
| Moss | 3b | 14.17 | 0.04 | 1.20 | 0.38 | 23.39 | 0.24 | 0.97 | 14.34 | 0.08 | 0.06 | 0.01 | 0.07 | 0.00 | 0.00 | 0.00 | 0.00 | 34.09 | 89.04 |
| Moss | 3b | 15.02 | 0.04 | 1.05 | 0.33 | 21.81 | 0.22 | 0.27 | 13.54 | 1.26 | 0.16 | 0.02 | 0.07 | 0.00 | 0.01 | 0.03 | 0.00 | 34.24 | 88.07 |
| Moss | 3b | 14.76 | 0.04 | 0.85 | 0.24 | 22.38 | 0.23 | 0.12 | 14.12 | 0.84 | 0.06 | 0.01 | 0.08 | 0.00 | 0.01 | 0.00 | 0.00 | 34.02 | 87.75 |
| Moss | 3b | 14.34 | 0.04 | 0.87 | 0.25 | 22.97 | 0.24 | 0.04 | 14.25 | 0.11 | 0.06 | 0.00 | 0.11 | 0.00 | 0.01 | 0.01 | 0.00 | 33.55 | 86.85 |
| Moss | 3b | 14.42 | 0.04 | 0.84 | 0.23 | 23.68 | 0.24 | 0.55 | 14.46 | 0.08 | 0.06 | 0.01 | 0.09 | 0.02 | 0.00 | 0.01 | 0.00 | 34.06 | 88.80 |
| Moss | 3b | 14.61 | 0.06 | 1.26 | 0.32 | 24.23 | 0.24 | 0.32 | 14.62 | 0.09 | 0.05 | 0.00 | 0.09 | 0.00 | 0.01 | 0.02 | 0.00 | 34.90 | 90.81 |
| Moss | 3b | 14.64 | 0.05 | 1.19 | 0.26 | 23.34 | 0.25 | 0.08 | 14.29 | 0.11 | 0.24 | 0.01 | 0.11 | 0.00 | 0.00 | 0.00 | 0.00 | 34.40 | 88.97 |
| Moss | 3b | 14.37 | 0.06 | 1.05 | 0.32 | 23.35 | 0.23 | 0.34 | 14.28 | 0.18 | 0.05 | 0.00 | 0.12 | 0.00 | 0.01 | 0.03 | 0.00 | 34.05 | 88.44 |
| Moss | 3b | 15.08 | 0.04 | 0.71 | 0.25 | 24.27 | 0.26 | 0.05 | 15.12 | 0.10 | 0.06 | 0.00 | 0.09 | 0.00 | 0.00 | 0.00 | 0.00 | 35.17 | 91.20 |
| Moss | 3b | 14.66 | 0.06 | 0.94 | 0.30 | 23.31 | 0.23 | 0.22 | 14.63 | 0.08 | 0.08 | 0.00 | 0.10 | 0.00 | 0.01 | 0.01 | 0.00 | 34.39 | 89.00 |
| Moss | 3b | 15.13 | 0.04 | 0.82 | 0.26 | 24.17 | 0.23 | 0.04 | 15.27 | 0.07 | 0.04 | 0.01 | 0.07 | 0.01 | 0.01 | 0.02 | 0.00 | 35.36 | 91.55 |
| Moss | 3b | 14.54 | 0.04 | 0.88 | 0.26 | 23.12 | 0.25 | 0.05 | 14.50 | 0.11 | 0.09 | 0.02 | 0.06 | 0.00 | 0.01 | 0.02 | 0.00 | 33.95 | 87.89 |
| Moss | 3b | 13.62 | 0.04 | 0.76 | 0.24 | 24.82 | 0.23 | 4.48 | 14.08 | 0.06 | 0.05 | 0.01 | 0.07 | 0.03 | 0.01 | 0.01 | 0.00 | 34.19 | 92.71 |
| Moss | 3b | 14.73 | 0.05 | 0.81 | 0.23 | 23.86 | 0.25 | 0.64 | 14.82 | 0.07 | 0.05 | 0.00 | 0.09 | 0.02 | 0.01 | 0.03 | 0.00 | 34.70 | 90.36 |
| Moss | 3b | 14.09 | 0.06 | 1.38 | 0.36 | 24.32 | 0.23 | 0.99 | 14.32 | 0.11 | 0.10 | 0.00 | 0.11 | 0.02 | 0.00 | 0.01 | 0.00 | 34.48 | 90.58 |
| Moss | 3b | 14.09 | 0.05 | 1.08 | 0.39 | 24.62 | 0.21 | 1.64 | 14.34 | 0.09 | 0.05 | 0.00 | 0.09 | 0.02 | 0.01 | 0.01 | 0.00 | 34.47 | 91.17 |
| Moss | 3b | 13.98 | 0.04 | 1.08 | 0.40 | 22.92 | 0.22 | 1.18 | 13.96 | 0.19 | 0.10 | 0.01 | 0.11 | 0.00 | 0.01 | 0.01 | 0.00 | 33.56 | 87.78 |
| Moss | 3b | 14.59 | 0.06 | 1.10 | 0.35 | 23.14 | 0.24 | 0.07 | 14.59 | 0.11 | 0.06 | 0.01 | 0.10 | 0.00 | 0.01 | 0.02 | 0.00 | 34.36 | 88.80 |
| Moss | 3b | 14.99 | 0.04 | 0.98 | 0.36 | 24.53 | 0.24 | 0.31 | 15.05 | 0.09 | 0.12 | 0.02 | 0.07 | 0.00 | 0.01 | 0.01 | 0.00 | 35.50 | 92.31 |

| Sample | Area | Si | Ti | Al | Cr | Fe | Mn | Ni | Mg | Ca | Na | K | P | Co | V | Zn | S | O | Total |
|---|---|---|---|---|---|---|---|---|---|---|---|---|---|---|---|---|---|---|---|
| Warrenton | 1a | 9.15 | 0.04 | 0.93 | 1.04 | 26.38 | 0.12 | 5.99 | 11.10 | 3.12 | 0.21 | 0.01 | 2.12 | 0.04 | 0.0 | 0.0 | 1.07 | 33.97 | 95.30 |
| Warrenton | 1a | 12.89 | 0.04 | 0.78 | 0.33 | 20.87 | 0.17 | 0.03 | 13.39 | 0.29 | 0.05 | 0.01 | 0.21 | 0.00 | 0.0 | 0.0 | 0.04 | 30.88 | 79.99 |
| Warrenton | 1a | 17.32 | 0.12 | 2.07 | 0.63 | 16.20 | 0.38 | 0.00 | 12.96 | 3.18 | 0.97 | 0.12 | 0.11 | 0.00 | 0.0 | 0.0 | 0.03 | 37.04 | 91.13 |
| Warrenton | 1a | 15.73 | 0.10 | 4.99 | 0.56 | 13.47 | 0.29 | 0.09 | 8.92 | 3.47 | 3.13 | 0.36 | 0.56 | 0.00 | 0.0 | 0.0 | 0.06 | 35.88 | 87.61 |
| Warrenton | 1a | 14.36 | 0.09 | 3.78 | 0.44 | 17.76 | 0.13 | 0.09 | 10.95 | 0.67 | 2.02 | 0.33 | 0.10 | 0.00 | 0.0 | 0.0 | 0.04 | 33.58 | 84.35 |
| Warrenton | 1a | 15.11 | 0.06 | 2.55 | 0.33 | 20.64 | 0.22 | 0.00 | 12.67 | 0.79 | 1.42 | 0.15 | 0.13 | 0.00 | 0.0 | 0.0 | 0.03 | 35.04 | 89.14 |
| Warrenton | 1a | 14.69 | 0.09 | 0.91 | 0.27 | 23.09 | 0.22 | 0.06 | 14.45 | 0.29 | 0.24 | 0.03 | 0.06 | 0.00 | 0.0 | 0.0 | 0.04 | 34.27 | 88.70 |
| Warrenton | 1a | 14.13 | 0.06 | 0.43 | 0.30 | 23.55 | 0.21 | 0.01 | 14.57 | 0.03 | 0.04 | 0.00 | 0.03 | 0.00 | 0.0 | 0.0 | 0.04 | 33.17 | 86.56 |
| Warrenton | 1a | 12.59 | 0.06 | 0.78 | 0.38 | 23.93 | 0.18 | 0.01 | 12.73 | 0.15 | 0.04 | 0.01 | 0.06 | 0.00 | 0.0 | 0.0 | 1.67 | 33.19 | 85.77 |
| Warrenton | 1a | 13.26 | 0.05 | 0.79 | 0.26 | 21.97 | 0.18 | 0.10 | 13.96 | 0.09 | 0.04 | 0.00 | 0.07 | 0.00 | 0.0 | 0.0 | 0.04 | 31.72 | 82.52 |
| Warrenton | 1a | 13.60 | 0.06 | 0.95 | 0.42 | 22.00 | 0.18 | 0.07 | 13.32 | 0.08 | 0.05 | 0.00 | 0.06 | 0.00 | 0.0 | 0.0 | 0.05 | 31.91 | 82.74 |
| Warrenton | 1a | 13.49 | 0.05 | 0.97 | 0.41 | 21.81 | 0.19 | 0.02 | 12.93 | 0.10 | 0.06 | 0.01 | 0.07 | 0.00 | 0.0 | 0.0 | 0.04 | 31.47 | 81.60 |
| Warrenton | 1a | 12.40 | 0.05 | 1.20 | 0.43 | 20.26 | 0.16 | 0.25 | 12.14 | 0.12 | 0.05 | 0.01 | 0.06 | 0.00 | 0.0 | 0.0 | 0.12 | 29.67 | 76.93 |
| Warrenton | 1a | 12.45 | 0.06 | 1.09 | 0.48 | 21.73 | 0.18 | 0.21 | 13.09 | 0.05 | 0.04 | 0.00 | 0.06 | 0.00 | 0.0 | 0.0 | 0.28 | 30.90 | 80.63 |
| Warrenton | 1a | 12.30 | 0.05 | 0.82 | 0.41 | 22.63 | 0.17 | 0.24 | 12.63 | 0.08 | 0.04 | 0.01 | 0.08 | 0.00 | 0.0 | 0.0 | 1.16 | 31.76 | 82.38 |
| Warrenton | 1a | 13.06 | 0.06 | 0.91 | 0.39 | 18.48 | 0.15 | 0.04 | 12.05 | 1.45 | 0.04 | 0.00 | 0.04 | 0.00 | 0.0 | 0.0 | 0.12 | 30.02 | 76.81 |
| Warrenton | 1a | 12.52 | 0.05 | 1.14 | 0.45 | 21.73 | 0.16 | 0.43 | 12.70 | 0.09 | 0.04 | 0.01 | 0.07 | 0.01 | 0.0 | 0.0 | 0.53 | 31.20 | 81.14 |

Continued on next page

| Sample | Area | Si | Ti | Al | Cr | Fe | Mn | Ni | Mg | Ca | Na | K | P | Co | V | Zn | S | O | Total |
|---|---|---|---|---|---|---|---|---|---|---|---|---|---|---|---|---|---|---|---|
| Warrenton | 1a | 12.29 | 0.05 | 1.01 | 0.37 | 19.64 | 0.16 | 0.04 | 12.37 | 0.17 | 0.03 | 0.01 | 0.05 | 0.00 | 0.0 | 0.0 | 0.05 | 29.15 | 75.39 |
| Warrenton | 1a | 13.16 | 0.04 | 0.62 | 0.25 | 21.00 | 0.18 | 0.01 | 12.93 | 0.08 | 0.04 | 0.00 | 0.07 | 0.00 | 0.0 | 0.0 | 0.04 | 30.45 | 78.87 |
| Warrenton | 1a | 12.28 | 0.04 | 0.75 | 0.24 | 20.73 | 0.16 | 0.81 | 13.30 | 0.08 | 0.06 | 0.00 | 0.05 | 0.00 | 0.0 | 0.0 | 0.07 | 29.98 | 78.55 |
| Warrenton | 1a | 12.92 | 0.03 | 0.78 | 0.25 | 20.25 | 0.17 | 0.03 | 12.82 | 0.13 | 0.06 | 0.01 | 0.07 | 0.00 | 0.0 | 0.0 | 0.04 | 30.07 | 77.63 |
| Warrenton | 1a | 12.75 | 0.05 | 0.85 | 0.32 | 20.66 | 0.16 | 0.27 | 12.86 | 0.08 | 0.05 | 0.00 | 0.07 | 0.00 | 0.0 | 0.0 | 0.04 | 30.16 | 78.31 |
| Warrenton | 1a | 12.26 | 0.05 | 0.99 | 0.37 | 20.18 | 0.16 | 0.47 | 12.61 | 0.07 | 0.04 | 0.00 | 0.06 | 0.00 | 0.0 | 0.0 | 0.05 | 29.50 | 76.81 |
| Warrenton | 1a | 12.55 | 0.06 | 0.85 | 0.30 | 20.17 | 0.17 | 0.35 | 12.62 | 0.11 | 0.05 | 0.00 | 0.10 | 0.00 | 0.0 | 0.0 | 0.04 | 29.72 | 77.09 |
| Warrenton | 1a | 12.23 | 0.04 | 0.76 | 0.24 | 19.46 | 0.15 | 0.01 | 12.51 | 0.13 | 0.05 | 0.00 | 0.06 | 0.00 | 0.0 | 0.0 | 0.06 | 28.83 | 74.52 |
| Warrenton | 1a | 13.17 | 0.04 | 0.67 | 0.40 | 23.79 | 0.18 | 0.04 | 14.13 | 0.30 | 0.01 | 0.01 | 0.02 | 0.00 | 0.0 | 0.0 | 1.02 | 33.68 | 87.48 |
| Warrenton | 1a | 13.15 | 0.05 | 1.40 | 0.50 | 21.70 | 0.18 | 0.24 | 13.07 | 0.22 | 0.05 | 0.00 | 0.06 | 0.00 | 0.0 | 0.0 | 0.10 | 31.75 | 82.46 |
| Warrenton | 1a | 15.62 | 0.05 | 1.07 | 0.40 | 18.86 | 0.16 | 0.06 | 12.46 | 3.25 | 0.08 | 0.00 | 0.08 | 0.00 | 0.0 | 0.0 | 0.04 | 34.12 | 86.25 |
| Warrenton | 1a | 14.65 | 0.05 | 1.17 | 0.44 | 17.37 | 0.14 | 0.03 | 11.30 | 3.51 | 0.05 | 0.00 | 0.10 | 0.00 | 0.0 | 0.0 | 0.14 | 32.20 | 81.16 |
| Warrenton | 1a | 13.42 | 0.04 | 0.78 | 0.29 | 21.83 | 0.18 | 0.04 | 13.97 | 0.07 | 0.03 | 0.01 | 0.06 | 0.00 | 0.0 | 0.0 | 0.05 | 31.87 | 82.66 |
| Warrenton | 1a | 13.45 | 0.04 | 0.61 | 0.23 | 21.88 | 0.17 | 0.17 | 13.64 | 0.10 | 0.03 | 0.00 | 0.04 | 0.00 | 0.0 | 0.0 | 0.04 | 31.50 | 81.90 |
| Warrenton | 1a | 14.76 | 0.04 | 0.56 | 0.21 | 18.87 | 0.15 | 0.02 | 12.37 | 2.90 | 0.04 | 0.00 | 0.05 | 0.00 | 0.0 | 0.0 | 0.09 | 32.41 | 82.46 |
| Warrenton | 1a | 12.88 | 0.05 | 0.53 | 0.26 | 20.38 | 0.17 | 0.02 | 11.67 | 0.08 | 0.06 | 0.01 | 0.05 | 0.00 | 0.0 | 0.0 | 0.04 | 29.05 | 75.25 |
| Warrenton | 1a | 13.02 | 0.04 | 0.65 | 0.25 | 21.23 | 0.17 | 0.02 | 13.61 | 0.08 | 0.04 | 0.00 | 0.07 | 0.00 | 0.0 | 0.0 | 0.04 | 30.85 | 80.07 |
| Warrenton | 1a | 12.45 | 0.04 | 0.82 | 0.28 | 21.16 | 0.16 | 1.20 | 12.77 | 0.07 | 0.04 | 0.00 | 0.09 | 0.01 | 0.0 | 0.0 | 0.06 | 30.14 | 79.27 |
| Warrenton | 1a | 11.78 | 0.04 | 0.82 | 0.26 | 18.83 | 0.16 | 0.03 | 12.24 | 0.07 | 0.04 | 0.00 | 0.06 | 0.00 | 0.0 | 0.0 | 0.05 | 27.99 | 72.37 |
| Warrenton | 1a | 11.95 | 0.04 | 0.82 | 0.24 | 18.89 | 0.14 | 0.05 | 11.83 | 0.08 | 0.05 | 0.01 | 0.06 | 0.00 | 0.0 | 0.0 | 0.05 | 27.95 | 72.17 |
| Warrenton | 1a | 11.90 | 0.05 | 0.76 | 0.25 | 19.28 | 0.15 | 0.04 | 12.05 | 0.08 | 0.04 | 0.00 | 0.09 | 0.00 | 0.0 | 0.0 | 0.05 | 28.13 | 72.87 |
| Warrenton | 1a | 13.79 | 0.06 | 0.77 | 0.27 | 21.89 | 0.19 | 0.03 | 12.73 | 0.16 | 0.26 | 0.04 | 0.07 | 0.00 | 0.0 | 0.0 | 0.06 | 31.61 | 81.92 |
| Warrenton | 1a | 13.64 | 0.05 | 1.12 | 0.34 | 22.15 | 0.17 | 0.05 | 13.42 | 0.12 | 0.12 | 0.02 | 0.06 | 0.00 | 0.0 | 0.0 | 0.05 | 32.22 | 83.53 |
| Warrenton | 1a | 13.82 | 0.05 | 1.13 | 0.42 | 23.73 | 0.18 | 1.04 | 13.71 | 0.12 | 0.10 | 0.01 | 0.06 | 0.01 | 0.0 | 0.0 | 0.04 | 33.35 | 87.77 |
| Warrenton | 1a | 15.48 | 0.06 | 0.95 | 0.37 | 25.41 | 0.21 | 0.05 | 15.23 | 0.37 | 0.07 | 0.03 | 0.06 | 0.00 | 0.0 | 0.0 | 0.08 | 36.45 | 94.83 |
| Warrenton | 1a | 15.83 | 0.05 | 0.84 | 0.42 | 25.84 | 0.23 | 0.06 | 15.78 | 0.31 | 0.13 | 0.02 | 0.06 | 0.00 | 0.0 | 0.0 | 0.04 | 37.20 | 96.82 |
| Warrenton | 1a | 16.41 | 0.04 | 1.34 | 0.28 | 25.57 | 0.22 | 0.03 | 15.42 | 0.29 | 0.75 | 0.06 | 0.03 | 0.00 | 0.0 | 0.0 | 0.02 | 38.04 | 98.50 |
| Warrenton | 1a | 13.52 | 0.07 | 0.54 | 0.24 | 22.78 | 0.20 | 0.02 | 14.26 | 0.10 | 0.14 | 0.01 | 0.08 | 0.00 | 0.0 | 0.0 | 0.06 | 32.30 | 84.31 |
| Warrenton | 1a | 13.31 | 0.05 | 0.64 | 0.30 | 22.88 | 0.20 | 0.07 | 14.44 | 0.09 | 0.05 | 0.00 | 0.06 | 0.00 | 0.0 | 0.0 | 0.05 | 32.25 | 84.39 |
| Warrenton | 1a | 14.72 | 0.04 | 1.20 | 0.33 | 24.32 | 0.19 | 0.09 | 13.87 | 0.73 | 0.50 | 0.02 | 0.13 | 0.00 | 0.0 | 0.0 | 0.84 | 36.08 | 93.06 |
| Warrenton | 1a | 14.55 | 0.05 | 1.12 | 0.38 | 24.40 | 0.19 | 0.11 | 14.68 | 0.08 | 0.10 | 0.02 | 0.06 | 0.00 | 0.0 | 0.0 | 0.09 | 34.80 | 90.62 |
| Warrenton | 1a | 14.31 | 0.05 | 1.94 | 0.38 | 23.66 | 0.21 | 0.60 | 13.85 | 0.15 | 0.52 | 0.06 | 0.09 | 0.00 | 0.0 | 0.0 | 0.05 | 34.81 | 90.69 |
| Warrenton | 1a | 13.81 | 0.06 | 1.29 | 0.34 | 22.57 | 0.20 | 0.03 | 13.73 | 0.11 | 0.11 | 0.03 | 0.06 | 0.01 | 0.0 | 0.0 | 0.05 | 32.90 | 85.31 |
| Warrenton | 1b | 13.06 | 0.04 | 0.53 | 0.17 | 20.48 | 0.16 | 0.03 | 13.54 | 0.74 | 0.11 | 0.01 | 0.04 | 0.01 | 0.0 | 0.0 | 0.05 | 30.73 | 79.68 |
| Warrenton | 1b | 13.15 | 0.04 | 0.98 | 0.15 | 19.69 | 0.18 | 0.03 | 12.79 | 1.17 | 0.38 | 0.03 | 0.04 | 0.00 | 0.0 | 0.0 | 0.05 | 30.81 | 79.49 |
| Warrenton | 1b | 13.90 | 0.05 | 1.44 | 0.23 | 20.81 | 0.17 | 0.01 | 12.62 | 0.39 | 0.86 | 0.09 | 0.07 | 0.00 | 0.0 | 0.0 | 0.14 | 32.34 | 83.11 |
| Warrenton | 1b | 13.72 | 0.04 | 1.11 | 0.37 | 22.89 | 0.17 | 0.39 | 13.85 | 0.10 | 0.06 | 0.00 | 0.09 | 0.00 | 0.0 | 0.0 | 0.04 | 32.88 | 85.70 |
| Warrenton | 1b | 14.71 | 0.04 | 0.52 | 0.32 | 24.17 | 0.20 | 0.23 | 14.78 | 0.12 | 0.03 | 0.01 | 0.04 | 0.00 | 0.0 | 0.0 | 0.03 | 34.33 | 89.55 |
| Warrenton | 1b | 14.13 | 0.03 | 0.76 | 0.50 | 24.77 | 0.19 | 0.27 | 15.30 | 0.28 | 0.05 | 0.01 | 0.12 | 0.00 | 0.0 | 0.0 | 0.39 | 35.17 | 91.96 |
| Warrenton | 1b | 13.35 | 0.05 | 0.86 | 0.31 | 22.49 | 0.18 | 0.22 | 14.00 | 0.16 | 0.05 | 0.00 | 0.10 | 0.00 | 0.0 | 0.0 | 0.06 | 32.22 | 84.05 |
| Warrenton | 1b | 13.45 | 0.04 | 1.36 | 0.34 | 22.05 | 0.18 | 0.06 | 13.74 | 0.09 | 0.14 | 0.01 | 0.07 | 0.01 | 0.0 | 0.0 | 0.04 | 32.38 | 83.96 |
| Warrenton | 1b | 13.31 | 0.04 | 0.94 | 0.26 | 22.60 | 0.18 | 0.74 | 13.89 | 0.07 | 0.05 | 0.00 | 0.07 | 0.00 | 0.0 | 0.0 | 0.04 | 32.21 | 84.40 |
| Warrenton | 1b | 13.11 | 0.04 | 1.14 | 0.33 | 21.64 | 0.17 | 0.10 | 13.29 | 0.07 | 0.08 | 0.00 | 0.06 | 0.00 | 0.0 | 0.0 | 0.05 | 31.36 | 81.45 |
| Warrenton | 1b | 12.81 | 0.05 | 1.27 | 0.31 | 20.57 | 0.17 | 0.04 | 12.59 | 0.22 | 0.04 | 0.00 | 0.07 | 0.00 | 0.0 | 0.0 | 0.04 | 30.39 | 78.57 |
| Warrenton | 1b | 13.32 | 0.06 | 1.15 | 0.26 | 21.45 | 0.18 | 0.04 | 13.29 | 0.11 | 0.16 | 0.02 | 0.09 | 0.00 | 0.0 | 0.0 | 0.04 | 31.60 | 81.77 |
| Warrenton | 1b | 13.30 | 0.06 | 1.25 | 0.32 | 21.71 | 0.18 | 0.24 | 12.81 | 0.10 | 0.09 | 0.01 | 0.08 | 0.00 | 0.0 | 0.0 | 0.05 | 31.48 | 81.68 |
| Warrenton | 1b | 14.81 | 0.06 | 0.79 | 0.21 | 23.90 | 0.20 | 0.16 | 14.35 | 0.11 | 0.21 | 0.04 | 0.05 | 0.00 | 0.0 | 0.0 | 0.04 | 34.36 | 89.29 |
| Warrenton | 1b | 13.90 | 0.08 | 0.93 | 0.34 | 23.67 | 0.20 | 0.06 | 14.36 | 0.09 | 0.04 | 0.02 | 0.05 | 0.00 | 0.0 | 0.0 | 0.16 | 33.54 | 87.44 |
| Warrenton | 1b | 13.14 | 0.07 | 0.70 | 0.24 | 22.22 | 0.18 | 0.24 | 13.68 | 0.07 | 0.05 | 0.01 | 0.07 | 0.00 | 0.0 | 0.0 | 0.06 | 31.47 | 82.20 |
| Warrenton | 1b | 14.90 | 0.08 | 0.95 | 0.35 | 21.77 | 0.17 | 0.73 | 13.51 | 1.94 | 0.15 | 0.01 | 0.06 | 0.01 | 0.0 | 0.0 | 0.13 | 34.53 | 89.30 |
| Warrenton | 1b | 12.71 | 0.07 | 1.77 | 0.46 | 20.42 | 0.16 | 0.28 | 12.02 | 0.38 | 0.53 | 0.06 | 0.25 | 0.01 | 0.0 | 0.0 | 0.10 | 31.02 | 80.23 |
| Warrenton | 1b | 13.06 | 0.07 | 1.25 | 0.38 | 21.25 | 0.17 | 0.07 | 12.49 | 0.09 | 0.06 | 0.00 | 0.06 | 0.00 | 0.0 | 0.0 | 0.14 | 30.92 | 80.00 |
| Warrenton | 1b | 13.20 | 0.06 | 1.28 | 0.35 | 21.77 | 0.17 | 0.40 | 13.00 | 0.07 | 0.22 | 0.03 | 0.08 | 0.00 | 0.0 | 0.0 | 0.16 | 31.79 | 82.58 |
| Warrenton | 1b | 13.24 | 0.06 | 1.08 | 0.25 | 20.76 | 0.18 | 0.15 | 12.61 | 0.14 | 0.25 | 0.02 | 0.06 | 0.00 | 0.0 | 0.0 | 0.06 | 30.86 | 79.72 |
| Warrenton | 1b | 12.76 | 0.05 | 1.44 | 0.54 | 21.39 | 0.18 | 0.11 | 13.27 | 0.24 | 0.08 | 0.03 | 0.07 | 0.00 | 0.0 | 0.0 | 0.06 | 31.36 | 81.59 |
| Warrenton | 1b | 13.50 | 0.04 | 1.14 | 0.42 | 24.12 | 0.19 | 1.28 | 13.80 | 0.06 | 0.06 | 0.01 | 0.02 | 0.01 | 0.0 | 0.0 | 0.06 | 33.19 | 87.91 |
| Warrenton | 1b | 16.18 | 0.05 | 0.70 | 0.25 | 20.65 | 0.15 | 0.17 | 12.43 | 3.99 | 0.10 | 0.01 | 0.27 | 0.00 | 0.0 | 0.0 | 0.87 | 36.67 | 92.49 |
| Warrenton | 1b | 16.45 | 0.06 | 0.71 | 0.23 | 19.80 | 0.14 | 0.11 | 11.88 | 4.77 | 0.12 | 0.01 | 0.07 | 0.00 | 0.0 | 0.0 | 1.04 | 36.68 | 92.08 |

Continued on next page

| Sample | Area | Si | Ti | Al | Cr | Fe | Mn | Ni | Mg | Ca | Na | K | P | Co | V | Zn | S | O | Total |
|---|---|---|---|---|---|---|---|---|---|---|---|---|---|---|---|---|---|---|---|
| Warrenton | 1b | 13.69 | 0.06 | 1.33 | 0.29 | 20.85 | 0.17 | 0.02 | 12.49 | 0.15 | 0.52 | 0.07 | 0.06 | 0.00 | 0.0 | 0.0 | 0.04 | 31.61 | 81.36 |
| Warrenton | 1b | 14.57 | 0.08 | 1.82 | 0.27 | 21.36 | 0.16 | 0.06 | 12.95 | 0.39 | 0.86 | 0.10 | 0.08 | 0.00 | 0.0 | 0.0 | 0.05 | 33.76 | 86.51 |
| Warrenton | 1b | 13.37 | 0.08 | 1.04 | 0.32 | 21.34 | 0.17 | 0.06 | 13.29 | 0.16 | 0.17 | 0.02 | 0.07 | 0.00 | 0.0 | 0.0 | 0.06 | 31.59 | 81.72 |
| Warrenton | 1b | 15.33 | 0.08 | 1.70 | 0.39 | 27.27 | 0.20 | 1.24 | 15.11 | 0.23 | 0.84 | 0.07 | 0.12 | 0.03 | 0.0 | 0.0 | 0.51 | 38.70 | 101.83 |
| Warrenton | 1b | 15.97 | 0.06 | 0.75 | 0.33 | 26.62 | 0.23 | 0.17 | 16.07 | 0.18 | 0.18 | 0.02 | 0.05 | 0.00 | 0.0 | 0.0 | 0.11 | 37.74 | 98.47 |
| Warrenton | 1b | 15.79 | 0.07 | 0.89 | 0.29 | 23.23 | 0.22 | 0.11 | 14.25 | 0.87 | 0.22 | 0.01 | 0.07 | 0.00 | 0.0 | 0.0 | 0.05 | 35.67 | 91.73 |
| Warrenton | 1c | 14.41 | 0.05 | 1.41 | 0.57 | 25.09 | 0.19 | 0.29 | 14.26 | 0.17 | 0.21 | 0.03 | 0.05 | 0.01 | 0.0 | 0.0 | 0.09 | 35.03 | 91.86 |
| Warrenton | 1c | 14.56 | 0.07 | 1.14 | 0.32 | 24.86 | 0.20 | 0.15 | 14.22 | 0.13 | 0.28 | 0.03 | 0.06 | 0.01 | 0.0 | 0.0 | 0.06 | 34.70 | 90.79 |
| Warrenton | 1c | 13.90 | 0.08 | 1.02 | 0.33 | 25.27 | 0.19 | 1.86 | 13.89 | 0.10 | 0.27 | 0.03 | 0.07 | 0.03 | 0.0 | 0.0 | 0.07 | 34.24 | 91.37 |
| Warrenton | 1c | 13.41 | 0.07 | 1.47 | 0.27 | 21.91 | 0.16 | 0.50 | 13.05 | 0.27 | 0.69 | 0.07 | 0.07 | 0.01 | 0.0 | 0.0 | 0.05 | 32.34 | 84.34 |
| Warrenton | 1c | 14.05 | 0.06 | 1.27 | 0.34 | 23.62 | 0.19 | 0.07 | 13.77 | 0.13 | 0.43 | 0.04 | 0.05 | 0.01 | 0.0 | 0.0 | 0.31 | 33.98 | 88.32 |
| Warrenton | 1c | 14.09 | 0.06 | 1.50 | 0.51 | 24.50 | 0.20 | 0.09 | 14.30 | 0.14 | 0.11 | 0.00 | 0.06 | 0.00 | 0.0 | 0.0 | 0.04 | 34.40 | 90.00 |
| Warrenton | 1c | 13.95 | 0.05 | 1.28 | 0.44 | 24.25 | 0.20 | 0.09 | 13.74 | 0.03 | 0.09 | 0.01 | 0.04 | 0.00 | 0.0 | 0.0 | 0.08 | 33.56 | 87.82 |
| Warrenton | 1c | 13.44 | 0.07 | 1.27 | 0.40 | 23.62 | 0.17 | 0.77 | 13.52 | 0.07 | 0.15 | 0.02 | 0.05 | 0.01 | 0.0 | 0.0 | 0.06 | 32.84 | 86.46 |
| Warrenton | 1c | 13.73 | 0.05 | 1.37 | 0.37 | 24.82 | 0.18 | 0.13 | 12.29 | 0.21 | 0.54 | 0.03 | 0.05 | 0.00 | 0.0 | 0.0 | 0.98 | 34.15 | 88.89 |
| Warrenton | 1c | 12.62 | 0.07 | 1.80 | 0.29 | 21.16 | 0.17 | 0.10 | 11.61 | 0.22 | 0.89 | 0.08 | 0.08 | 0.00 | 0.0 | 0.0 | 0.09 | 30.58 | 79.74 |
| Warrenton | 1c | 12.83 | 0.06 | 1.48 | 0.38 | 22.71 | 0.17 | 0.31 | 11.99 | 0.18 | 0.55 | 0.05 | 0.09 | 0.02 | 0.0 | 0.0 | 0.08 | 31.19 | 82.08 |
| Warrenton | 1c | 13.81 | 0.05 | 1.30 | 0.34 | 23.66 | 0.19 | 0.30 | 13.70 | 0.10 | 0.36 | 0.03 | 0.04 | 0.00 | 0.0 | 0.0 | 0.07 | 33.36 | 87.34 |
| Warrenton | 1c | 12.55 | 0.06 | 1.46 | 0.41 | 21.74 | 0.16 | 0.34 | 12.59 | 0.10 | 0.20 | 0.01 | 0.09 | 0.01 | 0.0 | 0.0 | 0.07 | 30.82 | 80.60 |
| Warrenton | 1c | 13.66 | 0.05 | 0.79 | 0.29 | 24.17 | 0.20 | 0.26 | 13.63 | 0.09 | 0.14 | 0.01 | 0.06 | 0.01 | 0.0 | 0.0 | 0.26 | 33.01 | 86.62 |
| Warrenton | 1c | 14.90 | 0.08 | 0.93 | 0.54 | 24.58 | 0.18 | 0.12 | 13.06 | 1.80 | 0.11 | 0.02 | 0.16 | 0.02 | 0.0 | 0.0 | 1.08 | 36.43 | 94.03 |
| Warrenton | 1c | 12.72 | 0.05 | 1.15 | 0.40 | 21.66 | 0.17 | 0.46 | 12.43 | 0.05 | 0.06 | 0.00 | 0.05 | 0.01 | 0.0 | 0.0 | 0.10 | 30.55 | 79.87 |
| Warrenton | 1c | 12.85 | 0.06 | 0.97 | 0.32 | 21.63 | 0.17 | 0.08 | 13.11 | 0.06 | 0.06 | 0.01 | 0.04 | 0.00 | 0.0 | 0.0 | 0.04 | 30.76 | 80.15 |
| Warrenton | 1c | 11.96 | 0.05 | 1.32 | 0.32 | 18.57 | 0.14 | 0.30 | 11.57 | 0.10 | 0.20 | 0.03 | 0.06 | 0.00 | 0.0 | 0.0 | 0.05 | 28.31 | 72.98 |
| Warrenton | 1c | 11.79 | 0.06 | 1.21 | 0.34 | 19.14 | 0.14 | 0.77 | 11.59 | 0.07 | 0.05 | 0.01 | 0.06 | 0.00 | 0.0 | 0.0 | 0.06 | 28.27 | 73.56 |
| Warrenton | 1c | 11.82 | 0.05 | 1.44 | 0.39 | 19.79 | 0.14 | 1.22 | 11.72 | 0.08 | 0.04 | 0.02 | 0.08 | 0.01 | 0.0 | 0.0 | 0.05 | 28.95 | 75.81 |
| Warrenton | 1c | 12.87 | 0.06 | 1.29 | 0.34 | 21.21 | 0.16 | 0.26 | 12.59 | 0.11 | 0.09 | 0.01 | 0.06 | 0.00 | 0.0 | 0.0 | 0.27 | 31.03 | 80.35 |
| Warrenton | 1c | 12.76 | 0.05 | 1.39 | 0.29 | 19.61 | 0.15 | 0.03 | 11.87 | 0.14 | 0.35 | 0.05 | 0.07 | 0.00 | 0.0 | 0.0 | 0.05 | 29.78 | 76.60 |
| Warrenton | 1c | 13.89 | 0.06 | 1.05 | 0.29 | 22.20 | 0.18 | 0.08 | 13.59 | 0.09 | 0.11 | 0.04 | 0.06 | 0.00 | 0.0 | 0.0 | 0.03 | 32.53 | 84.22 |
| Warrenton | 1c | 16.30 | 0.07 | 1.38 | 0.47 | 25.93 | 0.20 | 0.20 | 15.01 | 0.31 | 0.35 | 0.05 | 0.06 | 0.00 | 0.0 | 0.0 | 0.20 | 38.11 | 98.64 |
| Warrenton | 1c | 15.09 | 0.06 | 1.16 | 0.28 | 24.69 | 0.19 | 0.45 | 14.72 | 0.12 | 0.27 | 0.02 | 0.09 | 0.00 | 0.0 | 0.0 | 0.05 | 35.67 | 92.87 |
| Warrenton | 1c | 14.04 | 0.06 | 1.40 | 0.32 | 22.65 | 0.18 | 0.04 | 13.81 | 0.13 | 0.15 | 0.02 | 0.07 | 0.00 | 0.0 | 0.0 | 0.07 | 33.37 | 86.31 |
| Warrenton | 1c | 14.64 | 0.07 | 2.11 | 0.36 | 23.01 | 0.19 | 0.12 | 13.51 | 0.26 | 0.58 | 0.07 | 0.12 | 0.00 | 0.0 | 0.0 | 0.14 | 35.03 | 90.20 |
| Warrenton | 1c | 14.38 | 0.05 | 1.89 | 0.27 | 23.27 | 0.19 | 1.13 | 13.56 | 0.23 | 0.73 | 0.09 | 0.09 | 0.01 | 0.0 | 0.0 | 0.05 | 34.73 | 90.68 |
| Warrenton | 1c | 14.14 | 0.05 | 1.50 | 0.39 | 22.70 | 0.19 | 0.06 | 13.82 | 0.14 | 0.17 | 0.05 | 0.07 | -0.00 | 0.0 | 0.0 | 0.06 | 33.63 | 86.96 |
| Warrenton | 1c | 13.87 | 0.05 | 1.37 | 0.36 | 24.56 | 0.20 | 2.11 | 13.87 | 0.13 | 0.31 | 0.01 | 0.06 | 0.02 | 0.0 | 0.0 | 0.20 | 34.56 | 91.68 |
| Warrenton | 1c | 14.72 | 0.07 | 1.10 | 0.32 | 24.15 | 0.19 | 0.44 | 14.21 | 0.15 | 0.32 | 0.04 | 0.06 | 0.00 | 0.0 | 0.0 | 0.20 | 34.94 | 90.90 |
| Warrenton | 1c | 14.83 | 0.05 | 1.15 | 0.30 | 23.25 | 0.21 | 0.47 | 13.85 | 0.37 | 0.38 | 0.04 | 0.12 | 0.00 | 0.0 | 0.0 | 0.06 | 34.60 | 89.69 |
| Warrenton | 1c | 14.22 | 0.05 | 1.65 | 0.40 | 24.66 | 0.20 | 2.58 | 13.56 | 0.14 | 0.41 | 0.04 | 0.07 | 0.02 | 0.0 | 0.0 | 0.07 | 35.06 | 93.14 |
| Warrenton | 1c | 14.19 | 0.08 | 1.02 | 0.32 | 23.05 | 0.20 | 0.06 | 13.73 | 0.17 | 0.15 | 0.04 | 0.08 | 0.00 | 0.0 | 0.0 | 0.12 | 33.40 | 86.60 |
| Warrenton | 1c | 14.27 | 0.06 | 1.02 | 0.37 | 23.83 | 0.21 | 0.23 | 14.52 | 0.10 | 0.13 | 0.01 | 0.04 | 0.00 | 0.0 | 0.0 | 0.12 | 34.20 | 89.11 |
| Warrenton | 1c | 14.30 | 0.06 | 1.18 | 0.38 | 24.68 | 0.19 | 1.39 | 14.55 | 0.07 | 0.07 | 0.01 | 0.06 | 0.01 | 0.0 | 0.0 | 0.04 | 34.84 | 91.83 |
| Warrenton | 1c | 15.08 | 0.08 | 1.53 | 0.24 | 22.99 | 0.19 | 0.05 | 14.04 | 0.19 | 0.62 | 0.10 | 0.05 | 0.01 | 0.0 | 0.0 | 0.04 | 35.05 | 90.27 |
| Warrenton | 1c | 12.89 | 0.06 | 1.00 | 0.36 | 21.94 | 0.17 | 0.06 | 13.36 | 0.07 | 0.05 | 0.00 | 0.08 | 0.00 | 0.0 | 0.0 | 0.29 | 31.50 | 81.84 |
| Warrenton | 1c | 9.61 | 0.07 | 1.24 | 1.22 | 30.56 | 0.16 | 0.17 | 10.08 | 0.78 | 0.11 | 0.00 | 0.43 | 0.00 | 0.0 | 0.0 | 5.99 | 38.02 | 98.44 |
| Warrenton | 1c | 12.10 | 0.07 | 1.08 | 0.54 | 27.01 | 0.16 | 0.19 | 12.53 | 0.49 | 0.13 | 0.03 | 0.26 | 0.00 | 0.0 | 0.0 | 3.06 | 36.28 | 93.93 |
| Warrenton | 1c | 15.12 | 0.04 | 1.65 | 0.22 | 23.68 | 0.20 | 0.66 | 13.80 | 0.31 | 0.69 | 0.02 | 0.04 | 0.00 | 0.0 | 0.0 | 0.03 | 35.40 | 91.87 |
| Warrenton | 1c | 14.00 | 0.05 | 0.89 | 0.32 | 22.33 | 0.19 | 0.03 | 13.00 | 0.08 | 0.07 | 0.00 | 0.05 | 0.00 | 0.0 | 0.0 | 0.08 | 32.17 | 83.25 |
| Warrenton | 1c | 13.21 | 0.04 | 0.88 | 0.29 | 21.18 | 0.17 | 0.09 | 12.88 | 0.06 | 0.04 | 0.00 | 0.06 | 0.00 | 0.0 | 0.0 | 0.04 | 30.79 | 79.73 |
| Warrenton | 1c | 13.66 | 0.06 | 0.70 | 0.26 | 21.83 | 0.17 | 0.12 | 12.89 | 0.08 | 0.05 | 0.00 | 0.06 | -0.00 | 0.0 | 0.0 | 0.06 | 31.38 | 81.31 |
| Warrenton | 1c | 8.94 | 0.02 | 0.43 | 0.36 | 35.63 | 0.14 | 3.98 | 8.66 | 0.35 | 0.07 | 0.00 | 0.18 | 0.02 | 0.0 | 0.0 | 8.03 | 40.22 | 107.04 |
| Warrenton | 1c | 13.25 | 0.05 | 1.21 | 0.33 | 21.25 | 0.17 | 0.10 | 12.99 | 0.07 | 0.06 | 0.02 | 0.07 | 0.00 | 0.0 | 0.0 | 0.04 | 31.26 | 80.86 |
| Warrenton | 1c | 13.22 | 0.04 | 1.11 | 0.32 | 22.10 | 0.18 | 1.19 | 13.00 | 0.09 | 0.04 | 0.00 | 0.07 | 0.01 | 0.0 | 0.0 | 0.05 | 31.71 | 83.14 |
| Warrenton | 1c | 13.28 | 0.06 | 1.26 | 0.37 | 22.23 | 0.18 | 0.40 | 13.15 | 0.08 | 0.04 | 0.00 | 0.06 | 0.00 | 0.0 | 0.0 | 0.13 | 31.97 | 83.22 |
| Warrenton | 2a | 13.35 | 0.06 | 1.57 | 0.56 | 23.06 | 0.18 | 1.71 | 12.98 | 0.10 | 0.26 | 0.00 | 0.04 | 0.00 | 0.0 | 0.0 | 0.06 | 32.85 | 86.80 |
| Warrenton | 2a | 14.30 | 0.06 | 1.16 | 0.36 | 22.89 | 0.19 | 0.07 | 13.53 | 0.10 | 0.26 | 0.01 | 0.05 | 0.00 | 0.0 | 0.0 | 0.05 | 33.34 | 86.36 |
| Warrenton | 2a | 13.32 | 0.07 | 1.59 | 0.57 | 23.35 | 0.19 | 2.08 | 13.08 | 0.10 | 0.25 | 0.01 | 0.05 | 0.01 | 0.0 | 0.0 | 0.08 | 33.14 | 87.90 |
| Warrenton | 2a | 14.02 | 0.06 | 1.36 | 0.38 | 22.26 | 0.19 | 0.03 | 13.19 | 0.12 | 0.31 | 0.02 | 0.06 | 0.00 | 0.0 | 0.0 | 0.06 | 32.86 | 84.92 |

Continued on next page

| Sample | Area | Si | Ti | Al | Cr | Fe | Mn | Ni | Mg | Ca | Na | K | P | Co | V | Zn | S | O | Total |
|---|---|---|---|---|---|---|---|---|---|---|---|---|---|---|---|---|---|---|---|
| Warrenton | 2a | 14.29 | 0.06 | 1.07 | 0.30 | 22.38 | 0.18 | 0.04 | 13.59 | 0.15 | 0.29 | 0.04 | 0.04 | 0.00 | 0.0 | 0.0 | 0.07 | 33.17 | 85.68 |
| Warrenton | 2a | 11.21 | 0.06 | 1.02 | 0.69 | 29.17 | 0.17 | 0.64 | 11.39 | 0.44 | 0.13 | 0.02 | 0.33 | 0.00 | 0.0 | 0.0 | 4.94 | 38.16 | 98.38 |
| Warrenton | 2a | 11.46 | 0.06 | 0.76 | 0.45 | 27.92 | 0.16 | 0.58 | 12.00 | 0.67 | 0.11 | 0.00 | 0.54 | 0.01 | 0.0 | 0.0 | 4.19 | 37.36 | 96.27 |
| Warrenton | 2a | 12.55 | 0.06 | 0.51 | 0.37 | 25.14 | 0.17 | 0.32 | 11.67 | 0.39 | 0.08 | 0.00 | 0.06 | 0.05 | 0.0 | 0.0 | 1.49 | 32.48 | 85.33 |
| Warrenton | 2a | 14.51 | 0.05 | 0.97 | 0.52 | 22.97 | 0.18 | 0.03 | 13.89 | 0.18 | 0.06 | 0.02 | 0.04 | 0.00 | 0.0 | 0.0 | 0.07 | 33.72 | 87.23 |
| Warrenton | 2a | 14.09 | 0.03 | 0.87 | 0.53 | 23.58 | 0.18 | 0.82 | 13.89 | 0.17 | 0.07 | 0.01 | 0.02 | 0.00 | 0.0 | 0.0 | 0.05 | 33.47 | 87.78 |
| Warrenton | 2a | 14.13 | 0.06 | 1.63 | 0.46 | 21.97 | 0.18 | 0.03 | 13.24 | 0.19 | 0.56 | 0.07 | 0.06 | 0.00 | 0.0 | 0.0 | 0.19 | 33.51 | 86.27 |
| Warrenton | 2a | 13.49 | 0.07 | 1.60 | 0.57 | 22.55 | 0.19 | 0.43 | 13.15 | 0.12 | 0.32 | 0.02 | 0.04 | 0.00 | 0.0 | 0.0 | 0.33 | 33.10 | 85.98 |
| Warrenton | 2a | 13.60 | 0.06 | 1.34 | 0.45 | 22.04 | 0.18 | 0.30 | 13.33 | 0.15 | 0.28 | 0.03 | 0.04 | 0.00 | 0.0 | 0.0 | 0.12 | 32.56 | 84.50 |
| Warrenton | 2a | 14.18 | 0.07 | 1.76 | 0.29 | 20.62 | 0.17 | 0.01 | 12.70 | 0.23 | 0.79 | 0.12 | 0.08 | 0.00 | 0.0 | 0.0 | 0.05 | 32.80 | 83.88 |
| Warrenton | 2a | 13.94 | 0.06 | 1.51 | 0.27 | 21.00 | 0.17 | 0.03 | 13.13 | 0.18 | 0.59 | 0.09 | 0.06 | 0.00 | 0.0 | 0.0 | 0.07 | 32.58 | 83.69 |
| Warrenton | 2a | 13.69 | 0.06 | 1.76 | 0.31 | 20.99 | 0.18 | 0.52 | 12.41 | 0.22 | 0.66 | 0.09 | 0.06 | 0.00 | 0.0 | 0.0 | 0.09 | 32.27 | 83.31 |
| Warrenton | 2a | 13.68 | 0.07 | 1.25 | 0.38 | 21.75 | 0.18 | 0.07 | 13.55 | 0.17 | 0.16 | 0.02 | 0.05 | 0.00 | 0.0 | 0.0 | 0.08 | 32.46 | 83.87 |
| Warrenton | 2a | 13.23 | 0.06 | 1.44 | 0.48 | 21.79 | 0.18 | 0.15 | 13.59 | 0.13 | 0.06 | 0.01 | 0.06 | 0.00 | 0.0 | 0.0 | 0.07 | 32.16 | 83.42 |
| Warrenton | 2a | 10.87 | 0.04 | 0.89 | 0.31 | 17.55 | 0.14 | 0.02 | 11.02 | 0.17 | 0.04 | 0.01 | 0.05 | 0.00 | 0.0 | 0.0 | 0.09 | 25.95 | 67.14 |
| Warrenton | 2a | 12.61 | 0.05 | 1.13 | 0.37 | 20.25 | 0.19 | 0.10 | 12.68 | 0.07 | 0.06 | 0.00 | 0.05 | 0.00 | 0.0 | 0.0 | 0.11 | 30.08 | 77.74 |
| Warrenton | 2a | 11.97 | 0.06 | 0.92 | 0.28 | 19.19 | 0.16 | 0.02 | 11.97 | 0.09 | 0.30 | 0.01 | 0.07 | 0.00 | 0.0 | 0.0 | 0.07 | 28.39 | 73.50 |
| Warrenton | 2a | 12.01 | 0.06 | 0.90 | 0.28 | 19.04 | 0.16 | 0.12 | 12.04 | 0.09 | 0.23 | 0.03 | 0.07 | 0.01 | 0.0 | 0.0 | 0.07 | 28.45 | 73.57 |
| Warrenton | 2a | 13.36 | 0.04 | 1.06 | 0.37 | 17.78 | 0.15 | 0.02 | 12.06 | 2.07 | 0.05 | 0.00 | 0.10 | 0.00 | 0.0 | 0.0 | 0.20 | 30.71 | 77.97 |
| Warrenton | 2a | 12.21 | 0.04 | 1.16 | 0.33 | 19.05 | 0.15 | 0.29 | 11.45 | 0.28 | 0.04 | 0.00 | 0.06 | 0.00 | 0.0 | 0.0 | 0.07 | 28.54 | 73.65 |
| Warrenton | 2a | 12.37 | 0.04 | 1.11 | 0.32 | 19.50 | 0.17 | 0.22 | 11.93 | 0.08 | 0.04 | 0.00 | 0.07 | 0.00 | 0.0 | 0.0 | 0.06 | 29.03 | 74.95 |
| Warrenton | 2a | 12.10 | 0.04 | 1.04 | 0.30 | 19.00 | 0.15 | 0.16 | 11.92 | 0.10 | 0.05 | 0.01 | 0.07 | 0.00 | 0.0 | 0.0 | 0.05 | 28.48 | 73.48 |
| Warrenton | 2a | 12.14 | 0.05 | 1.06 | 0.33 | 19.03 | 0.14 | 0.03 | 11.81 | 0.06 | 0.05 | 0.00 | 0.06 | 0.00 | 0.0 | 0.0 | 0.07 | 28.46 | 73.31 |
| Warrenton | 2a | 11.97 | 0.06 | 1.01 | 0.39 | 19.54 | 0.15 | 0.11 | 12.16 | 0.08 | 0.05 | 0.00 | 0.07 | 0.00 | 0.0 | 0.0 | 0.07 | 28.68 | 74.34 |
| Warrenton | 2a | 12.83 | 0.06 | 0.81 | 0.30 | 20.07 | 0.18 | 0.02 | 12.34 | 0.09 | 0.15 | 0.02 | 0.06 | 0.00 | 0.0 | 0.0 | 0.06 | 29.71 | 76.70 |
| Warrenton | 2a | 12.67 | 0.06 | 1.05 | 0.32 | 21.55 | 0.17 | 1.73 | 12.48 | 0.10 | 0.21 | 0.02 | 0.05 | 0.01 | 0.0 | 0.0 | 0.07 | 30.76 | 81.25 |
| Warrenton | 2a | 12.40 | 0.05 | 0.89 | 0.41 | 20.49 | 0.17 | 0.03 | 12.54 | 0.07 | 0.04 | 0.00 | 0.06 | 0.00 | 0.0 | 0.0 | 0.26 | 29.84 | 77.26 |
| Warrenton | 2a | 12.80 | 0.05 | 1.17 | 0.38 | 20.44 | 0.15 | 0.20 | 12.46 | 0.10 | 0.22 | 0.03 | 0.07 | 0.00 | 0.0 | 0.0 | 0.13 | 30.40 | 78.60 |
| Warrenton | 2a | 11.29 | 0.06 | 1.27 | 0.51 | 19.09 | 0.16 | 0.92 | 11.53 | 0.47 | 0.07 | 0.01 | 0.43 | 0.01 | 0.0 | 0.0 | 0.07 | 28.48 | 74.35 |
| Warrenton | 2a | 11.88 | 0.06 | 1.18 | 0.30 | 19.00 | 0.17 | 0.99 | 11.47 | 0.33 | 0.05 | 0.00 | 0.05 | 0.01 | 0.0 | 0.0 | 0.05 | 28.37 | 73.91 |
| Warrenton | 2a | 12.41 | 0.05 | 1.15 | 0.31 | 19.20 | 0.16 | 0.03 | 11.72 | 0.09 | 0.06 | 0.00 | 0.08 | 0.00 | 0.0 | 0.0 | 0.10 | 28.91 | 74.27 |
| Warrenton | 2a | 11.99 | 0.04 | 1.03 | 0.28 | 18.53 | 0.16 | 0.20 | 10.94 | 0.09 | 0.05 | 0.00 | 0.06 | 0.00 | 0.0 | 0.0 | 0.09 | 27.61 | 71.06 |
| Warrenton | 2a | 9.77 | 0.05 | 1.22 | 0.31 | 16.75 | 0.14 | 0.10 | 9.86 | 0.23 | 0.12 | 0.00 | 0.08 | 0.00 | 0.0 | 0.0 | 0.10 | 24.14 | 62.88 |
| Warrenton | 2a | 12.02 | 0.05 | 1.09 | 0.28 | 19.39 | 0.15 | 0.14 | 12.18 | 0.08 | 0.06 | 0.00 | 0.05 | 0.00 | 0.0 | 0.0 | 0.07 | 28.69 | 74.23 |
| Warrenton | 2a | 11.30 | 0.05 | 1.27 | 0.28 | 20.47 | 0.14 | 0.80 | 10.75 | 0.10 | 0.09 | 0.02 | 0.07 | 0.01 | 0.0 | 0.0 | 1.19 | 29.32 | 75.87 |
| Warrenton | 2a | 11.72 | 0.05 | 1.09 | 0.29 | 18.92 | 0.14 | 0.39 | 11.14 | 0.07 | 0.05 | 0.01 | 0.06 | 0.00 | 0.0 | 0.0 | 0.15 | 27.74 | 71.83 |
| Warrenton | 2a | 11.44 | 0.04 | 0.97 | 0.28 | 18.26 | 0.15 | 0.47 | 10.99 | 0.07 | 0.06 | 0.01 | 0.06 | 0.01 | 0.0 | 0.0 | 0.09 | 26.95 | 69.84 |
| Warrenton | 2a | 11.54 | 0.04 | 0.65 | 0.25 | 20.88 | 0.15 | 0.14 | 12.57 | 0.09 | 0.04 | 0.00 | 0.04 | 0.00 | 0.0 | 0.0 | 0.89 | 29.65 | 76.94 |
| Warrenton | 2a | 12.62 | 0.06 | 0.64 | 0.23 | 20.11 | 0.17 | 0.04 | 11.87 | 0.04 | 0.05 | 0.01 | 0.04 | 0.00 | 0.0 | 0.0 | 0.07 | 28.92 | 74.87 |
| Warrenton | 2a | 12.14 | 0.05 | 0.80 | 0.26 | 18.84 | 0.16 | 0.08 | 11.57 | 0.06 | 0.06 | 0.01 | 0.06 | 0.00 | 0.0 | 0.0 | 0.09 | 28.02 | 72.17 |
| Warrenton | 2a | 12.77 | 0.03 | 0.84 | 0.28 | 20.14 | 0.18 | 0.06 | 12.37 | 0.07 | 0.04 | 0.00 | 0.04 | 0.00 | 0.0 | 0.0 | 0.05 | 29.59 | 76.44 |
| Warrenton | 2a | 12.52 | 0.04 | 0.66 | 0.25 | 19.91 | 0.16 | 0.03 | 12.16 | 0.05 | 0.04 | 0.02 | 0.07 | 0.00 | 0.0 | 0.0 | 0.06 | 28.96 | 74.91 |
| Warrenton | 2a | 12.66 | 0.05 | 0.77 | 0.28 | 20.47 | 0.16 | 0.02 | 12.55 | 0.06 | 0.06 | 0.00 | 0.06 | 0.00 | 0.0 | 0.0 | 0.07 | 29.67 | 76.87 |
| Warrenton | 2a | 12.62 | 0.05 | 0.77 | 0.28 | 20.38 | 0.17 | 0.29 | 12.40 | 0.08 | 0.04 | 0.02 | 0.07 | 0.00 | 0.0 | 0.0 | 0.06 | 29.58 | 76.79 |
| Warrenton | 2a | 11.79 | 0.04 | 0.79 | 0.28 | 19.04 | 0.16 | 0.07 | 11.68 | 0.07 | 0.04 | 0.00 | 0.06 | 0.00 | 0.0 | 0.0 | 0.07 | 27.71 | 71.78 |
| Warrenton | 2a | 12.33 | 0.06 | 0.86 | 0.32 | 20.16 | 0.15 | 0.36 | 12.18 | 0.06 | 0.04 | 0.00 | 0.06 | 0.00 | 0.0 | 0.0 | 0.07 | 29.14 | 75.78 |
| Warrenton | 2a | 12.74 | 0.04 | 0.76 | 0.26 | 20.56 | 0.16 | 0.25 | 12.26 | 0.06 | 0.04 | 0.01 | 0.07 | 0.00 | 0.0 | 0.0 | 0.05 | 29.61 | 76.87 |
| Warrenton | 2a | 12.55 | 0.05 | 1.31 | 0.41 | 20.34 | 0.18 | 0.11 | 12.20 | 0.07 | 0.04 | 0.00 | 0.04 | 0.00 | 0.0 | 0.0 | 0.07 | 29.84 | 77.21 |
| Warrenton | 2a | 11.14 | 0.04 | 0.77 | 0.23 | 18.01 | 0.14 | 0.14 | 11.22 | 0.10 | 0.06 | 0.01 | 0.04 | 0.00 | 0.0 | 0.0 | 0.06 | 26.34 | 68.31 |
| Warrenton | 2b | 13.63 | 0.06 | 1.95 | 0.32 | 21.41 | 0.17 | 1.12 | 12.00 | 0.23 | 1.02 | 0.09 | 0.08 | 0.01 | 0.0 | 0.0 | 0.05 | 32.49 | 84.63 |
| Warrenton | 2b | 13.44 | 0.06 | 1.53 | 0.29 | 20.80 | 0.16 | 0.65 | 12.35 | 0.17 | 0.78 | 0.07 | 0.08 | 0.01 | 0.0 | 0.0 | 0.06 | 31.71 | 82.16 |
| Warrenton | 2b | 12.26 | 0.05 | 1.61 | 0.45 | 19.71 | 0.15 | 1.29 | 11.15 | 0.44 | 0.48 | 0.06 | 0.08 | 0.03 | 0.0 | 0.0 | 0.20 | 29.79 | 77.75 |
| Warrenton | 2b | 20.38 | 0.07 | 11.04 | 0.14 | 2.90 | 0.08 | 0.01 | 3.66 | 4.97 | 7.96 | 0.93 | 0.06 | 0.00 | 0.0 | 0.0 | 0.03 | 41.47 | 93.68 |
| Warrenton | 2b | 24.20 | 0.17 | 3.90 | 0.46 | 4.13 | 0.17 | 0.03 | 11.76 | 8.28 | 2.39 | 0.28 | 0.08 | 0.00 | 0.0 | 0.0 | 0.10 | 44.78 | 100.72 |
| Warrenton | 2b | 13.01 | 0.06 | 1.34 | 0.28 | 19.67 | 0.17 | 0.21 | 10.93 | 0.18 | 0.46 | 0.06 | 0.06 | 0.00 | 0.0 | 0.0 | 0.10 | 29.59 | 76.11 |
| Warrenton | 2b | 11.71 | 0.05 | 1.59 | 0.24 | 16.50 | 0.14 | 0.10 | 9.67 | 0.20 | 0.67 | 0.07 | 0.07 | 0.00 | 0.0 | 0.0 | 0.07 | 26.59 | 67.67 |
| Warrenton | 2b | 12.26 | 0.06 | 1.78 | 0.23 | 17.20 | 0.14 | 0.06 | 10.13 | 0.21 | 0.90 | 0.09 | 0.08 | 0.00 | 0.0 | 0.0 | 0.06 | 27.96 | 71.16 |
| Warrenton | 2b | 12.27 | 0.06 | 1.63 | 0.29 | 17.31 | 0.15 | 0.08 | 10.12 | 0.21 | 0.76 | 0.08 | 0.08 | 0.00 | 0.0 | 0.0 | 0.07 | 27.86 | 70.98 |

Continued on next page

| Sample | Area | Si | Ti | Al | Cr | Fe | Mn | Ni | Mg | Ca | Na | K | P | Co | V | Zn | S | O | Total |
|---|---|---|---|---|---|---|---|---|---|---|---|---|---|---|---|---|---|---|---|
| Warrenton | 2b | 19.95 | 0.02 | 11.27 | 0.03 | 5.76 | 0.05 | 0.03 | 3.71 | 3.61 | 8.61 | 1.01 | 0.07 | 0.00 | 0.0 | 0.0 | 0.06 | 41.73 | 95.91 |
| Warrenton | 2b | 24.39 | 0.06 | 1.91 | 0.30 | 8.61 | 0.09 | 0.00 | 16.85 | 2.68 | 1.29 | 0.16 | 0.02 | 0.00 | 0.0 | 0.0 | 0.03 | 44.87 | 101.27 |
| Warrenton | 2b | 14.74 | 0.07 | 2.75 | 0.15 | 17.77 | 0.15 | 0.03 | 9.52 | 0.49 | 2.13 | 0.27 | 0.06 | 0.00 | 0.0 | 0.0 | 0.30 | 32.29 | 80.71 |
| Warrenton | 2b | 12.36 | 0.06 | 2.03 | 0.33 | 17.09 | 0.12 | 0.29 | 9.93 | 0.23 | 0.88 | 0.12 | 0.05 | 0.00 | 0.0 | 0.0 | 0.07 | 28.22 | 71.78 |
| Warrenton | 2b | 12.99 | 0.05 | 2.15 | 0.27 | 18.52 | 0.15 | 0.50 | 11.22 | 0.24 | 0.78 | 0.10 | 0.06 | 0.01 | 0.0 | 0.0 | 0.06 | 30.30 | 77.40 |
| Warrenton | 2b | 13.05 | 0.06 | 2.63 | 0.26 | 17.33 | 0.14 | 0.07 | 10.42 | 0.39 | 1.23 | 0.13 | 0.10 | 0.00 | 0.0 | 0.0 | 0.07 | 30.09 | 75.97 |
| Warrenton | 2b | 12.73 | 0.06 | 1.97 | 0.25 | 17.61 | 0.14 | 0.02 | 10.84 | 0.22 | 0.96 | 0.11 | 0.06 | 0.00 | 0.0 | 0.0 | 0.07 | 29.26 | 74.30 |
| Warrenton | 2b | 13.29 | 0.07 | 2.30 | 0.35 | 16.05 | 0.14 | 0.09 | 9.82 | 0.96 | 1.06 | 0.15 | 0.06 | 0.00 | 0.0 | 0.0 | 0.09 | 29.52 | 73.95 |
| Warrenton | 2b | 13.58 | 0.07 | 2.37 | 0.36 | 18.98 | 0.14 | 0.14 | 11.39 | 0.28 | 1.20 | 0.12 | 0.08 | 0.00 | 0.0 | 0.0 | 0.08 | 31.58 | 80.36 |
| Warrenton | 2b | 13.47 | 0.07 | 2.30 | 0.29 | 18.65 | 0.17 | 0.05 | 11.15 | 0.29 | 1.17 | 0.14 | 0.08 | 0.00 | 0.0 | 0.0 | 0.07 | 31.08 | 78.98 |
| Warrenton | 2b | 12.85 | 0.07 | 2.61 | 0.25 | 17.48 | 0.15 | 0.02 | 10.92 | 0.34 | 1.27 | 0.16 | 0.08 | 0.00 | 0.0 | 0.0 | 0.06 | 30.17 | 76.42 |
| Warrenton | 2b | 15.76 | 0.13 | 4.40 | 0.55 | 13.36 | 0.21 | 0.09 | 9.29 | 3.11 | 2.40 | 0.30 | 0.08 | 0.00 | 0.0 | 0.0 | 0.03 | 34.52 | 84.23 |
| Warrenton | 2b | 14.24 | 0.08 | 2.10 | 0.32 | 20.33 | 0.17 | 0.09 | 12.44 | 0.25 | 0.91 | 0.13 | 0.08 | 0.00 | 0.0 | 0.0 | 0.05 | 33.00 | 84.19 |
| Warrenton | 2b | 14.16 | 0.08 | 2.80 | 0.35 | 19.80 | 0.15 | 0.54 | 11.85 | 0.32 | 1.55 | 0.17 | 0.08 | 0.00 | 0.0 | 0.0 | 0.08 | 33.43 | 85.37 |
| Warrenton | 2b | 13.80 | 0.06 | 1.82 | 0.29 | 20.97 | 0.19 | 0.06 | 12.99 | 0.18 | 0.64 | 0.05 | 0.06 | 0.00 | 0.0 | 0.0 | 0.06 | 32.63 | 83.81 |
| Warrenton | 2b | 13.22 | 0.06 | 1.56 | 0.49 | 22.86 | 0.18 | 0.52 | 13.16 | 0.15 | 0.07 | 0.01 | 0.14 | 0.00 | 0.0 | 0.0 | 0.47 | 33.09 | 85.98 |
| Warrenton | 2c | 13.08 | 0.06 | 1.24 | 0.35 | 19.75 | 0.15 | 0.42 | 12.73 | 0.11 | 0.22 | 0.02 | 0.09 | 0.00 | 0.0 | 0.0 | 0.06 | 30.73 | 79.00 |
| Warrenton | 2c | 13.76 | 0.05 | 0.99 | 0.28 | 20.72 | 0.17 | 0.04 | 13.44 | 0.28 | 0.17 | 0.04 | 0.23 | 0.00 | 0.0 | 0.0 | 0.05 | 32.11 | 82.32 |
| Warrenton | 2c | 13.85 | 0.05 | 0.95 | 0.37 | 20.63 | 0.16 | 0.11 | 13.74 | 0.24 | 0.09 | 0.00 | 0.08 | 0.00 | 0.0 | 0.0 | 0.10 | 32.24 | 82.62 |
| Warrenton | 2c | 14.22 | 0.06 | 0.97 | 0.32 | 22.29 | 0.18 | 0.60 | 14.24 | 0.08 | 0.13 | 0.01 | 0.09 | 0.00 | 0.0 | 0.0 | 0.05 | 33.49 | 86.73 |
| Warrenton | 2c | 14.45 | 0.06 | 0.64 | 0.29 | 19.87 | 0.15 | 0.04 | 14.34 | 0.53 | 0.08 | 0.01 | 0.09 | 0.00 | 0.0 | 0.0 | 0.13 | 32.94 | 83.62 |
| Warrenton | 2c | 13.39 | 0.06 | 0.83 | 0.34 | 20.92 | 0.17 | 0.11 | 13.68 | 0.07 | 0.05 | 0.01 | 0.10 | 0.00 | 0.0 | 0.0 | 0.11 | 31.61 | 81.46 |
| Warrenton | 2c | 14.24 | 0.06 | 0.57 | 0.29 | 18.89 | 0.15 | 0.03 | 15.00 | 0.18 | 0.06 | 0.01 | 0.08 | 0.00 | 0.0 | 0.0 | 0.09 | 32.59 | 82.25 |
| Warrenton | 2c | 12.58 | 0.05 | 0.76 | 0.34 | 19.60 | 0.15 | 0.33 | 12.84 | 0.09 | 0.05 | 0.01 | 0.09 | 0.00 | 0.0 | 0.0 | 0.07 | 29.68 | 76.64 |
| Warrenton | 2c | 13.02 | 0.05 | 0.68 | 0.27 | 20.32 | 0.16 | 0.44 | 13.24 | 0.07 | 0.04 | 0.01 | 0.08 | 0.01 | 0.0 | 0.0 | 0.05 | 30.52 | 78.96 |
| Warrenton | 2c | 13.41 | 0.06 | 0.74 | 0.29 | 20.56 | 0.17 | 0.05 | 13.52 | 0.08 | 0.05 | 0.00 | 0.10 | 0.00 | 0.0 | 0.0 | 0.06 | 31.22 | 80.30 |
| Warrenton | 2c | 13.82 | 0.04 | 0.79 | 0.25 | 21.30 | 0.17 | 0.32 | 13.91 | 0.09 | 0.04 | -0.00 | 0.04 | 0.00 | 0.0 | 0.0 | 0.04 | 32.15 | 82.96 |
| Warrenton | 2c | 11.85 | 0.04 | 0.96 | 0.25 | 18.76 | 0.16 | 0.37 | 13.27 | 0.19 | 0.05 | 0.00 | 0.06 | 0.00 | 0.0 | 0.0 | 0.06 | 29.02 | 75.05 |
| Warrenton | 2c | 12.35 | 0.05 | 1.35 | 0.32 | 19.36 | 0.15 | 0.58 | 13.20 | 0.10 | 0.15 | 0.01 | 0.09 | 0.00 | 0.0 | 0.0 | 0.07 | 30.19 | 77.95 |
| Warrenton | 2c | 12.79 | 0.04 | 0.98 | 0.28 | 19.63 | 0.15 | 0.10 | 12.84 | 0.10 | 0.05 | 0.02 | 0.09 | 0.00 | 0.0 | 0.0 | 0.06 | 29.99 | 77.10 |
| Warrenton | 2c | 13.13 | 0.05 | 0.99 | 0.28 | 20.31 | 0.16 | 0.36 | 13.55 | 0.09 | 0.05 | 0.01 | 0.09 | 0.00 | 0.0 | 0.0 | 0.05 | 31.13 | 80.25 |
| Warrenton | 2c | 13.28 | 0.06 | 1.09 | 0.29 | 20.49 | 0.17 | 0.12 | 13.76 | 0.10 | 0.06 | 0.01 | 0.08 | 0.00 | 0.0 | 0.0 | 0.05 | 31.52 | 81.09 |
| Warrenton | 2c | 13.36 | 0.06 | 1.09 | 0.28 | 20.52 | 0.16 | 0.14 | 13.72 | 0.09 | 0.05 | 0.00 | 0.07 | 0.00 | 0.0 | 0.0 | 0.05 | 31.56 | 81.15 |
| Warrenton | 2c | 14.46 | 0.05 | 0.81 | 0.21 | 22.10 | 0.18 | 0.15 | 14.32 | 0.13 | 0.10 | 0.04 | 0.04 | 0.00 | 0.0 | 0.0 | 0.03 | 33.38 | 86.01 |
| Warrenton | 2c | 12.60 | 0.04 | 1.26 | 0.40 | 19.78 | 0.15 | 0.16 | 12.95 | 0.11 | 0.04 | -0.00 | 0.06 | 0.00 | 0.0 | 0.0 | 0.05 | 30.18 | 77.77 |
| Warrenton | 2c | 12.67 | 0.05 | 1.24 | 0.38 | 19.80 | 0.17 | 0.16 | 13.04 | 0.10 | 0.05 | 0.00 | 0.06 | 0.00 | 0.0 | 0.0 | 0.06 | 30.31 | 78.09 |
| Warrenton | 2c | 13.54 | 0.07 | 0.78 | 0.23 | 21.20 | 0.17 | 0.17 | 13.46 | 0.09 | 0.07 | 0.00 | 0.08 | 0.00 | 0.0 | 0.0 | 0.07 | 31.56 | 81.48 |
| Warrenton | 2c | 11.55 | 0.05 | 0.90 | 0.18 | 17.12 | 0.14 | 0.05 | 11.00 | 0.11 | 0.23 | 0.04 | 0.07 | 0.00 | 0.0 | 0.0 | 0.07 | 26.61 | 68.11 |
| Warrenton | 2c | 11.66 | 0.04 | 0.76 | 0.20 | 16.91 | 0.14 | 0.02 | 10.06 | 0.11 | 0.18 | 0.02 | 0.06 | 0.00 | 0.0 | 0.0 | 0.06 | 25.88 | 66.11 |
| Warrenton | 2c | 12.01 | 0.05 | 1.09 | 0.24 | 17.15 | 0.13 | 0.06 | 10.07 | 0.16 | 0.35 | 0.03 | 0.08 | 0.00 | 0.0 | 0.0 | 0.07 | 26.79 | 68.28 |
| Warrenton | 2c | 11.30 | 0.05 | 1.03 | 0.29 | 16.95 | 0.13 | 0.56 | 9.89 | 0.10 | 0.09 | 0.00 | 0.06 | 0.00 | 0.0 | 0.0 | 0.09 | 25.80 | 66.34 |
| Warrenton | 2c | 11.80 | 0.05 | 1.06 | 0.30 | 19.08 | 0.13 | 1.81 | 11.16 | 0.09 | 0.14 | 0.00 | 0.07 | 0.02 | 0.0 | 0.0 | 0.06 | 28.18 | 73.96 |
| Warrenton | 2c | 12.80 | 0.06 | 1.16 | 0.23 | 18.35 | 0.14 | 0.03 | 11.29 | 0.12 | 0.36 | 0.04 | 0.08 | 0.00 | 0.0 | 0.0 | 0.06 | 28.88 | 73.60 |
| Warrenton | 2c | 13.91 | 0.07 | 0.64 | 0.22 | 20.97 | 0.18 | 0.27 | 12.72 | 0.12 | 0.06 | 0.04 | 0.06 | 0.00 | 0.0 | 0.0 | 0.05 | 31.30 | 80.61 |
| Warrenton | 2c | 13.84 | 0.07 | 1.13 | 0.30 | 20.27 | 0.16 | 0.19 | 11.82 | 0.12 | 0.33 | 0.02 | 0.07 | 0.00 | 0.0 | 0.0 | 0.07 | 31.01 | 79.42 |
| Warrenton | 2c | 14.60 | 0.06 | 0.84 | 0.33 | 22.40 | 0.20 | 0.38 | 13.47 | 0.07 | 0.05 | 0.00 | 0.06 | 0.00 | 0.0 | 0.0 | 0.04 | 33.20 | 85.69 |
| Warrenton | 2c | 12.70 | 0.05 | 0.90 | 0.28 | 19.89 | 0.15 | 0.32 | 13.80 | 0.10 | 0.04 | 0.00 | 0.09 | 0.01 | 0.0 | 0.0 | 0.06 | 30.61 | 79.01 |
| Warrenton | 2c | 16.31 | 0.07 | 0.94 | 0.36 | 25.38 | 0.23 | 0.55 | 15.59 | 0.10 | 0.05 | 0.01 | 0.08 | 0.00 | 0.0 | 0.0 | 0.13 | 37.75 | 97.56 |
| Warrenton | 2c | 15.81 | 0.07 | 0.84 | 0.55 | 25.96 | 0.19 | 1.96 | 15.47 | 0.17 | 0.05 | 0.02 | 0.08 | 0.02 | 0.0 | 0.0 | 0.06 | 37.56 | 98.81 |
| Warrenton | 2c | 14.62 | 0.05 | 0.62 | 0.32 | 22.00 | 0.18 | 0.36 | 12.33 | 0.24 | 0.06 | 0.00 | 0.12 | 0.00 | 0.0 | 0.0 | 0.14 | 32.43 | 83.45 |
| Warrenton | 2c | 14.59 | 0.05 | 0.62 | 0.31 | 24.33 | 0.20 | 0.59 | 14.09 | 0.32 | 0.09 | 0.00 | 0.16 | 0.03 | 0.0 | 0.0 | 0.06 | 34.27 | 89.69 |
| Warrenton | 2c | 15.08 | 0.07 | 0.68 | 0.26 | 22.89 | 0.18 | 0.02 | 14.46 | 0.11 | 0.17 | 0.01 | 0.07 | 0.00 | 0.0 | 0.0 | 0.06 | 34.38 | 88.44 |
| Warrenton | 2c | 13.25 | 0.07 | 1.05 | 0.50 | 21.72 | 0.19 | 0.46 | 13.62 | 0.24 | 0.07 | 0.00 | 0.06 | 0.00 | 0.0 | 0.0 | 0.07 | 31.98 | 83.28 |
| Warrenton | 2c | 12.95 | 0.05 | 1.01 | 0.39 | 23.51 | 0.17 | 3.05 | 12.80 | 0.08 | 0.04 | 0.01 | 0.05 | 0.03 | 0.0 | 0.0 | 0.17 | 32.28 | 86.60 |
| Warrenton | 2c | 13.81 | 0.05 | 1.00 | 0.32 | 21.61 | 0.18 | 0.04 | 13.51 | 0.08 | 0.11 | 0.01 | 0.07 | 0.00 | 0.0 | 0.0 | 0.06 | 32.20 | 83.05 |
| Warrenton | 2c | 14.27 | 0.07 | 0.82 | 0.53 | 22.36 | 0.18 | 0.15 | 13.62 | 0.25 | 0.06 | 0.00 | 0.06 | 0.01 | 0.0 | 0.0 | 0.15 | 33.15 | 85.65 |
| Warrenton | 2c | 13.82 | 0.06 | 1.06 | 0.31 | 22.39 | 0.17 | 0.49 | 13.70 | 0.29 | 0.29 | 0.01 | 0.12 | 0.00 | 0.0 | 0.0 | 0.22 | 33.19 | 86.12 |
| Warrenton | 2c | 14.86 | 0.07 | 0.55 | 0.31 | 23.36 | 0.19 | 0.04 | 14.32 | 0.07 | 0.04 | 0.00 | 0.05 | 0.00 | 0.0 | 0.0 | 0.05 | 33.99 | 87.91 |

Continued on next page

| Sample | Area | Si | Ti | Al | Cr | Fe | Mn | Ni | Mg | Ca | Na | K | P | Co | V | Zn | S | O | Total |
|---|---|---|---|---|---|---|---|---|---|---|---|---|---|---|---|---|---|---|---|
| Warrenton | 2c | 13.91 | 0.07 | 0.99 | 0.42 | 21.88 | 0.17 | 0.06 | 13.85 | 0.09 | 0.06 | 0.00 | 0.08 | 0.00 | 0.0 | 0.0 | 0.05 | 32.66 | 84.31 |
| Warrenton | 2c | 14.11 | 0.08 | 1.16 | 0.33 | 21.57 | 0.18 | 0.15 | 13.47 | 0.13 | 0.38 | 0.05 | 0.07 | 0.01 | 0.0 | 0.0 | 0.06 | 32.81 | 84.54 |
| Warrenton | 2c | 9.48 | 0.03 | 0.37 | 0.20 | 37.19 | 0.14 | 0.16 | 10.21 | 0.05 | 0.05 | 0.00 | 0.03 | 0.03 | 0.0 | 0.0 | 9.33 | 42.76 | 110.03 |
| Warrenton | 2c | 13.52 | 0.04 | 0.96 | 0.41 | 25.03 | 0.19 | 1.66 | 13.99 | 0.06 | 0.04 | 0.01 | 0.03 | 0.01 | 0.0 | 0.0 | 1.06 | 35.04 | 92.06 |
| Warrenton | 2c | 13.71 | 0.06 | 1.09 | 0.36 | 21.20 | 0.16 | 0.07 | 13.99 | 0.12 | 0.05 | 0.00 | 0.09 | 0.00 | 0.0 | 0.0 | 0.05 | 32.41 | 83.37 |
| Warrenton | 2c | 13.71 | 0.06 | 1.09 | 0.37 | 21.43 | 0.18 | 0.07 | 13.95 | 0.14 | 0.05 | -0.00 | 0.10 | 0.00 | 0.0 | 0.0 | 0.05 | 32.46 | 83.65 |
| Warrenton | 2c | 12.95 | 0.05 | 1.50 | 0.42 | 22.27 | 0.17 | 1.98 | 13.87 | 0.07 | 0.05 | 0.01 | 0.09 | 0.03 | 0.0 | 0.0 | 0.04 | 32.64 | 86.11 |
| Warrenton | 2c | 13.00 | 0.06 | 2.44 | 0.55 | 22.58 | 0.16 | 1.72 | 13.82 | 0.14 | 0.07 | 0.01 | 0.11 | 0.01 | 0.0 | 0.0 | 0.06 | 33.68 | 88.41 |
| Warrenton | 2c | 13.74 | 0.05 | 1.55 | 0.36 | 22.16 | 0.17 | 0.71 | 14.08 | 0.09 | 0.16 | -0.00 | 0.09 | 0.01 | 0.0 | 0.0 | 0.04 | 33.38 | 86.60 |
| Warrenton | 2c | 13.69 | 0.06 | 1.12 | 0.25 | 20.86 | 0.17 | 0.07 | 14.01 | 0.09 | 0.08 | 0.01 | 0.09 | 0.00 | 0.0 | 0.0 | 0.05 | 32.26 | 82.80 |
| Warrenton | 2c | 14.28 | 0.04 | 1.08 | 0.28 | 21.59 | 0.17 | 0.20 | 14.30 | 0.10 | 0.17 | 0.01 | 0.07 | 0.00 | 0.0 | 0.0 | 0.04 | 33.35 | 85.69 |
| Warrenton | 2c | 14.26 | 0.05 | 1.08 | 0.27 | 21.61 | 0.18 | 0.03 | 14.33 | 0.10 | 0.12 | 0.02 | 0.08 | 0.00 | 0.0 | 0.0 | 0.04 | 33.30 | 85.47 |
| Warrenton | 2c | 13.77 | 0.05 | 1.09 | 0.26 | 21.51 | 0.17 | 0.17 | 14.13 | 0.10 | 0.05 | 0.02 | 0.10 | 0.00 | 0.0 | 0.0 | 0.05 | 32.65 | 84.14 |
| Warrenton | 2c | 13.11 | 0.05 | 0.71 | 0.22 | 20.08 | 0.16 | 0.01 | 13.16 | 0.08 | 0.03 | 0.01 | 0.08 | 0.00 | 0.0 | 0.0 | 0.05 | 30.38 | 78.13 |
| Warrenton | 2c | 14.50 | 0.06 | 0.68 | 0.27 | 22.84 | 0.18 | 0.03 | 14.73 | 0.08 | 0.05 | 0.00 | 0.07 | 0.00 | 0.0 | 0.0 | 0.04 | 33.79 | 87.32 |
| Warrenton | 2c | 14.76 | 0.04 | 0.77 | 0.30 | 23.25 | 0.19 | 0.05 | 14.94 | 0.08 | 0.06 | 0.00 | 0.07 | 0.00 | 0.0 | 0.0 | 0.04 | 34.42 | 88.97 |
| Warrenton | 3a | 12.74 | 0.05 | 1.26 | 0.36 | 21.25 | 0.15 | 0.08 | 13.03 | 0.13 | 0.34 | 0.03 | 0.05 | 0.00 | 0.0 | 0.0 | 0.08 | 30.93 | 80.50 |
| Warrenton | 3a | 14.12 | 0.06 | 0.67 | 0.29 | 23.08 | 0.20 | 0.11 | 13.98 | 0.08 | 0.04 | 0.01 | 0.06 | 0.00 | 0.0 | 0.0 | 0.03 | 32.94 | 85.67 |
| Warrenton | 3a | 14.39 | 0.07 | 0.49 | 0.26 | 23.39 | 0.19 | 0.10 | 14.50 | 0.09 | 0.07 | 0.01 | 0.07 | 0.00 | 0.0 | 0.0 | 0.03 | 33.53 | 87.19 |
| Warrenton | 3a | 13.13 | 0.07 | 0.80 | 1.90 | 22.93 | 0.19 | 0.48 | 13.74 | 0.90 | 0.06 | -0.00 | 0.29 | 0.01 | 0.0 | 0.0 | 0.18 | 33.42 | 88.09 |
| Warrenton | 3a | 14.26 | 0.06 | 0.32 | 0.34 | 21.98 | 0.20 | 0.08 | 13.95 | 0.40 | 0.06 | 0.00 | 0.10 | 0.00 | 0.0 | 0.0 | 0.09 | 32.72 | 84.55 |
| Warrenton | 3a | 13.51 | 0.06 | 1.56 | 0.54 | 22.43 | 0.19 | 1.20 | 13.51 | 0.42 | 0.43 | 0.05 | 0.07 | 0.02 | 0.0 | 0.0 | 0.04 | 33.24 | 87.25 |
| Warrenton | 3a | 14.03 | 0.07 | 0.78 | 0.34 | 22.97 | 0.20 | 0.02 | 14.09 | 0.07 | 0.06 | 0.01 | 0.06 | 0.00 | 0.0 | 0.0 | 0.04 | 32.99 | 85.73 |
| Warrenton | 3a | 14.28 | 0.07 | 0.76 | 0.35 | 23.22 | 0.21 | 0.03 | 14.21 | 0.07 | 0.06 | -0.00 | 0.04 | 0.00 | 0.0 | 0.0 | 0.04 | 33.39 | 86.72 |
| Warrenton | 3a | 14.66 | 0.04 | 3.52 | 0.61 | 14.83 | 0.19 | 0.02 | 9.72 | 2.86 | 1.83 | 0.22 | 0.09 | 0.00 | 0.0 | 0.0 | 0.03 | 32.84 | 81.48 |
| Warrenton | 3a | 12.57 | 0.08 | 2.87 | 0.43 | 20.02 | 0.17 | 0.33 | 11.99 | 0.25 | 0.89 | 0.07 | 0.06 | 0.00 | 0.0 | 0.0 | 0.05 | 31.47 | 81.25 |
| Warrenton | 3a | 12.77 | 0.08 | 3.13 | 0.38 | 18.72 | 0.14 | 0.29 | 11.04 | 0.35 | 1.53 | 0.15 | 0.07 | 0.00 | 0.0 | 0.0 | 0.16 | 31.36 | 80.18 |
| Warrenton | 3a | 12.25 | 0.08 | 1.51 | 0.38 | 21.31 | 0.16 | 1.87 | 12.46 | 0.14 | 0.38 | 0.05 | 0.05 | 0.02 | 0.0 | 0.0 | 0.05 | 30.75 | 81.47 |
| Warrenton | 3a | 13.47 | 0.07 | 1.49 | 0.56 | 21.77 | 0.17 | 0.07 | 13.08 | 0.21 | 0.52 | 0.04 | 0.06 | 0.00 | 0.0 | 0.0 | 0.04 | 32.29 | 83.83 |
| Warrenton | 3a | 13.38 | 0.07 | 2.47 | 0.47 | 18.14 | 0.14 | 0.12 | 11.02 | 1.31 | 0.95 | 0.11 | 0.04 | 0.00 | 0.0 | 0.0 | 0.04 | 31.22 | 79.49 |
| Warrenton | 3a | 12.59 | 0.08 | 4.04 | 0.48 | 19.01 | 0.14 | 0.68 | 11.35 | 0.44 | 1.39 | 0.16 | 0.07 | 0.01 | 0.0 | 0.0 | 0.04 | 32.20 | 82.68 |
| Warrenton | 3a | 13.60 | 0.08 | 0.97 | 0.27 | 21.89 | 0.16 | 0.05 | 13.47 | 0.16 | 0.35 | 0.02 | 0.07 | 0.00 | 0.0 | 0.0 | 0.03 | 32.05 | 83.16 |
| Warrenton | 3a | 12.39 | 0.09 | 1.20 | 0.37 | 22.33 | 0.17 | 0.25 | 13.04 | 0.07 | 0.06 | 0.00 | 0.07 | 0.00 | 0.0 | 0.0 | 0.58 | 31.52 | 82.16 |
| Warrenton | 3a | 13.15 | 0.07 | 1.60 | 0.31 | 21.37 | 0.16 | 0.08 | 13.48 | 0.17 | 0.34 | 0.02 | 0.07 | 0.00 | 0.0 | 0.0 | 0.03 | 32.00 | 82.88 |
| Warrenton | 3a | 13.15 | 0.06 | 0.84 | 0.45 | 22.00 | 0.17 | 0.17 | 12.97 | 0.05 | 0.04 | 0.00 | 0.06 | 0.00 | 0.0 | 0.0 | 0.03 | 31.08 | 81.08 |
| Warrenton | 3a | 13.94 | 0.14 | 5.79 | 0.31 | 16.33 | 0.12 | 0.02 | 9.97 | 1.19 | 2.83 | 0.28 | 0.07 | 0.00 | 0.0 | 0.0 | 0.03 | 34.19 | 85.19 |
| Warrenton | 3a | 12.76 | 0.09 | 1.12 | 0.28 | 22.02 | 0.16 | 0.69 | 13.33 | 0.08 | 0.10 | 0.01 | 0.05 | 0.02 | 0.0 | 0.0 | 0.03 | 31.23 | 81.96 |
| Warrenton | 3a | 13.21 | 0.10 | 2.59 | 0.25 | 20.45 | 0.16 | 0.08 | 11.84 | 0.24 | 1.32 | 0.11 | 0.06 | 0.00 | 0.0 | 0.0 | 0.29 | 32.36 | 83.08 |
| Warrenton | 3a | 12.68 | 0.10 | 1.57 | 0.34 | 21.18 | 0.16 | 0.27 | 12.34 | 0.08 | 0.17 | 0.00 | 0.06 | 0.00 | 0.0 | 0.0 | 0.09 | 30.68 | 79.71 |
| Warrenton | 3a | 11.80 | 0.09 | 1.66 | 0.33 | 19.94 | 0.16 | 0.20 | 12.17 | 0.09 | 0.07 | 0.00 | 0.07 | 0.00 | 0.0 | 0.0 | 0.04 | 29.17 | 75.79 |
| Warrenton | 3a | 12.32 | 0.09 | 1.68 | 0.33 | 20.46 | 0.17 | 0.03 | 12.64 | 0.17 | 0.07 | 0.00 | 0.12 | 0.00 | 0.0 | 0.0 | 0.03 | 30.27 | 78.39 |
| Warrenton | 3a | 12.47 | 0.09 | 2.02 | 0.26 | 19.76 | 0.17 | 0.43 | 11.74 | 0.17 | 0.60 | 0.05 | 0.08 | 0.00 | 0.0 | 0.0 | 0.05 | 30.21 | 78.11 |
| Warrenton | 3a | 12.44 | 0.09 | 1.54 | 0.32 | 21.19 | 0.18 | 0.78 | 12.58 | 0.33 | 0.32 | 0.01 | 0.19 | 0.00 | 0.0 | 0.0 | 0.04 | 30.91 | 80.92 |
| Warrenton | 3a | 12.56 | 0.10 | 1.42 | 0.28 | 21.59 | 0.18 | 0.99 | 12.78 | 0.09 | 0.20 | 0.02 | 0.06 | 0.01 | 0.0 | 0.0 | 0.09 | 31.00 | 81.34 |
| Warrenton | 3a | 14.73 | 0.08 | 4.27 | 0.28 | 15.83 | 0.13 | 0.00 | 10.50 | 3.32 | 1.96 | 0.06 | 0.09 | 0.00 | 0.0 | 0.0 | 0.02 | 34.42 | 85.69 |
| Warrenton | 3a | 14.02 | 0.12 | 3.89 | 0.28 | 19.32 | 0.15 | 0.01 | 11.50 | 0.89 | 1.77 | 0.09 | 0.07 | 0.00 | 0.0 | 0.0 | 0.02 | 33.90 | 86.03 |
| Warrenton | 3a | 14.31 | 0.07 | 3.99 | 0.27 | 19.54 | 0.16 | 0.01 | 11.84 | 1.51 | 1.04 | 0.07 | 0.05 | 0.00 | 0.0 | 0.0 | 0.02 | 34.53 | 87.40 |
| Warrenton | 3a | 16.51 | 0.29 | 11.15 | 0.45 | 7.68 | 0.04 | 0.00 | 7.49 | 9.08 | 2.43 | 0.02 | 0.09 | 0.00 | 0.0 | 0.0 | 0.01 | 40.88 | 96.13 |
| Warrenton | 3a | 13.22 | 0.07 | 1.39 | 0.21 | 20.88 | 0.17 | 0.04 | 12.82 | 0.15 | 0.45 | 0.05 | 0.08 | 0.00 | 0.0 | 0.0 | 0.03 | 31.29 | 80.84 |
| Warrenton | 3a | 14.35 | 0.07 | 1.02 | 0.25 | 24.50 | 0.20 | 0.00 | 14.74 | 0.10 | 0.12 | 0.01 | 0.06 | 0.00 | 0.0 | 0.0 | 0.02 | 34.38 | 89.82 |
| Warrenton | 3a | 14.28 | 0.06 | 0.83 | 0.21 | 24.15 | 0.21 | 0.01 | 14.87 | 0.08 | 0.10 | 0.01 | 0.06 | 0.00 | 0.0 | 0.0 | 0.02 | 34.08 | 88.97 |
| Warrenton | 3a | 14.21 | 0.06 | 1.02 | 0.27 | 22.89 | 0.19 | 0.00 | 13.74 | 0.15 | 0.14 | 0.02 | 0.05 | 0.00 | 0.0 | 0.0 | 0.02 | 33.12 | 85.88 |
| Warrenton | 3b | 12.55 | 0.06 | 1.04 | 0.41 | 20.08 | 0.17 | 0.35 | 13.23 | 0.08 | 0.08 | 0.01 | 0.07 | 0.00 | 0.0 | 0.0 | 0.04 | 30.27 | 78.44 |
| Warrenton | 3b | 13.07 | 0.04 | 0.65 | 0.37 | 20.70 | 0.17 | 0.10 | 13.43 | 0.08 | 0.04 | 0.00 | 0.05 | 0.00 | 0.0 | 0.0 | 0.05 | 30.70 | 79.47 |
| Warrenton | 3b | 13.68 | 0.04 | 0.76 | 0.32 | 21.29 | 0.17 | 0.07 | 13.42 | 0.12 | 0.28 | 0.02 | 0.06 | 0.00 | 0.0 | 0.0 | 0.05 | 31.73 | 82.00 |
| Warrenton | 3b | 14.17 | 0.07 | 0.83 | 0.44 | 22.98 | 0.20 | 0.20 | 14.84 | 0.12 | 0.10 | 0.01 | 0.07 | 0.01 | 0.0 | 0.0 | 0.04 | 33.83 | 87.90 |
| Warrenton | 3b | 15.12 | 0.07 | 0.98 | 0.27 | 23.76 | 0.19 | 0.07 | 15.10 | 0.13 | 0.36 | 0.04 | 0.08 | 0.00 | 0.0 | 0.0 | 0.04 | 35.45 | 91.67 |
| Warrenton | 3b | 15.03 | 0.07 | 1.05 | 0.29 | 23.84 | 0.20 | 0.38 | 15.05 | 0.13 | 0.40 | 0.03 | 0.08 | 0.00 | 0.0 | 0.0 | 0.03 | 35.48 | 92.07 |

Continued on next page

| Sample | Area | Si | Ti | Al | Cr | Fe | Mn | Ni | Mg | Ca | Na | K | P | Co | V | Zn | S | O | Total |
|---|---|---|---|---|---|---|---|---|---|---|---|---|---|---|---|---|---|---|---|
| Warrenton | 3b | 14.42 | 0.06 | 0.78 | 0.39 | 24.11 | 0.19 | 1.03 | 15.04 | 0.14 | 0.11 | 0.02 | 0.09 | 0.00 | 0.0 | 0.0 | 0.05 | 34.78 | 91.22 |
| Warrenton | 3b | 14.80 | 0.06 | 1.19 | 0.36 | 23.70 | 0.20 | 0.45 | 14.90 | 0.13 | 0.30 | 0.04 | 0.10 | 0.01 | 0.0 | 0.0 | 0.03 | 35.25 | 91.52 |
| Warrenton | 3b | 14.79 | 0.08 | 1.22 | 0.26 | 22.83 | 0.20 | 0.09 | 14.62 | 0.19 | 0.45 | 0.05 | 0.10 | 0.00 | 0.0 | 0.0 | 0.04 | 34.77 | 89.66 |
| Warrenton | 3b | 14.76 | 0.07 | 1.57 | 0.30 | 23.16 | 0.18 | 0.21 | 14.56 | 0.20 | 0.53 | 0.08 | 0.08 | 0.00 | 0.0 | 0.0 | 0.09 | 35.24 | 91.02 |
| Warrenton | 3b | 14.29 | 0.05 | 0.86 | 0.37 | 24.42 | 0.20 | 0.03 | 14.85 | 0.07 | 0.03 | -0.00 | 0.06 | 0.00 | 0.0 | 0.0 | 0.67 | 35.19 | 91.08 |
| Warrenton | 3b | 14.36 | 0.07 | 1.22 | 0.28 | 22.91 | 0.19 | 0.71 | 14.49 | 0.15 | 0.36 | 0.04 | 0.08 | 0.01 | 0.0 | 0.0 | 0.03 | 34.33 | 89.25 |
| Warrenton | 3b | 14.65 | 0.06 | 1.38 | 0.33 | 23.41 | 0.20 | 0.24 | 14.58 | 0.18 | 0.35 | 0.04 | 0.08 | 0.00 | 0.0 | 0.0 | 0.04 | 34.90 | 90.43 |
| Warrenton | 3b | 14.04 | 0.05 | 0.99 | 0.34 | 23.37 | 0.19 | 0.04 | 14.79 | 0.09 | 0.05 | 0.00 | 0.06 | 0.00 | 0.0 | 0.0 | 0.02 | 33.72 | 87.76 |
| Warrenton | 3b | 14.83 | 0.05 | 0.96 | 0.29 | 24.44 | 0.19 | 0.60 | 15.09 | 0.10 | 0.12 | 0.01 | 0.08 | 0.00 | 0.0 | 0.0 | 0.04 | 35.31 | 92.11 |
| Warrenton | 3b | 14.78 | 0.06 | 1.17 | 0.25 | 23.18 | 0.20 | 0.20 | 14.56 | 0.16 | 0.39 | 0.03 | 0.08 | 0.00 | 0.0 | 0.0 | 0.04 | 34.75 | 89.85 |
| Warrenton | 3b | 14.41 | 0.06 | 0.94 | 0.47 | 23.94 | 0.18 | 0.20 | 14.76 | 0.09 | 0.07 | 0.01 | 0.10 | 0.00 | 0.0 | 0.0 | 0.20 | 34.68 | 90.12 |
| Warrenton | 3b | 14.47 | 0.06 | 1.27 | 0.38 | 23.23 | 0.20 | 0.18 | 14.55 | 0.12 | 0.27 | 0.00 | 0.09 | 0.01 | 0.0 | 0.0 | 0.05 | 34.50 | 89.37 |
| Warrenton | 3b | 14.24 | 0.05 | 1.08 | 0.36 | 23.09 | 0.19 | 0.09 | 14.53 | 0.08 | 0.07 | 0.01 | 0.07 | 0.00 | 0.0 | 0.0 | 0.03 | 33.85 | 87.75 |
| Warrenton | 3b | 13.94 | 0.07 | 1.44 | 0.32 | 21.30 | 0.18 | 0.06 | 13.53 | 0.18 | 0.53 | 0.07 | 0.10 | 0.00 | 0.0 | 0.0 | 0.05 | 32.91 | 84.69 |
| Warrenton | 3b | 14.21 | 0.06 | 1.62 | 0.27 | 21.15 | 0.16 | 0.03 | 13.50 | 0.21 | 0.75 | 0.09 | 0.09 | 0.00 | 0.0 | 0.0 | 0.03 | 33.32 | 85.49 |
| Warrenton | 3b | 13.24 | 0.06 | 1.00 | 0.37 | 23.96 | 0.16 | 0.86 | 13.49 | 0.46 | 0.04 | 0.01 | 0.08 | 0.01 | 0.0 | 0.0 | 0.87 | 33.81 | 88.42 |
| Warrenton | 3b | 14.01 | 0.06 | 1.21 | 0.41 | 23.17 | 0.17 | 0.56 | 14.47 | 0.16 | 0.06 | 0.00 | 0.10 | 0.00 | 0.0 | 0.0 | 0.02 | 33.89 | 88.31 |
| Warrenton | 3b | 15.98 | 0.08 | 0.60 | 0.47 | 23.80 | 0.42 | 0.04 | 14.49 | 1.67 | 0.10 | 0.01 | 0.04 | 0.01 | 0.0 | 0.0 | 0.66 | 37.25 | 95.63 |
| Warrenton | 3b | 13.47 | 0.07 | 0.54 | 0.43 | 28.62 | 0.20 | 0.02 | 13.39 | 0.25 | 0.06 | 0.01 | 0.05 | 0.00 | 0.0 | 0.0 | 3.18 | 38.10 | 98.38 |
| Warrenton | 3b | 13.40 | 0.06 | 0.67 | 0.78 | 25.91 | 0.20 | 0.03 | 13.70 | 0.61 | 0.08 | 0.01 | 0.09 | -0.00 | 0.0 | 0.0 | 2.03 | 36.20 | 93.76 |
| Warrenton | 3b | 13.72 | 0.06 | 1.01 | 1.09 | 25.16 | 0.20 | 0.12 | 14.52 | 0.27 | 0.09 | 0.01 | 0.08 | 0.00 | 0.0 | 0.0 | 0.90 | 35.53 | 92.76 |
| Warrenton | 3b | 13.88 | 0.05 | 0.92 | 0.48 | 22.95 | 0.19 | 0.49 | 13.78 | 0.66 | 0.09 | 0.00 | 0.07 | 0.00 | 0.0 | 0.0 | 0.38 | 33.66 | 87.58 |
| Warrenton | 3b | 13.77 | 0.06 | 1.07 | 0.32 | 21.97 | 0.18 | 0.02 | 13.89 | 0.12 | 0.23 | 0.03 | 0.06 | 0.00 | 0.0 | 0.0 | 0.04 | 32.59 | 84.34 |
| Warrenton | 3b | 13.86 | 0.05 | 1.14 | 0.35 | 22.15 | 0.19 | 0.03 | 14.07 | 0.08 | 0.17 | 0.02 | 0.04 | 0.00 | 0.0 | 0.0 | 0.03 | 32.88 | 85.07 |
| Warrenton | 3b | 14.87 | 0.06 | 1.12 | 0.44 | 22.29 | 0.19 | 0.02 | 14.22 | 0.75 | 0.24 | 0.02 | 0.08 | 0.00 | 0.0 | 0.0 | 0.06 | 34.57 | 88.93 |
| Warrenton | 3b | 15.11 | 0.05 | 0.86 | 0.73 | 21.01 | 0.18 | 0.05 | 13.27 | 2.34 | 0.08 | 0.01 | 0.17 | 0.00 | 0.0 | 0.0 | 0.38 | 34.92 | 89.16 |
| Warrenton | 3b | 12.77 | 0.05 | 0.59 | 0.34 | 24.83 | 0.15 | 1.24 | 13.51 | 0.13 | 0.10 | 0.02 | 0.06 | 0.01 | 0.0 | 0.0 | 1.34 | 33.83 | 88.99 |
| Warrenton | 3b | 13.18 | 0.06 | 1.07 | 0.36 | 20.48 | 0.16 | 0.08 | 13.03 | 0.12 | 0.27 | 0.03 | 0.08 | -0.00 | 0.0 | 0.0 | 0.04 | 30.98 | 79.91 |
| Warrenton | 3b | 13.44 | 0.07 | 1.52 | 0.34 | 19.72 | 0.17 | 0.04 | 12.19 | 0.19 | 0.78 | 0.10 | 0.08 | 0.00 | 0.0 | 0.0 | 0.04 | 31.11 | 79.76 |
| Warrenton | 3b | 11.72 | 0.05 | 1.63 | 0.50 | 19.22 | 0.14 | 0.93 | 11.76 | 0.15 | 0.40 | 0.05 | 0.06 | 0.02 | 0.0 | 0.0 | 0.07 | 29.02 | 75.74 |
| Warrenton | 3b | 13.48 | 0.04 | 0.61 | 0.24 | 21.47 | 0.19 | 0.03 | 13.81 | 0.04 | 0.03 | 0.00 | 0.04 | 0.00 | 0.0 | 0.0 | 0.04 | 31.47 | 81.49 |
| Warrenton | 3b | 13.51 | 0.05 | 0.72 | 0.27 | 21.71 | 0.16 | 0.01 | 14.12 | 0.05 | 0.04 | 0.01 | 0.05 | 0.01 | 0.0 | 0.0 | 0.03 | 31.91 | 82.65 |
| Warrenton | 3b | 13.77 | 0.04 | 1.09 | 0.33 | 21.59 | 0.19 | 0.02 | 13.80 | 0.09 | 0.23 | 0.03 | 0.05 | 0.00 | 0.0 | 0.0 | 0.03 | 32.38 | 83.63 |
| Warrenton | 3b | 13.37 | 0.08 | 1.29 | 0.38 | 19.90 | 0.16 | 0.02 | 12.33 | 0.29 | 0.45 | 0.07 | 0.08 | 0.00 | 0.0 | 0.0 | 0.06 | 30.95 | 79.43 |
| Warrenton | 3b | 12.65 | 0.07 | 1.55 | 0.49 | 23.08 | 0.16 | 2.44 | 12.55 | 0.35 | 0.39 | 0.03 | 0.08 | 0.03 | 0.0 | 0.0 | 0.58 | 32.92 | 87.36 |
| Warrenton | 3b | 13.01 | 0.04 | 2.94 | 0.08 | 17.54 | 0.14 | 0.03 | 10.60 | 0.39 | 1.89 | 0.20 | 0.09 | 0.00 | 0.0 | 0.0 | 0.04 | 30.58 | 77.58 |
| Warrenton | 3b | 14.99 | 0.07 | 1.71 | 0.36 | 20.38 | 0.17 | 0.15 | 12.85 | 1.48 | 0.61 | 0.09 | 0.07 | 0.00 | 0.0 | 0.0 | 0.12 | 34.30 | 87.35 |
| Warrenton | 3c | 13.35 | 0.05 | 1.57 | 0.34 | 22.61 | 0.17 | 1.07 | 13.43 | 0.12 | 0.17 | 0.01 | 0.07 | 0.01 | 0.0 | 0.0 | 0.03 | 32.70 | 85.69 |
| Warrenton | 3c | 14.00 | 0.05 | 1.18 | 0.31 | 22.90 | 0.19 | 0.04 | 14.10 | 0.09 | 0.10 | 0.01 | 0.08 | 0.00 | 0.0 | 0.0 | 0.02 | 33.30 | 86.40 |
| Warrenton | 3c | 13.98 | 0.06 | 1.25 | 0.38 | 23.04 | 0.18 | 0.12 | 14.25 | 0.09 | 0.10 | 0.01 | 0.08 | 0.00 | 0.0 | 0.0 | 0.03 | 33.55 | 87.13 |
| Warrenton | 3c | 14.26 | 0.06 | 1.23 | 0.34 | 23.69 | 0.19 | 0.57 | 14.52 | 0.08 | 0.05 | 0.00 | 0.07 | 0.00 | 0.0 | 0.0 | 0.03 | 34.27 | 89.35 |
| Warrenton | 3c | 14.28 | 0.06 | 1.42 | 0.35 | 24.09 | 0.19 | 0.57 | 14.60 | 0.07 | 0.10 | 0.01 | 0.06 | 0.01 | 0.0 | 0.0 | 0.05 | 34.68 | 90.54 |
| Warrenton | 3c | 14.63 | 0.05 | 0.85 | 0.34 | 23.45 | 0.19 | 0.24 | 15.32 | 0.09 | 0.04 | 0.00 | 0.08 | 0.00 | 0.0 | 0.0 | 0.01 | 34.70 | 89.99 |
| Warrenton | 3c | 14.02 | 0.06 | 1.31 | 0.31 | 23.71 | 0.17 | 1.06 | 14.39 | 0.10 | 0.14 | 0.00 | 0.07 | 0.00 | 0.0 | 0.0 | 0.07 | 34.21 | 89.62 |
| Warrenton | 3c | 14.02 | 0.06 | 1.33 | 0.33 | 23.74 | 0.18 | 1.01 | 14.34 | 0.11 | 0.14 | 0.02 | 0.07 | 0.00 | 0.0 | 0.0 | 0.06 | 34.19 | 89.58 |
| Warrenton | 3c | 13.84 | 0.05 | 1.10 | 0.32 | 22.58 | 0.20 | 0.13 | 13.99 | 0.08 | 0.05 | 0.01 | 0.08 | 0.00 | 0.0 | 0.0 | 0.05 | 32.92 | 85.40 |
| Warrenton | 3c | 15.42 | 0.05 | 0.95 | 0.29 | 22.81 | 0.19 | 0.64 | 15.17 | 1.23 | 0.06 | 0.00 | 0.11 | 0.01 | 0.0 | 0.0 | 0.03 | 36.03 | 92.99 |
| Warrenton | 3c | 15.22 | 0.06 | 1.29 | 0.35 | 23.62 | 0.18 | 0.10 | 14.77 | 0.63 | 0.20 | 0.02 | 0.06 | 0.00 | 0.0 | 0.0 | 0.03 | 35.72 | 92.26 |
| Warrenton | 3c | 15.30 | 0.05 | 1.68 | 0.38 | 23.48 | 0.19 | 0.15 | 14.74 | 0.88 | 0.37 | 0.05 | 0.07 | 0.00 | 0.0 | 0.0 | 0.03 | 36.30 | 93.67 |
| Warrenton | 3c | 14.67 | 0.07 | 1.81 | 0.33 | 24.17 | 0.19 | 0.75 | 14.17 | 0.16 | 0.52 | 0.03 | 0.05 | 0.00 | 0.0 | 0.0 | 0.12 | 35.52 | 92.56 |
| Warrenton | 3c | 14.56 | 0.06 | 1.90 | 0.48 | 25.07 | 0.18 | 0.73 | 14.59 | 0.14 | 0.28 | 0.01 | 0.07 | 0.00 | 0.0 | 0.0 | 0.20 | 36.13 | 94.42 |
| Warrenton | 3c | 15.07 | 0.06 | 1.55 | 0.35 | 24.93 | 0.19 | 0.16 | 15.24 | 0.13 | 0.26 | 0.04 | 0.07 | 0.00 | 0.0 | 0.0 | 0.08 | 36.39 | 94.52 |
| Warrenton | 3c | 14.91 | 0.05 | 1.33 | 0.30 | 24.37 | 0.22 | 0.15 | 15.25 | 0.14 | 0.26 | 0.03 | 0.06 | 0.00 | 0.0 | 0.0 | 0.03 | 35.74 | 92.84 |
| Warrenton | 3c | 15.18 | 0.06 | 1.58 | 0.30 | 24.29 | 0.20 | 0.44 | 14.99 | 0.20 | 0.54 | 0.04 | 0.09 | 0.00 | 0.0 | 0.0 | 0.03 | 36.30 | 94.22 |
| Warrenton | 3c | 14.79 | 0.05 | 2.49 | 0.43 | 23.85 | 0.20 | 0.95 | 14.51 | 0.75 | 0.72 | 0.08 | 0.34 | 0.01 | 0.0 | 0.0 | 0.04 | 37.06 | 96.26 |
| Warrenton | 3c | 14.84 | 0.07 | 2.82 | 0.41 | 23.38 | 0.21 | 0.80 | 14.17 | 0.92 | 0.96 | 0.09 | 0.43 | 0.01 | 0.0 | 0.0 | 0.05 | 37.31 | 96.47 |
| Warrenton | 3c | 14.83 | 0.07 | 2.30 | 0.33 | 24.18 | 0.20 | 1.49 | 14.54 | 0.54 | 0.78 | 0.07 | 0.24 | 0.02 | 0.0 | 0.0 | 0.04 | 36.98 | 96.61 |
| Warrenton | 3c | 15.81 | 0.12 | 2.86 | 0.30 | 21.25 | 0.17 | 1.35 | 13.28 | 1.41 | 1.55 | 0.14 | 0.11 | 0.02 | 0.0 | 0.0 | 0.03 | 37.35 | 95.77 |

Continued on next page

| Sample | Area | Si | Ti | Al | Cr | Fe | Mn | Ni | Mg | Ca | Na | K | P | Co | V | Zn | S | O | Total |
|---|---|---|---|---|---|---|---|---|---|---|---|---|---|---|---|---|---|---|---|
| Warrenton | 3c | 15.41 | 0.09 | 2.79 | 0.29 | 22.87 | 0.19 | 2.31 | 13.37 | 0.59 | 1.44 | 0.15 | 0.06 | 0.02 | 0.0 | 0.0 | 0.04 | 37.17 | 96.78 |
| Warrenton | 3c | 15.69 | 0.09 | 3.37 | 0.24 | 21.14 | 0.18 | 0.89 | 12.67 | 0.67 | 1.94 | 0.19 | 0.08 | 0.01 | 0.0 | 0.0 | 0.04 | 36.89 | 94.09 |
| Warrenton | 3c | 15.43 | 0.07 | 1.61 | 0.21 | 23.54 | 0.20 | 0.87 | 14.08 | 0.19 | 0.74 | 0.09 | 0.08 | 0.01 | 0.0 | 0.0 | 0.05 | 36.00 | 93.16 |
| Warrenton | 3c | 14.96 | 0.06 | 0.94 | 0.23 | 24.22 | 0.19 | 1.15 | 14.46 | 0.10 | 0.17 | 0.01 | 0.09 | 0.01 | 0.0 | 0.0 | 0.04 | 35.15 | 91.79 |
| Warrenton | 3c | 14.36 | 0.06 | 2.14 | 0.48 | 24.77 | 0.20 | 1.46 | 14.42 | 0.29 | 0.14 | 0.02 | 0.20 | 0.02 | 0.0 | 0.0 | 0.11 | 36.17 | 94.84 |
| Warrenton | 3c | 14.53 | 0.05 | 2.35 | 0.53 | 24.71 | 0.21 | 1.19 | 14.56 | 0.60 | 0.20 | 0.02 | 0.32 | 0.01 | 0.0 | 0.0 | 0.06 | 36.80 | 96.15 |
| Warrenton | 3c | 13.74 | 0.06 | 1.83 | 0.29 | 21.55 | 0.17 | 0.77 | 13.10 | 0.18 | 0.58 | 0.06 | 0.07 | 0.00 | 0.0 | 0.0 | 0.05 | 32.96 | 85.41 |
| Warrenton | 3c | 13.78 | 0.06 | 1.62 | 0.29 | 21.53 | 0.18 | 0.86 | 13.15 | 0.18 | 0.56 | 0.04 | 0.05 | 0.01 | 0.0 | 0.0 | 0.03 | 32.81 | 85.14 |
| Warrenton | 3c | 13.61 | 0.05 | 1.54 | 0.28 | 21.05 | 0.15 | 0.11 | 12.95 | 0.14 | 0.36 | 0.03 | 0.05 | 0.00 | 0.0 | 0.0 | 0.04 | 31.96 | 82.30 |
| Warrenton | 3c | 13.55 | 0.04 | 1.12 | 0.28 | 21.37 | 0.18 | 0.02 | 13.31 | 0.20 | 0.08 | -0.00 | 0.06 | 0.00 | 0.0 | 0.0 | 0.04 | 31.78 | 82.03 |
| Warrenton | 3c | 13.14 | 0.04 | 1.45 | 0.37 | 21.85 | 0.17 | 0.38 | 13.51 | 0.12 | 0.05 | 0.00 | 0.06 | 0.00 | 0.0 | 0.0 | 0.04 | 31.97 | 83.16 |
| Warrenton | 3c | 14.34 | 0.03 | 1.67 | 0.30 | 18.58 | 0.15 | 0.15 | 12.12 | 2.22 | 0.41 | 0.04 | 0.08 | 0.00 | 0.0 | 0.0 | 0.03 | 32.55 | 82.67 |
| Warrenton | 3c | 13.38 | 0.04 | 1.71 | 0.31 | 20.87 | 0.16 | 0.17 | 12.89 | 0.14 | 0.41 | 0.04 | 0.06 | 0.00 | 0.0 | 0.0 | 0.03 | 31.82 | 82.02 |
| Warrenton | 3c | 16.99 | 0.04 | 0.96 | 0.24 | 16.74 | 0.13 | 0.04 | 11.71 | 5.00 | 0.06 | 0.00 | 0.08 | 0.00 | 0.0 | 0.0 | 0.04 | 35.08 | 87.13 |
| Warrenton | 3c | 16.22 | 0.04 | 1.19 | 0.31 | 16.01 | 0.13 | 0.06 | 11.34 | 5.20 | 0.11 | 0.01 | 0.08 | 0.00 | 0.0 | 0.0 | 0.04 | 34.08 | 84.82 |
| Warrenton | 3c | 13.24 | 0.06 | 0.87 | 0.30 | 20.85 | 0.17 | 0.03 | 12.54 | 0.09 | 0.08 | 0.00 | 0.05 | 0.00 | 0.0 | 0.0 | 0.04 | 30.52 | 78.86 |